NERDDC / SENRAC RESEARCH PROJECT

Origin, Evolution and Controls of Permian Reservoir Sandstones in the Southern Cooper Basin, South Australia

Author:

J.P. Schulz-Rojahn, M.Sc., B.Sc.(Hons.)

Thesis submitted to the University of Adelaide in fulfilment of the requirement for the degree of Doctor of Philosophy

National Centre for Petroleum Geology & Geophysics (NCPGG)/
Department of Geology & Geophysics

- November 1991 -

Statement of authenticity and availability

This thesis contains no material which has been accepted for the award of any other degree or diploma in any University. To the best of my knowledge and belief the thesis contains no material previously published or written by another person, except where due reference is made in the text.

If accepted for the award of the degree and, if applicable, I consent to the thesis being made available for photocopying and loan.

Jörg Schulz-Rojahn

Abstract

The Cooper Basin, containing Permo-Triassic sediments of fluvio-lacustrine and deltaic origin, is characterised by dominantly low-porosity, low-permeability reservoir sandstones for oil and gas occurring at burial depths between about 5400 and 12,000 feet subsea. Ambient core porosity averages 10.7 % and permeability 30 md, with over 75 % of sandstones having permeabilities less than 5 md. Despite its overall poor reservoir characteristics, the basin is one of Australia's major hydrocarbon provinces; ultimate sales gas reserves amount to about 6 TCF, and gas-liquids and oil reserves approach 310 MMSTB.

The objective of this thesis was to define the interaction of factors influencing reservoir quality in Permian sandstones of the southern Cooper Basin. A total of 887 core and ditch samples from 82 field and wildcat wells were investigated, including the Wancoocha, Daralingie, Toolachee, Strzelecki, Munkarie, Big Lake and Moomba Fields. In all, almost 900 feet of core were logged. The samples collected were studied using an array of different techniques such as optical petrography, X-ray diffraction, scanning electron microscopy, cathodoluminescence and oxygen/carbon isotope geochemistry. The results were integrated with over 7000 porosity and permeability values derived from 148 petroleum wells, as well as DST and production test data.

Diagenetic factors, sedimentary facies and basin architecture all influence reservoir quality. Principal cementing agents include authigenic quartz and various carbonate minerals, mostly siderite but also ankerite, dolomite and calcite. Authigenic clay minerals include illite, kaolinite, dickite, clinochlore and pyrophyllite.

Petrographic evidence enabled establishment of the diagenetic sequence for the authigenic minerals relative to the timing of hydrocarbon generation and migration in the study area. The results suggest the precipitation of several authigenic mineral phases occurred synchronous with, or postdating hydrocarbon migration. Mineral authigenesis involved both grain replacement and precipitation from migrating pore fluids. Pyrophyllite is considered to have formed under conditions of low-grade metamorphism in the central Nappamerri Trough (R_v max. > 5 %).

An early phase of silicification provided a rigid grain framework which mainly suppressed mechanical compaction in numerous moderate to well-sorted sandstones of point bar and crevasse splay origin. These sandstones represent the most common hydrocarbon reservoirs in the southern Cooper Basin, and despite multiple phases of silicification retain the highest average porosity and permeability. Effective primary intergranular porosity was retained in such reservoir facies particularly in marginal and midflank areas of the basin, but also in more basinal areas to depths approaching 10,000 feet. Other attractive targets for petroleum exploration include distributary delta mouthbar and shoreline sands. Where secondary dissolution pores occur in conjunction with primary pores, effective permeability is enhanced. Sandstones with abundant macroporosity can produce at initial flow rates in excess of 11 MMCFD.

With increasing depth of burial, there is a broad transition towards reservoirs dominated by microporosity associated with kaolin clays. Microporous rocks are characterised by core porosities as high as about 15 % but permeabilities of typically 2 md or less. Significantly, microporosity in sandstones of the Moomba and Big Lake Fields accounts for much of the total porosity in reservoirs which have produced more than a trillion cubic feet of gas. Where there are remnants of primary pores in microporous zones, DST flow rates of 2 MMCFD and more are recorded. Undoubtedly, the drilling of deeper targets has the potential to yield large commercial hydrocarbon discoveries in the study area. It is suggested that high-quality reservoir facies occur within low-permeability sequences.

Irreducible water associated with kaolin clays likely affects hydrocarbon reserve calculations. Pessimistic computation of S_w due to bound water of irreducible nature may lead to productive zones being by-passed because they appear water-wet.

Isotope results provide constraints on the modes of formation of carbonate cements in the study area. Likely carbon sources include atmospheric CO_2, thermal decarboxylation reactions, and bacterial fermentation reactions and/or methanogenesis. Siderite precipitation occurred throughout the Permian and may have continued into the Late Cretaceous.

Massive carbonate-cemented zones may serve as a guide to commercial hydrocarbon accumulations in the Eromanga Basin overlying the Cooper Basin. The formation of intensely carbonate-cemented zones in the Eromanga Basin is believed to be controlled by the injection of Cooper Basin carbon dioxide into the calcium-bearing Eromanga aquifers. The zones of intense carbonate cementation are considered to reflect the preferred migration pathways of the carbon dioxide and hence also the hydrocarbons. The delineation of such zones in the subsurface using seismic sections and wireline logs may prove to be an invaluable new exploration tool. The origin of the carbon dioxide is poorly understood but is believed to be at least partly related to thermal maturation reactions involving organic matter.

TABLE OF CONTENTS

LIST OF FIGURES

LIST OF TABLES

LIST OF PLATES

APPENDICES

CHAPTER ONE

INTRODUCTION

1.1 Economic background

Over the last two decades, Australia has enjoyed a high level of self-sufficiency in petroleum. This has reduced its needs for oil imports, and enabled the nation to become a net exporter of substantial quantities of both liquefied petroleum gas and natural gas. Recent statistics published by the Bureau of Mineral Resources (BMR) in Canberra, however, indicate that the potential exists for a significant decline in Australia's oil and gas production in the short to medium-range future. The country's remaining commercial reserves of crude oil and condensate are estimated at 1676 million barrels, representing only 8.5 years production at current rates (Powell et al., 1990). Commercial gas reserves amount to 16 trillion cubic feet (TCF) which represents 30 years' production at current rates (Powell et al., 1990).

According to the Australian Institute of Petroleum (AIP), the country's self-reliance in petroleum products may fall from approximately 84 percent at present to 33 percent within ten years, unless significant new petroleum reserves are located. This scenario would seriously affect the nation's balance of payments and foreign debt, with petroleum imports projected to rise to about $US 5.6 billion by 1999 - compared with little more than $US 1 billion this year.

For these reasons, the development of Australia's natural petroleum resources must rank among the nation's top economic priorities. The changing balance in the supply of fossil fuels highlights the growing need for new and innovative thinking in resource exploration. Petroleum reserves in either established or poorly explored regions can be increased by both refinement of old play concepts and development of new perceptions of prospectivity.

One of Australia's major onshore petroleum provinces is the Cooper Basin located in South Australia and Queensland. Since 1963, when the first commercial gas discovery was made at Gidgealpa, 100 gas and 10 oil fields have been discovered here, containing about 170 x 10^6 m^3 of sales gas (6 TCF) and 2000 kL of oil and gas liquids (300 MMSTB) (Laws, 1989). At present, two Australian states - South

Australia and New South Wales - are dependent on gas supplies from the region, total gas sales amounting to approximately 200 PJ per year (Laws, 1989).

Petroleum exploration in the basin has traditionally concentrated on drilling crestal features, resulting in the discovery of fields such as Moomba and Big Lake. However, as the basin enters its mature phase of exploration, structural prospects of economic size with simple four- or three-way dip closures continuously decrease in number. Significant future hydrocarbon discoveries are likely to be made through definition of alternative play styles with probable stratigraphic and/or diagenetic components. Similarly, improved production performance of existing fields in the basin will depend largely on a detailed knowledge of facies interrelationships, as well as the diagenetic controls affecting reservoir quality.

The present study focuses on the evolution of the reservoir sandstones in the southern Cooper Basin, addressing both their modes of deposition and diagenetic history. The work forms part of a co-ordinated research strategy involving staff and students of the University of Adelaide, and was carried out in close collaboration with the South Australian Department of Mines and Energy (SADME) and the Cooper Basin Consortium Group of Companies [1]. Project funding was provided by the State Energy Research Advisory Committee (SENRAC) and the National Energy Research, Development and Demonstration Council (NERDDC) [2].

1.2 Project objectives

Several research goals were set. First, the project aimed to identify the factors influencing reservoir quality in Permian sandstones of the southern Cooper Basin, hypothesised to include diagenesis, sedimentary processes and structural growth. A second objective was to establish the broad sequential order of authigenic clay and cement formation, with particular reference to the timing of hydrocarbon generation and migration. Further, the author wanted to determine the causal mechanisms controlling mineral authigenesis in the basin. Another major objective was to delineate regional diagenetic trends and changes in porosity-permeability character with depth, complementing field-specific data obtained by Alsop (1990), Eleftheriou (1990), Phillips (unpubl.), Sansome (1988) and Thomas (1990).

---

[1] Santos Ltd., Sagasco Resources Ltd., Delhi Petroleum Pty. Ltd. (Esso Australia Ltd.), Western Mining Corporation Ltd., Bridge Oil Ltd., Hartogen Energy Ltd., Crusader Ltd., TCPL, Adelaide Petroleum Ltd., Basin Oil N.L.

[2] NERDDC project number 1175

Project objectives were anticipated to help define the prospectivity of less explored areas in the Cooper Basin, as well as to provide industry with conceptual models to better exploit sandstone reservoirs in existing petroleum fields. The development of conceptual models for new or improved play definition in the basin was hoped to lead to their application by industry to other petroleum provinces.

1.3 Previous investigations

Relatively little information has been published regarding the factors influencing porosity and permeability in the Cooper Basin. A brief outline of the mineralogy and petrology of some Permian sandstones was provided by Smale & Trueman (1965) and later by Steveson & Spry (1973). Stanley & Halliday (1984) commented on diagenetic processes affecting reservoir quality in Early Permian sandstones in four deep wells in the Big Lake Field. On the basis of three wells, Martin & Hamilton (1981) discussed the composition, diagenesis and porosity characteristics of the Toolachee Formation. The most comprehensive regional study of diagenetic processes in the Cooper Basin, including the overlying Eromanga Basin, is provided by Wall (1987). This unpublished report was based predominantly on student research in selected oil and gas fields (Stern, 1984; Denton, 1985; Edwards, 1985; Menhennitt, 1985; Pianalto, 1985; Staughton, 1985; Walsh, 1985) and concluded that authigenic quartz and compaction were the major factors causing a reduction in porosity. Wild (1987) identified the diagenetic sequence in the Tirrawarra Sandstone of the Merrimelia and Tirrawarra Fields. Reservoir quality was found to be reduced by diagenetic processes including compaction and authigenic cements. Additional information is contained in isolated unpublished petrographic reports for the Cooper Basin Consortium Group of Companies.

1.4 Methods and work program

1.4.1 Study area

Work was focused on the southern and central portions of PEL 5 and 6 in the southern Cooper Basin as here the majority of wells have been drilled and most

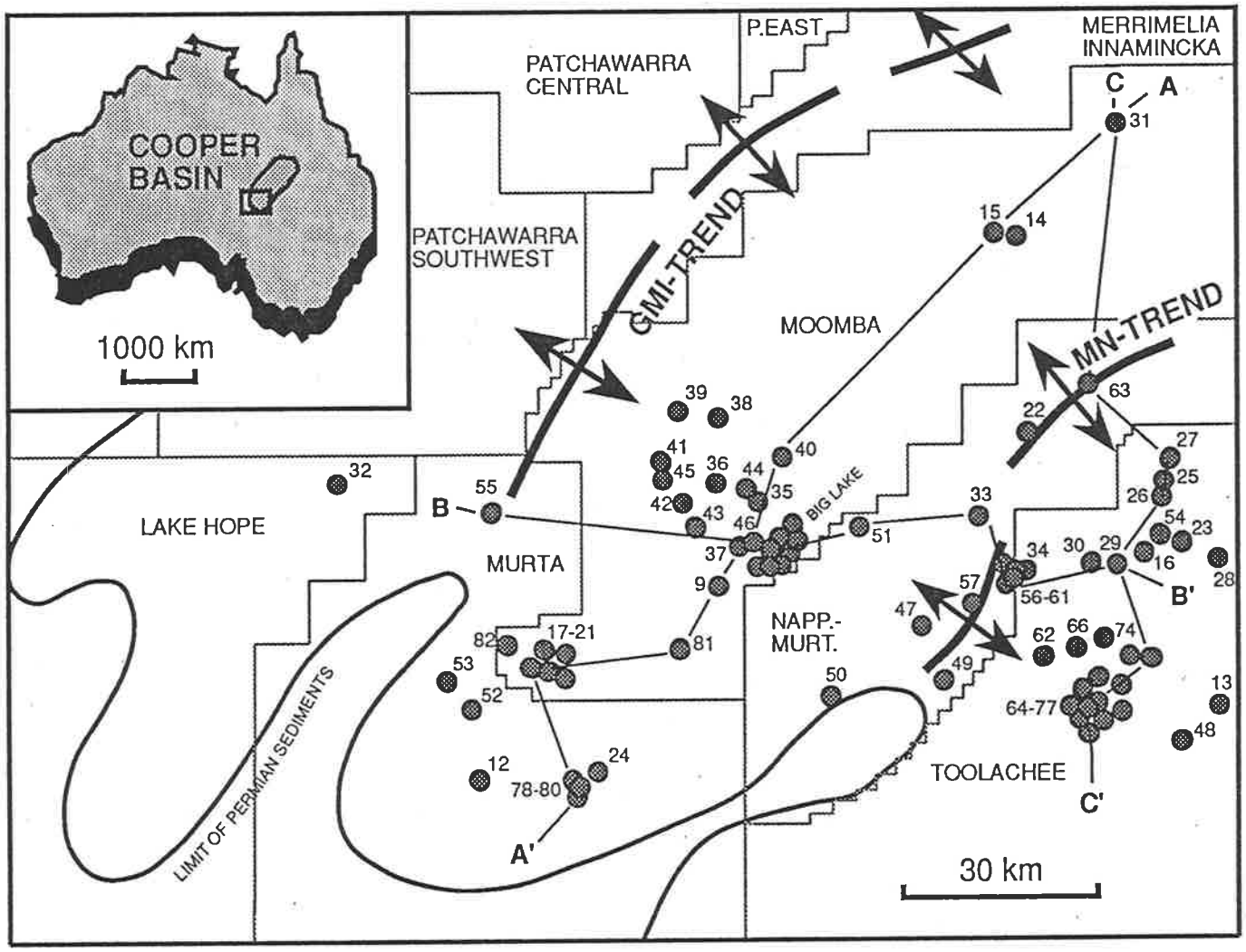

Figure 1.1 Locality plan of study area. For well names refer to Table 1.1 (Lines of section included as Enclosures 1-3) [MN = Murteree-Nappacoongee; GMI = Gidgealpa-Merrimelia-Innamincka].

petroleum reserves are located. The study area incorporates the Moomba, Nappacoongee-Murteree, Toolachee, Murta and Lake Hope petroleum blocks (Fig.1.1; Encl.1). Field and wildcat wells sampled are listed in Table 1.1

Geologically, the area of investigation occurs immediatly south of the Gidgealpa-Merrimelia-Innamincka (GMI) Trend and includes the Nappamerri and Tennaperra Troughs which are separated by the Murteree-Nappacoongee (MN) High (Fig.1.1; Encl.1). Wells from a variety of structural settings are incorporated into the project. Kirby and Burley represent wells from the basin depocentre whereas wells such as Wancoocha, Pando, Dirkala and Daralingie were drilled in more marginal areas of the basin. Numerous intervening field and wildcat wells were also investigated (Fig.1.1, Table 1.1).

1.4.2 Project participants

Results presented here synthesise the research efforts of the author as well as those of other NERDDC project participants. Table 1.2 lists the individuals involved in the study program, their principal research areas, and the number of samples collected and processed by each worker (see Appendix A for details). Where data obtained by these individuals is incorporated into the present study, due acknowledgements are given. However, to guarantee maximum database consistency, much of the data was re-examined by the author, including the entire NERDDC thin section database, all cathodoluminescence photomicrographs, and the bulk of the X-ray diffraction data. For this reason, a certain degree of unavoidable overlap exists between the work of the author and that of the other project participants. Investigative results obtained in the course of the present investigation are presented in Appendices C-K; for additional data the reader is referred to the work of Sansome (1988), Alsop (1990), Thomas (1990), Eleftheriou (1990), and Stuart et al. (1990).

1.4.3 Research strategy

The research procedures adopted to achieve the specific aims of the project are illustrated in Figure 1.2. The flow chart illustrates the sequential order of research stages accomplished during the course of the present investigation. Three main stages

Table 1.1 Wells sampled and number of core and ditch samples analysed from various formations during NERDDC project 1175 (for location of wells see Figure 1.1).

No.	Well	Napp.	Tool.	Dara.	Rose.	Eps.	Murt.	Patch.	Tirr.	Merr.	Pre-Per.
1	Big Lake-1	-	27	-	-	-	-	-	-	-	-
2	Big Lake-2	-	18	-	-	-	-	-	-	-	-
3	Big Lake-3	-	-	-	-	9	-	1	-	-	-
4	Big Lake-5	-	-	-	-	-	-	-	10	-	-
5	Big Lake-26	1	4	2	1	4	2	8	1	1	-
6	Big Lake-27	-	-	-	-	-	-	3	5	-	-
7	Big Lake-29	-	-	-	-	-	-	1	3	-	-
8	Big Lake-31	-	-	-	-	-	-	3	6	-	-
9	Big Lake-33	1	4	2	3	5	2	8	1	-	-
10	Big Lake-34	-	-	-	-	-	-	2	-	-	-
11	Big Lake-35	-	-	-	-	-	-	3	-	-	-
12	Boxwood-1	-	-	-	-	2	-	-	-	-	-
13	Brumby-1	-	-	-	-	-	-	5	-	-	-
14	Burley-1	-	9	-	-	-	-	-	-	7	-
15	Burley-2	1	11	3	2	9	2	8	1	1	-
16	Coochilara-1	-	-	-	-	2	-	3	-	-	-
17	Daralingie-1	1	15	1	-	2	-	4	-	1	1
18	Daralingie-2	1	1	1	-	2	-	1	-	1	1
19	Daralingie-9	-	-	-	-	-	-	3	-	-	-
20	Daralingie-19	-	-	-	-	-	-	4	-	-	-
21	Daralingie-22	-	-	-	-	-	-	3	-	-	-
22	Della-3	-	16	-	-	-	-	-	-	-	-
23	Dilchee-1	-	-	-	-	-	-	5	-	-	-
24	Dirkala-2	-	-	-	-	3	-	-	-	-	-
25	Dullingari-1	-	3	-	-	-	-	-	-	-	-
26	Dullingari-18	1	2	1	-	2	-	11	-	-	-
27	Dullingari-39	1	3	1	-	2	-	4	-	-	-
28	Kerna-1	-	-	-	-	6	-	7	-	-	-
29	Kidman-1	1	9	-	-	3	-	6	-	-	-
30	Kidman-2	-	1	-	-	-	-	-	-	-	-
31	Kirby-1	1	8	-	1	10	1	7	1	-	-
32	Lake Hope-1	-	-	-	-	3	-	-	-	-	-
33	Marabooka-1	1	3	-	-	-	-	8	-	-	-
34	Marana-1	-	4	-	-	-	-	-	-	-	-
35	Moomba-1	-	15	4	-	-	2	5	-	-	-
36	Moomba-3	-	15	6	-	-	-	-	-	-	-
37	Moomba-4	-	10	-	-	-	-	-	-	-	-
38	Moomba-5	-	4	3	-	-	-	-	-	-	-
39	Moomba-6	-	36	-	-	-	-	4	-	-	-
40	Moomba-7	1	13	4	-	3	-	5	-	-	-
41	Moomba-8	-	8	5	-	-	-	-	-	-	-
42	Moomba-9	-	13	4	-	-	-	-	-	-	-
43	Moomba-10	-	7	-	-	-	-	-	-	-	-
44	Moomba-52	-	4	-	-	-	-	-	-	-	-
45	Moomba-53	-	4	1	-	-	-	-	-	-	-
46	Moomba-57	1	4	3	-	3	-	5	2	-	-
47	Mudlalee-1	-	5	-	-	-	-	-	-	-	-
48	Munkarie-2	-	-	-	-	6	-	3	-	-	-

Table 1.1 (cont.)

49	Murteree-1	-	7	-	-	-	-	-	-	-	-
50	Murteree-C1	-	4	-	-	-	-	-	-	-	-
51	Namur-1	1	1	-	-	-	-	2	-	-	-
52	Pando-2	-	-	-	-	3	-	-	-	-	-
53	Pando North-1	-	-	-	-	4	-	-	-	-	-
54	Pira-2	-	2	-	-	-	-	4	-	-	-
55	Spencer-1	-	7	-	-	-	-	-	-	-	-
56	Strzelecki-1	-	18	-	-	-	-	15	-	-	-
57	Strzelecki-2	-	3	-	-	-	-	-	-	-	-
58	Strzelecki-5	-	3	-	-	-	-	-	-	-	-
59	Strzelecki-10	1	5	-	-	-	-	1	3	2	-
60	Strzelecki-15	-	4	-	-	-	1	-	-	-	-
61	Strzelecki-16	-	4	-	-	-	-	-	-	-	-
62	Tarwonga-2	-	-	-	-	3	-	-	-	-	-
63	Three Queens-1	1	3	2	-	2	-	6	-	-	-
64	Toolachee-1	1	6	1	-	3	-	10	-	-	-
65	Toolachee-3	1	3	-	1	2	-	28	-	-	-
66	Toolachee-5	-	-	-	-	-	-	13	-	-	-
67	Toolachee-6	-	-	-	-	-	-	10	-	-	-
68	Toolachee-8	-	-	-	-	-	-	5	-	-	-
69	Toolachee-9	-	-	-	-	-	-	6	-	-	-
70	Toolachee-12	-	-	-	-	-	-	6	-	-	-
71	Toolachee-15	-	-	-	-	-	-	5	-	-	-
72	Toolachee-18	-	-	-	-	-	-	8	-	-	-
73	Toolachee-19	-	-	-	-	-	-	6	-	-	-
74	Toolachee-21	-	-	-	-	-	-	4	-	-	-
75	Toolachee-32	-	-	-	-	4	-	-	-	-	-
76	Toolachee-34	-	-	-	-	5	-	-	-	-	-
77	Toolachee East-1	1	3	2	-	2	-	4	-	-	-
78	Wancoocha-1	-	-	-	-	5	-	4	-	-	-
79	Wancoocha-2	-	-	-	-	-	1	4	-	-	1
80	Wancoocha-4	-	-	-	-	-	1	6	-	-	1
81	Yalcumma-1	1	4	-	-	2	-	6	-	-	1
82	Yapeni-1	-	-	-	-	4	-	-	-	-	-

Abbreviations:

Napp. = Nappamerri Formation Tool. = Toolachee Formation Dara. = Daralingie Formation
Rose. = Roseneath Shale Formation Eps. = Epsilon Formation Murt. = Murteree Shale Formation
Patch. = Patchawarra Formation Tirr. = Tirrawarra Formation Merr. = Merrimelia Formation
Pre-Per. = Pre-Permian basement

Analysts	Capacity	Total number: Core	Ditch	Wells	Principal Study area(s):
Alsop, D.	M.Sc.	128	25	16	Toolachee Field
Eleftheriou, J.	M.Sc.	88	23	14	Strzelecki Field and vicinity
Lemon, N.	Staff	-	38	4	Sub-regional
Phillips, S.	Staff	106	79	13	Big Lake/Daralingie Fields
Sansome, A.	Honours	10	-	3	Daralingie Field
Thomas, A.	M.Sc.	161	33	12	Moomba Field
This study	Ph.D.	124	71	25	Sub-regional
	Total	617	269	82 *	

Table 1.2 List of analysts involved in NERDDC project 1175, principal study areas, and total number of core and ditch samples collected and processed by each worker. The number of wells studied by each project participant is also shown (*Duplicate wells exluded from total).

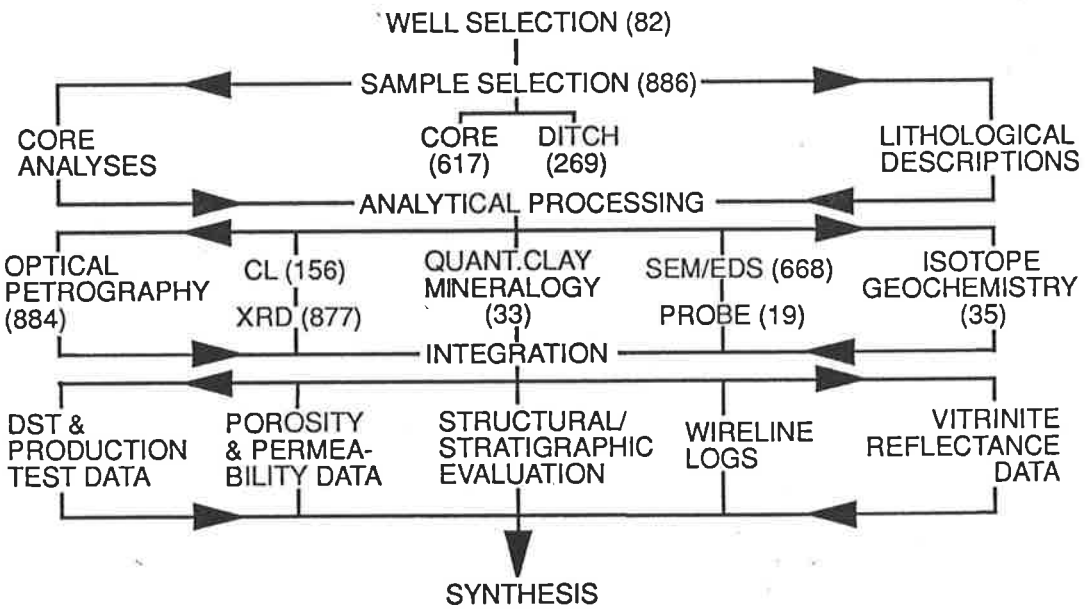

Figure 1.2 Flow diagram of research procedures adopted in the present investigation. Values in brackets refer to total number of wells/samples studied during NERDDC project 1175.

are distinguished: sample collection and data acquisition; analytical data processing; and integration of results with available geological/geochemical/geophysical information.

1.4.3.1 Sample collection and data acquisition

The first phase of NERDDC project 1175 involved the collection of both core and ditch samples from a large number of petroleum wells. In total, 617 core and 269 ditch samples were taken from 82 field and wildcat wells (Fig.1.2), covering a depth range from about 5600 to 12000 feet subsea (Fig.1.3) [3]. Based on available vitrinite reflectance data, most of these samples fall within the zone of oil generation and the wet gas window (Fig.1.4).

Research efforts were focused predominantly on the Toolachee, Epsilon and Patchawarra Formations, as these stratigraphic horizons represent the principal reservoir zones in the study area (Figs.1.5 & 2.3; Table 1.1; Appendix A). Secondary objectives included the Daralingie, Tirrawarra and Merrimelia Formations which also have proven hydrocarbon potential (Fig.2.3). A relatively small number of samples was further collected from the Nappamerri, Roseneath Shale and Murteree Shale Formations, including basement of pre-Permian origin (Fig.1.5; Table 1.1; Appendix A).

Cores selected for study were logged on a 1cm:1foot scale, noting sedimentary features, variations in grain size, grain sorting, and differences in sediment colour (Appendix J). An assessment of visual porosity trends was made and the location of core plugs noted (Appendix J). The majority of samples collected was taken at locations where core plug data is available; in many cases, new core analyses were carried out where porosity and permeability data did not already exist. Sampling of core material was based on lithology and grain size differences, palaeoenvironmental considerations, and where features of particular interest were observed, such as changes in porosity and permeability or rock colour.

Ditch cuttings were sampled to provide a continuous record of diagenetic changes with depth. Three regional, mutually intersecting traverses across the study area were initiated, incorporating selected wells from a variety of structural settings (Fig.1.1; Encl.1-3):

➢ Line A-A', a SW/NE traverse located along the central axis of the Nappamerri Trough, including wells from the basin margin and the basin depocentre:

---

[3] All depth values are in feet since imperial units currently remain in use by the Cooper Basin Consortium Group of Companies.

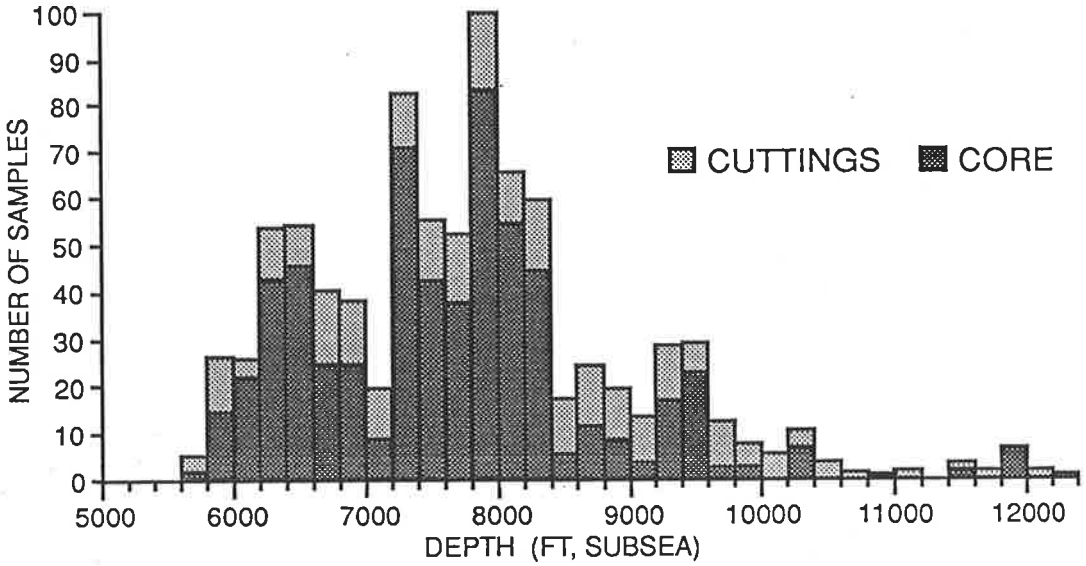

Figure 1.3 Sample distribution versus subsea depth of burial.

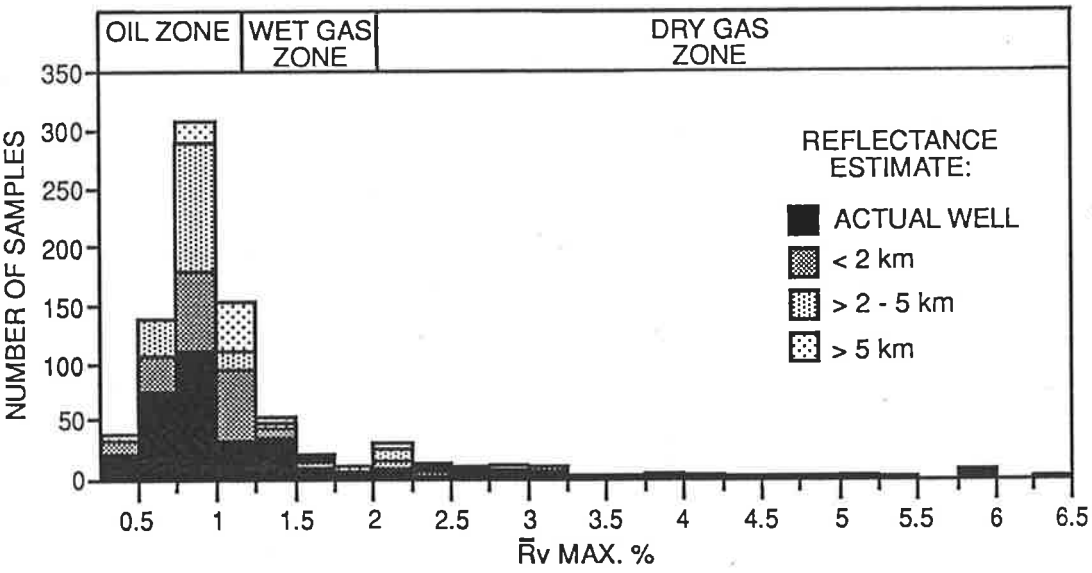

Figure 1.4 Sample distribution against vitrinite reflectivity of associated sediments. Most of the samples fall within the oil and the wet gas window. For some wells no vitrinite reflectance measurements were available; in such cases vitrinite reflectance data was extrapolated from the nearest well [Vitrinite reflectance data courtesy of Cooper Basin Consortium Group of Companies].

Wancoocha-4, Wancoocha-2, Daralingie-2, Daralingie-1, Yalcumma-1, Big Lake-33, Moomba-57, Moomba-7, Burley-2 and Kirby-1 (Enclosure 1). Wancoocha-2 is updip from Wancoocha-4 and contrasts oil-saturated reservoirs to water-wet sands in the Patchawarra Formation (Enclosure 1).

➢ Line B-B', an east-west traverse that includes wells from the GMI-Trend, the Nappamerri Trough and the Murteree-Nappacoongee High: Spencer-1, Moomba-57, Big Lake-26, Namur-1, Marabooka-1, Strzelecki-10 and Kidman-1 (Enclosure 2);

➢ Line C-C', of north-south orientation, incorporating Kirby-1, Three Queens-1, Dullingari-39, Dullingari-18, Kidman-1, Toolachee East-1, Toolachee-1 and Toolachee-3 (Enclosure 3).

Cross-sections were computer-generated utilising in-house Mincom Geolog software and SANTOS-licensed Vax software entitled 'Xsection'. Well-to-well correlation of stratigraphic intervals and facies associations was accomplished using gamma ray and sonic log signatures. All cross-sections incorporate available palynological data, drill stem test (DST) results and core information. The majority of major sandstone bodies identified from log response were sampled, in particular those for which DST or production test data exists. Identification of target sands was based on proximity to coal and/or shale marker horizons; driller's depth was offset relative to logger's depth by between approximately 5 to 40 feet for different wells. Appropriate depth corrections were applied.

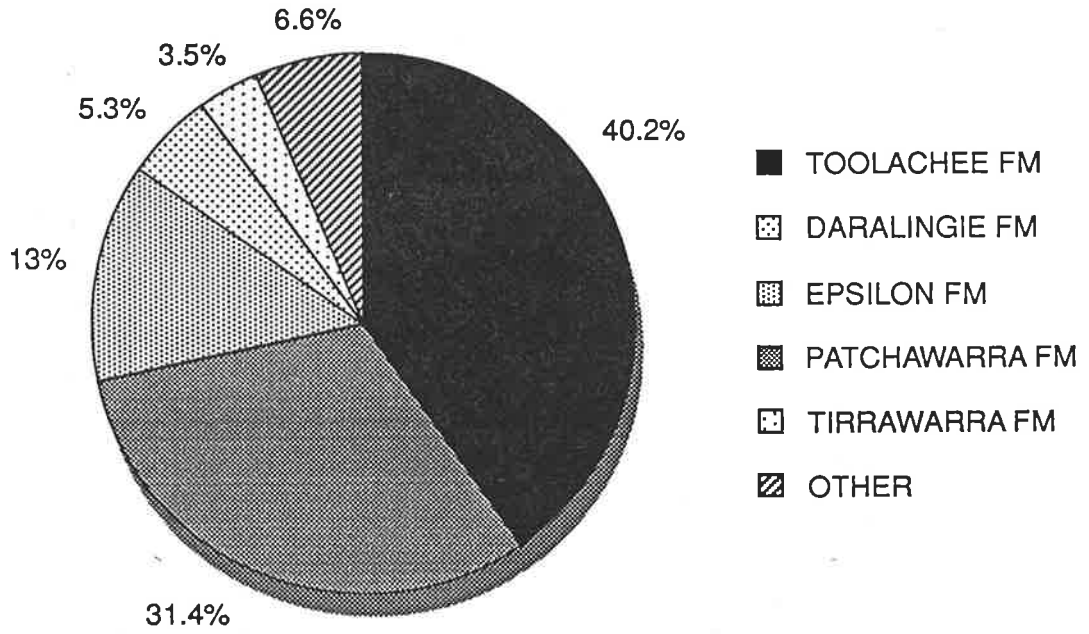

Figure 1.5 Pie-diagram showing stratigraphic origin of core and ditch samples collected during NERDDC project 1175.

1.4.3.2 Analytical procedures

An array of different techniques was used to characterise the samples collected. Routine analysis of samples involved optical petrography, scanning electron microscopy and X-ray diffraction. Ditch samples were generally not studied under the scanning electron microscope because of the fragmented nature of the sample material, rendering recognition of pore-cement relationships difficult. Other techniques employed to study the samples included cathodoluminescence (CL), oxygen and carbon isotope geochemistry, electron microprobe and quantitative clay analyses.

Detailed technical descriptions of laboratory procedures adopted are outlined below. Investigative results obtained from laboratory analyses have been summarised into a Dbase III+ database available on request from the National Centre for Petroleum Geology & Geophysics (NCPGG), Adelaide [4].

Optical petrography. All core samples and cuttings were prepared as thin sections. Blue dye was used during impregnation of the samples to facilitate the recognition of porosity. Petrographic descriptions were written for all core thin sections and photomicrographs taken of representative features. The modal mineralogical composition of several hundred thin sections was determined by point-counting, using between 700 and 1200 counts per section; for the remainder of thin sections, relative mineral abundances were determined using charts for visual estimation.

X-Ray Diffraction. Samples were mechanically ground in alcohol in a tungsten-carbide Siebtecnick mill for 30 seconds and then oven-dried at temperatures less than 100°C to minimise clay damage. Front-mounted powder pressings were run in a Siemens X-ray diffractometer at 50 kV and 35 mA, using Co K α radiation, at 4°/minute. Mineral identification was based on comparison with JCPDS files stored in CSIRO software ('XPLOT'). The illite-kaolin ratio was calculated by measuring the illite/muscovite peak height at ca. 10 Å and the kaolin peak height at 7 Å, then dividing double the illite peak height by the kaolin peak height. Kaolin type identification was accomplished by the presence or absence of the 27.3 Å peak, and the relative height of the 45.3 Å peak. In all cases, attempts were made to identify chlorite.

Scanning Electron Microscope (SEM) studies. Freshly fractured chips of core samples were mounted on aluminium stubs and then evaporatively coated with carbon (15 nm) and gold/palladium (20 nm). The samples were studied in a Philips 505/ ETEC Autoscan microscope operated at 20 kV. Features of interest were photographed using Kodak Panatomic-X black and white negative film (iso 32/16°).

---

[4] Address: National Centre for Petroleum Geology & Geophysics (NCPGG), GPO Box 498, Adelaide, South Australia 5001.

The elemental composition of each mineral photographed was determined using a Tracor Northern (TN 5500) Energy Dispersive Spectrometer (EDS).

Cathodoluminescence (CL). Polished thin sections of both core and ditch samples were prepared and cleaned to minimise pump-down time to operational vacuum levels at 0.07 to 0.01 Torr. A Technosyn model 8200 MK II generator and stage was used in conjunction with a Leitz Orthomat E automatic microscope camera. Cathodoluminescence micrographs were taken at < 1 to 30 minute exposure times in integral metering mode with high-speed Kodak Ektachrome slide or Fujicolor Super HR100 colour print film (1600 ASA). An electron gun voltage of 8 to 25 kV and a beam current of 200 to 600 mA was maintained. Reciprocity failure was compensated for by employing Orthomat E correction factors of 4 or 5.

O^{18}/O^{16} and C^{13}/C^{12} isotope ratios. The nodular siderite in sample CB-0062 was sampled on a cut surface using a small dental drill as described by Stevens & Clayton (1971). The remainder of the samples was crushed to a fine dry powder. For mass spectrometric analysis, carbon dioxide was extracted from the powdered samples by reaction with 100 per cent phosphoric acid (H_3PO_4) at 100°C under vacuum (McCrea, 1950), over reaction periods variable between 12 and 24 hours. The acid correction factors cited by Rosenbaum & Sheppard (1986) were used to compensate for the oxygen isotope fractionation occurring during the reaction with phosphoric acid. All isotope values are expressed as per mil (‰) values and refer to the University of Chicago Peedee Belemnite (PDB) standard (Craig, 1957).

Quantitative clay analysis. Detailed clay mineralogy was undertaken on 33 samples of variable lithology by Dr. S.E. Phillips of the NCPGG, Adelaide (unpublished data). Samples were hand-crushed, mechanically agitated in a dispersant solution of sodium hexametaphosphate and allowed to settle in a column of water following Stoke's Law to separate < 10 and < 20 micron fractions. The clay fraction was then flocculated with the use of NaCl, saturated with calcium, oven-dried and run both as powder pressing and an oriented sample. Oriented samples were prepared on ceramic plates, held under vacuum and saturated with Mg and glycerol. Traces were run from 3 to 30° 2 theta, at 1°/minute using Co K α radiation, in a Philips PW 1800 microprocessor-controlled diffractometer at 40 kV and 60 mA. Subsamples of the clay fractions were also prepared as oriented samples saturated with Ba for X-ray fluorescence spectometry (XRS). XRS analyses of major elemental composition and cation exchange capacity (CEC) were carried out on a Philips PW 1400 microprocessor-controlled instrument using algorithms developed by Dr. K.Norrish at CSIRO Division of Soils, Adelaide. The chemical data was then used in conjunction with the XRD results to semi-quantitatively calculate mineral abundances.

Electron Microprobe analyses. The elemental composition of carbonate cements and clays in 22 samples was determined by Dr. S.E. Phillips from the

NCPGG, Adelaide (unpublished data). Polished thin sections were evaporatively coated with carbon and analysed in a JEOL 733 Superprobe using 15 kV excitation voltage and an absorbed current of 3 nA. Following calibration using mineral and pure copper standards, quantitative analyses were triplicated using a KEVEX 7000 series energy dispersive Si(Li) detector.

Core analyses. A total of 145 core analyses were made by the Petroleum Services Section of AMDEL Core Services Pty. Ltd., Adelaide. One-inch diameter plugs were cut using tap water as the bit lubricant and coolant. All samples were trimmed square with offcuts retained. Residual hydrocarbons were extracted from the plugs using a 3:1 chloroform/methanol mix in a soxhlet extraction apparatus. After cleaning, the plugs were dried in a conventional dry oven at 100°C and then stored in a desiccator containing silica gel to cool to room temperature before proceeding with analysis. Permeability to air measurements (ambient) were determined by placing plug samples in a Hassler cell with a confining pressure of 250 psig (1725 kpa). A known pressure was then applied to the upstream sample face and the differential pressure (between the upstream and downstream faces) was monitored using a calibrated orifice and straight tube manometer. Permeability was then calculated using Darcy's Law.

To determine ambient porosity, the clean dry core plug was first placed in a matrix cup and grain volume determined by helium injection. A known volume of helium at a known pressure was expanded into the matrix cup, and the resulting pressure recorded. Grain volume was then determined using Boyle's Law, and bulk volume estimated by mercury immersion to calculate the volume percentage of pores.

Coal microscopy. A Leitz Ortholux II microscope was used to determine hydrocarbon fluorescence in polished thin sections, with a 510 nm barrier filter used in fluorescence mode (immersion oil = n_e^{23} = 1.5180 or DIN 58884).

1.4.3.3 Integration with geological and other data

In the third and final phase of the project, diagenetic results were integrated with available geological and geochemical data, as well as wireline logs (Fig.1.2).

Tectono-stratigraphic evaluation was deemed an integral part of reservoir characterisation. The structural position of reservoir intervals was determined through the combined use of (i) time-structure maps provided by SANTOS Ltd., and (ii) well-to-well correlation of stratigraphic intervals relative to sea level (Encls.1-3). Identification of generic facies was based on interpretation of core data and log character. Quantitative diagenetic results and porosity-permeability data were

correlated against sedimentological parameters such as grain size and sorting, and differentiated on the basis of facies associations.

The study was supplemented by over 7000 porosity and permeability values made available by the Cooper Basin Consortium Group of Companies and SADME [5] (see Chapter 5; Appendix K). The integration of diagenetic results with porosity-permeability data was considered critical to the delineation of reservoir trends in the basin.

The productive capability of specific reservoir zones was assessed using available DST and production test data derived from well completion reports. The study approach was anticipated to aid in the identification of generic porosity types favourable to oil and gas production.

Last, study results were integrated with existing vitrinite reflectance measurements (R_v max. %) derived from core samples and cuttings as compiled from well completion and consultant reports [6]. Estimation of thermal sediment maturity at any given depth was determined by constructing a line of best fit through available data points, and extrapolating back to the depth interval selected. In cases where no vitrinite reflectance data was available, reflectance measurements were estimated from the nearest well, details of which are provided in Appendix I.

---

[5] NERDDC project numbers 820 and 1033

[6] Keiraville Konsultants Pty. Ltd., A.J. Kantsler (University of Wollongong)

CHAPTER TWO

REGIONAL AND PETROLEUM GEOLOGY

2.1 Introduction

The Cooper Basin is a northeast trending intracratonic basin over 560 km long and 225 km wide, covering an area of approximately 130,000 km^2 (Fig.2.1). Stanmore (1989) considered it to be a Type 2A Complex Petroleum Basin as defined by Klemme (1980) whilst Yew & Mills (1989) described it as a 'rift basin'. Middleton & Hunt (1988) are of the view that the Cooper Basin is an 'interior sag basin' (Kingston et al., 1983) or 'flexural basin' as specified by Watts et al. (1982).

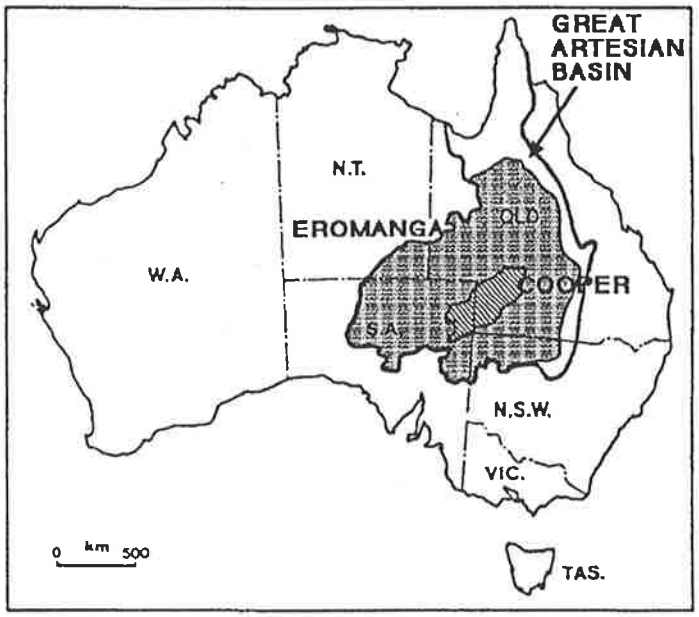

Figure 2.1 Location of Cooper and Eromanga/ Great Artesian Basins.

The contained Permo-Triassic sediments include shales, siltstones, sandstones and coals that were laid down in glacial, fluvial and lacustrine environments (Kapel, 1966, 1972; Martin, 1967a; Thornton, 1979). These clastics unconformably overlie the pre-Permian sedimentary rocks of the Warburton Basin, and metamorphic and igneous basement rocks (Battersby, 1976; Gatehouse, 1986) (Fig. 2.2). In turn, the Cooper Basin sediments are unconformably overlain by Jurassic and Cretaceous strata of the Eromanga Basin (Fig.2.2); the Eromanga Basin forms part of the 1.7 million square kilometre area of the Great Artesian Basin of central and northeastern Australia (Habermehl, 1980; Kantsler et al., 1983) (Fig.2.1). The

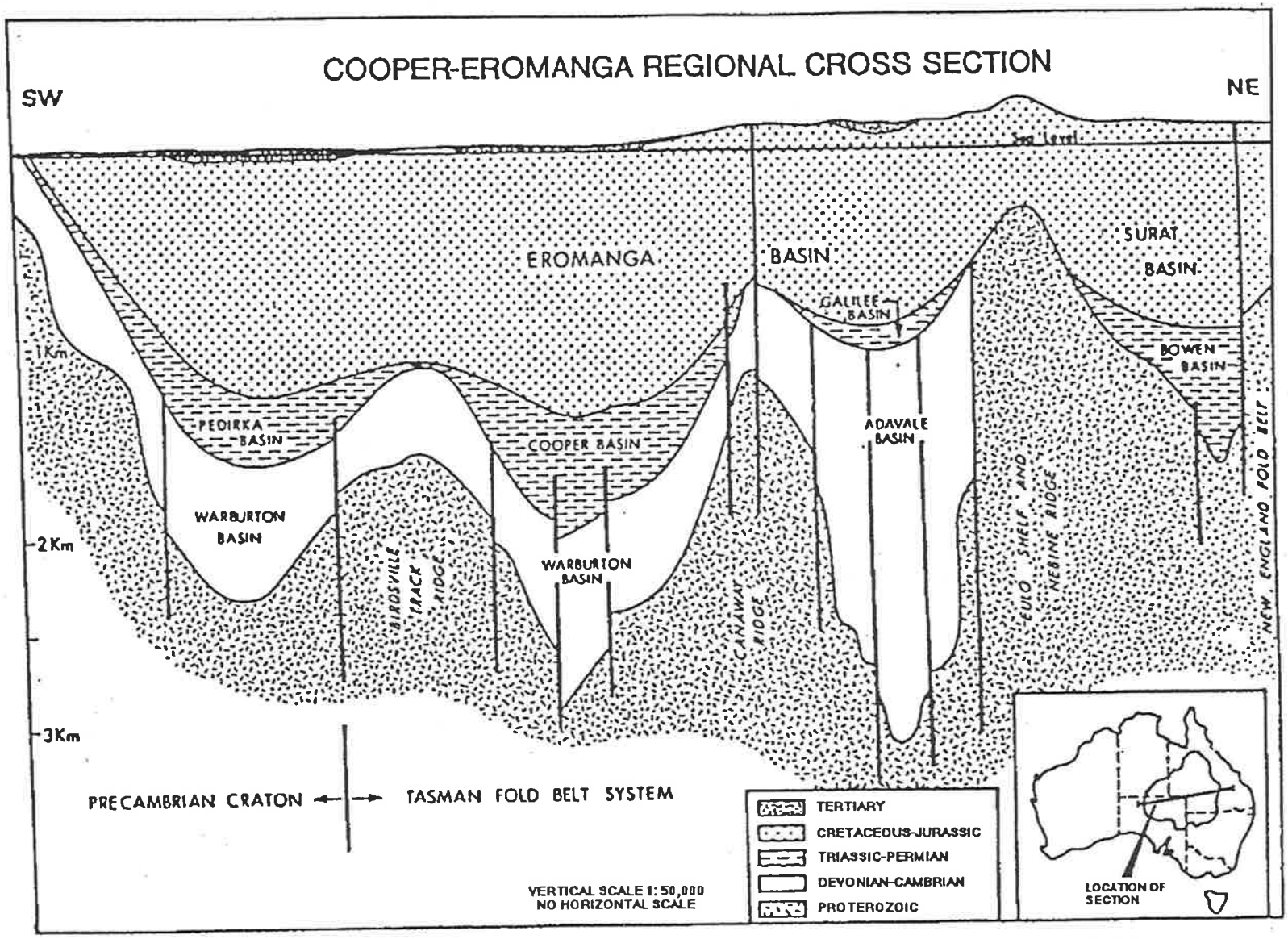

Figure 2.2 Regional cross-section of Cooper/Eromanga Basins (schematic) (modified from Santos Ltd.).

Cooper Basin is dominantly gas prone whereas the Eromanga Basin contains most of the oil in the region (Tupper & Burckhardt, 1990); significant gas in the Eromanga Basin has only been found in the Namur Gas Field in South Australia, and the Challum and Chookoo Fields in Queensland (cf. Yew & Mills, 1989; Fig.3).

2.2 Stratigraphy

The stratigraphy of the Cooper Basin has been outlined by numerous authors (Kapel, 1966, 1972; Martin, 1967a; Gatehouse, 1972; Youngs, 1975; Battersby, 1976; Stuart, 1976; Thornton, 1973, 1978, 1979; Kantsler et al., 1983; Gravestock & Morton, 1984; Williams et al., 1985; Heath, 1989; Powis, 1989; Gilby & Mortimore, 1989; Fairburn, 1989). Kapel (1966) first described the Permian strata which later was formally defined by Martin (1967a). The definition of the so-called Gidgealpa Group was revised and modified by Kapel (1972) and Gatehouse (1972). The subdivision of the Gidgealpa Group into its constituent formations was based upon both lithostratigraphic and palynological criteria (Paten, 1969; Price, 1973; Thornton, 1979) (Fig.2.3). Information pertaining to the regional pre-Permian stratigraphy is provided by Battersby (1976), Kantsler et al. (1983), Gatehouse (1986) and Roberts et al. (1990). The post-Triassic stratigraphy of the Cooper/Eromanga region is outlined by Nugent (1969), Exon & Senior (1976), Senior et al. (1978), Habermehl (1980), Senior & Habermehl (1980), Bowering (1982), Moore & Pitt (1984), Armstrong & Barr (1982, 1986), Wiltshire (1989), Passmore (1989), Gilby & Mortimore (1989), and Scholefield (1989).

2.2.1 Pre-Permian

About half of the petroleum wells drilled in the Cooper Basin penetrated pre-Permian sediments, the majority of which drilled less than 100 feet into these rocks before drilling was terminated (Gatehouse, 1986). Pre-Permian sediments include a sequence of Ordovician shales, siltstones and sandstones (Battersby, 1976; Gatehouse, 1986); Cambrian to early Ordovician carbonates (Battersby, 1976; Gatehouse, 1986; Roberts et al., 1990); and gently dipping 'Red Beds' of ?Cambrian or ?Devonian age, including a thick marine sandstone-shale sequence (Battersby,

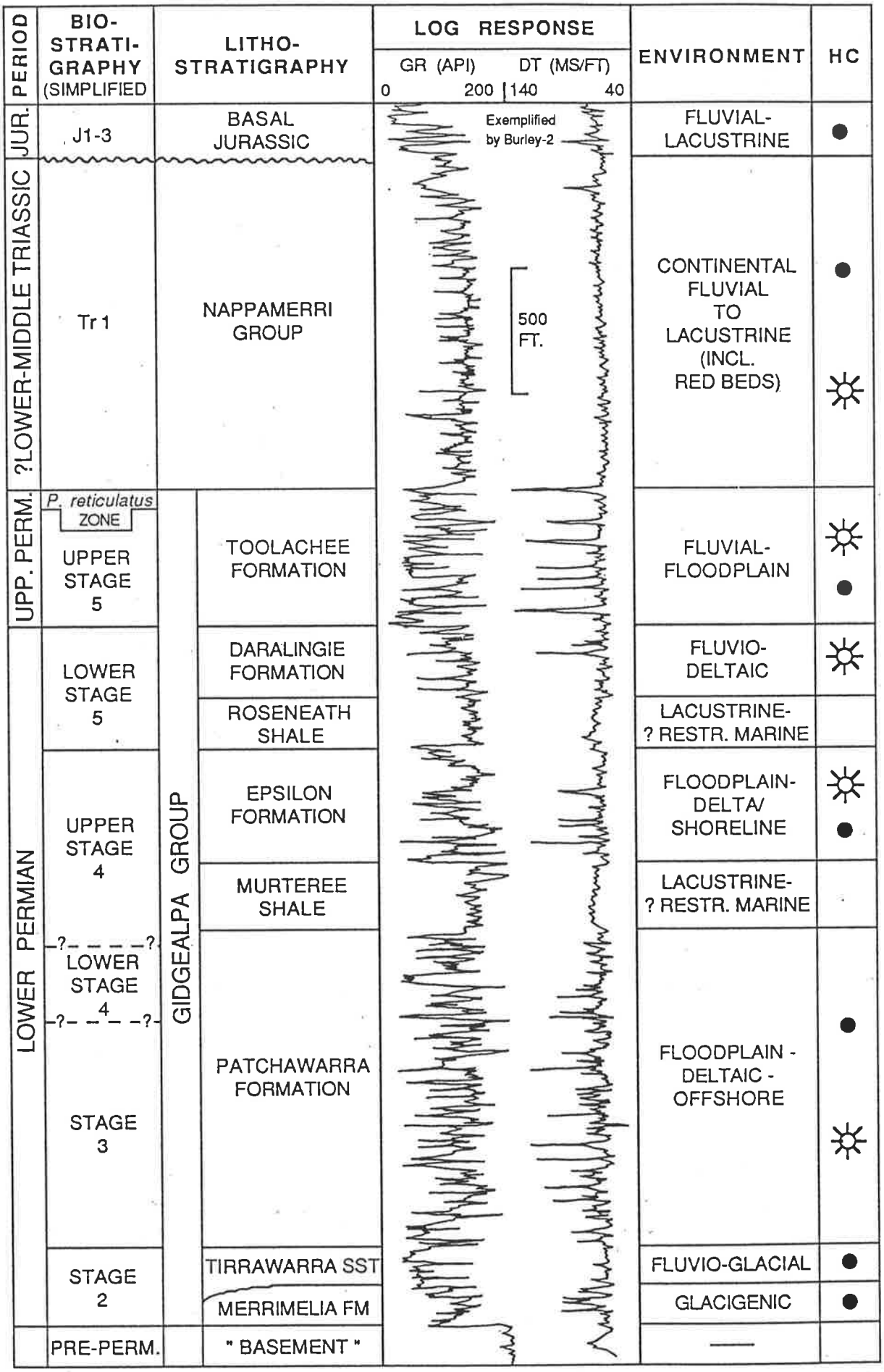

Figure 2.3 Cooper Basin stratigraphic nomenclature, typical log response, and proven hydrocarbon (HC) associations with various formations (after Evans, 1966; Martin, 1967a; Paten 1969; Papalia, 1969; Battersby, 1976; Gatehouse, 1972; Price, 1973; Stuart, 1976; Thornton, 1979; McKirdy, 1982c; Williams & Wild, 1984 a & b; Williams et al., 1985; Powis, 1989; Yew & Mills, 1989; Tupper & Burckhardt, 1990).

1976; Gatehouse, 1986). Volcanic rocks include Upper Proterozoic to Early Cambrian trachytic and andesitic lavas, tuffs and agglomerates (Battersby, 1976; Gatehouse, 1986). In some wells, drilling terminated in quartz-muscovite phyllite schists interpreted to be of Precambrian age (Gatehouse, 1986). Elsewhere, granitic basement was intersected, the age of which is contentious (Gatehouse, 1986) (cf. Table 6.6; discussion in section 6.5.8.1). The distribution of the various pre-Permian rock types is shown in Figure 2.4.

2.2.2 Permo-Triassic

The *Merrimelia Formation* is the basal unit in the Cooper Basin (Williams et al., 1985), and is considered to be of Late Carboniferous to Early Permian age (Cooper, 1981). It rests unconformably on older rocks. Locally, the Merrimelia Formation is in excess of 1000 feet thick and comprises a succession of conglomeratic sandstones that in some places are overlain by shales and siltstones (Thornton, 1979). Grund (1966) described the Merrimelia Formation as consisting of 'tillites' (diamictites), glaciofluvial, glaciolacustrine, interglacial and periglacial sediments resulting from two phases of Permo-Carboniferous glaciation. A glacial origin was also suggested by Martin (1967a), Kapel (1972) and Battersby (1976). More recently, Williams et al. (1985) identified a suite of paraglacial aeolianites in the Merrimelia Formation penetrated by wells within the Merrimelia Field. Thornton (1979) considered both the top and base of the Merrimelia Formation to be bound by an unconformity. However, detailed stratigraphic analysis by Williams & Wild (1984 a & b) has shown the glacigenic Merrimelia Formation to interfinger with the fluvioglacial braided stream deposits of the Tirrawarra Sandstone (cf. Enclosures 1-3). On this basis, Williams & Wild (1984 a & b) proposed the formal incorporation of the Merrimelia Formation into the basal Gidgealpa Group, a view that is adopted in the present study (Fig.2.3) (Enclosures 1-3).

The *Tirrawarra Sandstone* is considered to have a fluvial origin (Kapel, 1972; Gostin, 1973; Thornton, 1979), and consists of fine to medium grained, occasionally conglomeratic sandstones interbedded with minor amounts of carbonaceous siltstone, shale and very thin coals (Thornton, 1979). Gostin (1973) identified three units of braided stream and fluvial channel origin in the basal sediments of the Tirrawarra Field. A braided stream environment of deposition was also proposed by Thornton (1979).

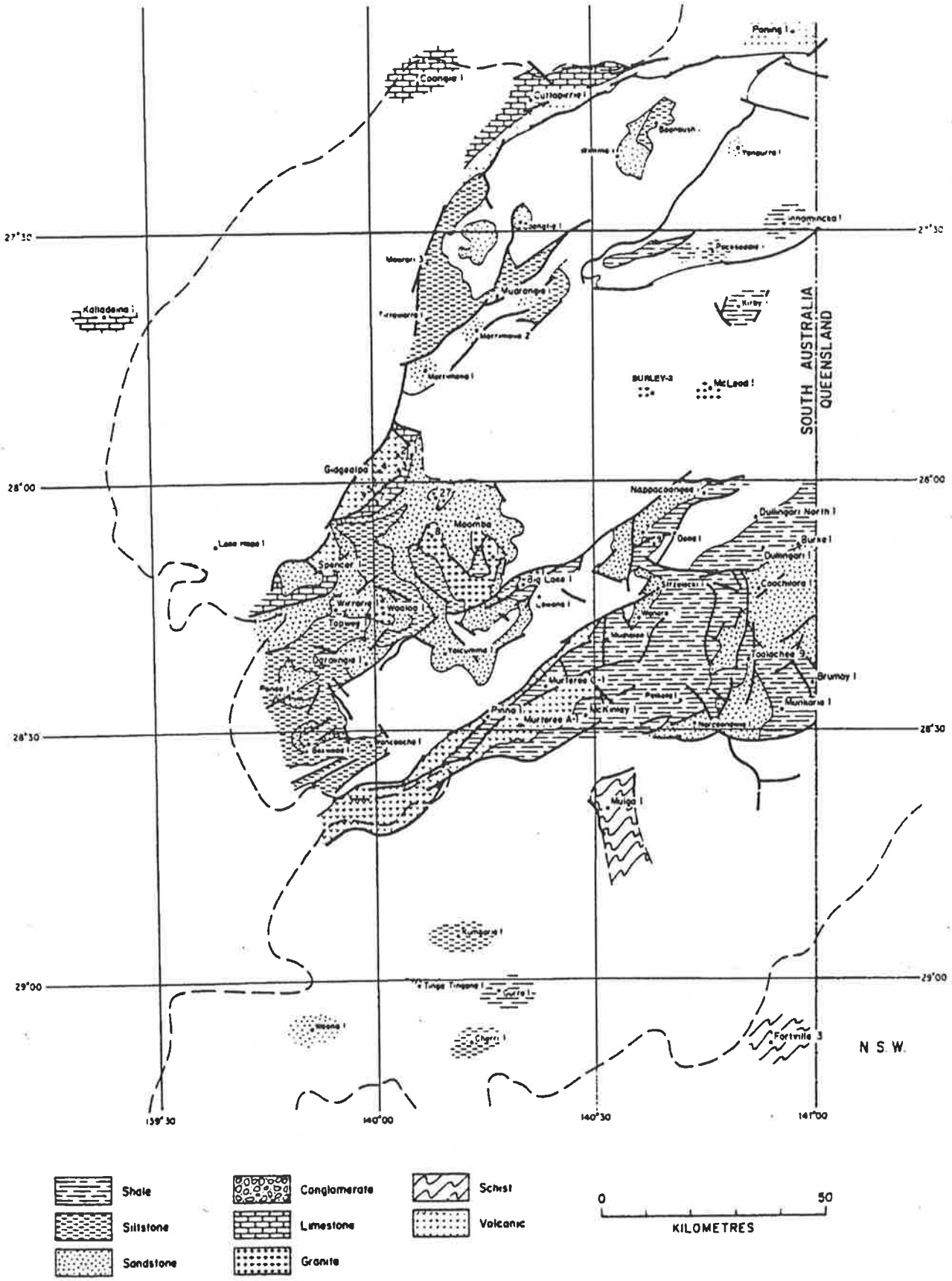

Figure 2.4 Distribution of rock types as interpreted from cores and cuttings in drill-holes penetrating Warburton Basin rocks. Minimal interpretation basis (revised and modified from Gatehouse, 1986).

The Tirrawarra Sandstone grades upward, and interfingers with the overlying sediments of the *Patchawarra Formation* (cf. Thornton, 1979; Fig.5). The Patchawarra Formation is composed of a rhythmic succession of sandstones, siltstones, shales and coals, and can exceed 1000 feet in thickness in the deeper parts of the basin (Enclosures 1 & 3). Locally, coal seams up to 80 feet in thickness have been recorded (Thornton, 1979) which points to low gradients of deposition (Stuart, 1976; Thornton, 1979). The Patchawarra Formation is characterised by considerable facies variations, with depositional environments ranging from floodplain through deltaic to offshore (Stuart, 1976; Thornton, 1979). Three basic units were distinguished by Gatehouse (1972). In the Patchawarra Trough, 'distributary sandstones' at the base of the Patchawarra Formation termed the Moorari Beds (Kapel, 1972) cannot be correlated elsewhere (Thornton, 1979) but may be equivalent to Gostin's (1973) upper Tirrawarra Sandstone unit (Battersby, 1976).

The *Murteree Shale* is typically between 100 and 200 feet thick, and comprises light to dark grey shales with interbedded micaceous siltstones (Thornton, 1979). It conformably overlies the Patchawarra Formation in most areas, although in a few wells there is evidence for a minor hiatus between the two (Battersby, 1976). Battersby (1976) considered the Murteree Shale to have been deposited in a series of lakes whereas Thornton (1979, p.24) thought that "there was virtually complete submergence of the basin under a single shallow body of water" during Murteree time. This body of water was either a restricted sea or a freshwater lake (Stuart, 1976; Thornton, 1979)

Conformably overlying the Murteree Shale is the *Epsilon Formation* which consists of sands and silts with thinly interbedded sandstones and coals (Thornton, 1979). Typically the sediments are fine to very fine grained and were laid down in floodplain to shoreline environments (Battersby, 1976). The Epsilon Formation averages about 200 feet in thickness and exhibits a gradual thinning towards the basin margin (Battersby, 1976). It is conformably overlain by the *Roseneath Shale* which has essentially the same lithological and palaeo-environmental characteristics as the Murteree Shale (Battersby, 1976; Thornton, 1979). The depositional basin was probably smaller than during deposition of the Murteree Shale, with the southwestern and northern parts of the basin not being submerged (Thornton, 1979).

The *Daralingie Formation*, generally less than 100 feet thick, is present in the deeper parts of the Cooper Basin where a complete Lower Permian section is present (Battersby, 1976) (Enclosures 1-3). It comprises a succession of thin sandstones, siltstones, shales and coals which reflect a regressive environment similar to the lower part of the Epsilon Formation (Thornton, 1979). The upper part of the Daralingie Formation contains thicker sands and coals which were deposited in lower deltaic and floodplain environments (Battersby, 1976).

The *Toolachee Formation* unconformably overlies the Daralingie Formation although in deeper areas the contact appears to be transitional between the two (Battersby, 1976) (Enclosures 1-3). The Toolachee Formation consists of freshwater sandstones, siltstones, shales and coals deposited in a floodplain environment (Battersby, 1976; Thornton, 1979; Fairburn, 1989). The sandstones are typically medium to coarse grained, often conglomeratic, and exhibit upward fining cross-beds indicative of point bar sequences (Stuart, 1976; Thornton, 1979; Stuart et al., 1988; Fairburn, 1989).

The final phase of sedimentation within the Cooper Basin resulted in the deposition of the *Nappamerri Group* (Powis, 1989). Papalia (1969) described these sediments as consisting of interbedded shales, siltstones and sandstones exhibiting red-bed characteristics and being of continental fluvial to lacustrine origin. The Nappamerri sediments are defined to range in age from Early to Middle Triassic by Papalia (1969) and Thornton (1979) but Powis (1989) considered the basal unit of the Nappamerri Group (the Arrabury Formation) to be of Late Permian to Early Triassic age. Unfortunately, the contact between the Toolachee and Arrabury Formations is ill-defined as diagrams in Powis (1989) show the contact as both conformable and unconformable (cf. Powis, 1989; Figs.3, 5, 6 & 9). In the present study, log characteristics support the view that the contact between the Toolachee Formation and the basal Nappamerri Group is conformable in the project area (Enclosures 1-3).

2.2.3 Post-Triassic

The Eromanga Basin overlying the Cooper Basin comprises a succession of Early Jurassic to Late Cretaceous sediments (Exon & Senior, 1976; Senior et al., 1978). The Jurassic sediments consist mainly of continental deposits of quartzose sandstone, carbonaceous siltstone and minor coal (Senior et al., 1978; Habermehl, 1980; Senior & Habermehl, 1980; Bowering, 1982; Armstrong & Barr, 1982, 1986). Cretaceous sediments include quartz-rich sandstone and siltstone of marine, paralic, lacustrine and fluvial origin (Exon & Senior, 1976; Moore & Pitt, 1984; Armstrong & Barr, 1982, 1986). The Eromanga sediments are in part mantled by Cainozoic stream sediments and sand dunes (Exon & Senior, 1976).

2.3 Structure

Knowledge of the structural geology of the Cooper Basin has been derived entirely from subsurface data (Kapel, 1966; Battersby, 1976). The majority of major fold complexes are oriented northeast-southwest (Stuart, 1976; cf. Fig.3; Thornton, 1979) (Fig.2.5). Local variance to this dominant trend exists. For example, in the Moomba area there is a secondary northwest-southeast synclinal pattern (cf. Stuart, 1976; Fig.3), and in the Toolachee area fold trends are almost north-south (Stuart, 1976; Thornton, 1979) (Fig.2.5). Folds are commonly doubly-plunging, and the tightness of folds increases with depth (Stuart et al., 1988).

Six major structural zones are identified on the basis of structure contour and isopach maps (Battersby, 1976; Thornton, 1979) (Fig.2.5). The zones include the Gidgealpa-Merrimelia-Innamincka (GMI) and Murteree-Nappacoongee (MN) anticlinal trends, the Patchawarra, Nappamerri and Tennaperra Troughs, and the area northeast of the Karmona anticlinal trend (Kapel, 1966; Stuart, 1976; Thornton, 1979) (Fig.2.5).

➢ The *GMI trend* is the most prominent anticlinal feature in the basin, comprising several major structural culminations (Fig.2.5); it is very steep-sided, largely fault controlled, and has a maxium relief of over 3000 feet. It is baldheaded of Gidgealpa Group sediments along most of its length (Thornton, 1979) (cf. Spencer-1, Enclosure 2).

➢ The *MN trend* is S-shaped (Fig.2.5), plunging northeast and southwest from Murteree. It has a maximum relief of about 2600 feet northwest of Della. Again, much of the upper portion of the Gidgealpa Group sediments is missing due to non-deposition or erosion (Thornton, 1979).

➢ The *Nappamerri Trough* is nearly 310 km long and up to 100 km wide (Fig.2.5). Both the interpreted maximum thickness of the Gidgealpa Group and the greatest sediment thickness intersected by drilling occurs in this structural province (Thornton, 1979) (cf. Kirby-1 and Burley-2, Enclosure 1).

➢ The *Patchawarra Trough* runs sub-parallel to the GMI anticlinal trend (Fig.2.5) and attains a maximum depth of about 10,500 feet below sea level at its northeastern extremity. Secondary asymmetrical fold structures such as Tirrawarra occur near the axis of the trough (Fig.2.5) (Stuart, 1976; Thornton, 1979).

➢ The *Tennaperra Trough* is the main synclinal feature along the southern flank of the Cooper Basin, curving around the northern end of the Toolachee anticlinal trend; towards the northeast, the Tennaperra Trough bifurcates into the Tickalara and Wolgolla anticlinal trends (Fig.2.5). It is fairly indistinct south of Murteree, and has a maximum depth of about 7200 feet below sea level in the vicinity of Burke-Dullingari (Thornton, 1979) (cf. Enclosure 3).

➢ The *Karmona anticlinal trend* separates the southern from the northern Cooper Basin; it is parallel with, and south of, the Arrabury Trough which also plunges westwards (Fig.2.5) (Thornton, 1979). The Karmona trend attains a maximum depth of about 6200 feet below sea level, and along its southern flank is partly defined by a fault with a maximum throw of more than 1500 feet at the level of the 'P' (near top Toolachee) Horizon; this fault forms part of a major lineament that transects the Australian continent (Thornton, 1979).

Faults are associated with the majority, if not all, of the major anticlinal structures in the Cooper Basin (Thornton, 1979), the faults becoming increasingly more abundant with depth (Stuart et al., 1988). At least some of the faults have very high angles of throw, and both normal and reverse fault styles occur. Normal faults are commonest, and generally do not penetrate the full Permian sequence as evident from seismic data (Hollingsworth et al., 1976; Thornton, 1979; cf. Gray & Roberts, 1984; Figs.4 & 8). The throw on some of the major faults appears not to have been consistently in one direction, as exemplified by the Big Lake Fault which separates the Moomba and Big Lake Fields (Battersby, 1976; Stuart, 1976; Thornton, 1979). Big Lake is on the upthrown side of the fault now, but contains over 650 feet more Permian sediment at the level of the 'P horizon than Moomba on the downthrown side. This indicates a relative structural inversion between the two fields (Thornton, 1979).

The structural characteristics of the Cooper Basin region have been attributed to rejuvenation of pre-existing basement structures (Wopfner, 1960; Sprigg, 1961), differential vertical tectonics (O'Driscoll, 1983), compressional tectonics and strike-slip motion (Stuart, 1976), as well as fold interference patterns, thrusting and compressional wrench tectonics (Kuang, 1985). Rejuvenation of pre-Permian faults along the flanks of many structures occurred contemporaneously with deposition (Battersby, 1976). As noted by Stuart (1976), there were both subtle and pronounced earth movements that took place immediatly prior to and during Permian time. Structural growth or fault movement in the Permian is reported by Martin (1967a), Kapel (1972), Gatehouse (1972), Thornton (1973, 1979), Gray & Roberts (1984), Stanmore (1989) and Heath (1989).

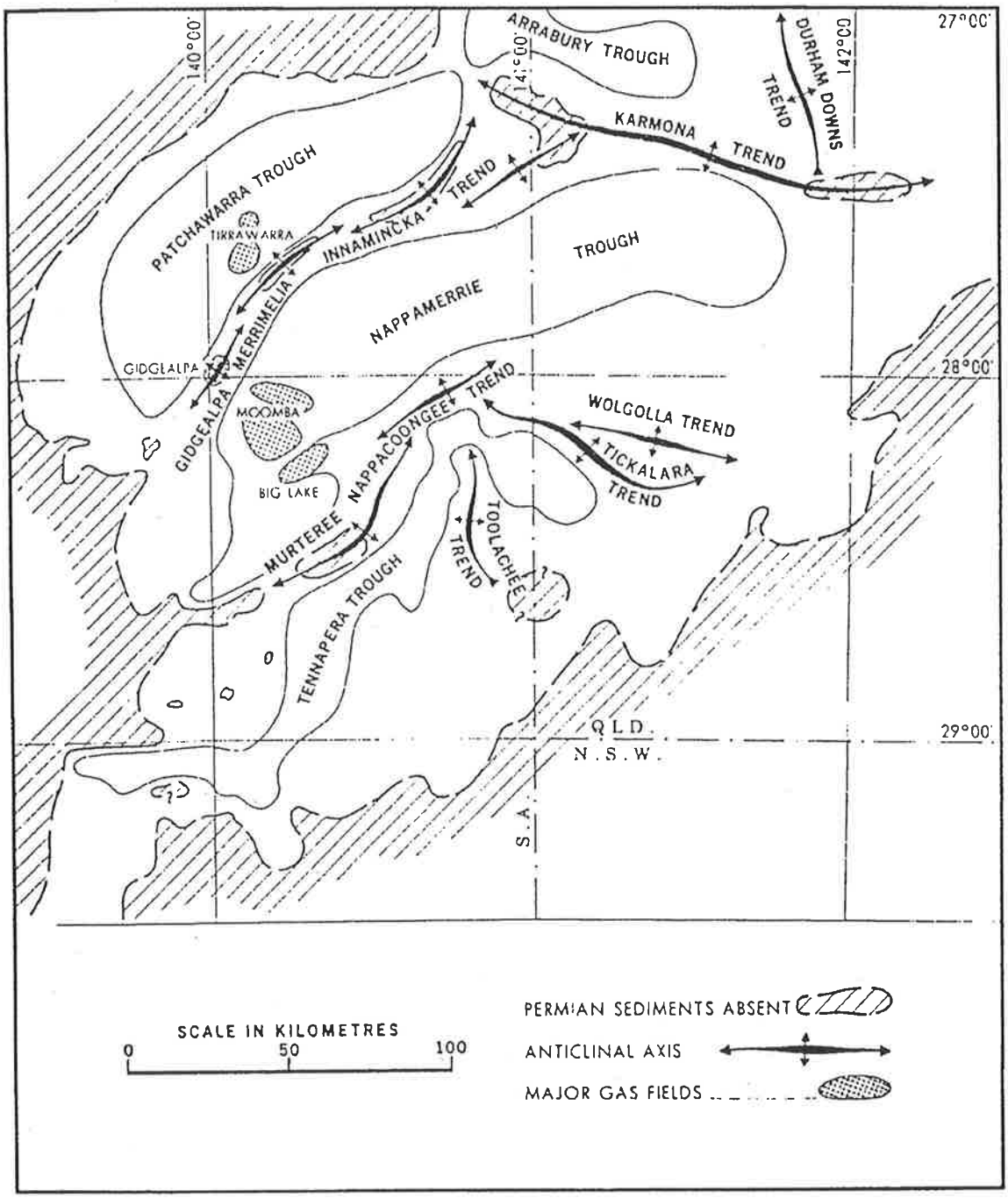

Figure 2.5 Cooper Basin - major structural elements (after Thornton, 1979).

2.4 Basin history

Initial Gidgealpa Group sedimentation commenced on an undulating land surface which probably was created by glacial scour (Thornton, 1979; Heath, 1989). The initiation of glaciation occurred in response to the gradual poleward drift of Australia during the late Palaeozoic (Veevers, 1984), and the development of mountain highlands in eastern Australia during the Kanimblan orogeny (Dulhunty, 1964; Sprigg, 1966; Frakes, 1979; Lambeck & Stephenson, 1986; Powell & Veevers, 1987). Glacigene sediments in the Cooper Basin are represented by the Merrimelia Formation (Grund, 1966; Martin, 1967a; Kapel, 1972; Battersby, 1976; Williams et al., 1985). According to Powell & Veevers (1987), such glacigene sediments of Permo-Carboniferous age in Australia represent the waning stages of glaciation when temperatures warmed and ice sheets retreated. This view appears supported by Dickins (1985) who considered that no conclusive evidence for glaciation can be found in Australia after the Sakmarian (Early Permian). However, other workers believe that glaciation in Australia continued with less intensity into the late Permian (Crowell & Frakes, 1971a,b; Crowell, 1978; Veevers, 1984) when there was a return to warmer conditions (Frakes, 1979).

The Tirrawarra Sandstone and Patchawarra Formation were deposited under conditions of diminishing topographic relief over geologic time (Thornton, 1979). During uppermost Patchawarra time, the Cooper Basin was invaded from the east by an inland 'sea' which deposited the Murteree Shale; this sea may have had distant connection to the Galilee and Bowen Basins and ultimately with the open sea (Stuart, 1976; Thornton, 1979). As this 'sea' retreated, shoreline sediments of the Epsilon Formation built out towards the east. A second transgressive pulse occurred, resulting in the deposition of the Roseneath Shale (Thornton, 1979). Finally, delta sediments of the Daralingie Formation prograded eastwards into this receding 'sea' (Thornton, 1979). While Daralingie deltaic deposition likely continued in deeper parts of the basin, a prolonged period of differential uplift and erosion occurred, affecting pre-existing palaeo-highs and resulting in the formation of numerous anticlinal closures prior to deposition of the Toolachee Formation (Battersby, 1976; Thornton, 1979; Heath, 1989). Gray & Roberts (1984) considered the major fault movements to have occurred during this time. On major anticlinal trends, much of the Permian section was removed from some culminations (Battersby, 1976; Thornton, 1979; Kantsler et al., 1983) (Enclosures 1-3). Evidence for an angular unconformity exhibited by the contact between the Toolachee Formation and underlying formations has been observed on seismic records (Hollingsworth et al., 1976; Gray & Roberts, 1984) and is confirmed by well correlations (Wopfner, 1966; Kapel, 1972; Pyecroft, 1973;

Thornton, 1979). Palynologic findings support a major hiatus in the geologic record up to about 12 Ma at the end of the Early Permian (Thornton, 1979) (Enclosures 1-3).

By the time deposition resumed, peneplanation of the Early Permian sequence (Thornton, 1973) had produced an essentially flat land surface, except "for a few hills" rising above the peneplain (Thornton, 1979, p.11). Thornton (1979) considers meandering rivers to have entered the basin from the west. These rivers deposited the sediments of the late Permian Toolachee Formation which locally can reach up to about 650 feet in thickness (Kantsler et al., 1983). Overall, Permian thickness variation is controlled by onlap, growth faulting, non-deposition, differential compaction, and erosion (Stuart, 1976; Battersby, 1976; Thornton, 1979; Kantsler et al., 1983; Gray & Roberts, 1984).

In the Triassic, subsidence continued and the Nappamerri sediments of continental fluviatile and lacustrine origin were deposited, including some red beds suggestive perhaps of a change in climate (Thornton, 1979) related to the northward drift of the Australian continent (Veevers, 1984). A major change in depocentre of the Cooper Basin at this time is suggested by the fact that Permian sediments are thickest in the southern Cooper Basin but the Triassic section thickens to the north indicating regional tilt (Battersby, 1976; Kantsler et al., 1983). Deposition of the Nappamerri Group was terminated by a major phase of uplift in the Late Triassic and Early Jurassic which resulted in the loss of up to 1640 feet of section in the southeastern portion of the Cooper Basin (Kantsler et al., 1983; Gray & Roberts, 1984) (Enclosures 1-3). This event led to accentuation of pre-existing structures (Heath, 1989).

The accumulation of Cooper Basin sediments was followed after an interval of erosion by deposition of the Eromanga Basin sediments. Several thousand feet of fluvial-lacustrine to marginal-marine rocks of Jurassic-Cretaceous age were laid down on an irregular erosional surface in a gently subsiding basin (Kantsler et al., 1983; Heath, 1989). Subsidence culminated with the relatively rapid deposition of the Cenomanian Winton Formation (Kantsler et al., 1983), after which the Cooper and Eromanga Basins were subjected to renewed basin-wide deformation (Heath, 1989). This phase of structural movement also enhanced pre-existing folds and faults formed by earlier structural movements in the Cooper Basin, and additionally resulted in the formation of younger Eromanga folds (Heath, 1989).

2.5 Exploration history

The prospectivity of the Cooper Basin region was originally promoted by Sprigg (1958). Exploration in the Cooper Basin first commenced in 1959 when Innamincka-1 was spudded. The first commercial gas discovery occurred at Gidgealpa in 1963. Moomba-1 was drilled in 1966 and discovered a gas field later proved to be the biggest in South Australia, containing some 1 TCF of sales gas (Heath, 1989). The Moomba plant was commissioned and gas started flowing to Adelaide in 1969. The first oil field was found in 1970 by Tirrawarra-1 which intersected liquids-rich gas in several Patchawarra reservoirs and oil in the Tirrawarra Sandstone. The commencement of Cooper Basin gas sales to Sydney was in 1976. In 1978, the Eromanga Basin overlying the Cooper Basin was established as an oil province with the discovery of a major oil pool in the Hutton Sandstone at Strzelecki-3 (Armstrong & Barr, 1982, 1986; Hollingsworth, 1989). To date, in excess of 4000 seismic lines totalling over 50,000 km have been acquired, and over 157 wildcat wells drilled in the Cooper/Eromanga Basins, with an overall success rate of 45 percent (Heath, 1989; cf. Figs.3-10). For a more comprehensive review of the exploration history of the region, the reader is referred to the work of Battersby (1976), Randal (1983), Armstrong & Barr (1982, 1986), Lindner (1986), Doyle & Howard (1988), Branson (1989), Heath (1989), and Hollingsworth (1989). The petroleum geology of major oil and gas fields is described by other authors (Greer, 1965; Wopfner, 1966; Martin, 1967b; Pyecroft, 1973; Battersby, 1976; Devine & Gatehouse, 1972; Middleton & Boardman, 1983; Pecanek & Paton, 1984; Gravestock & Morton, 1984; Bowering & Harrison, 1986; Paton & Zwigulis, 1988; Fairburn, 1989; Yew & Mills, 1989).

2.6 Hydrocarbon characteristics

Cooper Basin oils and condensates are typically medium to light (30° to 60° API), paraffinic, low in sulphur, with variable low to high wax contents; they also are characterised by high pristane/phytane ratios indicative of a land plant origin (Powell & McKirdy, 1972, 1973, 1975, 1976; Shibaoka et al., 1978; Connan & Cassou, 1980; Philp et al., 1981; Thomas, 1982; McKirdy, 1982c; Kantsler et al., 1983; Hunt et al., 1986, 1989). Most Permian oils contain significant dissolved gas, and none show any evidence of water washing on the basis of aromatic distribution (absence of

benzene and toluene) (Hunt et al., 1986, 1989). However, Triassic oils are reported to be water-washed at Merrimelia (Kantsler et al., 1983).

Hydrocarbon gases are of the paraffin series and include methane (C_1), ethane (C_2), propane (C_3), butane (C_4), and pentane and heavier molecules (C_{5+}), generally in decreasing order of abundance (Hunt et al., 1986, 1989). Non-hydrocarbon gas components include nitrogen, hydrogen, helium, hydrogen sulphide and carbon dioxide; only carbon dioxide and nitrogen are present in concentrations exceeding one percent (Hunt et al., 1986, 1989). Carbon dioxide contents generally vary between 10 to 20 percent, but are reported to exceed 40 percent by molar volume towards the depocentres of the basin (Kantsler et al., 1983; Cosgrove, 1987; Hunt et al., 1986, 1989) (cf. Fig.6.11). Further information relating to the composition and geochemical character of gaseous hydrocarbons in the Cooper Basin is presented by Schwebel et al. (1980), Rigby & Smith (1981), Kantsler et al. (1983), Bodard et al. (1985), Cosgrove (1987), and Hunt et al. (1986, 1989).

2.7 Reservoirs

Within the Gidgealpa Group sediments of the Cooper Basin, the Tirrawarra Sandstone holds the bulk of the oil reserves whereas the Toolachee and Patchawarra Formations hold most of the gas reserves (Armstrong, 1983). About 95 percent of the Cooper Basin oil is reservoired in the Tirrawarra Sandstone of the Tirrawarra Field (Heath, 1989) located outside the study area (Fig.2.6). Oil is also present in the Tirrawarra Sandstone and/or Patchawarra Formation in the Fly Lake-Brolga, Moorari, Kudrieke, Kanowana, Daralingie, Muteroo, Yanpurra, Mudrangie, and Wancoocha areas (Smyth, 1979; McKirdy, 1982c; Kantsler et al., 1983; Heath, 1989; Hunt et al., 1989; Yew & Mills, 1989) (Figs.2.6). The oil potential of the Merrimelia Formation was recently demonstrated at Malgoona-1A. In addition, oil is reservoired in the Toolachee Formation at Strzelecki and at Gidgealpa (McKirdy, 1982c), as well as in several fields located in the Queensland sector of the Cooper Basin (eg. Naccowlah South, Karmona) (Yew & Mills, 1989) (Fig.2.6). Oil is also found in Triassic reservoirs in the Merrimelia Field and at Chandos (McKirdy, 1982c; Kantsler et al., 1983; Bowering & Harrison, 1986; Paton & Zwigulis, 1988). Further, some 10 to 15 known gas fields in the Cooper Basin have the potential to contain commercial oil legs (Yew & Mills, 1989), however differentiation between oil and very wet gas under reservoir conditions is often difficult in the absence of pressure-volume-temperature (PVT) analysis (Hunt et al., 1989).

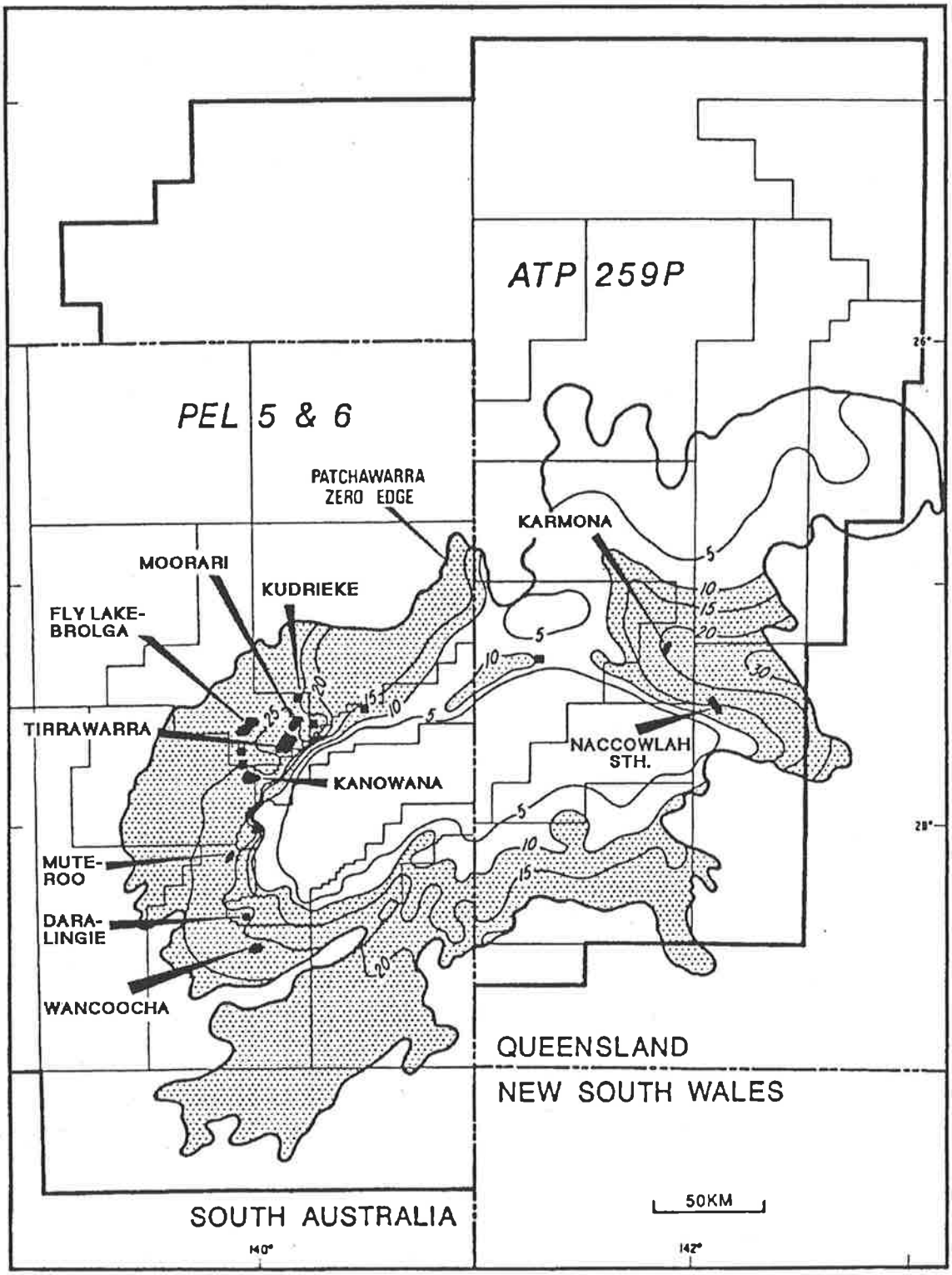

Figure 2.6 Contour map of gas wetness (% [C2-C4]/[C1-C4]) in Patchawarra Formation showing some occurrences of oil in the Toolachee, Patchawarra and Tirrawarra Formations (modified from Yew & Mills, 1989).

Virtually all formations in the Cooper Basin produce gas. About 40 percent of the gas reserves are located in the Toolachee and Daralingie Formations, 30 percent in the Patchawarra Formation, and 12 percent in the Tirrawarra Sandstone (Heath, 1989). Additional gas reserves occur in the Epsilon Formation and the Triassic sediments of the Nappamerri Group (McKirdy, 1982c; Kantsler et al., 1983).

Reservoir thickness is variable. The Tirrawarra Sandstone commonly ranges in thickness from 50 to 150 feet, whilst individual reservoirs in the other formations are generally thinner than 50 feet (Yew & Mills, 1989). There is a strong decrease in average porosity and permeability with depth (Battersby, 1976) (Fig.2.7 a &b). Whereas crestal areas generally have the best reservoir character (Yew & Mills, 1989), low-porosity, low-deliverability gas-saturated sandstones are predominant towards the basin depocentre (Fig.2.7 a &b) (Heath, 1989). Trends in Patchawarra reservoir quality broadly follow the main structural elements of the basin (Heath, 1989) (Figs.2.7 a & b). The bulk of the commercial petroleum discoveries occur in channel and point bar type sandstones; elsewhere hydrocarbons are trapped in sandstone bodies deposited in a regressive lake shoreline environment (Stuart, 1976; Battersby, 1976).

2.8 Traps

The bulk of the commercial hydrocarbon discoveries to date in the Cooper Basin occur in simple anticlinal or fault-bounded anticlinal structures. Such trap structures were described by Beddoes (1973), Battersby (1976) and Yew & Mills (1989). Structural relief is accentuated by differential compaction and 'drape-folding' in some areas (Thornton, 1979; Kantsler et al., 1983). Only a limited number of wells have been drilled specifically on stratigraphic targets (Thornton, 1979; Heath, 1989). An example of a small unconformity trap developed on the plunging nose of an anticline includes the Tirrawarra Sandstone at Merrimelia (Stanmore, 1989). Petroleum fields discovered in stratigraphic pinchout traps onto major highs (Stuart, 1976; Stanmore & Johnstone, 1988; Heath, 1989) include Wackett, Pondrinie and Naccowlah South (Stanmore, 1989). Elsewhere, intraformational facies changes and pinch-out traps unrelated to structural elevation provide attractive targets for petroleum exploration (Stuart, 1976; Stanmore, 1989). Effective fault traps on the high and low block sides are represented by the Karwin and Mudrangie discoveries respectively; the fault seal occurs intraformationally at Karwin whilst at Mudrangie the reservoir is

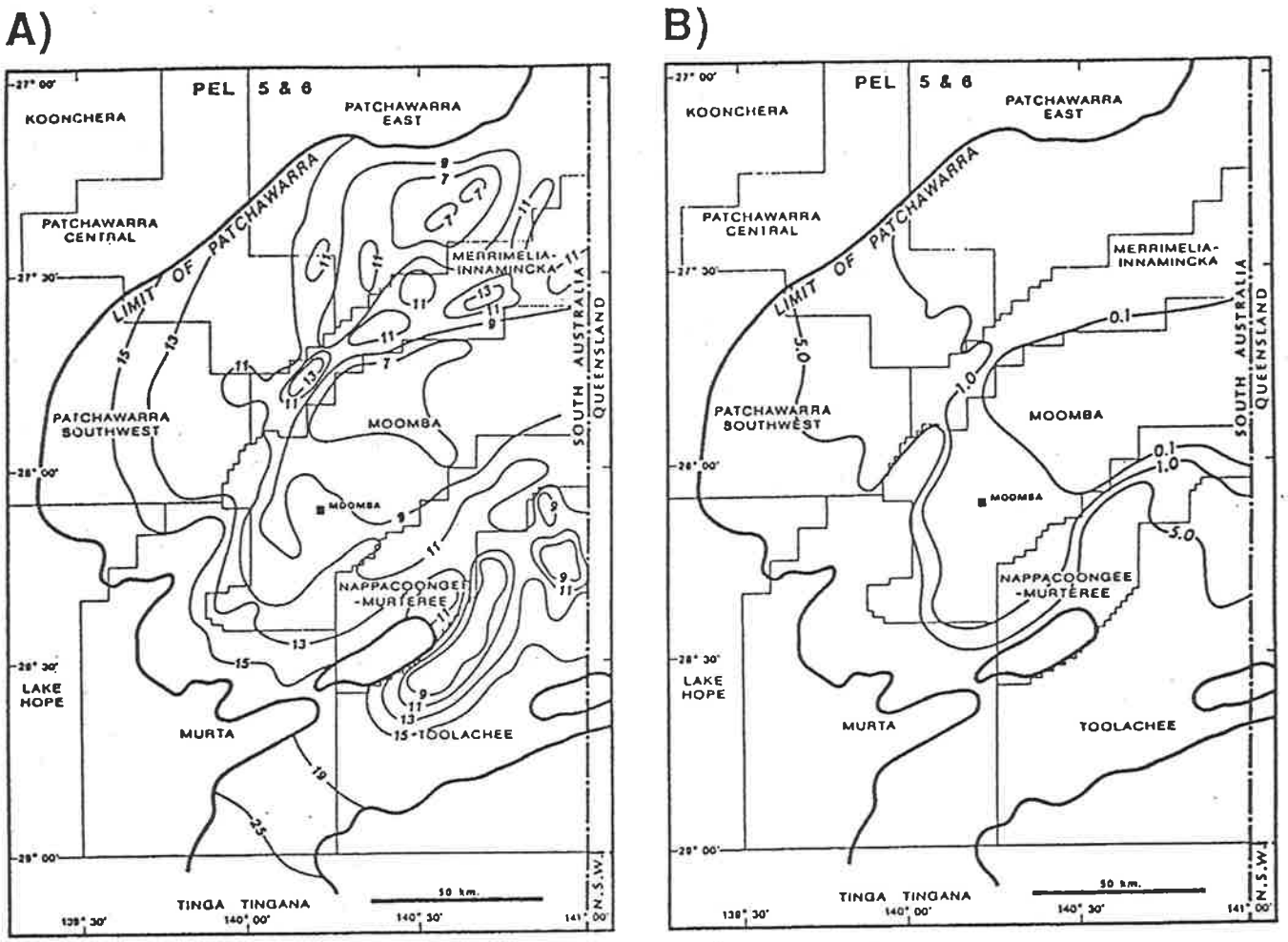

Figure 2.7 a & b (A) Average regional porosity (%) for the Patchawarra Formation; (B) Mean permeability (md) for the Patchawarra Formation (after: Heath, 1989).

juxtaposed against basement (cf. Stanmore, 1989; Figs.12-15). Low side fault plays also exist in areas bordering the GMI trend (Yew & Mills, 1989).

2.9 Seals

Good to excellent regional sealing units for the principal reservoir zones in the Cooper Basin are provided by the Murteree Shale, the Roseneath Shale and parts of the Nappamerri Group (Kantsler et al., 1983; Heath, 1989; Powis, 1989; cf. Gilby & Mortimore, 1989; Fig.11). The competent sealing capacity of the Murteree and Roseneath Shales, for example, is indicated by the fact that in the Toolachee, Kerna and Brumby Fields gas pools occur in the Patchawarra and Epsilon Formations below water-saturated Toolachee reservoirs (Heath, 1989). Local intraformational seals are also provided by the silts and shales which are intercalated with the reservoir sandstones (Stanmore, 1989) (Enclosures 1-3). The possibility that thick coal layers locally act as competent seals cannot be ruled out (G.Royle, Santos Ltd., pers.comm., 1988).

2.10 Sources

Many workers consider the abundant dispersed organic matter (DOM) in the shales and siltstones, and possibly the coals to represent the logical source of the gas and gas-liquids reservoired in the Cooper Basin sediments (Greer, 1965; Brooks et al., 1971; Battersby, 1976; McKirdy, 1989). Both the coals and the dispersed organic matter in the shales are dominated by vitrinite and inertinite (Type III kerogen), with subordinate amounts of sporinite and cutinite derived from a higher land plant assemblage (Hunt et al., 1989; Heath, 1989). Total organic carbon (TOC) contents generally vary between 1 and 5 percent (Schwebel et al., 1980; Smyth, 1983; Jenkins, 1989), although locally TOC values up to 25 percent and more are reported in the Permian coal measures (Gilby & Mortimore, 1989; Jenkins, 1989). Potential therefore exists for the generation of both liquid and gaseous hydrocarbons from organic matter in the Cooper Basin (Kantsler et al., 1983; Hunt et al., 1989). However, because of the dominance of Type III kerogen in the Permo-Triassic sediments, "specific yields of liquids are likely to be relatively low" (Kantsler et al., 1983, p.378). In particular,

the source of the oil is problematic in that no particularly oil-prone source rocks have been identified, compared with the ubiquitous gas-prone source rocks (Hunt et al., 1989; McKirdy, 1989). Oil pooled in Permian reservoirs possibly is derived from local concentrations of exinite and biodegraded organic material (mixed Type II/Type III kerogen) (Kantsler et al., 1983). The crude oil reservoired in the Tirrawarra Sandstone at Tirrawarra was most likely derived from the Patchawarra Formation, as indicated by both geochemical and geological considerations (Kantsler et al., 1983; Taylor et al., 1988; Hunt et al., 1989). An alternative suggestion put forward by Smyth (1983) is that the inertinite in dispersed organic matter, and possibly the coals, represent the primary source for the oils reservoired in the Cooper sediments.

2.11 Geothermal gradients

The present-day geothermal gradients in the Cooper/Eromanga region have been estimated from wireline logging runs and drill stem tests by various workers (Middleton, 1979; Kantsler et al., 1983; Pitt, 1986). The lowest temperature gradients (7.6-12.2 °C per 1000 feet, or 25-40 °C/km) occur in the Patchawarra Trough which is presumed to overlie a thick pre-Permian sedimentary section of relatively high thermal conductivity (Kantsler et al., 1983). The highest temperature gradients (13.7-18.3 °C per 1000 feet, or 45-60 °C/km) occur in and around the Nappamerri and Tennaperra Troughs, particularly in areas underlain by granite basement such as the Moomba and Big Lake Fields (Kantsler et al., 1978; Middleton, 1979; Schwebel et al., 1980; cf. Kantsler et al., 1983; Fig. 6).

2.12 Thermal history

Rank variation in the Nappamerri Trough was strongly influenced by palaeo-heat flow (Kantsler et al., 1983). An early heating event is identified in the Moomba-Big Lake area creating a maturity 'high' persisting into the Late Jurassic/Lower Cretaceous section, as indicated by subsidence/maturation history plots (Kantsler & Cook, 1979; Kantsler et al., 1983; cf. Fig.16). Outside the Nappamerri Trough, maturation of the Cooper Basin sediments can generally be modelled within the constraints of the present-day geothermal gradient (cf. Kantsler et al., 1983; Fig.17). A Permian to Late Triassic phase of high heat flow throughout the basin is indicated

by offsets in the vitrinite reflectance profile with depth at or near the Jurassic/Triassic unconformity surface (cf. Kantsler et al., 1983; Figs. 14 & 15). Kantsler et al. (1983) considered such offsets in the vitrinite reflectance profile to represent evidence for significant Late Triassic erosion, possibly up to 1640 feet in some areas. From Cretaceous times onwards, heat flow stabilised in the general area of the Eromanga Basin although a late rise in temperature may have occurred in the Pliocene (Kantsler & Cook, 1979). Fission track data indicates a general increase in temperature in the last 1 to 10 million years (Gleadow et al., 1989).

The causes for such heating events in the Cooper/Eromanga region are not fully understood. High initial heat flow associated with the initiation of basin subsidence may be the result of deep crustal metamorphism (Middleton, 1980) and/or crustal extension (McKenzie, 1978). In the Cooper Basin, already high levels of regional crustal heat flow were probably enhanced through radiogenic decay of granite basement (Middleton, 1979; Kantsler & Cook, 1979; Kantsler et al., 1983). Increased vitrinite reflectivity in the basal Jurassic section of some wells may possibly be due to local movement of hot connate water along deep-seated faults (Kantsler & Cook, 1979; Kantsler et al., 1983). Local variance of the thermal regime in post-Triassic times can hereby be attributed to dissipation of heat by the Jurassic aquifer system (Kantsler & Cook, 1979; Kantsler et al., 1983; Gleadow et al., 1989). A postulated Tertiary heating event is possibly the result of tectonism and/or drift of the Cooper/Eromanga region over a sub-crustal 'hot spot' (Kantsler & Cook, 1979; Kantsler et al., 1983). Thermal blanketing related to deposition of Late Cretaceous and Tertiary strata may also be the cause of a more recent thermal heating event (Gallagher, 1978).

2.13 Organic maturity

The predominance of land plant organic material in the Cooper Basin allows reliable assessment of the organic maturity by vitrinite reflectance (R_v %) (Kantsler et al., 1983; Hunt et al., 1989). To date, almost 300 wells exist for which vitrinite reflectance data is available in the Cooper/Eromanga region (Tupper & Burckhardt, 1990) (cf. Appendix I). Essentially, organic maturity increases with increasing burial depth, depth-reflectance gradients varying between different structural provinces (Shibaoka et al., 1973; Kantsler et al., 1983; Hunt et al., 1989) (Fig.2.8). Reflectance gradients are highest in the Nappamerri Trough and lowest in the Patchawarra Trough (Kantsler et al., 1983) (Fig.2.8). In the central Nappamerri Trough, vitrinite reflectance levels in excess of 4 percent are attained whereas in the low-temperature

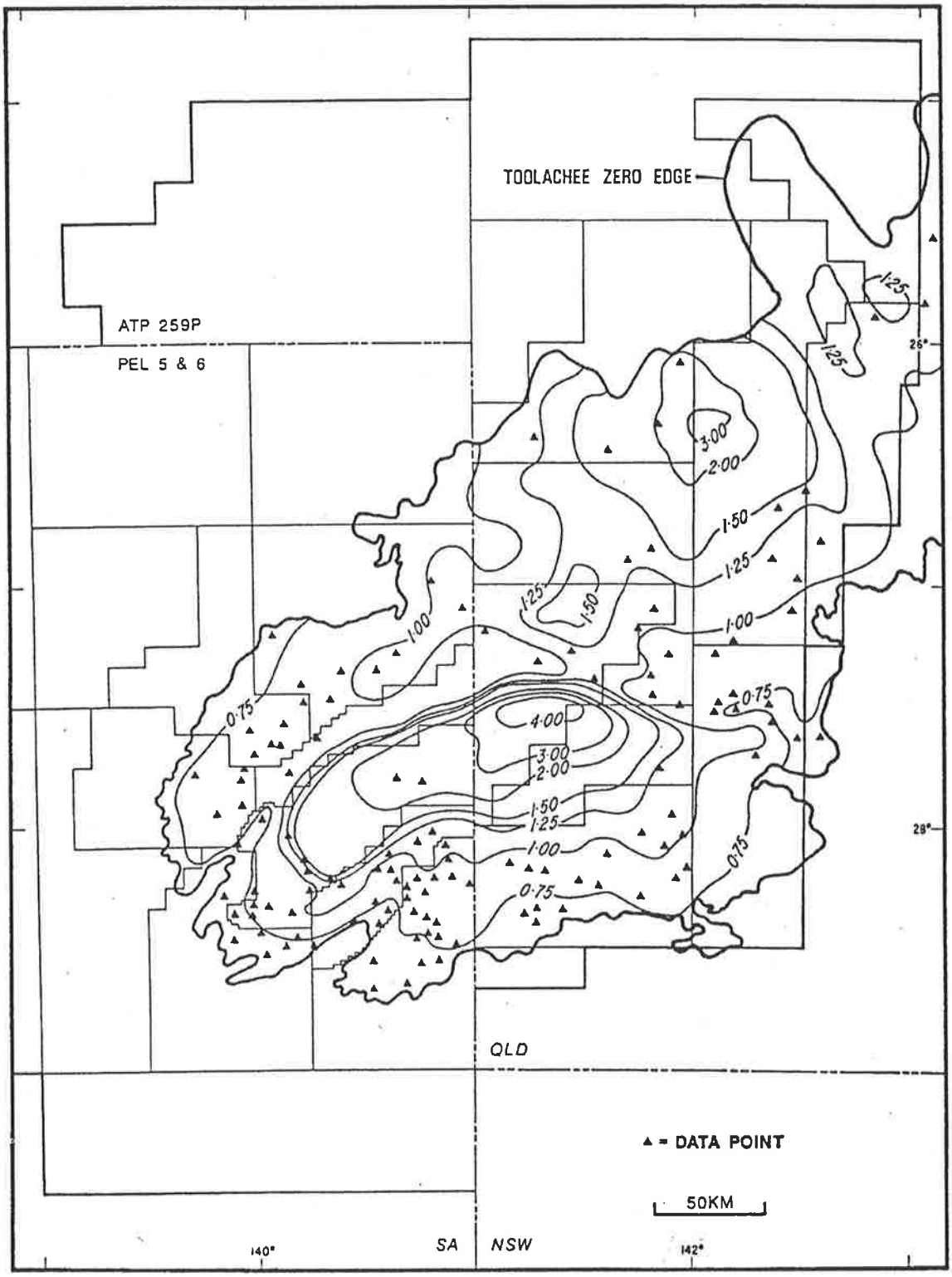

Figure 2.8 Spatial variation of vitrinite reflectance (Rv.%) for the top of the Toolachee Formation (after Hunt et al., 1989) (cf. Heath, 1989; Fig.17 for top of the Patchawarra Formation).

Patchawarra Trough vitrinite reflectance levels commonly are less than 1 percent (Kantsler et al., 1983; Hunt et al., 1989) (Fig.2.8). Although there are subtle differences of opinion between different workers regarding the treshold of significant hydrocarbon generation in the Cooper Basin (cf. Kantsler et al., 1983; Hunt et al., 1989; Tupper & Burckhardt, 1990), an overall consensus exists with respect to the level of organic maturation attained in the various structural provinces. The sediments in the Nappamerri Trough are currently mature for dry gas generation (Kantsler et al., 1983; Hunt et al., 1989; cf. Tupper & Burckhardt, 1990; Fig.15) and are well located to have charged many of the surrounding gas fields (Kantsler et al., 1983). In contrast, present-day maturation levels suitable for oil generation occur in the Patchawarra and Tennaperra Troughs, as well as in a narrow zone around the flanks of the Nappamerri Trough, and over much of the northern Cooper Basin (Kantsler et al., 1983; Tupper & Burckhardt, 1990). The far south and some flank areas of the Cooper Basin are generally immature for both liquid and gaseous hydrocarbon generation (Kantsler et al., 1983; Tupper & Burckhardt, 1990).

2.14 Timing of hydrocarbon migration

The hydrocarbons reservoired in the Cooper Basin were expelled over a wide maturity range and therefore the timing of expulsion varies across the basin (Kantsler et al., 1983; Tupper & Burckhardt, 1990). In the central Nappamerri Trough, oil expulsion from the Cooper sequence may have begun as early as in the Triassic, as evident from thermal modelling using oil maturity data (Tupper & Burckhardt, 1990). A different view is held by Kantsler et al. (1983) who consider that in the central Nappamerri Trough Permian source rocks passed through the zone of significant oil generation in the Cenomanian. In the Patchawarra Trough, Permian source rocks entered the oil window either after Cretaceous deposition (Kantsler et al., 1983) or in the early Late Cretaceous (Tupper & Burckhardt, 1990). Much of the Permian sequence in the Patchawarra Trough currently remains within the oil window (Kantsler et al., 1983; Tupper & Burckhardt, 1990).

Conflicting views also exist regarding the onset of significant gas generation in the Cooper Basin. Kantsler et al. (1983) believe that significant gas generation in the Nappamerri Trough commenced in the Cenomanian, whilst Tupper & Burckhardt (1990) believe this occurred from the Jurassic onwards. An even earlier timing of hydrocarbon generation is suggested by Battersby (1976, p.334) who commented that "[hydrocarbon migration] could have commenced as early as the end of Patchawarra Formation times" as indicated by the timing of trap formation in the basin. At least

portions of the Permian sequence presently continue to generate dry gas in the Nappamerri Trough (cf. Chapter 5) (Kantsler et al., 1983; Tupper & Burckhardt, 1990). Heath et al. (1989) attributed this to the increased thermal cracking of wet gas at increased formation temperatures. The Patchawarra Trough is either immature for gas generation, or gas generation is limited to deeper areas (Kantsler et al., 1983; Tupper & Burckhardt, 1990).

2.15 Hydrocarbon distribution

The distribution of hydrocarbons in the Cooper Basin is closely related to the maturity of the source rocks (Hunt et al., 1986, 1989). The Permian sequence is saturated with dry gas in the centre of the Nappamerri Trough, Permian reservoirs containing progressively wetter gas towards the basin margin (Norton, 1985; Heath et al., 1989; Yew & Mills, 1989) (Figs.2.6). This relationship is evident within fields. In the Dullingari Field, for example, wet Toolachee gas is found above dry Patchawarra gas (Heath, 1989). Most of the known oil occurrences are located in areas in which the gas wetness is about 10 percent or greater (Yew & Mills, 1989) (Figs.2.6). High-deliverability wet gas fields include the Daralingie, Bagundi-Aroona-Lepena, Kidman and Toolachee Fields, all found at relatively shallow structural depth near the basin margin (Heath, 1989). Examples of petroleum fields containing large dry gas reserves include the Big Lake and Moomba Fields (Battersby, 1976; Stanley & Halliday, 1984).

The percentage fill of Permian reservoirs changes rapidly from almost 100 percent in the Basin depocentre to very low values nearer the basin margin (Heath et al., 1989). Heath et al. (1989) attributed this to differences in source potential and reservoir maturity of the Cooper sediments, resulting in different volumes of hydrocarbons locally generated. Shallowest Permian gas in significant quantities occurs at a vitrinite reflectance level of R_v = 0.75 percent or within 10 km of sediments that are at a maturity of R_v = 0.8-0.9 percent (Heath, 1989).

2.16 Formation water characteristics

Formation waters in the reservoirs of the Cooper Basin are essentially solutions of sodium chloride and sodium bicarbonate in varying proportions, and are

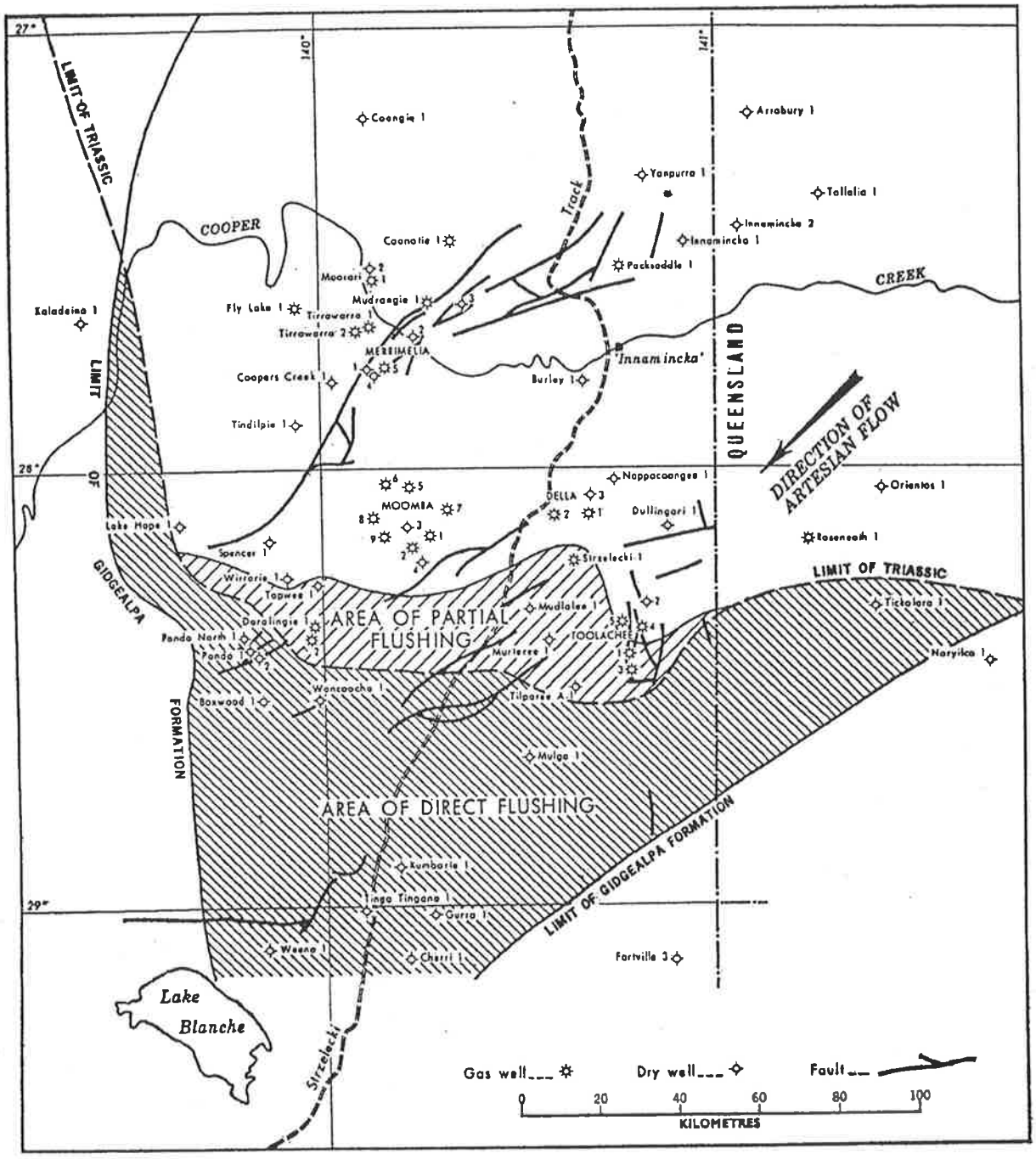

Figure 2.9 Limits of Triassic and Gidgealpa Group sediments and areas of flushing, southern Cooper Basin (modified from Youngs, 1975).

characterised by primary alkalinity (Porter, 1974). Salinities range from 1600 to a maximum of 20,000 ppm NaCl equivalent (Porter, 1974; Youngs, 1975; Battersby, 1976; Faehrmann, 1986), and isosalinity maps show an overall increase in salinity with depth (Porter, 1974; Battersby, 1976; Bowering & Burnett, 1980). The freshest Permian Formation waters are generally encountered where the absence of the Nappamerri sediments places permeable Permian zones in direct communication with the fresher overlying Mesozoic waters of artesian origin; such Mesozoic waters have salinities in the range of 1000 to 4000 ppm NaCl equivalent (Porter, 1974; Youngs, 1975; Battersby, 1976; Bowering & Burnett, 1980; Faehrmann, 1986). As stated by Youngs (1975, p.21), "flushing by artesian waters of the entire Gidgealpa Formation [has occurred] in the southern part of the Cooper Basin and, to a lesser extent, northwards into the centre of the basin. This is the direct result of the absence of the Triassic aquiclude from the southern area" (Fig.2.9). The direction of artesian groundwater flow in the Mesozoic aquifers overlying the study area is from the northeast (Fig.2.9), reflecting principal recharge from eastern Australia, mainly the Great Dividing Range (Habermehl, 1980) (Fig.6.14).

CHAPTER THREE

FACIES ANALYSIS & ENVIRONMENTAL INTERPRETATION

3.1 Introduction

A facies represents "the aspect, appearance, and characteristics of a rock unit, usually reflecting the conditions of its origin" (Bates & Jackson, 1987, p.232). The spatial interrelationships of features such as colour, bedding, composition, texture, fossils and sedimentary structures greatly assist in the identification of sedimentary depositional environments (Reading, 1978). In the present investigation, the lithofacies code of Miall (1978) was adopted for core descriptions (Table 3.1). In all, almost 900 feet of core were logged. Detailed core descriptions are presented in Appendix L.

3.2 Lithofacies distinguished

3.2.1 Gravels

Massive to crudely bedded gravels (lithofacies Gm) and matrix supported gravels (lithofacies Gms) are common in the study area. These lithofacies include intraformational conglomerates or channel lag deposits that formed by traction load in the upper flow regime (Miall, 1978). Several matrix supported gravels show evidence of imbrication, and most gravel lags are polymictic. Intraformational clasts comprise sand and siltstone pebbles, shaly fragments, and granules of coal. In gravel lags, these clasts are typical of bank collapse material indicative of multiple scouring and reworking of fluvial deposits (Stuart et al., 1988). Exotic clasts may also be present, and include pebbles of white quartzite, weathered granite of grey-red appearance, and

Lithofacies

Ge	Gravel: scour base
Gms	Gravel: matrix supported
Gm	Gravel: massive or crudely bedded
Sb	Sand: bioturbated
Sd	Sand: soft sediment deformation
Se	Sand: erosional scour
Sh	Sand: horizontal laminae
Sl	Sand: low angle crossbed
Sm	Sand: massive
Sp	Sand: planar cross-bedded
St	Sand: trough cross-bedded
Sx	Sand: cross-bedded (type unknown)
Sr	Sand: ripple marks
Sw/Fw	Interlaminated sands & muds (rippled)
Fb	Mudstones: bioturbated
Fd	Mudstones: soft sediment deformed
Fg	Mudstones: graded bedding
Fl	Mudstones: flat, finely laminated
Fm	Mudstones: fine massive
Fr	Mudstones: ripple mark
Fsc	Mudstones: laminated to massive
Fw	Mudstones: starved ripples
C	Coal & carbonaceous shale

Fill patterns

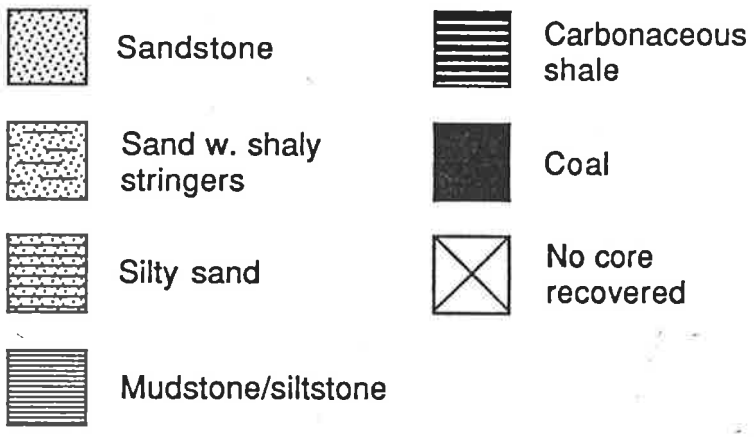

Table 3.1 Lithofacies code and fill patterns used for core descriptions. Lithofacies code adopted from Miall (1978).

fine black igneous material (?dolerite). Gravel facies are generally thin, in the order of 2 to 20 cm only.

3.2.2 Sandstones

Sandstones in the study area exhibit a variety of internal sedimentary structures. The types of lithofacies identified include: massive sands (Sm); sands that are horizontally bedded (Sh); sands that are cross bedded (St, Sp, Sx, Sr); sands characterised by soft sediment deformation (Sd); ripple-laminated sands which are intercalated with silts and muds (Sw/Fw); and bioturbated sands (Sb). Of these, cross bedded sands and ripple laminated sands are most common.

Massive sands (lithofacies Sm) are fine to coarse grained and devoid of any internal features. Such sediments were destratified either by fluid escape or bioturbation. Horizontally bedded sandstones (lithofacies Sh) range from fine to medium grain size, and are produced under conditions of parting or stream lineation in the upper flow regime (Miall, 1978).

Sands with planar cross-bedding (lithofacies Sp) are medium to fine grained, and characteristic of linguoid or transverse channel bars in the moderate to lower flow regime (Miall, 1978). Thin pebbly layers occasionally occur within this lithofacies. Crossbeds typically have an angle of inclination of less than 10 degrees and may contain some grain imbrication. Trough cross-bedded sands (lithofacies St) are coarse to fine grained, and locally are interstratified with finely laminated sediments of the lower flow regime.

Ripple cross laminated sands (lithofacies Sr) are abundant, and are typically very fine to fine grained. They represent the product of the lower flow regime, and were deposited under waning channel flow conditions (Galloway & Hobday, 1983). Ripple cross laminated sands often are interlaminated with bioturbated sands (lithofacies Sb), or fine silts and muds (Sw/Fw) which also may show evidence of bioturbation (below).

Sands characterised by soft sediment deformation (lithofacies Sd) are generally fine to very fine grained; sediment deformation is evident from disrupted or contorted laminae and bedding planes, microfaults, slump folds, and/or microthrusts. Such features may be the result of a combination of factors, including mass movement of sediments, subsidence due to compaction, and dewatering processes (Tucker, 1981).

3.2.3 Siltstones and mudstones

Some mudstones are massive and have little or no internal structure (lithofacies Fm), others are finely laminated (lithofacies Fl). Flat, finely laminated mudstones are commonest and often occur in association with the Fw/Sw lithofacies. Massive mudstones probably were deposited out of suspension in quiet waters; such mudstones often overlie lithofacies Fl and in turn can be overlain by lithofacies C (see below). Bioturbated mudstones (lithofacies Fb) are characterised by disrupted laminae and bedding planes; burrows are typically infilled by silt or very fine sand. Trace fossils vary from discrete, well-organised structures to vague bioturbation features. Irregular horizontal burrows in laminated siltstones resemble the *Planolites* association described by Pollard (1988) in coal-bearing sequences, who considered this trace fossil assemblage to be indicative of overbank/crevasse splay deposits and flood plain lake sediments. Other trace fossils in the present investigation are small mud-filled U-shaped burrows without spreiten. They resemble the *Arenicolites* association that also is typical of channel fill sequences (cf. Pollard, 1988). Narrow V-shaped burrows were ascribed by Stuart (1976) to delta shoreline sequences.

3.2.4 Coals and carbonaceous shales

Massive to carbonaceous coals (lithofacies C) are grey-black to black in colour and are made up of plant debris that has undergone coalification. Locally, silty intervals (carbonaceous shales) exist within the coal layers, and there is evidence of root traces. Coal seams are indicative of flood basin swamps, cutoff meanders, or delta marsh sediments (Walker & Cant, 1984; Serra, 1985).

3.3 Depositional settings

Two principal environments of deposition are distinguished in the cores that were logged in the present investigation, namely fluvial and deltaic deposits. The restricted number of depositional facies within the Permian sediments suggests a relatively simple sedimentational history for the Cooper Basin. The present study

supports earlier depositional models outlined by Kapel (1966), Gatehouse (1972), Battersby (1976), Stuart (1976), Thornton (1978, 1979), Stuart et al. (1988), and Fairburn (1989). The following discussion briefly highlights the key characteristics of the different depositional facies identified by the author in the study area. For a review of both modern and ancient fluviatile and deltaic systems, the reader is referred to the work of Allen (1970), Leeder (1973), Broussard (1975), Coleman (1976), Collinson (1978), Miall (1978, 1984), Elliott (1978), Tucker (1981), and Walker & Cant (1984). The recognition of sedimentary facies from wireline logs is discussed by Coleman & Prior (1982) and Serra (1985).

3.3.1 Fluvial environment

Fluvial deposits in their simplest form are fining upward sequences, generally with an abrupt base and a gradational top (Allen, 1970). Lateral accretion sediments comprise channel floor and point bar deposits that form part of the active channel sequence (Walker & Cant, 1984) (Fig.3.1). Vertical accretion deposits form outside the main channel in the flood basins, ox-bows and levees when the river overtops its banks (Walker & Cant, 1984) (Fig.3.1). A sequence model for lateral and vertical accretion deposits of meandering rivers is illustrated in Figure 3.2.

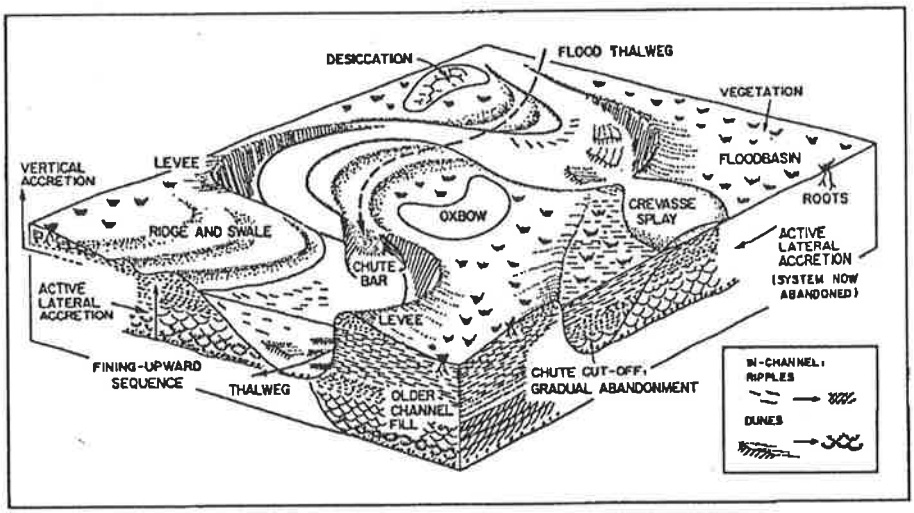

Figure 3.1 Block diagram showing morphological elements of a meandering river system. Erosion on the outside bend of a meander loop leads to lateral accretion on the opposite point bar. The dunes and ripples in the channel give rise to trough cross-bedding and ripple cross lamination respectively (insert, lower right), which are preserved in a fining upward sequence (after: Walker & Cant, 1984).

In the present study, vertical and lateral accretion deposits are evident in numerous cores from the Toolachee, Daralingie and Patchawarra Formations (cf. Figs. 3.3 & 3.4) (cf. Gravestock & Morton, 1984; Fig.6). A typical point bar sequence begins with a basal scour lag that is overlain by a channel lag deposit. The channel lag deposit is either massive or flatbedded (lithofacies Gm/Gms) and includes the gravelly component of the clastic load; it is interpreted to have formed during peak flood time. Above the lag, medium- to coarse grained, trough cross-bedded sandstones (lithofacies St) are generally preserved (Figs.3.2 & 3.4). The trough cross-bedded sandstones are indicative of mid-channel dune migration when the sand was transported along the channel floor as bedload (Walker & Cant, 1984) (Fig.3.1). Planar cross-bedded sands (lithofacies Sp) may also be present but these are less common; this lithofacies is produced by transverse bar migration (Stuart et al., 1988). Some sandstones lack internal sedimentary features (lithofacies Sm) and are interbedded with clastics that display trough or planar cross-bedding (Figs.3.3 & 3.4).

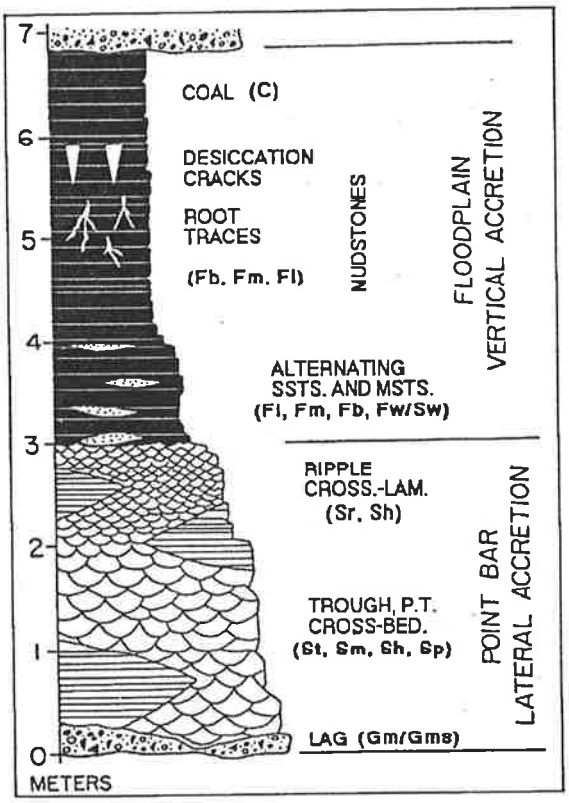

Figure 3.2 Model for lateral and vertical accretion deposits of meandering rivers. Lithofacies codes shown in brackets (modified from Walker & Cant, 1984).

Towards the point bar top, there is generally an upward decrease in relative grain size and scale of cross stratification (Figs.3.2, 3.3 & 3.4). Very fine to fine grained ripple cross-laminated sandstones (lithofacies Sr) are predominant in this part of the fluvial sequence (Figs.3.2, 3.3 & 3.4). These are interpreted to have been deposited under waning channel flow conditions (Galloway & Hobday, 1983). Ripple- and finely trough cross-laminated sands may be interbedded with horizontally laminated fine grained clastics (lithofacies Sh) (Figs.3.3 & 3.4); the latter are thought to have formed at shallow depth in higher velocity flow regimes (Walker & Cant, 1984).

Vertical accretion deposits comprise very fine to fine grained sands, silts, shales and minor coals (Figs.3.2, 3.3 & 3.4). The silts and clays are deposited on the floodplain by overbank sedimentation (Fig.3.1) (Tucker, 1981;

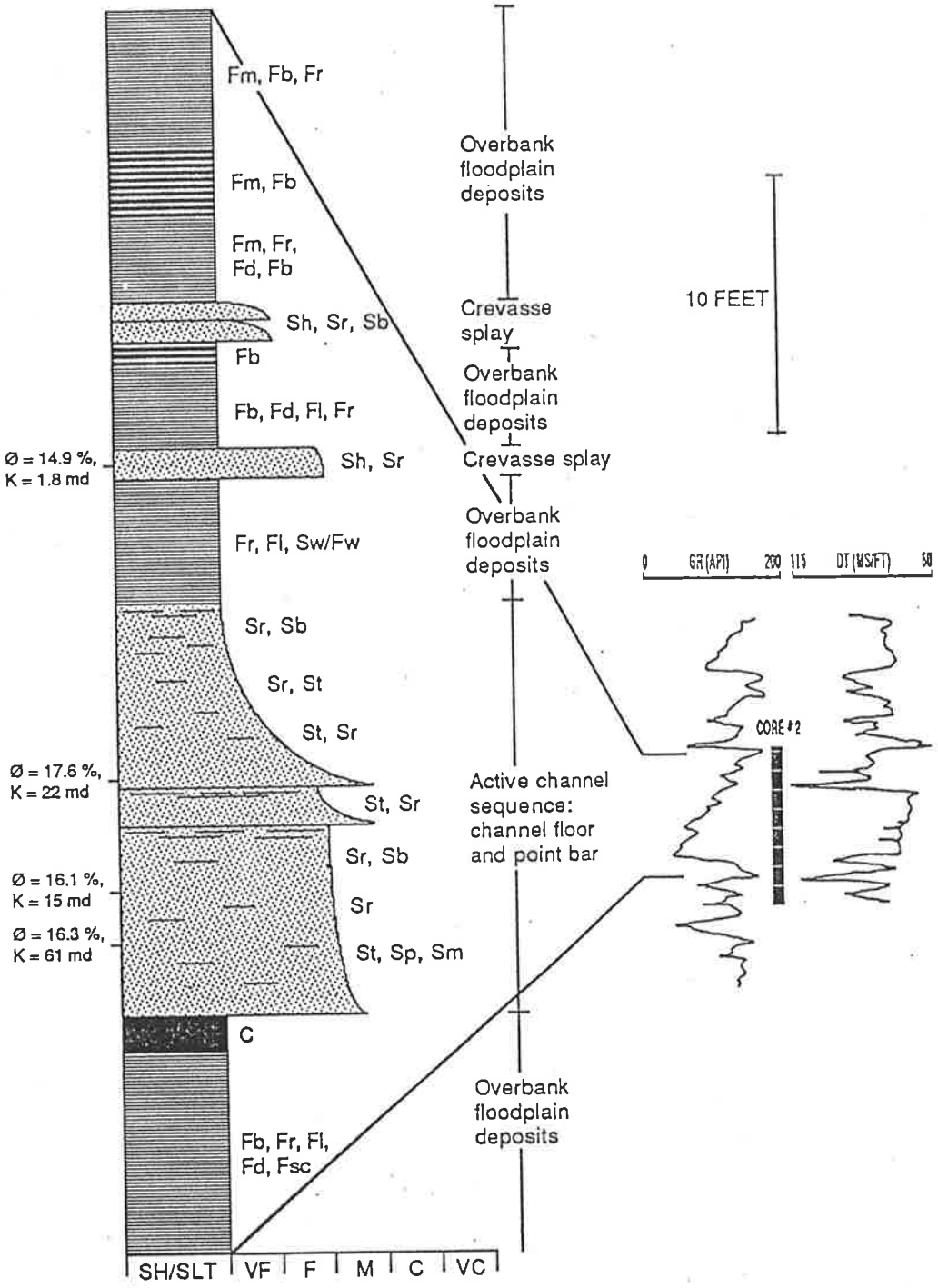

Figure 3.3 Example of a typical fluvial sequence as cored in the basal Patchawarra Formation at Wancoocha-1 (6160-6219'). Observe the characteristic gamma ray log response of this fining upward sequence. Active channel deposits of point bar origin grade upward into overbank floodplain sediments indicative of a meandering river system. Crevasse splay sandstones are found intercalated within the overbank deposits; the crevasse splay sandstones formed when the river breached its banks (Walker & Cant, 1984).

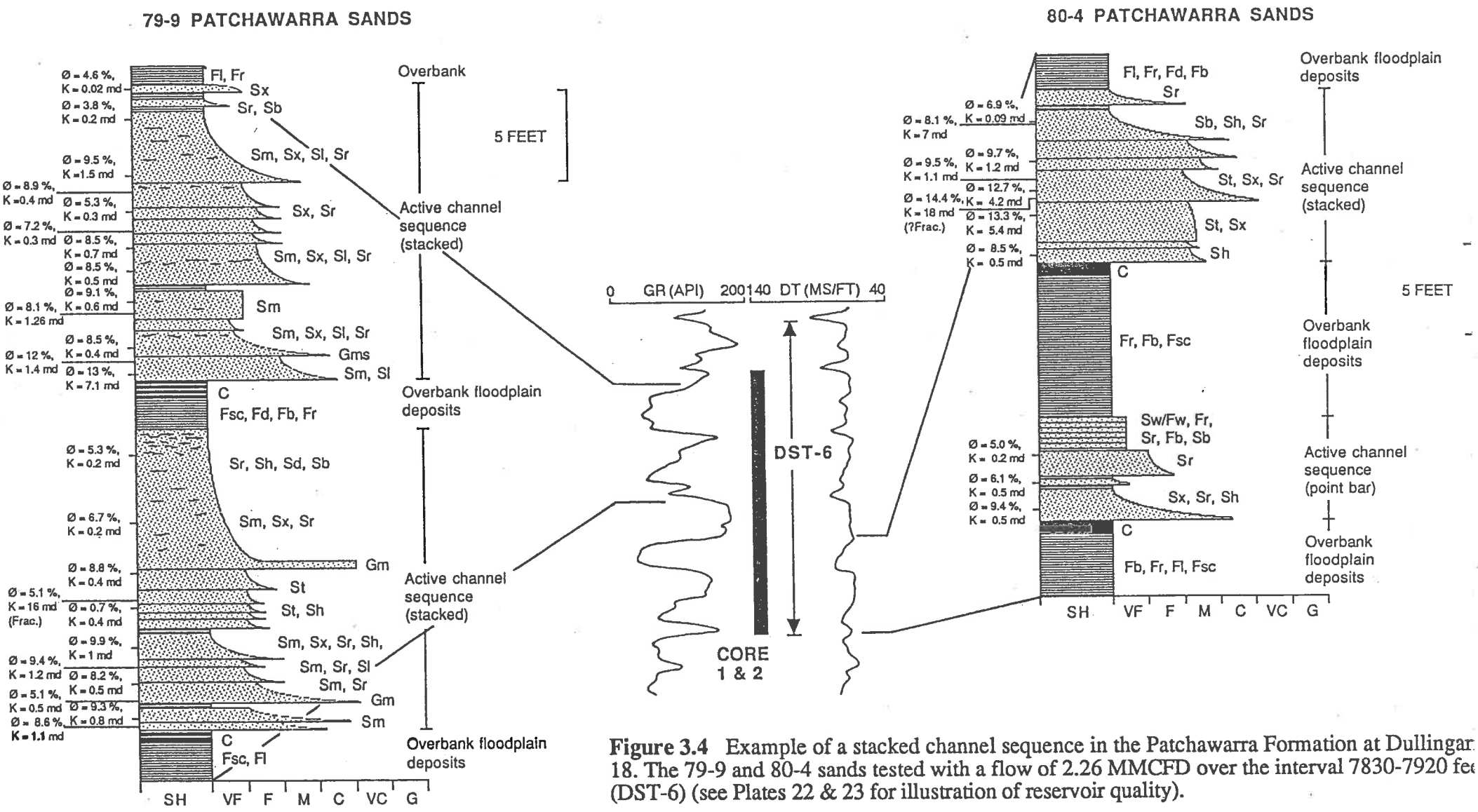

Figure 3.4 Example of a stacked channel sequence in the Patchawarra Formation at Dullingar 18. The 79-9 and 80-4 sands tested with a flow of 2.26 MMCFD over the interval 7830-7920 fe (DST-6) (see Plates 22 & 23 for illustration of reservoir quality).

Walker & Cant, 1984). They may be massive, finely laminated, and/or show evidence of bioturbation (lithofacies Fm, Fl, Fb) (Figs 3.2, 3.3 & 3.4). Locally, desiccation cracks occur which formed when the muds and silts dried out after the retreat of the flood (Fig.3.1). Fine sands are occasionally intercalated within the floodplain muds (lithofacies Fw/Sw, Fl, Fm, Fb) (Fig.3.3). Such sand can be deposited on levees adjacent to the channel when the river overtops its banks (Fig.3.1) (Tucker, 1981). Other sands are the result of catastrophic breaching of the levee that lead to crevassing (Fig.3.1) (Walker & Cant, 1984). Sands of crevasse splay origin are typically characterised by a sharp base, parallel laminations that may pass into ripple cross-laminations, and occasional root traces and trace fossils in the top of the splay beds (Walker & Cant, 1984) (cf. Fig.3.3). The uppermost portion of vertical accretion deposits comprise backswamp authochthonous coals and carbonaceous shales (lithofacies C) which may contain small rootlets and siderite nodules (Fig.3.2). The coals are indicative of humid climatic conditions and a high water table (Tucker, 1981; Serra, 1985).

Floodplain deposits are best-developed in fluvial meandering systems whereas braided rivers that migrate laterally leaving sheet-like or wedge-shaped deposits of channel and bar complexes preserve only minor amounts of floodplain material (Allen, 1965; Cant, 1982; Serra, 1985). A meandering point bar deposit is exemplified by the basal Patchawarra Formation intersected at Wancoocha-1 (Fig.3.3). Note that the gamma ray log profile exhibits an abrupt base and a gradational top (Fig.3.3); this is similar to the log characteristics of meandering point bar deposits described by Stuart (1976), Thornton (1979), Coleman & Prior (1982), and Serra (1985). In contrast, in the Patchawarra Formation at Dullingari-18, reservoir sands are characterised by multiple scouring and multistorey stacking suggestive of a more braided depositional environment (Fig.3.4). In this sequence, overbank deposits are generally poorly developed (cf. Figs.3.4 & 3.5). Differences in the depositional environment are suggested by the gamma ray log response. At Dullingari-18, the gamma ray exhibits a far less gradational upper contact than at Wancoocha (cf. Figs.3.4 & 3.5).

3.3.2 Deltaic environment

Deltaic sediments "are formed under subaerial and shallow marine or lacustrine environments and typically show a gradation into finer-grained offshore facies" (Miall, 1984, p.105). Typical delta front sub-environments as exemplified by the Mississippi Delta are illustrated in Figure 3.5. In the Cooper Basin, deltaic sediments exist where

fluviatile deposits pass laterally into lacustrine shale and siltstone (Moore & Castro, 1984). Lacustrine delta-fill sediments are locally well-developed in the Patchawarra, Epsilon and Daralingie Formations (Thornton, 1979; Moore & Castro, 1984). An example of delta front sandstones in the Daralingie Formation at Moomba is illustrated by Thornton (1979; cf. Figure 47).

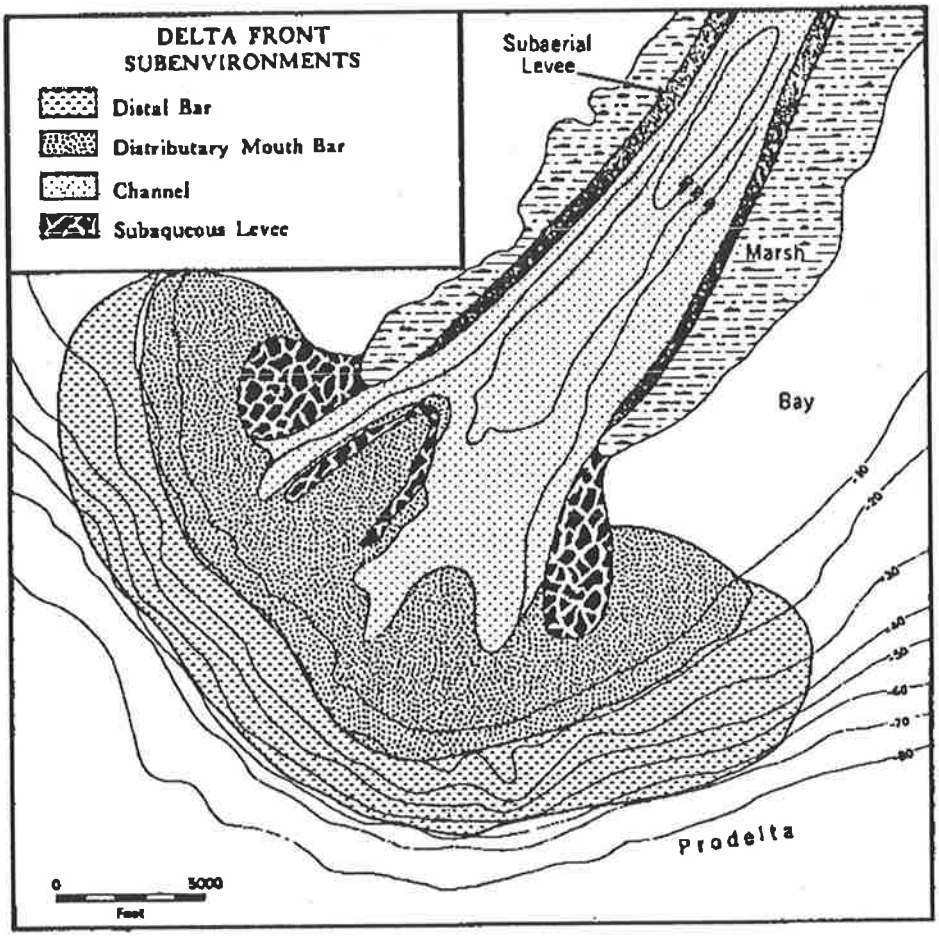

Figure 3.5 Sub-environments at a distributary mouth in a river-dominated delta, South Pass, Mississippi Delta (modified from Coleman & Gagliano, 1965).

Deltaic deposits are typically coarsening-upward sequences, produced by progradation of the delta front (Tucker, 1981; Serra, 1985) (Fig.3.6). Such deposits are characterised by a gamma ray signature exhibiting a gradational base and an abrupt top (Coleman & Prior, 1982; Serra, 1985). An example includes the basal Epsilon Formation intersected at Dirkala-2 (Fig.3.7). The sequence overlies argillaceous sediments of Murteree 'lake' origin (see Battersby, 1976; Thornton, 1979). Delta front sediments grade from muddy prodelta shales and silts to fine grained sandstones

interpreted to be of proximal distributary mouthbar/shoreline origin (Fig.3.7). The sequence is capped by interdistributary (delta plain) marsh sediments (Fig.3.7), thus representing a classical example of a river-dominated delta as described by Coleman & Prior (1980), Miall (1984) and Serra (1985) (cf. Fig.3.6). The prodelta shales and silts are grey-black to black in colour, and are characterised by fine laminations (lithofacies Fl), bioturbation (lithofacies Fb), soft sediment deformation (lithofacies Fd), and isolated ripple-laminated intervals (lithofacies Fr) (Fig.3.7). Interbedded within these lithofacies occur coarsening-upward silts and fine grained sandstones interpreted to be of distal distributary mouth bar origin. The distal bar sediments are lighter coloured, less argillaceous, and contain both wavy ripple-cross lamination and cross-bedding (lithofacies Sr/Fr and Sx) (Fig.3.7).

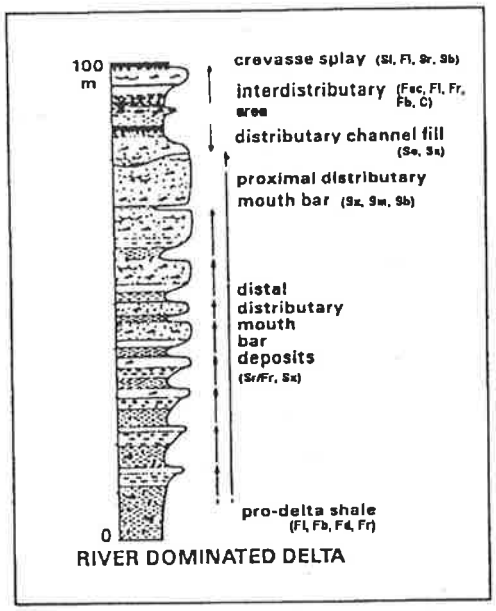

Figure 3.6 Vertical sequential evolution in a river-dominated delta. Lithofacies codes shown in brackets. Arrows indicate increasing grain size (modified from Serra, 1985).

The proximal distributary mouth bar/shoreline deposits overlying the distal bar and prodelta sediments are very fine to fine grained, and light grey to buff coloured; they gradually coarsen upward, are fair to well sorted, and exhibit abundant crossbedding (lithofacies Sx) resulting from variations in internal flow conditions (Fig.3.7) (Miall, 1984) [7]. Within the proximal mouth bar/shoreline sediments, there also occur massive sandstones with a lack of internal sedimentary features (lithofacies Sm) (Fig.3.7). Trace fossils locally exist (lithofacies Sb), and are characterised by narrow V-shaped burrows. Stuart (1976, p.39) commented that such "trace fossils are distinctly different from worm burrows which represent flood plain environments and show clearly that organisms lived in the distributary [delta] sediments with access to the sediment-water interface". The delta plain sediments consist of massive to finely laminated shales with occasional ripple laminated silty intervals (lithofacies Fsc, Fl and Fr) which may be bioturbated (lithofacies Fb). The top of the delta plain sequence at Dirkala-2 consists of a coaly interval (lithofacies C)

[7] The fine grain size appears to be a characteristic feature of all delta shoreline deposits that were logged in the present investigation, namely the Epsilon Formation at Kirby-1, Coochilara-1, Yapeni-1, Kerna-1 and Big Lake-3. Shoreline deposits are rarely more than medium grained, confirming earlier results by Stuart (1976). They also are typically well to very well-sorted and locally have superb reservoir character (cf. Figs. 3.7 & 3.8; Chapter 5).

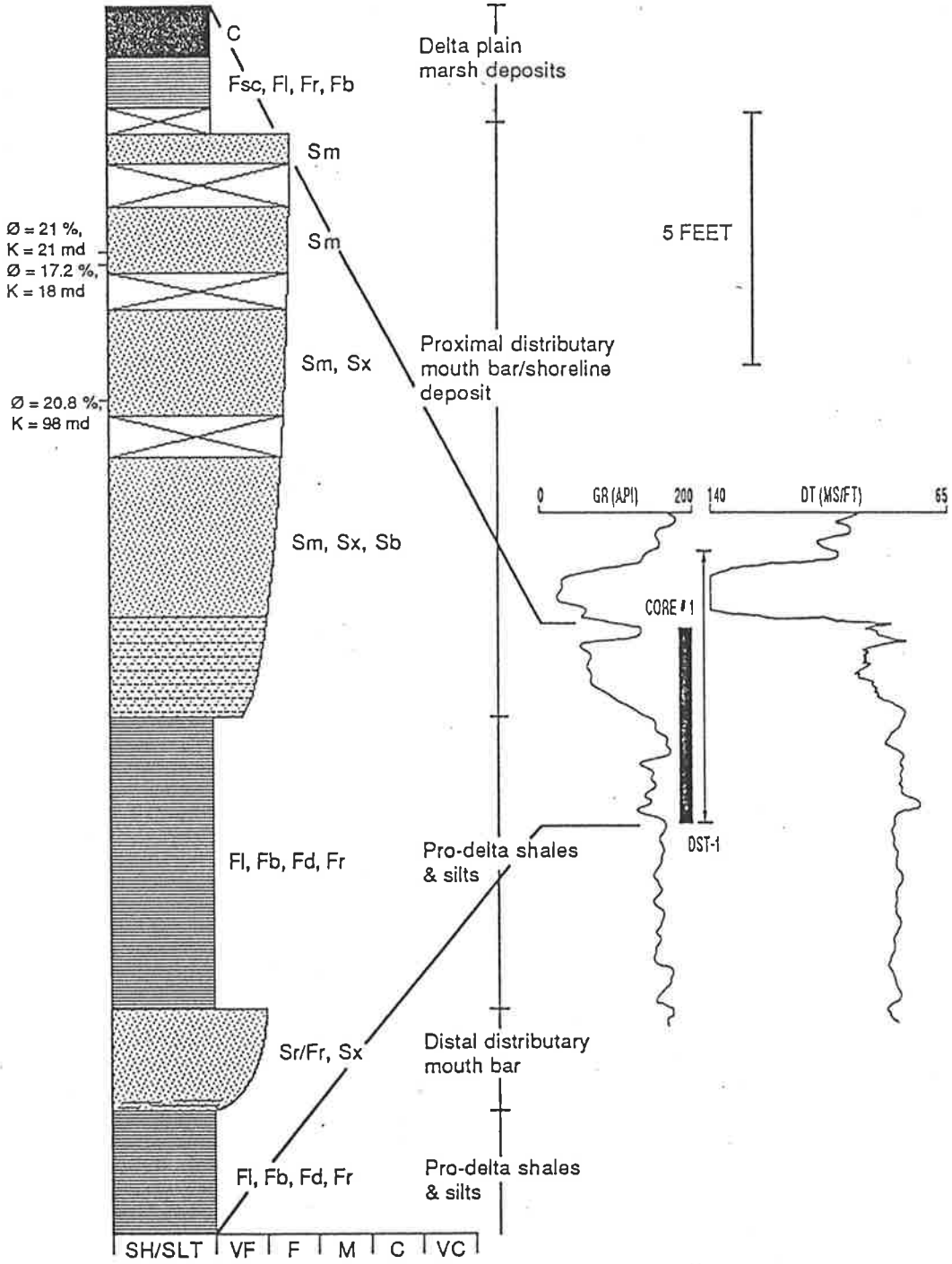

Figure 3.7 Example of a typical delta sequence as illustrated by the basal Epsilon Formation cored at Dirkala-2 (6188-6218'). The sequence coarsens upwards, giving rise to a gamma ray signature with a gradational base and an abrupt top. Note the fine grained nature of the sediments. DST-1 over the interval 6176-6218 feet tested with a flow of 6.9 MMCFD and 287 BCPD (API = 47.3° at 60° F).

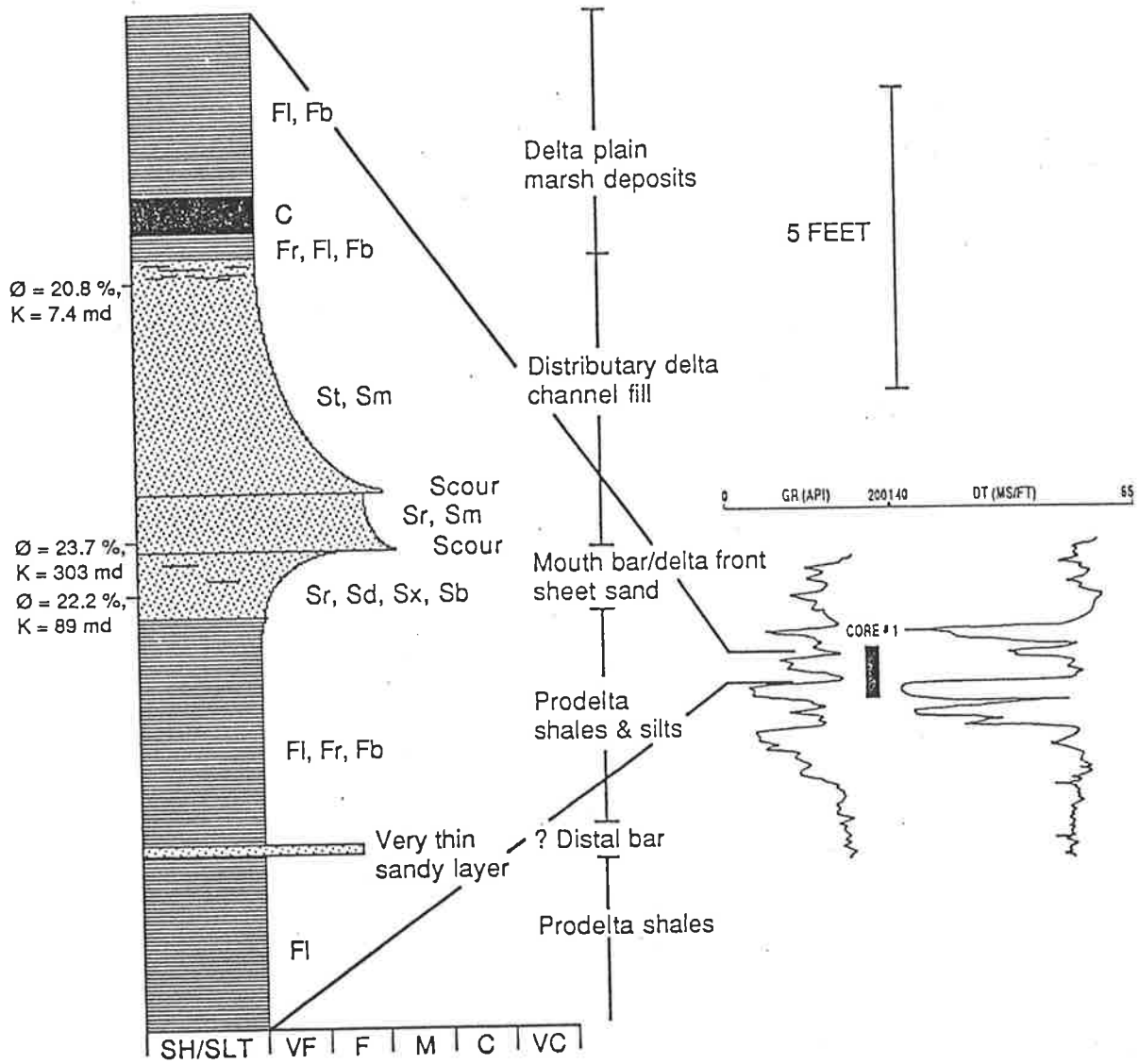

Figure 3.8 In the Epsilon Formation cored at Pando-2 (5806-5830'), a distributary channel fill sequence overlies a coarsening-upward mouthbar/delta front sheet sand. The distributary channel fill sequence could be mistaken for a channel lag deposit were it not for its distinct texture and stratigraphic level (cf. Stuart, 1976). A deltaic environment of deposition is clearly indicated by the gradational 'coarsening upward' gamma ray response of the sand body underlying the cored interval. A similar delta sequence is described by Tucker (1981; Fig.2.55).

representative of interdistributary delta marsh environments (Miall, 1984) (Fig.3.7). Interdistributary sediments were deposited under conditions of low energy, muddy sedimentation and abundant organic activity (Miall, 1984). Crevasse splays similar to those within fluvial overbank deposits locally exist within such sediments (Miall, 1984; Serra, 1985).

Distributary channel fills within delta plain sequences often exhibit similar gamma ray signatures to point-bar and channel lag deposits (Stuart, 1976; Coleman & Prior, 1982; Serra, 1985). This is because distributary channel fills represent essentially fining-upward deposits, often with a scoured base, cross-bedded sands and a swamp deposit on top (see Tucker, 1981; Fig.2.55) (Fig.3.8). However, distributary sandstones can usually be differentiated from point-bar and channel lag deposits by their texture and relative stratigraphic level (Stuart, 1976). In the Cooper Basin, the distributary channel fills are usually fine grained, and coarse scour lags within their basal beds are relatively uncommon (Stuart, 1976). An example includes part of the basal Epsilon Formation intersected at Pando-2 in the southern Cooper Basin (Fig.3.8). Overlying a thin coarsening-upward mouthbar/delta front sheet sand, a fining upward distributary channel sand occurs, characterised by medium to very fine grain size and several internal scour surfaces (Fig.3.8). On wireline logs, the sands are characterised by an abrupt upper and lower gamma ray contact; the sands occur interbedded within a sequence of coals and mudstones, and could be misinterpreted as a fluvial multistorey channel sequence within floodplain deposits (Fig.3.8). However, a deltaic origin of the sequence is suggested by the characteristic 'coarsening-upward' gamma ray signature of the underlying sands, and the available core data (Fig.3.8).

3.4 Detrital rock composition

The sandstones in the study area can be classified as sublitharenites and litharenites. Detrital quartz grains make up between about 40 and 70 percent of total rock composition as determined by point count. Monocrystalline detrital quartz grains are the most abundant; polycrystalline detrital quartz grains of igneous or metamorphic origin generally constitute less than 5 percent of total rock composition. Matrix consists typically of illitic clay, and can be in excess of 60 percent in some sandy mudstones or poorly sorted coarser sediments. Lithic rock fragments of sedimentary origin (eg. shale, coal or reworked sandstone clasts) vary in abundance between zero and five percent. Only rarely are lithics of volcanic or metamorphic origin observed. The latter comprise phyllites whilst the former include porphyritic rhyolite and rhyodacite (eg. Lake Hope-1). Detailed XRD work failed to identify any detrital feldspar, and differentiation between K-feldspar and plagioclase using that method was found to be effectively impossible in the study area. Similarly, SEM studies were found to be of very limited use for the same purpose. Most feldspars have long since weathered away, and only 'ghost' structures in kaolin matrix (cf. Plate 14 F) provide any indication of their former presence. However, feldspar remnants were occasionally identified under the conventional microscope and also with CL, indicating a residual feldspar content in *a few* samples of up to about 2-3 percent maximum (visual chart estimates). Petrographic work suggests these are almost exclusively alkali feldspars with only one recorded occurrence of plagioclase in the study area.

CHAPTER 4

DIAGENETIC ALTERATION OF PERMIAN RESERVOIR SANDSTONES

4.1 Introduction

Diagenesis is defined as the chemical and physical modification of sediments after deposition and prior to the onset of metamorphism (McBride, 1989). Diagenetic events include mechanical compaction, chemical compaction and cementation. In the Cooper Basin, all three types of diagenetic alteration are identified. The various diagenetic events are broadly similar throughout the study area, hence all Permian formations are discussed together. Emphasis is placed on cementing agents because of their complexity and important influence on porosity and permeability (Chapter 5). Study results presented here form an extension of the work of Schulz-Rojahn & Phillips (1989) and Schulz-Rojahn et al. (1991).

4.2 Results

4.2.1 Mechanical compaction

Houseknecht (1987, p.634) defined mechanical compaction as "the bulk volume reduction resulting from processes other than framework grain dissolution". Evidence for mechanical compaction includes the presence of bent mica flakes (Plates 1 D & E), grain rotation and slippage, and deformed lithic fragments seen in thin section. Mechanical compaction is more evident in poorly sorted, finer grained sandstones with detrital clay. These sandstones have minor to insignificant porosity.

Plate 1

Micrographs of features indicating mechanical and chemical compaction

A. Thin section micrograph of sutured grain boundary in a very poorly sorted sandstone of scour lag origin. Sutures represent the combined effect of mechanical and chemical compaction. Crossed nichols. Scale bar 1 mm. Sample CB-0027, Big Lake-27, Patchawarra Formation (9146' 6").

B. High-amplitude microstylolites cross-cutting a medium-grained sandstone derived from the basal portion of a point bar sequence. Note the lack of porosity and the in-situ alteration of some grains to illite (brown). Plane light. Scale bar 1 mm. Sample CB-0013, Kirby-1, Toolachee Formation (8953' 6").

C. Scanning electron micrograph of a stylolite between quartz overgrowths. This suggests there was some chemical compaction after silicification. Scale bar 10 μm. Sample CB-0079, Big Lake-34, Patchawarra Formation (9339' 2") [micrograph courtesy of S.E. Phillips].

D. Bent mica due to mechanical compaction. Scale bar 0.1 mm. Sample CB-0070, Big Lake-5, Patchawarra Formation (9417' 5") [micrograph courtesy of S.E. Phillips].

E. Thin section view of bent and broken (arrow) mica flake, indicating the effects of mechanical compaction. Crossed nichols. Scale bar 250 μm. Sample CB-0457, Moomba-5, Daralingie Formation (8232' 0").

F. Fine-grained argillaceous sandstone that has experienced intense mechanical and chemical compaction. Note the abundance of microstylolites and pressure dissolution seams. The sample is derived from the fining upward portion of a fluvial channel sequence. Plane light. Scale bar 1 mm. Sample CB-0029, Big Lake-27, Patchawarra Formation (9156' 9").

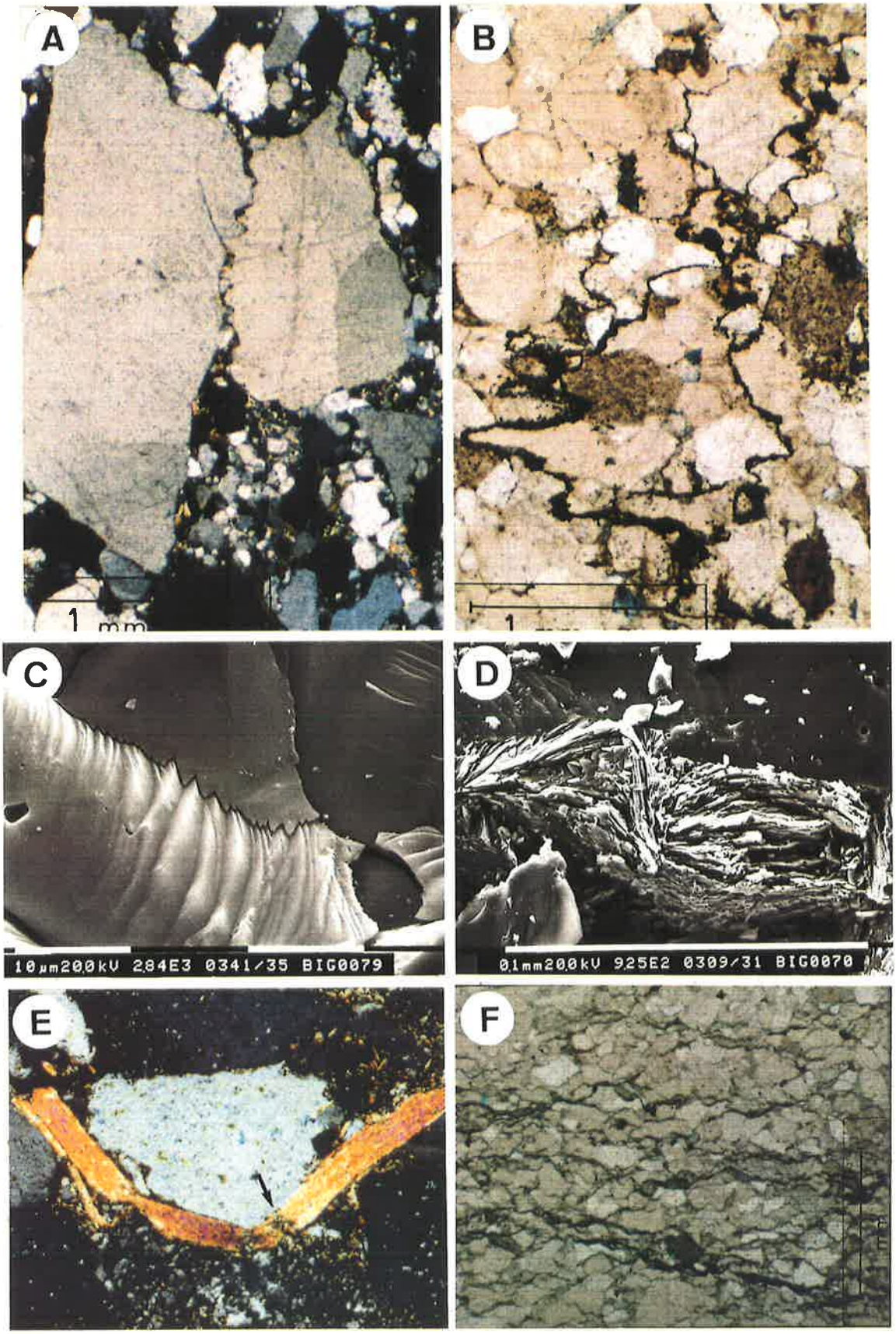
A
1 mm
B
1
C
10µm20.0kV 2.84E3 0341/35 BIG0079
D
0.1mm20.0kV 9.25E2 0309/31 BIG0070
E
F

4.2.2 Chemical compaction

Chemical compaction represents "the bulk volume reduction caused by the dissolution of framework grains at points of contact" (Houseknecht, 1987, p.634). Chemical compaction is evident in both hand specimen and from thin section studies from the presence of stylolites, sutured grain contacts and pressure dissolution seams (Plates 1 A, B, C & F). Dissolution seams and stylolites are typically highlighted by an accumulation of clay or other insoluble material (Braithwaite, 1988). In the present study, these features crosscut rock textures (including quartz overgrowths), indicating that some chemical compaction occurred after silicification in some sandstones. Sutured grain contacts are abundant in finer grained clayey sediments where quartz cementation is minimal, and between polycrystalline and adjacent monocrystalline quartz grains (see section 4.1.3.1). Generally, features due to chemical compaction are rare, and appear to be more abundant in the fine grained clayey sediments at depth as evident from lithological descriptions and petrographic work (Schulz-Rojahn & Phillips, 1989; Thomas, 1991; Stuart et al., 1991). Based on the available data, chemical compaction is of lesser importance than mechanical compaction. Rocks that underwent intense chemical compaction have very little porosity.

4.2.3 Cementation

Cementation is a major cause of reduction in porosity and permeability in the reservoir sandstones of the southern Cooper Basin. Cementation is defined as "the occlusion of intergranular volume by the precipitation of authigenic minerals, with no directly related reduction of bulk volume" (Houseknecht, 1987, p.634). In the present study, the authigenic minerals identified include quartz, carbonates and clays (Schulz-Rojahn & Phillips, 1989; Schulz-Rojahn et al., 1991).

4.2.3.1 Quartz

Authigenic quartz represents the most common cement type in the reservoir sandstones of the southern Cooper Basin. It is most abundant in coarser clastics

Plate 2

Micrographs of quartz cement (1)

A. SEM view of a medium-grained sandstone demonstrating the partial preservation of primary intergranular pores (arrow) where euhedral quartz overgrowths have developed. This sample was derived from the basal trough cross-bedded portion of a fluvial point bar sequence (stacked channel sands). Measured core porosity is 15.15 % and permeability 215 md. This sample is typical of many high-quality reservoir sandstones found dominantly along the basin margin and in midflank position. Scale bar 10 µm. Sample CB-0192, Murteree-1, Toolachee Formation (5981' 9.5").

B. Very fine-grained sandstone of deltaic origin with abundant primary porosity. Again, most detrital quartz grains are characterised by large euhedral quartz overgrowths. Measured core porosity is 23.7 % and permeability 303 md. Scale bar 0.1 mm. Sample CB-0104, Pando-2, Epsilon Formation (5814' 10").

C. The same sample shown in (B) above. Note that large euhedral quartz overgrowths have partly intergrown. Towards the centre of the micrograph, a large quartz prism can be seen (A). Primary porosity is prominent although locally it is reduced by authigenic clays that partly block pore throats (see D). Where clays cover detrital grains (arrow), overgrowths are poorly developed (cf. Plates 3 A, C & D). Scale bar 0.1 mm.

D. Close-up view of (C) above (insert). The pore throats can be seen to be partly blocked by authigenic ?kaolin interstratified with illite. However, porosity and permeability values suggest the clays in this sample have only a negligible influence on overall reservoir quality. The rock has excellent reservoir potential. Scale bar 10 µm.

E. In this very coarse-grained sandstone, euhedral quartz overgrowths are particularly prominent. Despite this, primary intergranular porosity (arrow) has been partially retained. Note coexistence of fine quartz druse (D) with large quartz rhombohedra. Scale bar 0.1 mm. Sample CB-0425, Toolachee-18, Patchawarra Formation (7327' 3") [micrograph courtesy of D. Alsop].

F. Quartz overgrowths can be seen to be interlocking in this SEM view of a fine-grained sandstone. Remnants of primary porosity (P) exist in this micrograph, but pore aperture radii are greatly reduced by quartz cementation. Scale bar 10 µm. Sample CB-0182, Wancoocha-1, Patchawarra Formation (6218' 5").

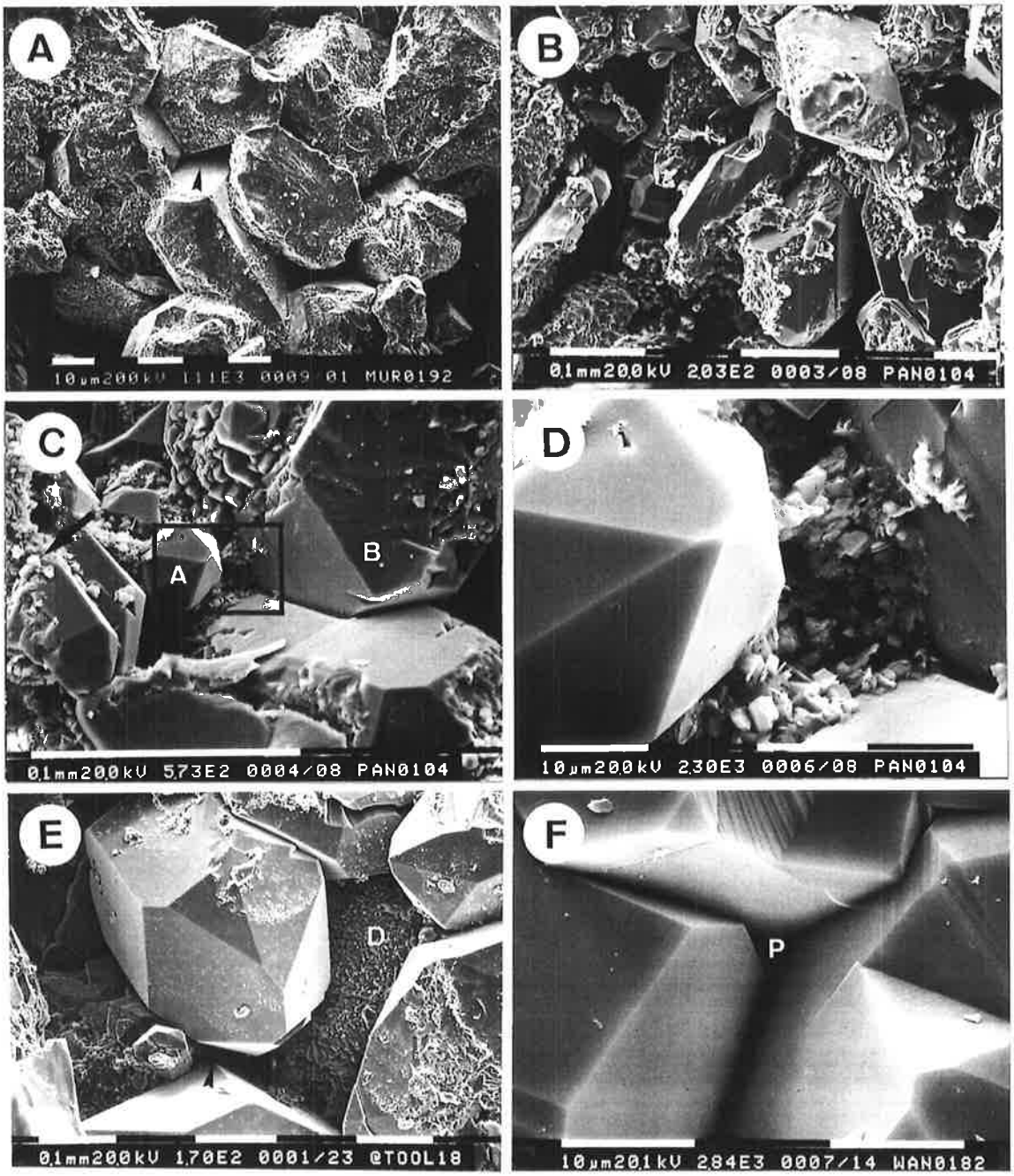
A
10µm20.0kV 1.11E3 0009 01 MUR0192
B
0.1mm20.0kV 2.03E2 0003/08 PAN0104
C
A
B
0.1mm20.0kV 5.73E2 0004/08 PAN0104
D
10µm20.0kV 2.30E3 0006/08 PAN0104
E
D
0.1mm20.0kV 1.70E2 0001/23 @TOOL18
F
P
10µm20.1kV 2.84E3 0007/14 WAN0182

devoid of significant amounts of clay (cf. Plates 5 E & 12 E). It occurs as syntaxial overgrowths on detrital quartz grains, frequently with euhedral terminations (Plates 2 C, D, E & F, 18 E). In thin section, overgrowths are distinguished by 'dust' linings or clay rims over detrital grains (Plates 7 A & B, 21 C), and by euhedral crystal faces and straight contacts between adjacent grains (Plates 7 C & 18 E). Detrital quartz grains commonly exhibit abundant inclusions whereas overgrowths are relatively free of inclusions (Plate 3 B). SEM studies reveal that many of the overgrowths have rhombohedral and prismatic terminations (Plates 2 C & E, 3 A). The large terminations develop where there are no constraints on the space available for precipitation (McBride, 1989). However, not all quartz grains exhibit overgrowths, and on some grains only incipient overgrowths are evident (Plates 3 A & C). The latter are characterised by a fine quartz druse, consisting of numerous small, closely spaced prisms which protrude into the adjacent pore space (Plate 3 D). Many of the grains characterised by druse are at least partially coated with illite. Grains exhibiting clay coatings sometimes coexist with grains showing extensive euhedral overgrowths (Plate 3 D). These overgrowths may be covered by V-shaped depressions (Plate 13 A). Despite the presence of overgrowths, in numerous samples primary intergranular porosity is partially retained (Plates 2 A, B & F) (see Chapter 5).

Cathodoluminescence (CL) work enabled the identification of the relative abundance of quartz overgrowths which are rarely apparent in thin section (cf. Plates 4 A & B). For this reason, CL is now considered an essential tool in the petrographic description of sedimentary rocks (eg. Sibley & Blatt, 1976; Houseknecht, 1988). In the samples studied, there is up to about 30 percent authigenic quartz. Only deeper sandstones are completely cemented by quartz (Plates 4 A, 5 D, 6 C & D). There appears to be a broad increase in the proportion of quartz overgrowths in clean well-sorted sandstones from the basin margin to midflank and basinal areas of the basin (cf. Plates 6 A, B, C & D; 4 A & D).

CL colours of detrital quartz grains vary from dull reddish-brown to red and light blue. Locally, such as in the Toolachee Field, rare bright-red luminescent detrital quartz grains are also evident (Plates 4 C & 5 A). The dull reddish-brown detrital quartz grains are most common. In the view of Marshall (1988), such grains reflect a dominantly metamorphic source. The provenance of the bright-red luminescent grains is uncertain, but there are examples with zonations in colour which may be due to inherited overgrowths derived from a previous sedimentary environment; such grains exhibit abraded edges (Plate 4 C). Bright-blue quartz luminescence tends to fade with long exposure to the electron beam, and is most abundant in the Nappamerri Trough. These blue coloured detrital quartz grains may be plutonic or volcanic in provenance (Marshall, 1988). The interpretation is in accordance with fluid inclusion data obtained by Bone & Russell (1988) and Russell & Bone (1989) for Cooper Basin sandstones,

Plate 3

Micrographs of quartz cement (2)

A. Large quartz rhombohedra (A) and fine quartz druse (B) can coexist on the same detrital grain. Scale bar 0.1 mm. Sample CB-0180, Wancoocha-1, Patchawarra Formation (6200' 11").

B. In thin section, quartz overgrowths can sometimes be distinguished from detrital quartz grains by the relative lack of fluid inclusions (arrows). Plane light. Scale bar 250 µm. Sample CB- 0015, Kirby-1, Epsilon Formation (9703' 0").

C. Clay coatings inhibit quartz cementation. In this example, large quartz rhombohedra have grown where there is no clay. The same relationship is evident in CL in other samples (eg. Plates 12 E & G) Scale bar 10 µm. Sample CB-0199, Dirkala-2, Epsilon Formation (6201' 11").

D. Euhedral quartz prisms developed on the margins of a detrital quartz grain. Note the larger overgrowth on the adjacent grain (A). The smaller prisms demonstrate the selective and impaired development of overgrowths at specific sites. Scale bar 0.1 mm. Sample CB-0117, Big Lake-1, Toolachee Formation (7687' 6").

E. Close-up view of authigenic quartz. Large euhedral quartz rhombohedra and prims envelop smaller ones. It would appear that overgrowth formation is favoured at specific sites. Scale bar 1 µm. Sample CB-0104, Pando-2, Epsilon Formation (5814' 10").

F. Under cathodoluminescence (CL), quartz overgrowths can clearly be distinguished from the detrital quartz grains. Quartz cement is non-luminescent or only faintly luminescent. Detrital quartz grains exhibit a variety of colours ranging from pale-blue to pink to brown. The large dark areas are the edge of the sample (araldite), and the small bright-blue areas represent kaolin clay. The sample is derived from the hydrocarbon-bearing Patchawarra 57-0 sandstone at Wancoocha. The interval tested with a flow of 2.2 MMCFD and 1747 BOPD (42° API at 60 °F). Hydrocarbon production occurs from remnant primary pores (arrow) that are seen to contain contain dead oil in thin section. Note 'floating' texture of detrital grains in quartz cement suggesting early silicification prior to significant compaction. Scale bar 0.3 mm. Sample CB-0695, Wancoocha-2, Patchawarra Formation (5710-5720').

G. 'Economic basement 'of pre-Permian origin in the Wancoocha area is tight, this sandstone is completely cemented by quartz. This downgrades the pre-Permian reservoir potential in the Wancoocha area. The black areas represent the edge of the sample. Crossed nichols. Scale bar 1mm. Sample CB-0697, Wancoocha-2 (5750-5760').

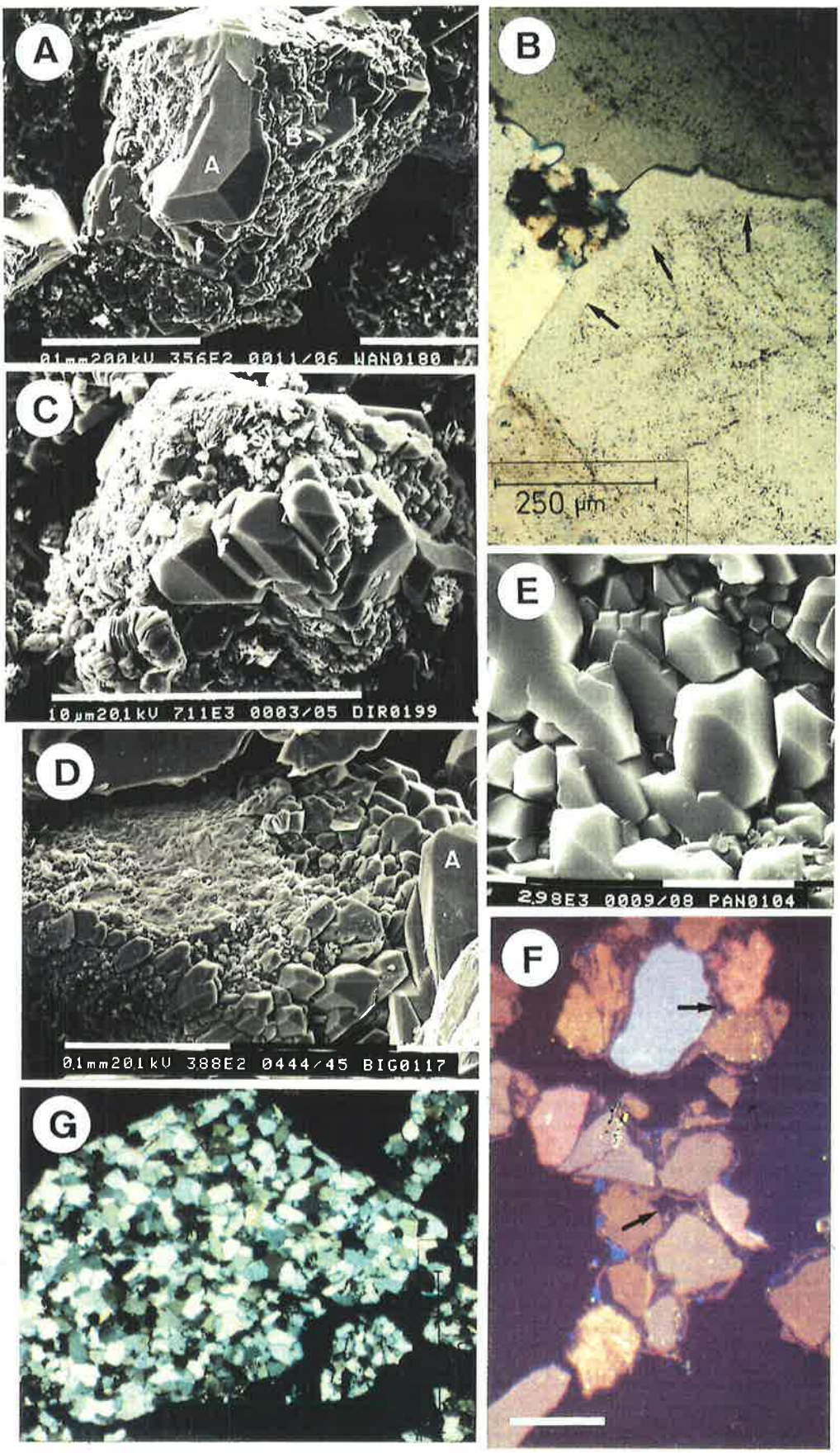
A
A
B
0.1mm20.0kV 356E2 0011/06 WAN0180
B
250 µm
C
10µm20.1kV 711E3 0003/05 DIR0199
D
A
0.1mm20.1kV 388E2 0444/45 BIG0117
E
2.98E3 0009/08 PAN0104
F
G

indicating the detrital quartz has homogenisation temperatures greater than about 300 °C.

Quartz cement is typically non-luminescent, or only faintly luminescent (Plates 3 F, 4 A, C & D, 5 A-E). Nonetheless, vague euhedral outlines and zonations within the authigenic quartz are often distinguished (Plate 5 D). Multiple overgrowths are generally only apparent on one side of detrital quartz grains suggesting preferential growth at certain sites. At least three major phases of overgrowth development are recognised (Plate 4 D), although up to six phases have been recorded. The three main phases of quartz crystallisation distinguished include (Plates 4 & 5):

➢ An early phase (Q1), characterised by luminescence colours varying from black-brown to medium-brown to medium orange-brown. It is of uneven distribution and irregular thickness, sometimes filling microfractures in detrital quartz grains (Plates 4 D & 5 A). This phase of overgrowth development acts as a grain-supporting framework in many samples.

➢ A second phase of quartz cement development (Q2) with luminescence colours varying from brown-greenish to dark bluish-purple; the bluish-purple cement phase precedes the rarer brown-greenish phase. Q2 generally is the most extensive of all overgrowth generations, representing the final pore-filling silicification event in many sandstones. On some detrital grains, it is the only cement phase present.

➢ A final phase of authigenic quartz (Q3), generally light-brown in CL colour and more continuous in distribution than earlier phases. This phase is difficult to discern from the first phase of overgrowth development (Q1) in cases where the second phase (Q2) is absent.

The factors controlling differences in quartz cathodoluminescence colour and intensity are not fully understood. Marshall (1988) suggested variations in the chemistry of water from which the quartz precipitated. A similar view is held by Sprunt (1981) who suggested red quartz luminescence is common in crystals with low titanium concentrations and high iron concentrations, whereas the reverse was considered true for blue luminescence. Differences in luminescence colour in quartz are also attributed to crystal irregularities and defects (Nickel, 1978), crystallisation temperatures (Marshall, 1988), length of exposure to the electron beam (Ramseyer et al., 1988), film type and reciprocity factor selected.

The overwhelming majority of CL samples is characterised by very loose grain packing, irrespective of stratigraphic origin, burial depth or geographic location (Plates 3 F, 4 A-D, 5 D & E, 6 A-D). Individual detrital grains commonly 'float' in a matrix of authigenic quartz (eg. Plates 4 A, 5 E, 6 D). Where detrital grains touch, there is a clear predominance of tangential grain contacts with infrequent occurrences of long contacts in some samples. Possible evidence for pressure dissolution in the form of concavo-convex or irregularly sutured grain boundaries is rare or absent. Only in a

Plate 4

Micrographs of quartz cement (3)

A. Detrital quartz grains are pale-blue to cream in luminescence, whilst the overgrowths are brownish. The very bright blue is kaolin. Note that the detrital grains 'float' in quartz cement, suggesting silicification was initiated early in the diagenetic history, prior to significant compaction. Measured core porosity in this sample is about 4.0 % and permeability 0.33 md. The rock is extensively silicified, all of the porosity is microporosity that occurs interstitially between clays particles (eg. Plate 13 C). The sample is derived from a massive sandstone of point bar origin. Scale bar 0.35 mm. Sample CB-0058, Burley-2, Patchawarra Formation (11383' 6").

B. Same field of view as (A) above in plane light. The comparison demonstrates that the proportion of overgrowths is very difficult to detect with the optical microscope. Scale bar 0.35 mm.

C. Some quartz overgrowths which are discontinuous and anhedral are probably inherited (arrow) in this medium-grained sandstone derived from the lower portion of a point bar sequence. Polycrystalline quartz (P) does not have overgrowths, and there are sutured boundaries where overgrowths are absent. Red, partially altered grains probably represent feldspars. Measured core porosity in this sample is 14.3 % and permeability 18.5 md. Scale bar 0.35 mm. Sample CB-0535, Toolachee-6, Patchawarra Formation (7638' 0") [micrograph courtesy of D. Alsop].

D. Multiple stages are evident in the development of some quartz overgrowths (arrows). At least three events are recorded in this medium-grained trough cross-bedded sandstone of point bar origin, elsewhere up to six phases of silicification can be detected. Note abundant macropores (black); primary porosity is predominant. At the bottom left, a secondary pore infilled with kaolin (blue) can be seen. Scale bar 0.3 mm. Sample CB-0342, Toolachee-1, Patchawarra Formation (6891' 3") [micrograph courtesy of D. Alsop].

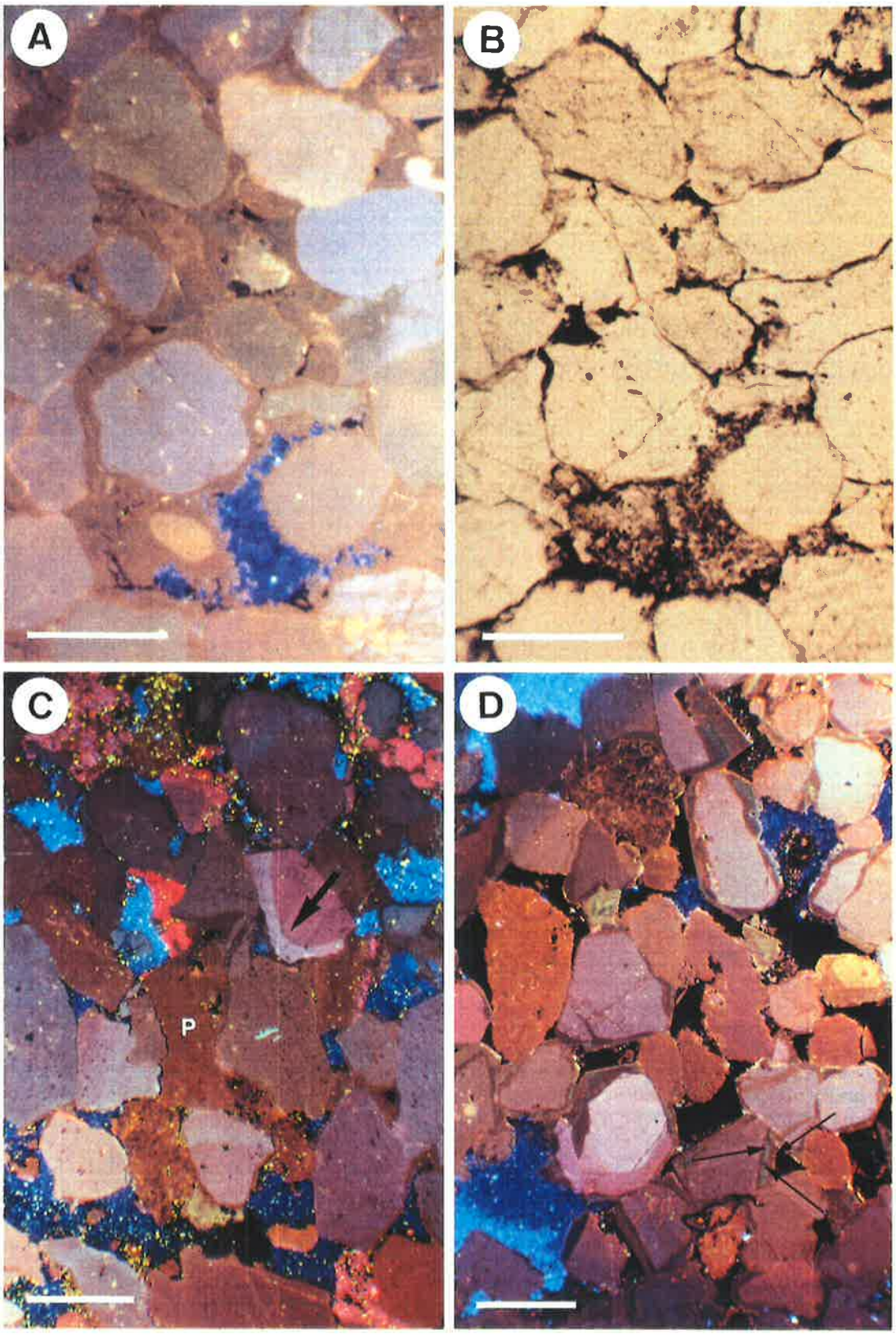
A
B
C
P
D

handful of samples studied by CL is there evidence for compaction and intense intergranular pressure solution (Plates 5 B & C). Such samples are characterised by a very dense grain packing as well as by abundant long and irregular sutured pressure dissolution contacts between grains; the average number of contacts per grain is very high, up to eight (Plates 5 B & C). These samples display a very low authigenic quartz content, unlike other samples studied, and there is almost no intergranular porosity preserved (Plates 5 B & C).

Petrological evidence of liquid hydrocarbon migration is apparent in samples from the Big Lake, Strzelecki, Toolachee, Daralingie, Moomba and Wancoocha Fields, as well as a number of wildcat wells. Thin sections viewed under plane light rarely show fluid inclusions in quartz overgrowths that appear to contain dead bitumen (Plates 7 A & B). It is impossible to discern which phase of quartz overgrowth is associated with the bitumen since the latter does not luminesce under CL. Dead bitumen/oil also often lines remnants of primary pores; the pore margins are outlined by euhedral quartz overgrowths (Plates 7 A, B & C). At Wancoocha, no differences in the amount of silicification between water-wet and oil-saturated sandstones in the Patchawarra Formation were detected (cf. Plates 3 F & 6 B). Similarly, no diagenetic changes immediatly above or below gas/water contacts are noticeable in the Moomba and Strzelecki Fields (Thomas, 1990; Eleftheriou, 1990; Schulz-Rojahn et al., 1991).

4.2.3.2 Carbonates

Carbonate cements are widespread in the reservoir sandstones of the southern Cooper Basin, being present in over 90 percent of clastics. Carbonate types identified from bulk XRD analyses include siderite, ankerite, dolomite, ferroan dolomite, and calcite. Siderite is by far the commonest carbonate mineral present, being almost 17 times more abundant than all other carbonate varieties included together (Fig.4.1). The total carbonate content in some samples exceeds 70 percent as determined by point counting (eg. Plates 11 A & 23 A).

The carbonate concentration varies rapidly in lateral and vertical distribution; intensely carbonate-cemented zones can be within centimetres of areas where there is little or no carbonate cement. Carbonate-cemented reservoirs are found at all depths throughout the study area, and occur up to about 12,000 feet of burial in the central Nappamerri Trough. Siderite occurs in all formations in every well investigated (Fig.4.2a). Ankerite, dolomite and Fe-dolomite cements concentrate in isolated wells towards the southern portion of the Nappamerri Trough (Pando North, Wancoocha,

Plate 5

Micrographs of quartz cement (4)

A. Fractures within detrital quartz grains are typically healed by two generations of quartz cement (arrow). Red grains in this coarse-grained sublitharenite do not represent feldspars as they can be seen to be surrounded by quartz overgrowths. Note the thinning or absence of quartz cements adjacent to patches of kaolin (blue). Black areas represent macropores. Measured core porosity is 14.2 % and permeability 15.5 md. The sample is derived from the trough cross-bedded portion of a point bar sequence. Scale bar 0.5 mm. Sample CB-0167, Toolachee-3, Patchawarra Formation (7428' 0") [micrograph courtesy of D. Alsop].

B. Sutured grain contacts are abundant where quartz cements are absent. In this medium-grained sandstone of point bar origin, some of the contacts are lined by insoluble residue (arrows). Almost all porosity is microporosity associated with kaolin (blue). Measured core porosity is 7.9 % and permeability 3.93 md. Scale bar 0.3 mm. Sample CB-0394, Moomba-3, Toolachee Formation (7912' 9").

C. CL micrograph of a fine- to medium-grained, poorly sorted sandstone showing a high degree of intergranular pressure solution. Note the relative lack of authigenic quartz and the predominance of long irregular sutured grain contacts. In this section, no porosity is evident. The sample is derived from a thin channel lag deposit. Scale bar 0.3 mm. Sample CB-0093, Della-3, Toolachee Formation (6698' 9").

D. In this trough cross-bedded sample of point bar origin, distinct zonations and euhedral terminations (arrow) are visible within quartz overgrowths. This suggests there were several distinct phases of quartz cementation in the study area. Quartz overgrowths first grew into primary pore space (arrow), then tightly cemented the rock. Scale bar 0.3 mm. Sample CB-0043, Burley-1, Toolachee Formation (8875' 10").

E. The loose grain packing at the time quartz cementation was initiated is highlighted by this micrograph. Numerous grains 'float' in a matrix of authigenic quartz. Where detrital grains touch, there is a clear predominance of tangential grain contacts. It would appear early introduction of authigenic quartz provided rigidity to reduce the effects of compaction. Black areas represent remnant primary pores, including possibly some secondary porosity (S). Notice the absence of clay. Measured core porosity is 14.2 % and permeability 15.5 md. The sample originates from the through cross-bedded portion of a fluvial point bar deposit. Scale bar 0.3 mm. Sample CB-0167, Toolachee-3, Patchawarra Formation (7428' 0") [micrograph courtesy of D. Alsop].

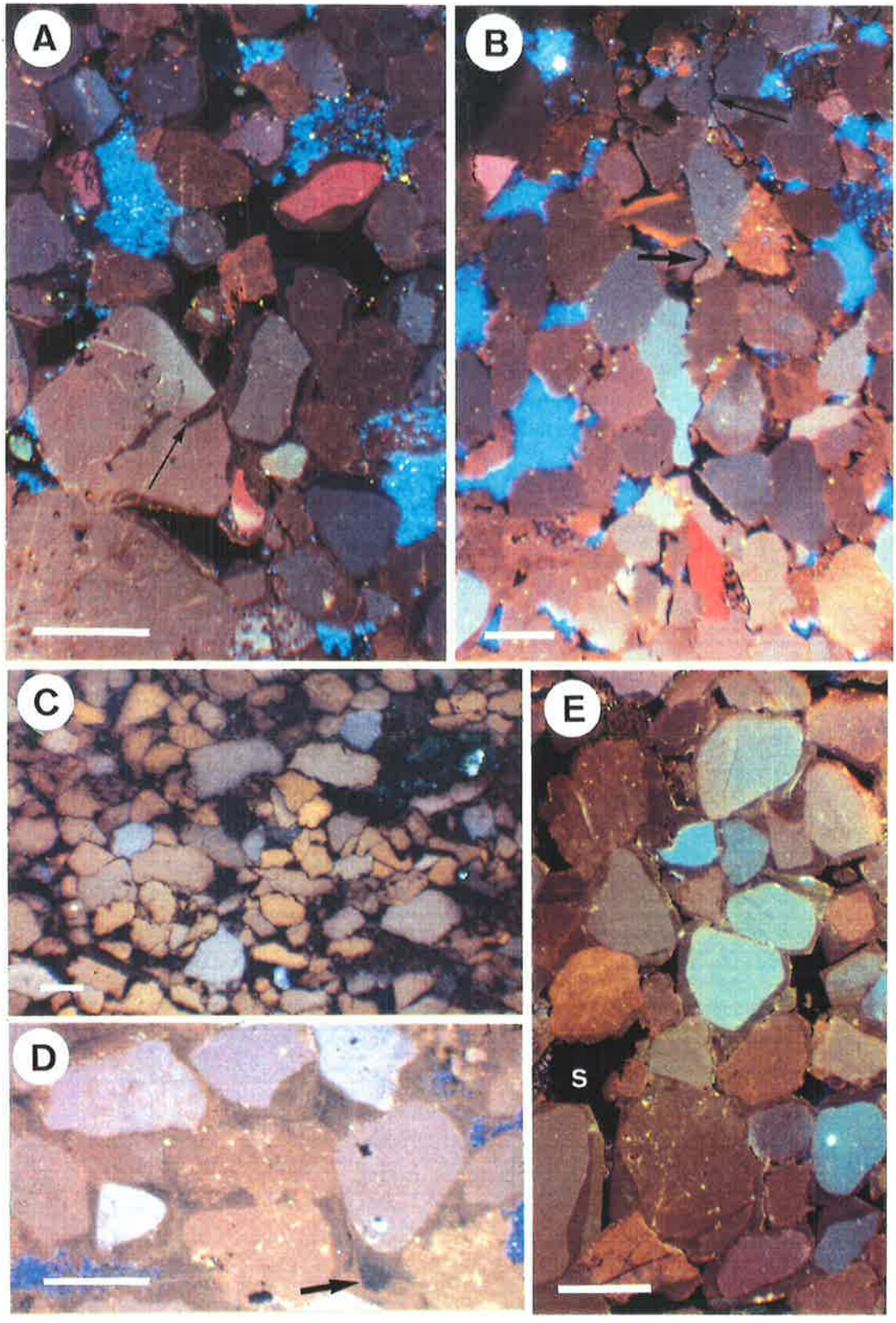
A
B
C
D
E
S

Murteree, Boxwood, Daralingie) (Fig.4.2 b & c). Ankerite and dolomite also occur sporadically at Moomba, Burley and Kirby, and the Dullingari Field (Fig.4.2 b & c). These Mg-rich carbonates are not restricted to any one formation, nor are they pervasive throughout the formations where they have been recognised; they appear to be most abundant in the Toolachee and Epsilon Formations. Calcite concentrates at shallower depths in wells located near the southern extremity of the study area, either along the basin margin (Wancoocha) or along structural highs (Daralingie) (Fig.4.2d). Calcite is also found sporadically in the south and east of the Toolachee Field in the Toolachee, Epsilon and Patchawarra Formations (Fig.4.2d). The only other localities from which calcite has been recorded is the Merrimelia Formation in Burley-1 (one core sample) and the basal Nappamerri Formation at Kirby (one ditch sample) (Fig.4.2d).

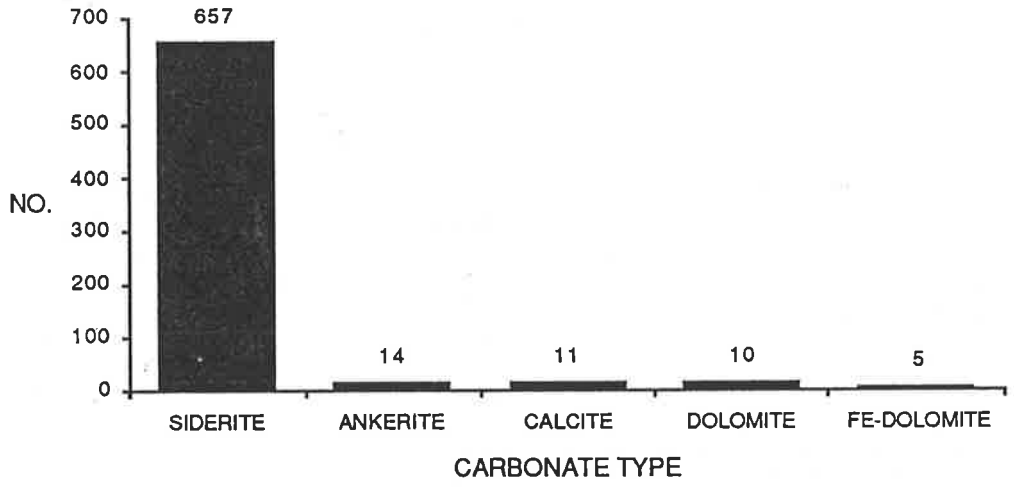

Figure 4.1 Relative abundance of carbonate types in the reservoir sandstones of the southern Cooper Basin, as identified from bulk XRD analyses (NO. = Number of samples) [data compiled from Sansome (1988), Alsop (1990), Eleftheriou (1990), Thomas (1990), Phillips (NCPGG, unpubl.data), this study].

In hand specimen, siderite-cemented zones generally are easily identified. Core samples are stained deep red to rust brown when the siderite is oxidised, or yellowish when fresh. The siderite has a variety of forms, it occurs as bands several centimetres thick, as isolated blotches, as pervasive cement, and outlining bedding. In the Toolachee Formation, one example of a siderite band up to 15 cm thick was observed.

Petrographic and SEM studies reveal that the siderite has several different crystal habits, including anhedral micrite (Plates 8 A & F; 9 C, D & E), microspar (Plate 8 B), and rhombohedral and scalenohedral spar (Plates 8 C, D & E; 9 A & B).

Plate 6

Reservoir silicification with depth

The CL photomicrographs shown here illustrate the change in reservoir silicification from the basin margin to the basin depocentre, as exemplified by four medium-grained, moderatly to well-sorted sandstones containing little or no clay. Similar cement relationships with depth are evident in other samples in the study area (cf. Plates 4 A & D, 5 E). Loose grain packing is evident in numerous samples irrespective of stratigraphic origin or depth of burial.

A. In marginal and midflank areas of the Cooper Basin, quartz cementation is incomplete. In this example from the Toolachee Field, quartz cement provided rigidity to resist the effects of compaction but did not occlude all porosity (black). Measured core porosity is 14.2 % and permeability 15.5 md. Scale bar 0.3 mm. Sample CB-0167, Toolachee-3, Patchawarra Formation (7428' 0") [micrograph courtesy of D. Alsop].

B. Near the basin margin at Wancoocha, a similar relationship to (A) is apparent. There are abundant remnants of primary pores (arrows). In thin section, some of the primary pores are seen to be infilled with dead bitumen/oil. Black areas in this micrograph represent the edge of the sample. Scale bar 0.3 mm. Sample CB-0702, Wancoocha-4, Patchawarra Formation (5780-5790').

C. In the central Nappamerri Trough, reservoir silicification appears to be much more pronounced in clean well-sorted sandstones than in similar samples derived from shallower depths. In this example, there is only a single isolated remnant of primary porosity (arrow). The amount of authigenic quartz is estimated to be 26 percent. Scale bar 0.3 mm. Sample CB-0824, Burley-2, Toolachee Formation (9040-9050').

D. In the Tirrawarra Formation at Kirby-1, well-sorted reservoir sandstones are completely cemented by quartz. In this sample, quartz cement constitutes about 30 percent of total rock composition. Silicification completely eliminated primary pores. Black areas represent the edge of the sample. Scale bar 0.3 mm. Sample CB-0723, Kirby-1, Tirrawarra Formation (12400-12410').

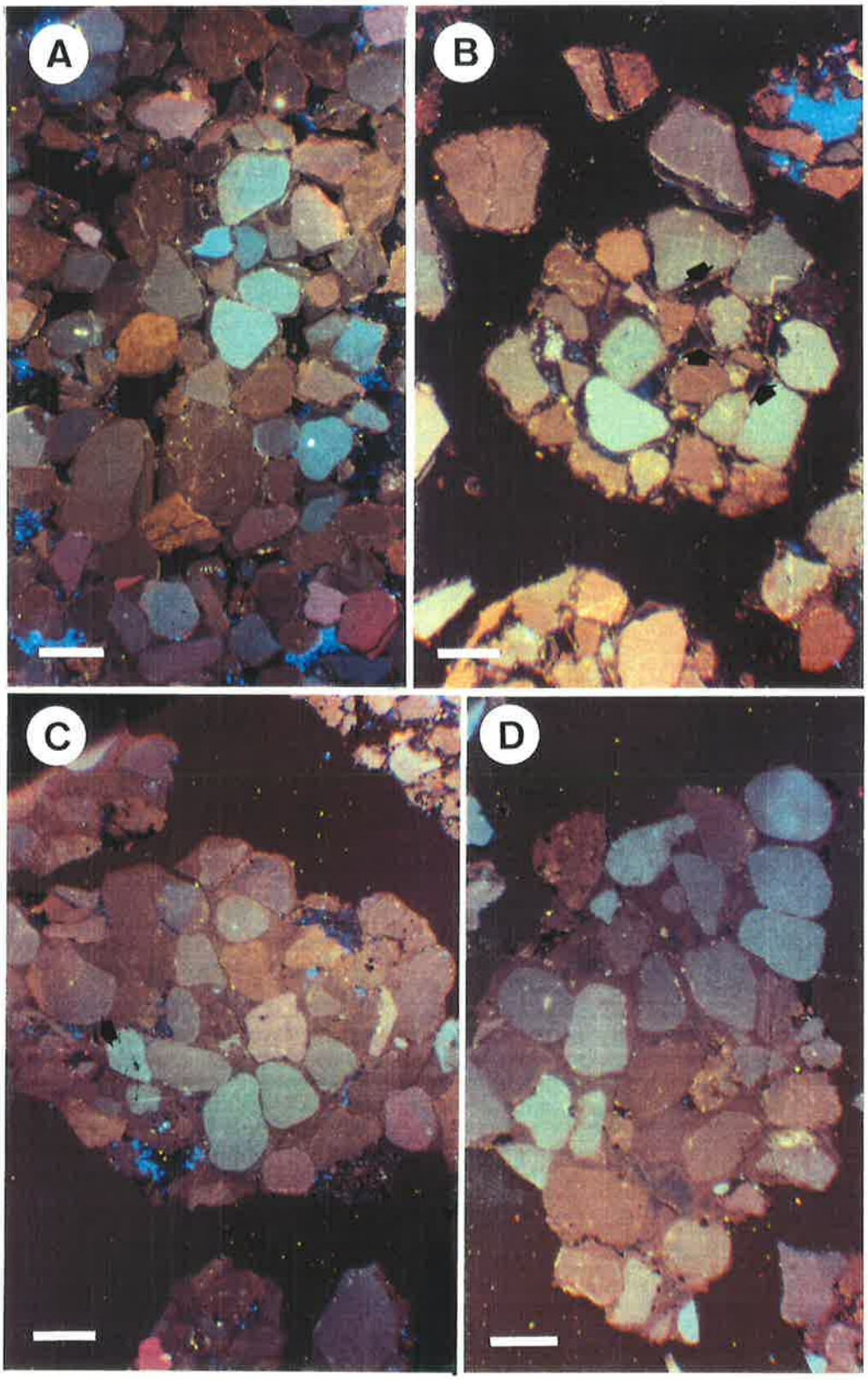
A
B
C
D

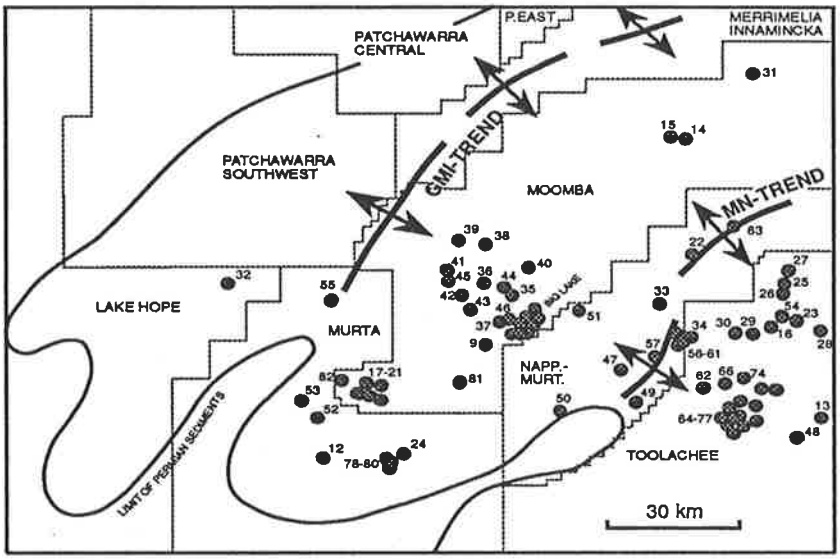

Figure 4.2a Distribution of siderite cements in the southern Cooper Basin (for well code see Table 1.1) (data source: this study, Sansome [1988], Alsop [1990], Eleftheriou [1990], Thomas [1990], Phillips [NCPGG, unpubl.].

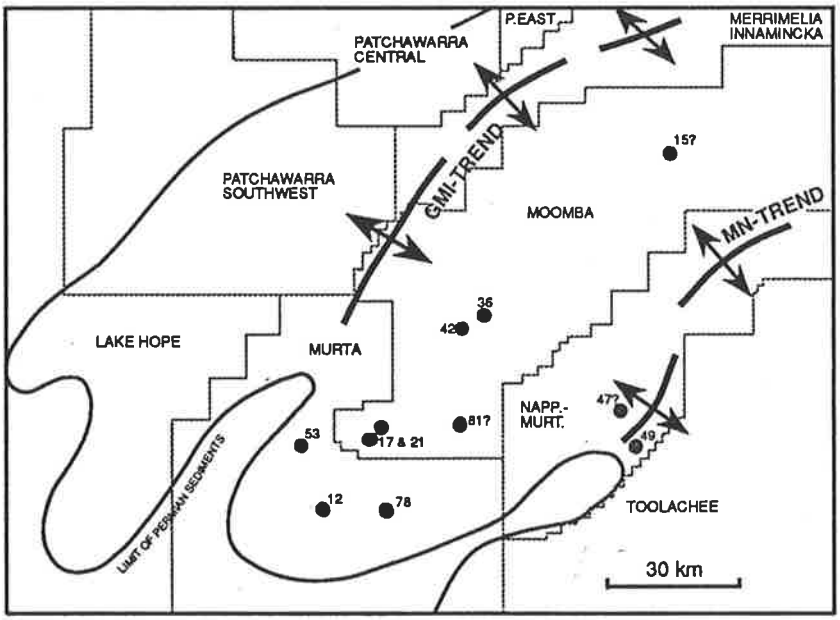

Figure 4.2b Distribution of ankerite cements in the southern Cooper Basin (for well code see Table 1.1) (data source: this study, Sansome [1988], Alsop [1990], Eleftheriou [1990], Thomas [1990], Phillips [NCPGG, unpubl.].

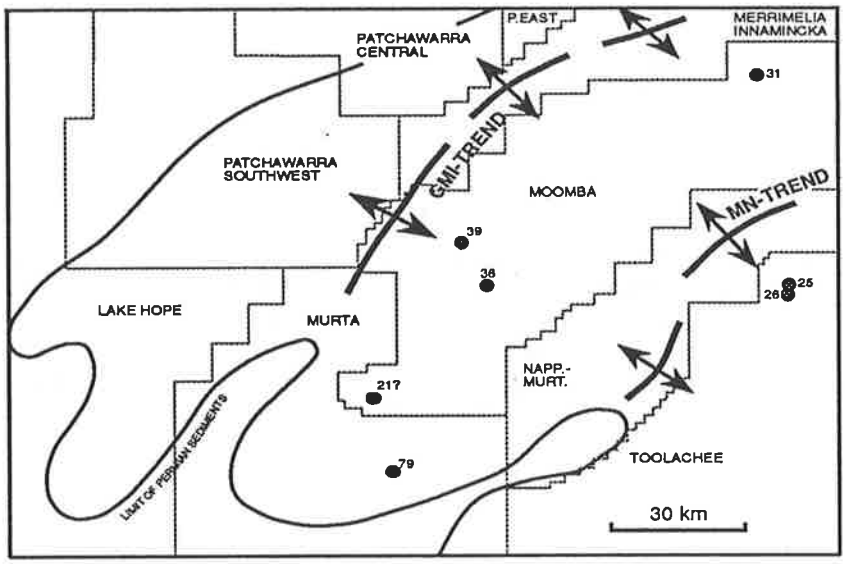

Figure 4.2c Distribution of dolomite and Fe-dolomite cements in the southern Cooper Basin (for well code see Table 1.1) (data source: this study, Sansome [1988], Alsop [1990], Eleftheriou [1990], Thomas [1990], Phillips [NCPGG, unpubl.].

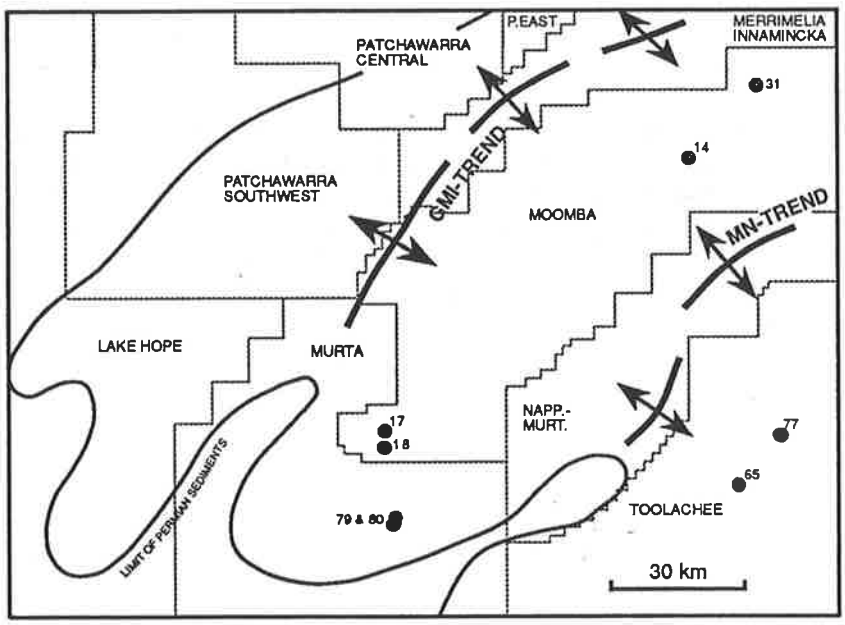

Figure 4.2d Distribution of calcite cements in the southern Cooper Basin (for well code see Table 1.1) (data source: this study, Sansome [1988], Alsop [1990], Eleftheriou [1990], Thomas [1990], Phillips [NCPGG, unpubl.].

Plate 7

Thin section micrographs of dead bitumen/oil staining

A. Dead bitumen/oil is evident trapped as dust linings in quartz overgrowths (O) and filling remnants of primary pores (P). Approximately 4 % of the total composition of this medium-grained sandstone is rock bitumen. The major phase of liquid hydrocarbon migration appears to postdate the formation of the quartz overgrowths in this area. Plane light. Scale bar 250 µm. Sample CB-0394, Moomba-3, Toolachee Formation (7912' 9") [micrograph courtesy of A. Thomas].

B. Evidence of liquid hydrocarbon migration is also apparent at the Strzelecki Gas Field. In this medium-grained sandstone, dead bitumen/oil is trapped as dust linings (O) and lining pores (P). Plane light. Scale bar 250 µm. Sample CB-0465, Strzelecki-1, Toolachee Formation (6360' 11") [micrograph courtesy of J. Eleftheriou].

C. The rounded globular nature of this pore-lining bitumen suggests that it is dead oil. Note that the major phase of migration appears to postdate the formation of the euhedral quartz overgrowths in this coarse-grained sandstone. Plane light. Scale bar 100 µm. Sample CB-0580, Moomba-9, Toolachee Formation (7788' 0") [micrograph courtesy of A. Thomas].

D. Patchy distribution of bitumen (black) in this coarse-grained sandstone is possibly due to migration of liquid hydrocarbons (?condensates) into pores that were already filled with kaolin (brown). Alternatively, the kaolin precipitated out of pore waters that contained hydrocarbons. Plane light. Scale bar 100 µm. Sample CB-0602, Moomba-52, Toolachee Formation (7844') [micrograph courtesy of A. Thomas].

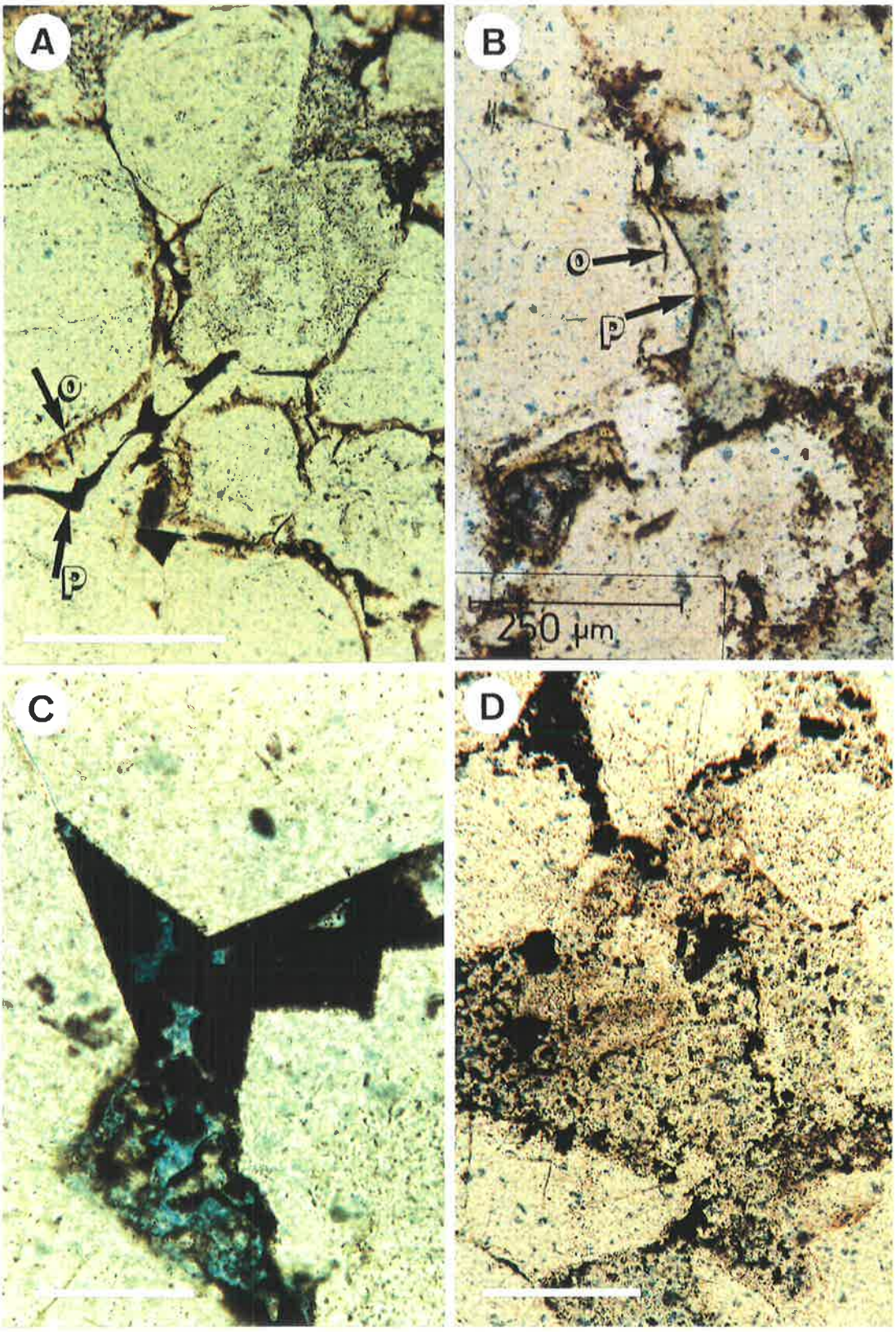
A
O
P
B
O
P
250 µm
C
D

Compositional variation is indicated by trace amounts of Mg, Mn, and Ca. The other carbonate types are characterised by an exclusively sparry crystal habit.

The micritic siderite is commonly found in shales, silts and fine-grained sandstones, often adjacent to clays and occasionally in the vicinity of coals and/or organic matter (Plate 9 E). Typically, the micritic siderite occurs as a finely dispersed cement in the ground matrix or as wavy bands following laminations (Plate 9 C), or as small isolated blotches (Plate 8 F). The blotches are near-spherical in shape and vary in diameter from 0.15 mm to 1.2 cm, which is commonly larger than the average grain size (Plate 8 F). Where micrite is present there is minimal evidence of quartz overgrowth development and frequently detrital quartz grains with embayed edges 'float' within micrite. Some intra-formational rip-up clasts are composed predominantly of micritic siderite. The clasts are typically subangular to rounded, and may be up to 30 mm in diameter when associated with scour lags. Where siderite occurs as distinct bands in some of the finer-grained bioturbated sands, penetrative U-shaped burrows do not contain siderite, but are filled with clean quartz sand [8].

Microspar cements can only be identified under extreme magnification under the optical microscope, or by backscatter electron imagery (see Chapter 6). They are intimately mixed with micrite, and display radial fabrics where emanating from micritic blotches and zones (Plates 21 A & B).

Sparry carbonates generally are found in fine to coarse sandstones with low clay contents. Locally, sparry carbonates form pervasive cements that engulf quartz grains with embayed edges (Plates 11 A & B, 23 A & B); 'ghost' remnants of dissolved grains are sometimes evident in the spar cement. Mostly however the sparry carbonates are of patchy distribution within the samples, occasionally filling large irregular-shaped areas (Plate 9 F). Rarely sparry carbonates can be seen to surround detrital mica (Plates 10 C & D). Under the SEM, sparry carbonates occur as single rhombs up to 0.25 mm in diameter (Plates 8 C, D & E), or in clusters of crystals (Plates 9 A & B) which may show minor evidence of dissolution (Plate 9 G). Spar is occasionally seen to surround the margins of micritic blotches, indicating spar postdates the formation of micrite (Plate 8 A).

In some samples, siderite cements are intimately associated with dead oil (Plates 11 A, B, C & D) that is characterised by yellow fluorescence under the UV microscope. The oil is found around the margins of pores filled with carbonate spar (Plate 11 D), or finely dispersed within the carbonate matrix (Plates 11 A, B & C). The oil also occurs in irregular-shaped voids within the siderite cement (Plates 11 A & B).

---

[8] The delicate structure of bioturbated siderite bands prohibits photographic reproduction.

Plate 8

Micrographs of carbonate cements (1)

A. Thin section micrograph (crossed nichols) of a fine-grained, siderite-cemented sandstone. Sparry siderite surrounds a micritic blotch. Cement stratigraphy indicates that spar cements postdate the formation of micrite. Note the embayed edges of quartz grains associated with the spar. Scale bar 250 μm. Sample CB-0085, Della-3, Toolachee Formation (6653' 3").

B. Siderite microspar (brown) filling primary pore space (arrow) between quartz grains (q) in a very fine grained sandstone. XRD results suggest the rock contains both calcite and siderite. Note the embayed edges of quartz grains associated with the microspar. Plane light. Scale bar 100 μm. Sample CB-0700, Wancoocha-4, Patchawarra Formation (5760-5770').

C. SEM view of euhedral siderite (S) filling primary pore space between quartz overgrowths (Q). Note presence of kaolin booklets (arrow) around the margins of the pore. Scale bar 0.1 mm. Sample CB-0574, Brumby-1, Patchawarra Formation (7404' 3") [micrograph courtesy of D. Alsop].

D. Euhedral authigenic siderite crystal growing in primary pore space. Scale bar 10 μm. Sample CB-0167, Toolachee-3, Patchawarra Formation (7428' 0") [micrograph courtesy of D. Alsop].

E. Authigenic euhedral ankerite crystal intergrown with quartz cement (Q). Scale bar 10 μm. Sample CB-0176, Wancoocha-1, Epsilon Formation (5818' 5").

F. Micrite and ?microspar siderite blotches (brown and golden-brown) in a poorly sorted sandstone. Note the oversized nature of some of the blotches (arrow) suggesting grain replacement and/or displacive carbonate precipitation. The sample is derived from overbank/floodplain deposits. Plane light. Scale bar 1mm. Sample CB-0014, Kirby-1, Toolachee Formation (9859' 0").

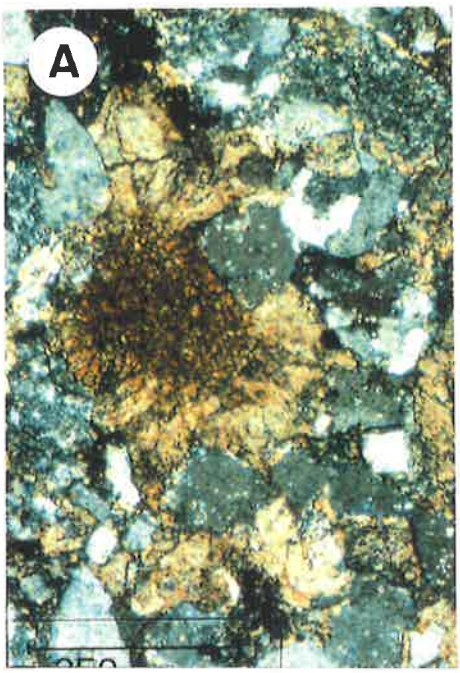
A


C
Q
S
q
01mm200kV 326E2 0004/58 BRUM 1

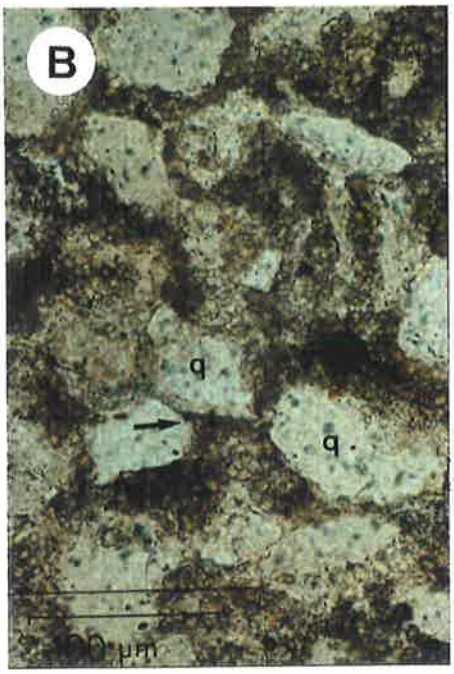
B
q
q


D

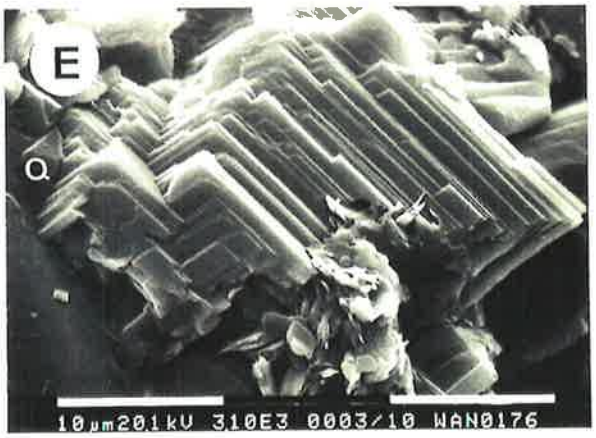
E
Q
10µm20kV 310E3 0003/10 WAN0176

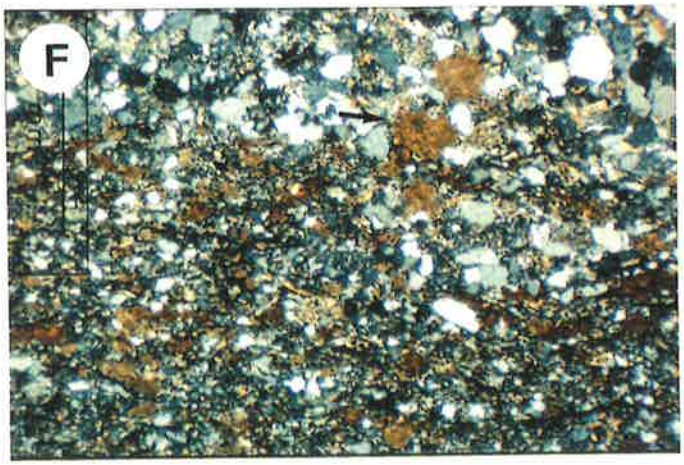
F

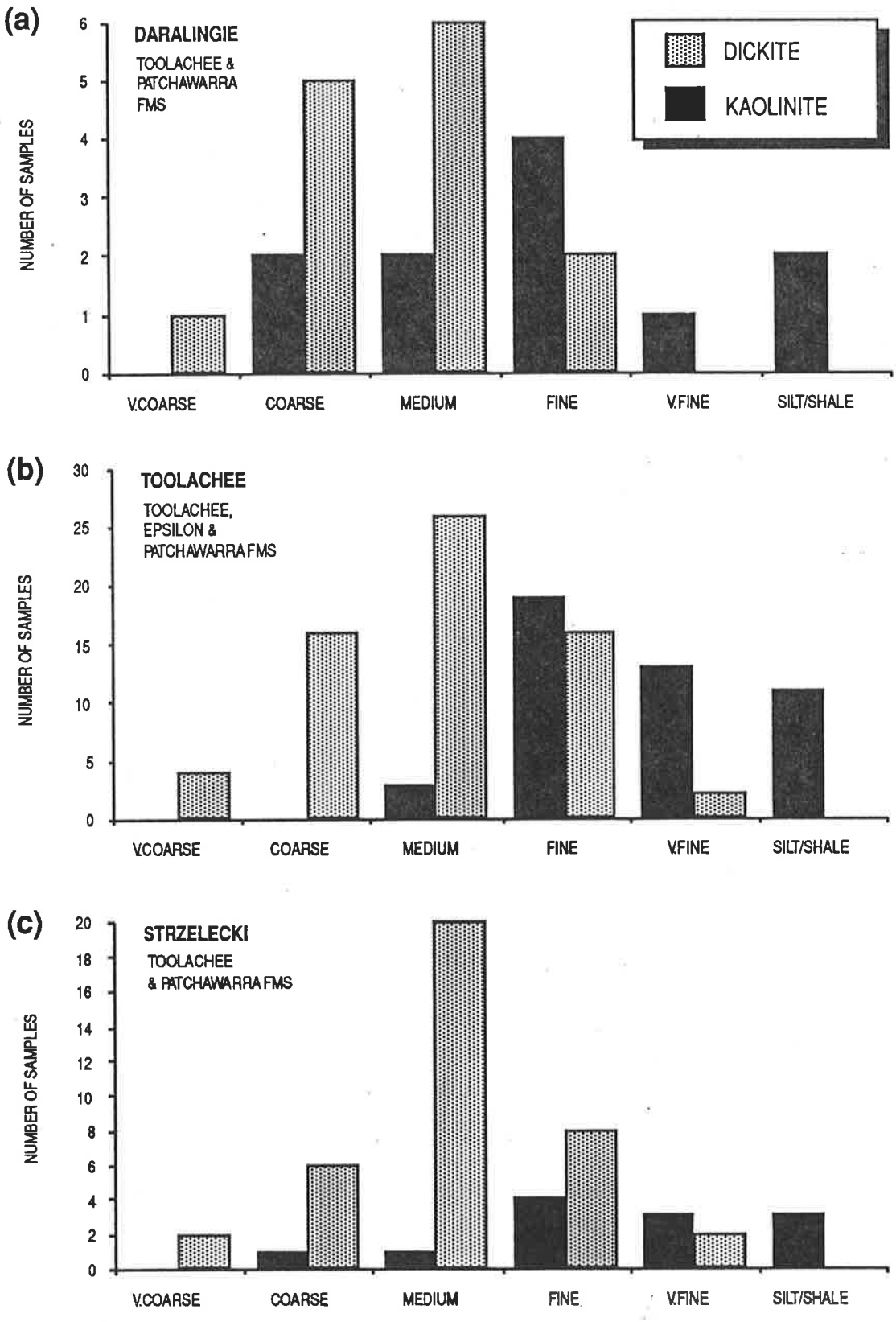

Figure 4.3 a-f Relative proportions of dickite and kaolinite for different grain sizes in the Daralingie (a), Toolachee (b) and Strzelecki (c) Fields, southern Cooper Basin. Dickite concentrates in the coarser sediments whereas the reverse is true for kaolinite [data source: this study, Schulz-Rojahn & Phillips (1989), Alsop (1991), Eleftheriou (1991)].

- continue overleaf -

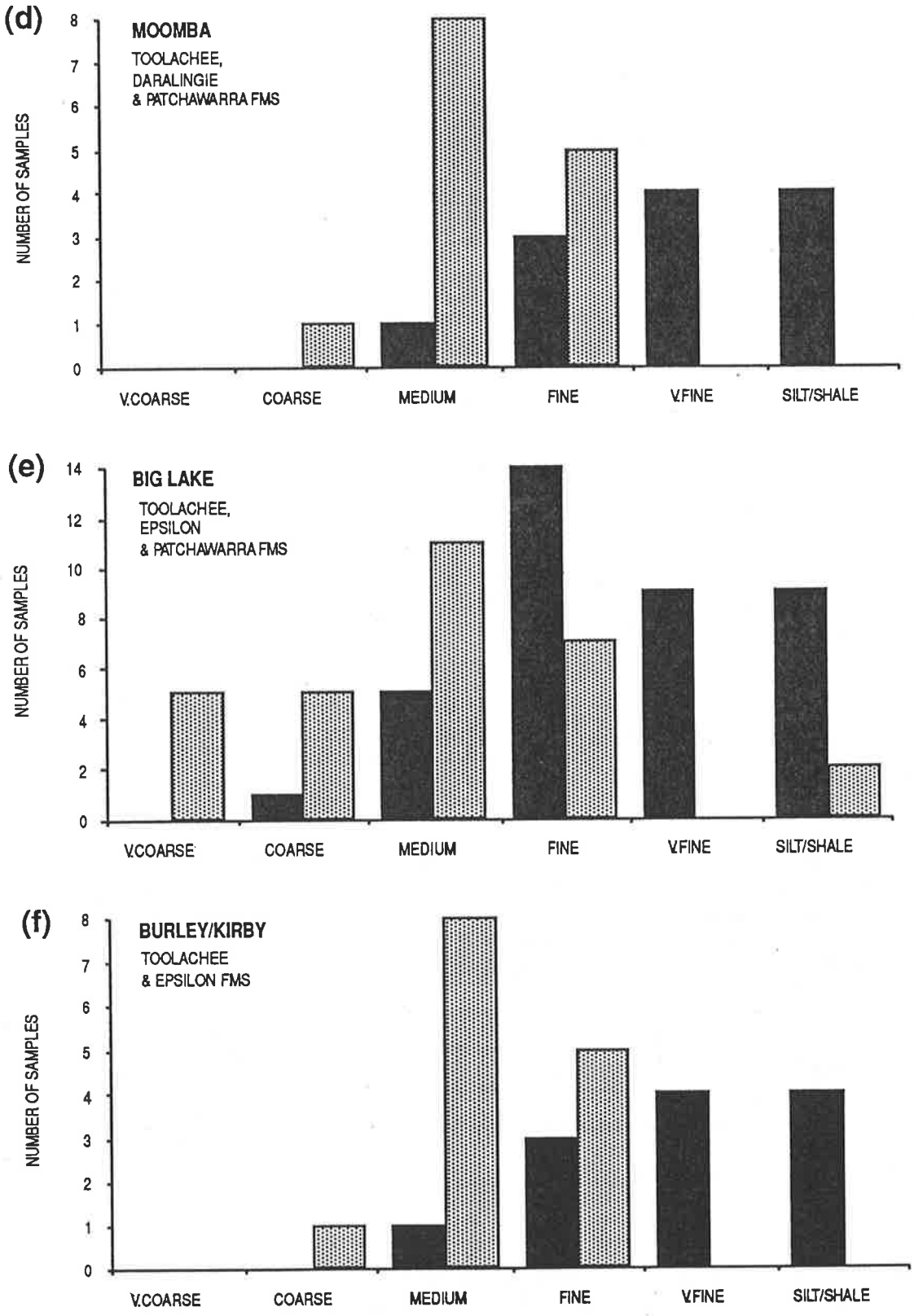

Figure 4.3 d-f (cont.) Relative proportions of dickite and kaolinite for different grain sizes in the Moomba (d), Big Lake (e) and Burley/Kirby (f) areas, southern Cooper Basin. For legend see previous page. Based on diagenetic investigation of core samples [data source: this study, Schulz-Rojahn & Phillips (1989), Thomas (1991)].

Plate 9

Micrographs of carbonate cements (2)

A. Sparry siderite rhombs (light-golden) between quartz grains (Q) in a fine grained sandstone. Note dust rims (arrow) associated with some of the quartz overgrowths. Crossed nichols. Scale bar 250 μm. Sample CB-0745, Dullingari-18, Patchawarra Formation (7847' 2").

B. Close-up view of (A) above (insert).

C. Micritic siderite (brown) occurring as wavy bands following laminations in a fine grained sandstone. Organic stringers are black. Crossed nichols. Scale bar 1mm. Sample CB-0018, Kirby-1, Epsilon Formation (9730' 10").

D. Thin section micrograph of radial siderite blotches (brown). Crossed nichols. Scale bar 1mm. Sample CB-0252, Moomba-6, Toolachee Formation (8152' 0").

E. Nodular siderite blotches (S) associated with thin coal stringers (black) in a siltstone. This is a common observation suggesting there may be a link between organic maturation reactions and carbonate precipitation. Unfortunately, isotopic evidence is ambiguous in this regard (Chapter 6). Plane light. Scale bar 1mm. Sample CB-0074, Big Lake-29, Patchawarra Formation (9325' 0").

F. CL micrograph showing patchy distribution of bright luminescent calcite cements (arrows) in a fine grained sandstone. In contrast, siderite cements are non-luminescent. This is because iron acts as a quencher of cathodoluminescence in carbonate minerals (Barker & Dalziel, 1991). Scale bar 0.5 mm. Sample CB-0278, Mudlalee-1, Toolachee Formation (5887' 10").

G. Siderite rhombohedra intergrown with, or ?replacing another mineral. Note the pitted nature of the surface indicating partial dissolution. Such evidence for dissolution is rare. Scale bar 10 μm. Sample CB-0105, Pando-2, Epsilon Formation (5819' 11").

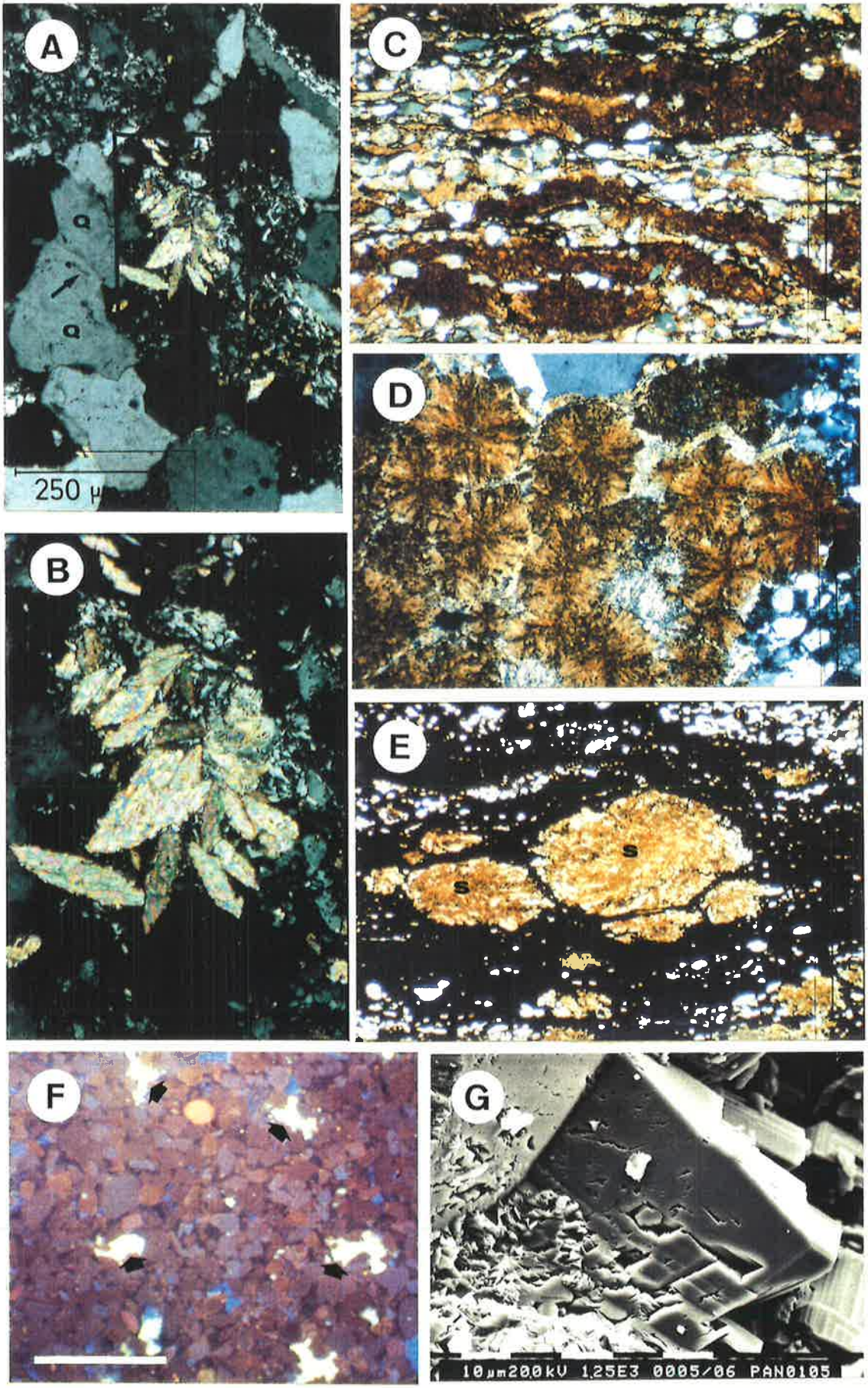
A
Q
Q
250 μ
C
D
B
E
S
S
F
G
10μm200kV 1.25E3 0005/06 PAN0105

4.2.3.3 Clays

Based on bulk and clay fraction XRD analyses, there are five clay species present in the Cooper Basin sediments: kaolinite, dickite, illite, clinochlore IIB, and pyrophyllite.

Dickite and kaolinite form part of the kaolin sub-group of clay minerals, and are the most abundant clay minerals present. Based on XRD results, kaolin is found in at least 98 percent of core and ditch samples. In thin section, kaolin concentrates in what appears to be oversized (secondary) pores (Plates 20 B & E); silicification is minimal where there is abundant kaolin (Plates 12 E & G, 14 E). Occasionally, there are 'ghost' remnants of dissolved minerals found in association with kaolin clay patches (Plate 14 F). Under CL, red-luminescent detrital feldspar grains of corroded appearance are sometimes seen surrounded by kaolin (Plate 14 E). Rarely is there dead bitumen within the kaolin matrix; the bitumen occurs both as isolated patches and finely dispersed throughout the matrix (Plate 7 D). Based on point-count data, kaolin constitutes up to about 18 percent of total rock composition in some samples (Appendix L). Dickite can represent up to at least 70 percent and kaolinite 62 percent of the total clay fraction (S. Phillips, NCPGG, unpublished data) (Table 4.1; Appendix G).

The occurrence of kaolinite and dickite is related to grain size (Fig.4.3a-f). Kaolinite is most abundant in shales, siltstones and fine-grained sandstones whereas dickite concentrates in coarser sediments (Schulz-Rojahn & Phillips, 1989). This trend is broadly consistent for all petroleum fields and formations in the southern Cooper Basin (Alsop, 1990; Eleftheriou, 1990; Thomas, 1990; Stuart et al., 1990) (Fig.4.3a-f). However, XRD analyses of ditch cuttings show a distinct lack of dickite (Fig.4.4). The implication is that dickite is being preferentially washed out from the ditch samples in the stream of drilling mud that brings the ditch cuttings to the surface.

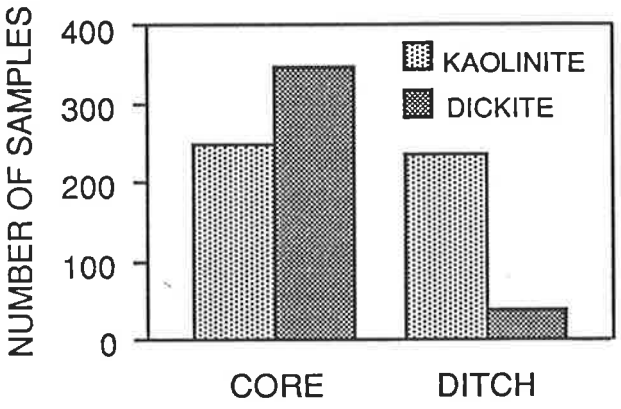

Figure 4.4 Relative abundance of kaolinite and dickite in core and ditch samples. Dickite is preferentially washed out from the ditch cuttings.

Under the SEM, the kaolinite and dickite are evident as subhedral to euhedral booklets which infill pores and may completely block pore throats (Plate 12 A). Typically, the contact

Plate 10

Micrographs of carbonate cements (3)

A. Mica in this coarse-grained sublitharenite is being altered in several different ways. The mica flake which has been replaced by illite is deformed due to compaction (I) and the apparently unaltered mica contains micritic siderite (arrow). Crossed nichols. Scale bar 250 μm. Sample CB-0315, Toolachee-3, Patchawarra Formation (7211' 0").

B. Same sample as (A) above. The micrograph shows siderite (light patches) replacing mica (elongate dark grey), surrounding area is quartz. Back-scattered electron micrograph. Scale bar 10 μm [micrograph courtesy of S.Phillips].

C. In thin section, mica flakes (M) can sometimes be seen to be surrounded by carbonate spar (S). XRD results suggest the carbonate in this sample is siderite. The mica is weakly pleochroic displaying faint brown colours upon stage rotation, indicating it is biotite. It is possible the supply of Fe for the sparry siderite became available during the alteration of biotite. Plane light. Scale bar 250 μm. Sample CB-0012, Kirby-1, Toolachee Formation (8949' 0").

D. Same field of view as in (C) above. Crossed nichols. Scale bar 250 μm.

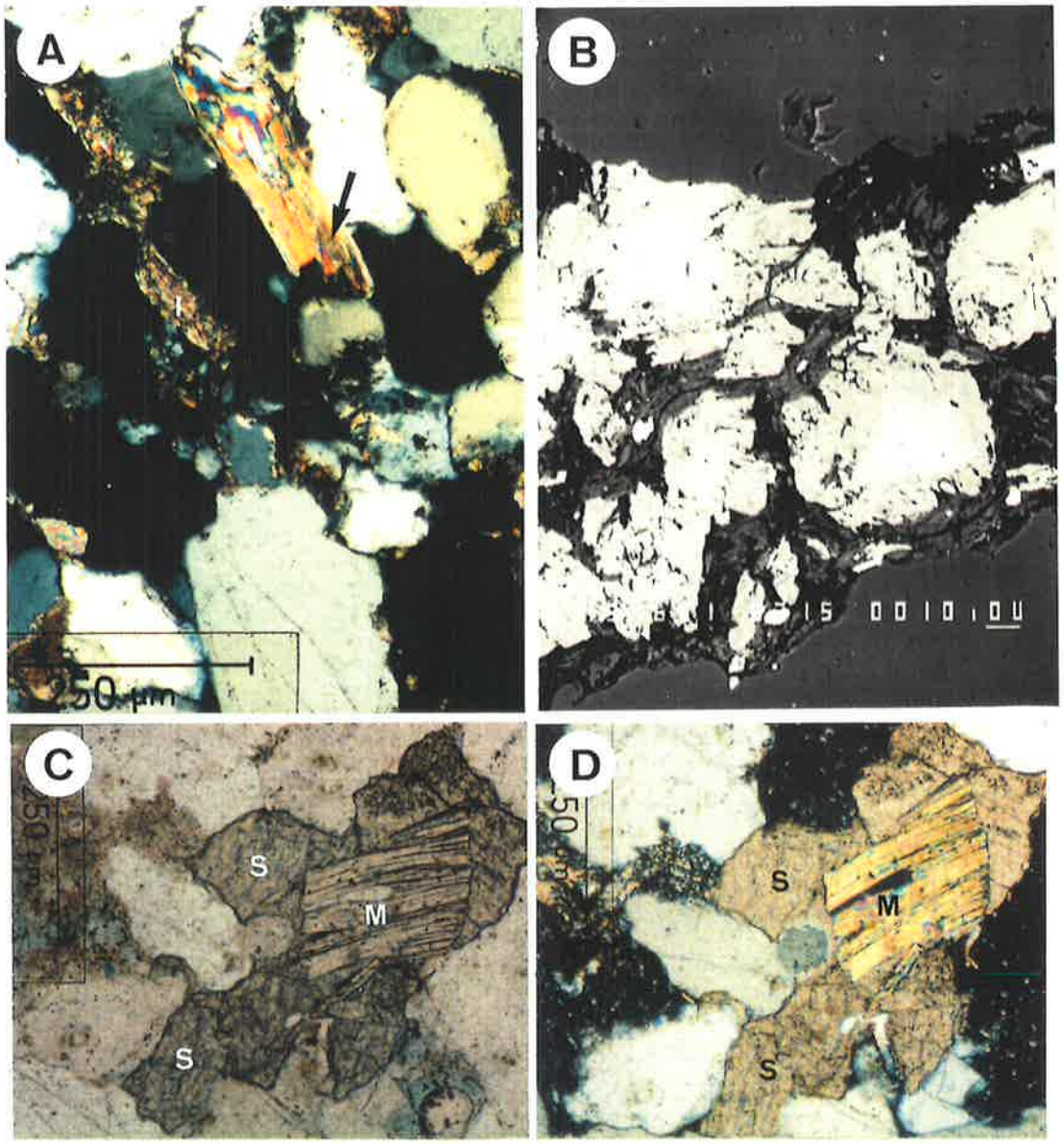
A
250 µm
B
C
S
M
S
D
S
M
S

Table 4.1
Quantitative calculations of the relative proportions (%) of clay minerals in clastic samples derived from the southern Cooper Basin. These calculations are based on XRD and XRF analyses of the < 5 and < 10 micron size fractions [data courtesy of S. Phillips, NCPGG, in: Stuart et al., 1990].

Sample	Well	Formation	Depth (ft.KB)	Q	Sid	M/I	Kao	Pyr	Chl
CB-0002	Big Lake-3	Epsilon	8248' 6"	21	3	49 I	19 K	0	0
CB-0006	Big Lake-3	Epsilon	8270' 6"	40	3	57 B	14 D	0	0
CB-0007	Big Lake-3	Epsilon	8274' 10"	19	2	44 B	28 K	0	0
CB-0012	Kirby-1	Toolachee	8949' 0"	31	7	33 M	26 D	0	0
CB-0019	Big Lake-31	Patchawarra	9492' 0"	19	2	54 I	29 K	0	0
CB-0036	Burley-1	Toolachee	8794' 7"	35	0	53 M	11 D	0	14
CB-0058	Burley-2	Patchawarra	11383' 6"	16	0	27 I	0	51	11
CB-0060	Kirby-1	Epsilon	9717' 0"	31	3	45 M	30 K	0	0
CB-0061	Big Lake-3	Epsilon	8232' 9"	16	21	43 B	23 K	0	0
CB-0067	Big Lake-5	Tirrawarra	9411' 2"	11	0	16 I	69 D	0	5
CB-0077	Big Lake-29	Tirrawarra	9666' 0"	9	0	67 I	22 D	0	3
CB-0079	Big Lake-34	Patchawarra	9339' 2"	69	0	34 B	8 K	0	15
CB-0116	Big Lake-1	Toolachee	7669 ' 0"	38	1	31 M	39 D	0	0
CB-0117	Big Lake-1	Toolachee	7687' 6"	41	1	26 M	37 D	0	0
CB-0126	Big Lake-1	Toolachee	7744' 6"	19	2	43 B	35 K	0	0
CB-0131	Big Lake-1	Toolachee	7771' 6"	22	2	45 B	35 K	0	0
CB-0134	Big Lake-1	Toolachee	7798' 0"	38	2	47 B	28 D	0	0
CB-0136	Big Lake-1	Epsilon	8605' 7"	20	3	55 B	25 K	0	0
CB-0149	Big Lake-2	Toolachee	7489' 6"	27	2	34 I	41 K	0	0
CB-0159	Big Lake-2	Toolachee	7659' 1"	25	16	43 B	22 K	0	0
CB-0162	Toolachee-3	Patchawarra	7345' 3"	21	1	10 M	68 D	0	0
CB-0168	Toolachee-3	Patchawarra	7437' 9"	15	2	19 B	62 K	0	0
CB-0180	Wancoocha-1	Patchawarra	6200' 11"	20	2	52 B	29 B	0	0
CB-0202	Moomba-6	Toolachee	8267' 4"	44	20	37 M	25 B	0	0
CB-0205	Moomba-6	Daralingie	8339' 4"	20	2	57 B	16 B	0	0
CB-0209	Moomba-6	Daralingie	8357' 1"	29	2	57 B	16 K	0	0
CB-0218	Daralingie-1	Toolachee	6405' 9"	12	2	38 B	42 K	0	0
CB-0226	Daralingie-1	Toolachee	6464' 8"	22	5	46 M	30 K	0	0
CB-0233	Daralingie-22	Patchawarra	7464' 10"	33	2	21 B	50 D	0	0
CB-0236	Kerna-1	Epsilon	7683' 11"	31	2	54 M	21 B	0	0
CB-0298	Strzelecki-10	Toolachee	6336' 10"	20	2	30 M	53 B	0	0
CB-0302	Marana-1	Toolachee	6324' 0"	23	2	36 M	37 D	0	0
CB-0309	Kidman-1	Toolachee	6608' 6"	30	0	33 M	38 D	0	4

Abbreviations:
Q = Quartz Sid = Siderite M/I = Mica/illite Kao = Kaolin Pyr = Pyrophyllite
Chl = Chlorite M = Mica I = Illite B = Both K = Kaolinite D = Dickite

Plate 11

Dead oil associated with siderite cements

A. Occasionally, siderite cements in Permian sandstones are intimately associated with dead oil. In this example from Wancoocha, dead oil characterised by yellow fluorescence under the UV coal microscope is finely dispersed within the carbonate matrix (golden-brown). Quartz grains (Q) are white. Either the liquid hydrocarbons migrated into a submicroscopic network of pores between the carbonate crystals, or the siderite precipitated synchronous with oil migration from pore waters carrying hydrocarbons (section 4.3.5). Isotopic evidence does not favour a hydrocarbon-derived origin of the carbonate cements (Chapter 6). Plane light. Scale bar 250 μm. Sample CB-0699, Wancoocha-4, Patchawarra Formation (5690-5700').

B. Same field of view as (A) above. Crossed nichols. Scale bar 250 μm.

C. Close-up view of fine siderite microspar (brown) showing intimate association with dead oil (black). It is unclear whether the carbonate cement crystallised around the oil, or whether the oil migrated into submicroscopic pores (blue) within the carbonate matrix. Again, the presence of oil was confirmed in consultation with Ms. D. Padley (Univ. of Adelaide) by examination of the sample in UV mode under the coal microscope; the oil was characterised by moderate to intense yellow fluorescence. Scale bar 100 μm. Sample CB-0228, Daralingie-19, Patchawarra Formation (7428' 4").

D. In this example, dead oil (black) is found around the margins of a pore filled with siderite cement (brown), indicating the carbonate formed after oil migration into the pore network. Surrounding areas are quartz (Q). The oil has yellow fluorescence under the coal microscope. Plane light. Scale bar 100 μm. Sample CB-0745, Dullingari-18, Patchawarra Formation (7847' 2").

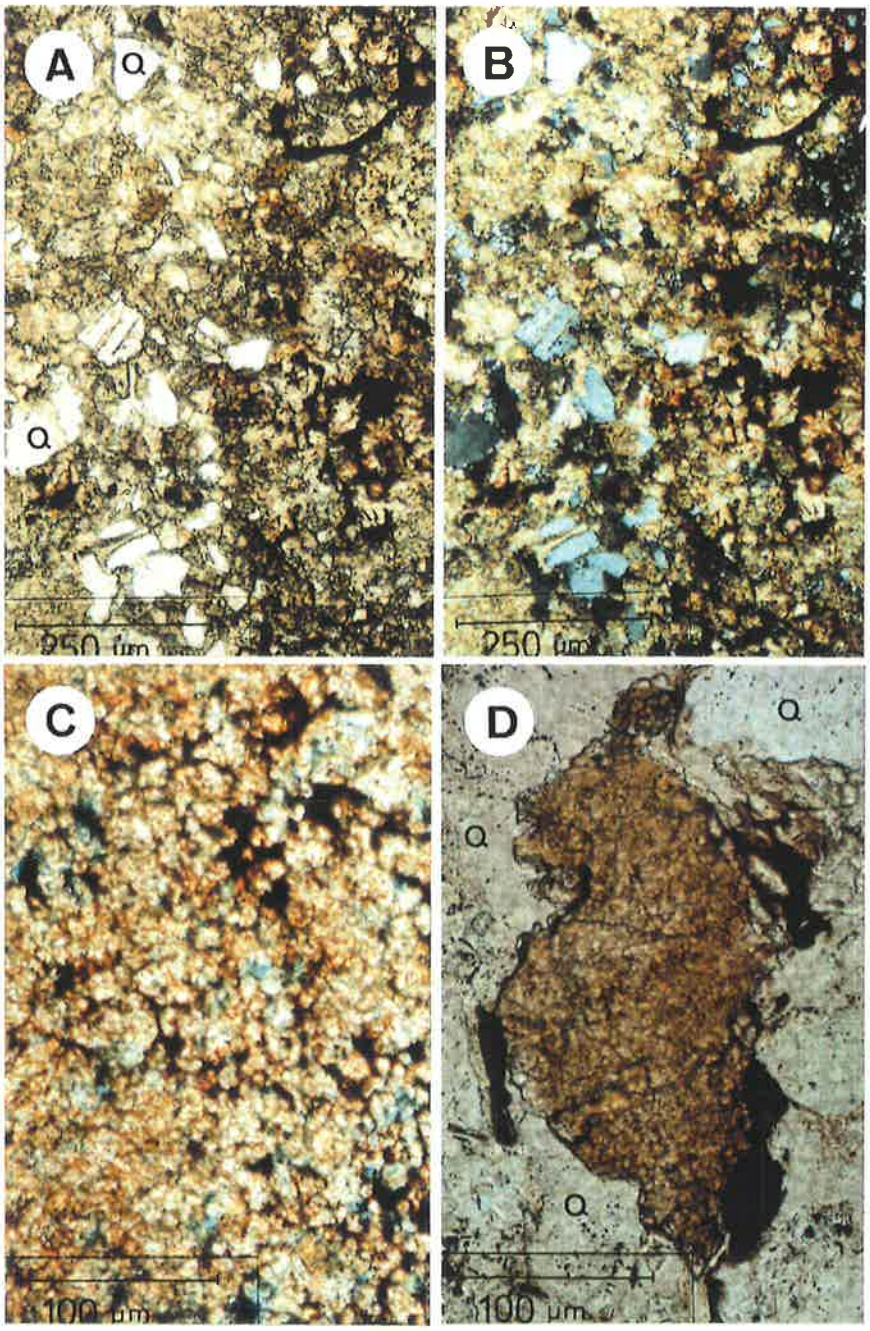
A
Q
Q
250 µm
B
250 µm
C
100 µm
D
Q
Q
Q
100 µm

between quartz overgrowths and kaolin is very jagged as kaolin is frequently intergrown with the outer margin of quartz overgrowths (Plates 12 C & D, 13 A & D); rarely is kaolin engulfed completely by overgrowths (Plate 13 D). At least three different sizes of kaolin are evident under the SEM, namely 1-2 μm, 10-15 μm and 30-50 μm. The middle size range is by far the most abundant and consists of subhedral or blocky booklets characterised by random orientation (Plates 13 B & C). The larger crystals, concentrating in the centre of pores, are frequently vermiform in habit and consist of stacked pseudohexagonal plates with ragged edges (Plate 13 E). These euhedral crystals are most common in samples containing abundant dickite. The smallest variety of kaolin crystals is relatively rare and typically consists of subhedral to anhedral pseudohexagonal plates and very short booklets (Plate 13 D). Rarely can blocky kaolin be seen growing between mica flakes (Plates 13 F & 14 A). Honeycombed remnants of feldspars are generally filled with anhedral booklets of kaolin (Plates 14 B, C & D). Kaolinisation of feldspars is extensive in the Tirrawarra Conglomerate at Big Lake (Plates 16 C & D) and many other areas in the southern Cooper Basin.

Illite concentrates in the matrix of finer grained rocks throughout the southern Cooper Basin, in particular shales and siltstones associated with overbank and floodplain deposits (Fig.4.5). In these sediments, illite generally occurs as closely packed, small anhedral platelets suggestive of a detrital origin (Plate 15 A).

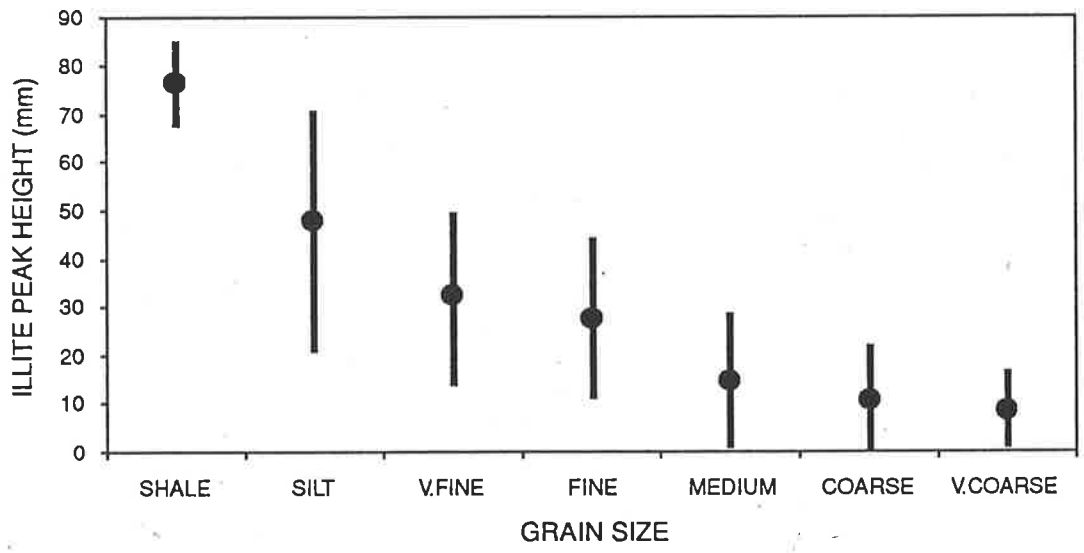

Figure 4.5 Variation in illite content as indicated by XRD against grain size. Finer grained sediments contain a higher proportion of illite than coarse clastics. This is supported by petrographic and SEM work. Calculated mean (circle) and standard deviation (bar) for different grain sizes based on 312 core samples (data source: this study, Alsop [1990], Eleftheriou [1990], Thomas [1990], Phillips [NCPGG, unpubl. data]).

Plate 12

Micrographs of kaolin clay (1)

A. Precipitation of kaolin (K) in pore spaces and adjacent pore throats reduces porosity and permeability. Intergrowth of kaolin and quartz overgrowths is evident from jagged contact. Scale bar 0.1mm. Sample CB-0029, Big Lake-27, Patchawarra Formation (9156' 9").

B. Close-up view of small kaolin booklets (< 5 μm) intergrown with quartz cement. Scale bar 10 μm. Sample CB-0180, Wancoocha-1, Patchawarra Formation (6200' 11").

C. The jagged nature of the contact between quartz cement and kaolin clay shown in (A) is a common phenomenon throughout the study area. In this example, the delicate intergrowth between the quartz cement and the kaolin is further highlighted under extreme magnification under the SEM. Scale bar 10 μm. Sample CB-0236, Kerna-1, Epsilon Formation (7683' 11").

D. In thin section, the intergrowth of kaolin (grey-black) with quartz cement (Q) can only be seen under extreme magnification. Plane light. Scale bar 250 μm. Sample CB-0015, Kirby-1, Epsilon Formation (9703' 0").

E. The abundance of kaolin in some sandstones is highlighted when viewed under CL. Large oversized pores in this fine- to medium-grained sandstone of point bar origin are filled with dickite (blue), as determined from XRD traces. Note that a certain degree of interconnection is established between the kaolin clay patches although tortuosity between individual micropores is likely to be high. Isolated occurrences of macroporosity exist. Measured core porosity is 13.5 % and permeability 4.6 md. There is a widespread lack of quartz cement in this kaolin-rich rock. Scale bar 0.3 mm. Sample CB-0328, Toolachee-3, Patchawarra Formation (7340' 0") [micrograph courtesy of D. Alsop].

F. Rarely can microporosity (blue) between the kaolin booklets (light-grey) be seen in thin section. Area on right represents a detrital quartz grain (Q). Scale bar 100 μm. Sample CB-0750, Dullingari-18, Patchawarra Formation (7896' 7").

G. In samples in which there is abundant kaolin (blue), quartz cement (arrows) is generally absent or only thinly developed around quartz grains, as exemplified by this medium-grained sandstone from the central Nappamerri Trough (cf. Plate 12 A & C). Scale bar 0.4 mm. Sample CB-0043, Burley-1, Toolachee Formation (8875' 10").

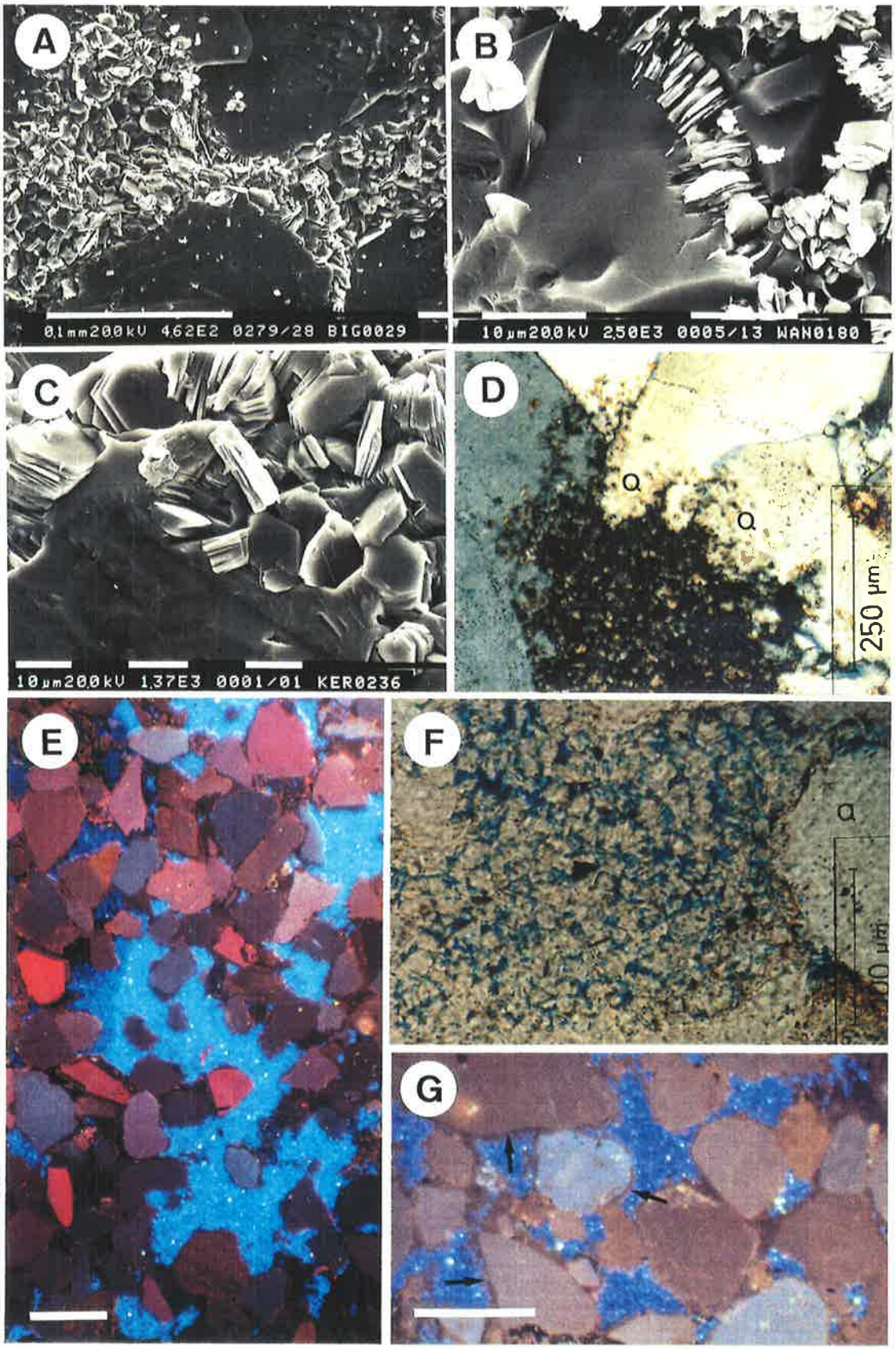
A
0.1mm20.0kV 462E2 0279/28 BIG0029
B
10µm20.0kV 2.50E3 0005/13 WAN0180
C
10µm20.0kV 1.37E3 0001/01 KER0236
D
Q
Q
250 µm
E
F
a
G

XRD analyses indicate illite is a dioctahedral 2M1 variety with a relatively broad base to the 10 Å peak, indicative of either a poorly crystalline nature or possible interstratification with other minerals [9]. Rarely under the SEM can illite be seen with a fibrous, lath- or lettuce-like habit indicative of an authigenic origin (Plates 15 B, C, D, E & F) [10]. In the clay fractions analysed by XRD, illite and muscovite are differentiated on the basis of peak sharpness, and mica is found to be more common in shallower samples (Table 4.1). Authigenic illite typically concentrates in deeper buried sediments where it forms as a replacement product of unstable rock fragments and/or feldspars (Plate 15 B), and as the residue of degraded micas (Plate 15 E); it rarely lines pores (Plate 15 F). Distinctive large hydromuscovite flakes [11] occur in the Tirrawarra Conglomerate at Big Lake, indicating a granitic or metamorphic source provenance in close proximity (Plates 16 C & D).

Trace to minor amounts of clinochlore (Fe-rich chlorite) are present in some areas of the southern Cooper Basin. Clinochlore concentrates towards the deeper part of the Nappamerri Trough at Burley and Kirby, and also in the Patchawarra, Tirrawarra and Merrimelia Formations at Big Lake (Appendix E) where it forms up to 15 percent of the clay fraction (Table 4.1). Electron microprobe analyses of clinochlore (Table 4.2) give a composition similar to brunsvigite (Deer et al., 1975) but XRD indicates it is an Fe-rich clinochlore IIB. It would appear that there has been considerable substitution of Fe^{2+} for Mg (S.Phillips, NCPGG, pers. comm.). The authigenic origin of clinochlore is clearly evident under the SEM. Clinochlore occurs as euhedral rosettes and pseudohexagonal plates which line and infill pores (Plates 17 A & B), and it is present replacing ferromagnesian minerals (Plate 17 C). Samples with high proportions of clinochlore IIB typically have a low siderite content and contain little kaolin (Table 4.1).

Pyrophyllite is also restricted in geographic distribution to the central Nappamerri Trough where it is observed in isolated sandy intervals of the Epsilon and Patchawarra Formations at Burley-2 (Table 4.3). The abundance of pyrophyllite is greatest in deeper samples of the Patchawarra Formation where it forms up to 6 percent of the total rock composition. Kaolin is absent where pyrophyllite is commonest (Schulz-Rojahn & Phillips, 1989) (Plate 17 C). Typically, pyrophyllite occurs as euhedral radiating plates that fill secondary pores and replace quartz (Plates 17 C, D, E & F). Rarely it is observed filling pores that have been lined by clinochlore (Plate 17 D), suggesting pyrophyllite is of authigenic origin and postdates clinochlore. Electron microprobe results of pyrophyllite indicate some substitution of Al by Mg,

---

[9] Authigenic illite is usually the 1M polytype and should produce a sharp 10 Å peak (Srodon & Eberl, 1984).

[10] Where present, this illite morphology can coexist with the platy illite variety.

[11] Identification based on electron microprobe analyses by Dr. S. E. Phillips (NCPGG, unpubl. data).

Plate 13

Micrographs of kaolin clay (2)

A. Kaolin and quartz overgrowths are commonly intergrown as in this example, due to their contemporaneous precipitation. The surface of the quartz overgrowth is covered in chemically etched V-shaped pits. Scale bar 10 μm. Sample CB-0016, Kirby-1, Epsilon Formation (9714' 3").

B. Ragged-edged vermiform kaolin, 10 to 15 μm in diameter. Micropores occur between the kaolin booklets. Scale bar 10 μm. Sample CB-0036, Burley-1, Toolachee Formation (8794' 7").

C. The euhedral nature of the kaolin booklets is suggestive of an authigenic origin. The kaolin in this sample is considered to have precipitated under ideal conditions from aqueous solution. Notice the well-developed micropores between the kaolin booklets. Scale bar 10 μm. Sample CB-0180, Wancoocha-1, Patchawarra Formation (6200' 11").

D. Two different sizes of kaolin are evident (A and B). Small crystals of kaolin are trapped within the quartz overgrowth (arrow) and concentrate on the outer wall of the pore. Moderate-size pseudohexagonal kaolin plates are also intergrown with quartz overgrowths (P). Scale bar 0.1mm. Sample CB-0117, Big Lake-1, Toolachee Formation (7687' 6").

E. Large vermiform dickite (> 30 μm) identified from XRD traces concentrates in the centre of oversized pores. Note that medium-sized kaolin crystals (about 10 μm) occur adjacent to the larger variety. Kaolinite crystals tend to be smaller than dickite booklets. Scale bar 10 μm. Sample CB-0117, Big Lake-1, Toolachee Formation (7687' 6") [micrograph courtesy of S. Phillips].

F. Blocky kaolinite (arrow) growing between biotite flakes. Scale bar 10 μm. Sample CB-0117, Big Lake-1, Toolachee Formation (7687' 6").

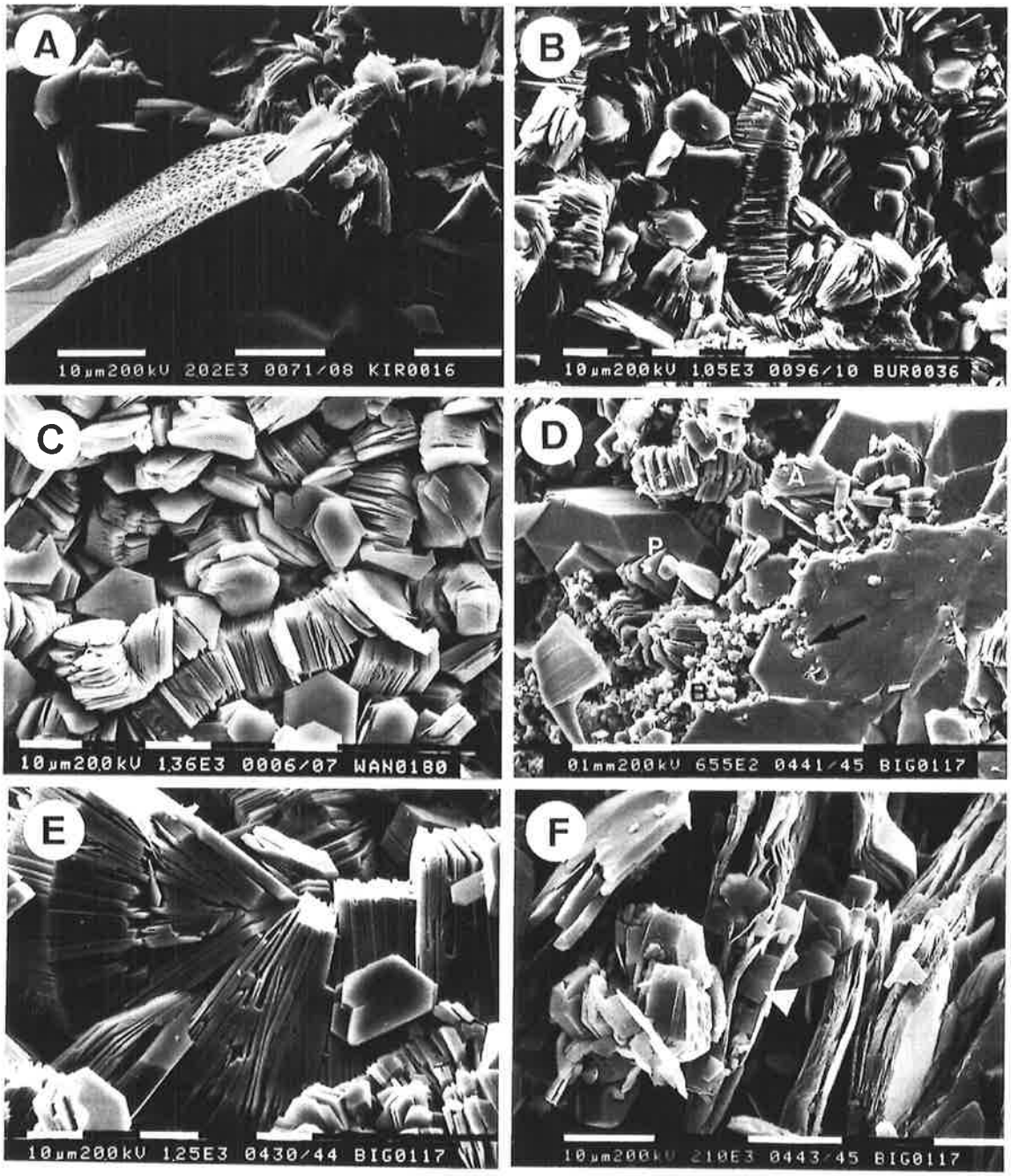
A
10µm200kV 202E3 0071/08 KIR0016
B
10µm200kV 105E3 0096/10 BUR0036
C
10µm200kV 136E3 0006/07 WAN0180
D
A
P
B
01mm200kV 655E2 0441/45 BIG0117
E
10µm200kV 125E3 0430/44 BIG0117
F
10µm200kV 210E3 0443/45 BIG0117

Na, K and Fe (S. Phillips, NCPGG, in: Stuart et al., 1991) (Table 4.4). This relationship is a common feature of pyrophyllite analyses (Deer et al., 1975; Ianovici et al., 1981). In rocks containing pyrophyllite, no feldspar remnants were encountered.

Table 4.2 Electron microprobe analyses of clinochlore [data courtesy of Dr. S.E. Phillips, NCPGG, unpubl.data].

Sample	SiO_2	Al_2O_3	FeO	MgO
		(weight % oxide)		
CB-0057	27.1	30.0	19.2	8.1
[Burley-2,	21.9	23.3	30.2	5.5
Epsilon Fm.]	22.2	26.9	30.7	6.3
	24.8	26.9	21.8	6.9
	22.7	26.3	24.5	6.0
CB-0058	22.1	22.2	26.3	8.4
[Burley-2,	23.8	23.1	28.5	9.0
Patchawarra Fm.]	23.5	23.0	26.1	8.5

4.3 Discussion

4.3.1 Sources of silica and timing

The present study has highlighted several important observations regarding the nature of reservoir silicification in the southern Cooper Basin. The loose grain packing of most sandstones at the time authigenic quartz was introduced suggests that reservoir silicification was initiated prior to significant compaction, under relatively shallow diagenetic burial conditions (Schulz-Rojahn & Phillips, 1989). Further, sandstones which are well cemented by quartz overgrowths are almost totally devoid of solution effects, as was first noted by Martin & Hamilton (1981). This conflicts with views expressed by Steveson & Spry (1973) who considered solution and interpenetration of

Plate 14

SEM, CL and thin section micrographs of micas and feldspars altering to kaolin

A. Kaolin crystals have grown between mica flakes to produce vermiform kaolin. EDS analyses of the kaolin show an absence of K, whilst the intervening micas still retain some K. Scale bar 10 µm. Sample CB-0067, Big Lake-5, Tirrawarra Conglomerate (9411' 2") [micrograph courtesy of S. Phillips].

B. K-feldspar covered by a honeycomb texture. This texture is typical of many feldspars that are being altered to kaolin. Scale bar 0.1 mm. Sample CB-0008, Big Lake-3, Patchawarra Formation (9860' 6") [micrograph courtesy of S. Phillips].

C. Close-up view of (B) above. Within the depressions of the honeycomb texture, there exist kaolin booklets. Scale bar 0.1 mm.

D. In this example of feldspar altering to kaolin, the feldspar remnants look like illite. Scale bar 10 µm. Sample CB-0068, Big Lake-5, Tirrawarra Conglomerate (9415' 7") [micrograph courtesy of S. Phillips].

E. Under CL, corroded feldspar grains (red) are commonly seen to be surrounded by kaolin (blue). Observe the lack of overgrowths on the adjacent quartz grains (purple to brown). Scale bar 0.3 mm. Sample CB-0745, Dullingari-18, Patchawarra Formation (7847' 2").

F. 'Ghost' remnants of labile components that were dissolved during diagenesis are sometimes evident in the sandstones of the southern Cooper Basin. In this example, a 'ghost' outline of a dissolved ?feldspar grain within a kaolin matrix (brown) is highlighted by organic matter/bitumen (arrows). Plane light. Scale bar 250 µm. Sample CB-0015, Kirby-1, Epsilon Formation (9703' 0").

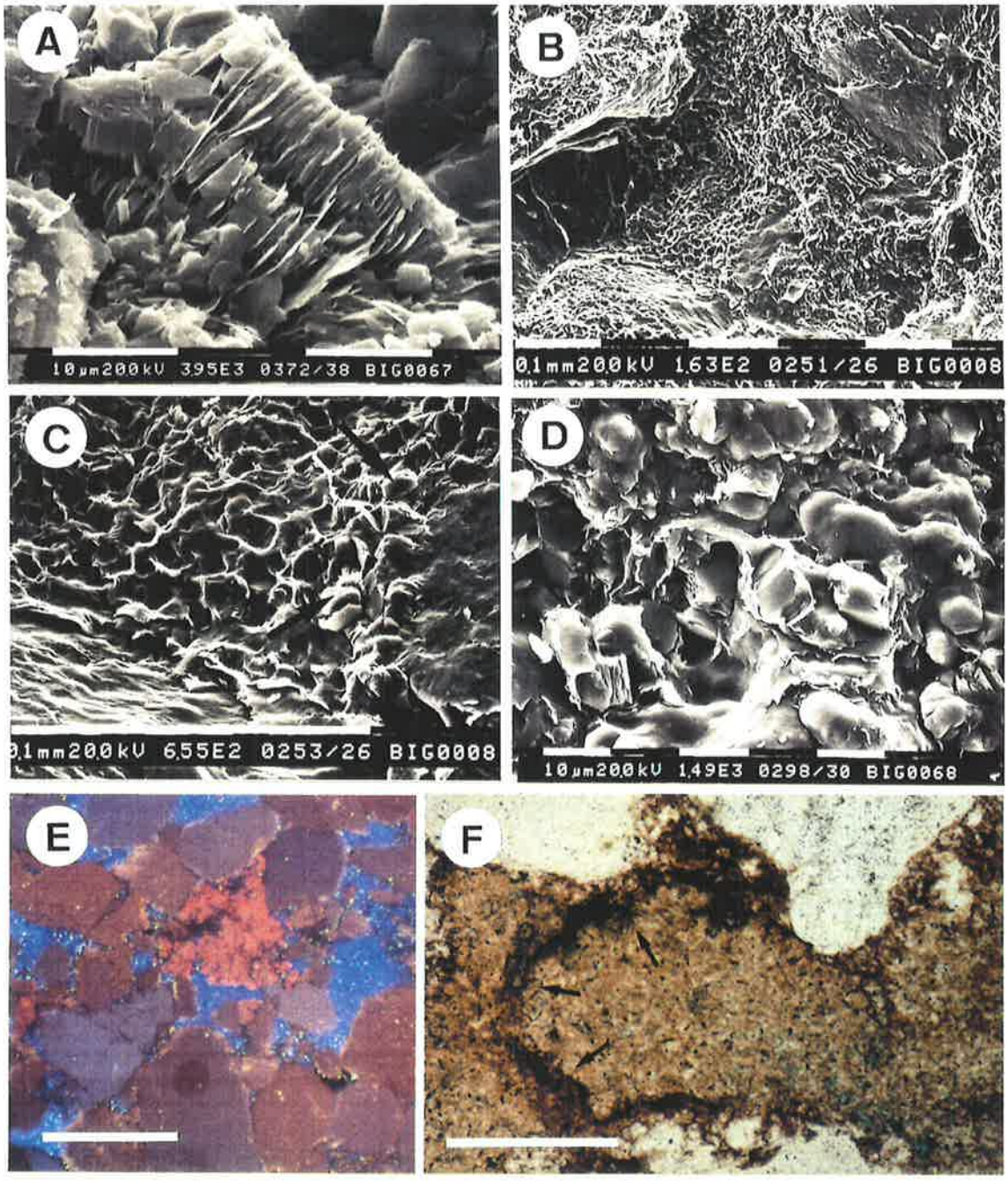
A
10µm20.0kV 3.95E3 0372/38 BIG0067
B
0.1mm20.0kV 1.63E2 0251/26 BIG0008
C
0.1mm20.0kV 6.55E2 0253/26 BIG0008
D
10µm20.0kV 1.49E3 0298/30 BIG0068
E
F

Table 4.3 Occurrence of pyrophyllite in the central Nappamerri Trough (Burley-2), as based on XRD results. Petrographic evidence suggests it may occur in other samples from the same well. Pyrophyllite is commonly associated with clinochlore IIB.

Sample	Depth (ft.KB)	Formation	Associated mineralogy (XRD)
CB-0058	11383' 6"	Patchawarra	Quartz, illite/muscovite, clinochlore IIB
?CB-0838	10200-10'	Epsilon	Quartz, kaolinite, illite/muscovite, siderite, clinochlore IIB
?CB-0842	10670-80'	Patchawarra	Quartz, kaolinite, illite/muscovite, siderite, clinochlore IIB
?CB-0843	10800-10'	Patchawarra	Quartz, dickite, illite/muscovite, siderite, clinochlore IIB
CB-0846	11600-10'	Patchawarra	Quartz, illite/muscovite, clinochlore IIB

Table 4.4 Electron microprobe analyses of pyrophyllite derived from the Patchawarra Formation at Burley-2 (sample CB-0058) [data courtesy of Dr. S. E. Phillips, NCPGG, unpubl.].

SiO_2	Al_2O_3	MgO	Na_2O	K_2O	FeO
		(weight % oxide)			
67.0	29.2	0.2	0.4	-	-
68.6	29.7	0.3	0.5	-	-
67.9	29.4	0.3	0.3	0.1	-
66.5	28.7	0.2	0.8	1	0.1
68.3	29.5	0.2	0.4	0.1	-
68.1	29.4	0.2	0.4	-	-
68.1	29.7	0.4	0.5	0.2	-
69.2	30	0.3	0.4	0.1	-

Plate 15

SEM and thin section micrographs of illite

A. Closely packed, platy crystal habit of detrital illite, significantly reducing porosity and permeability in a fine-grained sandstone. In shales and silty clastics, it is frequently difficult to see anything other than these platelets under the SEM. Microporosity is insignificant or absent in association with this type of illite. Scale bar 10 μm. Sample CB-0055, Burley-2, Epsilon Formation (10205' 9").

B. Illite also occurs where it replaces grains. In this example, it is not as well compacted as detrital varieties. Scale bar 0.1 mm. Sample CB-0005, Big Lake-3, Epsilon Formation (8265' 10") [micrograph courtesy of S. Phillips].

C. Fibrous authigenic ?illite occurs as pore lining in this medium-grained sandstone. The presence of minor Ca, Fe and K together with Si and Al suggest that this mineral may be interstratified. Note the microporosity between the illite laths. Scale bar 10 μm. Sample CB-0058, Burley-2, Patchawarra Formation (11383' 6").

D. Pore-filling lettuce-like illite which is interpreted as authigenic in origin. Again, note associated microporosity. This type of illite is rare. Scale bar 10 μm. Sample CB-0180, Wancoocha-1, Patchawarra Formation (6200' 11").

E. Elongate detrital mica flake which has partly been replaced by illite (thin fibrous 'film' on mica surface - arrow). In the clay fractions analysed by XRD, illite and muscovite are differentiated on the basis of peak sharpness; illite concentrates in deeper buried sediments throughout the basin. Crossed nichols. Scale bar 100 μm. Sample CB-0009, Kirby-1, Toolachee Formation (8935' 0").

F. Authigenic illite engulfing euhedral quartz prism (Q) and growing into primary pore space (P). Scale bar 10 μm. Sample CB-0589, Moomba-9, Toolachee Formation (7870' 0") [micrograph courtesy of A.Thomas].

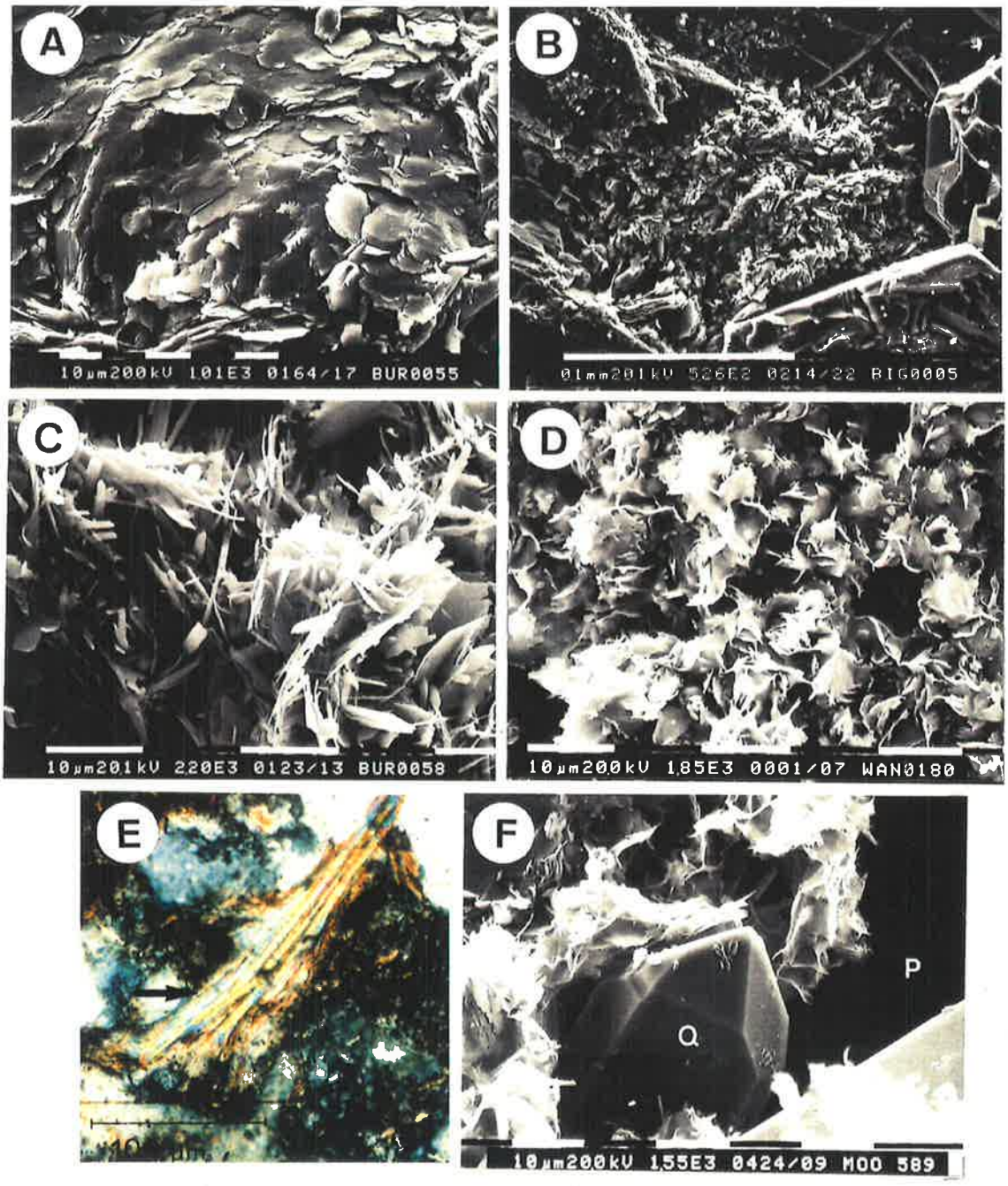
A
10µm200kV 101E3 0164/17 BUR0055
B
01mm201kV 526E2 0214/22 BIG0005
C
10µm201kV 220E3 0123/13 BUR0058
D
10µm200kV 1.85E3 0001/07 WAN0180
E
F
P
Q
10µm200kV 1.55E3 0424/09 MOO 589

quartz to constitute the primary source of silica to affect the sandstones in the Tirrawarra and Gidgealpa areas [12].

The study also highlighted the existence of several distinct phases of quartz crystallisation, as evident by zonation of authigenic quartz under CL (Schulz-Rojahn & Phillips, 1989). The implication is that cementation by quartz proceeded episodically and from formation waters of variable chemical composition. Another observation is that there is a high proportion of quartz overgrowths in coarser sediments devoid of significant amounts of clay (Schulz-Rojahn & Phillips, 1989). This could suggest that quartz cementation is selective to more permeable beds deposited in high-energy environments. As stated by McBride (1989, p.82), "the greater permeability of coarser beds dictates that they can provide the largest fluid flux and, thus, a possibility of sequestering more silica for overgrowths than finer beds". An alternative, not necessarily conflicting interpretation is that the clays inhibited quartz cementation by isolating detrital grains from water capable of precipitating quartz overgrowths (Heald & Larese, 1974; McBride, 1989).

Study results further suggest that reservoir silicification broadly increases from the basin margin to the depocentre, and only deeply buried sandstones are fully cemented by quartz. A similar observation was made by Martin & Hamilton (1981) who noted that quartz cementation is more advanced in deep wells in the Toolachee Formation. Any model attempting to explain the origin of authigenic quartz in the study area must account for these observations.

Quartz cement originated either from within the basin or from an external source, or both. Silica may have been derived internally by the dissolution of feldspar grains and their replacement by more stable minerals such as kaolinite (Fothergill, 1955; Hower et al., 1976; Hawkins, 1978). Depending on the type of feldspar, between 40 and 48 percent of silica can be released in this way and may be reprecipitated as interstitial quartz cement (Bjørlykke, 1984, 1988; Morad & Aldahan, 1987a). This mechanism would account for the abundance of kaolinite in the study area, its association with feldspar remnants, and the intergrowth of kaolin and quartz overgrowths: as feldspars were dissolved, there was a contemporaneous precipitation of kaolin and quartz.

Kaolinisation undoubtedly provided at least some of the silica required for quartz cementation, particularly in sediments originally enriched in detrital feldspars. However, quantitative calculations indicate that this source alone cannot account for the authigenic quartz in the majority of sandstones. The total abundance of kaolin minerals does not generally exceed 15 percent of any one sample (Appendix L), hence

---

[12] Steveson & Spry (1973) based their interpretation on conventional petrographic data. They comment that "most of the sandstones [in the Tirrawarra and Gidgealpa areas] are characterised by large volumes of extremely well-connected quartz...the average number of contacts per grain is very high and grain boundaries are normally concavo-convex or long" (Steveson & Spry, 1973, p. 88).

Plate 16

Thin section micrographs of the Tirrawarra Conglomerate at Big Lake

A. General view. The Tirrawarra Conglomerate at Big Lake is generally coarse grained and very poorly sorted. Clays constitute a significant proportion of this rock. On wireline logs, the Tirrawarra Conglomerate locally resembles a shale. Measured core porosity is 1.2 % and permeability < 0.1 md. Crossed nichols. Scale bar 1 mm. Sample CB-0069, Big Lake-5, Tirrawarra Conglomerate (9417' 5").

B. Close-up view of (A). Many of the detrital grains have rims of illite (light). There are large areas of kaolin clay patches (K) in this sample. The kaolin is thought to be an end product of the beakdown of feldspars. Crossed nichols. Scale bar 250 μm. Sample CB-0069, Big Lake-5, Tirrawarra Conglomerate (9417' 5").

C. Distinctive large hydromuscovite flakes (high birefringence; identification based on probe analyses) are characteristic of the Tirrawarra Conglomerate, indicating a granitic or metamorphic source provenance in close proximity. Probe analyses of the hydromuscovite give an average composition of 46.4 wt. % SiO_2, 39.8 wt. % Al_2O_3, 0.3 wt. % FeO, 0.3 wt. % MgO, 1.1 wt. % K_2O and 0.5 wt. % Na_2O. The remainder would be H_2O (S.E. Phillips, NCPGG, unpubl. data). XRD and XRF analyses of the < 5 and < 10 micron size fractions suggest illite constitutes 67 percent and dickite 22 percent of the clay matrix in this sample; chlorite is also present in trace quantities (Table 4.1). Crossed nichols. Scale bar 1 mm. Sample CB-0077, Big Lake-29, Tirrawarra Conglomerate (9666' 0").

D. Close-up view of large hydromuscovite flakes (high birefringence colours) in a kaolin-rich matrix (grey). Crossed nichols. Scale bar 1 mm. Sample CB-0075, Big Lake-29, Tirrawarra Conglomerate (9661' 8").

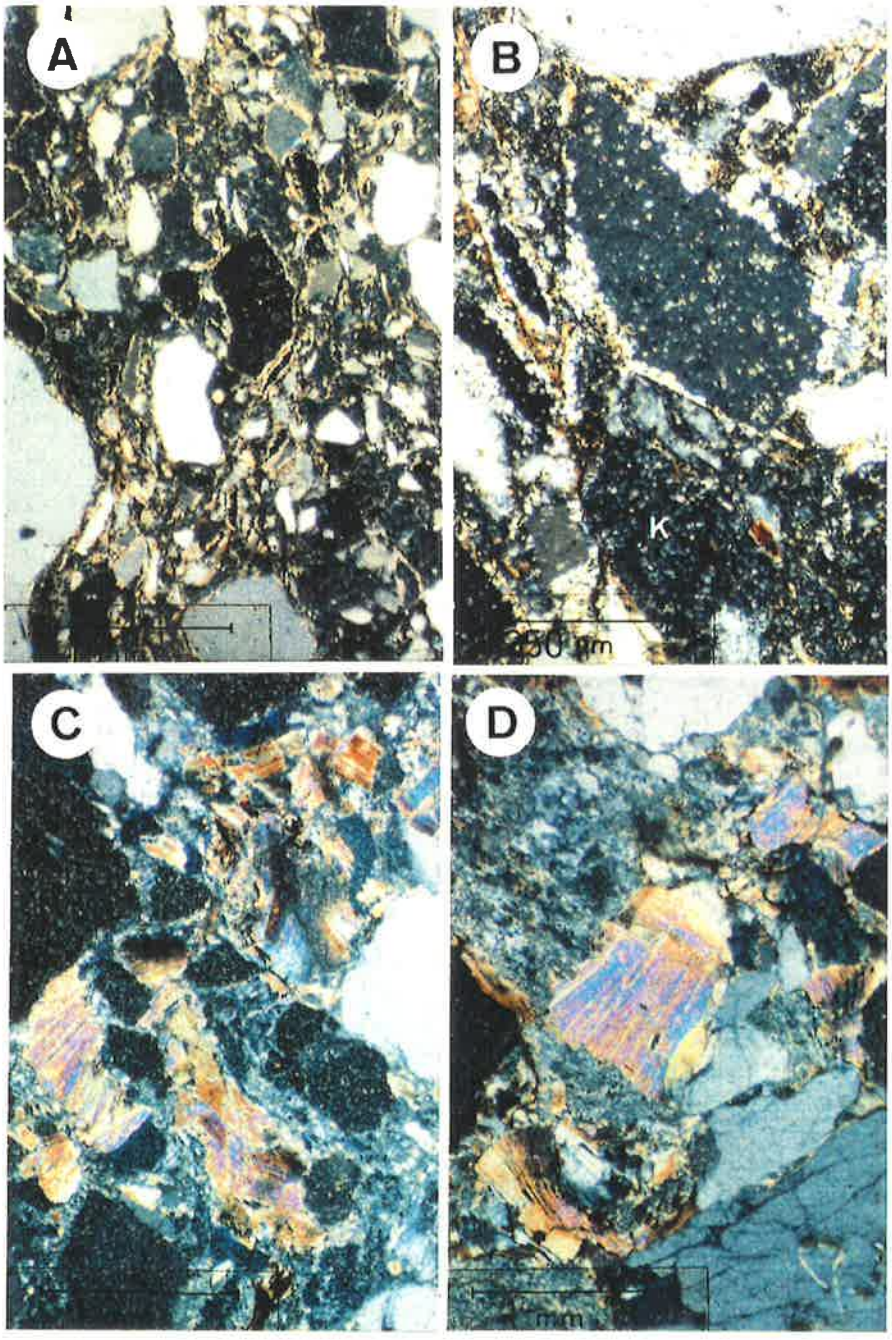
A
B
K
C
D
mm

the amount of quartz released locally through this mechanism could not have been greater than approximately 6 to 7 percent of total rock composition. These calculations indicate that a considerable proportion of the authigenic quartz can not be accounted for in coarse grained samples through this mechanism alone.

A further possibility is that replacement of silicates by carbonate provided a source of silica for quartz cementation (Walker, 1960; Burley & Kantorowicz, 1986). Other workers consider shale bodies to represent a major source of silica for authigenic quartz (Füchtbauer, 1967b; Land & Dutton, 1978; Hayes, 1979). In support of this theory is the fact that shale pore waters often contain high concentrations of dissolved silica (Lerman, 1979). Such high silica concentrations may be the result of dissolution of silt- and clay-size quartz grains in the shales (Dapples, 1967b; Füchtbauer, 1978). An alternative interpretation is that silica released into the shale pore waters is the product of clay mineral reactions. An example includes the smectite to illite transformation that takes place at temperatures between 50 to 120 °C, and involves the progressive release of Si^{4+} and other ions from smectite (Towe, 1962; Siever, 1962; Perry & Hower, 1970; Hower et. al., 1976; Boles & Franks, 1979). The amount of free silica released through this mechanism is 2.2 grams of quartz per 100 grams of clay transformed (Towe, 1962). Similarly, the illitisation of kaolinite where K is available has the potential to release small amounts of silica (Aldahan & Morad, 1986; Eslinger & Pevear, 1988).

Since there are large volumes of argillaceous sediments which frequently interfinger with the sandstones in the Cooper Basin, it is possible that clay transformation has contributed to the supply of authigenic quartz in the sandstones. Bulk XRD analyses and investigation of the less than 5 and 10 μm size clay fractions have not detected any smectite. However, Stanley & Halliday (1984) report the presence of trace amounts of illite-smectite in the Patchawarra and Tirrawarra Formations at Big Lake. Minor amounts of smectite clay are also present in some Toolachee samples along the Murteree-Nappacoongee High but were ascribed by Martin (1980) and Martin & Hamilton (1981) to infiltration of drilling mud into the core.

In the present investigation, illite seen under the SEM typically forms anhedral plates which are suggestive of a detrital origin and not the authigenic origin hypothesised by clay transformation. Furthermore, the release of silica through clay mineral transformations is likely to be dependent on compactional dewatering of the shales with a consequent upward flow of silica-enriched waters. It is difficult to envisage how quartz precipitation could have occurred through this mechanism in those parts of the southern Cooper Basin where there is evidence from CL work that the sands were little affected by compaction when authigenic quartz was first introduced.

Plate 17

Micrographs of pyrophyllite and clinochlore

A. Euhedral pseudohexagonal plates of clinochlore IIB lining voids. Scale bar 10 μm. Sample CB-0058, Burley-2, Patchawarra Formation (11383' 6") [micrograph courtesy of S. Phillips].

B. Rosettes and pseudohexagonal plates of clinochlore IIB attached to the surface of a quartz grain (Q). Scale bar 10 μm. Sample CB-0058, Burley-2, Patchawarra Formation (11383' 6").

C. Thin section micrograph of highly birefringent pyrophyllite filling oversized pores and embaying the edges of adjacent quartz grains. Chlorite grain replacement (C) is evident in the centre of the micrograph. Measured core porosity in this sample is 4.1 % and permeability 0.33 md. The porosity occurs interstitially between the clinochlore and pyrophyllite platelets. Crossed nichols. Scale bar 1 mm. Sample CB-0058, Burley-2, Patchawarra Formation (11383' 6").

D. Back-scattered image of pore rimmed with clinochlore IIB and filled with pyrophyllite. Cement stratigraphy indicates that pyrophyllite postdates clinochlore. Compositions of each mineral were checked with the electron microprobe. Scale bar 100 μm. Sample CB-0058, Burley-2, Patchawarra Formation (11383' 6") [micrograph courtesy of S. Phillips].

E. Radial clusters of platey pyrophyllite as seen in the SEM. The soft nature of this mineral means that it is easily damaged during sample preparation. When it is damaged, pyrophyllite has a morphology that is indistinguishable from detrital illite. Scale bar 0.1 mm. Sample CB-0058, Burley-2, Patchawarra Formation (11383' 6").

F. Close-up view of radiating pyrophyllite. Note etching of the surface of an adjacent quartz grain (Q). Scale bar 0.1 mm. Sample CB-0058, Burley-2, Patchawarra Formation (11383' 6") [micrograph courtesy of S. Phillips].

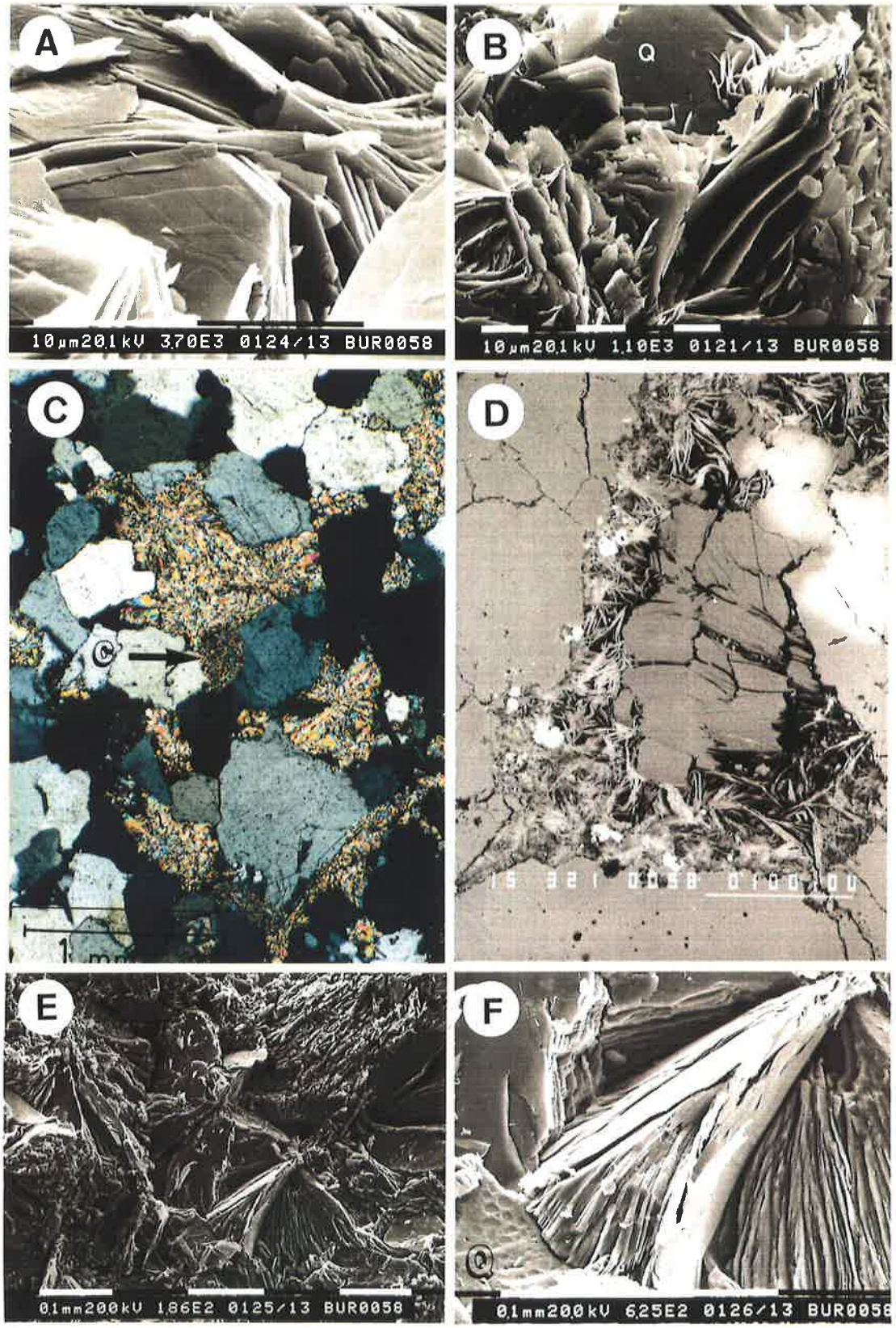
A
10µm20.1kV 3.70E3 0124/13 BUR0058
B
Q
10µm20.1kV 1.10E3 0121/13 BUR0058
C
C
D
E
0.1mm200kV 1.86E2 0125/13 BUR0058
F
Q
0.1mm20.0kV 6.25E2 0126/13 BUR0058

Other sources of silica ascribed to compaction, such as stylolitisation (Füchtbauer, 1978; Bjørlykke, 1991) and intergranular pressure solution (Hayes, 1979; Houseknecht, 1988) are also unlikely to be major sources of silica in those areas where authigenic quartz developed prior to significant compaction. However, it is possible that chemical compaction and clay transformation have contributed to the later stages in the development of the quartz overgrowths. These sources may be of importance at depth in the southern Cooper Basin. Such sources could account for the generally higher proportion of quartz overgrowths in sandstones towards the basin depocentre. Late-diagenetic quartz cements probably precipitated at elevated temperatures. This is in accordance with fluid inclusion data by Bone & Russell (1988) and Russell & Bone (1989), suggesting homogenisation temperatures for some authigenic quartz in Cooper Basin sediments to be in the order of 100 to 150 °C [13].

Quartz solubility increases with increasing pH (Krauskopf, 1959; Blatt et al., 1972; Knauss & Wolery, 1988) and overburden pressure (Willey, 1974), therefore the presence of oriented V-shaped depressions indicative of chemical etching suggests that alkaline conditions prevailed at certain times at depth. Only in the large euhedral quartz overgrowths are these features evident. Although dissolution is not extensive it may also have provided a source of silica for later overgrowths. Alkaline conditions would have prevailed during carbonate precipitation: these pH levels are attained commonly after early diagenesis during progressive burial (Siever, 1979).

In view of the apparently limited nature of potential silica sources operative prior to compaction within the Cooper Basin, the influence of meteoric waters must be considered. It is suggested that early quartz cementation was made possible through sub-surface invasion of atmospheric waters enriched in silica. Similar models have been proposed for other basins (Siever, 1959; Sibley & Blatt, 1976; McBride, 1987; Bjørlykke, 1984, 1988; Ayalon & Longstaffe, 1988).

Large-scale mass transport of dissolved mineral components will be favoured by high fluid flux where adequate porosity and permeability exist. This is likely to occur in clastic sequences at shallow to intermediate burial depths under the influence of high groundwater flow rates (Bjørlykke, 1979, 1988). High groundwater flow rates up to several thousand metres per year are associated with unconfined shallow aquifers [14] (Giles, 1987). Volumetric calculations indicate that in the range of 10^4 to 10^5 pore volumes of water are necessary to introduce 5 to 15 percent cement in each cubic centimetre of rock (von Engelhardt, 1967; Land & Dutton, 1978; Bjørlykke, 1979, 1983; Dutton & Land, 1988a). Such high volumes of water from internal sources are not available in most basins (Bjørlykke, 1979; Land & Dutton, 1979;

---

13 There is no data to suggest which phase(s) of quartz overgrowth development precipitated at these elevated temperatures.

14 Confined aquifers have much lower flow rates, in the order of 1 to 30 metres per year (Giles, 1987).

Land, 1984). Up to 90 percent of modern groundwaters are reported to be supersaturated with respect to quartz (Livingstone, 1963; Davis, 1964). The dissolved silica content of surface or ground waters is generally in the order of 10 to 20 ppm (Davis, 1964; Payne, 1968), averaging 13 ppm (Blatt, 1979), but can be as high as between 50 and 100 ppm (Blatt, 1979; Land, 1984). However, only slightly more than 6 ppm are required before quartz precipitation is possible (Blatt, 1979). Similarly, temperature equilibrium data (Blatt, 1979; Dapples, 1979b; Holland & Malinin, 1979) emphasize that quartz could precipitate under relatively low temperature diagenetic conditions. These hypotheses support the suggestion that initial quartz development was an early diagenetic event in the majority of sandstones in the southern Cooper Basin. Some overgrowths developed prior to significant compaction and this silica probably was derived from groundwaters. The silica released by kaolinisation, possible clay transformation, chemical compaction and silicate replacement by carbonates may be responsible for later phases of silicification.

4.3.2 Carbonates

The micritic and sparry siderite are considered to have different origins because of their relatively rare mutual coexistence and distinct lithological associations. Micrite is typical of carbonate cements in the vadose zone, whilst spar and blocky cements are associated with deeper burial in the phreatic zone (James & Choquette, 1984).

Equilibrium models indicate that siderite precipitation is favoured by waters of low oxidation potential with extremely low concentrations of dissolved sulphide, high concentrations of dissolved carbonate, near-neutral pH, and a high Fe^{2+}/Ca^{2+} ratio (Garrels & Christ, 1965; Berner, 1964; Curtis, 1967; Curtis & Spears, 1968). According to Berner (1981) and Bahrig (1989), such conditions are likely to prevail in fine-grained lake and swamp sediments enriched in organic matter. This is in accordance with numerous occurrences of micritic siderite observed in modern sediments. For example, recent freshwater occurrences of micritic siderite have been reported from the Atchafalaya River Basin of Louisiana (Ho & Coleman, 1969), and from the inland moors and river bogs of Denmark (Postma, 1977, 1982; Jakobsen, 1987). Pye (1984) and Shotyk (1988) have reported that micritic siderite precipitation can occur at depths of less than 1 metre below the sediment-surface interface. Channelling and erosion by rivers and creeks could easily rework clasts containing siderite from this depth. Rip-up clasts similar to those in the Cooper Basin sediments have been reported from both modern (Pye, 1984) and ancient sediments (de Boer &

Collins, 1988). The siderite in these clasts is typically micritic and thus is interpreted as a primary precipitate. Furthermore, the presence of burrows (filled with clean sands) cutting across siderite bands suggest that either the siderite accumulated in a zone subject to bioturbation or the burrow had a different diagenetic history to the siderite bands. Ho & Coleman (1969) noted a positive correlation between the number of siderite nodules and the presence of organic matter in a recent freshwater clay-rich sequence. In the present study, the association of micritic siderite with organic-rich argillaceous sediments and coals suggests that the release of CO_2 from decomposing organic matter may have been involved in siderite precipitation (Schulz-Rojahn & Phillips, 1989) (cf. results in Chapter 6). Alternatively, the formation of Fe-rich carbonates in swamp environments may be controlled by the reduction of ferric oxyhydroxides by organic matter (Postma, 1977, 1981). A third possibility is that bacterial fermentation reactions were involved in early diagenetic carbonate precipitation (Irwin et al., 1977; Irwin, 1980). Differentiation between these models is presently not possible (see discussion in Chapter 6).

For the supply of iron, numerous potential sources can be envisaged. Iron was probably present in the lake and river waters. In modern rivers, iron may be present in concentrations exceeding 30 ppm (Dapples, 1979b). The iron can be absorbed on clays and detrital grains (Ho & Coleman, 1969; McBride, 1987), or occur in the form of organic colloidal complexes (Blatt et al., 1972). It is also possible that the decomposition of plant material in swamp environments released some of the metal cations required for siderite precipitation (Ho & Coleman, 1969). Modern swamp and lake sediments have been reported to contain iron concentrations exceeding 20 percent (Postma, 1977, 1982; Schwertmann et al., 1987).

During later diagenesis, iron could have been derived from the decomposition of phyllosilicates such as biotite, illite or chlorite (Blatt et al., 1972; Füchtbauer, 1978). Alternatively, iron was liberated during shale compaction (Boles & Franks, 1979). These sources of iron probably contributed to the formation of the spar and microspar siderite varieties, including possibly ankerite.

Sparry cements of patchy distribution occupy large, irregular-shaped areas in some sandstones (Plate 9 F), suggesting the spar precipitated in secondary pores resulting from the dissolution of framework grains. Evidence of silicate replacement by carbonates includes quartz grains with embayed edges, and 'ghost' remnants of grains within the carbonate cement. The high proportion of carbonate cement (>70 %) in some sandstones is a further indicator that carbonate precipitation was not restricted to pore space within the reservoir rock but involved the active dissolution of framework grains. Replacement of quartz by carbonate cement has been reported elsewhere (Lambert-Aikhionbare, 1982; Bubenicek, 1983).

The sources of Mg, Mn, and/or Ca required for dolomite, ankerite and calcite formation are uncertain. As for quartz cements, multiple sources probably influenced the precipitation of the carbonate cements. The potential role of clay minerals in dolomite formation was highlighted by Kahle (1965). Boles (1978) suggested that the transformation of smectite to illite releases calcium, iron and magnesium. Magnesium may also be released from kerogen after burial (Desborough, 1978). An important source of calcium could also be the breakdown of Ca-feldspars (Irwin, 1980). Alternatively, carbonate material may have been introduced directly into the Permian sediments through vertical movement of carbonate-enriched fluids from the underlying Cambrian rocks (Youngs, 1975). Vertical motion of pore fluids could have been accomplished by compactional dewatering (Magara, 1976, 1981), thermal convection currents (Wood & Hewlett, 1982), or 'seismic pumping' accompanying fault movements (Sibson et al., 1975). However, in the present study no clear relationship exists between the distribution of carbonate cements and the Cambrian Warburton Basin limestones (cf. Figs.4.2 a-d and Fig.2.4). This may argue against the hypothesis that Cambrian limestones influenced carbonate genesis in the Cooper Basin (cf.Ch.6). Evidence for biogenic carbonate material in the study area is entirely absent.

Another option is that carbonate material was derived from the overlying Eromanga Basin (Schulz-Rojahn & Phillips, 1989) that forms part of the Great Artesian aquifer system (Habermehl, 1980). These aquifers are widely reported to be calcium- and magnesium-bearing (Habermehl, 1984; Collerson et al., 1988; Herczeg et al., 1988). Downward movement of Eromanga groundwaters may have carried carbonate ions into the Permian sequence (Schulz-Rojahn & Phillips, 1989). This hypothesis is feasible considering that Permian strata have been partly flushed by artesian waters from the overlying Jurassic aquifers (Porter, 1973, 1974; Youngs, 1975). Although the data set is limited in this study, calcite cements appear to concentrate in shallower Permian sediments near the basin margin and along structural highs in the southern Cooper Basin. These areas represent those most affected by flushing (Porter, 1973, 1974; Youngs, 1975), supporting the hypothesis that invasion of groundwater from the Eromanga aquifers may have been involved in calcite precipitation in Permian strata. The mechanism may have preferentially affected the coarser grained clastics with adequate porosity and permeability which would explain the dominant association of spar with sandstones. Distributional patterns for ankerite and dolomite suggest they too could have formed in this way although alternative interpretations are possible. Isolated occurrences of calcite in clastics at Burley and Kirby in the central Nappamerri Trough reflect possible local sources of Ca^{2+}.

4.3.3 Clays

The euhedral habit of kaolin is indicative of the authigenic origin of this clay type. Kaolinite is characteristic of low to moderate temperature environments (Hurst & Kunkle, 1985), and may form at relatively shallow depths of burial; it is stable between pH 5.2 and pH 8 (May et al., 1979; Hurst, 1980). This range broadly corresponds to the pH stability field of quartz. Hence, the precipitation of quartz overgrowths and kaolinisation could have proceeded simultaneously, explaining the frequent intergrowth of kaolin with the outer margin of quartz overgrowths. Furthermore, kaolinite now is thought to form in open diagenetic environments during periods of meteoric flushing (Hancock & Taylor, 1978; Sommer, 1978; Bjørlykke et al., 1979; Bjørlykke, 1988; Glasmann et al., 1989). Under such conditions, feldspars and micas could be readily converted to kaolinite. In the present study, it would appear that loss of K from the feldspars has resulted in the precipitation of kaolin in pockets on the surface of the feldspars, creating a 'honey-comb' texture. Continuation of this process would result in feldspars being completely altered to kaolin (including possibly some illite). SEM studies by Morad & Aldahan (1987b) suggest that it is kaolinite rather than dickite which forms as the alteration product of feldspars.

Lombardi & Sheppard (1977) found that when kaolinite and dickite coexist, dickite crystals are typically larger than kaolinite. This hypothesis is applicable to the Cooper Basin sediments where comparison of kaolin morphology as seen under the SEM with XRD analyses clearly demonstrates that the larger euhedral crystals are dickite. The size and vermiform nature of dickite imply that this mineral formed under ideal conditions. Dickite is generally considered the more stable polymorph of the kaolin group (Larsen & Chilingar, 1983) although the conditions under which it forms are not well understood. According to Kisch (1983), replacement of kaolinite by dickite appears to be favoured by high porosity and permeability, and formation of dickite may be related to groundwater heated by igneous activity. Brindley & Porter (1978) also attribute dickite formation to precipitation from hot waters ascending along fractures. More recently, Loughnan & Roberts (1986) hypothesised that dickite precipitated from migrating groundwater in the Illawarra Coal Measures of the Sydney Basin. They suggested that the large crystal size was due to slow precipitation caused by a lack of Si in the groundwaters. In the Cooper Basin, the concentration of dickite in coarser-grained clastics favours the hypothesis that dickite has precipitated from migrating fluids. The fact that dickite is not intergrown with quartz overgrowths and occurs as pore filling suggests it may have formed when the amount of Si was diminished in the ground waters and slow crystallisation was possible.

Several different mechanisms are thought to be responsible for the abundance of illite. Martin & Hamilton (1981), Stanley & Halliday (1984) and Hamilton (1989) considered that the illite was mainly authigenic in origin. Based on crystal habit and spatial distribution, much of the illite in the present study is interpreted to have a detrital origin. A similar view was put forward by Smale & Trueman (1965). This explains the high proportion of illite in fine grained sandstones, siltstones and shales associated with overbank and flood plain deposits. The distribution of detrital illite is considered to be related to the hydraulic regime and sediment provenance of the depositional environment. The alignment of the illite plates is a function of sorting by currents as well as later mechanical compaction. Only minor amounts of illite are of authigenic origin as a product of in situ alteration, as seen in thin section and the SEM. Rarely does illite in the study area show a fibrous habit which could be attributed to the transformation of smectite with depth (Hower et al., 1976; Boles & Franks, 1979; Eslinger & Pevear, 1988; Pearson & Small, 1988; O'Shea & Frape, 1988) or direct precipitation from pore fluids (Guven et al., 1980). Authigenic illite typically develops in near-neutral fluids (Huang et al., 1986) with total dissolved solids (TDS) greater than seawater (Harder, 1974). The elements necessary for the formation of illite may be derived from the dissolution of K-feldspars and/or micas (Perry & Hower, 1970; Perry, 1974; Hurst & Irwin, 1982; Pearson & Small, 1988; O'Shea & Frape, 1988). Hower et al. (1976) found an increase of illite content with depth, accompanied by a proportional decrease of feldspar and kaolinite. The fact that fibrous illite in the southern Cooper Basin occurs in more deeply buried sediments is consistent with its precipitation from solution as kaolinite, K-feldspars and/or mica are altered with increasing depth (Schulz-Rojahn & Phillips, 1989). Such processes are not necessarily related to temperature (Srodon & Eberl, 1984) but may also be triggered by a decrease in the rate of influx of acidic fluids (Huang et al., 1986).

Clinochlore is interpreted as an authigenic mineral based on its euhedral crystal habit. Sarkisyan (1972) suggested ferrous chlorites form by transformation of trioctahedral hydromicas and biotite. Other workers consider clinochlore formation to be an end product of smectite transformation (Eslinger & Pevear, 1988). Chlorite authigenesis has also been attributed to the release of Fe and Mg by illitisation and subsequent reaction with kaolinite in sandstones at temperatures less than 100 °C (Boles & Franks, 1979). Further, chlorite can form due to the recrystallisation of illite, illite-smectite and rarely kaolinite (Velde & Medhioub, 1988). In the latter case, an additional source of Fe would be required (Schulz-Rojahn & Phillips, 1989). In the present study, kaolin and siderite abundances are relatively low in sediments which contain clinochlore (Table 4.1). This suggests there may be a reaction involving these minerals that produces Fe-rich chlorite. Eslinger & Pevear (1988) demonstrated that the abundance of both chlorite and illite commonly increases with depth. Hurst (1985)

suggested clinochlore formation is temperature-controlled during burial diagenesis. The fact that clinochlore is a IIB polytype indicates that it has possibly formed under conditions of low-grade metamorphism (Hayes, 1970; Carroll, 1970).

The presence of pyrophyllite in some samples, commonly in association with clinochlore, appears to mark the poorly defined boundary between diagenesis and regional metamorphism. This is indicated by the restricted geographic occurrence of pyrophyllite in the basin: the mineral is found only towards the depocentre of the central Nappamerri Trough, characterised by a high present-day geothermal gradient in excess of about 16 °C per 1000 feet (50 °C/km) (Table 4.5). A significant degree of thermal alteration is confirmed by high vitrinite reflectance levels in this area, such that virtually the entire Permian section falls within the zone of dry gas generation, or beyond (Kantsler et al., 1983). In the case of the Patchawarra Formation, vitrinite reflectance levels (R_v max.) in excess of 6 percent are reported (Cook, 1985) (Table 4.5), well within the zone of metamorphism (greenschist facies) as defined by Tissot & Welte (1978). The association of pyrophyllite with low-grade metasediments has been reported elsewhere, including Switzerland (Frey, 1978; Wieland, 1979), Spain (Lécolle & Roger, 1976; Goméz-Pugnaire et al., 1978), and the Caribbean (Frey et al., 1988). Pyrophyllite formed in this type of geologic setting is interpreted as a reaction product between kaolin and quartz (Kossovskaya & Shutov, 1963; Reed & Hemley, 1966; Ianovici et al., 1981; Zaykov et al., 1988). The absence of kaolin from samples containing abundant pyrophyllite confirms that a similar mechanism may have operated in the Nappamerri Trough. Based on experimental thermodynamic data, pyrophyllite neomorphism is favoured by temperatures between 290 to 420 °C, at pressures varying between 1 and 3 kb (Hemley & Jones, 1964; Reed & Hemley, 1966; Althaus, 1969; Velde & Kornprobst, 1969; Thompson, 1970; Haas & Holdaway, 1973; Helgeson et al., 1978; Chatterjee et al., 1984; Berman et al., 1985) (Table 4.6). These temperatures are higher than bottomhole temperatures (240 °C) recorded in the central Nappamerri Trough (Table 4.5) [15]. However, results obtained by Reed & Hemley (1966) suggest that pyrophyllite may form at lower temperatures when reaction rates are slow. Furthermore, Frey et al. (1988) suggested that the presence of carbon dioxide and methane in the pore fluids can reduce the activity of water and thus lead to a lower estimate of the temperature at which pyrophyllite forms. Pyrophyllite is considered to have formed under conditions of low-grade metamorphism in the central Nappamerri Trough [16]. A similar interpretation is put forward by other workers in different basins (Winkler 1964, 1965, 1970; Kossovskaya & Shutov, 1970; Clauer & Lucas, 1970).

---

15 Bottomhole temperatures are generally lower than the real formation temperature (Rider, 1986).

16 Possibly the low or medium pressure range of the lower greenschist facies (Winkler, 1979; Chopin & Schreyer, 1983; Frey et al., 1988).

Table 4.5 Temperature and vitrinite reflectance data for petroleum wells drilled in the central Nappamerri Trough (BHT = bottom-hole temperature; Geo.Grad. = geothermal gradient, extrapolated from logging runs and drill stem tests) [data compiled from well completion reports, courtesy of Cooper Basin Consortium Group of Companies].

Well	Base Permian (feet KB)	BHT (°C)	Geo.Grad. (°C/km)	R_v max. at base Permian (%)	Comment
Burley-1	11975+	210-226	52-56	≥ 6.5	-
Burley-2	12020	237.2	58.3	> 6.2	-
Kirby-1	12685+	193.3	44.6+	≥ 4.8	-
McLeod-1	12292	215.6	51	≥ 5.0	No core cut in Permian section

4.3.4 Diagenetic sequence for authigenic minerals

Despite the regional nature of sampling and the different stratigraphic sequences considered, relatively little variation was evident in the diagenetic products. Similar cement types and clay species affect the reservoir quality of the Permo-Triassic formations throughout the study area. The apparent lack of differences in diagenetic events may be attributed to the fact that some of the sandstones are interconnected and fluids may have migrated vertically between formations.

The proposed diagenetic sequence for the authigenic minerals in the southern Cooper Basin is illustrated in Figure 4.6. Precipitation of micritic siderite in the vadose zone represents the earliest diagenetic event, initiated shortly after deposition. Silicification occurred during at least several phases. The first phase of quartz overgrowth development occurred prior to significant compaction in the shallow subsurface, and represents an early cementation event. Precipitation of overgrowths progressed through several other phases of diagenesis including the kaolinisation of feldspars and micas. Chemical compaction is considered to be a late diagenetic event,

Table 4.6 Experimental thermodynamic equilibrium data compiled from various sources highlighting the temperature conditions required for pyrophyllite formation under varying pressures and over different reaction periods.

	Pyrophyllite formation temperatures (°C) at:					
Source:	500 bars	1 kbar	2 kbar	3 kbar	≥ 4 kbar	Time
Hemley & Jones (1964)	-	385 max.	-	-	-	?
Velde & Kornprobst (1969)	-	292-310 ± 5	303-315 ± 4	-	-	23-120 days
Althaus (1969)	340	368	380	-	405 (6.9 kbar)	6 weeks to 6 months
Thompson (1970)	-	325 ± 20	345 ± 10	-	375 ± 15 (4 kbar)	1 week - 3 months
Haas & Holdaway (1973)	-	-	345-380	-	400-420 (7 kbar)	8-30 days
Chatterjee et. al. (1984)	-	-	-	320-395	520 (12 kbar)	1 day -
					400 (4 kbar)	28 days
Reed & Hemley (1966)	-	≤ 300	-	-	-	1 year
Helgeson et al. (1978)	-	-	-	315-420	-	?
Berman et al. (1985)	-	-	-	305-395	-	?

and silica released through this mechanism may have reprecipitated locally, particularly in sandstones in the deeper portions of the basin. In other areas, where compaction occurred prior to the precipitation of overgrowths, intense intergranular dissolution occurred. Some feldspars and micas were altered to kaolinite, liberating the elements required for slow precipitation of dickite from solution as the supply of Si became limited. Thus dickite formation postdates that of kaolinite.

Alkaline conditions prevailed after the formation of large euhedral quartz overgrowths causing their partial dissolution. Sparry carbonates were possibly precipitated during this period. Compositional variations in the carbonates reflect changes in the chemistry of the migrating pore fluids. Petrographic data is insufficient to establish the relative timing of sparry siderite, calcite, ankerite and dolomite formation in relation to other authigenic mineral phases (cf. discussion in Chapter 6).

Authigenic illites probably formed during periods of deeper burial when smectite, kaolinite and/or K-feldspars were altered. It is possible the shift from kaolinite to illite stability is the result of cutoff of meteoric recharge and resultant stagnation of entrained meteoric water (Huang et al., 1986). The final diagenetic events are depth and temperature related, with the formation of clinochlore IIB and pyrophyllite in the central Nappamerri Trough. Pyrophyllite formed under conditions of low-grade (?lower greenschist) metamorphism as a reaction product of kaolin and quartz in the central Nappamerri Trough.

4.3.5 Relative timing of hydrocarbon generation and migration

Petrographic evidence provides clues to determining the relative timing of hydrocarbon generation and migration in relation to mineral authigenesis in the study area (Fig.4.6). Dead oil/bitumen was found associated with authigenic minerals in sandstones from the Wancoocha oil field and the Moomba, Big Lake, Strzelecki, Toolachee and Daralingie gas fields, as well as several wildcat wells. This suggests liquid hydrocarbons have migrated through, and not been trapped, in sandstones in many of these areas. Instead, large volumes of liquid hydrocarbons generated in the Cooper Basin probably were trapped in the superjacent Eromanga Basin, as suggested by abundant evidence of geochemical and other nature (Jenkins, 1989; Gilby & Mortimore, 1989; Heath et al., 1989; Yew & Mills, 1989). Some of the liquid hydrocarbons may also have been 'cracked' and converted to gas during metagenesis (Tissot & Welte, 1978), particularly in the more deeply buried sediments of the Cooper Basin. Oil in the project area presently occurs in commercial quantities only in

the Patchawarra Formation at Wancoocha; a thin oil leg is further present in the same formation at Daralingie (Yew & Mills, 1989) and at Strzelecki (McKirdy, 1982c).

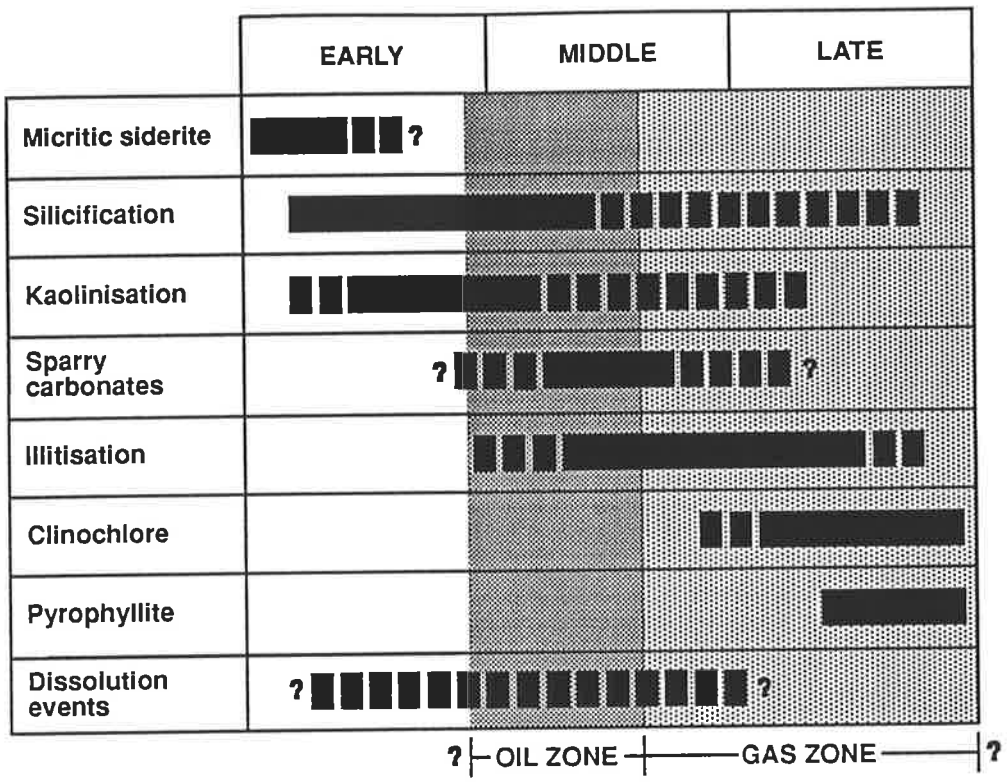

Figure 4.6 Paragenetic sequence for authigenic minerals in the Permian reservoir sandstones of the southern Cooper Basin in relation to early, middle and late diagenesis. The approximate timing of oil and gas generation and migration is indicated. Sparry cements include siderite, ankerite, dolomite and calcite. The timing of microspar development is uncertain but is believed to occur after the formation of micrite and prior to, or synchronous with sparry cement genesis (cf. Chapter 6) (modified from Schulz-Rojahn & Phillips, 1989).

Petrographic evidence suggests fluid inclusions in quartz overgrowths may contain dead oil/bitumen. Similar results are reported by Bone & Russell (1988) for sandstones in the Cooper Basin. Hence, silicification appears to coincide with oil migration, although it could not be ascertained which phase of overgrowth development is associated with this event. The fact that dead bitumen/oil frequently occurs in primary pores between euhedral quartz overgrowths indicates the main phase of liquid hydrocarbon migration postdated quartz cementation in many areas (Schulz-Rojahn et al., 1991). This is supported by the observation that no differences in silicification between hydrocarbon-bearing and water-wet reservoir intervals were observed in the Wancoocha, Moomba and Strzelecki Fields (Thomas, 1990; Eleftheriou, 1990; Schulz-Rojahn & Phillips, 1991). The data emphasises that the

development of quartz overgrowths in these areas had ceased by the time hydrocarbons migrated into the reservoirs. However, it is possible that in other parts of the basin quartz cementation proceeded during later stages of diagenesis, including chemical compaction.

There may have been one single continuous phase of liquid hydrocarbon generation associated with the final stage of quartz cementation, culminating after quartz overgrowth formation in some parts of the southern Cooper Basin. Alternatively, it is possible there were earlier minor phases of petroleum generation synchronous with quartz cementation which are evident as fluid inclusions. Some fluid inclusions within the quartz overgrowths may also contain gaseous hydrocarbons.

Oil characterised by yellow fluorescence under the UV microscope is associated with siderite cements in several clastics from throughout the study area. In sandstones where the oil is found around the margins of pores filled with carbonate spar, cement stratigraphy clearly indicates that the siderite spar formed after oil migration into the reservoir rock. In other sands, oil is found intimately mixed with the carbonate spar/microspar matrix, rendering identification of the relative sequence of events more difficult. One possibility is that the oil migrated into submicroscopic pores within the carbonate cement in which case the siderite predates oil migration. The pores may be remnant pores between individual carbonate crystals, or secondary pores resulting from minor dissolution of the carbonate cement (as possibly indicated by their irregular size and shape), or a combination of the two. An alternative explanation is that carbonate genesis occurred synchronous with oil migration, the siderite precipitating from pore waters carrying hydrocarbons. This raises the question whether there may be a hydrocarbon-derived origin of the carbonate cements in the study area, as suggested by other authors for different basins (Donovan 1974a; Donovan et al., 1974; Gould & Smith, 1978; Duchscherer, 1982; Al-Shaieb & Lilburn, 1982; Oehler & Sternberg, 1984; Dimitrakopoulos & Muehlenbachs, 1985, 1987; Hovland et al., 1987; Prikryl et al., 1988). The hydrocarbons may have acted as a source of carbon for carbonate precipitation. This possibility is further discussed in Chapter 6 in the light of carbon isotope data.

In contrast to the spar and microspar cements, the micritic siderite in the study area is not associated with dead bitumen/oil, implying that micrite formed prior to liquid hydrocarbon generation. This is in accordance with the interpretation that micritic siderite represents an early diagenetic product and precipitated in the shallow subsurface (Schulz-Rojahn & Phillips, 1989), long before liquid hydrocarbon generation was initiated.

Kaolin clay patches also occasionally contain dead bitumen. This suggests liquid hydrocarbons (?condensates) were able to migrate into the submicroscopic

network of pores that exists between the kaolin booklets (Chapter 5), indicating kaolinisation took place prior to hydrocarbon migration in some areas. Again, an alternative interpretation is possible, namely that kaolinisation and hydrocarbon emplacement took place simultaneously in the reservoir rocks; liquid hydrocarbons became trapped within the kaolin matrix as the clays precipitated out of the pore waters. Differentiation between these two models is presently not possible.

Authigenic illite is relatively uncommon, and no clear textural relationships exist to determine the timing of illite formation in relation to the onset of hydrocarbon generation and migration in the study area. Illite is considered to have formed during the intermediate and late stages of diagenesis, probably synchronous with gas/condensate generation although possibly earlier (Fig.4.6).

Clinochlore and pyrophyllite are thought to have precipitated after oil generation. The two clay species occur only in the central Nappamerri Trough containing abundant dry gas (Kantsler et al., 1983). Dry gas (dominantly methane) can be produced from organic matter in great quantities at vitrinite reflectance levels exceeding 2.0 percent (Tissot & Welte, 1978). Such thermal maturity levels (and greater) are presently attained in the central Nappamerri Trough (Kantsler et al., 1983) (Table 4.5), hence gaseous hydrocarbons are probably still being generated in this area at the present time. For this reason, the formation of clinochlore and pyrophyllite is considered to have occurred synchronous with the generation of gaseous hydrocarbons in this area (Fig.4.6). The possibility exists that the formation of clinochlore and pyrophyllite is an on-going process at depth in the central Nappamerri Trough today.

CHAPTER FIVE

POROSITY AND PERMEABILITY

5.1 Introduction

Various workers have commented on the nature of porosity in the southern Cooper Basin. Steveson & Spry (1973) believe that evidence of primary porosity is almost completely absent in sandstones from the Tirrawarra and Gidgealpa Field areas. They consider most of the porosity to be of secondary origin. A similar view is held by Stanley & Halliday (1984, p.182) who state that "secondary porosity is the dominant [porosity] type in all sandstones" in some deep wells in the Big Lake Field. In contrast, Martin & Hamilton (1981) report abundant remains of primary porosity in some sandstones from the Toolachee Formation in the southern Cooper Basin. These workers are of the opinion that there is only sporadic development of secondary porosity, with some interstitial microporosity between clay particles in this region. Similarly, Heath (1989) attributes regional porosity trends in the southern Cooper Basin to essentially primary porosity distribution. A more complex porosity interrelationship is highlighted by Schulz-Rojahn & Phillips (1989) who describe both primary and secondary porosity, and stress the importance of microporosity associated with clays in the same area.

In the present chapter, the nature of porosity in the southern Cooper Basin is more closely investigated. An understanding of the types of porosity from which hydrocarbons may be produced is considered paramount to both petroleum exploration and field development operations. Knowledge of the controls affecting porosity and permeability can enhance reservoir-quality prediction in the subsurface and improve exploration success ratios. Generic porosity recognition may also impact on reservoir stimulation techniques and reserve calculations.

For documentation of the nature of reservoir styles in the southern Cooper Basin, the chapter is divided into three main parts. Part I, based on statistical investigation of available core analysis data, focuses on the porosity and permeability characteristics of the Permian sediments. Broad regional aspects of reservoir quality

are discussed, presenting the reader with a basic understanding of porosity-permeability trends with depth, and for various stratigraphic intervals. A comparison is made to other petroleum provinces throughout the world. Part II focuses on diagenetic results obtained from techniques such as optical petrography, cathodoluminescence, scanning electron microscopy, and X-ray diffraction. Generic porosity types are outlined, and their productive capability is assessed by integration of petrographic data with DST results. Thin section data is correlated against burial depth and thermal sediment maturity. The influence of sedimentary facies relationships on reservoir quality is evaluated. Part III synthesises study results from the previous two sections into a regional model of porosity distribution. The factors controlling porosity and permeability are discussed, with particular emphasis on implications for improved play definition in the basin. Potential problems pertaining to wireline log evaluation and production operations in the Cooper Basin are highlighted.

5.2 Part I: Statistical investigation of core plug data

5.2.1 Data source

A total of 7122 porosity and 6773 permeability values [17] from 148 field and wildcat wells located in PEL 5 & 6 in South Australia were incorporated into the present investigation (Fig.5.1; Table 5.1). Study wells selected include wells from the Toolachee, Nappacoongee-Murteree, Murta, Moomba, Lake Hope, Merrimelia-Innamincka, Patchawarra Southwest, Patchawarra Central, and Patchawarra East petroleum blocks (Fig.5.1). The porosity-permeability data was obtained from the Cooper Basin Consortium Group of Companies, as well as the South Australian Department of Mines and Energy [18] (see Morton, 1989; Gravestock & Alexander, 1988, 1989); the data pool was supplemented by 145 core plugs taken during NERDDC project 1175 (Appendices D & J).

The bulk of the core plugs originates from the Toolachee and Patchawarra Formations; other stratigraphic intervals represented include the Nappamerri, Daralingie, Epsilon, Tirrawarra and Merrimelia Formations (Fig.5.2). An additional 1023 porosity and 963 permeability values were derived from the Jurassic/Cretaceous sediments of the superjacent Eromanga Basin. The depth range covered is from

[17] Derived from whole-core analyses under laboratory conditions
[18] NERDDC project numbers 820 and 1033

Table 5.1
List of Cooper Basin wells incorporated into the present porosity-permeability study. Refer to Figure 5.1 for well locations (italics). Values in brackets represent number of core analyses included per well.

1 Andree-1 (11)
2 Andree-2 (47)
3 Beanbush-1 (55)
4 Big Lake-1 (98)
5 Big Lake-2 (202)
6 Big Lake-3 (41)
7 Big Lake-4 (15)
8 Big Lake-5 (28)
9 Big Lake-27 (81)
10 Big Lake-29 (19)
11 Big Lake-31 (42)
12 Big Lake-32 (49)
13 Big Lake-33 (14)
14 Big Lake-34 (15)
15 Big Lake-35 (39)
16 Big Lake-45 (44)
17 Boxwood-2 (1)
18 Brolga-1 (106)
19 Burke-1 (73)
20 Burke-3 (22)
21 Burke-4 (37)
22 Burley-1 (17)
23 Burley-2 (30)
24 Coochilara-1 (11)
25 Coonatie-1 (16)
26 Corkwood-1 (71)
27 Cuttapirrie-1 (9)
28 Daralingie-1 (43)
29 Daralingie-2 (105)
30 Daralingie-3 (13)
31 Daralingie-4 (9)
32 Daralingie-7 (57)
33 Daralingie-8 (11)
34 Daralingie-9 (56)
35 Daralingie-15 (32)
36 Daralingie-19 (16)
37 Daralingie-22 (32)
38 Della-1 (60)
39 Della-2 (97)
40 Della-3 (11)
41 Della-4 (106)
42 Della-5a (84)
43 Della-6 (69)
44 Dilchee-1 (16)
45 Dirkala-1 (26)
46 Dullingari-1 (5)
47 Dullingari-2 (10)
48 Dullingari-11 (12)
49 Dullingari-16 (67)
50 Dullingari-17 (118)
51 Dullingari-19 (39)
52 Dullingari-23 (53)
53 Dullingari-24 (19)
54 Dullingari-25 (14)
55 Dullingari-44 (19)
56 Dullingari North-1 (67)
57 Dullingari North-2 (20)
58 Dullingari North-3 (13)
59 Fly Lake-2 (164)
60 Fly Lake-3 (108)
61 Fly Lake-4 (158)
62 Fly Lake-6 (26)
63 Gidgealpa-3 (3)
64 Gidgealpa-16 (78)
65 Innamincka-1 (27)
66 Jack Lake-1 (70)
67 Kerna-1 (37)
68 Kidman-2 (53)
69 Kirby-1 (19)
70 Kudrieke-1 (140)
71 Lake Hope-1 (2)
72 Marsilea-1 (19)
73 McKinlay-1 (52)
74 McLeod-1 (27)
75 Merrimelia-5 (140)
76 Merrimelia-6 (160)
77 Merrimelia-7 (58)
78 Merrimelia-8 (40)
79 Merrimelia-15 (38)
80 Moomba-1 (104)
81 Moomba-3 (109)
82 Moomba-4 (65)
83 Moomba-5 (48)
84 Moomba-6 (97)
85 Moomba-7 (63)
86 Moomba-8 (126)
87 Moomba-9 (72)
88 Moomba-10 (103)
89 Moomba-15 (6)
90 Moomba-18 (19)
91 Moomba-19 (64)
92 Moomba-26 (7)
93 Moomba-27 (11)
94 Moomba-45 (41)
95 Moomba-46 (27)
96 Moomba-47 (60)
97 Moomba-48 (32)
98 Moomba-52 (85)
99 Moomba-53 (110)
100 Moomba North-1 (19)
101 Moomba South-1 (1)
102 Moorari-1 (58)
103 Moorari-5 (73)
104 Mudera-1 (74)
105 Mudlalee-2 (5)
106 Mudrangie-1 (91)
107 Munkarie-1 (12)
108 Munkarie-4 (53)
109 Murteree-1 (19)
110 Nappacoongee-2 (61)
111 Nungeroo-1 (22)
112 Packsaddle-1 (6)
113 Packsaddle-2 (14)
114 Packsaddle-3 (5)
115 Pelketa-1 (7)
116 Pinna-1 (36)
117 Strzelecki-1 (81)
118 Strzelecki-2 (38)
119 Strzelecki-3 (84)
120 Strzelecki-4 (233)
121 Strzelecki-5 (116)
122 Strzelecki-10 (46)
123 Strzelecki-15 (26)
124 Strzelecki-16 (42)
125 Tilparee-A1 (34)
126 Tirrawarra-8 (40)
127 Toolachee-1 (36)
128 Toolachee-2 (11)
129 Toolachee-3 (135)
130 Toolachee-4 (29)
131 Toolachee-5 (96)
132 Toolachee-6 (108)
133 Toolachee-7 (43)
134 Toolachee-8 (10)
135 Toolachee-9 (34)
136 Toolachee-12 (14)
137 Toolachee-14 (2)
138 Toolachee-15 (33)
139 Toolachee-18 (30)
140 Toolachee-19 (42)
141 Toolachee-21 (5)
142 Wancoocha-1 (7)
143 Wancoocha-3 (24)
144 Wancoocha-4 (26)
145 Wantana-1 (43)
146 Wilpinnie-1 (50)
147 Woolkina-1 (12)
148 Yapeni-1 (23)

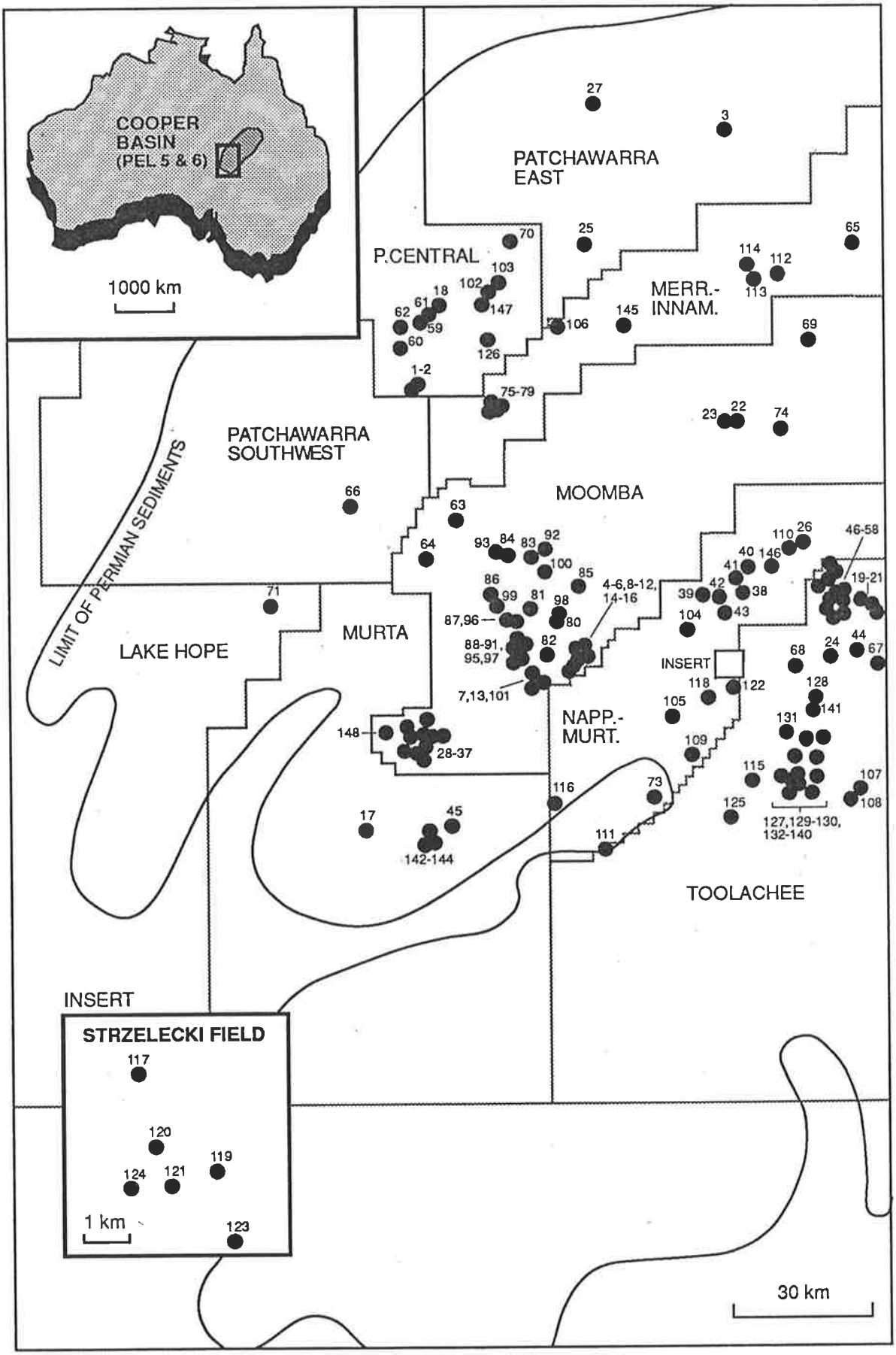

Figure 5.1 Location of study wells from which porosity and permeability data was derived [Numbers refer to well codes shown in Table 1.1].

approximately 2800 to 11800 feet subsea (Fig.5.3). Various structural provinces are represented, including the Gidgealpa-Merrimelia-Innamincka and the Nappacoongee-Murteree anticlinal trends, and the Patchawarra, Nappamerri and Tennaperra Troughs (Fig.5.1). The data set incorporates porosity and permeability values from marginal and mid-flank areas of the basin, as well as the basin interior. Petroleum fields represented include Big Lake, Daralingie, Della, Dullingari/Burke, Fly Lake, Merrimelia, Moomba, Munkarie, Strzelecki, Toolachee and Wancoocha (Table 5.1).

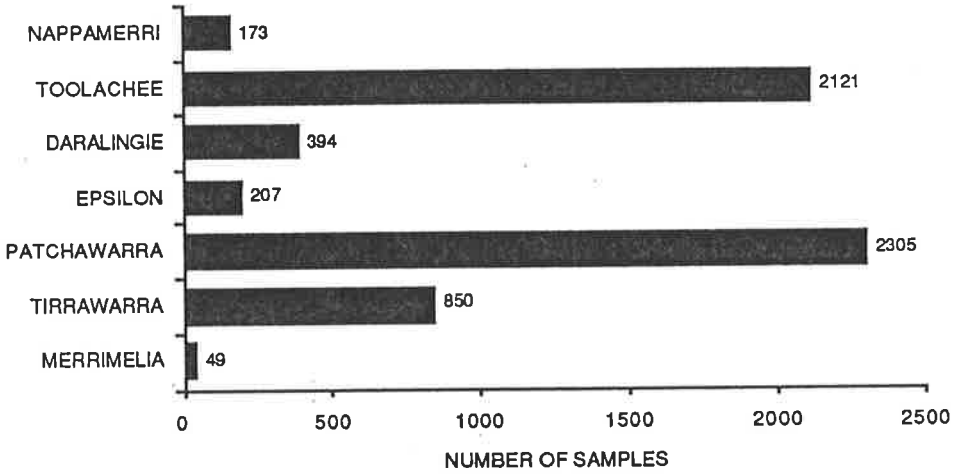

Figure 5.2 Stratigraphic distribution of Cooper Basin core plugs. The bulk of the data is derived from the Toolachee and Patchawarra Formations.

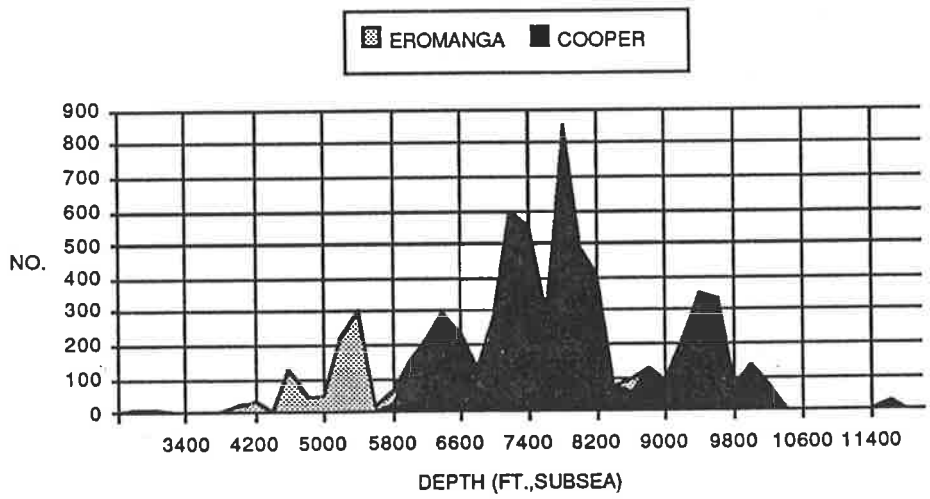

Figure 5.3 Core plug distribution versus subsea burial depth, Cooper and Eromanga Basins [No. = number of samples].

The porosity-permeability data was compiled and processed using Mincom Geolog software, and is available on request in ASCII format from the National Centre for Petroleum Geology & Geophysics (NCPGG), Adelaide. The raw data is included in Appendix K. All core analyses were made under ambient laboratory conditions; depth references are standardised to subsea depths.

5.2.2 Data limitations

A number of problems arise when evaluating conventional core plug data. A draw-back is that porosity and permeability measurements were routinely made at atmospheric pressures [19] , and do not strictly reflect true in-situ reservoir conditions. As a result, both core porosity and core permeability measurements may be up to an order of magnitude too high (Thomas & Ward, 1972; Walls et al., 1982). These measurements are shown in Table 5.2 where the effect of overburden pressure on porosity/permeability values is demonstrated: both core porosity and permeability measurements are lowered as a function of increasing net overburden pressure (NOB). Other factors which may potentially enhance core analysis measurements in the laboratory include the artificial drying of clays, gas slippage (Klinkenberg) effects, and the loss of aqueous pore fluids as compared to high irreducible water saturations (S_{Wirr}) at reservoir conditions (Jones & Owens, 1980; Morton, 1989).

A further potential problem in evaluating porosity-permeability data is that core material may undergo extensive mechanical stress during core recovery, slabbing, or cutting of core plugs; this may result in artificially high fracture permeabilities, and sometimes also fracture porosities. An example includes the Epsilon Formation cored at Burley-2 where an anomalously high, fracture-induced permeability measurement (48 md) was obtained in a sequence of low-permeability (< 1md) clastics (Fig. 5.4). Such fractures frequently are sub-parallel to stylolite seams, of tensional nature, and form in response to unloading of the rock parallel to the direction of maximum stress (Nelson, 1981). The fractures are not always easily detected because of their sub-microscopic size (see section 5.2.3).

For the above mentioned reasons, porosity and permeability statistics cited in the present investigation should be considered as maximum values which is to be taken into account when considering the following discussion.

---

19 Ambient pressure adopted by service companies for routine core analysis max. 2758 kPa (Morton, 1989) (see Chapter 1).

Table 5.2
Comparison of core plugs for which ambient and overburden porosities and permeabilities were measured. Wells from marginal, basinal and intermediate positions are contrasted [ambient = 2758 kPa; NOB = net overburden pressure; see below] [Data made available by the South Australian Department of Mines and Energy (NERDDC project 1033)].

	Depth (ft.logger)	Porosity (%) (ambient)	(NOB)	Permeability (md) (ambient)	(NOB)
Wancoocha-3 [1]: Patchawarra Fm [marginal]	5788.5	10.5	10.1	0.261	0.015
	5790.5	9.1	9	0.045	0.003
	5793.5	14.9	14.2	1.5	1.1
	5794.5	14.5	13.9	1.5	0.986
	5795	10.2	9.6	0.204	0.05
	5796	13.2	12.7	7	5.3
	5797.5	17.2	16.7	14.4	10.8
	5799.5	19.1	18.4	24.8	19.2
	5800.5	17.5	17	12.4	9
	5802	20.3	19.7	64	51
Dullingari-16 [2]: Toolachee Fm [intermediate]	7030	14.5	13.6	110	90
	7032.5	12.6	12.3	26	20.1
	7034	14.5	13.9	213	170
	7040	6.7	6.4	0.062	0.006
	7052	9.1	8.4	2.9	2.1
	7053.5	11.5	11	165	134
	7060	8.7	7.9	0.845	0.162
	7061.5	14.5	13.9	152	107
	7062.5	12	11.4	7.9	5.3
	7063	14.1	13.4	111	87
Big Lake-31 [3]: Tirrawarra Fm [basinal]	9962.5	8.8	8	0.565	0.228
	9965.5	8.9	8.1	0.433	0.107
	9971.5	7.5	6.5	0.198	0.071
	9980	8.7	7.9	0.499	0.151
	9981	7.3	6.7	0.184	0.046
	9984	9.2	8.3	0.675	0.182
	9987.5	9.9	9	0.638	0.228
	10202.5	2.6	2.6	0.014	0.01
	10205	2.1	1.9	0.23	0.001
	10216.5	8.2	7.4	0.396	0.82

[1] NOB = 18000 kPa
[2] NOB = 26998 kPa
[3] NOB = 38310 kPa

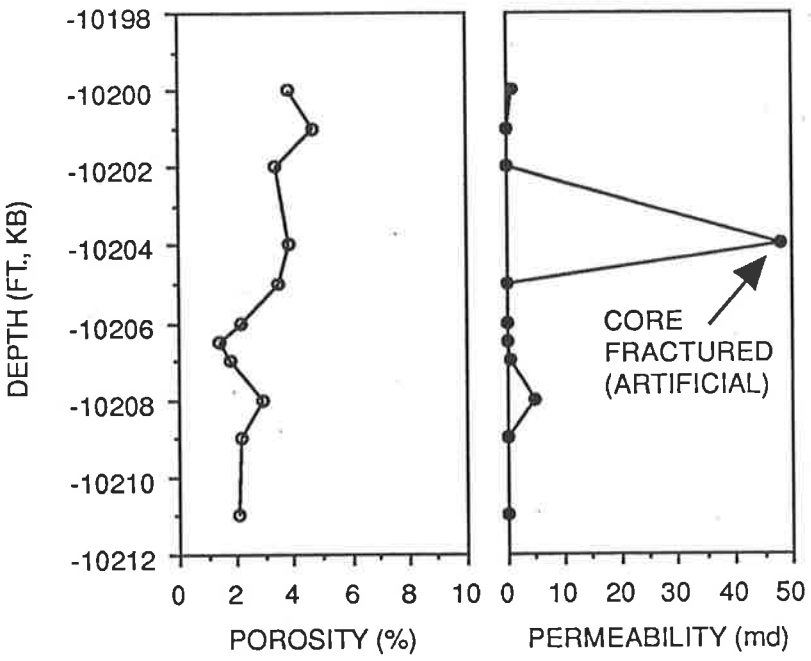

Figure 5.4 Effect of mechanical fracturing on porosity/permeability measurements, as observed in core material derived from the Epsilon Formation at Burley-2.

5.2.3 Results

5.2.3.1 General reservoir character

Measured core porosities in the Cooper Basin range up to 27.7 percent; associated permeabilities may be as high as 6820 md (Fig.5.5a; Table 5.6 a & b). On average, however, the basin is characterised by much lower-quality reservoir sandstones. Mean core porosity is 10.7 percent (Fig.5.5a) and average permeability 30.3 md (Fig.5.6). Over 75 percent of clastics have permeabilities no greater than 5 md, and just 7 percent have permeabilities exceeding 100 md (Table 5.3).

In comparison, the superjacent oil-prone Eromanga Basin has generally much better reservoir characteristics. Core porosities range up to almost 40 percent (Fig.5.5b), and permeabilities as high as 10200 md have been measured. Average porosity in the Eromanga Basin is 15.9 percent (Fig.5.5b) and mean permeability 369 md (Fig.5.6). In this basin, over 60 percent of clastics have permeabilities exceeding 100 md (Table 5.3).

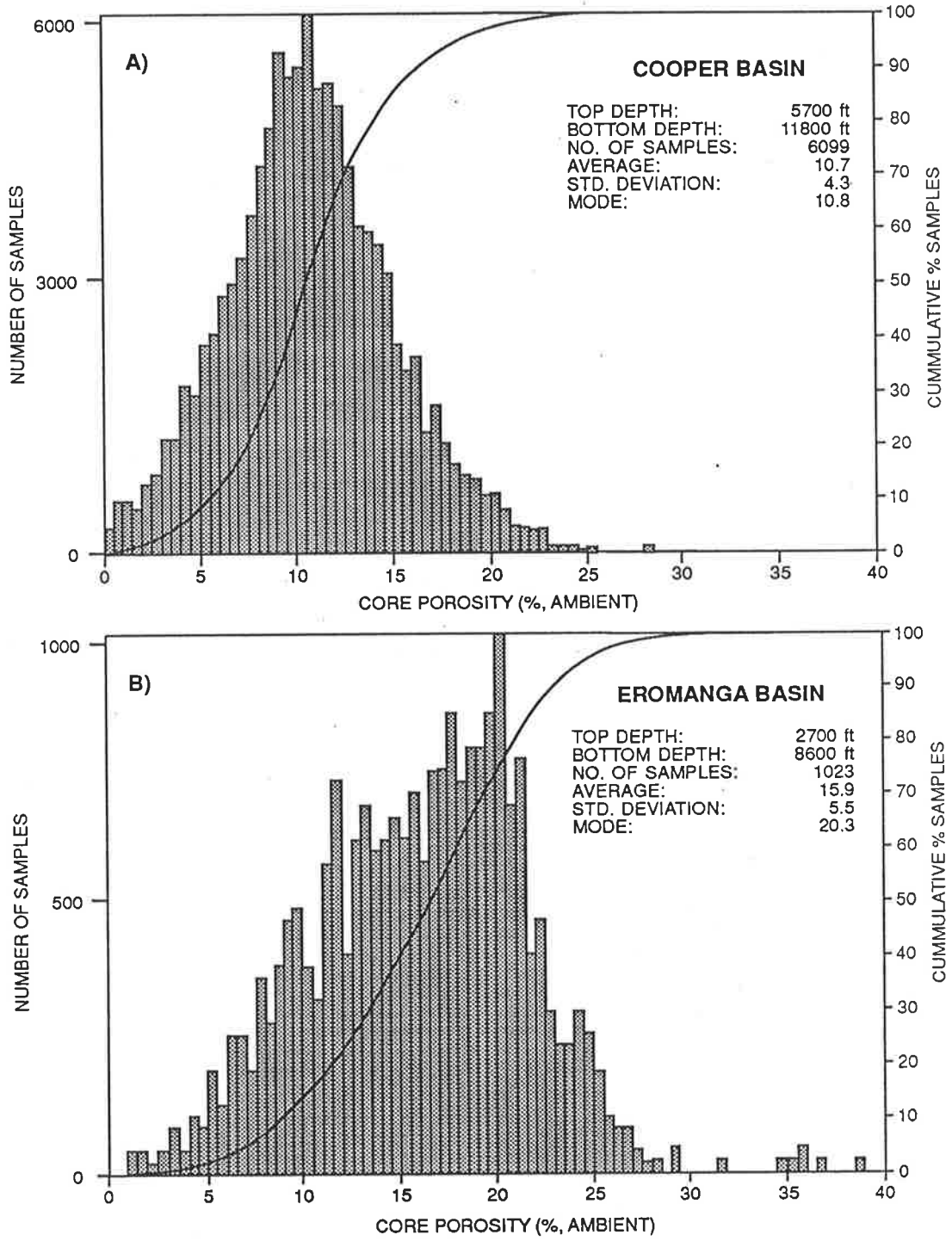

Figure 5.5 Frequency histogram and cummulative curve of porosity distribution in the Cooper (A) and Eromanga (B) Basins.

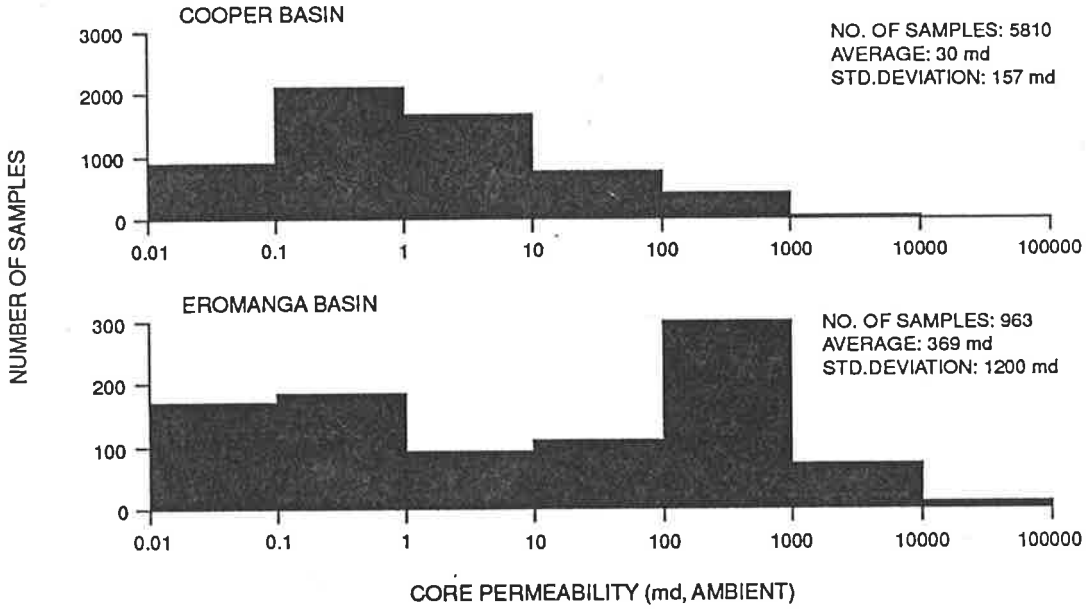

Figure 5.6 Frequency histogram showing permeability characteristics of the Cooper and Eromanga Basins. Note predominance of low-permeability clastics in the Cooper Basin.

	Number of samples		Cumm. % samples	
Permeability (md)	Cooper Basin	Eromanga Basin	Cooper Basin	Eromanga Basin
0.1 or less	813	173	14	18
0.1 - 2	2847	193	63	38
2 - 5	727	48	75.5	43
5 - 10	262	38	80	47
10 - 50	581	77	90	55
50 - 100	174	38	93	59
100 - 500	290	231	98	83
500 - 1000	99	87	99.7	92
1000 - 5000	11	58	99.9	98
5000 - 10000	6	10	100	99
10000 - 50000	0	10	100	100

Table 5.3 Comparison of permeability characteristics for Cooper and Eromanga Basin clastics. The bulk of reservoir sands in the Cooper Basin have permeabilities less than 10 md whereas the reverse is true for the Eromanga Basin sediments.

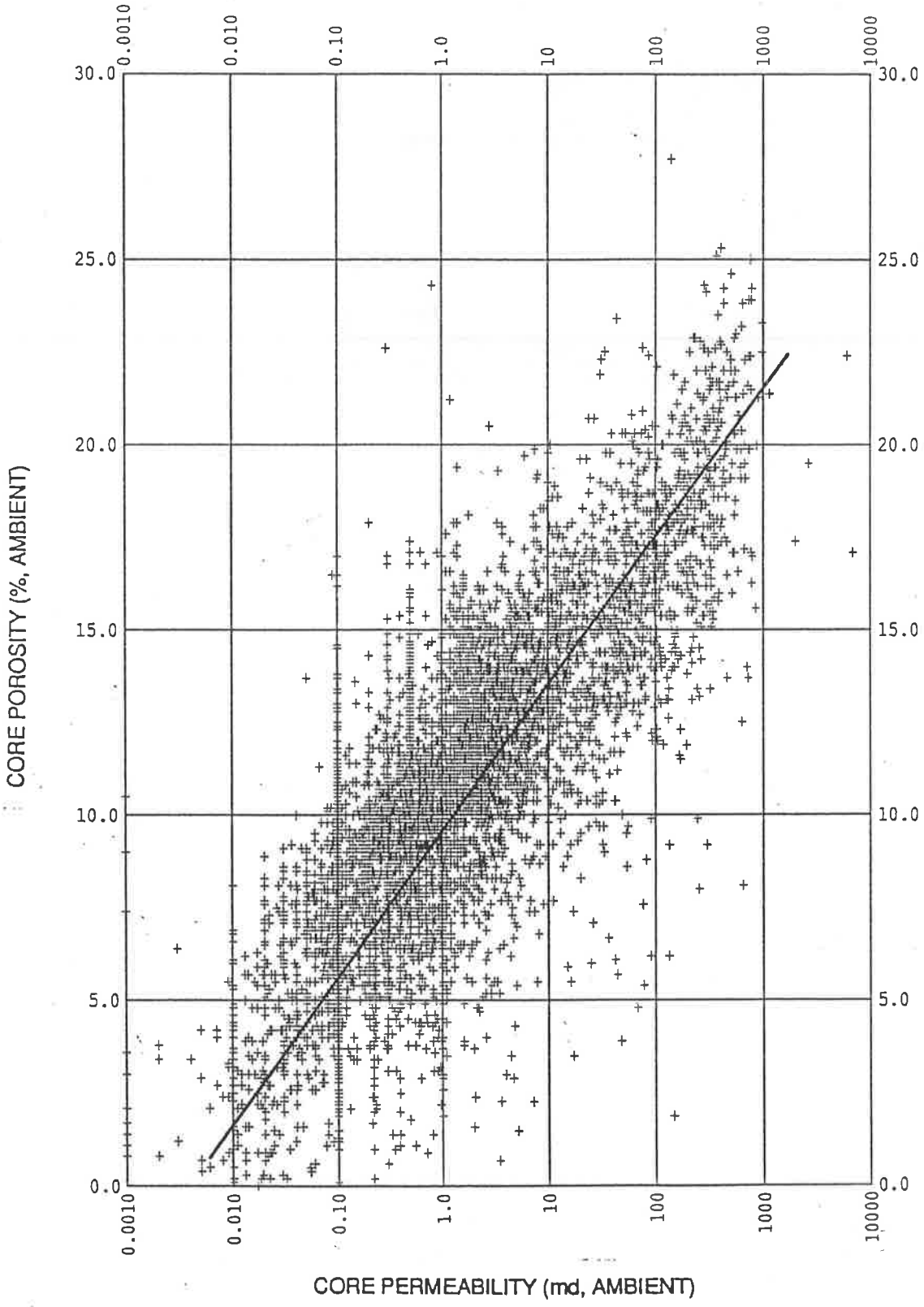

Figure 5.7 Crossplot of core porosity (%) versus core permeability (md).

5.2.3.2 Porosity versus permeability

Figure 5.7 illustrates the relationship between core porosity and permeability - core permeability broadly increases with increasing reservoir porosity. The crossplot can be used to provide an estimate for mean and maximum reservoir permeability expectable at any given porosity value. The indicated line suggests that mean permeability changes by a factor of about 10 for each 4 percent change in porosity (Fig.5.7).

5.2.3.3 Stratigraphic variability

Few differences in porosity character are apparent between the various stratigraphic horizons of Permo-Triassic age (Table 5.4a). The stratigraphic intervals exhibit similar mean porosity values, the highest porosity average being associated with the Toolachee Formation. The same formation also gave the highest overall porosity value (27.7 percent).

In contrast, when the general permeability character of the formations is studied, subtle differences are noted (Table 5.4b). There is a broad decrease in mean permeability with formations of increasing geologic age. Again, the Toolachee Formation has the best overall reservoir potential, being associated with the highest-permeability sands; mean permeability of this formation is 49 md as compared to only 6 md for the Tirrawarra Formation, and 1.1 md for the Merrimelia Formation (Table 5.4b). Permeability values greater than 1000 md were measured exclusively in clastics of the Toolachee, Daralingie and Patchawarra Formations (Table 5.4b).

5.2.3.4 Lateral changes

Lateral reservoir character is not uniform but broad trends are apparent (Fig. 5.8 a & b; Table 5.5 a & b). In general, the best-quality reservoir sands are present in the marginal and mid-flank areas of the basin. Average porosity values in Toolachee sandstones are similar in the Daralingie, Della and Strzelecki Fields, ranging between about 13 to 15 percent; mean porosity values in Patchawarra sands vary between

Table 5.4a
Statistical comparison of core porosity data (%) derived from various stratigraphic horizons of Permo-Triassic age, southern Cooper Basin.

Formation	Min.	Max.	Mean	St.dev.	No.
Nappamerri	2	22.6	10.6	4.2	173
Toolachee	0.1	27.7	11.7	4.3	2121
Daralingie	0.6	23.8	9.3	4.7	394
Epsilon	0.5	22.5	9.2	4.8	207
Patchawarra	0.2	24.3	10.4	4.2	2305
Tirrawarra	0.4	22.5	10.1	3.7	850
Merrimelia	0.4	15.3	9.3	3.6	49

Table 5.4b
Statistical comparison of core permeability data (md) derived from various stratigraphic horizons of Permo-Triassic age, southern Cooper Basin.

Formation	Min.	Max.	Mean	St.dev.	No.
Nappamerri	<0.01	766	34	107	159
Toolachee	<0.001	6820	49	205	2020
Daralingie	0.01	1262	42	139	403
Epsilon	<0.001	396	22	62	193
Patchawarra	<0.001	6077	20	145	2223
Tirrawarra	<0.01	313	6	21	763
Merrimelia	<0.001	10	1.1	1.8	49

approximately 12 to 13 percent in the same areas, including the Toolachee Field (Fig. 5.8a; Table 5.5a). A high porosity average (15.6 percent) is further associated with Patchawarra sands in the Wancoocha Field, located in close vicinity to the basin margin (Fig.5.1). Towards the basin interior, average porosity values decline. In the Moomba Field, mean reservoir porosity is 9.5 percent in the Toolachee Formation, and 6.6 percent in the Patchawarra Formation. A similar porosity relationship is apparent for the Big Lake Field (Fig.5.8a; Table 5.5a). Relatively little core material was taken from wells drilled in the central Nappamerri Trough, however available data suggests mean porosity is 6.5 percent in Toolachee sandstones from the Burley and Kirby wells; the average porosity of Patchawarra sands intersected at Burley-2 is 2 percent (Fig.5.8a; Table 5.5a).

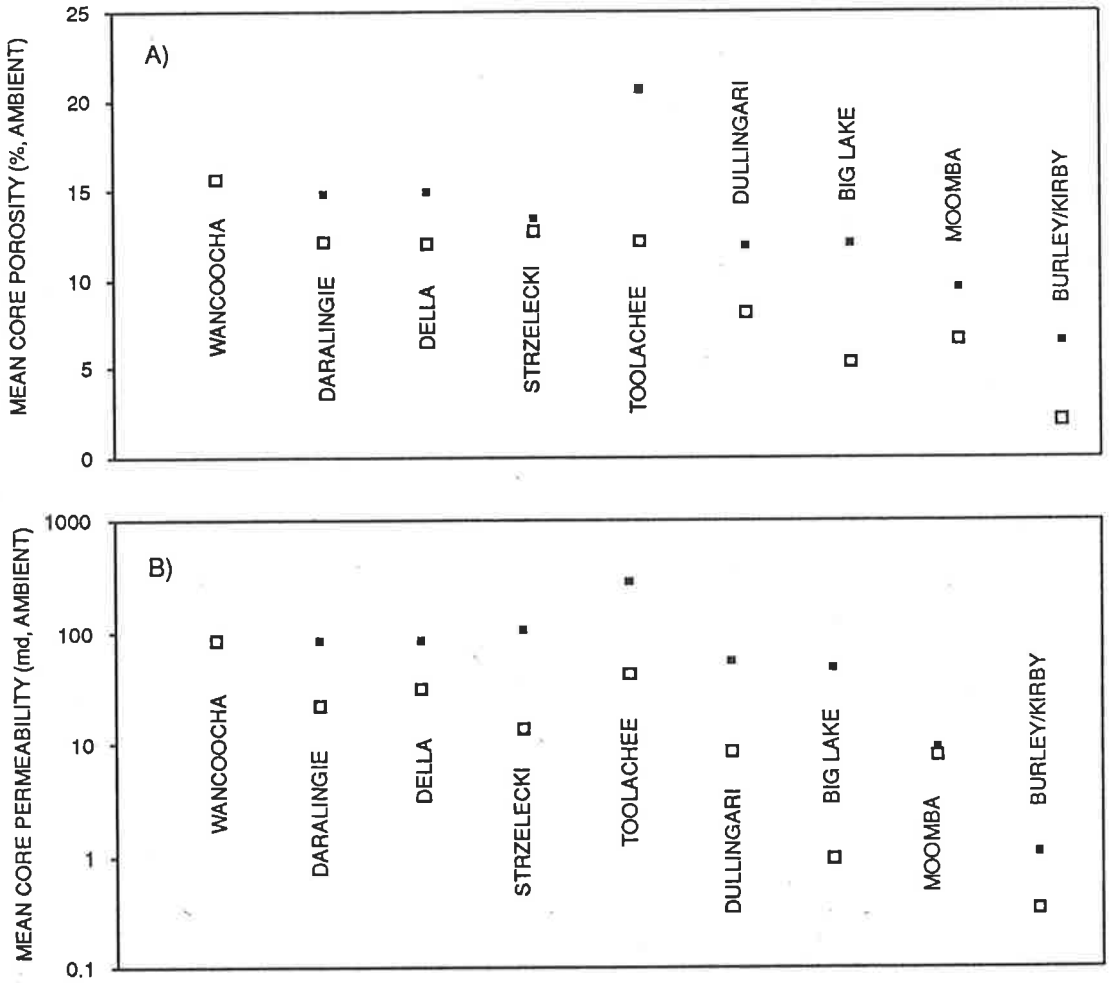

Figure 5.8a,b Values of average core porosity (a) and core permeability (b) for a variety of petroleum fields in the southern Cooper Basin (black squares = Toolachee Formation; open squares = Patchawarra Formation) (see Table 5.5 a & b for depth ranges for each petroleum field).

Table 5.5a
Comparison of porosity (%) data derived from core plug analyses from a variety of petroleum fields, southern Cooper Basin.

Formation	Depth (ft., subsea)	Min.	Max.	Mean	St.Dev.	No.
Daralingie Field						
Toolachee	6265-6360	2.8	20.3	14.8	4.6	17
Patchawarra	7130-7440	0.2	22.6	12.1	3.9	323
Della Field						
Toolachee	6100-6570	4.4	27.7	14.9	4.5	377
Patchawarra	6525-6560	6	14	12	2.2	16
Wancoocha Field						
Toolachee *	-	-	-	-	-	-
Patchawarra	5700-6090	7.2	20.3	15.6	3.9	29
Strzelecki Field						
Toolachee	5865-6230	3	23.2	13.4	3.2	264
Patchawarra	6330-6390	3.2	18.3	12.6	3.2	26
Toolachee Field						
Toolachee	5855-5870	19.4	22	20.6	1.1	3
Patchawarra	6695-7405	0.2	23.4	12.06	4.1	620
Dullingari Field						
Toolachee	6605-7000	4.9	19	11.8	3	79
Patchawarra	7735-8360	0.7	17.6	8.1	3.2	348
Big Lake Field						
Toolachee	7330-7720	0.1	21.6	11.9	4.3	327
Patchawarra	8480-9545	0.4	10.7	5.3	2.1	95
Moomba Field						
Toolachee	7480-8200	0.1	19.4	9.5	3	779
Patchawarra	8880-9700	1.5	19.8	6.6	5.1	19
Burley/Kirby						
Toolachee	8600-9070	0.2	14.5	6.46	3.89	28
Patchawarra	11195-11225	0.04	4.3	2	1.67	13

* Toolachee Formation absent

Table 5.5b
Comparison of permeability (md) data derived from core plug analyses from a variety of petroleum fields, southern Cooper Basin.

Formation	Depth (ft., subsea)	Min.	Max.	Mean	St.Dev.	No.
Daralingie Field						
Toolachee	6265-6360	0.019	666	84.5	155	17
Patchawarra	7130-7440	<0.001	1121	21.7	90	323
Della Field						
Toolachee	6100-6570	<0.01	974	84	173.5	353
Patchawarra	6525-6560	0.001	150	30.5	42.5	16
Wancoocha Field						
Toolachee *	-	-	-	-	-	-
Patchawarra	5700-6090	0.03	739	82.7	158	29
Strzelecki Field						
Toolachee	5865-6230	<0.001	6820	103	476	264
Patchawarra	6330-6390	0.1	90	13.9	21.3	26
Toolachee Field						
Toolachee	5855-5870	236	298	275	27.9	3
Patchawarra	6695-7405	<0.01	6077	42.2	267	574
Dullingari Field						
Toolachee	6605-7000	<0.01	300	54.1	82	79
Patchawarra	7735-8360	<0.01	269	8.5	32.2	348
Big Lake Field						
Toolachee	7330-7720	<0.01	865	47.9	112	326
Patchawarra	8480-9545	<0.01	16	0.93	2.5	95
Moomba Field						
Toolachee	7480-8200	<0.01	718	9.11	48.6	759
Patchawarra	8880-9700	0.06	88	7.95	21.1	19
Burley/Kirby						
Toolachee	8600-9070	0.001	5.7	1.08	1.51	28
Patchawarra	11195-11225	0.013	3.5	0.34	0.96	13

* Toolachee Formation absent

The lateral variation in porosity values is reflected by the permeability data from the various petroleum fields (Fig. 5.8b; Table 5.5b). Mean permeability values decrease from marginal and midflank areas of the basin towards the deep interior. In the Daralingie, Della, Strzelecki and Toolachee Fields, average permeabilities in Toolachee sandstones vary between about 84 and 275 md (Fig.5.8b; Table 5.5b). At Big Lake, mean permeability is 48 md for the same stratigraphic interval, and in the Moomba Field 9.1 md. Toolachee sandstones from the Burley and Kirby wells have an average permeability value of about 1 md. A similar trend is apparent for the Patchawarra sandstones, mean permeability values decreasing from as high as 83 md in marginal positions (Wancoocha) to less than 1 md in the Nappamerri Trough (Big Lake, Burley-2) (Fig.5.8b; Table 5.5b).

5.2.3.5 Vertical changes

The relationship between porosity/permeability and depth is illustrated in Figures 5.9 to 5.12. Crossplots of porosity/permeability versus depth show a broad, but not very clearly defined trend (Fig.5.9a,b). In general, both porosity and permeability decrease towards greater burial depths (Fig.5.9a,b). There is, however, a wide range of porosity/permeability values at any given depth, highlighting the complexities involved in understanding the controls affecting reservoir quality in the basin. For example, at a depth of about 8000 feet, core porosities vary between almost zero and 24 percent (Fig.5.9a); associated permeabilities range between less than 0.01 to more than 100 md (Fig.5.9b). The results suggest that other factors, besides depth of burial, influence reservoir quality in the basin on a regional scale.

When the porosity/permeability data is averaged over 200-ft intervals, the broad deterioration of reservoir quality with depth is more apparent (Figs.5.10, 5.11a,b; Table 5.6a,b). Figure 5.10 illustrates the porosity-depth curve for the Cooper Basin sediments. Based on a visual line of best fit, the average loss of porosity is fairly gradual, corresponding to a gradient of about 1.5 percent per 1000 feet (Fig.5.10). However, an alternative porosity gradient is possible, characterised by three distinct phases (Fig.5.10). In the first phase, mean porosity loss with depth is relatively rapid, from about 15 percent at 5800-6000 feet to approximately 10 percent at 8000 feet. In the second phase, average reservoir porosity remains relatively constant at 9 to 10 percent to depths approaching 10200 feet. Finally, based on a statistically small number of samples only, mean porosity diminuishes to less than 2 percent at burial depths close to 12000 feet (Fig.5.10; Table 5.6a).

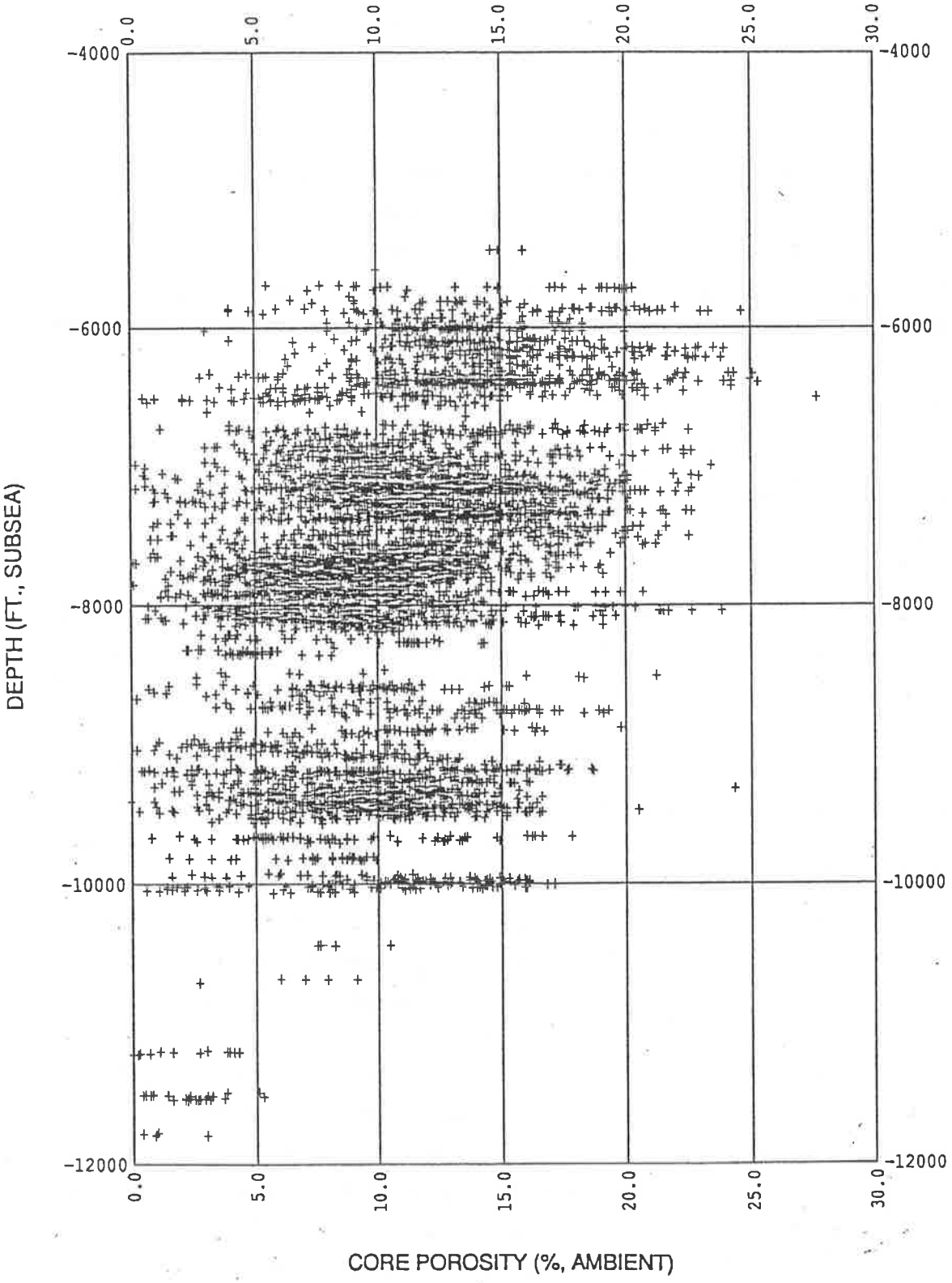

Figure 5.9a Crossplot of core porosity (%) versus subsea depth, PEL 5 & 6, southern Cooper Basin [data derived from 148 petroleum wells].

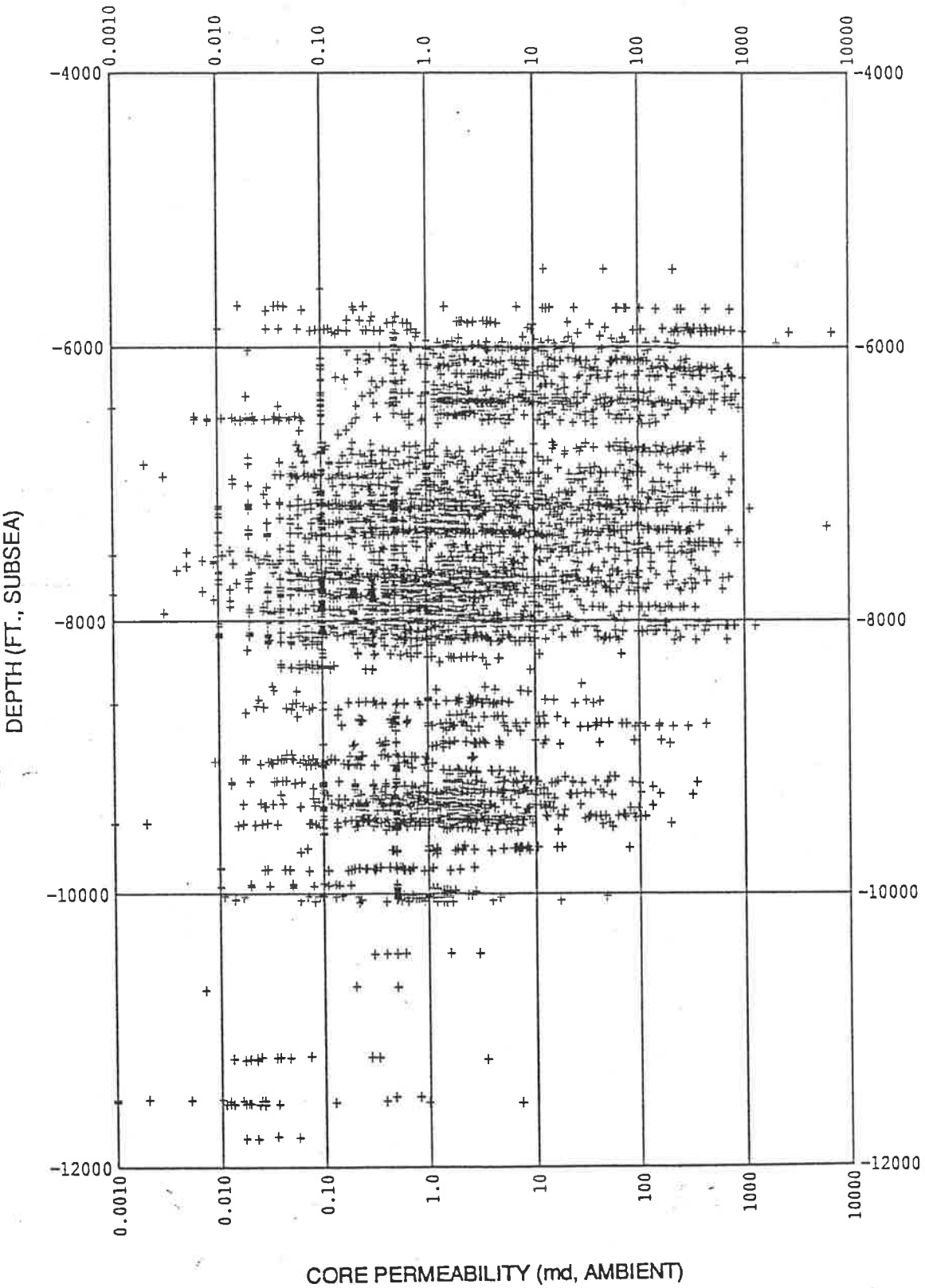

Figure 5.9b Crossplot of core permeability (md) versus subsea depth, PEL 5 & 6, southern Cooper Basin [data derived from 148 petroleum wells].

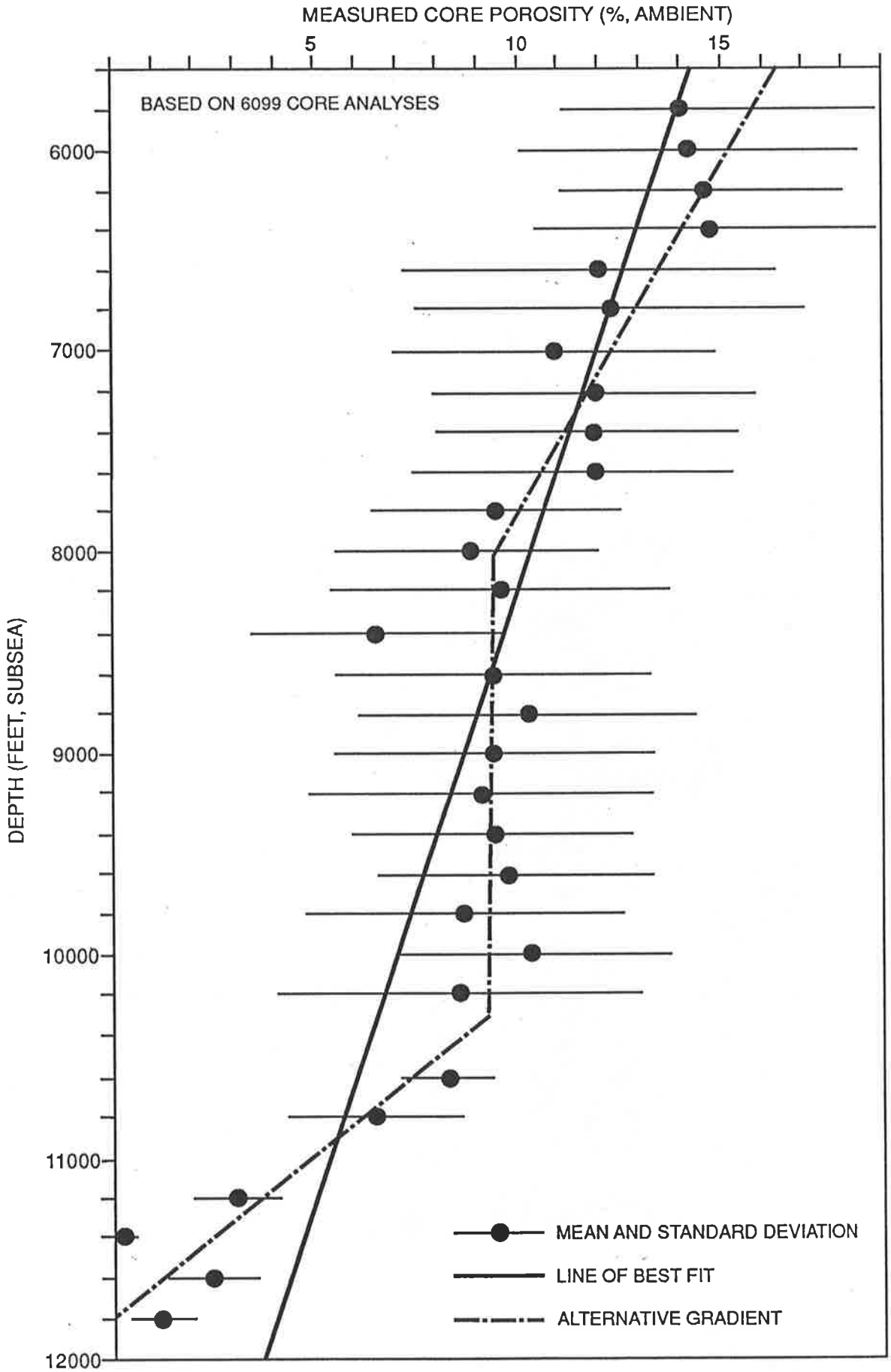

Figure 5.10 Mean reservoir porosity versus depth from whole-core analyses for Permian sediments, southern Cooper Basin. Plug data was averaged over 200-feet intervals and plotted at the mid-points of those intervals (filled circles). See text for full discussion.

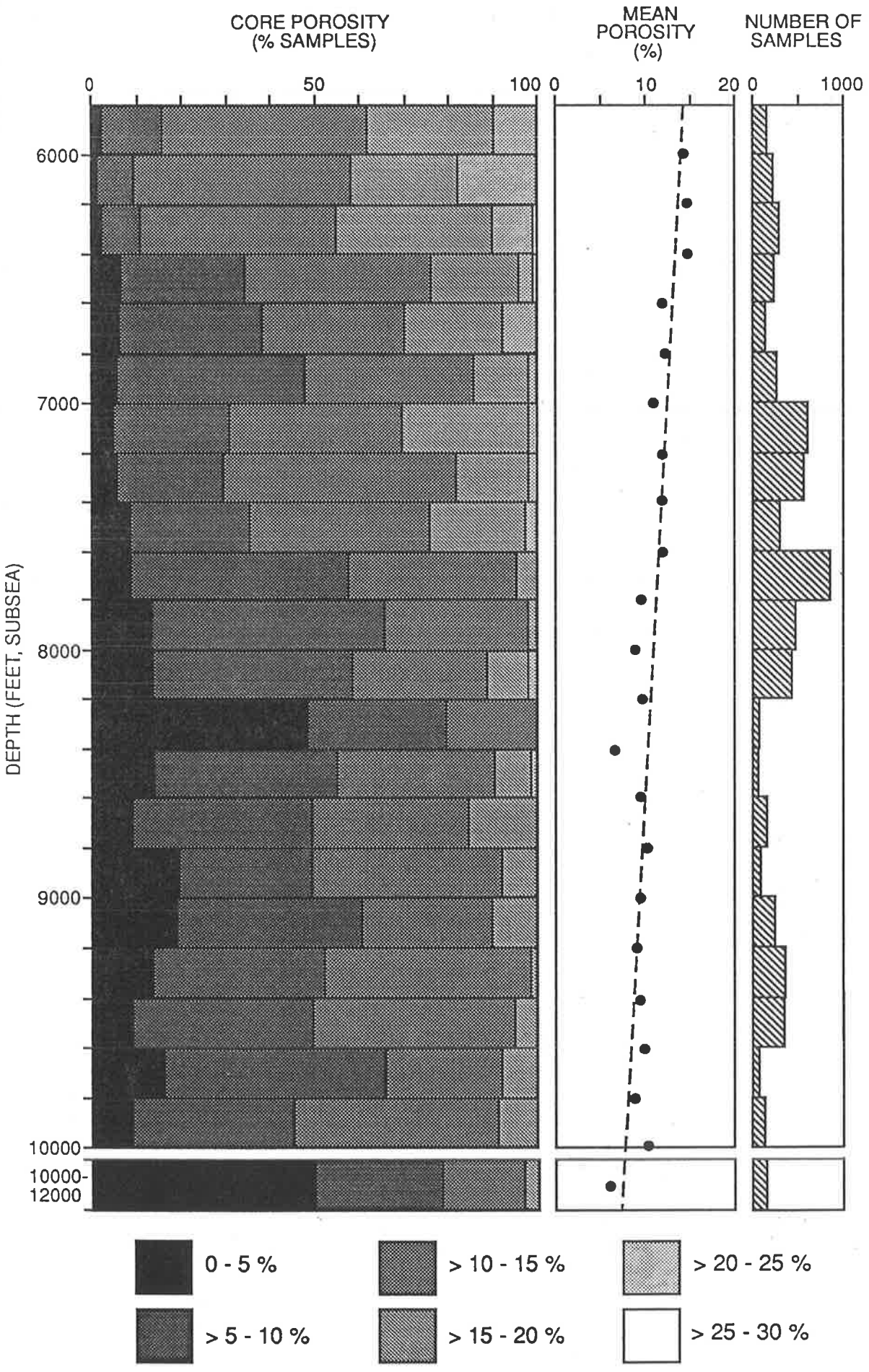

Figure 5.11a Porosity variation with depth. Clastics with porosities greater than 15 percent decrease in abundance towards the more deeply buried parts of the basin. Compare porosity gradient with mean deterioration in permeability character shown in Figure 5.11b.

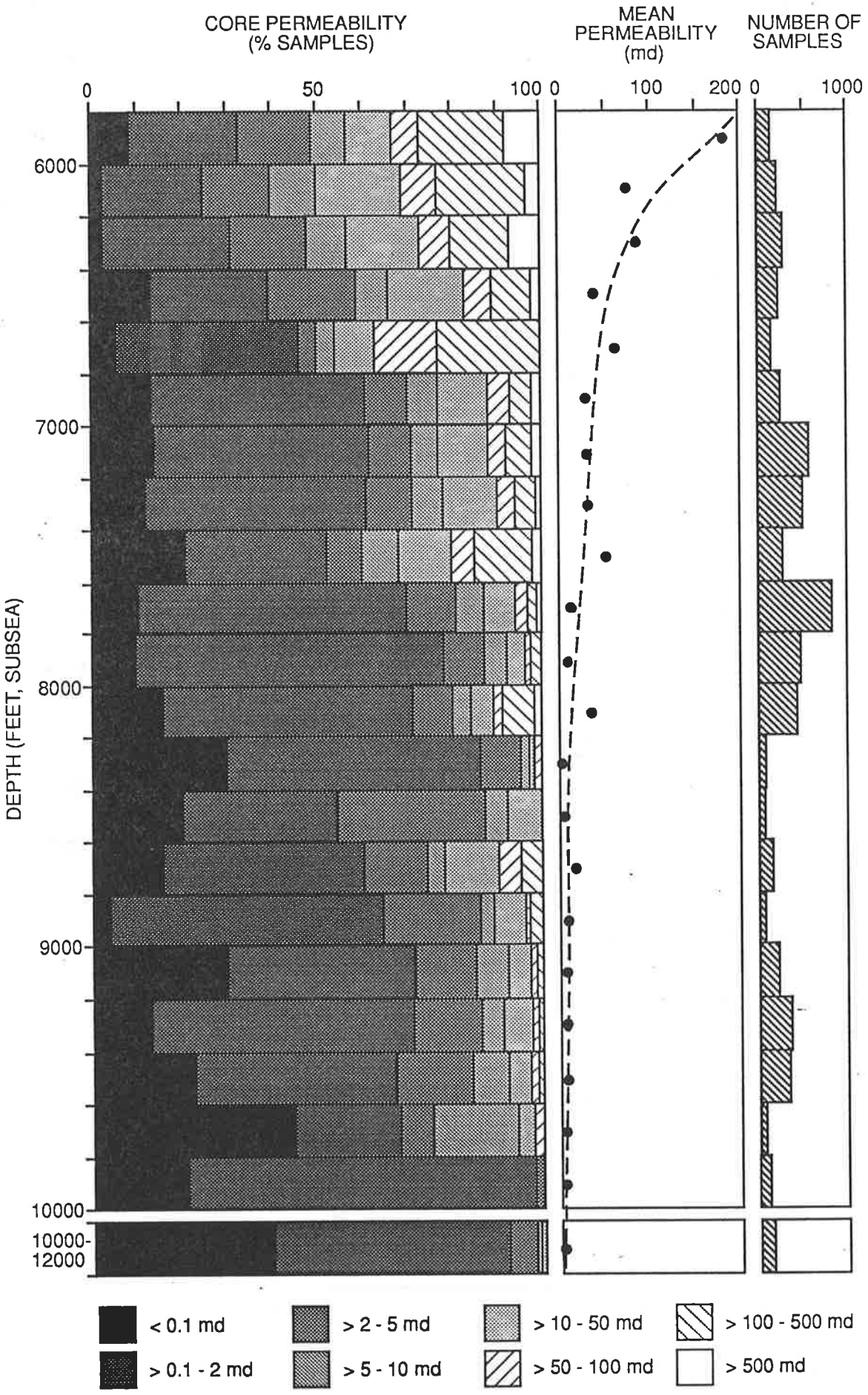

Figure 5.11b Permeability variation with depth. Note increase in predominance of clastics with permeabilities of 2 md or less towards the deeper parts of the basin. Compare with porosity trends shown in Figure 5.11a.

Table 5.6a
Statistical analysis of measured core porosity (%) with increasing burial depth in the southern Cooper Basin.

Depth (ft.,subsea)	Min.	Max.	Mean	St.Dev.	No.
5600-5800	5.5	20.3	14	4.9	30
5800-6000	4	24.6	14.2	4.2	141
6000-6200	3	23.9	14.6	3.5	205
6200-6400	2.8	25.3	14.7	4.2	295
6400-6600	0.5	27.7	11.8	4.6	233
6600-6800	1.2	22.5	12.3	4.8	132
6800-7000	0.2	23.4	10.9	4	269
7000-7200	0.2	22.9	11.9	4	600
7200-7400	0.9	22.6	11.8	3.7	555
7400-7600	0.8	22.5	11.9	4.5	295
7600-7800	0.1	19.4	9.5	3.2	846
7800-8000	0.1	20.7	8.8	3.3	480
8000-8200	0.6	23.8	9.6	4.3	405
8200-8400	2.2	14.3	6.5	3.1	69
8400-8600	0.7	21.2	9.4	3.9	61
8600-8800	0.2	19.3	10.3	4.2	131
8800-9000	0.1	19.8	9.4	4	90
9000-9200	0.2	18.7	9.1	4.3	227
9200-9400	0.9	24.3	9.4	3.5	352
9400-9600	0	20.5	9.8	3.2	335
9600-9800	0.8	17.8	8.7	4	69
9800-10000	1.5	17.1	10.4	3.4	138
10000-10200	0.6	17.2	8.6	4.5	80
10200-10400	-	-	-	-	-
10400-10600	7.5	10.5	8.3	1.04	6
10600-10800	2.7	9.1	6.5	2.2	5
10800-11000	-	-	-	-	-
11000-11200	1.1	4.3	3.1	1.1	8
11200-11400	0.3	0.7	0.3	0.23	5
11400-11600	0.4	5.3	2.5	1.17	27
11600-11800	0.4	3	1.2	0.9	5
11800-12000	-	-	-	-	-

Table 5.6b
Statistical analysis of measured core permeability (md) with increasing burial depth in the southern Cooper Basin.

Depth (ft.,subsea)	Min.	Max.	Mean	St.Dev.	No.
5600-5800	0.016	739	79	160	29
5800-6000	<0.001	6820	184	649	140
6000-6200	<0.05	730	76	137	205
6200-6400	<0.001	974	85	180	271
6400-6600	0.0001	904	38	103	225
6600-6800	<0.1	368	62	96	131
6800-7000	0.0001	766	30	96	260
7000-7200	<0.001	1121	32	100	563
7200-7400	0.0001	6077	32	281	487
7400-7600	<0.001	865	52	122	247
7600-7800	0.001	718	13	57	824
7800-8000	<0.001	340	8	32	480
8000-8200	<0.005	1262	36	131	415
8200-8400	0.0001	67	1.8	8.1	69
8400-8600	<0.001	42.2	3.7	7.5	61
8600-8800	<0.02	425	17	53	131
8800-9000	0.0001	195	8	30	76
9000-9200	<0.001	344	6	27	206
9200-9400	<0.005	313	6	23	346
9400-9600	0.001	196	6	19	335
9600-9800	0.0001	78	3.6	9.9	67
9800-10000	<0.001	2.8	0.57	0.57	106
10000-10200	<0.05	48*	1.6	5.8	75
10200-10400	-	-	-	-	-
10400-10600	0.3	3	1.07	0.97	6
10600-10800	0.007	0.5	0.34	0.2	5
10800-11000	-	-	-	-	-
11000-11200	0.022	0.33	0.11	0.12	8
11200-11400	0.013	3.5	0.7	1.4	5
11400-11600	0.001	7.1	0.4	1.3	27
11600-11800	<0.001	0.055	0.026	0.018	5

In contrast, the decline in mean reservoir permeability with depth displays a very different gradient (cf. Fig.5.10, 5.11 a & b). Average reservoir permeability decreases very rapidly within the first 1000 feet of the Cooper Basin sediments, from 184 md at 6000 feet to 32 md at 7000 feet. Permeability decline then becomes more gradual, reaching 6 md at 9600-9800 feet. Beyond 10000 feet of burial - again based on a relatively small number of core plugs - mean permeability is 1.6 md or less (Fig.5.11b; Table 5.6b).

The decline in mean porosity with depth may be attributed to the decreasing abundance of clastics with porosities greater than 15 percent; in particular, clastics in the 20-25 and 25-30 percent porosity categories are progressively eliminated towards the deeper parts of the basin (Fig.5.11a). Similarly, the decline in mean reservoir permeability with depth is a function largely of the decreasing abundance of sands with high permeabilities (> 50 md), especially sands with permeabilities greater than 100 md (Fig.5.11b). There is a broad corresponding increase in low-permeability clastics: At 6000 feet, only about 32 percent of clastics have permeabilities of 2 md or less; at depths greater than 10000 feet, more than 90 percent of core analyses fall into this category (Fig.5.11b). Importantly, however, the data suggests that high-quality reservoir facies, characterised by permeabilities of up to 100 md or more, may persist to depths approaching 10000 feet or beyond; such facies occur within sandstone sequences dominated by low-permeability sandstones (Fig.5.11b).

5.2.3.6 Comparison to other petroleum provinces

The generally low-quality nature of the Cooper Basin reservoir sandstones is highlighted when comparing the present results to those obtained by other workers for various clastic petroleum provinces throughout the world. In Figure 5.12, the mean deterioration in reservoir porosity with depth is shown for a number of basins with proven hydrocarbon potential, as compiled from the existing literature.The porosity-depth gradient in the Cooper Basin is not unlike that of many other basins, including the Bass Basin (Meszoly et al., 1986), the Texas Gulf Coast (Loucks et al., 1984), and the North Sea (Selley, 1978; Bjørlykke et al., 1988) (Fig.5.12). Importantly however, the Cooper Basin differs from numerous other petroleum provinces by being characterised by reservoir sandstones which fall within the lower end of the existing porosity spectrum: mean reservoir porosity in the Cooper Basin is considerably less than that of many other basins buried to similar depths (Fig.5.12). For example, the Sacramento and San Joaquin Basins of California have average reservoir porosities of about 21 percent at 8000 feet of burial (Zieglar & Spotts,

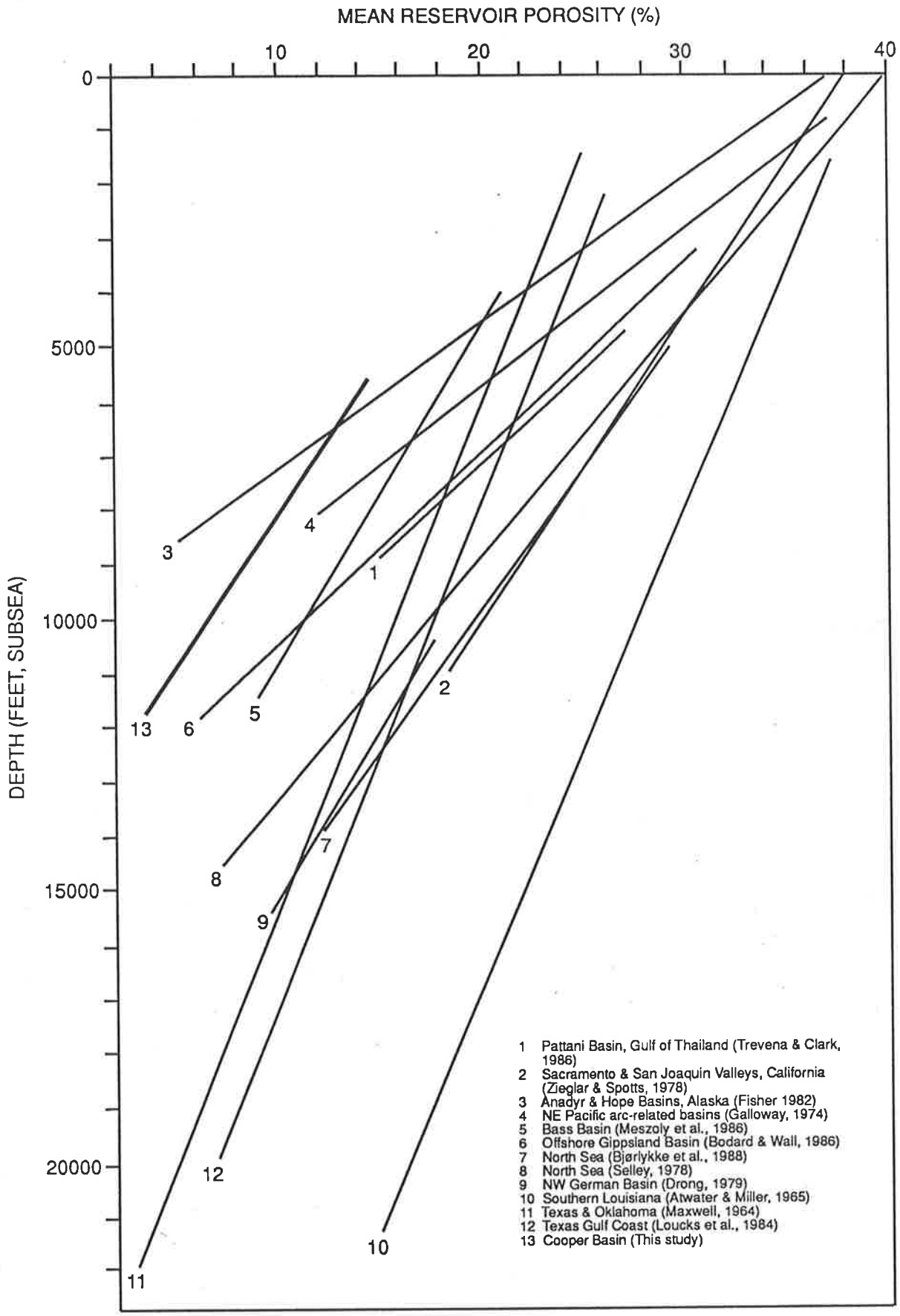

Figure 5.12 Relationship between mean reservoir porosity and depth for various clastic petroleum provinces throughout the world.

1978), more than twice that of the Cooper Basin clastics at equivalent depths. Further examples are shown in Figure 5.12.

Such wide variation in porosity-depth trends for different basins is likely to be the product of a complex interplay of factors, including differences in age, tectonic history, structural styles, facies, diagenesis, and thermal regimes. This naturally complicates a direct comparison of reservoir character between different hydrocarbon provinces, and must be kept in perspective relative to the above discussion.

Permeability-depth trends based on a statistically significant number of core plugs for different basins were not available in the literature; hence, no direct comparison between the Cooper Basin clastics and those from other petroleum provinces could be made.

5.3 Part II: Laboratory results

5.3.1 Types of porosity

Three types of porosity are distinguished in the reservoir sandstones of the southern Cooper Basin. These include microporosity, primary intergranular porosity and secondary dissolution porosity (macroporosity). Their characteristics and interrelationships are briefly discussed [20].

5.3.1.1 Primary porosity

Primary porosity represents the dominant porosity type in numerous reservoir sandstones of the southern Cooper Basin. Remnants of original depositional porosity are found in fine to coarse grained sandstones generally low in clay content (Plates 2 A & B, 18 A). Such sandstones are characterised by prominent euhedral quartz overgrowths that grew from detrital quartz grains into primary pores, reducing but not occluding initial porosity (Plates 2 E & F, 5 E, 18 E). In samples which display intense intergranular pressure solution and only minor development of quartz overgrowths, primary intergranular porosity is absent (Plate 5 C). The size of pore

[20] The assessment of porosity in ditch cuttings is often problematic since there is evidence to suggest some clays were preferentially washed out of pores (Fig.4.4). In the present discussion, attention is therefore largely focused on core samples.

Plate 18

Micrographs of macroporosity

A. This medium-grained sandstone of point bar origin is derived from a gas-producing interval that tested with a flow of up to 9.2 MMCFD. Blue araldite was used to highlight porosity. Remnants of primary pores are common, but some oversized pores of secondary origin are also evident (arrows). In some pores, dead oil/bitumen can be seen (black). Note the fair grain sorting and lack of clay. The sample is typical of many high-quality reservoir sandstones found along the basin margin and in midflank position in the southern Cooper Basin (cf. Plates 1-5). Measured core porosity is 18.1 % and permeability 434 md. Plane light. Scale bar 1 mm. Sample CB-0597, Moomba-10, Toolachee Formation (7775' 0").

B. Secondary porosity is evident from the oversized pore (blue araldite). However, some remnant of primary porosity is suggested by the euhedral nature of overgrowths, similar to those seen under the SEM (Plate 1 A & B). This type of porosity interrelationship was not commonly observed in the central Nappamerri Trough. Plane light. Scale bar 250 µm. Sample CB-0013, Kirby-1, Toolachee Formation (8953' 6").

C. Carbonate spar that has undergone partial dissolution, as indicated by the irregular and serrated outline of the mineral (cf. Plate 8 G). Blue areas represent secondary porosity. Such evidence for carbonate dissolution is rare in the the study area. Plane light. Scale bar 100 µm. Sample CB-0033, Big Lake-27, Tirrawarra Formation (9504' 2").

D. There is petrographic evidence to suggest that remnants of primary porosity exist to great depths in mature, well to moderatly sorted sandstones in the central Nappamerri Trough. In this micrograph, primary pores are indicated by the euhedral nature of the overgrowths (arrow). Large blue area towards bottom right corner of the micrograph is not porosity but marks the edge of the sample. Altough clays tend to be washed out in the stream of drilling mud that brings the ditch cuttings to the surface (Chapter 4), this is not believed to be the case in the present example due to the high textural maturity of this rock. Plane light. Scale bar 250 µm. Sample CB-0719, Kirby-1, Patchawarra Formation (10710-10720').

E. This sample is derived from the basal 56-9 Patchawarra sand below the oil-water contact at Wancoocha. The euhedral nature of the overgrowths indicates the presence of abundant primary porosity (P). In adjacent areas, the primary pores are partly filled with dead bitumen/oil. No difference in porosity character is evident between samples from this interval and those from the oil-saturated zone found updip at Wancoocha-2 (cf. Plate 2 F). Plane light. Scale bar as for (D) (250 µm). Sample CB-0703, Wancoocha-4, Patchawarra Formation (5790-5800').

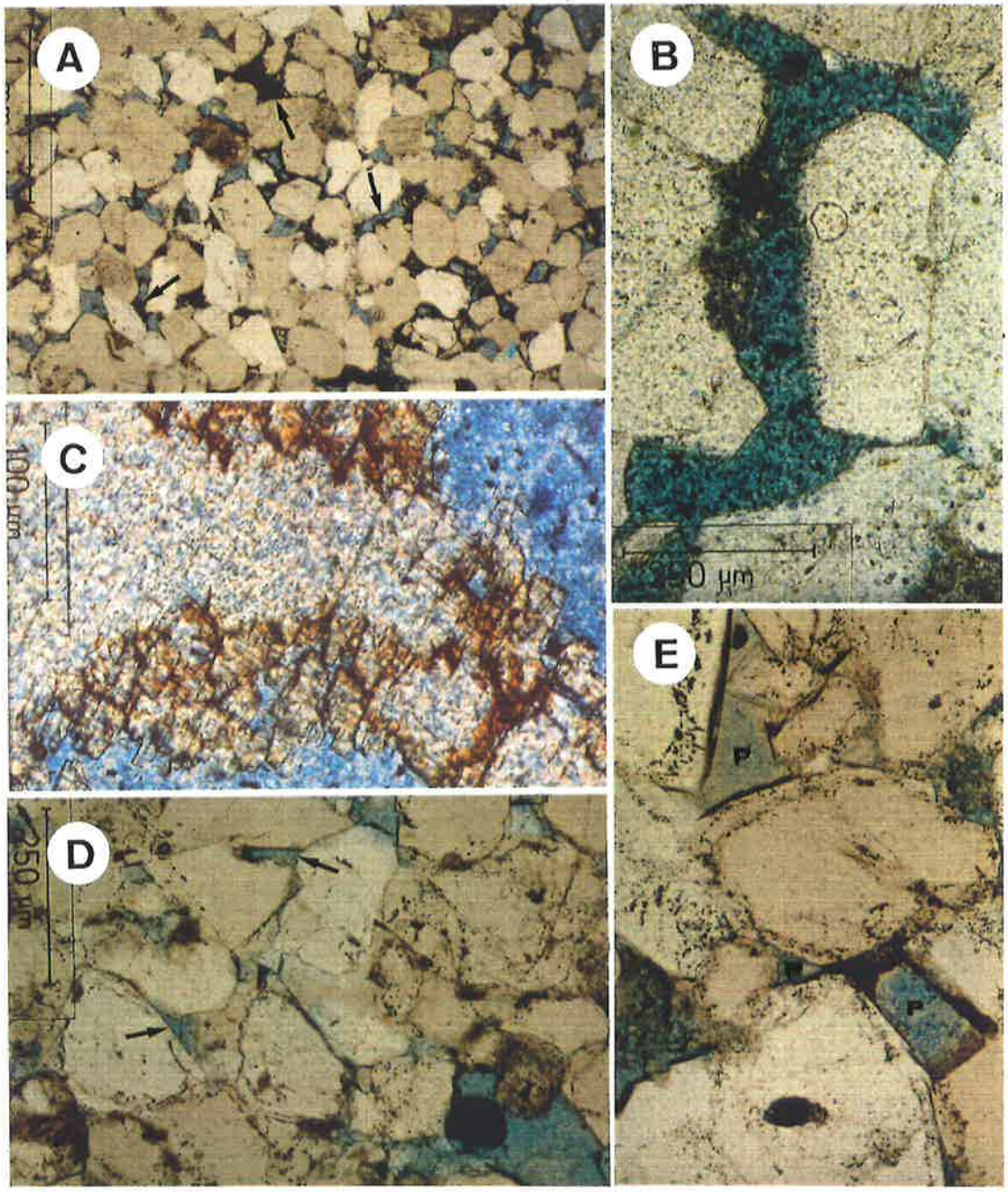
A
B
C
D
E
100 µm
250 µm
P
P

diameters is variable, ranging from a few microns (Plate 2 F) to more than 250 μm. Frequently, pore throats are reduced or blocked by authigenic clays (Plates 2 C & D, 15 F, 20 F). In some samples, there is up to 18 percent primary porosity, allowing for a high degree of interconnection between primary pores (Plates 2 A & B).

5.3.1.2 Secondary porosity

Secondary porosity generally constitutes a volumetrically minor component compared to primary porosity although locally secondary porosity is significant (Table 5.7). The identification of secondary porosity is based on criteria outlined by Schmidt et al. (1977) and Schmidt & McDonald (1979b). Secondary porosity is distinguished by the presence of oversized pores [21], frequently of irregular shape or elongate appearance (Plates 18 A & B), rock fractures, and dissolution remnants of minerals in pores (Plate 18 C). Oversized pores are predominant and are attributed to the dissolution of labile rock components such as feldspars and lithic fragments (volcanic and sedimentary), contributing up to 10 percent of total rock composition in some samples [22] (Martin & Hamilton, 1981; Schulz-Rojahn & Phillips, 1989). The diameter of individual secondary pores occasionally exceeds 1 mm (Plate 20 E). Evidence for carbonate cement dissolution is rare and localised (Plates 9 G & 18 C). Secondary pores are generally poorly interconnected because of their erratic distribution (Martin & Hamilton, 1981).

Rock or grain fractures are uncommon and are typically cemented by quartz; at least two phases of fracture silicification are distinguished in CL in some samples (Plate 5 A). The fractures occasionally contain rock bitumen, suggesting that some fracturing of reservoir rocks existed at the time of hydrocarbon migration in the southern Cooper Basin.

5.3.1.3 Microporosity

Microporosity is sometimes defined as pores with pore-aperture radii less than 0.5 μm (Pittman, 1979; Hamilton & Wilson, 1981; Tieh et al., 1986). In the present

---

21 Oversized pores alone represent a poor criterion to distinguish secondary porosity in thin section as the same effect may be produced by grain plucking during sample collection and/or preparation.

22 Many such pores are completely infilled by authigenic clay (chiefly kaolin) (cf. Plates 4D, 12 E & 20E); these pores were classified as microporosity.

Plate 19

Micrographs of reservoir dominated by microporosity (1)

The 79-9 and 80-4 Patchawarra sands of fluvial origin at Dullingari-18 tested with a flow of 2.26 MMCFD at 415 psi on a 1/2" top choke over the interval 7830-7920 feet (see Fig.3.4). Diagenetic results and core data indicate that hydrocarbon production occurs from reservoir sandstones dominated by microporosity associated with kaolin clay, and local remnants of macroporosity.

A. In this fine-grained sandstone characterised by planar lamination, no porosity is visible in thin section yet measured core porosity is 8.9 %; associated permeability is 0.4 md. Dark-brown patches represent kaolin clay. XRD results suggest the kaolin clay type in this sample is kaolinite rather than dickite. Plane light. Scale bar 1 mm. Sample CB-0745, Dullingari-18, Patchawarra Formation (7847' 2").

B. Remnants of primary porosity (arrows) are visible in this medium-grained sandstone of moderate sorting. Secondary pores are largely infilled by kaolin (K) clay (brown patches). XRD data suggests dickite is the dominant kaolin clay type. Measured core porosity is 13 % and permeability 7.1 md. The sample is derived from a channel floor sequence. Plane light. Scale bar 1 mm. Sample CB-0746, Dullingari-18, Patchawarra Formation (7857' 6").

C. In the SEM, the clay-rich nature of the reservoir rock shown in (B) is highlighted. Note the general lack of large pores (compare with Plate 1 A & B). Scale bar 1 mm.

D. Close-up scanning electron micrograph view of (B). Only isolated remnants of primary pores exist (P). Large euhedral overgrowths (O) protrude from a detrital quartz grain (Q) into primary pore space. Many of such pores are infilled by kaolin. Scale bar 0.1 mm.

E. Close-up SEM view of abundant kaolin clay booklets. Note associated microporosity. Scale bar 0.1 mm. Sample CB-0747, Dullingari-18, Patchawarra Formation (7869' 7").

F. Same sample as in (E) above. In thin section, no porosity is visible in this fine-grained, poorly-sorted sandstone but there is abundant kaolin clay (brown patches). Measured core porosity is 5.1 % and permeability 16 md. It would appear that all of the core porosity is microporosity. The relatively high permeability value in this sample is the result of an artificially-induced microfracture associated with a thin microstylolite zone evident in hand specimen. Scale bar 1 mm.

G. SEM view of (F). Abundant kaolin is visible between detrital quartz grains (Q). Scale bar 1 mm.

H. When zooming-in, the euhedral nature of the kaolin booklets is evident. Micropores among the clay particles are up to 15 μm in diameter. XRD results suggest dickite is the dominant kaolin clay type in this sample. Scale bar 10 μm. Sample CB-0747, Dullingari-18, Patchawarra Formation (7869' 7").

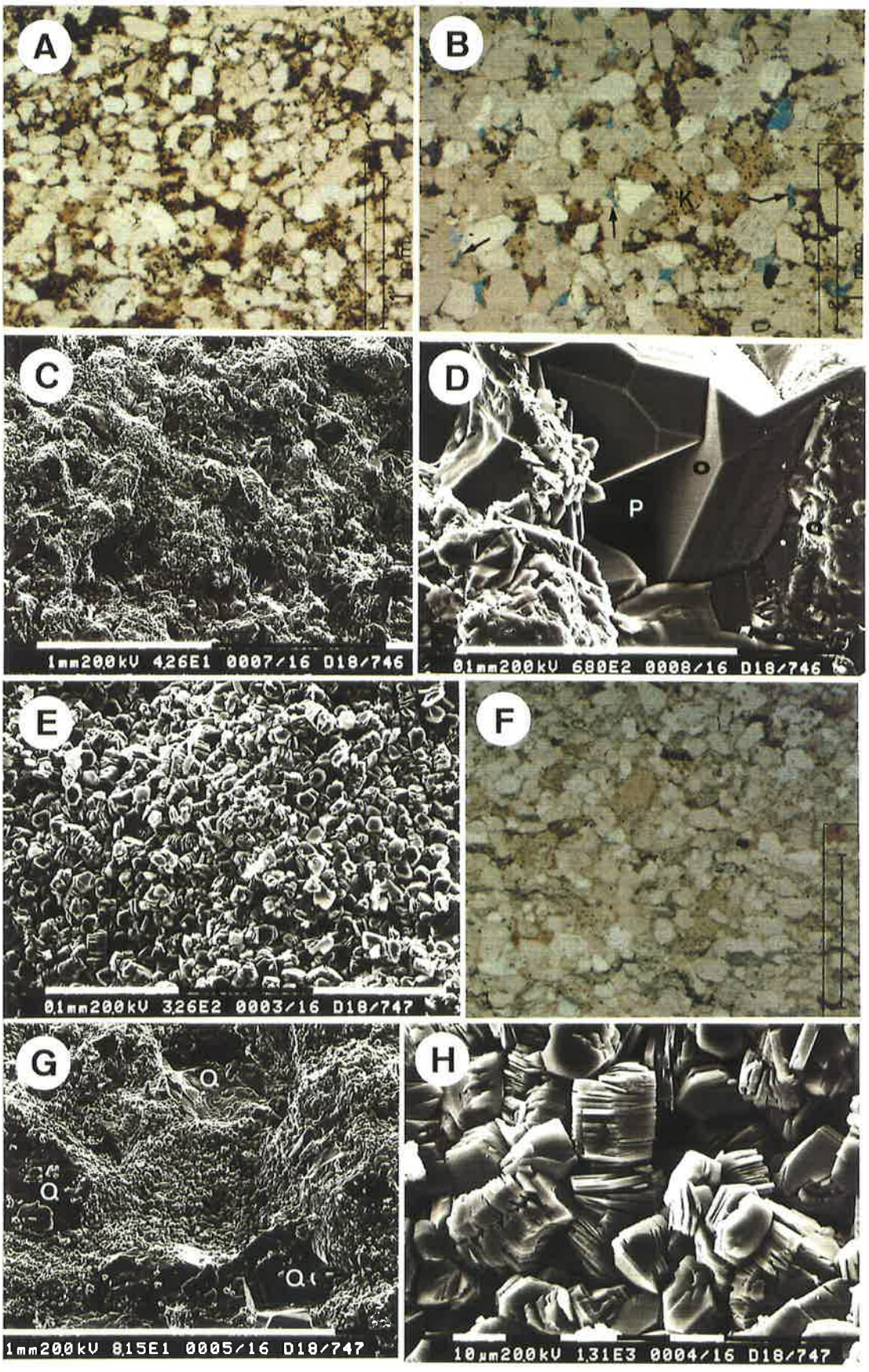
A
B
K
C
1mm20.0kV 4.26E1 0007/16 D18/746
D
P
Q
0.1mm20.0kV 6.80E2 0008/16 D18/746
E
0.1mm20.0kV 3.26E2 0003/16 D18/747
F
G
Q
Q
Q
1mm20.0kV 8.15E1 0005/16 D18/747
H
10µm20.0kV 1.31E3 0004/16 D18/747

investigation, the definition is extended to include all porosity that occurs interstitially between clay particles. Such clay micropores can be of hybrid nature, being part primary and part secondary in origin: primary micropores are associated with clays that precipitated in primary pore space; micropores of secondary origin occur where clays formed as the product of mineral alteration and/or replacement.

Microporosity is most common in association with kaolin clays (Plates 12F, 13B & C , 19 H), but to a lesser extent also occurs in association with authigenic illite of fibrous, lath- or lettuce-like habit, as seen under the SEM (Plates 15 C, D & E). Detrital illite significantly reduces microporosity due to the closely packed, platy crystal habit of the mineral (Plate 15 A). Micropores are insignificant in association with clinochlore or pyrophyllite (Plates 17 B, E & F).

The largest micropores occur between individual dickite booklets; microporosity is relatively poorly developed among the subhedral and more blocky kaolinite crystals thought to have formed as a replacement product of feldspar (section 4.3.3). Pore diameters range between less than 1 μm to 30 μm but commonly are around 10 μm. Generally, dickite concentrates in the relatively high-porosity, high-permeability clastics whereas kaolinite is associated with the lower quality reservoir rocks (Fig.5.13).

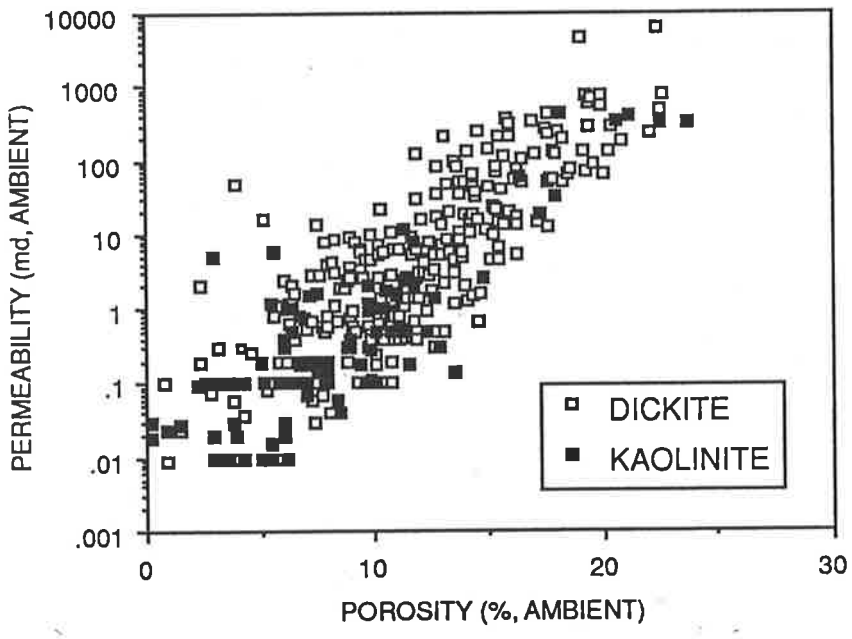

Figure 5.13 Porosity-permeability character (core) of kaolinite- and dickite-bearing rocks. Dickite concentrates in the higher quality reservoir clastics. Because of its euhedral nature and large crystal size, dickite is associated with high microporosity. The high microporosity contributes to the overall reservoir character of the sandstones in the southern Cooper Basin. Identification of kaolin type is based on XRD results [includes some data from Alsop (1990), Phillips (NCPGG, unpubl.), Eleftheriou (1990), Thomas (1990)].

Plate 20

Micrographs of reservoir dominated by microporosity (2)

A. In this medium-grained moderatly-sorted sandstone, no porosity is evident in thin section. However, there is abundant kaolin clay (brown), interpreted to be dickite on the basis of XRD traces. Measured core porosity is 9.9 % and permeability 1 md. The sample is derived from the cross-bedded portion of a point bar sequence. Plane light. Scale bar 1 mm. Sample CB-0748, Dullingari-18, Patchawarra Formation (7872' 0").

B. Secondary pores of oversized nature are infilled by kaolin (K) in this medium-grained sandstone characterised by planar bedding. XRD data suggests the kaolin clay is dominantly dickite. Again, no porosity is visible in thin section although measured core porosity is as high as 9.7 %; associated core permeability is 1.2 md. Plane light. Scale bar as for (A). Sample CB-0749, Dullingari-18, Patchawarra Formation (7894' 5").

C. General SEM view of (B). The rock is clay-rich, without macroporosity. There is an abundance of kaolin. Scale bar 1 mm.

D. Medium-grained, fairly poorly sorted sandstone of massive appearance derived from the middle portion of a point bar sequence. Kaolin clay is abundant (brown), interpreted to be dominantly dickite on the basis of XRD data. Remnants of primary pores are present (arrow). The large blue area in the top right corner of the micrograph is not porosity but the result of sample damage during laboratory work. Measured core porosity is approximately 13.3 % and permeability 5.4 md. Plane light. Scale 1 mm. Sample CB-0750, Dullingari-18, Patchawarra Formation (7896' 7").

E. Thin section view of (D). Large oversized secondary pore infilled by kaolin (K). Plane light. Scale bar 1 mm.

F. Close-up scanning electron micrograph view of (D) showing primary pore space infilled by authigenic kaolin booklets. In this case, it is unclear whether the kaolin precipitated in the primary pore or whether it collapsed into the pore structure during sample preparation. Scale bar 0.1 mm.

G. General SEM view of (D). Primary pores (arrow) are evident in this medium-grained sandstone. Some kaolin clay was probably lost during sample preparation. Scale bar 1 mm.

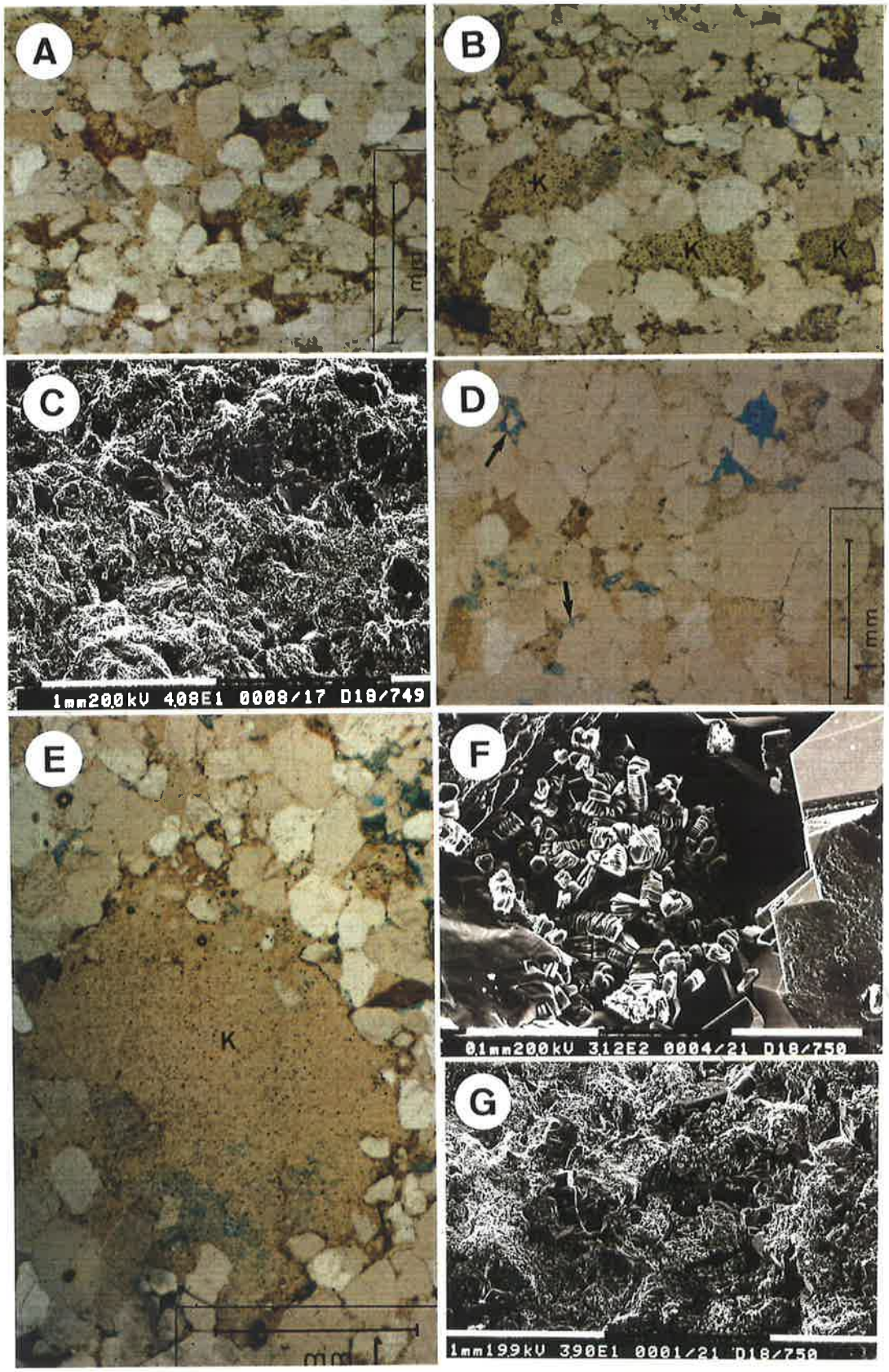
A
B
K
K
K
C
1mm20.0kV 4.08E1 0008/17 D18/749
D
1mm
E
K
mm
F
0.1mm20.0kV 3.12E2 0004/21 D18/750
G
1mm19.9kV 3.90E1 0001/21 D18/750

Only rarely can microporosity be seen in thin section (Plate 12 F). The abundance of microporosity in Cooper Basin clastics is highlighted by the fact that visual estimates of porosity in thin section when compared to core plug data generally do not show a good correlation (Steveson & Spry, 1973; Martin & Hamilton, 1981; Schulz-Rojahn & Phillips, 1989) (Fig.5.14 a & b). Point-counting consistently underestimates the measured core porosity (Fig.5.14a). However, when the estimated amount of kaolin minerals seen in thin section is added to observed thin section macroporosity, a much better correlation of data is achieved (Fig.5.14b). The relationship suggests that a large proportion of total porosity is microporosity associated with kaolinite and dickite in the study area (Schulz-Rojahn & Phillips, 1989). A similar method was applied by Hankel et al. (1989) to quantify microporosity in reservoir sandstones of the Medicine Hat Gas Field in southeastern Alberta. In the present study, microporosity is estimated to constitute up to about 15 percent of bulk rock composition in some samples. In numerous reservoir sandstones, microporosity is the only porosity type present (Plates 19 A & F, 20 B).

5.3.2 Porosity interrelationships

Primary and secondary porosity may coexist together with microporosity in the same sample. For example, in thin section one area may be dominated by kaolin with only minor quartz cement, and immediatly adjacent to this area detrital quartz grains may be 'floating' in a thick quartz cement without appreciable amounts of kaolin clay (Plates 4 D & 5 A). The result is that remnants of primary pores are found juxtaposed to zones characterised by abundant microporosity (Plates 4 D & 19 B). Sandstones with remnants of primary porosity also tend to be those in which secondary porosity is most common (Plates 5 A & 18 A). A similar observation was made by Johnston & Johnson (1987) for the lower Eocene Wilcox Sandstone of Louisiana.

The close coexistence of porosity types, often within millimetres of each other in the same sample, must be taken into account when evaluating core plug data. The different porosity types combine to influence porosity and permeability measurements as evident when petrographic data is compared to available core porosity and permeability values (Fig.5.15). The broad linear relationship between core porosity and permeability discussed in section 5.2.3.2 is related to the abundance of porosity types seen in thin section. The highest quality reservoir rocks are those dominated by primary porosity; such sands often have permeabilities exceeding several hundred millidarcys, and porosities typically in the range of 10-25 percent (Fig.5.15). In

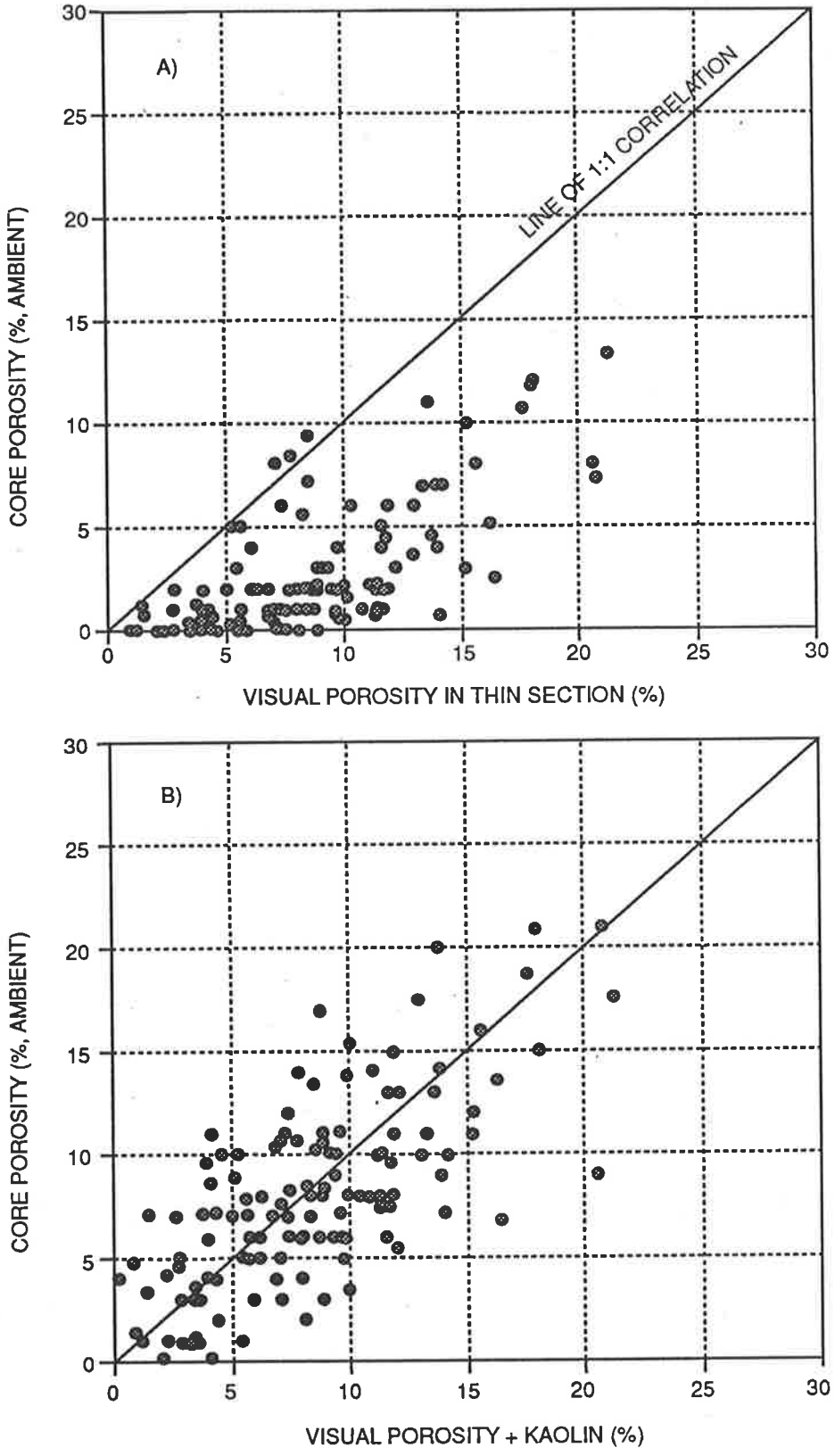

Figure 5.14 a & b Crossplot of core plug porosity versus thin section porosity (a) with the addition of the estimated amount of kaolin minerals (b). The graph includes data from a multitude of wells, including Burley-1, Burley-2, Kirby-1, Della-3, Yapeni-1, Pando-2, Murteree-C1, Dullingari-1, Dullingari-18, Wancoocha-1, Boxwood-1, Tarwonga-2, Kerna-1, Coochilara-1, Mudlalee-1, and Spencer-1; data from a string of Moomba wells is further incorporated from the work of Thomas (1990).

contrast, clastics in which there only is microporosity have a relatively poor reservoir character. These microporous sands have permeabilities typically less than 2 md and porosities in the range of 0.5 to 15 percent (Fig.5.15). Clastics containing both abundant microporosity and some macroporosity represent an intermediate category, with some degree of overlap in porosity-permeability character between the different types of reservoir rock (Fig.5.15).

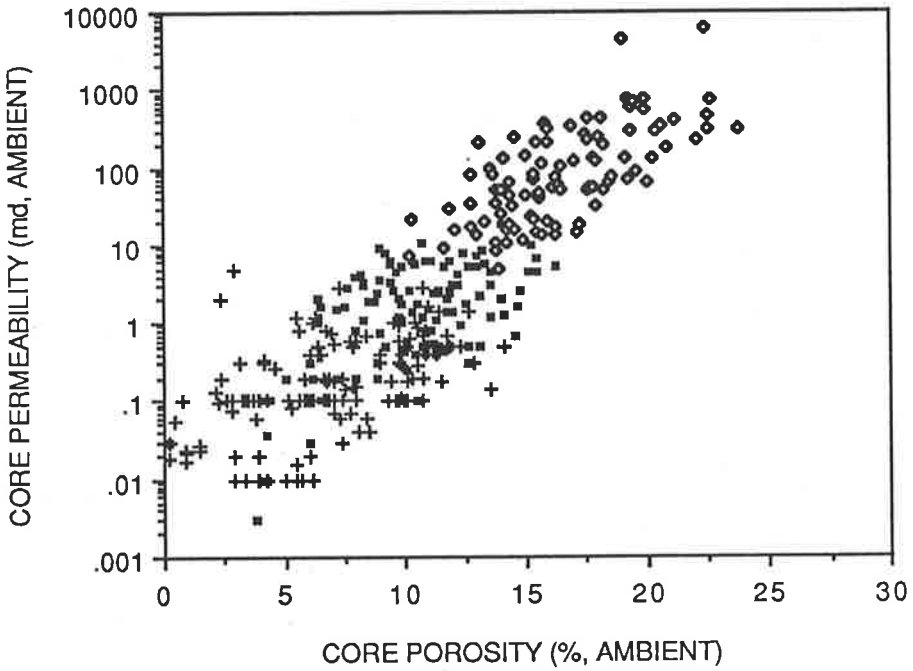

Figure 5.15 Influence of abundance of porosity types seen in thin section on core porosity and permeability measurements. The diagram represents the key to understanding the nature of porosity in the sandstones of the southern Cooper Basin when evaluating core plug data (symbols: cross = sandstones which exclusively contain microporosity; black squares = sandstones with abundant microporosity and trace/minor primary and/or secondary porosity; diamond = sandstones dominated by primary porosity with some secondary porosity and/or microporosity).

5.3.3 Initial deliverability rates of porosity types

The ability of the various porosity types distinguished in the Permian sandstones to produce hydrocarbons was examined by comparing diagenetic results with DST and production test data (Table 5.7). The data suggests that hydrocarbon production is generally derived from a complex mixture of porosity types. Many

hydrocarbon-bearing reservoir sandstones contain both primary and secondary porosity, as well as microporosity (Table 5.7). Although this complicates assessment of the effectiveness of the various porosity types identified, a broad pattern of initial hydrocarbon production is distinguished.

The reservoir sandstones characterised by the highest flow rates are those containing abundant primary porosity. Primary pores provide for a high degree of porosity interconnection, resulting in high effective rock permeabilities that contribute to numerous flow results of commercial significance. For example, a gas-bearing Patchawarra sandstone at Daralingie-9, characterised by abundant primary porosity, tested with a flow of 11.35 MMCFD at 2180 psi on a 1/2" choke over the interval 7244-7314 feet (Table 5.7). Similar good flow results are reported from other sandstone intervals in which primary porosity is abundant (Table 5.7). Primary porosity is also the dominant porosity type in the Patchawarra 57-0 sandstone from which oil production (42° API at 60 °F) occurs at Wancoocha (Table 5.7; Plate 3 F).

The role of secondary porosity in hydrocarbon production is more difficult to assess due to the more erratic distribution of this type of porosity. The presence of secondary pores undoubtedly enhances the storage capacity of many reservoir rocks for oil and gas. Martin & Hamilton (1981) considered the interconnection between secondary pores to be limited. However, where secondary pores occur in conjunction with primary pores, effective permeability is enhanced. Table 5.7 indicates that sandstones with combined primary/secondary porosity produce gas at flow rates generally greater than about 5 MMCFD. Secondary porosity may locally be important for hydrocarbon production.

Gas-bearing sandstones dominated by microporosity can produce at initial flow rates between 20 and 500 MCFD [23] (Table 5.7). However, where there are trace remnants of primary pores in microporous sands, the efficiency of hydrocarbon recovery is much improved and flow rates several orders of magnitude higher are recorded (Table 5.7). For example, the Patchawarra 79-9 and 80-4 sands intersected in Dullingari-18 over the interval 7830-7920 feet tested with a flow of 2.26 MMCFD at 415 psi on a 1/2" top choke (Table 5.7) (see Fig.3.4). These reservoir sands contain abundant kaolin and are characterised by a predominance of microporosity, with isolated occurrences of remnant primary pores in some samples (Plates 19 & 20). Initial flow results in the order of about 2 MMCFD are recorded from other reservoir intervals dominated by microporosity in the study area, including kaolin-rich sands in the Moomba Field (Table 5.7). In some wells, minor quantities of condensate were also recovered from rocks with a high microporosity component (Table 5.7). The results indicate that kaolin-rich rocks containing abundant microporosity are locally favourable to low- and medium-order gas production, and possibly also condensate

[23] Prior to fracturing.

Table 5.7 Initial deliverability results of generic porosity types distinguished in the study area, as evident from intervals for which DST data is available [depth ranges given refer to logger's depth]. Porosity types and abundances are derived from petrographic data [Appendix D]. The amount of microporosity is estimated from the abundance of kaolin clay seen in thin section [PP = primary porosity; SP = secondary porosity; MP = microporosity; No. = number of samples].

Well	DST No.	Test results	Porosity types (s): PP	SP	MP	No.
Wancoocha-2 Patchawarra Fm. [Cuttings]	# 3 [5678-5746']	GTS 4 mins. @ 2.2 MMCFD. OTS 13 mins. @ 1747 BOPD (44.1 API)	Abundant	?? Present	Trace	3
Dirkala-2 Epsilon Fm [Core 1]	# 1 [6176-6218']	GTS @ 6.9 MMCFD, Rec. 287 BCPD (47.3 API), 45' C	Abundant to very abundant	Trace to minor	Trace to minor	3
Della-3 Toolachee Fm. [Cores 1 - 3]	# 3 & 4 [6560-6743']	GTS max. 22 mins. @ 60 MCFD Rec. max. 300' W, 6300' GCW	Trace to very abundant	Absent to minor	Minor to abundant	16
Toolachee-3 Patchawarra Fm. [Core 1]	# 4 [7162-7260']	GTS 2 mins. @ 5.9 MMCFD Rec. 120' C	Absent to trace, locally significant	Absent to ? minor	Minor to fair	7
Toolachee-3 Patchawarra Fm. [Cores 2 & 3]	# 5 [7274-7376']	GTS 4 mins. @ 8.6 MMCFD Rec. 100' C	Generally abundant, locally absent	Absent to minor	Minor to abundant	10
Toolachee-3 Patchawarra Fm. [Cores 4 & 5]	# 6 [7404-7474']	GTS 7 mins. @ 450 MCFD Rec. 1112' W	Absent, abundant in one sample	Mostly absent, local trace	Minor to abundant	11
Daralingie-1 Toolachee Fm. [Cores 1 & 2]	# 1 [6374-6465']	GTS 55 mins. @ RTSTM. MTS 69 mins. Rec. 6354' W	Mostly abundant, absent in some samples	Trace to minor	Minor to abundant	15
Daralingie-9 Patchawarra Fm. [Cores 1 & 2]	# 1 [7244-7314']	GTS @ 11.35 MMCFD Rec. 15' C, 35' GCW	Abundant to very abundant	Present	Minor to abundant	3

Table 5.7 (cont.)

Daralingie-19 Patchawarra Fm. [Core 1]	# 1 [7392-7492']	NFTS, Rec. 393' SOGCM	Absent to trace	Absent to ? trace	Minor to abundant	3
Daralingie-22 Patchawarra Fm. [Core 1]	# 1 [7415-7509']	NFTS, Rec. 5427' W	Trace to abundant	Absent	Minor to abundant	3
Coochilara-1 Epsilon Fm. [Core 1]	# 2 [7538-7587']	GTS 23 mins. @ 150 MCFD Rec. 546' GCM	Absent, local trace	Absent	Trace to minor	3
Kidman-1 Toolachee Fm. [Core 1]	# 1 [6596-6640']	GTS 1 min. @ 9551 MCDF Rec. 232' C, 29' W	Very abundant	Absent to minor	Trace to ? minor	4
Kerna-1 Epsilon Fm. [Core 1]	# 2 [7659-7714']	GTS @ 0.546 MMCFD Rec. 2231 GCM	Mostly absent, local trace	Generally absent, one sample with trace	Fair	6
Kerna-1 Patchawarra Fm. [Core 2]	# 4 [8096-8155']	GTS @ 3.7 MMCFD Rec. 35' C, 420' GCM	Mostly absent, local trace	Absent	Minor to abundant	7
Dullingari-18 Patchawarra Fm. [Cores 1 & 2]	# 6 [7816-7917']	GTS @ 2.26 MMCFD Rec. 430' SGCM	Mostly absent, local trace	?? Trace	Fair to abundant	7
Dilchee-1 Patchawarra Fm. [Core 1]	# 5 [8267-8308']	NGTS. Rec. 50' MW, 60' SGCM	Absent to trace	Absent	Minor to abundant	5
Big Lake-1 Toolachee Fm. [Cores 2 - 4]	# 5 [7728-7844']	GTS 5 mins. @ 6.15 MMCFD Rec. 40' W	Mostly absent, locally abundant	Mostly absent, abundant in some samples	Fair to abundant	19
Big Lake-2 Toolachee Fm. [Core 1]	# 1 [7410-7546']	GTS 2 mins. @ 9.3 MMCFD Rec. 100' W	Absent, abundant in one sample	Absent, abundant in one sample	Fair to abundant	6
Big Lake-2 Toolachee Fm. [Cores 2 & 3]	# 2 [7548-7617']	GTS 3 mins. @ 10.4 MMCFD Rec. 100' W	Mostly absent, locally abundant	Fair to ? abundant	Fair to abundant	7

Table 5.7 (cont.)

Big Lake-2 Toolachee Fm. [Cores 4 - 6]	# 3 [7628-7750']	GTS 3 mins. @ 9.8 MMCFD Rec. 60' W	Absent	Absent to trace	Fair to abundant	5
Big Lake-27 Patchawarra Fm. [Cores 5 & 6]	# 3 [9117-9175']	GTS 9 mins. @ 0.064 MMCFD Rec. 341' MW, 409' WM	? Absent	? Absent	Trace to minor	3
Big Lake-35 Patchawarra Fm. [Core 1]	# 2 [9211-9247']	GTS 14 mins. @ 0.24 MMCFD Rec. 1000' SGCMW	Absent to trace	Absent to ? trace	Trace to minor	3
Moomba-1 Toolachee Fm. [Cores 1 & 2]	# 2 [7596-7683']	NGTS Rec. 40' MW, 10' M	Mostly absent to trace	Absent, possible trace	Minor to abundant	5
Moomba-1 Toolachee Fm. [Core 3]	# 4 7820-7879']	GTS 4 mins. @ 1.8 MMCFD Rec. 385' GCM	Generally absent to trace, one sample with minor	Absent	Fair to abundant	6
Moomba-1 Toolachee Fm. [Core 4]	# 5 [7878-7923']	GTS 2 mins. @ 5.8 MMCFD Rec. 20' W, 65' MW, 10' GCM	Absent to very abundant	Minor	Fair to abundant	3
Moomba-1 Daralingie Fm. [Core 6]	# 7 [7988-8043']	NGTS Rec. 15' MW, 518' M	Absent to ? trace	Absent	Fair	5
Moomba-1 Patchawarra Fm. [Core 8]	# 12 [9196-9258']	NGTS Rec. 1100' WC, 100' MW	Absent	Absent	Fair	5
Moomba-3 Toolachee Fm. [Cores 2 & 3]	# 1 [7879-7939']	GTS 29 mins. @ RTSTM Rec. 150' M	Absent to minor	Absent	Minor to abundant	6
Moomba-3 Toolachee Fm. [Core 4]	# 2 [7950-7991']	GTS 25 mins. @ 45 MCFD Rec. 180' M	Trace	? Fair	Minor to abundant	3
Moomba-3 Toolachee Fm. [Core 5]	# 3 [7988-8044']	GTS 4 mins. @ 38 MCFD Rec. 180' VSGCM	Mostly absent, abundant in one sample	Absent to ? minor	Fair to abundant	4

Table 5.7 (cont.)

Moomba-4 Toolachee Fm. [Core 2]	# 3 [7892-7913']	GTS 17 mins. @ 44 MCFD Rec. 260' GCM, 100' GCMW, 160' SGCW	Absent	Absent	Abundant	2
Moomba-4 Toolachee Fm. [Core 3]	# 5 [7909-7972']	GTS 29 mins. @ RTSTM Rec. 310' GCM+MW, 3515' GCW	Absent to minor	Absent to trace	Minor to abundant	2
Moomba-4 Toolachee Fm. [Cores 4 & 5]	# 6 [7988-8014']	NGTS Rec. 170' M, 130' SGCMW	Absent to minor	Absent	Minor to abundant	4
Moomba-5 Toolachee Fm. [Core 1]	# 4 [8045-8114']	GTS & WCTS 5 mins. @ 4.5 MMCFD	Absent to trace	Absent to trace	Mostly abundant	4
Moomba-6 Toolachee Fm. [Core 1]	# 1 [8003-8064']	GTS 14 mins. @ 192 MCFD Rec. 290' SLMW	Absent to trace	Absent	Fair to abundant	3
Moomba-6 Toolachee Fm. [Cores 2 & 3]	# 2 [8073-8142']	GTS 4 mins. @ 1.51 MMCFD Rec. 370' GCM	Absent, ? possible trace	Absent to ?? trace	Fair to abundant	7
Moomba-6 Toolachee Fm. [Core 4]	# 4 [8136-8190']	GTS 8 mins. @ 1.8 MMCFD Rec. 612' GCM	Absent to trace	? Trace	Fair to abundant	6
Moomba-6 Tool./Dara.Fms. [Cores 5 & 6]	# 5 [8196-8294']	GTS 3 mins. @ 5.35 MMCFD Rec. 150' GCM	Absent to abundant	Minor to abundant	Fair to abundant	11
Moomba-6 Daralingie Fm. [Cores 7 & 8]	# 6 [8318-8382']	GTS 30 mins. @ 87 MCFD Rec. 300' M	Generally absent, abundant in one sample	Trace to ? abundant	Minor to abundant	8
Moomba-6 Patchawarra Fm. [Core 9]	# 7 [9029-9082']	NGTS Rec. 2000' WC, 200' GCMW	Absent to very abundant	Minor to ? abundant	Fair	4
Moomba-7 Toolachee Fm. [Cores 1 - 5]	# 1 - 4 [8011-8253']	GTS @ max. 485 MCFD Rec. max. 432' GCM	Absent to trace	Absent	Minor to abundant	11

Table 5.7 (cont.)

Moomba-8 Toolachee Fm. [Cores 1 & 2]	# 2 [7782-7836']	GTS 7 mins. @ 5.3 MMCFD Rec. 606' M	Absent to very abundant	Absent	Mostly abundant	5
Moomba-8 Toolachee Fm. [Cores 3 & 4]	# 3 [7849-7926']	GTS 2.5 mins. @ 7.5 MMCFD Rec. 90' W	Mostly absent, very abundant in one sample	Absent	Generally abundant	5
Moomba-8 Toolachee Fm. [Core 5]	# 4 [7929-8023']	GTS 3.5 mins. @ 2.15 MMCFD Rec. 440' SGCM, 90' MW	Absent to abundant	Absent	Minor to v. abundant	3
Moomba-9 Toolachee Fm. [Cores 2 & 3]	# 1 [7736-7858']	GTS 4 mins. @ 2.4 MMCFD Rec. 650' GCM	Trace to abundant	Absent to trace	Mostly abundant to v. abundant	6
Moomba-9 Tool./Dara. Fms. [Cores 4 & 5]	# 2 [7861-7937']	GTS 3 mins. @ 4.6 MMCFD Rec. 220' W	Trace to v. abundant	Absent to ? trace	Fair to abundant	8
Moomba-9 Daralingie Fm. [Core 6]	# 3 [7941-8086']	GTS 4 mins. @ 9.1 MMCFD Rec. 30' W	Minor to abundant	Absent	Fair to abundant	2
Moomba-10 Toolachee Fm. [Cores 2 - 4]	# 3 & 4 [7689-7980']	GTS @ 7.8 to 9.2 MMCFD. Rec. max 150' MW.	Generally abundant, sometimes absent	Minor	Fair to abundant	7
Kirby-1 Epsilon Fm. [Core 2]	# 5 [9678-9738']	NGTS. Rec. 2768' water cushion, 30' drilling mud	Absent to trace	Absent	Minor to abundant	6
Burley-2 Epsilon Fm. [Core 3]	# 5 [10194-10235']	NGTS. Rec. 920' mixed mud, 568' WC	Absent	Absent	Abundant	5

production in the Cooper Basin (Table 5.7). In contrast, the delicate structure of the clays and the tortuosity of the micropore network are thought to prohibit oil production.

5.3.4 Porosity and permeability trends

A complex interrelationship of factors controls reservoir quality in the southern Cooper Basin. The important role of diagenesis has already been addressed (Chapter 4). Porosity and permeability were found to be reduced by reservoir cementation as well as mechanical and chemical compaction (Chapter 4). Additional factors that influence porosity and permeability include depth of burial, thermal sediment maturity, and sedimentary and textural parameters related to the palaeoenvironment of deposition of the Permian sediments.

5.3.4.1 Burial depth

A broad regional pattern of porosity distribution emerges when studying all available petrographic data from core samples. This is illustrated in figures 5.16 and 5.17. The two diagrams highlight differences in the type and abundance of porosity observed in thin section in relation to burial depth. There is a systematic decrease in the abundance of primary porosity towards the deeper portions of the basin whereas the proportion of microporous sands increases with depth (Fig.5.16). Secondary porosity broadly follows the distributional pattern of primary porosity (Fig.5.17). Beyond about 8400 feet, based on limited data, rocks which exclusively contain microporosity are predominant (Fig.5.16). Importantly, however, isolated remnants of primary pores are recorded in sandstones to depths approaching 10,000 feet in the central Nappamerri Trough (Fig.5.16), and possibly deeper as evident from ditch cuttings (Plate 18 D) (Appendix D). In such rocks there also exist local traces of secondary porosity (Fig.5.17) (Appendix D).

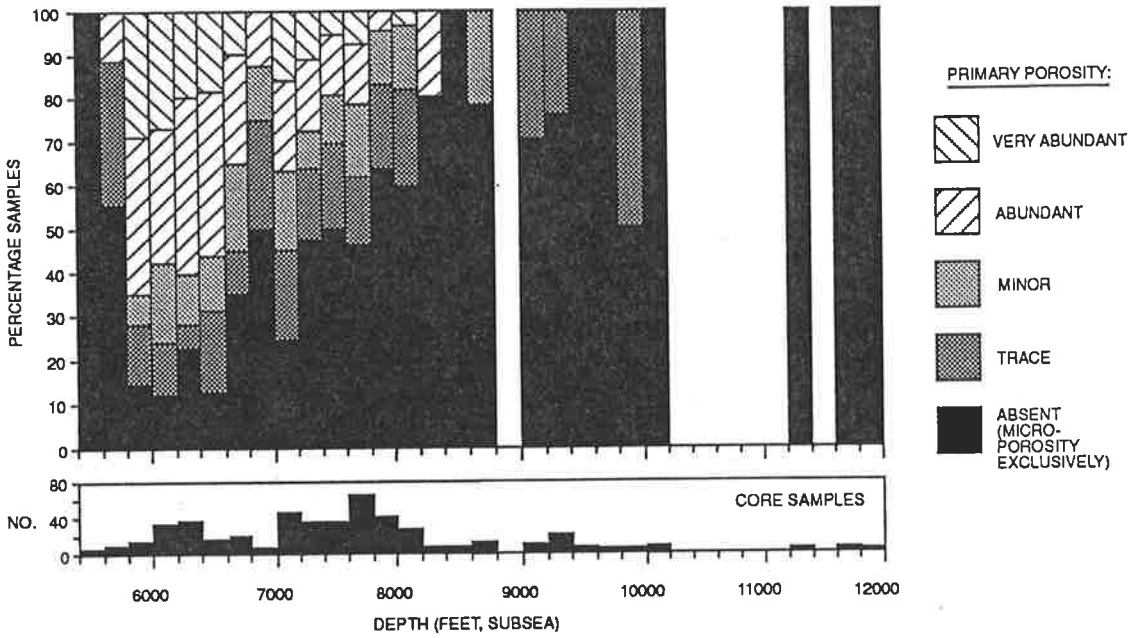

Figure 5.16 Relationship between primary porosity and microporosity with depth. The proportion of clastics with abundant primary porosity decreases towards the basin depocentre whereas microporous rocks increase in overall abundance. Porosity abundances were estimated from thin sections (Appendices D & J) [No. = Number of samples].

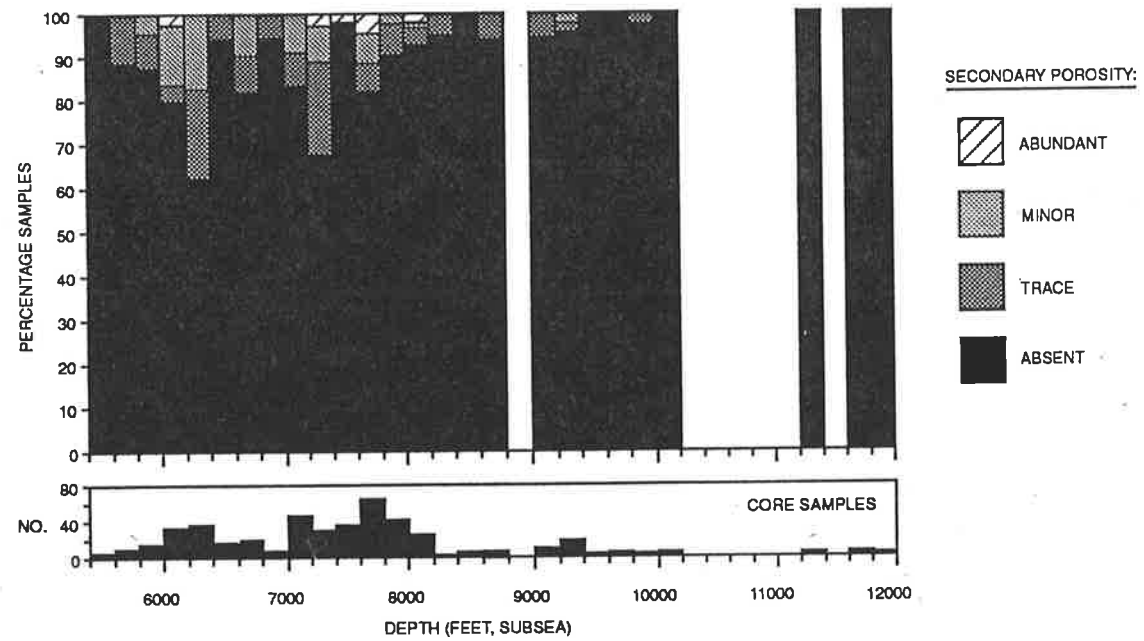

Figure 5.17 Relationship between secondary porosity and depth. The distribution of secondary porosity broadly follows that of primary porosity (cf. Fig.5.16). Porosity abundances were estimated from thin sections (Appendices D & J) [No. = Number of core samples].

5.3.4.2 Thermal sediment maturity

An attempt was made to study the influence of thermal sediment maturity on porosity and permeability. For this purpose, petrographic data from core samples was correlated against vitrinite reflectivity (R_v max. %) (Appendix I). The results show that between vitrinite reflectance levels of about 0.5 and 1.25 percent, macroporosity is a significant component of reservoir quality in many Permian sandstones (Fig.5.18). Between vitrinite reflectance levels of 1.25 and 2.0 percent, macroporosity is greatly reduced in abundance and most reservoir rocks are microporous. Beyond reflectance levels of 2.0 percent, based on a limited set of data, only trace remnants of macroporosity exist in some samples (Fig.5.18). Hence, available data suggests that both the zone of oil generation and the wet gas window as defined by Tissot & Welte (1978) [24] coincide with higher quality reservoir facies in the study area. In contrast, the zone of dry gas generation is associated with reservoir sequences dominated by microporosity.

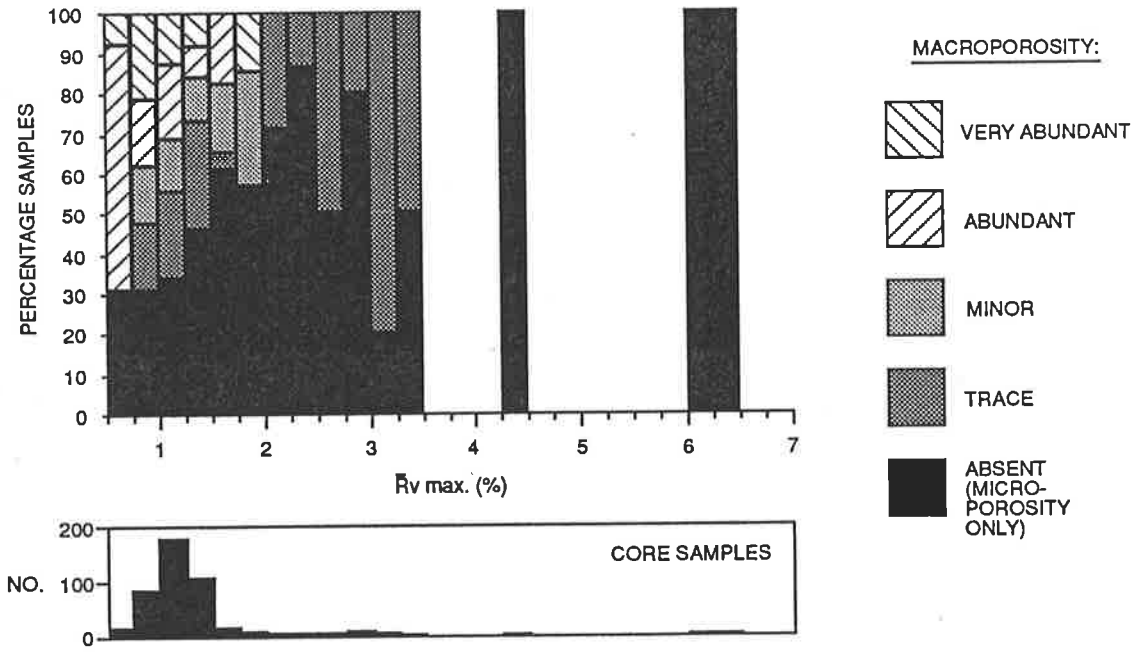

Figure 5.18 Relationship between macro- and microporosity versus vitrinite reflectivity of associated sediments (Appendix I) [NO. = Number of core samples] [Vitrinite reflectance data courtesy of Cooper Basin Consortium Group of Companies].

---

[24] Tissot & Welte (1978) place the zone of peak oil generation between vitrinite reflectance levels of 0.5 to 1.3 %, and the wet gas window between 1.3 and 2.0 %. Tissot & Welte (1978) consider the dry gas zone to commence at reflectance levels exceeding 2.0 %.

Table 5.8a Variation in reservoir porosity with grain size [No. = number of samples; Av. = average; St.Dev. = standard deviation].

Grain size	Min.	Max.	Av. (%)	St.Dev.	No.
Silt	0.2	10.7	3.41	3.3	20
Very fine	0.2	23.7	7.6	4.4	50
Fine	0.8	21.2	8.7	4.4	116
Medium	0.4	22.5	11.4	4.3	134
Coarse	4	22.6	13.5	4.6	63
V.coarse	1.2	22.4	10	5.7	27

Table 5.8b Variation in reservoir permeability with grain size [No. = number of samples; Av. = average; St.Dev. = standard deviation].

Grain size	Min.	Max.	Av. (md).	St.Dev.	No.
Silt	0.001	0.9	0.16	0.28	20
Very fine	<0.1	303	7.15	42.8	50
Fine	0.0001	396	12.3	54.16	116
Medium	0.001	720	38.4	101.2	134
Coarse	0.001	4380	177.1	571.4	63
V.coarse	0.01	6077	246.7	1166.2	27

5.3.4.3 Sedimentary facies and textural parameters

As a broad generalisation, core porosity increases with increasing grain size (Table 5.8a), and there is a similar relationship between grain size and permeability (Table 5.8b). Thus, sands of medium to coarse grain size are generally more porous and permeable than fine grained clastics (Schulz-Rojahn & Phillips, 1989). Similar results were reported by Steveson & Spry (1973), Martin & Hamilton (1981), and Staughton (1985). Sorting also plays an important role in influencing reservoir quality in the Permian sediments (Table 5.9). Well-sorted sands generally have higher porosities and permeabilities than their more poorly sorted equivalents of similar grain size (Table 5.9). This conflicts with data presented by Martin & Hamilton (1981) who considered that no clear relationship exists between sorting and permeability in some Cooper Basin reservoirs.

Textural parameters such as grain size and sorting are related to the palaeo-environment of deposition of the Permian sediments. When porosity/permeability data is differentiated on the basis of facies associations identified from log profiles and lithological core descriptions, general trends in reservoir character are apparent (Table 5.10 a & b). High-quality reservoir facies are associated with the basal part of channel and point bar sequences (Table 5.10 a & b). In particular, basal scour lags and channel floors as well as trough cross-bedded coarser sands that form part of the lateral accretion deposits of meandering rivers (Walker & Cant, 1984) have the highest average porosity and permeability values (Table 5.10 a & b). Trough cross-laminated finer sands also are characterised by relatively good reservoir quality (Table 5.10 a & b). Lower average porosity-permeability values are associated with point bar tops characterised by ripple cross-laminated sands, and sands with planar lamination (Table 5.10 a & b). The poorest reservoir potential in the fluvial sequences of the Cooper Basin is associated with vertical accretion deposits; these include floodplain and levee deposits that are generally fine-grained and clay-rich, and not very permeable (Table 5.10 b). However, within these sequences occur sandstones of crevasse splay origin that locally have a relatively high porosity and permeability character (Table 5.10 a & b).

Relatively little porosity/permeability data is available for sediments that originated in a deltaic environment of deposition. Existing information suggests proximal delta mouthbar/shoreline deposits and distributary delta channel fill sediments locally have excellent reservoir potential in the Cooper Basin (Table 5.10 a & b) (Plate 2B). In some very fine to fine grained, clean, well-sorted sandstones deposited in such environments, porosities as high as 22.5 percent and permeabilities approaching 400 md have been recorded (Tables 5.10b). Based on limited data,

Table 5.9
Influence of sorting on porosity and permeability for different grain sizes. Based on correlation of 376 core plugs with petrographic data [No. = number of samples; Av. = average; St.Dev. = standard deviation].

		POROSITY (%)				PERMEABILITY (md)			
Sorting	No.	Min.	Max.	Av.	St.Dev.	Min.	Max.	Av.	St.Dev.
VERY FINE & FINE SANDS									
v.poor & poor	79	0.2	16.2	6.5	3.7	0.01	5.3	0.31	0.7
fair-medium	73	0.2	20	8.9	4.1	0.01	63	3.59	10.15
well & v.well	25	0.7	23.7	10.9	6.8	0.01	396	59.2	120.9
MEDIUM SANDS									
v.poor & poor	42	0.9	19.1	10.6	4.1	0.01	133	10.3	25.2
fair-medium	53	0.9	18.3	11.5	3.6	0.01	215	24.7	51.9
well & v.well	17	6.8	22.5	15	4.25	0.1	720	133	195.5
COARSE & VERY COARSE SANDS									
v.poor & poor	71	1.2	22.6	11.7	5.3	0.01	773	80.3	174.6
fair-medium	12	8	17.6	13.2	2.9	0.57	325	74.5	106.4
well & v.well	4	13.3	20.4	17.9	3.2	20.3	565	227	257.9

Table 5.10a
Porosity trends for different facies associations. Data based on statistical investigation o 334 core plugs [data source: this study, Phillips (NCPGG, unpubl.), Thomas (1990), Alsop (1990)].

	NO.	Min.	Max.	Av.	St.Dev.
LATERAL ACCRETION: CHANNELS & POINT BARS					
scour lag/ channel floor	40	4.1	20.3	12	5
trough cross-bedded coarse sands	78	2.9	20.3	11.7	4.6
trough cross-laminated finer sands	18	7	13.1	11	2
ripple cross-laminated sands	25	3.8	12.8	8.3	2.4
sands with planar lamination	29	1.1	19.5	8.71	3.5
VERTICAL ACCRETION: CHANNEL ABANDONMENT & OVERBANK FLOODING					
flood plains & levees	58	0.2	12.4	5.2	3.25
crevasse splays	15	2.6	12	7	2.7
SANDS OF DELTA/SHORELINE ORIGIN					
distributary channel & proximal mouthbar/ shoreline sands	34	8.2	22.5	17.3	3.3
distal mouth bars	12	2.8	13.2	8.7	2.8
mouthbars: undifferentiated	61	2.8	17.4	11	3.3
pro-delta shales & delta plain deposits	4	3.7	7.3	5.75	1.6

Table 5.10b
Permeability trends for different facies associations. Data based on statistical investigation of 334 core plugs [data source: this study, Phillips (NCPGG, unpubl.), Thomas (1990), Alsop (1990)].

	NO.	Min.	Max.	Av.	St.Dev.
LATERAL ACCRETION: CHANNELS & POINT BARS					
scour lag/ channel floor	40	0.184	575.7	81.6	155
trough cross-bedded coarse sands	78	0.013	666	52.4	128.5
trough cross-laminated finer sands	18	0.4	212	27.9	74
ripple cross-laminated sands	25	0.036	17.3	2.4	4.8
sands with planar lamination	29	0.011	124	5.5	23.7
VERTICAL ACCRETION: CHANNEL ABANDONMENT & OVERBANK FLOODING					
flood plains & levees	58	0.001	8.1	0.5	1.7
crevasse splays	15	0.056	42	7	14.3
SANDS OF DELTA/SHORELINE ORIGIN					
distributary channel & proximal mouthbar/ shoreline sands	34	0.07	396	112.7	109.2
distal mouth bars	12	0.019	3.58	0.54	1.15
mouthbars: undifferentiated	61	0.009	60.5	9	16
pro-delta shales & delta plain deposits	4	0.01	0.1	0.078	0.045

reservoir quality deteriorates towards the distal end of delta fronts. Prodelta shales and delta plain marsh deposits have low porosities and permeabilities (Table 5.10 a & b). No information is available for crevasse splay sandstones in delta plain deposits; however, by analogy with their fluvial counterparts such crevasse splays may have local reservoir potential.

The distribution of clays is critical in influencing reservoir quality in the various depositional settings. Martin & Hamilton (1981) reported that permeability decreases with increasing clay content. In the present study and that of Schulz-Rojahn & Phillips (1989), finer grained samples were found to generally have higher proportions of detrital illite (Figs. 4.5 & 5.19). This is consistent with hydraulic regimes in depositional environments such as flood plain levees and distal offshore delta bars. Where illite contents are high, porosity and permeability are typically low (Figs. 5.20 & 5.21). Inversely, porosity and permeability are generally higher in samples which contain more kaolin, as evident from illite/kaolin ratios calculated from XRD traces (Figs. 5.20 & 5.21) (Schulz-Rojahn & Phillips, 1989). This broad trend is related to the increased abundance of dickite with associated microporosity in coarser grained sediments (Figs. 4.3 a-f & 5.13), and the occurrence of kaolinite which is more common in siltstones and fine sands (Fig. 4.3 a-f).

5.4 Part III: Discussion

5.4.1 General

The integration of core plug data with petrographic results provides valuable clues to determining the nature and distribution of porosity in the southern Cooper Basin. Based on a large database, kaolin-rich reservoir sandstones with no porosity visible in thin section have permeabilities of typically 2 md or less; such sands are essentially microporous (Fig.5.15). Statistical information indicates that almost two-thirds of all Permian clastics in the study area fall into this category (Fig.5.11b; Table 5.3). This is perhaps surprising considering over 100 petroleum fields containing about 6 TCF of sales gas and 300 MMSTB of oil and gas liquids have been discovered in the Cooper Basin since 1963 (Laws, 1989). The abundant occurrence of microporosity explains the generally low quality nature of the Permian reservoir sandstones (Fig. 5.11 a & b).

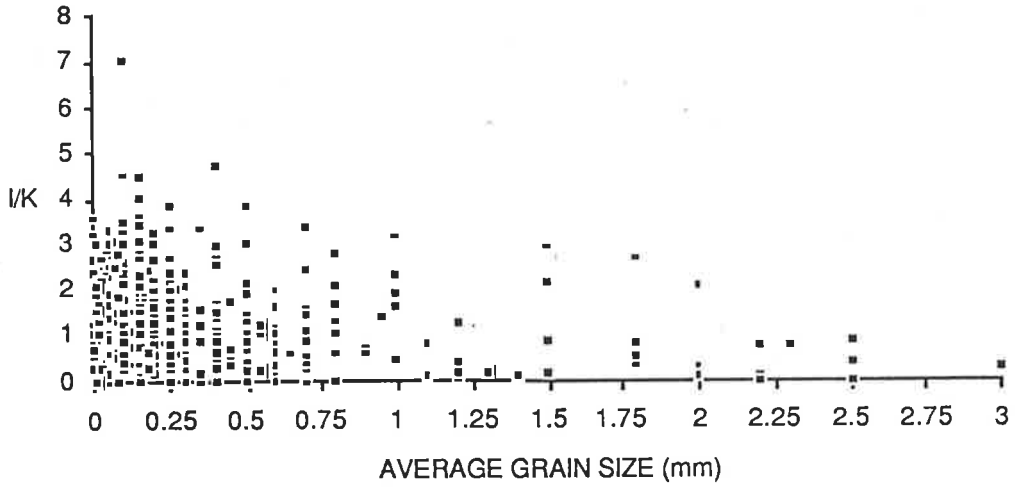

Figure 5.19 Crossplots of grain size versus illite/kaolin ratios for all core samples [data source: this study, Alsop (1990), Thomas (1990), Eleftheriou (1990), Phillips (NCPGG, unpubl.)].

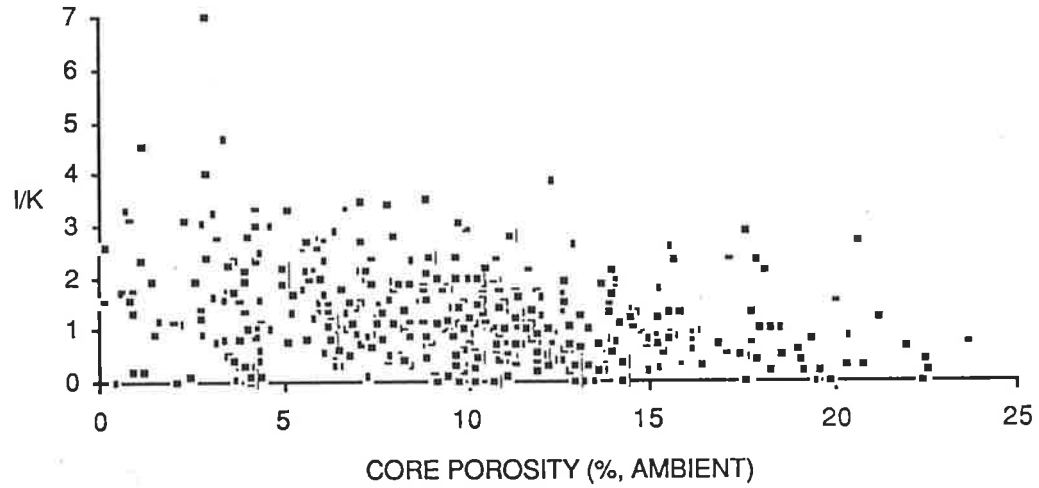

Figure 5.20 Crossplot of core porosity versus illite/kaolin ratios for all core samples [data source: this study, Alsop (1990), Thomas (1990), Eleftheriou (1990), Phillips (NCPGG, unpubl.)].

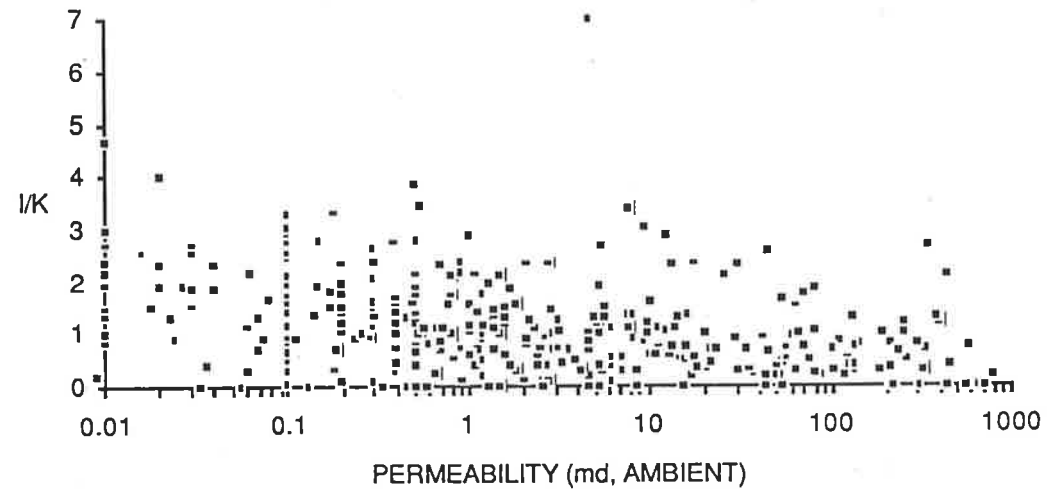

Figure 5.21 Crossplot of core permeability versus illite/kaolin ratios for all core samples [data source: this study, Alsop (1990), Thomas (1990), Eleftheriou (1990), Phillips (NCPGG, unpubl.)].

Microporous rocks are reported from numerous other petroleum provinces around the world, including the Permian Basin of New Mexico (Broadhead, 1984), the Piceance Basin of Colorado (Brown et al., 1986), the Appalachian Basin (Laughrey & Harper, 1986), the Greater Green River Basin of Wyoming, Colorado and Utah (Law et al., 1986), the Medicine Hat area in southeastern Alberta (Hankel et al., 1989), and offshore Gabon (Pittman & King, 1986). In Australia, high microporosity in clays was recently reported by Hawlader (1990a &b) for the reservoir sandstones of the Surat Basin; microporosity was found to be the volumetrically most important type of porosity (Hawlader, 1990b). Microporosity may also be widespread in other petroleum provinces in Australia, including the Eromanga Basin (cf. Table 5.3).

In the Cooper Basin, available petrographic data suggests the proportion of rocks dominated by microporosity increases in abundance towards the basin depocentres (Fig.5.16) (Schulz-Rojahn et al., 1991). This is reflected in the permeability data from the Permian sediments: clastics with permeabilities of 2 md or less roughly triple in abundance from the basin margin to its interior (Fig.5.11b).

In midflank and marginal areas of the Cooper Basin, reservoir quality is dominated by remnants of primary intergranular porosity (Schulz-Rojahn et al., 1991). Such sandstones greatly contribute towards the reservoir potential of the Cooper Basin as they typically have permeabilities of 10 md or greater (Fig. 5.15). In the study area, approximately 20 percent of all clastics fall into this category (Table 5.3). Higher-quality clastics generally also contain secondary porosity which resulted from the dissolution of labile grains (Martin & Hamilton, 1981; Stanley & Halliday, 1984; Schulz-Rojahn & Phillips, 1989).

The partial preservation of primary porosity is attributed to the introduction of an early quartz cement in coarser sediments. The quartz overgrowths acted as a rigid framework to resist the effects of compaction: quartz cementation reduced but did not occlude original depositional porosity (Schulz-Rojahn & Phillips, 1989; Schulz-Rojahn et al., 1991). In finer grained rocks where illite was abundant, quartz overgrowths were probably inhibited (Heald & Larese, 1974; McBride, 1989), thus allowing compaction to occur and primary porosity to be reduced (Schulz-Rojahn & Phillips, 1989).

The importance of quartz cement in diminuishing the effects of compaction in clastic sequences has been recognised elsewhere (eg. Houseknecht, 1984; McBride, 1989). In the Hartshorne Sandstone of North America, for example, samples with abundant quartz cement have better reservoir quality than many lesser cemented sands, the latter of which underwent major loss of porosity by intergranular pressure solution and compaction (Houseknecht, 1984). In the Cooper Basin, a similar process is

indicated by the fact that samples with a lack of authigenic quartz are invariably well-compacted and have almost no porosity visible in thin section (section 4.2.3.1).

The factors influencing the development and preservation of secondary porosity in the subsurface are less well-understood. There are numerous variables that are of importance in this context. In the regolith, these variables include controls on sediment provenance and depositional environment. Subsurface variables are related to the influence of meteoric versus connate water, structure, pressure, and temperature (Schulz-Rojahn & Phillips, 1989).

Giles (1987) considered development of secondary porosity to occur either in a closed system where the components become unstable under a given set of conditions or in an open system where mass transport is possible. Evidence favours the latter model for at least some of the secondary porosity created in the study area (Schulz-Rojahn & Phillips, 1989). Fluids of meteoric origin, although likely to be saturated with respect to silica, may be undersaturated with respect to other components. Hence, proximity to meteoric fluid flux may promote mineral dissolution, particularly in sandstones with high initial porosity (Bjørlykke, 1988). This may account for the common association of secondary porosity with coarser sandstones containing abundant primary porosity in the study area. Initial reservoir silicification that resulted from meteoric influx probably occurred simultaneously with the creation of secondary porosity (Schulz-Rojahn & Phillips, 1989). Some labile components were dissolved whereas others were altered and replaced by authigenic minerals; such labile components include feldspars, lithic fragments and to a lesser extent carbonate cements (Martin & Hamilton, 1981; Schulz-Rojahn & Phillips, 1989). The formation of secondary pores likely occurred during several stages of diagenesis (Fig.4.6).

The above considerations suggest there is a general transition in the nature of porosity with depth in the Cooper Basin (cf. Figs. 5.11b, 5.16 & 5.17). At least three broad porosity zones are identified (Fig.5.22), helping to explain changes in the porosity/permeability-depth curves in the study area (Figs. 5.10, 5.11 a & b):

➢ Zone I rims the marginal areas of the southern Cooper Basin and also occurs along structural highs; it is confined to depths of about 7000 feet or less. Zone I is characterised by abundant primary porosity, including erratic occurrences of secondary porosity. The proportion of rocks containing exclusively microporosity is low.

➢ Zone II marks the transition between porosity zones I and III, and occurs at intermediate structural depths (≥ 7000 to about 8400 feet). Primary porosity is much reduced but still represents a significant component of total porosity in many reservoir

rocks. Secondary porosity is of local significance. Microposity is proportionally more important.

➢ Zone III occurs towards the basin depocentres at depths exceeding about 8400 feet. Much of the central Nappamerri Trough falls within this zone. Microporosity associated with kaolin clay represents the dominant porosity type. However, isolated remnants of both primary and secondary porosity exist in some sandstones.

A possible fourth porosity zone is distinguished in the Patchawarra Formation at Burley-2 in the central Nappamerri Trough (Fig.5.22). In this area, petrographic and electron microprobe work suggest pyrophyllite forms at the expense of kaolin (section 4.2.3). As pyrophyllite is characterised by euhedral radial plates that fill pores and block pore throats (Plates 17 C, D, E & F), microporosity is effectively eliminated in pyrophyllite-bearing rocks. Hence, towards the deep central portions of the basin reservoir quality appears to be locally reduced by clay mineral reactions.

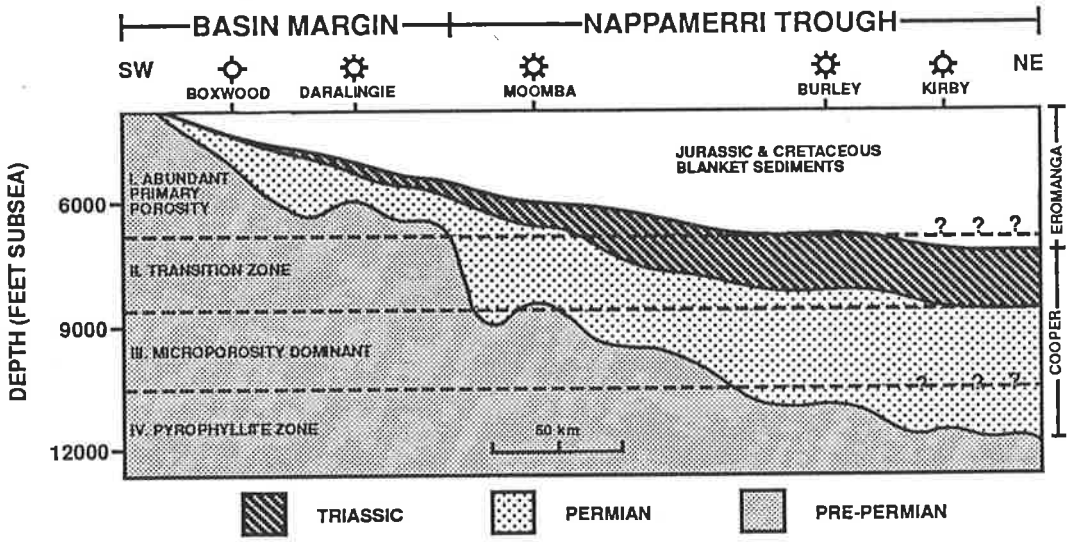

Figure 5.22 Schematic diagram illustrating broad transition in generic porosity types with depth in the southern Cooper Basin. Microporosity associated with kaolin clay is predominant in the central portions of the basin whereas reservoirs characterised by abundant primary porosity exist along the basin margin and in midflank position (interpretation based on combined investigation of petrographic results and core plug data).

The transition from sandstones dominated by primary porosity to those dominated by microporosity is not attributed to an overall increase in the kaolin content with depth. Overwhelming evidence from optical petrography and XRD work suggests kaolin occurs throughout the study area, and does not concentrate in the deeper portions of the basin (section 4.2.3.3). Instead, the general disappearance of clastics containing abundant remnants of primary pores is attributed to a greater degree of reservoir silicification in the more deeply buried sediments of the study area. This view is supported by the fact that only deeper samples are completely cemented by quartz, as indicated by CL and thin section studies (section 4.1.3.1) (Plates 4 A, 5 D, 6 C & D). A similar interpretation was put forward for the Toolachee Formation by Martin & Hamilton (1981) who considered reservoir silicification to increase with depth. Importantly, however, reservoir silicification with depth appears not to have been a strictly linear process, and some deeply buried sandstones escaped complete cementation by quartz, as indicated by thin section observations in the present study (Fig.5.16) (Plates 6 C, 18 B & D).

A number of other factors influence the decrease in average porosity/permeability with depth in the Cooper Basin. Of especial importance is compaction related to net overburden pressure (cf. Table 5.2). Mechanical compaction in Permian sandstones is evident from bent mica flakes, rearrangement of detrital grains and deformation of lithic fragments (section 4.1.1); such compaction resulted in denser grain packing and reduction of porosities in clayey sediments. In clean, moderate to well sorted sandstones mechanical compaction was largely suppressed by the introduction of early diagenetic quartz, as indicated by CL work (section 4.1.3.1). During later diagenesis, chemical compaction resulted in sutured grain contacts and stylolites in some sandstones. Again, mostly the finer grained clayey sediments were affected (section 4.1.2). A further important factor that influences the average deterioration in reservoir quality with depth in the Cooper Basin is clay authigenesis. Authigenic illite, clinochlore and pyrophyllite concentrate in sediments towards the basin depocentres (section 4.2.3.3). These clays block pore throats, effectively reducing porosity and permeability. Locally, reservoir quality is also destroyed by carbonate cementation, however there is no evidence to suggest carbonate cements actually increase in abundance with depth.

Last, the general basinward decrease in reservoir quality in the study area may further be attributed to broad facies changes from marginal areas to the depocentre of the Cooper Basin. Sediments deposited towards the interior of the basin are generally more distal and finer grained than their counterparts from shallower depths (Stuart, 1976). Downbasin facies changes of strata from fluviatile to 'lake' environments results in generally decreasing sandstone percentages towards the depocentres (Stuart et al., 1988). This general facies interrelationship is considered to be reflected in the

porosity-permeability data. Factors relating to the distribution of facies (Stuart, 1976), grain size, sorting and perhaps grain fabric all combine to influence reservoir character in the centre of basin deposition. In view of their more clay-rich nature, it is also apparent that distal facies are generally more prone to compaction than proximal sediments that tend to concentrate in up-flank position. This relationship helps to explain why features due to compaction are more pronounced at depth in the study area (Chapter 4). Also, towards the interior of the basin, meteoric flushing was probably not as vigorous, and silica was most likely gradually depleted from ground waters moving laterally due to precipitation along the margins. Hydrogeological and hydrochemical variability would have resulted in a lesser overall extent of early reservoir silicification in distal facies, also contributing to an increased porosity loss by compaction in many such sediments.

The lack of change of mean core porosity over the interval 8,000-10,000 feet (cf. Fig.5.10) may be due to sample bias. Alternatively, chemical diagenetic processes dominate the porosity character over this interval. This is unlikely however in view of the fact that no regional diagenetic modifications of such nature were observed in the study area. A more plausible explanation is that this interval marks an equilibration in bulk compaction of the Permian sediments.

5.4.2 Implications for petroleum exploration and development

5.4.2.1. General play concepts

The recognition that at least one phase of early silicification provided a rigid grain framework which prevented the process of compaction from irreversibly occluding porosity in many sandstones is of importance for play definition in the Cooper Basin. Despite multiple phases of silicification, primary porosity is mainly preserved in medium- to well-sorted sandstones in marginal and midflank areas of the study area. Such sandstones have the best overall reservoir potential, and in the foreseeable future will undoubtedly continue to provide numerous small to medium-sized oil and gas discoveries. Existing petroleum fields that produce from reservoir sandstones characterised by abundant primary porosity include the Wancoocha, Daralingie, Della, Toolachee and Strzelecki Fields, explaining the high porosity-permeability values in these areas (Table 5.5 a & b).

Petrographic studies support a meteoric model for early quartz cementation (Schulz-Rojahn & Phillips, 1989). Mature sandstones with low detrital clay contents and high initial porosities conducive to fluid flows are likely to have been the preferred migration conduits of the atmospheric waters. Facies associations befitting these criteria include the lower and middle portions of laterally accreted point bar deposits (Table 5.10 a & b). In such reservoir facies, the unimpeded flow of atmospheric waters enriched in silica is thought to have resulted in early reservoir silicification that

mostly lead to the suppression of compaction during later burial. The development of quartz overgrowths was made possible by the general absence of detrital clays. SEM and petrographic studies confirm the presence of well-developed quartz overgrowths in point bar sequences with good porosity and permeability in the southern Cooper Basin (eg. Plates 2 A, 4 D, 5 E & 18 A). As a result, point bars provide excellent targets for petroleum exploration in many parts of the study area, including marginal areas of the Cooper Basin, structural highs, and onlapping older strata near the depositional edge of the basin. Such sandstone sequences may also occur as downflank exploration plays. However, channel lag and point bar sandstones are less common towards the Nappamerri Low where such sediments grade laterally and intertongue with rocks more typical of deltaic and 'lake' deposition (Stuart, 1976).

Similar to sandstones of fluvial nature, sands of deltaic origin locally are characterised by abundant primary porosity (Plate 2 B) and permeabilities exceeding several hundred millidarcies (Table 5.10b). The best reservoir facies of deltaic nature include the distributary mouthbar/shoreline sands and interdistributary channel fill sediments (Table 5.10 a & b). CL and SEM studies confirm the loose grain packing at the time authigenic quartz was first introduced; again, the introduction of early diagenetic quartz is considered to have resisted the effects of compaction in these deposits. Importantly however, such high quality delta reservoir sands often are fine to very fine grained (Chapter 3; section 5.3.4.3). High-quality reservoir facies of fine-grained nature are anomalous since in the present study fine grained rocks in other depositional settings were found to be either completely cemented by quartz or very argillaceous, explaining their low overall porosity and permeability values (Table 5.8 a & b).

The general lack of detrital clay in the distributary mouthbar/shoreline sands and interdistributary channel fills is related to the high degree of sorting of these sands (Chapter 3). Clays were winnowed out by stream and/or wave action. Why such reservoir facies are not completely cemented by quartz despite their fine grained nature is believed to be related to their stratigraphic occurrence. Due to their more isolated nature, these sands are relatively poorly interconnected; they are considered to have become encased in shales because of 'lake' fluctuations related to differential subsidence and climatic variation (Stuart, 1976). As a result, the delta front sands were probably effectively shut off from the cementing influence of migrating pore fluids soon after deposition and the onset of early reservoir silicification. This assisted in the preservation of primary intergranular porosity in many of these fine grained sandstones. For this reason, well-developed distributary mouthbar/shoreline sands and interdistributary channel fill sediments will likely have economic significance for future exploration and development in the Cooper Basin. Delta-front sandstones have already proved their economic potential, such as in the Epsilon Formation at Big Lake

(Stuart, 1976; Taylor et al., 1991). At Dirkala-2, a hydrocarbon flow of 6.9 MMCFD and 287 BCPD was recorded from a very fine to fine proximal distributary mouthbar/shoreline sand in the basal Epsilon Formation (cf. Fig.3.7). Similarly, at the top of the Patchawarra Formation in Moomba-6, in excess of 7 MMCFD were recovered from a thin shoreline sand interval. This sandstone is overpressured (Battersby, 1976), and despite its depth (> 9000 feet) has abundant intergranular porosity (Stuart et al., 1990). Sands of deltaic origin may represent attractive targets for deep petroleum exploration.

The concept that initial reservoir silicification was an early event may be important in the development of other new and unconventional downflank exploration plays. Quartz cementation is thought to have begun prior to significant compaction, and there is evidence from CL data to suggest that some overgrowths on detrital grains are inherited; such overgrowths show abraded margins (section 4.2.3.1). These considerations may suggest that, following initial quartz overgrowth development in the shallow diagenetic realm, some sandstones were reworked [25]. This could have been accomplished, for example, by syndepositional earth movements that took place during Permian time; such syndepositional structural adjustments in the Cooper Basin are reported by Martin (1967a), Kapel (1972), Gatehouse (1972), Thornton (1973), Battersby (1976), Stuart (1976), and Fairburn (1989). Importantly, down-dip sedimentation of reworked clastics that experienced early reservoir silicification could have lead to the preservation of higher-quality reservoir facies in flank locations. The following speculative model is suggested: during the reworking of Permian sandstones in crestal areas, individual quartz grains that were loosely cemented by quartz broke up *but inherited part of the overgrowth*; such grains then were redeposited in downflank position where renewed quartz cementation was initiated by meteoric flushing. A second phase of overgrowth development was introduced which served as a framework to suppress mechanical compaction during later burial. The inherited overgrowths *effectively increased average grain size, resulting in an overall improvement of reservoir quality in the reworked sediments* since porosity/permeability are broadly related to grain size (Table 5.8 a & b).

In the Cooper Basin, it is possible that such a broad concept may help explorationists in the selection of new drilling targets. The model may be applicable to down-flank exploration plays in the vicinity of structures that show evidence of syndepositional movement during Permian time.

A further important recognition is that effective primary intergranular porosity was retained to great depths in some sandstones (Schulz-Rojahn et al., 1991).

---

[25] The possibility also exists that the detrital quartz grains with inherited overgrowths were derived from the hinterland craton. However, there is no evidence to suggest that such inherited overgrowths are more abundant near the basin margin, perhaps arguing against this hypothesis. The source origin of the inherited overgrowths requires isotopic resolution.

Evidence from core samples suggests remnants of original depositional porosity and some secondary porosity are present to depths approaching at least 10,000 feet. This offers encouragement to the petroleum industry for the drilling of deeper targets. It is interpreted that higher-quality reservoir facies ('sweet spots') occur within sandstone sequences dominated by low-permeability clastics. A similar phenomenon is reported from other petroleum provinces around the world (eg. Laughrey & Harper, 1986). In the Norphlet Formation of Alabama, for example, primary porosity is retained to depths in excess of 20,000 feet (Dixon et al, 1989; Ajdukiewicz et al., 1991). These findings provide ground for optimism in the search for deep basin reservoirs in the study area.

Another encouraging factor is that the pore filling kaolin in coarser sediments has significant microporosity. Undoubtedly, microporosity serves as storage space for gaseous hydrocarbons and contributes to long-term production in many petroleum fields. For example, microporosity in sandstones of the Moomba and Big Lake Fields accounts for much of the total porosity in reservoirs which have produced more than a trillion cubic feet of gas (Thomas, 1990; Stuart et al., 1990; Schulz-Rojahn et al., 1991); these fields comprise nearly 40 percent of the proven and probable gas reserves in South Australia (Morton, 1989). Scanning electron microscope studies support this conclusion by exhibiting the interconnection of pores between authigenic kaolin crystals, individual micropores being up to 30 microns in diameter (Chapter 4; section 5.3.1.3). Gaseous hydrocarbons could easily be stored in such pores because of the small molecular diameter of methane and other light hydrocarbons (Table 5.11). The small molecular diameter of the hydrocarbons also assists in sub-economic to economic gas flows from microporous rocks (Table 5.7). This is supported by laboratory results indicating kaolin is permeable to gas (Michaels & Lin, 1954). Where there are remnants of primary pores in microporous zones, initial flow rates in excess of 2 MMCFD are recorded. This upgrades the petroleum potential of the central Nappamerri Trough and other portions of the Cooper Basin where microporosity is predominant.

The importance of low-permeability clastics similar to those found in the Cooper Basin has increased tremendously in recent years. Reservoirs that were once too tight now are being re-evaluated in the light of new technology, such as hydraulic fracture stimulation (Stanley & Halliday, 1984; Magus et al., 1983; Brown et al., 1986). It is well-known that some of the largest gas fields in North America produce from low-porosity, low-permeability sandstones in downdip structural locations (Masters, 1979; Spencer, 1989) (Table 5.12). For example, the Canadian Milk River Field reservoir, containing recoverable reserves in the order of about 9 TCF, is a Late Cretaceous sandstone with an average permeability of 1 md (Masters, 1979; Magus et al., 1983). Other examples of low-permeability clastics (< 1.5 md) with large

commercial hydrocarbon accumulations are listed in Table 5.12. The data shows that average well production from 'tight' gas reservoirs generally is in the order of 100 to 1000 MCFD (Table 5.12). Such flows of relatively low volumes are often sustainable for 15 to 20 years (Laughrey & Harper, 1986). In the Cooper Basin, DST flow results of 1000 MCFD or less are not uncommon (Table 5.7). By analogy, the low-permeability clastics in the Cooper Basin can be developed, although they probably require reservoir stimulation before economic levels of production can be obtained. In recent years, hydraulic fracture stimulation has been successfully applied to reservoir sandstones of the Moomba Field (Thomas, 1990), the Big Lake Field (Stanley & Halliday, 1984), and the Tirrawarra Field (Salter, 1989). In the Patchawarra Formation at Big Lake-26, for example, gas flows increased from about 700 MCFD to 2.4 MMCFD after fracture stimulation (Stanley & Halliday, 1984). Another example is the Daralingie Formation intersected at Moomba-53 that did not sustain a gas flow on completion but after fracture stimulation flowed gas at a rate exceeding 3 MMCFD (Thomas, 1990). Other low-quality reservoir zones suitable for fracture stimulation were identified by Stanley & Halliday (1984) in the central Nappamerri Trough. The present study results support the conclusion that low-permeability clastics may be commercially exploitable in the deeper portions of the Cooper Basin.

Table 5.11 Approximate, effective molecular diameters of selected petroleum compounds and some reference molecules in Ångström (after: Tissot & Welte, 1978).

Molecule	Effective diameter in Å	Molecule	Effective diameter in Å
He	2.0	CH_4	3.8
H_2	2.3	benzene	4.7
Ar	2.9	*n*-alkanes	4.8
H_2O	3.2	cyclo-hexane	5.4
CO_2	3.3	complex ring structures	10 - 30
N_2	3.4	asphaltene molecules	50 - 100

$1\ nm = 10^{-9}\ m = 10\ Å$

In view of the fact that dickite crystals are typically larger than kaolinite (Chapter 4), and that dickite tends to concentrate in coarser sediments (Figs.4.3 a-f), the importance of proximal facies in microporous sequences is highlighted; dickite-bearing rocks have higher associated microporosity, and may theoretically store

Table 5.12 Reservoir parameters of low-permeability clastic gas fields in North America.

	San Juan Basin [1]	Milk River [2]	Appalachian Basin [3]	Pecos Slope [4]	Wattenberg Field [5]	Piceance Basin [6]
Location	New Mexico	Canada	Pennsylvania	New Mexico	Colorado	Colorado
Reservoir	Mesaverde & Dakota	Milk River	Medina Gp.	Abo	Dakota	Cozette, Corcoran & Rollins
Reservoir age	Cretaceous	Cretaceous	U.Devonian & Lr. Silurian	Permian	Cretaceous	Cretaceous
Average porosity (%)	7-10	15	0.5-12	5.0-15	9.5	2.6-22
Average permeability (md)	0.15-1.5	1	0.01-2.0	0.0067	0.3	0.002-0.04
Water saturation (%)	34-35	45	N.A.	N.A.	44	N.A.
Average pay (ft.)	60-80	60	N.A.	18+	25	N.A.
Original reservoir pressure (psi)	1360-3000	445	N.A.	N.A.	2750	N.A.
Average depth (ft.)	5400-7000	1100	1800-3400?	3800-4800	8000	3000-4000
Recoverable reserves (TCF)	7-11 [7]	9	N.A.	200 BCF	1.3	N.A.
Average well production (MCFD)	250-300	100	700-1000 (50-500 [8])	400	225	1131?
Well spacing (acres)	320	320	N.A.	160	320	N.A.

[1] Allen (1955), Pritchard (1973), Deischl (1973), Masters (1979); [2] Masters (1979); [3] Laughrey & Harper (1986) and references cited therein; [4] Scott et al. (1983), Broadhead (1984); [5] Matuszçzak (1973a,b), Masters (1979), Jones & Owens (1980); [6] Brown et al. (1986); [7] Infill drilling to change spacing from 320 acres to 160 acres may increase reserves 70% to 19 TCF in the Mesaverde reservoir (Long, 1977); [8] Prior to reservoir stimulation by hydraulic fracturing.

greater volumes of hydrocarbons than microporous sequences dominated by kaolinite. Depending on original rock composition, however, kaolinite may locally be very abundant. Environments favourable to the accumulation of feldspars are considered to be most conducive to the creation of microporosity associated with kaolinite (Schulz-Rojahn & Phillips, 1989). Such areas may have local reservoir potential.

Wireline log and mudlog gas analyses confirm that much of the Permian section in the central Nappamerri trough is gas-saturated [26]. The present study has shown that much of the microporous zone falls within the dry gas window (Fig.5.17). Hence, the possibility exists that dry gas is still being generated in this portion of the basin at the present time (section 4.3.5). Important in this context is that the relatively closed nature of low-permeability reservoirs imposes likely constraints on the ability of gas to migrate appreciable distances from the interbedded source rocks over a short geologic time. This effectively removes temporal restrictions of hydrocarbon generation and migration with respect to the development trap structures in tight sandstone sequences (Law et al., 1986), further encouraging the pursuit of basin-centred gas traps in the Cooper Basin sediments. Undoubtedly, the drilling of deeper targets has the potential to yield large commercial hydrocarbon discoveries in the study area.

5.4.2.2 Potential wireline log problems

The recognition that a significant proportion of porosity in the southern Cooper Basin is microporosity associated with kaolin clays has important implications for wireline log evaluation in this area, and possibly other petroleum provinces in Australia such as the Eromanga, Surat, Pedirka, Amadeus, Sydney, Otway and Bass Basins. Clay minerals within the pore system of a reservoir sandstone affect the electrochemistry and physical properties of the rock (Wescott, 1983; Laughrey & Harper, 1986). In particular, common parameters calculated from wireline logs - such as clay volume (V_{sh}), porosity (Ø), water saturation (S_w) and hydrocarbon saturation (S_{hc}) - are likely to be affected.

---

26 Information obtained from well completion reports, courtesy of Cooper Basin Consortium Group of Companies.

5.4.2.2.1 V_{sh} determination

An estimate of the shale (or clay) volume (V_{shale}) of a reservoir sandstone is routinely derived from the deflections of the gamma ray (GR) curve using the equation

$$V_{sh} = \frac{GR - GR(min)}{GR(max) - GR(min)}$$

where GR(max) = 100 % shale and GR(min) = 0 % shale (Rider, 1986; Bowler, 1988). The gamma ray provides a measure of a formation's natural radioactivity emanating from uranium, potassium and/or thorium. In particular, the potassium content of the clay minerals varies considerably. Illites contain by far the greatest amount, while kaolinite has very little or none (Table 5.13). As stated by Rider (1986, p. 63), "the consequence of this is that clay mixtures with a high kaolinite ...content will have lower potassium radioactivity than clays made up essentially of illite". The implication is that the total clay content of a reservoir rock may be underestimated by the gamma ray log where kaolin is present (Bowler, 1988).

5.4.2.2.2 Porosity determination

Empirically derived porosity values using the gamma ray (GR) - sonic (Δt) tool combination are in good agreement with core values of porosity in the Cooper Basin (Porter & Crocker, 1972; Vegh, 1975; Porter, 1976; Morton, 1989). By implication, the porosity log does not differentiate between different porosity types but measures total porosity ($\emptyset_T$). This creates problems for the geological interpretation of the petrophysical data. A calculated log porosity of, say, 10 percent in a reservoir sandstone may be attributed as much to a rock dominated by microporosity as to a sandstone in which primary porosity is predominant. Clearly, differentiation between different porosity types in a reservoir rock is of crucial importance for both play definition and assessment of reservoir quality in the subsurface. Microporosity is unfavourable to oil production, thus downgrading the potential for commercial oil discoveries in kaolin-rich sandstones. Clay in the rock structure may cause anomalously high porosity readings (Spencer, 1985). Hence, non-recognition of microporosity may lead to over-optimistic assessment by explorationists of reservoir quality in rocks with a high proportion of kaolin clay (Schulz-Rojahn & Phillips, 1989; Schulz-Rojahn & Stuart, 1991). This is important in the context of tight

exploration plays when commercial porosity cut-off values are particularly critical (Schulz-Rojahn & Phillips, 1989).

Table 5.13 Potassium in clay minerals: chemical content [from: Serra (1979), Dresser Atlas (1983)].

Mineral	% by weight	Average %	Construction
Illite	3.51 - 8.31	5.2	K, Al, Silicate
Kaolinite	0.00 - 1.49	0.63	Al, Silicate
Smectite	0.00 - 0.60	0.22	Ca, Na, Mg, Fe, Al, Silicate
Chlorite	0	0	Mg, Fe, Al, Silicate

5.4.2.2.3 Water saturation calculations

A further key problem for log evaluation relates to the high irreducible water saturation associated with microporosity (Keike & Hartmann, 1973; Almon & Schultz, 1979; Hutcheon, 1983; Wescott, 1983; Ranganathan & Tye, 1986; Laughrey & Harper, 1986; Tieh et al., 1986; Pittman, 1979, 1989; Schulz-Rojahn & Stuart, 1991). Clays contain lattice-water which forms part of the clay mineral structure (Table 5.14), as well as adsorbed water clinging to the clay surface; micropores among the clay particles also hold water by capillary forces (Rider, 1986; Pittman, 1989). Such water can be considered to be 'bound', or physically immobile water; it is an order of magnitude more conductive than the pore waters and decreases resistivity readings (Almon, 1979; Wescott, 1983; Spencer, 1985; Laughrey & Harper, 1986). Electric logs, which measure resistivity for the purpose of calculating water saturation (S_w) cannot presently differentiate between bound and movable ('free') water in clay-rich sequences (Almon & Schultz, 1979; Pittman, 1989). Consequently, values for S_w may compute too pessimistic, and productive zones may be by-passed because they

appear water-wet (Pittman, 1989). As stated by Pittman (1979, p.170), "log calculations may indicate water saturations are too high for a productive interval... [although] the reservoir may be capable of essentially water-free production because the water is predominantly irreducible". For example, it is well-known that very fine grained sandstones with high irreducible water contain producible hydrocarbons in the Tertiary sequences of the Gulf Coast Basin and Niger Delta; these reservoirs are present in what were initially considered to be dry holes because of water saturations calculated at 55 to 60 percent (Dr. W.J. Stuart, NCPGG, pers.comm., 1989). High S_w values (> 70 %) are also reported from clay-rich sequences characterised by abundant microporosity in the Upper Jurassic Cotton Valley Sandstone of East Texas (Wescott, 1983) (Table 5.15a). Wescott (1983) commented that log-calculated water saturations are subject to large errors in this region because of the bound water associated with the clays. Further, Ranganathan & Tye (1986) were able to show that calculated water saturation increases with increasing clay content and abundance of microporosity in the Late Cretaceous Shannon Sandstone of Wyoming. In this reservoir zone, water saturation is as high as 60 percent in clastics characterised by abundant microporosity, as compared to only 10-24 percent in sandstones where microporosity is low (Table 5.15b). Again, much of the water saturation is considered to be irreducible where microporosity is predominant (Ranganathan & Tye, 1986). An analoguous situation to these petroleum provinces likely exists in the Cooper Basin and other basins in Australia.

Clay type	% water (av.)
Illite	8
Kaolinite	13
Chlorite	14
Smectite	18-22

Table 5.14 Structural water in clays (after Weaver & Pollard, 1973). This excludes adsorbed water clinging to the clay surface under reservoir conditions, and water held in micropores between clay particles by capillary forces.

5.4.2.2.4 Hydrocarbon reserve estimates

Misleading results of log calculations of water saturation are problematic for realistic determination of hydrocarbon reserves (Schulz-Rojahn & Stuart, 1991). This is because water saturation is inversely related to the saturation in hydrocarbons (S_{hc}) of a reservoir zone (Rider, 1986):

Table 5.15a
Effect of diagenetic facies on log porosity and calculated water saturation, as exemplified by the Cotton Valley Sandstone (Upper Jurassic), East Texas (modified from Wescott, 1983).

Diagenetic facies	Characteristics	Porosity (log)	Water saturation (Sw)
'Type I'	Well-cemented by quartz and calcite	< 3 %	15 - 75 %
'Type II'	Clay-rich, high microporosity	3 - 10 %	> 75 %
'Type III'	Abundant secondary porosity	> 10 %	25 - 75 %

Table 5.15b
Effect of diagenetic facies on core/thin section porosity and calculated water saturation, as exemplified by the Shannon Sandstone (Late Cretaceous) of the Hartzog Draw Field, Wyoming (data compiled from Ranganathan & Tye, 1986).

Diagenetic facies	Characteristics	Porosity	Water saturation (Sw)
'Type I'	Sparse clay (< 2%), low microporosity	Core: 14-19 % Thin section: 8 % (average)	10 - 24 %
'Type II'	Some dispersed clay, most porosity is microporosity	Core: 11-15 % Thin section: generally less than 3 %	15 - 45 %
'Type III'	Abundant dispersed clay, microporosity is high	Core: 7-10 % Thin section: nil.	30 - 60 %

$$S_{hc} = 1 - S_w$$

Hence, if values for S_w compute too high because of bound water, the volume of hydrocarbons within a pay zone may proportionally be underestimated. This highlights the importance of the identification of the type(s) of porosity in a reservoir sequence. Non-recognition of microporosity may lead to pessimistic assessment of hydrocarbons in-place, and influence perceptions of prospectivity in the Cooper Basin and elsewhere.

5.4.2.3. Potential hydrocarbon recovery problems

The important role of diagenesis in hydrocarbon recovery is addressed by various authors (Pittman, 1979; Almon & Davies, 1981; Thomas, 1981; Hutcheon, 1983). Sandstone reservoirs are affected by production operations, and rock-fluid interactions can severely impair the porosity-permeability characteristics of a hydrocarbon-bearing interval (Kantorowicz et al., 1986). In the Cooper Basin, the potential recovery problems associated with early Permian gas reservoirs in the Big Lake Field were outlined by Stanley & Halliday (1984). Additional information pertaining to the influence of reservoir mineralogy on hydrocarbon recovery in different basins is presented by Keighin (1979), Almon & Davies (1979, 1981), Thomas (1981), Kantorowicz et al. (1986), and Pittman & King (1986). Briefly, potential recovery problems in the Cooper Basin include:

➢ *Migrating fines*. Microporosity associated with clay minerals increases the tortuosity of the pore network making the clay particles prone to dislodgement by high hydrocarbon flow rates. As a result, the clay particles may block pore throats, shutting off flow in that part of the rock (Hutcheon, 1983; Stanley & Halliday, 1984). This is characteristic of kaolin and less commonly so of chlorite and illite. The problem can be overcome by both decreasing flow rates and using clay stabilisers (Almon & Davies, 1979, 1981).

➢ *Fresh water sensitivity*. Both kaolin and illite are sensitive to the introduction of fresh water which can cause permeability impairment (Pittman & King, 1986). The same applies to trace amounts of illite-smectite detected in the sandstones of the Big Lake area; illite-smectite is also sensitive to sodium chloride waters (Stanley & Halliday, 1984).

➢ *HCl sensitivity*. Iron-rich chlorite, illite, siderite and ferroan dolomite exposed to acid treatment will dissolve and precipitate iron hydroxide gel ($Fe(OH)_3$), greatly reducing effective permeability (Almon & Davies, 1977, 1979; Keighin, 1979; Stanley & Halliday, 1984). If acids are employed, the problem can be overcome by using weak HCl (< 12 %) and iron-chelating and oxygen-scavenging agents and surfactants (Stanley & Halliday, 1984).

➢ *HF sensitivity*. Carbonate cements such as calcite and dolomite react with HF acids to form calcium fluoride (CaF_2) (Almon & Davies, 1979; Stanley & Halliday, 1984). Davies (1980) suggested that HF may be used in formations with less than 5 percent carbonate cements.

CHAPTER SIX

CARBON AND OXYGEN ISOTOPE INVESTIGATION OF CARBONATE CEMENTS

6.1 Introduction

In the present chapter, the genesis of the carbonate cements in the southern Cooper Basin is more closely investigated by stable carbon and oxygen isotope analysis, as well as electron microprobe work. This is done to shed more light on the factors controlling carbonate cementation in the southern Cooper Basin, supplementing results presented in Chapter 4.

The study so far has shown that carbonate cementation is complex. Several varieties of carbonate cements are distinguished. The dominant carbonate variety is siderite, with other less frequently distinguished carbonate types including ankerite, dolomite, Fe-dolomite, and calcite (cf. Fig.4.1). The carbonate cements vary rapidly in lateral and vertical abundance, and their distribution is not systematically related to depth of burial or restricted to specific formations. Locally, total carbonate content is as high as 70 per cent and more, and can result in the complete elimination of porosity and permeability in some reservoir sandstones. This renders prediction of reservoir quality at depth most difficult.

However, there are other reasons why knowledge of the genesis and distribution of carbonate cements in siliciclastic reservoirs is of importance to the petroleum industry. Massive carbonate-cemented zones may form restrictions to fluid flow and create updip seals in reservoir sands (Donovan, 1974a; Boles & Ramseyer, 1987; Bjørlykke et al., 1989). In contrast, the dissolution of carbonate cements enhances reservoir quality at depth in many basins (eg. Meszoly et al., 1986; Dickinson, 1988). The subsurface presence of carbonate-cemented zones can also negatively affect seismic data quality by resulting in velocity anomalies rendering geophysical interpretation problematic for explorationists (Anderson, 1985; Pinchin & Bayly, 1989). Further, carbonate cements may negatively influence field development as they can precipitate in the tubing string of producing wells, resulting in a pressure drop and a decline in hydrocarbon production (Boles & Ramseyer, 1987). In recent

years, the idea has also been put forward that carbonate cements in clastic sequences may serve as a guide to hydrocarbon accumulations (Donovan, 1974a; Donovan et al., 1974; Smith, 1978; Al-Shaieb & Lilburn, 1982; Fullagar, 1989).

The above considerations highlight the need to know more and in greater detail how the carbonate cements form. Determination of the mechanism(s) that control carbonate cementation can assist petroleum exploration in the Cooper Basin and elsewhere. Stable carbon and oxygen isotope geochemistry provides data to assess the diagenetic timing, temperature range of crystallisation, and source origin of the carbonate cements [27]. Electron microprobe results provide clues to the chemical evolution of these cements. This is of importance for the regional assessment of pore water compositions during carbonate formation, and in turn can provide insight into brine evolution in the Cooper Basin over geologic time.

6.2 Previous studies

Carbonate cements in the Cooper Basin have to a lesser extent previously been isotopically investigated by Gould & Smith (1979), Wall (1987), and Bone (University of Adelaide, unpubl. data). Gould & Smith (1979) studied one siderite sample from Brolga-1 whereas Bone (unpubl.) investigated eight siderites from the Mudrangie-1 and Tirrawarra-1 wells; Wall (1987) examined nine siderite samples and one calcite sample from a variety of hydrocarbon fields in the southern Cooper Basin. The studies of Gould & Smith (1979) and Bone (unpubl.) focused exclusively on nodular micrites associated with shales and coals, whereas the nature of the carbonates studied by Wall (1987) is unspecified. Gould & Smith (1979) interpreted the nodular micrite to be the product of the early post-depositional environment. Similarly, Wall (1987) concluded that most of the siderites formed early in the diagenetic paragenesis at relatively low temperatures, although Wall (1987) conceded some probably also originated from higher temperature fluids.

6.3 Sample origin and procedures

35 core samples derived from 21 petroleum wells located throughout the southern Cooper Basin were selected for C^{13}/C^{12} and O^{18}/O^{16} isotope analysis of the

[27] For a comprehensive review of the subject, the reader is referred to the work of Fritz & Fontes (1980, 1986) and Faure (1986).

carbonate cements (Table 6.1) (Appendix H). The data pool is supplemented by electron microprobe analyses of 21 core and ditch samples from 18 wells carried out by Dr. S.E. Phillips (NCPGG) (Appendix F).

Table 6.1 Origin and nature of samples chosen for oxygen and carbon isotope analysis, and the results obtained. For locality plan of wells see Figure 1.1 (ss = subsea; sst. = sandstone).

Sample Number	Well Name	Depth (ft.,ss)	Formation	Lithology	$\partial^{13}C$ (PDB)	$\partial^{18}O$ (PDB)	T(°C) [-15]*	T(°C) [-16]*
CB-0020	Big Lake-31	9348	Patchawarra	Fine sst.	-6.03	-22.1	70.2	64
CB-0062	Big Lake-3	8103	Epsilon	Siltstone	-3.03	-16.8	39.5	34.8
CB-0075	Big Lake-29	9535	Tirrawarra	Conglomerate	-7.67	-17.7	44	39
CB-0085	Della-3	6431	Toolachee	Fine sst.	-3	-15.4	32.5	28
CB-0105	Pando-2	5679	Epsilon	Medium sst.	-10.9	-17.4	42.2	37.3
CB-0120	Big Lake-1	7589	Toolachee	Fine sst.	-1.3	-14.7	29.5	25.2
CB-0140	Pando North-1	5977	Epsilon	Fine sst.	-11 [1]	-17.1 [1]	55.1 [2]	49.7 [2]
CB-0189B	Murteree-1	5815	Toolachee	Shale	-1.45	-16.3	37	32.4
CB-0189T	Murteree-1	5815	Toolachee	Very coarse sst.	-2.65	-16.1	36	31.4
CB-0258	Moomba-6	8062	Toolachee	Fine sst.	-1.81	-14.9	30.4	26.1
CB-0274	Strzelecki-15	6082	Toolachee	Very fine sst.	-2.91	-16.7	39.1	34.3
CB-0315	Toolachee-3	6993	Patchawarra	Medium sst.	-4.75	-18.6	49	43.8
CB-0317	Toolachee-3	7008	Patchawarra	Siltstone	-0.4	-17.8	44.3	39.3
CB-0345	Toolachee-1	6717	Patchawarra	Very fine sst.	-3.88	-17.6	43.5	38.5
CB-0346	Toolachee-1	6720	Patchawarra	Very fine sst.	-3.88	-17.1	41	36.1
CB-0398	Moomba-3	7799	Toolachee	Medium sst.	-5.7	-18.9	50.5	45.3
CB-0404	Moomba-3	7864	Toolachee	Very coarse sst.	-11.3	-20.7	77.5 [2]	71 [2]
CB-0410	Moomba-3	7948	Daralingie	Fine sst.	-9.45	-20.4	59.4	53.7
CB-0415	Toolachee-5	7076	Patchawarra	Very fine sst.	-4.5 [1]	-17.4 [1]	43.1	38.1
CB-0458	Strzelecki-1	6108	Toolachee	Medium sst.	-4.72	-17.4	42.4	37.5
CB-0486	Dilchee-1	8031	Patchawarra	Medium sst.	-5.69 [1]	-19.1 [1]	51.6	46.2
CB-0493	Strzelecki-1	6338	Patchawarra	Fine sst.	-1.46	-15	30.9	26.5
CB-0494	Strzelecki-1	6356	Patchawarra	Very fine sst.	-2.35	-15.5	33	28.5
CB-0495	Strzelecki-1	6362	Patchawarra	Very fine sst.	-0.56	-14.6	28.9	24.6
CB-0497	Strzelecki-1	6367	Patchawarra	Fine sst.	-1.04	-14	26.1	21.9
CB-0520	Moomba-7	7934	Toolachee	Medium sst.	-3.26	-17.6	43.4	38.4
CB-0529	Toolachee-6	7183	Patchawarra	Siltstone	-0.16	-17.1	40.8	36
CB-0536	Toolachee-6	7411	Patchawarra	Coarse sst.	-9.33	-20.2	57.7	52.1
CB-0551	Toolachee-1	5862	Toolachee	Coarse sst.	-6.88	-17.4	42.6	37.6
CB-0554	Toolachee-1	6290	Epsilon	Siltstone	-3.41	-16.1	35.9	31.3
CB-0556	Toolachee-34	6681	Epsilon	Fine sst.	-5.45	-17.2	41.5	36.6
CB-0558	Toolachee-34	6695	Epsilon	Very fine sst.	-2.4	-16.1	35.9	31.3
CB-0567	Munkarie-2	6599	Epsilon	Medium sst.	-4.57	-18.2	46.8	41.7
CB-0571	Munkarie-2	6964	Patchawarra	Very fine sst.	-3.67	-17.4	42.5	37.6
CB-0574	Brumby-1	7127	Patchawarra	Very coarse sst.	-3.2	-18.5	48.1	43

* Expressed as per mil values (‰) relative to PDB
[1] Average value (see Appendix H)
[2] Dolomite fractionation factor used (Land, 1983)

The work programme is supplemented by XRD results and petrographic data. Analytical methods and research procedures adopted are outlined in Chapter 1.

Isotope work is almost exclusively restricted to the siderite cements, because of the overwhelming abundance of these cements (Fig.4.1). However, two samples containing ankerite were also incorporated into the study programme. The electron microprobe study focuses on siderite, ankerite and dolomite cements.

6.4 Results

6.4.1 X-ray diffraction

The minerals identified from XRD traces in the samples selected for isotopic analysis are shown in Table 6.2. The minerals include quartz, kaolinite, dickite, illite, ankerite and/or siderite. Ankerite was identified only in samples CB-0404 and CB-0140. In sample CB-0140, abundant ankerite co-exists with minor siderite, in the remainder of samples carbonate composition is mono-mineralic. However, in samples CB-0062 and CB-0085 compositional variations within the siderite are indicated by peak doublets. Illite/muscovite is of a 2M1 variety with a relatively broad base to the 10 Å peak.

6.4.2 Optical petrography

Examination under the optical microscope reveals the samples to contain various types of carbonate cements as based on crystal habit and crystal size (Table 6.3). Rhombohedral and scalenohedral spar, anhedral micrite, and subhedral microspar are distinguished (Plates 8 & 9), and all may occur together in the same sample. Only in eight samples is the carbonate cement restricted to a single petrographic variety (Table 6.3). Siderite may adopt any of the crystal habits whereas ankerite occurs only as sparry cement and possibly also as microspar. The micritic siderite variety is found in shales, silts and fine-grained sandstones, whereas sparry carbonates are generally associated with fine to coarse sandstones with low clay

Table 6.2
Bulk X-ray diffraction results of samples analysed (Abbreviations: QZ = quartz, KAO = kaolinite, DI = dickite, ILL = illite/muscovite, ANK = ankerite, SID = siderite; T = trace, M = minor, SD = sub-dominant, CD = co-dominant, D = dominant).

Sample Number	QZ	KAO	DI	ILL	ANK	SID
CB-0020	D	M	-	M	-	SD
CB-0062	M	T	-	T	-	D
CB-0075	D	M	-	M	-	M
CB-0085	D	M	?T	M	-	CD
CB-0105	D	SD	-	SD	-	SD
CB-0120	D	T	-	T	-	SD
CB-0140	D	M	-	M	CD	M
CB-0189B	T	?T	-	T	-	D
CB-0189T	D	M	-	M	-	SD
CB-0258	D	M	-	M	-	CD
CB-0274	D	SD	-	SD	-	M
CB-0315	D	-	M	T	-	SD
CB-0317	D	SD	-	SD	-	CD
CB-0345	D	-	M	M	-	M
CB-0346	D	-	SD	SD	-	M
CB-0398	D	-	M	M	-	SD
CB-0404	D	-	M	M	M	-
CB-0410	SD	T	-	M	-	D
CB-0415	D	SD	-	SD	-	SD
CB-0458	D	-	T	T	-	SD
CB-0486	D	M	-	M	-	M
CB-0493	D	M	-	M	-	M
CB-0494	D	M	-	M	-	SD
CB-0495	D	M	-	T	-	SD
CB-0497	D	M	-	T	-	SD
CB-0520	D	-	T	T	-	SD
CB-0529	D	SD	-	SD	-	CD
CB-0536	D	-	SD	M	-	CD
CB-0551	D	-	SD	M	-	M
CB-0554	D	SD	?T	M	-	CD
CB-0556	D	-	SD	M	-	SD
CB-0558	D	M	?T	SD	-	SD
CB-0567	D	-	SD	T	-	M
CB-0571	D	-	M	M	-	CD
CB-0574	D	-	SD	T	-	CD

Table 6.3
Variations in carbonate cement morphology as evidenced by petrographic results (The same abbreviations are in use as in Table 6.2).

Sample Number	Spar	Micro-spar	Micrite
CB-0020	SD	D	T
CB-0062	M	D	T
CB-0075	D	-	-
CB-0085	D	M	M
CB-0105	D	M	-
CB-0120	D	M	SD
CB-0140	D	M	-
CB-0189B	-	-	D
CB-0189T	D	SD	M
CB-0258	M	T	D
CB-0274	D	-	-
CB-0315	D	M	-
CB-0317	-	SD	D
CB-0345	T	D	M
CB-0346	D	M	-
CB-0398	D	T	T
CB-0404	D	-	-
CB-0410	D	M	-
CB-0415	M	T	-
CB-0458	D	-	-
CB-0486	D	M	-
CB-0493	M	M	T
CB-0494	D	M	M
CB-0495	D	T	T
CB-0497	D	SD	SD
CB-0520	D	M	-
CB-0529	-	SD	D
CB-0536	D	-	-
CB-0551	D	M	-
CB-0554	M	D	M
CB-0556	D	T	-
CB-0558	T	D	SD
CB-0567	D	-	-
CB-0571	D	M	T
CB-0574	D	-	-

content (section 4.2.3.2). The sparry carbonates can in places be seen to surround micritic siderite blotches (Schulz-Rojahn & Phillips, 1989) (Plate 8 A).

6.4.3 Electron microprobe

Electron microprobe analyses demonstrate considerable elemental zonation within most carbonates. This is evident by variations in Mg, Mn, Ca and Fe content (Appendix F). Such variations were not apparent in thin section. Striking differences are observed when backscattered electron images are compared to the same areas studied in thin section (Plate 21 A & B).

6.4.3.1 Siderites

Siderite cements rarely consist of one chemical phase. The first cement phase is typically low in Mg-content and later phase(s) have higher Mg-concentrations (Plate 22 D). This relationship is evident in siderite cements irrespective of morphology or crystal size, as micrite, microspar and spar all exhibit similar compositional variation. The implication is that differences in crystal habit do not preclude the possible co-precipitation of these carbonate varieties. In the case of one sample derived from the Epsilon Formation at Wancoocha-1, at least seven fluctuations in Mg-content are observed in spar cement (Plate 22 D), indicating precipitation from pore waters of changing chemistry. Micritic siderite in many samples has recrystallised to microspar, as both low- and high-Mg varieties of bladed microspar are intermixed with micrite. In general, micrite is slightly more MgO-rich than associated spar in all the petroleum fields studied. In cases where siderites have formed within mica flakes (Plate 10 A & B), compositional zonation due to variations in Mg-content is also evident. It is likely that alteration of mica has produced a source of Fe for the siderite.

Subtle differences in siderite chemistry are evident between the various stratigraphic horizons of Permo-Triassic age and between the various petroleum fields (Fig.6.1a-c) (Appendix F). In the Toolachee Formation, sparry siderites at Moomba and Big Lake vary significantly in composition, yet the micrite in both fields is similar in composition (Fig.6.1a). This suggests that the formation of the micritic siderites occurred under chemically similar conditions throughout much of the study area

Plate 21

Micrographs of carbonate cement morphologies

A. Radiating laths of microspar surrounded by bladed micrite in a fine-grained laminated siltstone. Crossed nichols. Scale bar 250 µm. Sample CB-0476, Kerna-1, Patchawarra Formation (8118' 6").

B. Approximately the same field of view as (A) above. A back-scattered electron image showing compositional variation as colour differences. Light areas represent low-Mg siderite whereas darker areas are high-Mg siderite. Scale bar 100 µm [micrograph courtesy of S. Phillips].

C. Dust rims on quartz grains (arrows) indicate the presence of overgrowths. Euhedral siderite (S) crystals can be seen in primary pore space (blue). Plane light. Scale bar 250 µm. Sample CB-0458, Strzelecki-1, Toolachee Formation (6309' 3") [micrograph courtesy of J. Eleftheriou].

D. Same field of view as (C) above under crossed nicols.

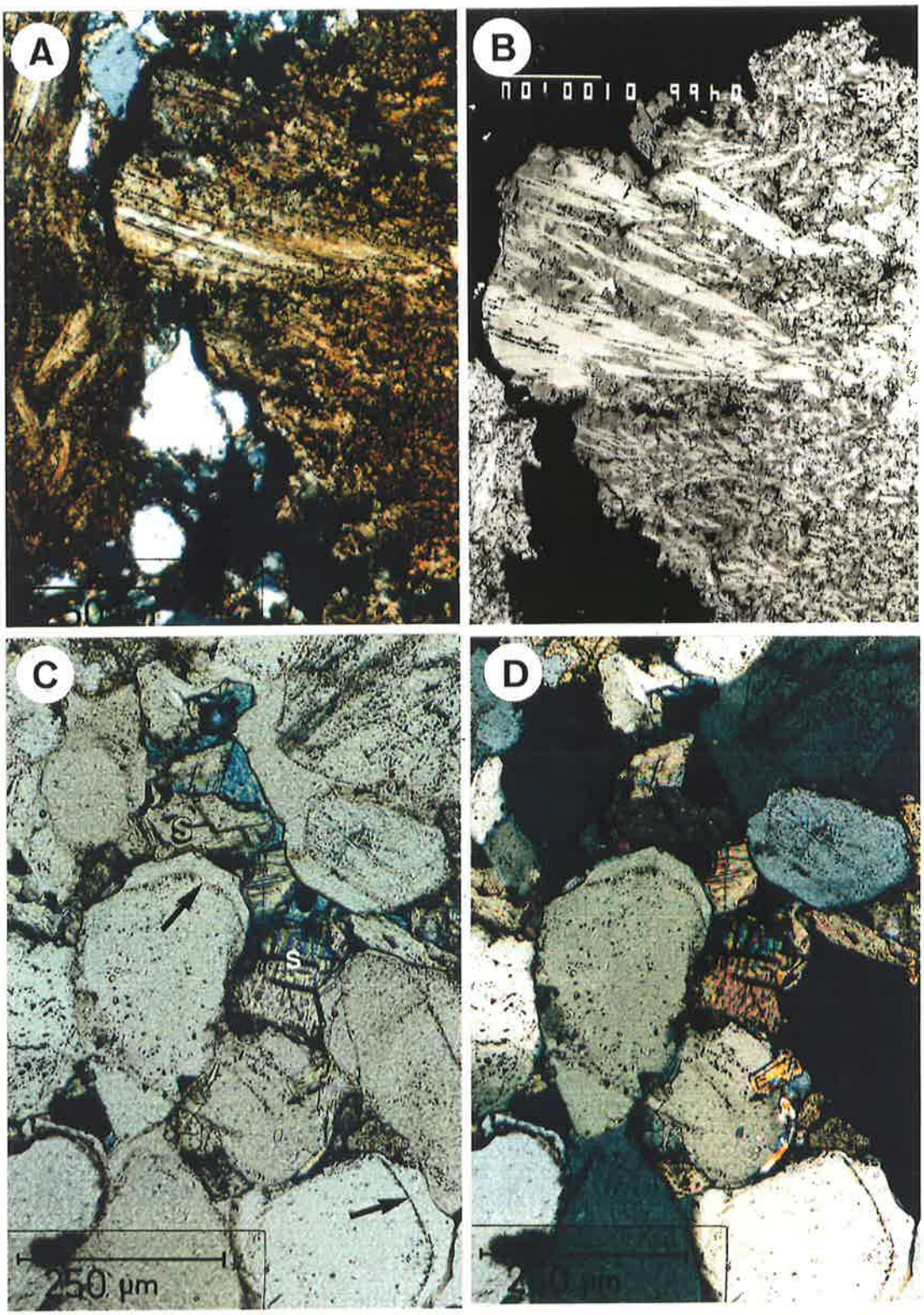
A
B
C
S
S
250 µm
D

whereas the sparry siderites formed under conditions that were more subject to local fluctuations in water chemistry. In the Strzelecki Field, carbonates from the Toolachee Formation contain slightly more MnO than in other fields, which may be related to the higher MnO content of the carbonates from the Epsilon Formation in that field (Fig.6.1a).

Siderites in the Epsilon Formation also vary considerably in composition (Fig.6.1b). This is best exemplified by the samples from the Big Lake Field. Here, two distinct groupings of micrite/microspar are evident, characterised by differences in the relative proportions of FeO and MgO, and to a lesser extent MnO (Fig.6.1b). Based on cement stratigraphy established from backscatter electron images, the siderites with the high FeO/low MgO content represent the first precipitates. A continuum between the high FeO/low MgO and low FeO/high MgO end member compositions of the siderites is observed in samples from the Toolachee Field.

Interestingly, the siderites analysed from wells located in relative proximity to the basin margin are characterised by high MnO contents (Fig.6.1b). At Wancoocha, for example, up to 6.4 wt % MnO is noted, higher than anywhere else sampled in the basin. Similarly, MnO content is fairly high (up to 2.2 wt %) in siderites from the Toolachee Field. In contrast, siderites from the Big Lake Field and Kirby-1 have the lowest MnO concentrations. Such wide variability in MnO content of the siderites is to be expected in vicinity of the basin margins where fluctuations in water chemistry are likely due to meteoric influences.

In the Patchawarra Formation, the samples analysed are characterised by low MnO contents (Fig.6.1c). Two broad compositional groups are apparent but this may be a function of the number of samples. Significantly, there is less MgO in the Patchawarra samples at Big Lake than in siderites from the Epsilon Formation at the same field (cf. Fig.6.1 b & c). This may mean that dissolution of Patchawarra siderites is not the source of carbonate for the Epsilon Formation.

6.4.3.2 Ankerites and dolomites

The chemical composition of ankerite and ferroan dolomite cements in comparison to siderite cements is illustrated in Figure 6.1d. In thin section, calcite and ferroan dolomite occur as spar cements in which quartz grains have a floating texture (section 4.2.3.2; Plate 23). Back-scattered images of ferroan dolomite spar revealed remnants of siderite spar engulfed by dolomite (Plate 23 C). These siderites are both low- and high-Mg varieties with textures indicative of neomorphic dolomite partially

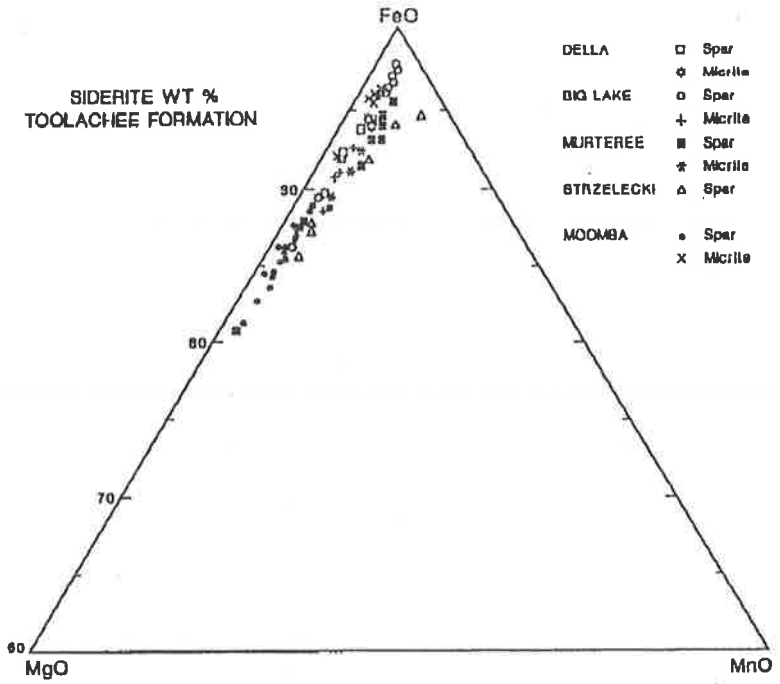

Figure 6.1a Electron microprobe analyses, siderite cements, Toolachee Formation (data courtesy of Dr. S.E. Phillips).

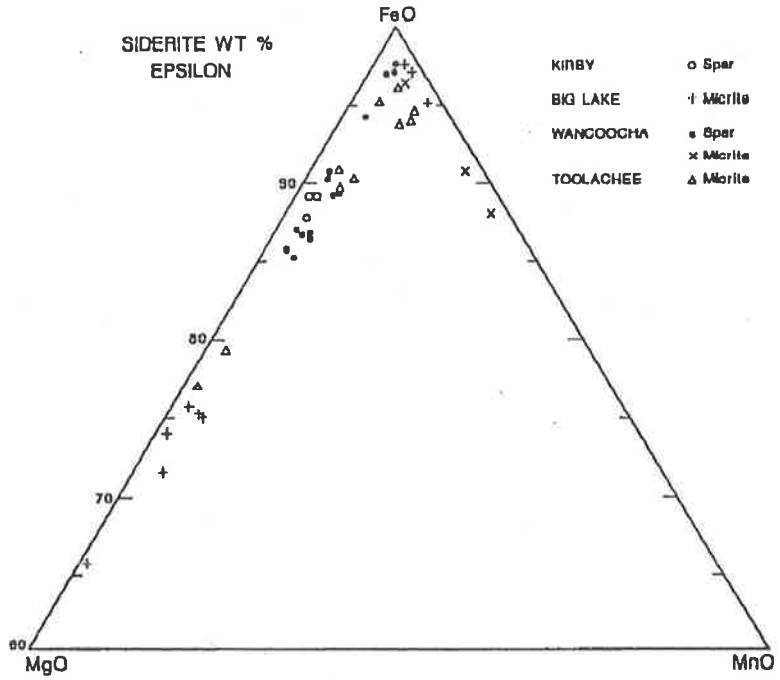

Figure 6.1b Electron microprobe analyses, siderite cements, Epsilon Formation (data courtesy of Dr. S.E. Phillips).

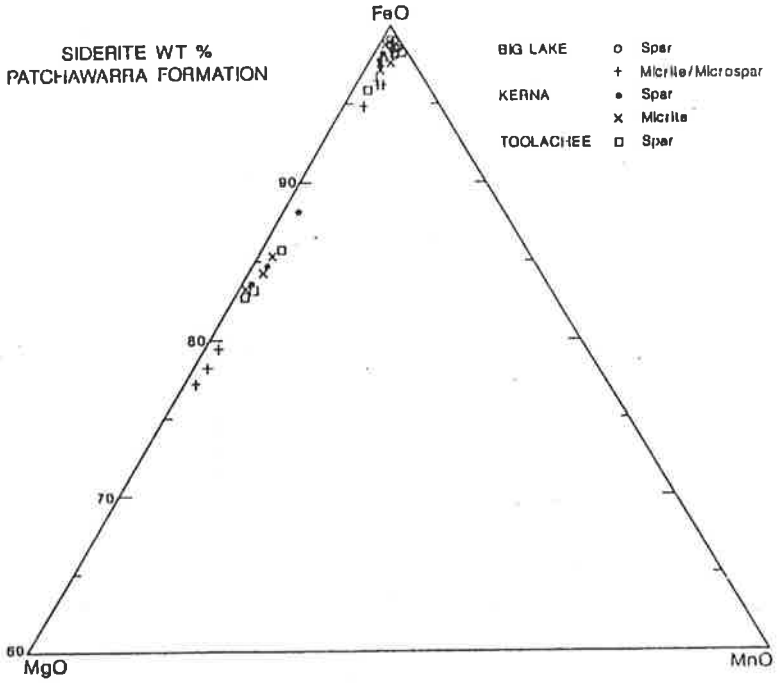

Figure 6.1c Electron microprobe analyses, siderite cements, Patchawarra Formation (data courtesy of Dr. S.E. Phillips).

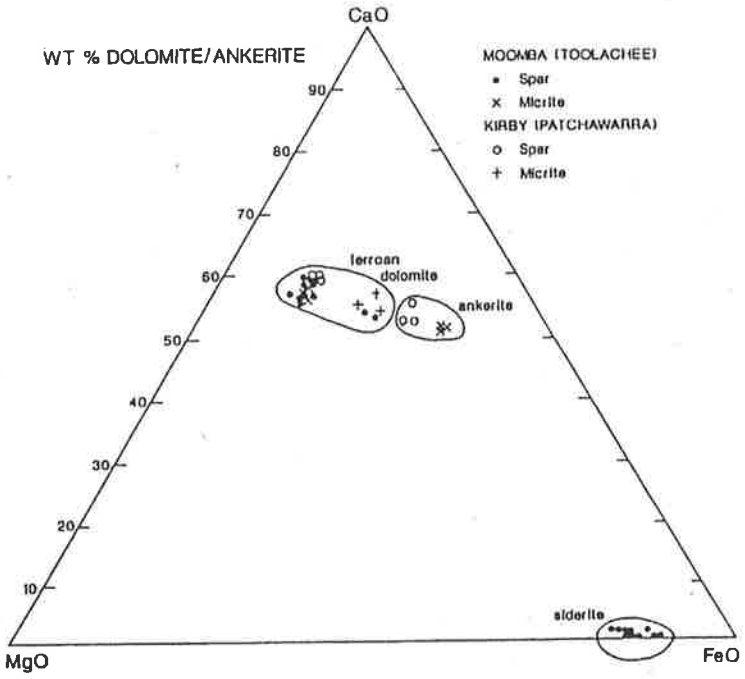

Figure 6.1d Electron microprobe analyses: dolomite, ankerite and siderite cements (data courtesy of Dr. S.E. Phillips).

Plate 22

Examples of compositional zonation in siderite

A. In thin section under crossed nichols, there are apparently two different siderite cements in this fine-grained sandstone: the reddish-brown micrite (R) and the high birefringence spar cement (C). Embayed edges are present on some detrital quarz grains. Compaction has deformed a metamorphic rock fragment (M). Scale bar 250 µm. Sample CB-0120, Big Lake-1, Toolachee Formation (7709' 6").

B. Similar field of view as (A) above under the electron microprobe indicates that there is no difference in siderite composition, the red area has simply been oxidised. The oxidised micritic siderite is replacing the metamorphic rock fragment (arrow). Quartz grains are mid-grey in colour. Scale bar 100 µm [micrograph courtesy of S. Phillips].

C. Fine-grained sandstone cemented by siderite micrite and microspar. Dark areas represent organic matter and/or rock bitumen. Crossed nichols. Scale bar 250 µm. Sample CB-0176, Wancoocha-1, Epsilon Formation (5818' 5").

D. Similar field of view to (C) above in back-scattered mode under the electron microprobe. Microspar forms as a cement with at least seven different fluctuations in composition. Light areas represent low-Mg siderite and darker areas are high-Mg siderite. The final cement is high-Mg siderite. Some of the cement phases have a high proportion of Mn. Scale bar 10 µm [micrograph courtesy of S. Phillips].

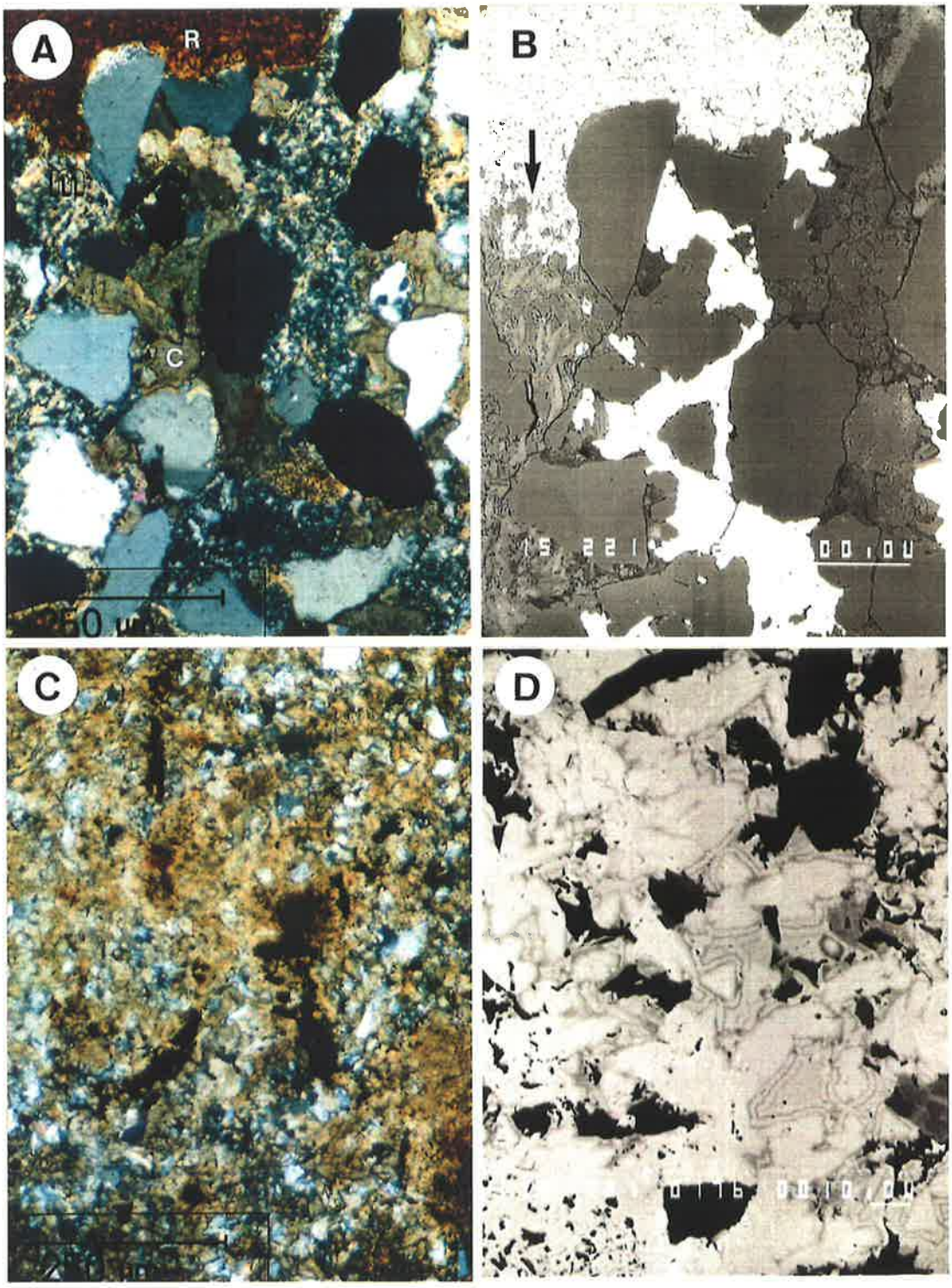
A
R
C
B
C
D

replacing an earlier siderite cement. In the Patchawarra Formation at Kirby-1, both ankerite and dolomite are present and textures show that ankerite here has also been replaced by neomorphic dolomite (Plate 23 D).

6.4.4 $^{18}O/^{16}O$ and $^{13}C/^{12}C$ isotope analysis

Stable carbon and oxygen isotope data is listed in Table 6.1 and graphically portrayed in Figure 6.2 on a cross-plot of $\partial^{13}C$ versus $\partial^{18}O$. Carbon isotope results for siderite are widely scattered, ranging from -0.16 to -10.93, with a mean of -3.98 ± 2.66 per mil. Ankerite is isotopically lighter than the siderite, with the two samples from Moomba-3 and Pando North-1 having $\partial^{13}C$ values of -11.32 and -11.03 per mil respectively (Table 6.1). Oxygen isotope results for the siderites also show considerable variation, ranging from about -14 to -22, with a mean of -17.2 ± 1.76 per mil. The pure ankerite sample from Moomba-3 gave a $\partial^{18}O$ result of -20.7 whereas the sample from Pando North-1 containing both ankerite and a trace of siderite yielded a value of -17.14 per mil (Table 6.1).

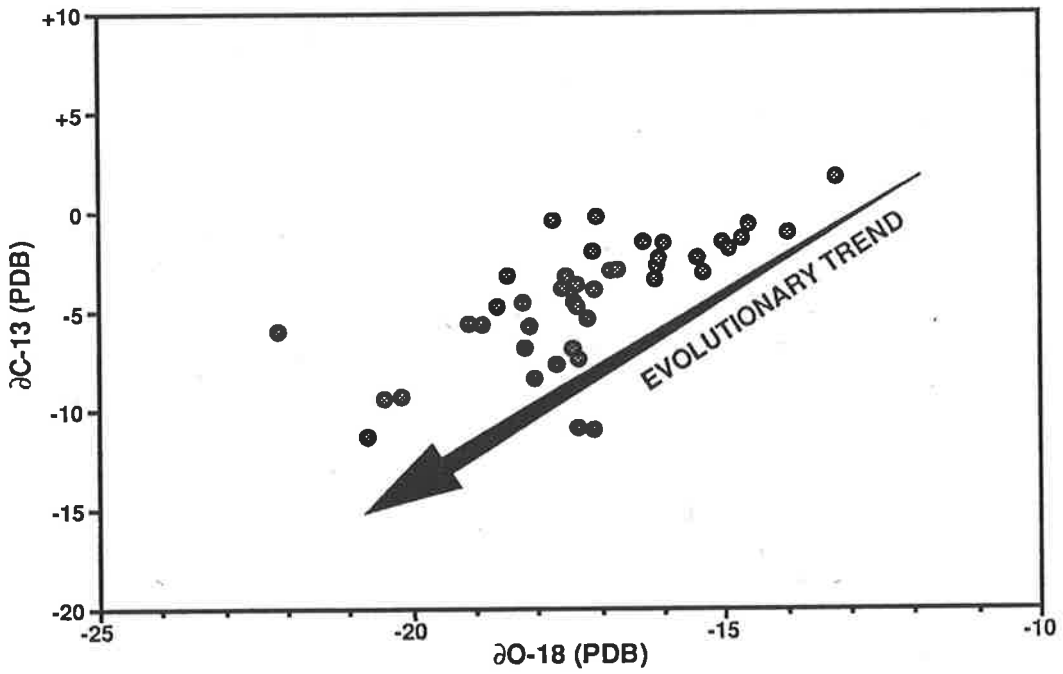

Figure 6.2 Crossplot of $\partial^{13}C$ versus $\partial^{18}O$ (PDB). Note broad evolutionary trend - see text for discussion (six data points courtesy of Dr. Y.Bone, University of Adelaide, unpubl. data).

Plate 23

Micrographs of ferroan dolomite and ankerite cements

A. Detrital quartz grains floating in ferroan dolomite spar. Note the embayed edges on quartz grains indicating replacement. A similar relationship is evident in calcite-cemented samples. Crossed nichols. Scale bar 250 μm. Sample CB-0578, Moomba-9, Toolachee Formation (7696' 0").

B. A back-scattered micrograph of the same field of view as (A) above. The dolomite cement is mid-grey. Note the lighter coloured patches of siderite in the cement. Both low- and high-Mg varieties of siderite (arrow) are being replaced by neomorphic spar. Scale bar 100 μm [micrograph courtesy of S. Phillips].

C. Remnants of siderite (light) in a dolomitic spar cement (mid-grey). Dark-grey patches represent detrital quartz grains. Back-scattered electron image. Scale bar 100 μm. Sample CB-0404, Moomba-3, Toolachee Formation (8016' 4") [micrograph courtesy of S. Phillips].

D. Remnants of ankerite (arrows) rimming quartz grains (Q) and engulfed by neomorphic dolomite spar. Back-scattered electron image. Scale bar 100 μm. Sample CB-0721, Kirby-1, Patchawarra Formation (11610-11620') [micrograph courtesy of S. Phillips].

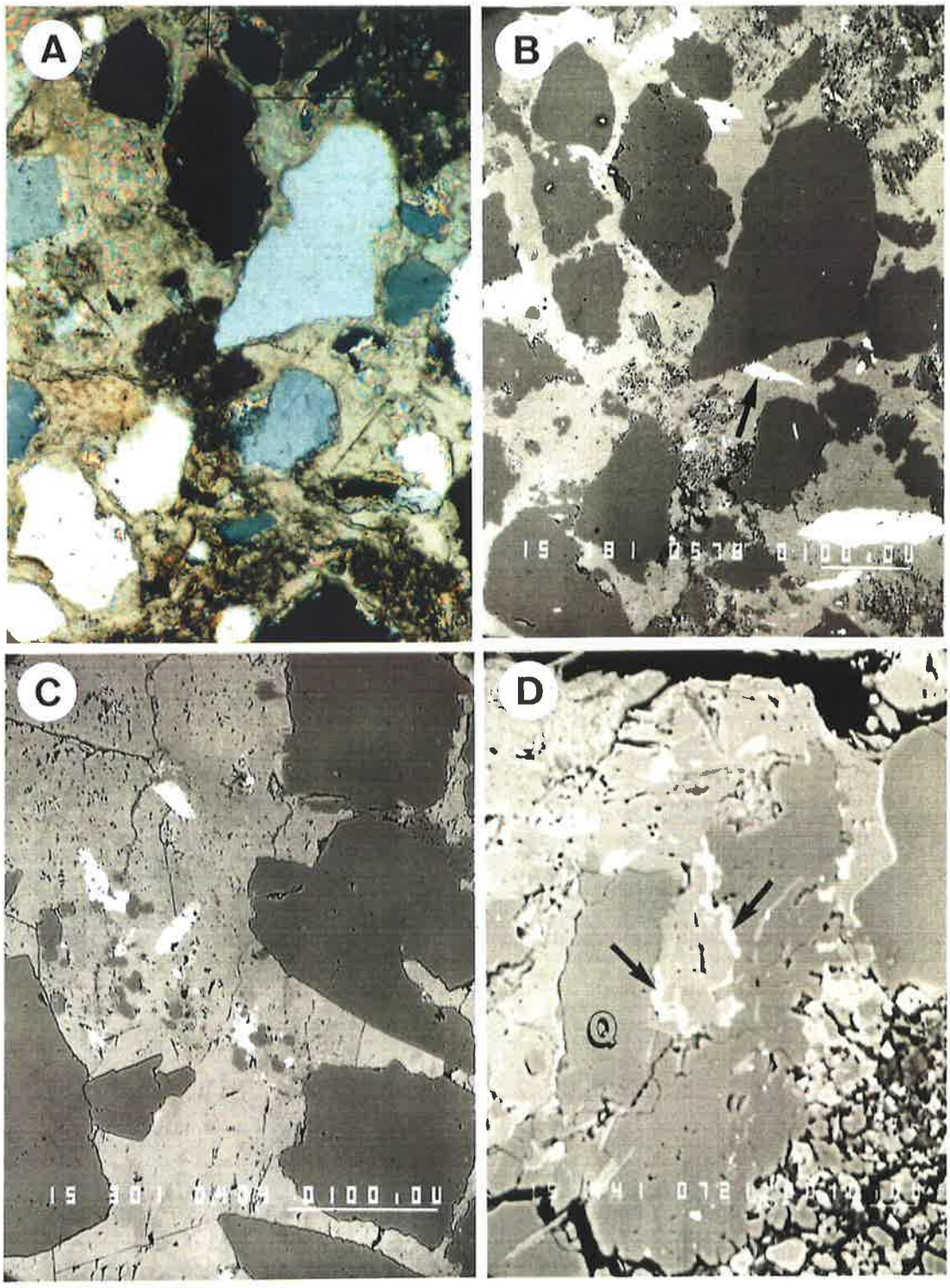
A
B
C
D
Q

Taken as a whole, a broad correlation exists between $\partial^{13}C$ and $\partial^{18}O$ values suggestive of an evolutionary trend in the isotope ratios and the conditions of formation of the carbonate cements. This is evidenced by the $\partial^{13}C$ values for the carbonates generally becoming more negative with increasing depletion in oxygen-18 (Fig.6.2). A further weak correlation exists between $\partial^{18}O$ values and depth of burial (Fig.6.3). The lightest $\partial^{18}O$ values are attained towards greater burial depths where carbonate samples are characterised by a wider scatter of data than in less deeply buried clastics (Fig.6.3).

The influence of sedimentary facies is apparent from the overall tendency for $\partial^{13}C$ values to become lighter with increasing grain size (Fig.6.4; Table 6.4a). For example, siderites found in shales or siltstones have a mean $\partial^{13}C$ value of -1.69 ± 1.48 per mil whereas siderite cements associated with coarse grained clastics have an average $\partial^{13}C$ value of -8.1 ± 1.73 per mil (Fig.6.4; Table 6.4a).

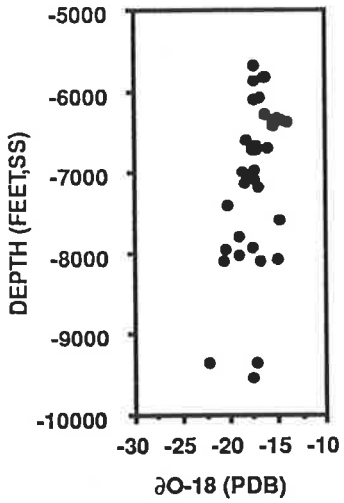

Figure 6.3 Relationship between $\partial^{18}O$ and depth.

A parallel, although less well-defined trend is apparent for the mean $\partial^{18}O$ character of the siderites when grouped according to grain size, the lighter $\partial^{18}O$ values being associated with the coarser grained sediments (Table 6.4a). An apparent exception represents the very coarse grained clastics of basal scour lag origin (Table 6.4a) but this is poorly understood because of the small number of samples collected from this category. It is possible the coarse clastics are 'contaminated' by carbonate-cemented micritic shale or mudstone rip-up grains that were not detected during visual/petrographic inspection of the samples. Evidence for this is derived from near-identical isotope signatures between sample CB-0189T which represents part of a basal scour lag and the directly underlying miciritic shale band (CB-0189B) (Table 6.1).

The isotopic character of the siderites associated with the different grain sizes is largely a function of the carbonate type present (Fig.6.5; Table 6.4b). Samples in which siderite spar is dominant are isotopically lighter than samples in which micrite or microspar are most prominent. For example, samples dominated by siderite spar have a mean $\partial^{13}C$ character of -5.81 per mil, whereas those dominated by micrite or microspar have a mean of -0.67 per mil. Samples in which there is a mixture of siderite types are characterised by an intermediate value (mean $\partial^{13}C$ = -2.82 per mil) (Fig.6.5; Table 6.4b). Again, a similar relationship is evident for the $\partial^{18}O$ character of the siderite cements, although considerable overlap in isotopic range is noted between the various categories (Table 6.4b).

Table 6.4 a -c
Statistical comparison of isotope results for siderite cements in the southern Cooper Basin according to (a) grain size, (b) siderite morphology, and (c) stratigraphic horizon.

a)

Grain size	∂C-13 (PDB) n	Min.	Max.	Mean	SD	∂O-18 (PDB) Min.	Max.	Mean	SD
Shale/silt	5	-3.41	-0.16	-1.69	1.48	-17.8	-16.1	-16.8	0.65
Very fine	8	-4.5	-0.56	-3.02	1.25	-17.6	-14.6	-16.6	1.08
Fine	8	-9.45	-1.04	-3.69	3.01	-22.1	-14	-16.7	2.99
Medium	7	-10.9	-3.26	-5.66	2.46	-19.1	-17.4	-18.2	0.73
Coarse	2	-9.33	-6.88	-8.1	1.73	-20.2	-17.4	-18.8	1.93
Very coarse	3	-7.67	-2.65	-4.5	2.75	-18.5	-16.1	-17.4	1.2

b)

Type	∂C-13 (PDB) n	Min.	Max.	Mean	SD	∂O-18 (PDB) Min.	Max.	Mean	SD
Spar dominant	15	-10.9	-2.91	-5.81	2.5	-20.4	-16.7	-18.1	1.1
Micrite and/or microspar exclusively	3	-1.45	-1.45	-0.67	0.68	-17.8	-16.3	-17.1	0.71
Combination	15	-6.03	-0.56	-2.82	1.58	-22.1	-14	-16.4	2.07

c)

Formation	∂C-13 (PDB) n	Min.	Max.	Mean	SD	∂O-18 (PDB) Min.	Max.	Mean	SD
Toolachee	11	-11.3	-1.3	-4.1	2.97	-20.7	-14.7	-16.9	1.77
Epsilon	7	-11	-2.4	-5.83	3.66	-18.2	-16.1	-17	0.75
Patchawarra	15	-9.33	-0.16	-3.39	2.52	-22.1	-14	-17.5	2.15

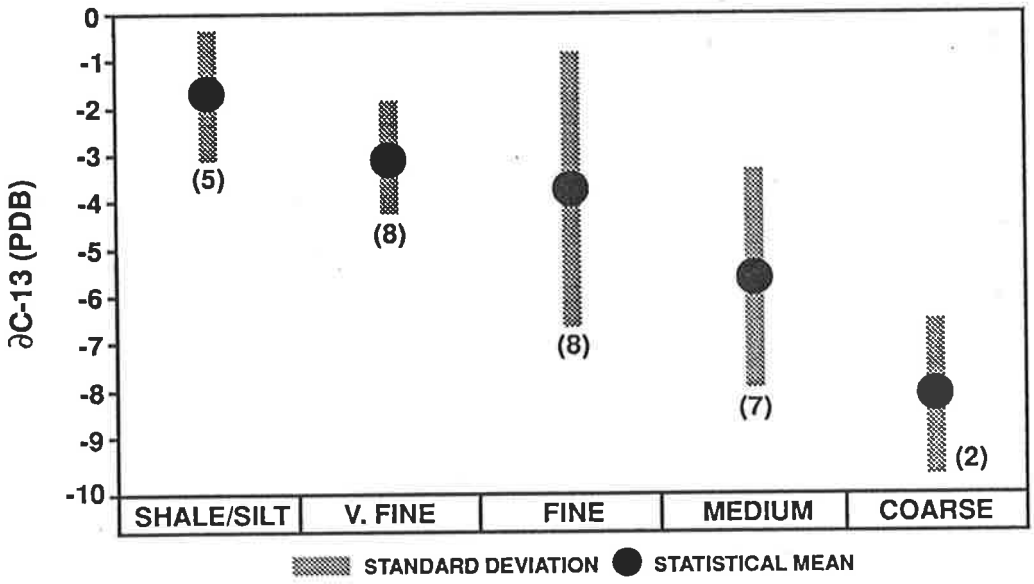

Figure 6.4 Statistical variation in $\partial^{13}C$ signature of siderite cements in relation to mean sediment grain size. Values in brackets refer to number of samples in each category. For further details refer to Table 6.4a.

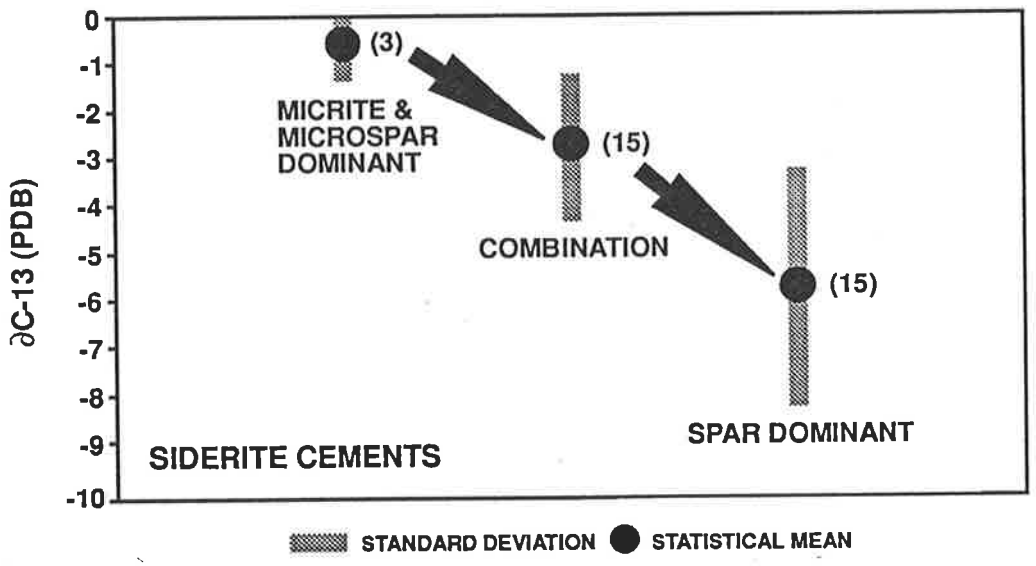

Figure 6.5 Statistical comparison of $\partial^{13}C$ character of siderite cement morphologies identified by optical petrography and with the electron microprobe. Values in brackets refer to number of samples in each category. For further detail see Table 6.4b. Arrows depict evolutionary trend in siderite evolution - see text.

Between formations, little difference is apparent in the $\partial^{13}C$ and $\partial^{18}O$ character of the siderites, with similar isotopic ranges and means noted between the various stratigraphic horizons (Table 6.4c). However, when the data is examined on the basis of structural setting, subtle differences are apparent in the isotopic signature of the siderite cements (Fig.6.6). Siderites along the Murteree-Nappacoongee anticlinal trend are characterised by heavier $\partial^{18}O$ values than their counterparts from the more deeply buried Nappamerri and Tennaperra Troughs. Similarly, $\partial^{13}C$ results for the siderite cements from the Murteree-Nappacoongee High are, on average, less negative than those derived from the more basinal parts of the study area. This is not merely a reflection of siderite type (cf. Table 6.3), and may indicate subtle differences in the controls affecting carbonate cementation in the various structural provinces of the Cooper Basin. It is, however, pointed out that samples derived from the Murteree-Nappacoongee Trend are biased towards the Strzelecki Field (see Table 6.1).

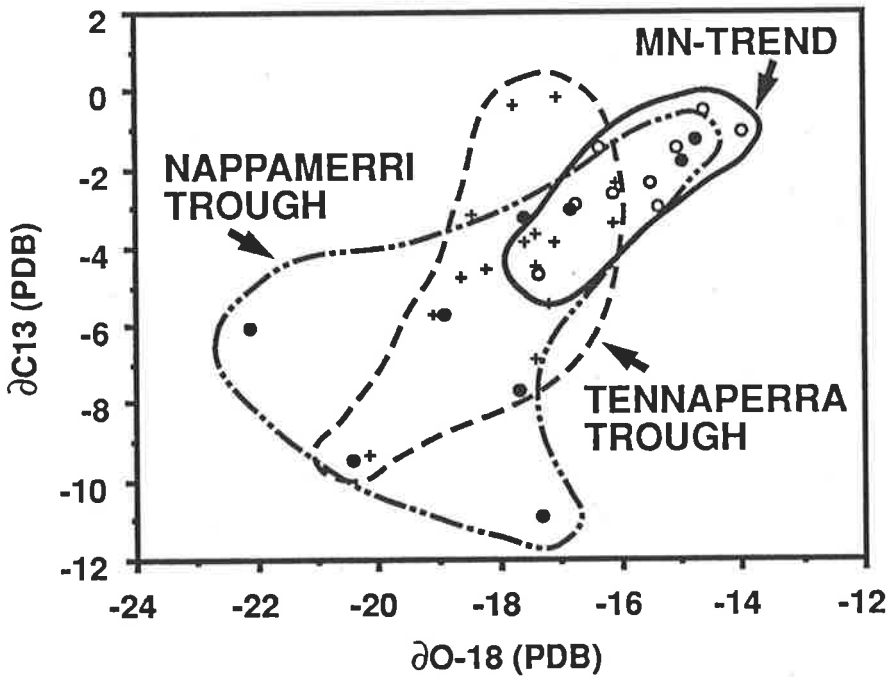

Figure 6.6 Crossplot of $\partial^{13}C$ and $\partial^{18}O$ (PDB) results of siderite cements, differentiated on the basis of structural setting. The most negative isotope values occur towards the basin depocentres. See text for explanation (MN = Murteree-Nappacoongee).

6.5 Discussion

6.5.1 Sequence of formation of authigenic carbonates

Petrographic data and evidence derived from X-ray diffraction and electron microprobe work highlight the complex nature of the carbonate phases in the sandstones. Multiple cement generations are distinguished, suggestive of a wide range of conditions under which the carbonates formed.

Micritic siderites in the Permian reservoirs of the Cooper Basin were interpreted by Gould & Smith (1979) and Schulz-Rojahn & Phillips (1989) to be the product of the early diagenetic environment. Sparry carbonate varieties were considered to be relatively late diagenetic precipitates (Martin & Hamilton, 1981; Schulz-Rojahn & Phillips, 1989). The results in the present investigation confirm these interpretations, however in the light of new evidence a more detailed carbonate paragenesis can now be established, as illustrated in Figure 6.7.

Low-Mg varieties recognised in backscatter images typically are surrounded by higher-Mg siderites, hence the low-Mg siderites represent the earliest formed diagenetic precipitates. Unfortunately, it is difficult to establish whether higher-Mg micritic siderite is replacing the low-Mg variety, or whether it is an additional phase of carbonate cement that precipitated from solution. The fact that microspar and spar also are characterised by such compositional variations lends support to the view that these larger crystals are 'aggrading neomorphic spar' (Bathurst, 1975) which has replaced the finer crystal sizes. However, there are examples at Wancoocha of microspar cements that appear to have precipitated out of aqueous solution. This evidence, combined with that for neomorphic processes, highlights the complex origin of the carbonates, involving both replacement and precipitation.

Based on petrographic and electron microprobe evidence, ferroan dolomite is a neomorphic spar replacing siderite and ankerite. As a result, the overall diagenetic sequence within the carbonates can be interpreted as changing from low-Mg siderite to high-Mg siderite, to ankerite and then to dolomite (Fig.6.7). Following this trend, calcite formed as the last carbonate cement (Fig.6.7). An almost identical sequence of precipitation of authigenic carbonates was suggested by Matsumoto & Iijima (1981) in some coalfields of Japan (see their Table 1). The sequence reflects a progressive change in water chemistry as Fe was lost and Mg and Ca increased in concentration. However, changes in siderite chemistry from low- to high-Mg varieties in the Cooper Basin do not form a continuum with the precipitation of ankerite and ferroan dolomite (Figs. 6.1d & 6.7). This sharp break in composition may be attributed to a major

change in water chemistry at the time when ankerite and ferroan dolomite were precipitated, namely an increase in CaO and MgO content of the basin waters. The increase in CaO content may lend support to the theory that some of the later-formed sparry carbonates (ankerite, dolomite and calcite) precipitated in response to post-Triassic influx of Ca^{2+}-bearing aquifer waters from the Great Artesian Basin overlying the Cooper Basin (section 4.3.2). Increases in MgO-content by late-stage carbonate precipitates have been reported from Jurassic concretionary siderites in Alaska; such increases were attributed to factors such as replacement, variations in water chemistry and increases in temperature (Mozely, 1989).

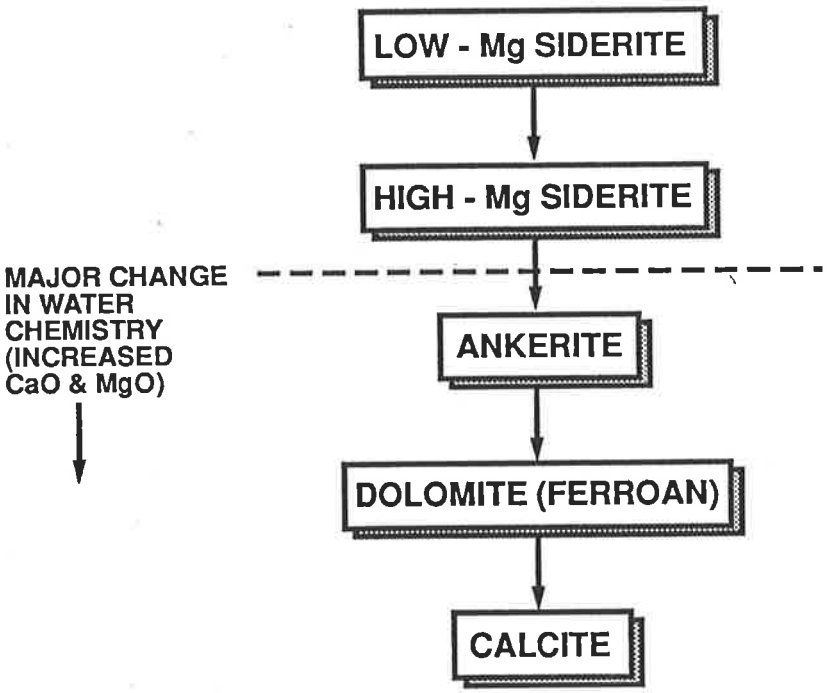

Figure 6.7 Generalised sequence of carbonate formation, based on cement stratigraphy established using the electron microprobe and petrographic microscope. Compare to Figure 6.1d.

6.5.2 Controls of carbonate formation

The fact that the different carbonate varieties occur together in the same sample creates problems in the evaluation of the isotope data. The different carbonate generations can not be separated chemically, and the small size and delicate

intergrowth of the carbonate crystals preclude mechanical separation. Consequently, the samples are not isotopically homogeneous, *but the isotopic character of each sample reflects the average of the sum of carbonate phases present.* This is important in recognising the limitations of the isotope data, and represents a problem frequently not discussed in comparable isotopic studies by other workers. Nonetheless, a number of important conclusions may be drawn from the isotope data.

The $\partial^{18}O$ values of the carbonates reflect meteoric or modified meteoric waters from high palaeolatitude (see Craig, 1961a,b). This interpretation is in accordance with independent geological evidence which confirms that Australia was located at high southern latitudes during much of the Palaeozoic (Frakes, 1979; Veevers, 1984). The implication is that the carbonate cements in the Cooper Basin equilibrated under near-atmospheric conditions, or during periods of freshwater flushing, and/or from water which at least in part retained its meteoric character in the subsurface; high latitude meteoric water possibly sourced the basinal brines.

The ill-defined trend in $\partial^{18}O$ values becoming lighter with depth is typical of many carbonate cements in a variety of basins from throughout the world (eg. Irwin, 1980; Milliken et al., 1981; Pitman et al., 1982; Curtis et al., 1986; Dickinson, 1987, 1988). The negative trend may be interpreted in two alternate ways: carbonate formation resulted from equilibration with pore waters at progressively elevated temperatures, or the $\partial^{18}O$ of the porewaters in which the carbonates precipitated changed towards lighter values over time as the basin evolved. The latter model is not considered plausible for a number of reasons.

If it is assumed that cementation in the Cooper Basin proceeded in an open diagenetic system, in which meteoric fluids were able to penetrate deeply into the Permo-Triassic section, the $\partial^{18}O$ of the formation fluids from which the carbonates precipitated is likely to have reflected that of Permian, or more recent atmospheric waters. This would suggest a shift towards heavier $\partial^{18}O$ values over time in view of the progressive northward drift of Australia since the Permian (Veevers, 1984), and the pronounced latitude effect on the isotopic compositions of meteoric waters (Craig, 1961a,b). The view is supported by the work of Bird & Chivas (1988a) who demonstrate that the isotopic composition of meteoric water in Australia has been getting progressively heavier since the late Palaeozoic.

Similarly, if a closed hydrologic system is envisaged for the Cooper Basin, in which there is no continuous meteoric recharge, a shift to a more positive $\partial^{18}O$ of the formation water over time is again suggested. This is because isotopic fractionation during diagenetic reactions causes a net transfer of oxygen-16 to diagenetic products, progressively changing the $\partial^{18}O$ character of the pore waters towards heavier values where the water/rock ratio is low (Kharaka & Carothers, 1986). Authigenic minerals that form in a closed diagenetic system therefore eventually adopt progressively more

positive $\partial^{18}O$ values with depth because of decreased availability of oxygen-16 for cementation (cf. Dickinson, 1987, 1988).

In the southern Cooper Basin, carbonate cementation is not considered to have proceeded in a strictly 'closed' diagenetic system. Theoretically, the carbonates may only be argued to have precipitated in reservoirs of restricted hydrodynamic circulation if (a) cementation proceeded soon after the reservoirs were hydrodynamically sealed, and (b) no isotopic re-equilibration occurred after precipitation. This is because only immediatly after a reservoir is hydrodynamically sealed and the $^{18}O/^{16}O$ ratio of the pore water is still low may cements precipitate which are characterised by a negative shift in $\partial^{18}O$ with depth.

It is exceedingly unlikely, however, that such a mechanism could account for the formation of carbonate cements in the present investigation in view of the negative $\partial^{18}O$ trend persisting over several thousand feet of burial. In addition, many carbonates show evidence of having undergone partial or complete recrystallisation, yet the $\partial^{18}O$ shows no sign of re-equilibration with closed-system (^{16}O-depleted) waters.

A generally 'open-system' diagenetic environment in the southern Cooper Basin appears supported by various lines of evidence. For example, there is a widespread lack of overpressured zones in the basin, even though some localised exceptions are noted (eg. the uppermost Patchawarra Formation at Moomba-6; Battersby, 1976). Also, flushing of Permian reservoir sandstones by meteoric waters from the superjacent Eromanga Basin is well-documented for the southern portion of the Cooper Basin (Porter, 1973, 1974; Youngs, 1975). Similarly, there is evidence to suggest that quartz cementation in the southern Cooper Basin was at least partly controlled by sub-surface invasion of meteoric waters enriched in silica (Schulz-Rojahn & Phillips, 1989; section 4.3.1).

On the basis of these considerations, it is suggested that the carbonate cements formed in an 'open', or at least partially 'open' hydrochemical system where diagenetic reactions caused little change to the $\partial^{18}O$ of the pore waters. The subtle trend of the maximum $\partial^{18}O$ values becoming more negative with depth is considered to simply reflect an increase in the temperatures of formation of the carbonate cements (see section 6.5.3). The considerable scatter of values found at any particular depth can hereby be explained by the variability of carbonate types and abundances. Samples which are dominated by sparry carbonates typically are more depleted in oxygen-18 than their fine-grained counterparts (Table 6.4b), which is considered to be a function of the higher precipitation temperatures at which the sparry carbonate cements formed (section 6.5.3). This suggests the sparry carbonates are closest to equilibrium with present formation waters whereas the finely crystalline siderites in the argillaceous sediments are generally furthest from their point of equilibration with present

conditions of burial. The implication is that the micrite and microspar carbonate varieties may survive complete recrystallisation to depths of up to 8000 feet or more, which is in accordance with petrographic data and results obtained from electron microprobe work.

The interpretation of the stable carbon isotope data is more ambiguous, as a number of potential carbon sources may be envisaged which could have been involved in carbonate precipitation. This is illustrated in Figure 6.8 which shows the common carbon isotopic composition of various natural products, as derived from the literature. As can be seen, the $\partial^{13}C$ character of the carbonates (about +2 to -12) overlaps in range with that of a number of potential carbon sources.

For example, the carbon required for carbonate precipitation could have partly been derived from an atmospheric source ($\partial^{13}C$ = -11 to -6 per mil; Keeling, 1958, 1961a). This interpretation is consistent with the meteoric origin inferred for the water from which the carbonates precipitated, and the open-system diagenetic environment of the southern Cooper Basin during carbonate cementation. Such a carbon source was previously suggested by Wall (1987). A further possibility is that surface-derived groundwater may have transported ^{13}C-depleted, soil-derived carbon into the diagenetic realm ($\partial^{13}C$ = -29 to -10 per mil; Broecker & Olson, 1960; Galimov, 1966; Hendy, 1971; Kunkler, 1969; Lebedew et al., 1969; Pearson & Hanshaw, 1970; Rightmire & Hanshaw, 1973; Deines, 1986). However, in view of the generally heavier $\partial^{13}C$ signature of the carbonate cements, this source alone cannot satisfactorily account for the present isotope character of the carbonates.

The carbonate cements with the isotopically light $\partial^{13}C$ signatures may also be the product of organic carbon sources. ^{13}C-depleted carbon is released during the maturation of organic matter involving a variety of different processes (oxidation, decarboxylation, CO_2 from methane generation, etc.; Irwin et al., 1977; Hudson, 1977; Carothers & Kharaka, 1980; Kharaka et al., 1983). Coals, for example, have $\partial^{13}C$ signatures varying between about -28 and -15 per mil (Jeffery et al., 1955; Craig, 1953), the more ^{13}C-enriched values approaching those of some of the later-formed carbonate cements in the Cooper Basin. Similarly, carbon dioxide produced during the thermal decarboxylation of organic matter is expected to have a $\partial^{13}C$ that is more negative than -20 per mil (Gould & Smith, 1980). Other workers consider $\partial^{13}C$ values of CO_2 derived from thermocatalytic decarboxylation and other abiotic reactions to be as positive as -10 per mil (Claypool & Kaplan, 1974; Irwin et al., 1977), possibly even as heavy as -6.0 per mil (Chivas et al., 1984). Clearly, ^{13}C-depleted organic carbon of such origin may account for the isotopic signature of many of the carbonate cements investigated, particularly if mixed with isotopically heavier carbon derived from other sources.

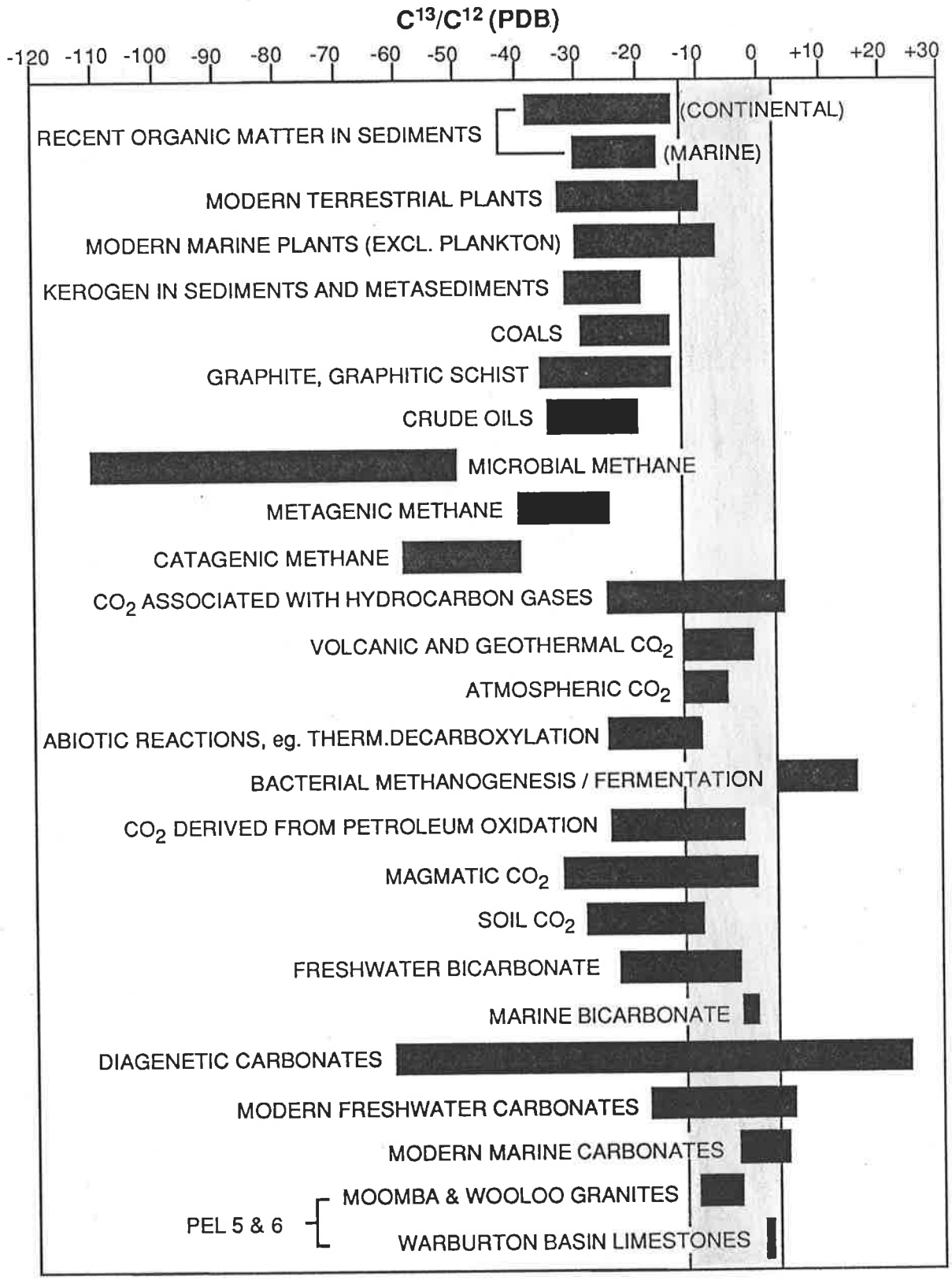

Figure 6.8 Common carbon isotopic composition of various natural products. Shaded area corresponds to range of carbon isotope values obtained for Cooper Basin carbonate cements (siderites and ankerites).

Data compiled from Allard et al. (1977), Baertschi (1957), Carothers & Kharaka (1980), Clayton & Degens (1959), Craig (1953,1954), Degens & Epstein (1964), Deines (1986) and references cited therein, Deuser & Degens (1967), Fuex (1977), Gross (1964), Hendy (1971), Hoefs (1973), Hudson (1977), Huebner (1981), Irwin et al. (1977), Kennicutt et al. (1987), Karaka et al. (1983), Keeling (1958), Kvenvolden & Squires (1967), Kvenvolden & Pettinga (1989), Laier (1988), Lyon & Hulston (1984), Münnich & Vogel (1959), Oana & Deevey (1960), Rigby & Smith (1981), Sackett (1964), Silverman (1964), Silverman & Epstein (1958), Smith (1978), Stahl (1977), Stahl & Carey (1975).

A further possibility is that the carbonates incorporated carbon of volcanic or geothermal origin, or a juvenile source. Such carbon has a $\partial^{13}C$ character generally between -12 and 0 per mil [28] (Deines, 1986; Kreulen, 1980; Eglinton & Murphy, 1969), a range which closely overlaps with that for the Cooper Basin carbonates. A volcanic origin of the carbon involved in carbonate precipitation is possible in view of the extensive subsurface distribution of pre-Permian volcanics in the southern Cooper Basin (Gatehouse, 1986; see Fig.2.4). Permian volcanic activity is exemplified by the basaltic sill intersected in the Gidgealpa Group sediments at Warnie East-1 in the Queensland sector of the Cooper Basin. Granite basement is found in several other parts of the region (see Table 6.6; Fig.2.4), characterised by a $\partial^{13}C$ signature between -10.5 and -4.0 per mil (Rigby & Smith, 1981).

Still another possible source of carbon for carbonate cementation represent the limestone sequences of the Warburton Basin underlying parts of the Cooper Basin (Fig.2.4). These limestones have a $\partial^{13}C$ composition between 0 and +1.3 per mil which is typical of marine carbonates (Rigby & Smith, 1981).

Heavy $\partial^{13}C$ values may also be produced during bacterial fermentation processes or methanogenesis (Fritz et al., 1971; Irwin et al., 1977; Siegel et al., 1987). Such processes are characterised by $\partial^{13}C$ values as positive as +15 per mil. In the present investigation, mixing of carbon from these sources with other, more ^{13}C-depleted carbon sources may be responsible for producing the stable carbon isotope character of the micrite and possibly also microspar carbonate varieties.

Unfortunately, discrimination between the various carbon sources is presently not possible. Most likely, the carbonates formed under a complex range of conditions involving a mixture of different carbon sources. Accordingly, the positive correlation between $\partial^{13}C$ and $\partial^{18}O$ values of the siderites, suggestive of an evolutionary change in the source of carbon during carbonate formation, may be interpreted in alternate ways. A possible explanation is that carbon derived from bacterial fermentation processes/methanogenesis decreased in importance as burial temperatures increased and the basin subsided. Instead, carbon of more negative $\partial^{13}C$ character became more important. The source of such ^{13}C-depleted carbon is problematic but could have been derived from the maturation of organic matter, pre-Permian basement, and/or influx of meteoric waters during geologic history.

In this context, the isotopically distinct character of the siderites derived from the Murteree-Nappacoongee (MN) anticlinal trend may possibly be explained. The generally more positive $\partial^{18}O$ values are interpreted to reflect lower temperatures of precipitation than for the carbonates derived from downflank positions. The relatively heavy $\partial^{13}C$ composition of the siderites probably signifies a greater input of carbon derived from bacterial fermentation processes as well as carbon of atmospheric origin.

---

[28] On average between -5 to -7 per mil (Deines, 1986, and references cited therein).

The latter source is consistent with meteoric influences. In contrast, the siderites that formed in the Nappamerri and Tennaperra Troughs probably received a greater contribution of carbon from thermal maturation reactions involving organic matter and/or basement sources (see section 6.5.8 for further assessment of these possibilities).

6.5.3 Precipitation temperatures

For the calculation of carbonate equilibrium fractionation temperatures, an estimation of the $\partial^{18}O$ of the original water must be made. Accordingly, a $\partial^{18}O$ value of between -15 and -16 per mil was adopted for Permian meteoric waters, based on the following considerations:

- The estimated palaeolatitude of central Australia was about 75° to 70° South during the Early Permian to Early Triassic period (McElhinny, 1969; Embleton, 1981; Embleton & McElhinny, 1982; Veevers, 1984). Modern-day meteoric waters at similar latitudes (Dansgaard, 1964) have a similarly ^{18}O-depleted character.

- Evaporative and altitudinal effects on the isotopic composition of the meteoric waters (Yurtsever & Gat, 1981) may be neglected. The Cooper Basin is characterised by fluvio-lacustrine sediments with thick interbedded coal measures, suggestive of a climate dominated by high precipitation rates and a palaeotopography of essentially low relief.

- The $\partial^{18}O$ estimate compares well with data by Smith et al. (1983) who measured ∂D values in Australian coals and calculated the Permian meteoric water composition to have been about -16 per mil. Similarly, Gould & Johnson (unpubl.) derived an Upper Permian meteoric $\partial^{18}O$ value of between -15 and -15.6 per mil for the Bowen Basin by the same method. A similar $\partial^{18}O$ meteoric water composition is adopted by other workers for the Australian Permian (Botz et al., 1986; Sun & Eadington, 1987; Bird & Chivas, 1988b).

On this basis, using the equation for siderite isotope fractionation by Carothers et al. (1988),

$$10^3 \ln a = 3.13 (10^6 \times T^{-2}) - 3.50$$

and assuming a mean $\partial^{18}O$ value of -16 per mil for Permian meteoric water, siderite formation temperatures are calculated to vary between about +22 and +64 °C (Table 6.1). If a mean meteoric $\partial^{18}O$ value of -15 per mil is assumed, formation temperatures

for siderite range between ca. +26 and +70 °C (Table 6.1). Temperatures of formation for ankerite are more difficult to assess because an explicit experimental relationship for ankerite-water is unavailable. Chemically most closely related is dolomite. Hence, an estimation of ankerite formation temperatures may be made if the isotope fractionation factor for dolomite (Land, 1983) is assumed:

$$10^3 \ln a = 3.2 (10^6 \times T^{-2}) - 1.50$$

Using this equation, formation temperatures for ankerite are estimated to vary between about +50 and +71 °C if a $\partial^{18}O$ value of -16 per mil is adopted, and between +55 and +77 °C if $\partial^{18}O$ = -15 per mil. The lower temperature estimate is derived from the sample containing both ankerite and a trace of siderite. Hence, the sample in which there is only ankerite probably provides a more realistic estimate of the temperature conditions of formation of the ankerite cements. The data suggests that the ankerites formed relatively late in the paragenetic history, at more elevated temperatures than many of the siderites, as is also indicated by the cement stratigraphy.

For the different siderite generations, temperature estimates vary considerably but are generally lower for samples in which micrite is predominant than for samples in which siderite spar is the dominant carbonate variety present. The isotope data suggests that the micritic siderites formed at relatively low temperatures in the shallow diagenetic realm, supporting the views expressed by Gould & Smith (1979), Wall (1987) and Schulz-Rojahn & Phillips (1989). A 15-cm thick micritic siderite band from the Toolachee Formation from Murteree-1 gave a temperature estimate of between +32 and +37 °C, depending on the original $\partial^{18}O$ water value used (Table 6.1). Other samples in which micrite or microspar is predominant suggest formation temperatures between about +25 and +44 °C, again depending on the $\partial^{18}O$ value selected (cf. Tables 6.1 & 6.3). The low temperature estimates are in accordance with sedimentological evidence derived from core material, suggesting that at least some of the micritic siderites are early diagenetic precipitates. Such lines of evidence include intra-formational rip-up clasts composed of micritic siderite, and bioturbated micrite bands which indicate precipitation near the sediment-surface interface (Schulz-Rojahn & Phillips, 1989; section 4.2.3.2). However, the sedimentological evidence would suggest that some micrites formed at temperatures lower than suggested by the isotope data. This is because the calculated minimum temperature for the formation of fine-grained siderites is about 25 °C, yet some siderite-cemented zones were within reach of burrowing organisms and subject to reworking by sedimentological processes in subarctic to cool-temperate climatic conditions, at least during the Early Permian. It is more likely that the sediment temperature within the first few metres of burial was that of Permian cold waters (+15 °C maximum; Rao, 1981), and that the earliest formed

micritic siderites precipitated under conditions that more closely approximated this temperature value. Unfortunately, no samples from bioturbated micrite bands or micrite rip-up clasts were included in the present investigation to test the validity of this assumption. However, stable isotope results from Bone (University of Adelaide, unpubl. data) confirm the view that some micritic siderites in the Cooper Basin formed at temperatures lower than suggested by the present isotope data. A nodular siderite sample from the Epsilon Formation at Mudrangie-1 gave a temperature estimate of between +14.5 and +18.4 °C, for an original $\partial^{18}O$ water value of -16 and -15 per mil respectively. A similar low-temperature origin is inferred for siderites forming in modern swamp environments in northern Europe (Postma, 1977, 1982; Jakobsen, 1987). In Australia, micritic or nodular siderites of low-temperature origin are reported from the Permian sediments of the Sydney Basin (Botz et al., 1986), the Bowen Basin (Gould & Johnson, unpubl.), and the Jurassic sediments of the Eromanga Basin (Eadington et al., 1989).

The temperature conditions of formation of the coarser carbonate varieties are more difficult to assess. Samples which exclusively contain siderite spar give temperature estimates varying between +32.5 and +70.25 °C if a $\partial^{18}O$ value of -15 per mil is assumed, and between +28 and +64 °C if $\partial^{18}O$ = -16 per mil. In samples in which siderite spar occurs in association with siderite microspar and/or micrite, a wide range of values is observed, covering both extremes of the temperature spectrum. For example, the lowest temperature estimate for siderite crystallisation (+22 °C) is derived from a sample in which both spar and microspar occur together. In contrast, in the sample which gave the highest temperature estimate for siderite formation (+70.25 °C), spar, microspar and micrite all co-exist (Tables 6.1 & 6.3). Such wide variability in the estimation of formation temperatures in samples containing multiple siderite generations is not surprising considering their observed compositional and morphological differences suggestive of different physico-chemical conditions prevalent at the time of their formation. The range in temperature estimates reflects a mixture of $\partial^{18}O$ signatures that resulted from precipitation and recrystallisation throughout diagenesis.

A further problem in assessing the formation temperatures of the more coarsely crystalline carbonate varieties lies in the possibility that these carbonates may not have precipitated in pore waters of Permian meteoric $\partial^{18}O$ composition (cf. section 6.5.1). Indiscriminate adoption of an original $\partial^{18}O$ value of -15 or -16 per mil for all carbonate temperature calculations may be too simplistic. According to Bird & Chivas (1988a), the $\partial^{18}O$ composition of meteoric water in Australia became progressively heavier with decreasing geologic age. Consequently, the precipitation temperatures of carbonate cements that precipitated in post-Permian times will not be accurately reflected. Expressed differently, whereas early formed carbonates in the present

investigation are considered to give comparatively realistic temperature estimates, formation temperatures for later formed diagenetic carbonates may be under-estimated if a constant 'Permian' $\partial^{18}O$ value is assumed through geologic time.

The difficulty lies in estimating the original $\partial^{18}O$ water composition which may have been involved in carbonate precipitation in the basin. To date, no $\partial^{18}O$ analyses of modern formation waters in the Cooper Basin are available, hence even the isotopic 'end-composition' is uncertain. It is possible that locally the present-day $\partial^{18}O$ character of formation waters in the Cooper Basin approximates that of the superjacent Great Artesian Basin where it is close to -6.6 per mil over large areas (Airey et al., 1979). This is plausible in the southern portion of the basin where Porter (1973, 1974) and Youngs (1975) showed that the absence of Triassic caprocks has allowed hydraulic interconnection between the Permian and the artesian aquifers. If it is assumed that some of the carbonate cements precipitated in response to meteoric flushing from the Great Artesian Basin, and an original $\partial^{18}O$ value of -6.6 per mil is adopted, the maximum temperature of siderite formation could be as high as about +140 °C. This figure, however, is greater than the present bottom-hole temperature of many wells, suggesting it is an over-estimate. Also, the data discussed in Chapter 4 shows that the distribution of siderite cements is ubiquitous throughout the southern Cooper Basin, and not restricted to those areas known to have been flushed by meteoric waters (cf. Figs. 2.9 & 4.2a). This argues against the possibility that the bulk of the sparry siderites formed in response to flushing by the Great Artesian Basin waters, in contrast perhaps to some of the other carbonate varieties.

A possible constraint on the timing of siderite formation in the Cooper Basin is provided by the association of siderite spar and microspar with dead oil in some samples (Chapter 4). This may suggest the coarser siderite varieties formed prior to, or synchronous with the main phase of oil generation and migration. According to Kantsler et al. (1983), peak generation of hydrocarbons in the Nappamerri Trough occurred in Mid to Late Cretaceous times. More recently, Tupper & Burckhardt (1990) suggested that oil expulsion from the Cooper sequence began as early as the Triassic in this area. Hence, some of the siderites could have formed as late as the Triassic or possibly the Late Cretaceous.

6.5.4 Burial depths of formation of authigenic carbonates

The Cooper Basin has a present-day geothermal gradient ranging from about 25 to 60 °C per kilometre (7.6 to 18 °C per 1000 feet), with the highest gradients (>

45 °C/km) found in and around the Nappamerri and Tennaperra Troughs, particularly in areas underlain by granite basement (Kantsler et al., 1983) (section 2.11). Using the present geothermal gradient and the isotopic temperatures, a crude estimate of the maximum burial depths over which the carbonates formed may be made. This requires an estimation of the surface temperatures during the Permian. According to Taylor et al. (1989), the climate was probably one of wet, cool summers and freezing winters, as evidenced by the type and abundance of inertodetrinite and alginite in the inertinite-rich Permian coals of Australia. Evidence for glaciation in the Australian Permian is widespread and includes striated and faceted boulders, tillites, glacial pavements, varves, glendonites, and the occurrence of dropstones (Sprigg, 1966; Crowell & Frakes, 1971a,b, 1975; Crowell, 1978; Frakes, 1979; Draper, 1983; Dickins, 1985). Towards the Late Permian, a return to warmer conditions occurred (Frakes, 1979).

On this basis, a wide range of mean Permian surface temperatures is adopted, ranging from 0 to +20 °C. This is similar to Permian palaeotemperature estimates reported by Lowenstam (1964) and Rao (1981).

Using a maximum temperature estimate of siderite formation of +70 °C, and adopting a surface temperature of zero degrees as well as a linear geothermal gradient of 60 °C/km, carbonate formation is calculated to have occurred over a burial depth of about 1.2 kilometres (3940 feet). If a lower geothermal gradient is assumed (30 °C/km), the depth at which some of the carbonates precipitated may have exceeded 2 kilometres (6560 feet). Similarly, if a surface temperature of +20 °C is adopted, the maximum depth of carbonate formation is calculated to have varied between somewhat less than 1 km to almost 1.7 km (3280 to 5580 feet).

However, in view of the possibility that the temperature estimates for some of the later formed carbonates are too low, the estimation of maximum burial depths of carbonate formation may also be too conservative. Nonetheless, the data confirms that at least some of the later-formed siderites and ankerites are likely to have precipitated in post-Permian times. This is evident from subsidence history plots constructed by various workers for the southern Cooper Basin, including the Big Lake area (Kantsler et al., 1983; Fig.16), Moomba-3 (Pitt, 1986, Fig.17), Kirby-1 (Kantsler et al., 1986, Figs.2 & 13), and Burley-2 (Tupper & Burckhardt, 1990, Fig.14). The data from these workers indicates that burial depths for Permian sediments of 1-2 km (3280-6560 feet) were first attained in the Big Lake-Moomba area in the Jurassic or Cretaceous (Kantsler et al., 1983; Pitt, 1986), although possibly earlier in the central Nappamerri Trough (Kantsler et al., 1986; Tupper & Burckhardt, 1990).

6.5.5 Comparison to $\partial^{13}C$ character of hydrocarbons

Stable carbon isotope results are available in the literature for a series of Cooper Basin crude oils and condensates, as well as gaseous hydrocarbons. In view of the possibility that the formation of carbonate cements is related to the thermal maturation of organic matter, and the observed association of dead oil with some carbonates (section 4.2.3.2; Plate 11 A-D), a comparison is made between the $\partial^{13}C$ character of the carbonate cements with that of hydrocarbons occurring naturally in the Cooper Basin (Fig.6.9a). This approach is adopted to test the possibility of a direct genetic link existing between carbonate cement formation and hydrocarbon generation and migration in the Cooper Basin. A hydrocarbon-related origin of carbonate cements is postulated by various workers for other petroleum provinces around the world (Donovan 1974a; Donovan et al., 1974; Gould & Smith, 1978; Duchscherer, 1982; Al-Shaieb & Lilburn, 1982; Oehler & Sternberg, 1984; Dimitrakopoulos & Muehlenbachs, 1985, 1987; Hovland et al., 1987; Prikryl et al., 1988).

Saturate and aromatic hydrocarbons pooled in Cooper Basin sediments of variable stratigraphic position were examined by McKirdy (1982c, 1984) from a large number of petroleum wells. Oils and condensates studied include a wide range of API gravities, varying from 28.2° to 57.2° API. $\partial^{13}C$ results for saturate hydrocarbons were found to range between -29.61 and -24.76, and those of the aromatic hydrocarbon fraction between -25.64 and -23.98 per mil (Fig.6.9a). The stable carbon isotopic composition of liquid hydrocarbons from the Cooper Basin was also examined by Rigby & Smith (1981) who studied 50 samples. $\partial^{13}C$ values varied from about -27 to -22 per mil, with an average $\partial^{13}C$ composition of -24 ± 1.1 per mil (Rigby & Smith, 1981) (Fig.6.9a). Similar $\partial^{13}C$ isotopic ranges are reported for Permian oils by Vincent et al. (1985) and Michaelsen & McKirdy (1989).

Gaseous hydrocarbons were isotopically investigated by Rigby & Smith (1981) and Vincent et al. (1985). Rigby & Smith (1981) examined the $\partial^{13}C$ composition of 24 gas samples from Permian sediments of variable stratigraphic position in the southern Cooper Basin. $\partial^{13}C$ values for methane were found to vary between -42.9 and -27.4, and those for ethane between -28.3 and -21.3 per mil (Fig.6.9a). Similarly, two methane samples analysed by Vincent et al. (1985) from the Jackson-Naccowlah area yielded $\partial^{13}C$ results of -34.2 and -33.4 per mil respectively (Fig.6.9a).

The data demonstrates that the carbonate cements in the Cooper Basin are isotopically much heavier than both the liquid and gaseous hydrocarbons (Fig.6.9a). This argues against the possibility that the hydrocarbons significantly influenced carbonate diagenesis. Hydrocarbon-derived carbonate cements generally have an

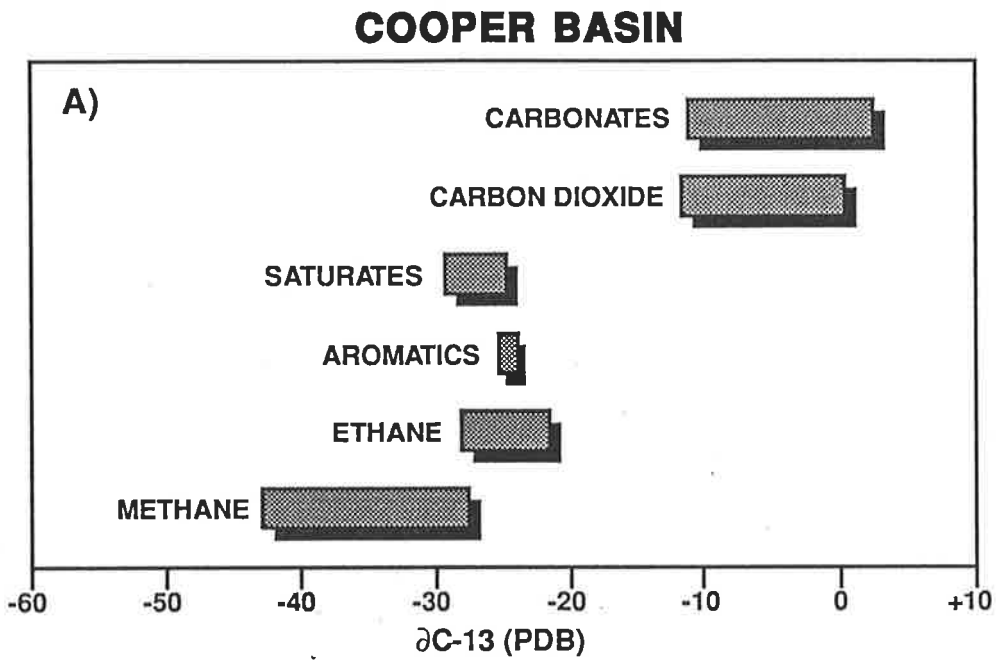

Figure 6.9a Comparison of $\partial^{13}C$ character for liquid and gaseous hydrocarbons, carbon dioxide and carbonate cements in the Cooper Basin [Data sources: this study, McKirdy (1982c, 1984), Rigby & Smith (1981), Vincent et al. (1985), Wall (1987)].

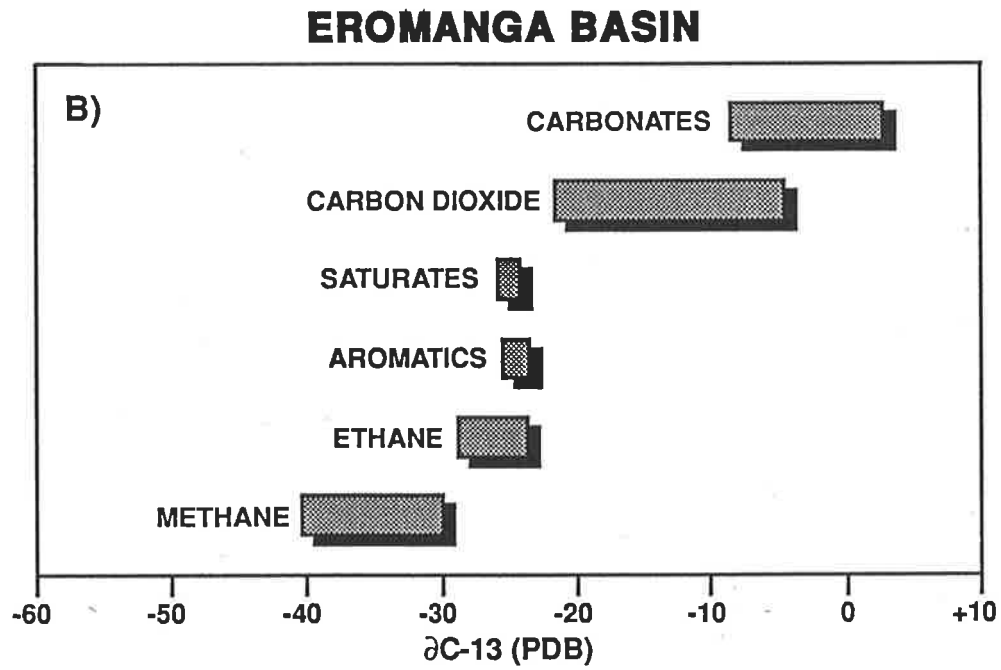

Figure 6.9b Comparison of $\partial^{13}C$ character for liquid and gaseous hydrocarbons, carbon dioxide and carbonate cements in the overlying Eromanga Basin [Data sources: Cox (1984a,b), Eadington et al. (1989), McKirdy (1982c, 1984), Rigby & Smith (1981), Vincent et al. (1985), Wall (1987)].

isotopically light signature approaching the $\partial^{13}C$ of associated hydrocarbons (Table 6.5), because of the incorporation of carbon from that source into the carbonate lattice (Donovan, 1974a; Donovan et al., 1974; Gould & Smith, 1978; Smith, 1978; Al-Shaieb & Lilburn, 1982; Oehler & Sternberg, 1984; Hovland et al., 1987; Prikryl et al., 1988). Such cements commonly have $\partial^{13}C$ values more negative than about -25 (Donovan et al., 1974; Al-Shaieb & Lilburn, 1982; Oehler & Sternberg, 1984; Prikryl et al., 1988), and occasionally as negative as -61 per mil (Hovland et al., 1987) (Table 6.5). However, in recent years the idea has also been put forward that hydrocarbon-derived carbonates may be characterised by strongly positive $\partial^{13}C$ values, up to +14.3 per mil [29] (Dimitrakopoulos & Muehlenbachs, 1987) (Table 6.5).

The mechanism for producing carbonate cements either very depleted or very enriched in carbon-13 from a hydrocarbon source is not fully understood. Most workers believe a form of chemical or biochemical oxidation of liquid/gaseous hydrocarbons is involved, taking place largely at shallow depths of burial (Table 6.5). In the Cooper Basin, geochemical evidence for the oxidation of hydrocarbons is hitherto unreported. Furthermore, the fact that the hydrocarbon-derived carbonate cements reported in the literature are dominated by calcite whereas the most common carbonate type in the Cooper Basin is siderite may argue against the possibility that hydrocarbons greatly influenced the formation of carbonate cements in the Cooper Basin.

6.5.6 Comparison to $\partial^{13}C$ signature of carbon dioxide

The stable carbon isotope composition of carbon dioxide associated with gaseous hydrocarbons in the southern Cooper Basin was determined by Rigby & Smith (1981) for a total of 24 samples from 17 wells. $\partial^{13}C$ values were found to range between +0.3 and -11.7 per mil, with a mean of -6.42 ± 2.4 per mil (Figs.6.9a & 6.10c). Further isotope analyses are reported by Vincent et al. (1985) for two carbon dioxide samples from the Jackson-Naccowlah area in the north-eastern portion of the southern Cooper Basin. In this area, the carbon dioxide was found to have a $\partial^{13}C$ composition of -7.5 and -10.1 per mil respectively (Figs.6.9a & 6.10c).

Significantly therefore, the stable carbon isotope character of the carbon dioxide overlaps in range with that of the carbonates in the Cooper Basin (cf.

---

[29] The study is based solely on interpretation of isotope data from carbonate cements; no supportive evidence of any other kind is presented by Dimitrakopoulos & Muehlenbachs (1987), contrary to the work of many of the other authors.

Table 6.5 $\partial^{13}C$ signatures of hydrocarbon-derived carbonate cements and associated hydrocarbons, as compiled from the literature.

			$\partial^{13}C$ (‰, PDB)			
Region	**Stratigraphic horizon / age**	**Carbonate type(s)**	**Carbonates**	**Associated hydrocarbons**	**Mechanism**	**Source**
Ashland Field, Arkoma Basin, Oklahoma	Hartshorne Sandstone (Pennsylvanian)	Calcite (? some dolomite & siderite)	-29 to -22	-44.9 to -38.7 (methane)	Near-surface oxidation of seeping hydrocarbons	Oehler & Sternberg [1984]
Pockmarks, North Sea	Recent	Calcite	-61.1 to -52.2	Greater than -44 (methane)	Near-surface oxidation within sediment pores	Hovland et al. [1987]
Barrow Sub-basin, W. Australia	Winning Group (Early Cret.)	Calcite	-27.4 to ?	-28.3 to -22.3 (crude oils)	Microbiologic oxidation of crude oils	Gould & Smith [1978]; Smith [1978]
Alberta, Canada	Mannville Group (Early Cret.)	Calcites & Fe-calcites	-1.2 to + 14.3	N.A.	2-step oxidation process of bio-degraded oil (near-surface)	Dimitrakopoulos & Muehlenbachs [1987]
Damon Mound, Texas	Pliocene/ Pleistocene	Calcite	-31.1 to -14.4	-28.3 to -23 (Gulf crude)	'From liquid hydrocarbons' (near-surface)	Prikryl et al. [1988]
Oregon/Washington Basin, USA	Recent	Mg-Calcite, dolomite & aragonite	-66.7 to -34.9	-80 (biogenic methane)	Biogenic methane oxidised at shallow depths of burial	Ritger et al. [1987]

Fig.6.10a-c). This relationship was previously noted by Wall (1987) who considered the carbon dioxide to be the product of the dissolution of siderite cements. More recently, this possibility was also raised by Hunt et al. (1989). However, the present investigation clearly demonstrates that there is a marked difference in frequency distribution between the siderite cements and the carbon dioxide, the former having a heavier isotopic mean than the latter (cf. Fig. 6.10 b & c). This is contrary to the views expressed by Wall (1987) who considered the $\partial^{13}C$ mean of the carbon dioxide to be similar to that of the siderites. Hence, it would appear that the bulk of the siderite cements did not undergo dissolution giving rise to the carbon dioxide in the Cooper Basin, as otherwise a closer match between the mean $\partial^{13}C$ character of the siderite and the carbon dioxide would be expected [30]. However, the carbonates which are isotopically lighter than about -4 per mil overlap with the $\partial^{13}C$ values of the carbon dioxide (cf. Fig. 6.10 b & c) which may suggest that these carbonates are more prone to dissolution than their isotopically heavier counterparts. This hypothesis appears supported by the observation that the carbonates most depleted in ^{13}C generally represent the sparry carbonates associated with the coarser grained sediments (Fig.6.4; Table 6.4) in which aqueous flow conducive to mineral dissolution is facilitated.

Two main considerations, however, indicate that this model may not be correct and that the dissolution of carbonate cements alone cannot satisfactorily account for the bulk of the carbon dioxide in the Cooper Basin:

1. The present diagenetic investigation of over 880 core and ditch samples was unable to ascertain the existence of zones of intense carbonate dissolution in the subsurface (cf. sections 4.2.3.2 & 5.3.1.2). Carbonate leaching was observed only sporadically, and was found to be mostly insignificant and localised (Plates 9 G & 18 C). A similar view is held by Martin & Hamilton (1981) who noted only minor dissolution of siderite cements in the Toolachee Formation in the southern Cooper Basin. The work of Schulz-Rojahn & Phillips (1989) and Stuart et al. (1990) is in accordance with this interpretation.

2. The carbon dioxide concentrations in the reservoirs of the central Nappamerri Trough and the Patchawarra Trough locally exceed 50 percent molar volume, representing the highest in the Cooper Basin (Kantsler et al., 1983; Hunt et al., 1989) (Fig.6.11). Accordingly, if the carbon dioxide is chiefly derived from the dissolution of the carbonate cements, the basin depocentres should represent zones of intense carbonate leaching, containing sandstones with abundant dissolution porosity. This is clearly not the case. Reservoir quality deteriorates with depth (Heath, 1988; section 5.2.3.5), and many reservoirs towards the basin depocentres are tight. Intensely carbonate-cemented zones are prominent to depths approaching 12000 feet

---

30 The possible temperature dependence of fractionation factors for the system $FeCO_3$-CO_2-H_2O is unknown (cf. Usdowski, 1982).

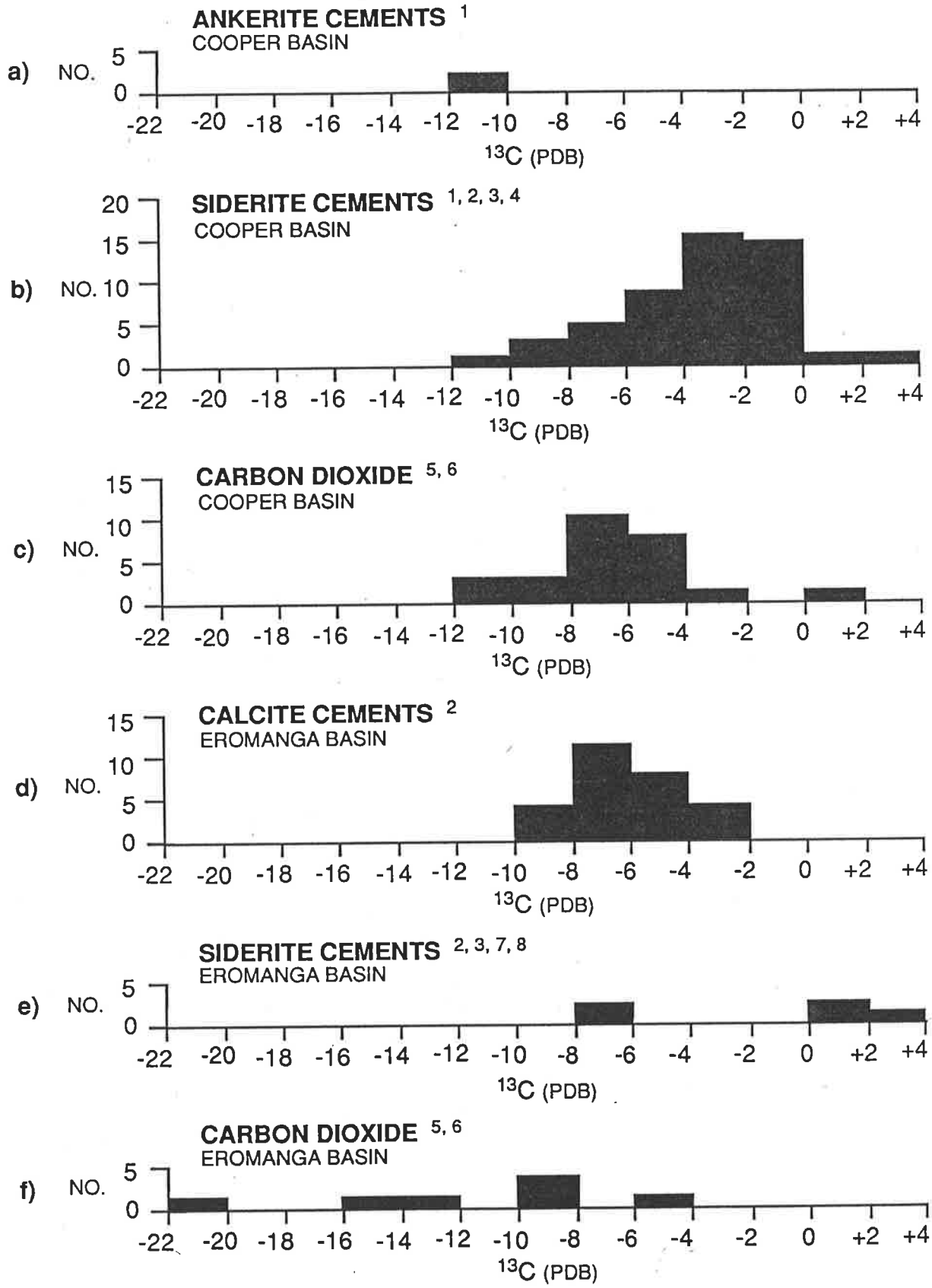

Figure 6.10 a - f Frequency comparison of stable carbon isotope values for carbonate cements and carbon dioxide in the Cooper/Eromanga Basins. For explanation see text. [NO. = Number of samples] [data sources: 1 = This study; 2 = Wall (1987); 3 = Bone (unpublished); 4 = Gould & Smith (1979); 5 = Rigby and Smith (1981); 6 = Vincent et al. (1985); 7 = Eadington et al. (1989); 8 = Green et al., (1989)].

of burial in the central Nappamerri Trough (section 4.2.3.2)). On this basis, it is evident that carbonate dissolution in the subsurface is controlled by neither depth nor temperature.

For these reasons, an alternative source of carbon dioxide in the Cooper Basin must be considered, and is more fully discussed in section 6.5.8.

6.5.7 Comparison with Eromanga Basin

The Eromanga Basin, of Lower Jurassic [31] to Late Cretaceous age, overlies the Cooper Basin and contains clastic sediments of continental, paralic and shallow marine origin characterised by good oil potential. For a composite review of the geology and exploration history of the Eromanga Basin the reader is referred to the work of Armstrong & Barr (1982, 1986).

Similar to the Cooper Basin, carbonate-cemented zones in the Eromanga sequence are common, and have been described in varying detail by Ambrose et al. (1982, 1986), Mount (1982), Scholefield (1983), Gravestock et al. (1983), Menhennitt (1985), Staughton (1985), Anderson (1985), Wall (1987), Gilby & Mortimore (1989), Eadington et al. (1989) and Green et al. (1989). From these workers, it is evident that calcite is by far the dominant carbonate variety, with other carbonate types identified including siderite, ankerite and dolomite. The carbonates can form pervasive cements of poikilotopic texture which locally reduce porosity to almost zero (Gravestock et al., 1983). There is petrographic evidence to suggest that some replacement of framework grains has occurred (Ambrose et al., 1982, 1986; Gravestock et al., 1983). Locally, total carbonate abundances are as high as 70 to 85 per cent in a single thin section (Gravestock et al., 1983; Staughton, 1985; Wall, 1987). In some areas, carbonate-cemented zones exceed several hundred feet in thickness, as evident from lithological descriptions and log character (Staughton, 1985; Anderson, 1985; Wall, 1987). Such massive carbonate-cemented zones are particularly prominent in the Adori Sandstone, the Hutton Sandstone and the Birkhead Formation (Staughton, 1985; Wall, 1987). The carbonate cements vary strongly in lateral and vertical abundance, rendering prediction of their extent and location in the subsurface difficult. This is exemplified by the Spencer South-1 well in the Murta Block where in excess of 195 feet of carbonate cemented zone was intersected in the basal Namur Sandstone. In contrast, about 500 metres north at Spencer-3 only about

---

31 Possibly Upper Triassic (Powis, 1989).

26 feet of carbonate cement was encountered at the same stratigraphic level [32]. The erratic thickness and distribution of the carbonate-cemented zones create problems for the accurate prognosis of formation tops in the basin, as thick carbonate sequences may result in seismic velocity pull-ups in the order of 10 milliseconds or more. Such velocity anomalies may artificially increase the area of structural closure, distort the reservoir shape and result in the pay zone being missed during drilling (Anderson, 1985).

However, despite their obvious importance for petroleum exploration, little is known about the origin of these carbonate cements. Conflicting ideas have been put forward by various workers. Gravestock et al. (1983) considered the carbonate cements in the Hutton Sandstone to represent early diagenetic calcrete horizons ('duricrusts') formed between intermittent episodes of sandy fluvial sedimentation under warm climatic conditions. This view was disputed by Wall (1987) on the basis of isotopic evidence which suggests the carbonates precipitated at temperatures between 55 and 135 °C [33], thus excluding a near-surface or calcrete origin. Most recently, Green et al. (1989) presented petrological evidence indicating the carbonates formed relatively late during burial diagenesis, post-dating the formation of quartz overgrowths.

Isotopically, the carbonate cements in the Eromanga reservoirs resemble those of the Cooper Basin, having a similar $\partial^{13}C$ range (cf. Fig.6.10 a & b, d & e). Based on only a handful of samples, the siderites in the Eromanga Basin have $\partial^{13}C$ values between -7.11 and +2.76 per mil (Wall, 1987; Eadington et al., 1989; Green et al., 1989; Bone, University of Adelaide, unpubl. data). Associated calcites are characterised by a $\partial^{13}C$ composition of between - 8.4 and -2.2 per mil, as determined for a total of 27 samples mostly from the Adori Sandstone (Wall, 1987). The mean $\partial^{13}C$ of the Eromanga calcites is - 5.8 ± 2 per mil, differing from that of the siderite cements in the Cooper Basin which are generally isotopically heavier (cf. Fig.6.10 b,d).

Based on this data, a hydrocarbon-derived origin of the calcites and siderites in the Eromanga sequence is not likely, following a similar line of argument as outlined in section 6.5.5. Liquid and gaseous hydrocarbons pooled in Eromanga Basin sandstones are isotopically much lighter than associated carbonates (Fig.6.9b). This is evident from the work of McKirdy (1982 a & c, 1984, 1985, 1987), Cox (1984 a & b) and Vincent et al. (1985). Saturate hydrocarbons in Eromanga reservoirs have $\partial^{13}C$ values ranging from about -26.1 to -24.2, and aromatic hydrocarbons from -25.5 to -23.3 per mil. The stable carbon isotope composition of methane is variable between -

---

32 Data courtesy of Santos Ltd. well completion reports.

33 Estimated isotopic compositions of basinal waters $\partial^{18}O$ = -6 to -9 per mil (Wall, 1987), as compared to $\partial^{18}O$ = -6.6 per mil for present-day formation waters in the Eromanga Basin aquifers (Airey et al., 1979).

40.4 and -29.9, whereas ethane has $\partial^{13}C$ values between -28.8 and -23.6 per mil (Fig.6.9b).

With respect to the carbon dioxide reservoired in the Eromanga Basin, relatively few $\partial^{13}C$ analyses are published in the existing literature. Rigby & Smith (1981) report the results of five CO_2 analyses from the southern Cooper Basin, and Vincent et al. (1985) provide two more results from the Jackson-Naccowlah area in ATP 259P in southwestern Queensland. The limited data suggests that the carbon dioxide in the Eromanga Basin has a widely variable $\partial^{13}C$ composition, between -4.6 and -21.8 per mil (cf. Figs. 6.9b & 6.10f). The carbon dioxide appears to be generally isotopically lighter than the CO_2 in the Cooper Basin reservoirs (Vincent et al., 1985), although there is some overlap between the two (cf. Fig. 6.10 c & f). When compared to the Eromanga calcites and siderites, the carbon dioxide in the Eromanga Basin shows poor correlation (cf. Fig.6.10 d-f). However, *there is a close similarity between the $\partial^{13}C$ character of the carbonate cements in the Eromanga Basin and the carbon dioxide reservoired in the Cooper Basin.* This suggests a generic link exists between the calcite cements in the Eromanga Basin and the carbon dioxide in the southern Cooper Basin.

Two alternative models may be invoked to explain the similarity in the stable carbon isotope character between the two (Fig.6.12). In the first model, carbonate cements in the Eromanga Basin are dissolved during the creation of secondary porosity, giving rise to the carbon dioxide presently reservoired in the Cooper Basin by downward motion of CO_2-charged groundwaters. In the second model, the carbon dioxide is derived from the Cooper Basin, migrates up-sequence, and controls the formation of the calcite cements in the Eromanga Basin by providing the source of carbon required for carbonate precipitation.

The first hypothesis appears supported principally by two lines of evidence. First, it has been demonstrated that flushing of the Permian strata by artesian waters from the overlying Jurassic aquifers has taken place in the southern portion of the Cooper Basin (Porter, 1973, 1974; Youngs, 1975). Second, various workers have commented on the presence of dissolution porosity in the Eromanga Basin reservoirs, considered to be produced at least partly by the leaching of carbonate cements (Ambrose et al., 1982; Mount, 1982; Staughton, 1985; Wall, 1987; Gilby & Mortimore, 1989; Green et al., 1989). However, overall evidence clearly suggests that the carbon dioxide in the Cooper Basin was not sourced from the Eromanga Basin.

First, extensive dissolution of carbonate cements in the Eromanga sediments is far from positively ascertained, as evidence based on petrographic investigation or SEM work has hitherto not been presented in the published literature. Also, the considerable thickness of carbonate-cemented zones in many parts of the basin suggests that the overall physico-chemical conditions presently favour carbonate

precipitation, not dissolution. Present carbon dioxide levels in the Eromanga reservoirs are low, in the order of 1 to 5 percent (Armstrong & Barr, 1982, 1986; Vincent et al., 1985). In the Cooper Basin, the highest carbon dioxide concentrations (in excess of 40 percent) are attained towards the deeply buried, central portions of the basin (Kantsler et al., 1983; Hunt et al., 1989) (Fig.6.11), furthest away from the influence of the Eromanga Basin aquifers. Clearly, there is a broad inverse relationship between carbon dioxide concentrations and areas flushed by meteoric waters (cf. Figs. 2.9 & 6.11). For example, where complete flushing has taken place in the Toolachee formation, carbon dioxide levels are relatively low, generally 10 percent or less. In contrast, in areas in which there is no evidence of meteoric flushing at the same stratigraphic level, carbon dioxide concentrations are much higher, in the order of 15 percent or more (cf. Figs. 2.9 & 6.11). Last, the isotopic character of the carbon dioxide in the Eromanga reservoirs differs from that in the Cooper Basin, being generally more depleted in ^{13}C (cf. Figs.6.10 c & f).

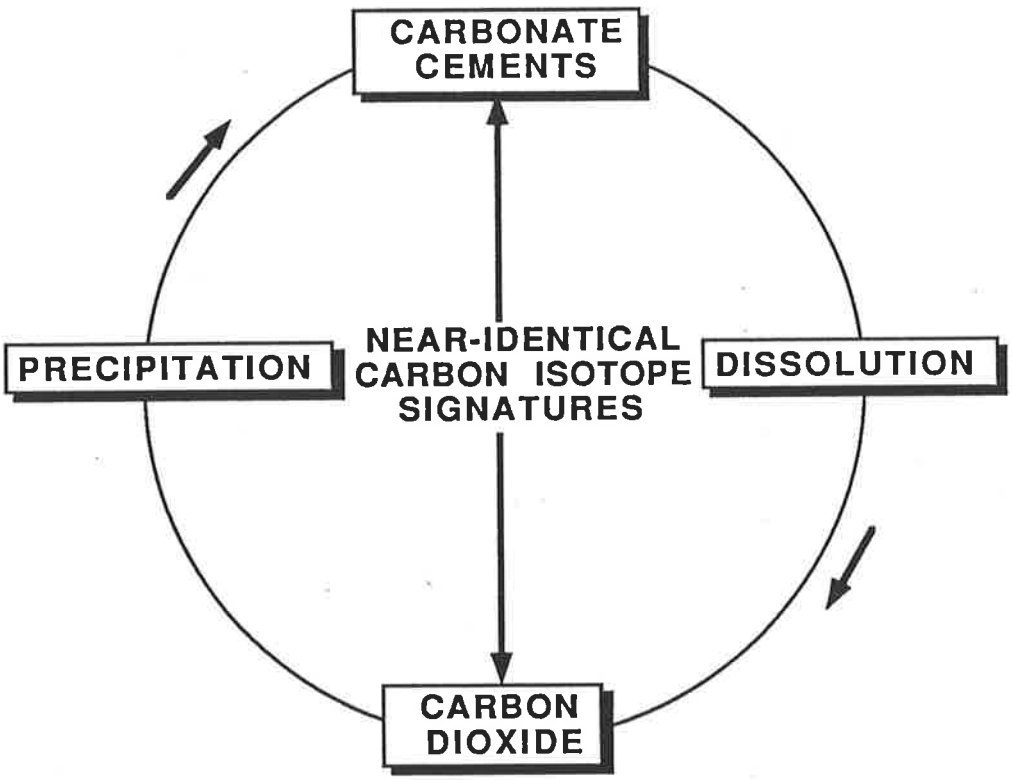

Figure 6.12 The carbonate cements (calcites) in the Eromanga Basin have a near-identical $\partial^{13}C$ signature to the carbon dioxide reservoired in the Cooper Basin. Two explanations are possible: The Eromanga carbonates became dissolved giving rise to the CO_2 presently reservoired in the Permo-Triassic sediments, or the carbon dioxide in the Cooper Basin controls carbonate genesis in the Eromanga Basin.

For these reasons, a model involving carbonate dissolution and flushing by CO_2-charged waters must be rejected. Instead, the second model is favoured to explain the similarity in $\partial^{13}C$ character between the carbon dioxide in the Cooper Basin and the calcite cements in the Eromanga Basin. In this model, the formation of calcite cements in the Eromanga Basin is controlled by the injection of Cooper Basin carbon dioxide into the overlying Ca^{2+}-bearing aquifers of the Great Artesian Basin (or equivalent) [1] of which the Eromanga Basin forms a part (Fig.6.13).

This view represents a radical two-fold departure from conventional thinking. First, the generally low carbon dioxide concentrations in the Eromanga Basin reservoirs was hitherto silently interpreted to indicate that updip migration of carbon dioxide from Cooper Basin sediments to overlying Jurassic-Cretaceous strata has not been volumetrically significant (eg. Kantsler et al., 1983). Kantsler et al. (1983, p.386) postulated that "migration processes" discriminate against carbon dioxide in favour of light hydrocarbon gases on the basis of local occurrences of low CO_2, dry-gas in Eromanga reservoirs above high CO_2 gas in Triassic and Permian reservoirs. Second, carbon dioxide is conventionally considered to control carbonate *dissolution*, not carbonate precipitation (eg. Dixon et al., 1989).

Based on theoretical considerations, there certainly is no reason why carbon dioxide from the Cooper Basin should not have migrated up-sequence into the Eromanga reservoirs. There is abundant geochemical and other evidence to suggest that a large proportion of the hydrocarbons pooled in the Eromanga sequence are sourced from the Cooper Basin sediments (Jenkins, 1989; Gilby & Mortimore, 1989; Heath et al., 1989; Yew & Mills, 1989). Clearly, if the Permian-sourced hydrocarbons were capable of migrating updip into the Jurassic-Cretaceous sediments, it is difficult to see why the carbon dioxide from the Cooper Basin should not have been equally capable of doing so, following the laws of buoyancy. This is supported by the small diameter of the carbon dioxide molecule (3.3 Å), smaller than that even of methane (3.8 Å), the simplest hydrocarbon molecule (Tissot & Welte, 1978) (Table 5.11). This should, if anything, have facilitated the updip migration of carbon dioxide, not the reverse. Carbon dioxide likely migrated updip, either in gaseous form or dissolved in water. In the latter case, processes related to diffusion and/or advective flow could been responsible for the transportation of CO_2 into shallower sequences. However, compactional pore water flow is unlikely to have been a dominant force in recent geological times as significant dewatering of clastics is typically a relatively early geological phenomenon iniated soon after burial (Tissot & Welte, 1978).

---

34 The isotopic equilibrium and the effective fractionation on CO_2-degassing and calcite precipitation is discussed by Usdowski (1982). Experimental results show the isotopic composition of the calcite is virtually identical with that of the dissolved carbonate (Usdowski, 1982).

The model would seem to be supported by the observation that there is an inverse relationship between carbon dioxide concentrations and areas flushed by meteoric waters in the study area. Hydraulic interconnection between the Cooper and Eromanga basins is made possible where there is no effective Triassic cap rock (Youngs, 1975). The absence of an effective Triassic seal is likely to have facilitated the upward escape of CO_2 from the Cooper Basin sediments (Fig.6.13). Similarly, the fact that carbon dioxide concentrations are low along structural highs (cf. Figs. 6.11 & 2.5) where there is minimum separation between the Permian and Jurassic-Cretaceous sediments due to depositional thinning and/or erosion indicates a similar mechanism may have applied here. Interestingly, Habermehl (1986b) also noted that carbon dioxide concentrations are relatively high in water samples from several wells in the Canaway Fault area. This suggests the carbon dioxide may have migrated updip along fault zones in the basin.

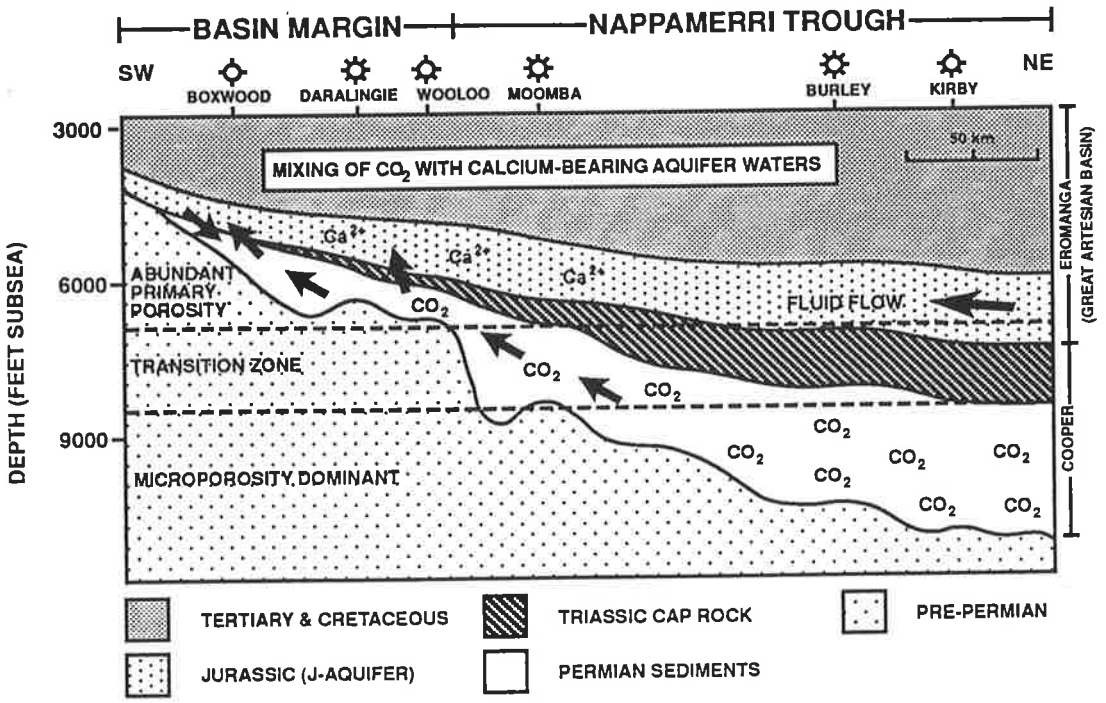

Figure 6.13 Model proposed to explain the similarity in $\partial^{13}C$ character between the carbon dioxide in the Cooper Basin and the calcite cements in the Eromanga Basin. Cooper Basin carbon dioxide migrates vertically into the calcium-bearing J-aquifers of the Eromanga/Great Artesian Basin, leading to formation of thick carbonate-cemented zones. Upward escape of carbon dioxide is facilitated where there is no effective Triassic seal, or where separation between the Permian and Jurassic sediments is minimal due to depositional thinning and/or erosion. Reservoir quality is a key factor in controlling carbon dioxide abundances (see text).

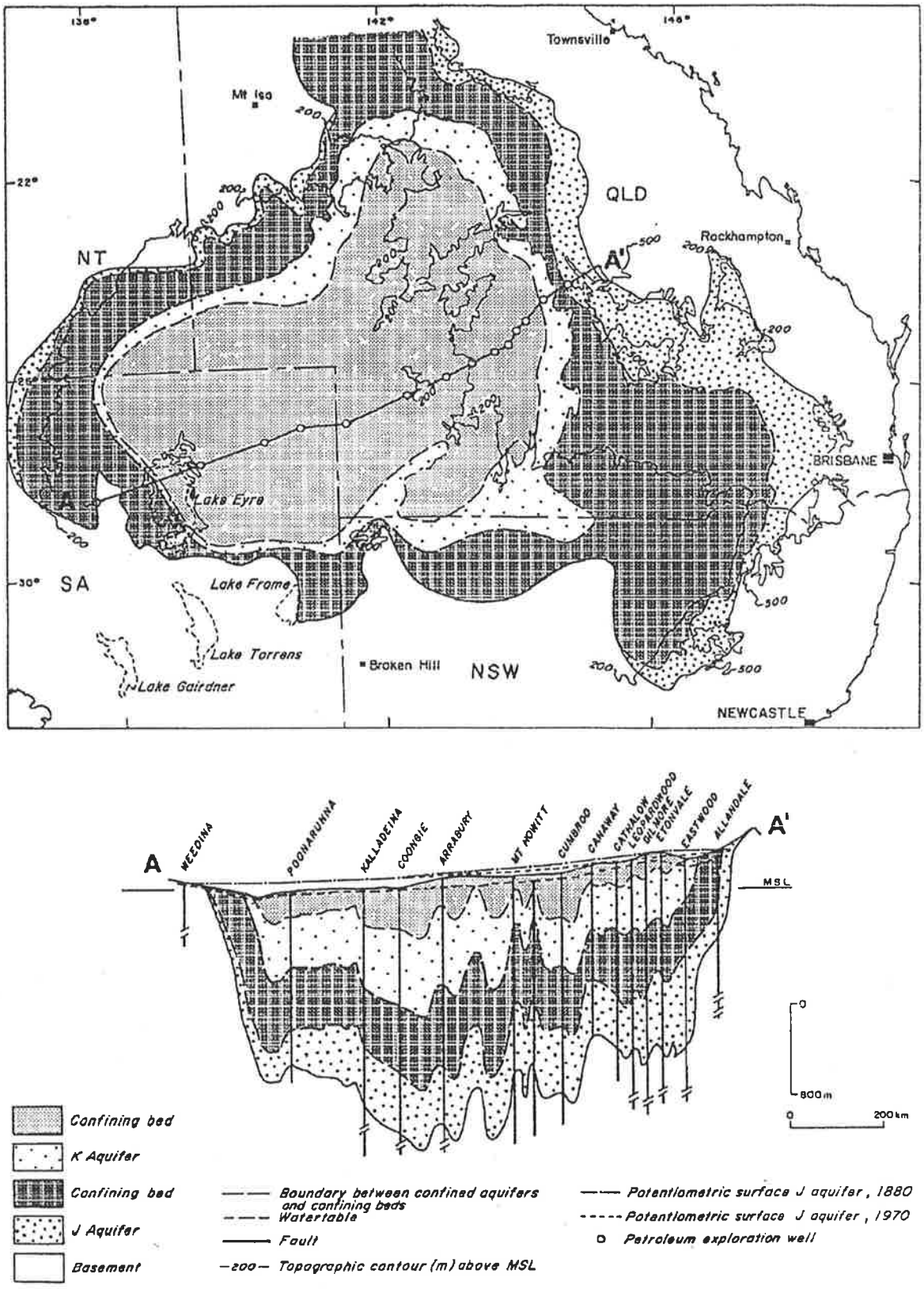

Figure 6.14 Lateral extent of simplified hydrogeological units and cross-section of the Great Artesian Basin (modified from: Habermehl, 1980).

In this context, a brief examination is warranted concerning the hydrogeology of the Eromanga/Great Artesian Basin aquifer system.

The Great Artesian Basin, underlying about 22 per cent of the Australian continent, is one of the largest artesian basins in the world (Habermehl, 1980) (Fig.6.14). It is a multi-layered, confined groundwater basin exclusively of meteoric origin which comprises the Eromanga, Surat and Carpentaria Basins, as well as portions of the Bowen and Galilee Basins. The basin is uplifted along its eastern margin and tilted southwesterly (Habermehl, 1986b) (Fig.6.14). Principal recharge occurs from this direction, resulting in a predominantly southwesterly flow direction (Fig.6.15). Minor recharge also occurs from the western margin (Habermehl, 1980), and possibly the northwest (Randal, 1978) (Fig.6.15).

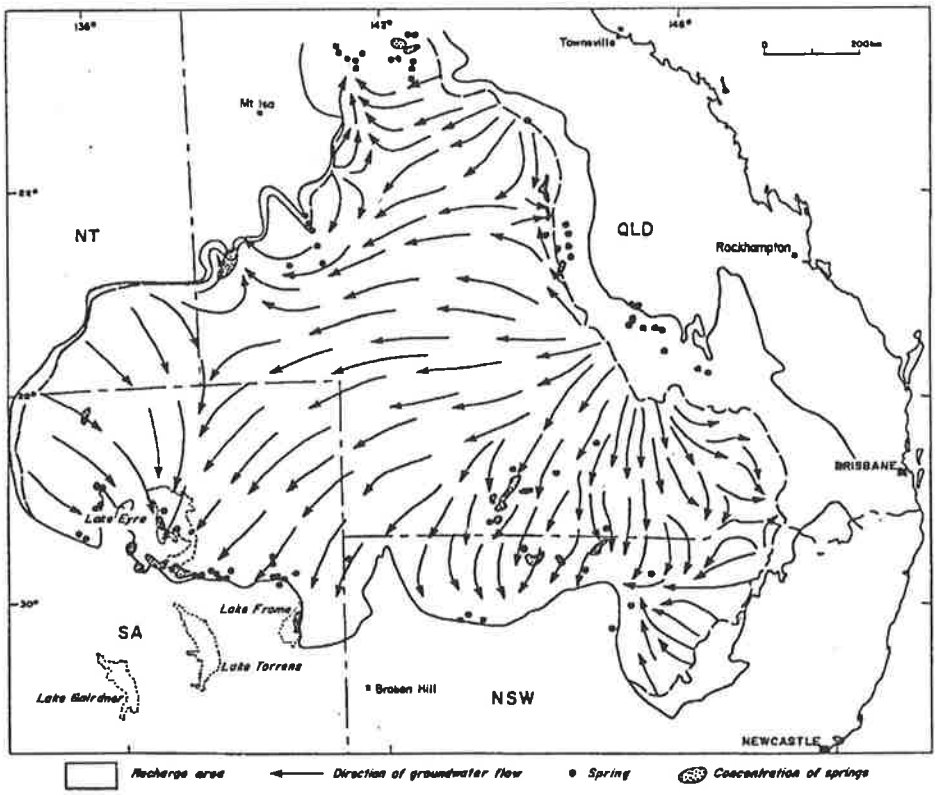

Figure 6.15 Recharge and natural discharge areas (artesian springs) and directions of regional groundwater flow in the Great Artesian Basin (after: Habermehl, 1980).

The principal aquifers are of Jurassic and Cretaceous age, designated the J- and K-aquifers respectively by Habermehl (1980). In the Eromanga Basin, the main continuous aquifer is the J-aquifer which comprises principally the Namur and Hutton Sandstones but also the Birkhead Formation, the Adori Sandstone and the Westbourne Formation (Fig. 6.16). It is evident that these stratigraphic horizons also represent

those in which thick carbonate-cemented zones are prominent. The J-aquifer reaches depths of almost 5000 feet in some parts of the Eromanga Basin, and is in close stratigraphic proximity to the Permo-Triassic sediments of the Cooper Basin.

Chemically, the groundwater in the Great Artesian Basin is mostly of the Na-HCO_3-Cl type, although some Na-Cl-SO_4 type water also occurs along its western margin (Habermehl, 1986d). Ca^{2+} concentrations are variable, but over large parts of the Great Artesian Basin aquifers are close to saturation with respect to calcite (Collerson et al., 1988). The water chemistry of the aquifers reflects changes with distance and age away from the recharge areas of the Great Artesian Basin (Habermehl, 1984; Herczeg et al., 1988; Collerson et al., 1988). Hydrologically young waters near the recharge areas have higher Ca^{2+} and Mg^{2+} concentrations than older water from more central parts of the basin, and the discharge areas (Habermehl, 1984; Herczeg et al., 1988; Collerson et al., 1988). The implication is that Ca^{2+} and Mg^{2+} are being removed from aqueous solution, by formation of authigenic minerals such as calcite and dolomite. This is feasible since the pH of the formation waters towards the centre of the Eromanga Basin is of a generally basic nature (pH = 7.4 to 8.6) [35], conducive to carbonate precipitation (cf. Tucker, 1981).

The unimpeded flow of groundwater carrying mineral components required for carbonate authigenesis is favoured by both the reservoir characteristics and the hydrodynamics of the Great Artesian Basin. The aquifers of the constituent geological basins are continuous and hydrologically interconnected (Habermehl, 1980). Sandstone porosities in the Eromanga Basin range up to 38 percent, and permeabilities may be as high as several darcys (section 5.2.3.1). Lateral groundwater flow rates in the Great Artesian Basin are in the order of 1 to 5 metres per year (Habermehl, 1980; Senior & Habermehl, 1980). Results obtained from radioactive dating suggest groundwater residence times are relatively short, in the order of only 1.4 million years or less (Bentley et al., 1986). According to Habermehl (1980, p.26), there was continuous meteoric recharge "from geological to modern times".

This raises the question when the Great Artesian Basin was formed, a topic of some conjecture. In the view of Bowering (1982), the artesian aquifer system was established following uplift and exposure of the intake beds as a result of the Kosciuskan Orogeny during the Plio-Pleistocene. This would indicate either that the carbonates formed in very recent geologic time, or that an artesian aquifer system existed prior to the Kosciuskan Orogeny. Other workers favour an earlier origin of the aquifer system. Wopfner (1960) is of the opinion that the western margin of the Eromanga Basin became uplifted as early as the pre-Middle Jurassic. This suggests there may have been a gentle easterly hydraulic gradient, opposite to the present gradient (Bowering, 1982). Most recently, Wall (1987) speculated that there was an

[35] Source: Santos Ltd.

earlier Tertiary, northward tilted aquifer system in the southern portion of the Eromanga Basin.

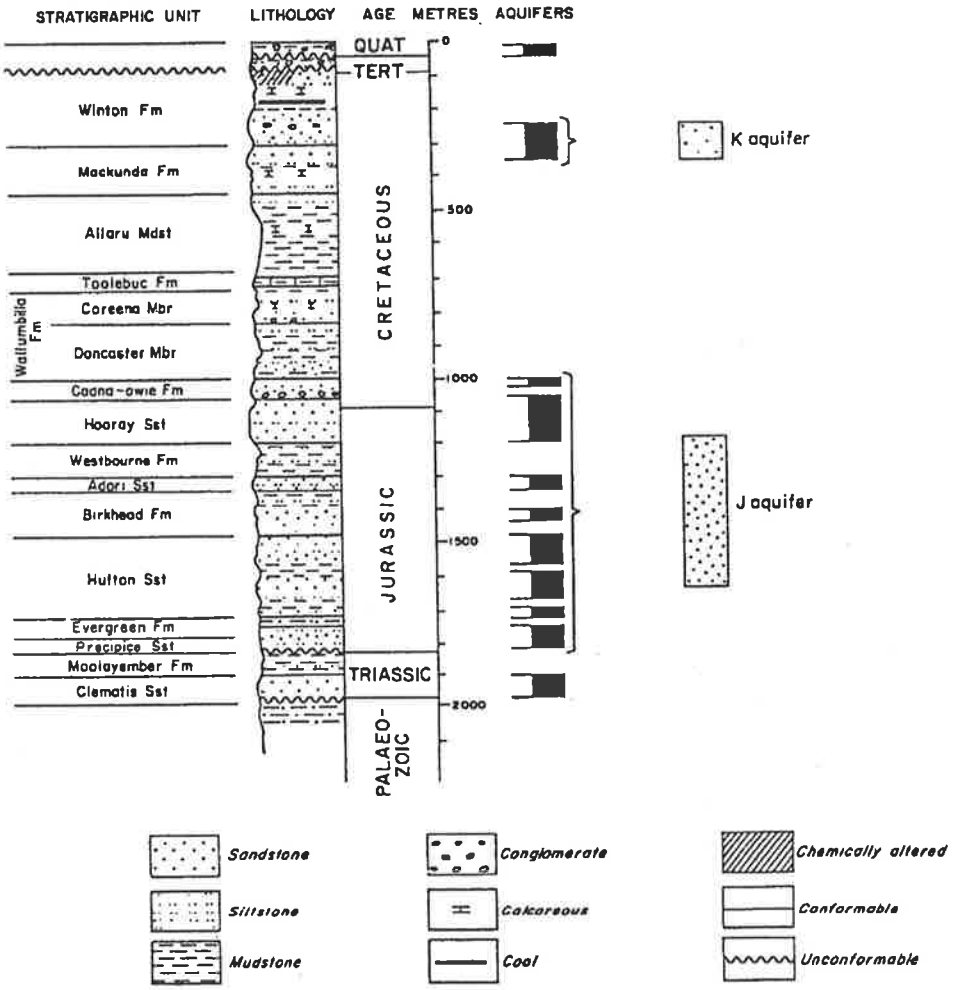

Figure 6.16 Schematic lithostratigraphic column and simplified aquifer groups of the Great Artesian Basin of which the Eromanga Basin forms a part (after: Habermehl, 1980).

Such lack of consensus regarding the timing of inception of the Great Artesian aquifer system (or equivalent) is unfortunate; it complicates assessment of the likely timing of carbonate cementation in the Eromanga Basin. Clearly more research is required to fully evaluate the hydrogeological and diagenetic history of the basin.

Theoretical evidence in support of the model proposed for carbonate cementation in the Eromanga Basin is presented by Smith & Ehrenberg (1989). The

workers suggest that the pH in clastic reservoirs is controlled primarily by aluminosilicate equilibria, not CO_2 levels as widely believed. Similar data was put forward by Hutcheon (1989). With the pH thus fixed independently, an increase in CO_2 concentration could result in carbonate precipitation. Smith & Ehrenberg (1989) suggested this would occur at temperatures lower than about 100 to 120 °C. This view is in good agreement with isotope data presented by Wall (1987) who considered the calcite cements in the Adori Sandstone of the Eromanga Basin to have formed at temperatures between 75 and 121 °C, or less. Alternatively, the pH of the aquifer system may be externally buffered by carboxylic acids and acid anions released from organic matter during thermal decarboxylation (Surdam et al., 1989). An increase in CO_2 concentration under such conditions would also result in carbonate precipitation (cf. Surdam et al., 1989, Fig. 9). One or both of these mechanisms may be applicable.

Interestingly, there is evidence to suggest that the proposed mechanism of carbonate cementation in the Eromanga Basin is not an isolated phenomenon but may be applicable to other basins. In the south of Texas, for example, abundant calcite and dolomite cements exist in meteoric aquifers of Mesozoic age that have evolved towards carbonate saturation by downdip hydrostatic flow (Woronick & Land, 1985). Underlying these aquifers are Triassic clastics containing abundant CO_2 as well as small amounts of hydrocarbons. Woronick & Land (1985) suggest, on the basis of isotopic evidence, that periodic injection of these CO_2-rich brine waters caused precipitation of the observed carbonate phases in the Mesozoic aquifers. Importantly however, the workers failed to recognise the potential role played by CO_2 in carbonate formation: "the only mechanism for carbonate precipitation we can suggest is CO_2 loss accompanying methane degassing since simple mixing of the two fluids we have proposed should result in dissolution, not precipitation" (Woronick & Land, 1985, p.273).

The example highlights the need to re-examine existing concepts of carbonate cementation in clastic sequences generally, since the significance of CO_2 in the genesis of carbonate cements may hitherto have been overlooked.

6.5.8 Origin of carbon dioxide

In the light of evidence presented, a detailed examination is warranted concerning the origin of carbon dioxide in the study area. An origin involving the dissolution of carbonate cements has already been addressed; such source was considered insignificant. However, other possibilities exist. For example, Rigby & Smith (1981) suggested the carbon dioxide was derived from a granite source. Alternatively, carbon dioxide may have originated from the thermal breakdown of Cambrian limestones in the underlying Warburton Basin (Rigby & Smith, 1981; Kantsler et al., 1983). A third possibility is that the carbon dioxide

originated from organic matter during maturation-related processes (Schwebel et al., 1980; McKirdy, 1982d). The various models shall be critically reviewed below.

6.5.8.1 Granites

Rigby & Smith (1981) observed a close similarity in $\partial^{13}C$ character between four granite samples from Wooloo-1 and the Moomba Field [36] and the carbon dioxide in the Cooper Basin. CO_2 released from the granites on pyrolysis or by treatment with phosphoric acid yielded $\partial^{13}C$ values between -4.0 and -10.5 per mil, a range which "encompasses 80 per cent of the natural [CO_2] gas samples analysed" (Rigby & Smith, 1981, p.227). In their view, this suggested that the carbon dioxide in the Cooper Basin was sourced from magmatic fluids, or from accessory carbonate minerals associated with the basement granites.

There are, however, a number of objections which may be raised with respect to the validity of Rigby & Smith's (1981) model:

1. There is a problem with the timing of granite emplacement relative to the onset of Permian sedimentation in the Cooper Basin. Geological evidence strongly suggests that crustal emplacement of granite in the region was followed by a prolonged phase of erosion and deep weathering prior to deposition of Permian strata. In PEL 5 & 6, granitoid rocks encountered at Big Lake-1, Burley-2, McLeod-1, Roseneath-1, Topwee-1, Wooloo-1 and a string of Moomba wells all intersected some weathered material, with the possible exception of Moomba-57 where it may have been eroded away (Table 6.6). At Moomba-56, at least 154 feet of highly weathered granite was intersected before reaching total depth. Available evidence suggests that such weathering profiles may be a regional feature, as exemplified by Ashby-1 in the Queensland sector of the Cooper Basin (Table 6.6). This suggests the granites were probably exposed at the Permo-Triassic unconformity surface in many parts of the basin. Hence, even if the granite magmas were accompanied by a CO_2-H_2O fluid phase during their ascent in the crust as suggested by Rigby & Smith (1981), much if not all of the carbon dioxide would have been lost to the atmosphere long before Cooper Basin sedimentation was initiated.

---

[36] The data of Rigby & Smith (1981) suggests Moomba-10 intersected granite basement at a depth of about 9500 feet (see their Table 2). This is inaccurate since Moomba-10 reached total depth in Gidgealpa sediments at 8140 feet; no granite basement was penetrated by this well. The mistake is attributed to a printing error. The authors are believed to refer to Moomba-1 which intersected granite basement between 9322 and 9519 feet KB.

Table 6.6 Listing of some wells that intersected pre-Permian granitoid basement i PEL 5 & 6 and ATP 259P, Cooper Basin. Note that most granites and granodiorites ar characterised by weathering zones of variable thickness. The recognition of weatherin profiles is based on lithological descriptions and log response. Data compiled from we completion reports and various authors [1 = Fanning (1987); 2 = Martin (1967b); 3 Webb (1974)].

Well Name	Top Depth (ft., drill.)	Thickness weathered zone (ft.)	Radio-metric age (Ma)	Description
Ashby-1	6947	62+	N.A.	Coarse granite
Big Lake-1	9792	?226 [a]	N.A.	Altered ?granodiorite with large quartz phenocrysts
Burley-2	12020	78	N.A.	Granodiorite (undiff.)
Ella-1	4048	?	408 ± 2 [1d]	Medium to coarse granite
McLeod-1	12292	?44	310 ± 17 [c]	Coarse to very coarse granite
Moomba-1	9322	125	305 ± 8 [2d] 333-362 [3e]	Granite (undiff.)
Moomba-8	9062	?	N.A	Granite (undiff.)
Moomba-27	9878	102	N.A.	Granodiorite (undiff.)
Moomba-56	10340	154+	N.A.	Granite (undiff., amount of weathering decreasing with depth)
Moomba-57	10289	?	N.A.	Granite (undiff.)
Moomba-58	9883	181	N.A.	Granite (undiff.)
Moomba-59	?9363	?50	N.A.	Medium to coarse granite
Moomba-63	9518	?36 [b]	N.A.	Coarse to v. coarse granite
Roseneath-1	7121	10	N.A.	Coarse granite
Topwee-1	7290	20+	N.A.	Coarse granite
Wooloo-1	7526	?	N.A.	Coarse granite, 'weathered towards top'

[a] based on sonic log response
[b] based on increased rate of drilling penetration
[c] U-Pb dating of zircon
[d] K-Ar dating of biotite
[e] Rb-Sr dating (whole-rock)

The duration of granite exposure is problematic, but probably was in the order of at least several several million years. Available K-Ar, U-Pb and Rb-Sr radiometric data suggests the granites vary in age between 305 and 408 Ma (Table 6.6). This would suggest a post Late Ordovician-Carboniferous time of emplacement. However, Gatehouse (1986) raised the possibility that the granites could also be of Precambrian age on the basis of more regional geological considerations. Hence, depending on the age of the granites, between about 19 and 300 million years may have been available in which the granites could have developed a weathering profile, and in which CO_2 could have escaped to the atmosphere.

2. A major underlying assumption of Rigby & Smith's (1981) model is that the Cooper Basin is devoid of any other major sources of carbon dioxide, and that the present $\partial^{13}C_{CO_2}$ character is not the result of mixing of carbon dioxide of different source origins. This is exceedingly unlikely in view of a wealth of data suggesting that both liquid and gaseous hydrocarbons were sourced in situ in the sediments of the Cooper Basin (Kantsler et al., 1983; Heath et al., 1989; Hunt et al., 1989; Yew & Mills, 1989; Jenkins, 1989; Tupper & Burckhardt, 1990). In the author's assessment, at least *some* carbon dioxide is likely to have been released during the thermal maturation of organic matter, as carbon dioxide is a common by-product of petroleum-generative processes (Tissot & Welte, 1978; Hunt, 1979). Other potential sources of carbon dioxide exist and are addressed elsewhere (cf. Fig.6.8). Clearly, if the carbon dioxide resulted from multiple sources, the observed similarity in $\partial^{13}C$ character between the granite samples and the carbon dioxide is fortuitous and an *a priori* granite origin of CO_2 may no longer be inferred on the basis of the isotope data.

3. Granite basement is absent in the low temperature, but CO_2-rich Patchawarra Trough (Kantsler et al., 1983) (cf. Figs.2.4 & 6.11). There is further a distinct lack of correlation between granite lithologies and carbon dioxide concentrations in the Nappamerri Trough (cf. Figs. 2.4 & 6.11) .

4. Further speculation by Rigby & Smith (1981) that carbon dioxide may have been present in the fluid phases which accompanied the ascent of the granites into the crust is problematic. As emphasized by Holloway (1976, p.1518), "significant amounts of CO_2 in the fluid phase accompanying a magma should leave some record of its presence - for example, in fluid inclusions". Rigby & Smith (1981) were, however, unable to ascertain this. Despite an attempt at studying such fluid inclusions, Rigby & Smith (1981) failed to provide irrevocable evidence for the presence of carbon dioxide having accompanied the ascent of the granites into the crust.

5. Strong doubts also exist regarding the 'igneous' origin of the carbonates associated with the granites. Rigby & Smith (1981) implied that the carbonates formed directly or indirectly from the granite magmas, possibly as "the products of invasion by carbon dioxide from greater depths" (Rigby & Smith, 1981, p.227). The workers

identified siderite as the dominant accessory carbonate mineral. This is, however, a most unusual carbonate variety to occur in association with granites (S.Turner, University of Adelaide, pers. comm.). The possibility therefore exists that these siderites are not magmatic or hydrothermal precipitates related to igneous activity. Instead, the carbonates may have been introduced into the granites as pore-filling cement by percolating ground waters. This is plausible in view of the widespread occurrence of siderite cements in the sandstones of the southern Cooper Basin. The similarity in $\partial^{13}C$ character between the siderites associated with the granites and those occurring in the Permo-Triassic sediments may argue in favour of this interpretation.

6. Rigby & Smith (1981) further raised the possibility that dissolution of the carbonates associated with the granites may have acted as a source of carbon dioxide in the Cooper Basin. Although theoretically possible, no evidence of carbonate dissolution in the granites has hitherto been presented. Also, it appears unlikely that such a source could account for the considerable volumes of carbon dioxide found in the basin as carbonate mineralisation in granites is typically insignificant. This is supported by the data of Rigby & Smith (1981) which shows that the carbonate carbon yields from the granites are exceedingly low, in the order of 0.01 to 0.22 per cent only. The total volumes of carbon dioxide released through dissolution of carbonate minerals associated with granites would, of course, depend on the subsurface extent of the granites in the Cooper Basin area. To date, however, positive identification of granite basement in the region is restricted to only a few locations (Fig.2.4), and evidence from seismic data is absent or ambiguous.

6.5.8.2 Warburton Basin limestones

The Cambrian carbonates of the Warburton Basin also theoretically represent a potential source of carbon dioxide for the superjacent Cooper Basin (Rigby & Smith, 1981; Kantsler et al., 1983). According to Kantsler et al. (1983), the carbonates could have undergone dissolution because of thermal activity from deep seated igneous intrusions, metamorphism, or volcanic activity. Recently, the model received new stimulus from the work of Roberts et al. (1990) who demonstrated the presence of dissolution porosity in some limestones of the Kalladeina Formation. The workers speculated that dissolution of carbonates along the Gidgealpa structure was caused by magnesium-rich fluids derived from volcanic rocks which directly underlie the limestones. However, it is unlikely that such a mechanism could account for the bulk of the carbon dioxide reservoired in the Cooper Basin. Evidence for this is derived

from the data of Rigby & Smith (1981) which shows that Cambrian carbonates from Kalladeina-1 are characterised by a typically marine $\partial^{13}C$ signature (0 to +1.3 per mil), much heavier than the mean $\partial^{13}C$ character of the Cooper/Eromanga carbon dioxide (cf. Figs. 6.8, 6.10 c & f). On this basis, a carbon dioxide origin involving predominantly dissolution of Warburton carbonates may be excluded (Rigby & Smith, 1981). However, the possibility that some carbon dioxide originated from Cambrian limestones may not entirely be ruled out, as the carbon dioxide may have mixed with isotopically lighter CO_2 derived from humic organic matter (Kantsler et al., 1983) and/or other sources (see Fig.6.8). Such mixing could account for the present isotope composition of the carbon dioxide.

Another problem exists with the timing of secondary porosity development in relation to the inception of the Cooper Basin. At least some of the dissolution porosity in the Warburton Basin is related to subaerial exposure and karst development (Roberts et al., 1990). Clearly, such porosity development must have predated the formation of the Permo-Triassic sediments and can therefore not have contributed to the carbon dioxide concentrations in the Cooper Basin. However, the timing of vuggy porosity development in the dolomites of the Kalladeina Formation (Roberts et al., 1990) remains unclear and requires further research. It is possible that the creation of such porosity contributed to the carbon dioxide in the Cooper Basin. However, the fact that the Cambrian limestones are separated from the sediments of the Cooper Basin by an unconformity spanning more than 200 million years downgrades this possibility.

Last, there is no obvious relationship between carbon dioxide concentrations and the known subsurface distribution of Cambrian limestones which may further argue against a prominent CO_2 origin from that source (cf. Figs. 2.4 and 6.11).

6.5.8.3 Organic maturation processes

An organic origin of the carbon dioxide in the Cooper Basin was suggested by Schwebel et al. (1980) who noted a good correlation between CO_2 content and vitrinite reflectivity in the Nappamerri Trough: with greater thermal maturity the carbon dioxide was found to increase. On this basis, Schwebel and co-workers proposed the carbon dioxide originated from the thermal degradation of humic organic matter within the Permian coal measures. The higher CO_2 content in the Patchawarra Trough was attributed to a different temperature history in that area (Schwebel et al., 1980).

Rigby & Smith (1981) and Hunt et al. (1989) dispute this interpretation by arguing that with increasing coalification the concentration of carbon dioxide produced would be expected to decrease, not the reverse. This is because the oxygen content of coal diminishes with increasing coal maturity, effectively limiting the amount of carbon dioxide which can be produced at greater maturity levels (Fig. 6.17).

In the Cooper Basin, reservoir temperature and thermal sediment maturity both increase with depth (Kantsler et al., 1983). In essence, therefore, Rigby & Smith (1981) and Hunt et al. (1989) imply that a maturation-related origin of the carbon dioxide in the Cooper Basin could only be argued for if CO_2-concentrations were greater at shallower depths of burial than towards the deeper, more central parts of the basin, contrary to the trend that is actually observed. Following this logic, a CO_2 origin involving the thermal maturation of organic matter may almost categorically be ruled out for numerous petroleum provinces throughout the world, since the carbon dioxide content commonly increases with depth and temperature in clastic basins (Franks & Forester, 1984; Lundegard & Land, 1986; Smith & Ehrenberg, 1989). This deduction is, at best, controversial. Certainly in basins with proven hydrocarbon potential considerable volumes of CO_2 are likely to have been generated during the maturation of organic matter.

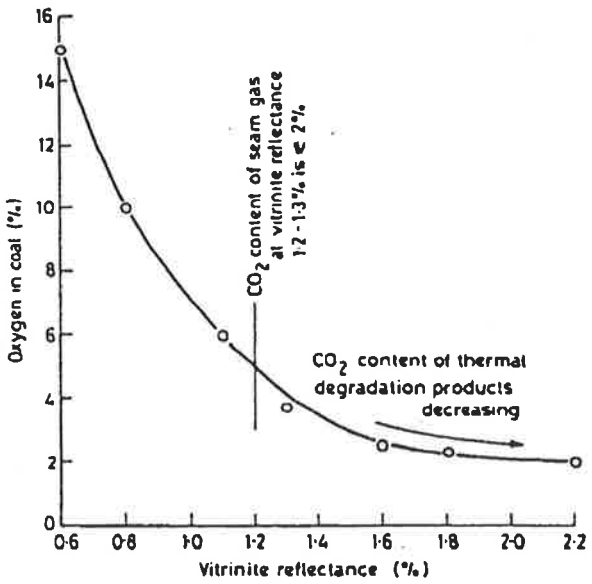

Figure 6.17 Decrease in oxygen content of coal with increasing coal maturity. Data of Seyler as quoted in Van Krevelen & Schuyer (1957) (reprinted in: Rigby & Smith, 1981).

Further, the present investigation has indicated that Cooper Basin carbon dioxide may have escaped into the Eromanga Basin sediments where it was involved in carbonate precipitation. It follows *that modern carbon dioxide concentrations in the Cooper Basin and elsewhere may not just be a function of CO_2 source, but also the reservoir characteristics and the sealing capacity of the associated sediments*. In this context, it may be significant that the central Nappamerri Trough, characterised by some of the highest CO_2 concentrations in the Cooper Basin (Fig.6.11), is dominated by microporosity with low effective permeabilities (section 5.4.1). A similar relationship

may apply for some areas in the Patchawarra Trough where carbon dioxide levels also are anomalously high (cf. Figs.6.11 & 6.18). In contrast, towards the flanks and the structural highs of the southern Cooper Basin abundant primary porosity is preserved, resulting in sandstones characterised by high effective porosities and permeabilities (section 5.4.1; Figs.5.16 & 5.22). It is in these areas that the lowest carbon dioxide concentrations are observed, lending support to the view that here CO_2 could more easily escape from the Permian sediments than towards the basin depocentres (Fig.6.13).

On the basis of these considerations, the increase in CO_2 content with depth and thermal maturity is clearly not a valid argument against the thermal degradation of organic matter having significantly contributed to the carbon dioxide in the Nappamerri Trough, as suggested by Rigby & Smith (1981) and Hunt et al. (1989). This is because carbon dioxide produced at relatively low thermal maturity levels may simply have become 'trapped' in low-quality reservoir clastics that subsequently underwent subsidence and more thermal heating; this may explain the present-day association of high CO_2-concentrations with the more deeply buried sediments of the Nappamerri Trough that are characterised by high vitrinite reflectance levels (Fig.6.19) [37].

---

37 Hunt et al. (1989, p.517) point out that "there appears to be a distinct dependence between CO_2 and depth and maturity in the Nappamerri Trough, but no relationship at all in the Patchawarra Trough" (cf. Figs. 6.18 & 6.19). The workers provide no explanation for this phenomenon.

The following comments are made:

1. Most of the data values presented by Hunt and co-workers from the Patchawarra Trough come from a relatively narrow depth interval (about 8000 to 10000 feet) (Fig.6.18). In contrast, CO_2 analyses derived from the Nappamerri Trough span a much wider depth range (approx. 5200 to 11000 feet) (Fig.6.18). Hence, it is perhaps little surprising that the CO_2-depth trend from the latter structural province is more 'well-defined' in view of the broader depth spectrum represented. More data is probably required to fully evaluate the nature of carbon dioxide distribution versus depth in the Patchawarra Trough.

2. The data in Chapter 5 has shown that the onset of the diagenetic zone dominated by microporosity in the southern Cooper Basin commences at depths exceeding about 8400 feet. Within this dominantly microporous zone, there still exist some reservoir sandstones characterised by abundant macropores. Hence, it is possible that the variation in reservoir quality is reflected in differences in the concentration of carbon dioxide in the Patchawarra Trough and elsewhere. High abundances of carbon dioxide may reflect areas where there is a predominance of microporosity (CO_2 escape made difficult) whereas low concentrations may indicate clastics of higher reservoir quality (CO_2 escape facilitated). Hence, the lack of dependence between CO_2 abundance and depth in the Patchawarra Trough (Fig.6.18) may be simply a function of the rapid lateral and vertical variation in reservoir quality in this area, although alternative explanations are possible [eg. differences in CO_2 source(s), thermal regimes, type and quantity of organic matter etc.].

3. With respect to the absence of correlation between CO_2 abundance and reservoir maturity in the Patchawarra Trough (Fig.6.19), it is pointed out that correlation of these two parameters may not necessarily be meaningful. The discussion has already shown that, even if the maturation of organic matter represents the sole source of carbon dioxide in the Cooper Basin, CO_2 abundance may be controlled as much by the nature of the regional reservoir character as the level of thermal maturation attained within the source sediments. On this basis, the "distinct dependence" between CO_2 and maturity in the Nappamerri Trough may be fortuitous. In other words, the assumption that thermal sediment maturity alone influences CO_2 concentration in the basin is probably too simplistic. A wide variation in 'trends' between CO_2 abundance and reservoir maturity between the Nappamerri and Patchawarra Troughs (Fig.6.19) is consistent with this interpretation.

Another argument put forward by Rigby & Smith (1981) to disclaim a CO_2 source involving organic maturation centres on the isotopic signature of the carbon dioxide gases. The authors comment that the $\partial^{13}C$ value of the carbon dioxide in the Cooper Basin remains relatively constant at -6.9 ± 2.9 per mil. In their view, this is incompatible with an organic source since the $\partial^{13}C$ value of the carbon dioxide should more closely approach the $\partial^{13}C$ value of carbon dioxide generated during the decarboxylation of coals [38], particularly in areas of the basin where the CO_2 concentration is high.

The argument is partly based on the assumption that "the carbon dioxide contents of natural gases represent the total carbon dioxide generated and *retained* [author's emphasis] since the earliest stages of gas production" (Rigby & Smith, 1981, p.226). This may, of course, not be correct as suggested above. Further, Rigby & Smith (1981) did not consider the possibility that the $\partial^{13}C$ character of the carbon dioxide may have evolved over geologic time, masking its true source origin. The carbon dioxide may initially have well been characterised by a $\partial^{13}C$ signature resembling that of coals, the $\partial^{13}C$ character then becoming progressively modified towards more positive values as the basin evolved [39]. This hypothesis appears supported by Rigby & Smith's (1981) own data, as illustrated in Figure 6.20. There is a broad trend suggesting the $\partial^{13}C$ nature of CO_2 in the Cooper/Eromanga region becomes, on the whole, heavier towards greater burial depths (Fig.6.20). Certainly the carbon dioxide reservoired in Eromanga clastics is generally isotopically lighter than CO_2 in Permian reservoirs (Vincent et al., 1985; cf. Figs. 6.10 c & f, 6.20).

The trend can be explained in alternate ways.

At shallow depths, there may be abundant carbon dioxide of recent organic origin, explaining the presence of $\partial^{13}C$ values of CO_2 as negative as -21.8 (Vincent et al., 1985) in some parts of the Eromanga Basin. The hypothesis is supported by the fact that vitrinite reflectance measured at the base Mesozoic is in the range of 0.6 to 1.2 percent over large parts of the basin (see Kantsler et al., 1983; their Fig. 8), coinciding with the zone of peak generation of carbon dioxide from coal (Fig.6.17). The relatively wide range in stable carbon isotope composition of the carbon dioxide in the

---

38 Rigby & Smith (1981) quote a value of -24 per mil in accordance with data obtained by Gould & Smith (1980) for brown coals. However, other workers have suggested some coals are characterised by considerably heavier $\partial^{13}C$ values, up to about -15 per mil (see section 6.5.2 and Figure 6.8).

39 It could be argued that this hypothesis contradicts the CO_2 migration-precipitation model outlined in section 6.5.7, since the model is based heavily on the present isotopic similarity of the carbon dioxide in the Cooper Basin and the calcite cements in the Eromanga Basin. However, it must be kept in mind that the formation of the carbonate cements in the Eromanga Basin may be a relatively recent geological phenomenon since the Great Artesian Basin aquifer system may have been established as late as in the Plio-Pleistocene (Bowering, 1982). The carbon dioxide in the Cooper Basin at that time is unlikely to have had a very different $\partial^{13}C$ composition from that of today.

Eromanga Basin (see Fig.6.10f) may possibly be attributed to mixing of CO_2 from alternative sources, including CO_2 of atmospheric source.

The transition from isotopically light to isotopically heavy CO_2 with depth may simply be a temperature-related fractionation effect (cf. Hoefs, 1973; Fig.9). It could also be due to the preferential removal of $^{12}C_{CO_2}$ from the carbon dioxide system towards the basin depocentres over geologic time. The mechanism for preferential removal of $^{12}C_{CO_2}$ may hereby be dependent on thermodynamic molecular properties related to atomic mass. As stated by Faure (1986, p.430), "bonds formed by the lighter of two isotopes are weaker and are therefore more easily broken, making the molecule with the lighter isotope more reactive than a similar molecule containing the heavier isotope". For example, $^{12}C_{CO_2}$ could have been preferentially incorporated into the lattice of carbonate cements during late-stage burial diagenesis in the Cooper Basin, effectively enriching the residual carbon dioxide pool in ^{13}C. In support of this model may be the fact that the later-formed sparry siderites and ankerites in the basin have a more negative $\partial^{13}C$ character than their fine-grained counterparts (Fig.6.5; Table 6.4).

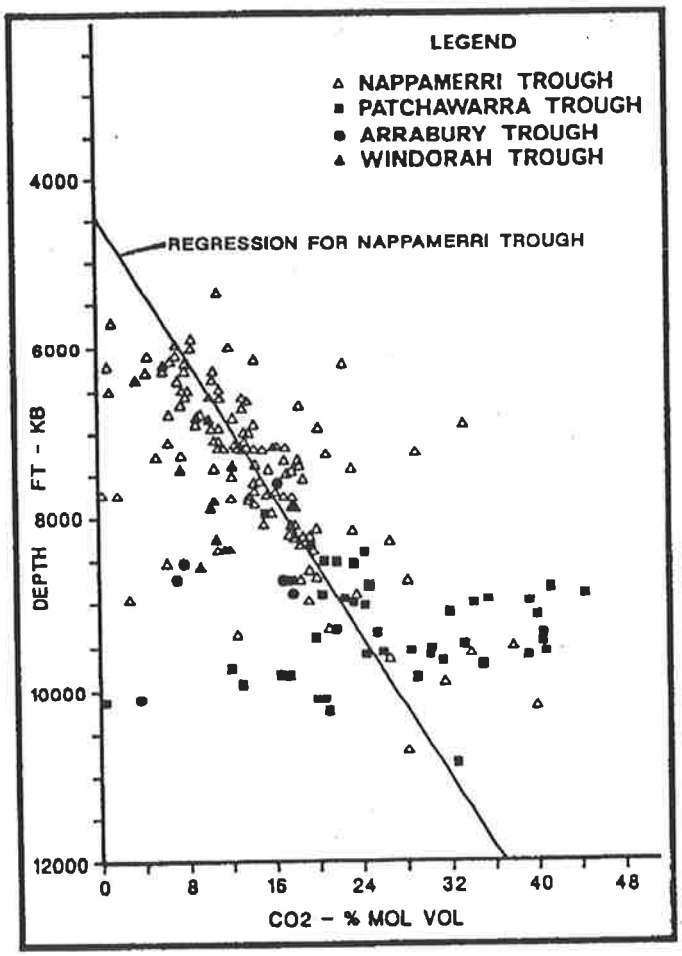

Figure 6.18 Carbon dioxide and reservoir depth for Cooper Basin gas reservoirs from all formations (after: Hunt et al., 1989).

Alternatively, it is possible that $^{12}C_{CO_2}$ was more readily able to escape updip into shallower sequences than $^{13}C_{CO_2}$ because of differences in molecular size; $^{13}C_{CO_2}$ over time became concentrated in the central Nappamerri Trough and other more deeply buried parts of the Cooper Basin that are characterised by low overall reservoir quality. The preferential escape of carbon dioxide molecules containing ^{12}C from the

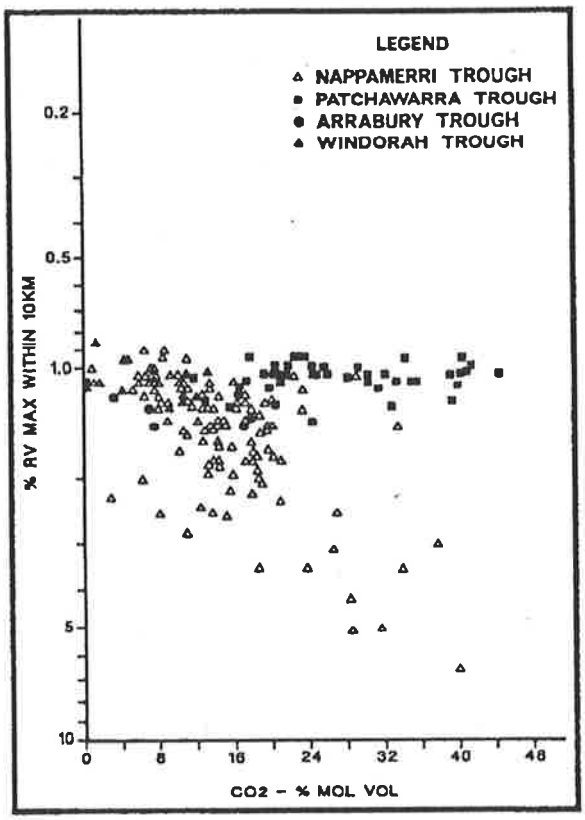

Figure 6.19 Carbon dioxide and reservoir maturity for Cooper Basin gas reservoirs from all formations (after: Hunt et al., 1989).

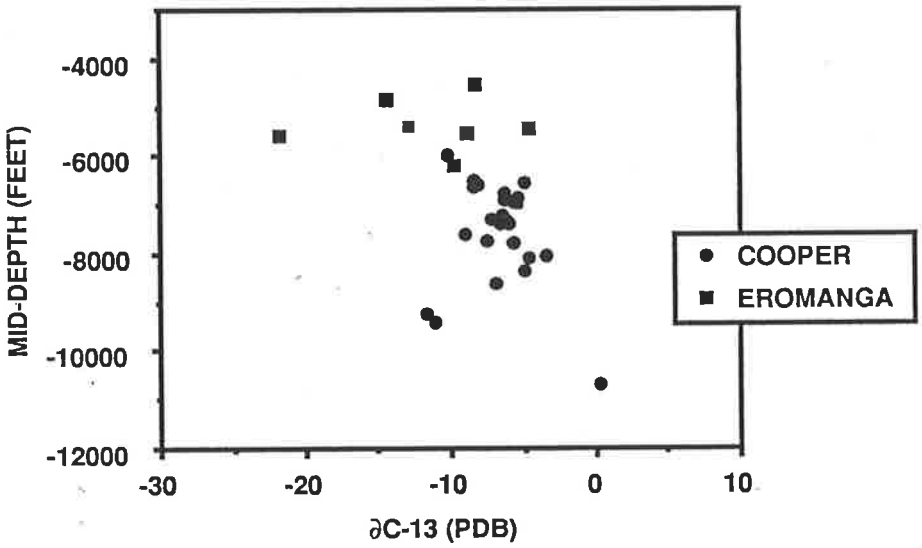

Figure 6.20 Change in $\partial^{13}C$ character of carbon dioxide with depth, Cooper and Eromanga Basins. Depth values represent mid-depths from DST intervals (data from: Rigby & Smith, 1981; Vincent et al., 1985).

basin depocentres could thus have contributed to the isotopically light carbon dioxide content of shallower sequences.

A third explanation is that the carbon dioxide of organic origin, rich in ^{12}C, blends with carbon dioxide rich in ^{13}C as the depth increases. Such mechanism was proposed by Koncz (1983) to account for the isotopic composition of Hungarian natural gases; the source of ^{13}C-enriched carbon dioxide was considered to be "in greater depth in the lithosphere" (Koncz, 1983, p.45). In the present context, a source of ^{13}C-enriched carbon dioxide could be the limestones of the Warburton Basin. A carbonate source was also proposed by Hankel et al. (1989) to account for $\partial^{13}C$ carbon dioxide values approaching zero per mil in deeper formations in the Medicine Hat Gas Field in southeastern Alberta. In the Cooper Basin, the only other source of ^{13}C-enriched carbon that can readily lead to a $\partial^{13}C$ value of CO_2 as heavy as +0.3 towards the depocentre (Kirby-1; Rigby & Smith, 1981) would be the micrite and microspar siderite varieties discussed in section 6.4.4 (see Fig.6.5); however, these show no evidence of dissolution.

Differentiation between these various models is presently not possible and requires more research. However, the discussion clearly demonstrates that an organic origin of the carbon dioxide reservoired in the Cooper Basin cannot presently be excluded, contrary to the views expressed by some workers. The debate highlights that the origin and evolution of the carbon dioxide gases in this petroleum province may be considerably more complex than hitherto portrayed in the existing literature.

6.5.9 Implications for petroleum exploration

The model presented in section 6.5.7 for the mechanism of carbonate cementation in the Eromanga Basin may assist petroleum exploration. The model suggests the carbonates form at sites of CO_2-expulsion from the Cooper Basin into the overlying Eromanga aquifers; Cooper Basin carbon dioxide is considered to have provided the source of carbon required for carbonate precipitation in the Eromanga Basin. Hence, zones of intense carbonate cementation may reflect the preferred migration pathways of the carbon dioxide, and also the hydrocarbons since both are likely to have migrated along similar conduits. Furthermore, massive carbonate-cemented zones may highlight areas where CO_2 became trapped en route to the atmosphere, helping to identify reservoir zones where hydrocarbons may have accumulated. There certainly is evidence to suggest that massive carbonate cements are prominent in many petroleum fields in the Eromanga Basin, the carbonates being

frequently found in main structure-flanking position where the hydrocarbons are reservoired. In the Namur Sandstone of the Gidgealpa Field, for example, calcite-cemented zones are as thick as 190 feet or more (Anderson, 1985). Seismic amplitude anomalies above the Birkhead horizon indicate that carbonate cementation is mainly restricted to crestal positions (Anderson, 1985). Similarly, in the Adori Sandstone of the Strzelecki Field, Staughton (1985) and Wall (1987) report calcite-cemented zones in excess of 295 feet thick. Staughton (1985, p.66) states that here the "carbonate cement content is significantly higher within the crestal reservoir compared to the underlying water-bearing zone" in the Namur Sandstone. Similarly, Wall (1987, p.27) commented that "[such calcite-cemented] zones appear to diminish in thickness and intensity troughwards down the flanks of structures". Wall (1987) attributed this at least partly to the dissolution of carbonate cements, however the present study demonstrates that an alternative interpretation is possible.

In this context, the question is raised whether the carbon dioxide may have acted as a carrier of hydrocarbons in the Cooper/Eromanga Basins. In the Norton Basin of Alaska, for example, Kvenvolden & Claypool (1980) argue that the migration of hydrocarbons was controlled by a CO_2 gas-drive mechanism. An analoguous situation may exist in the present study area. This view is shared by McKirdy (1989) who recently emphasised the potentially important role played by carbon dioxide in the mobilisation of liquid hydrocarbons from terrestrial organic matter in the Cooper Basin. McKirdy (1989) suggested that a CO_2-rich gas phase had facilitated stripping of liquid hydrocarbons from coaly source beds in Permian sediments of the Patchawarra Trough. The above considerations provide new stimulus for this idea.

CHAPTER SEVEN

CONCLUSIONS AND RECOMMENDATIONS

The Cooper Basin, containing Permo-Triassic sediments of fluvial, deltaic and lacustrine origin, is characterised by dominantly low-porosity, low-permeability reservoir sandstones for oil and gas. Ambient core porosity averages 10.7 percent and permeability 30 md, with over 75 percent of sandstones having permeabilities less than 5 md. Despite its overall poor reservoir characteristics, the basin ranks as one of Australia's most important petroleum provinces; ultimate sales gas reserves amount to about 6 TCF, and gas-liquids and oil reserves approach 310 MMSTB.

Remnants of original depositional porosity, dissolution porosity and microporosity are distinguished in the Permian sandstones. The occurrence and distribution of these porosity types is related to a complex interplay of factors, including sedimentary facies, diagenesis and basin architecture.

Primary porosity is common in fine to medium grained, moderate to well sorted sandstones low in detrital clay content. Individual pore diameters range from only a few microns to over 250 μm. Remnants of original depositional porosity are preserved because an early phase of silicification provided a rigid grain framework that mainly suppressed mechanical compaction in sandstones of point bar origin. Early quartz cementation is thought to have been made possible by subsurface invasion of meteoric waters enriched in silica. Sandstones characterised by abundant primary pores have core porosities between 10 and 25 percent, and permeabilities typically greater than 10 md, up to a maximum of several thousand millidarcys.

Secondary porosity is of subordinate importance to primary porosity and mostly of sporadic occurrence. It results from the dissolution of framework grains such as feldspars and lithic fragments; evidence for carbonate cement dissolution is rare and localised. Occasionally, secondary pores exceed 1 mm in diameter. Secondary porosity tends to concentrate in samples that also contain primary porosity. It is believed that high initial sediment porosities facilitated meteoric fluid flux which promoted mineral dissolution.

Microporosity is defined to include all porosity that occurs interstitially between clay particles. Clay types identified in the study area include kaolinite, dickite,

illite, clinochlore and pyrophyllite. Microporosity is insignificant in association with clinochlore and pyrophyllite. Detrital illite significantly reduces microporosity due to the closely packed, platy crystal habit of the mineral. Authigenic illite of fibrous, lath- or lettuce-like habit has only minor microporosity. Almost all of the microporosity in the study area is associated with authigenic kaolinite and dickite. The largest micropores occur between euhedral dickite booklets; microporosity is relatively poorly developed among the subhedral and more blocky kaolinite crystals. Kaolin morphology is related to the mode of formation of these two clay types. Kaolinite formed as an alteration product of feldspars whereas dickite is thought to have precipitated out of aqueous solution. Individual kaolin pore diameters range between less than 1 μm and 30 μm but commonly are around 10 μm. Sandstones dominated by microporosity are very abundant and account for at least two-thirds of all clastics in the study area; the abundance of microporosity explains the generally low-quality nature of the Cooper Basin reservoir rocks. Microporous clastics have core porosities as high as 15 percent but core permeabilities of typically 2 md or less.

The three porosity types occur together in numerous clastics. However, study results suggest there is a general transition in the nature of porosity with depth in the Cooper Basin. Three broad porosity zones are distinguished: (1) along the basin margin and in mid-flank structural positions at depths less than about 7000 feet, primary porosity is most common; (2) at intermediate structural depths (about 7000-8400 feet), a transition zone is identified with no clear predominance of porosity types; (3) towards the basin depocentres at depths exceeding about 8400 feet, the overwhelming majority of sandstones are microporous. However, isolated remnants of primary pores and some secondary pores are recorded to depths of at least 10,000 feet in some sandstones; such clastics occur in essentially microporous sequences. A possible fourth porosity zone is distinguished in the Patchawarra Formation intersected at Burley-2 in the central Nappamerri Trough. Here pyrophyllite replaces kaolin, effectively destroying microporosity in sandstones at depths around 11,000 feet. However, more core samples are required to confirm this trend.

The mean loss of porosity is approximately 1.5 porosity units per 1000 feet of burial; reservoir porosity decreases from about a 14 percent average at 6000 feet to less than 3 percent at 12,000 feet. The decline in mean permeability is more rapid from 184 md at 6000 feet to 32 md at 7000 feet; at a depth of about 9800 feet, average permeability is 6 md, and beyond 10,000 feet it is less than 2 md. Again, more data is required from the central Nappamerri Trough and other deep portions of the Cooper Basin to fully evaluate the reservoir character in these areas.

The general deterioration of reservoir quality with depth is partly related to the broad transition in the nature of porosity towards the basin depocentres. Other factors

that account for the general reduction of porosity and permeability with depth in the Permian sandstones from the basin margin to the basin depocentres include:

➢ *Cementation*. There is a general reduction of primary pore space with depth as a function of increased reservoir silicification, as evident from petrographic and CL work. Silica required for quartz cementation during later diagenesis was probably derived from the kaolinisation of feldspars, clay mineral transformations, chemical compaction, and replacement of silicates by carbonates. The carbonates locally significantly reduce porosity and permeability, however there is no evidence to suggest carbonate cements actually increase in abundance with depth.

➢ *Clay authigenesis*. Authigenic illite, clinochlore and pyrophyllite concentrate in the deeper portions of the basin. Authigenic illite replaces micas, feldspars and clays. Clinochlore and pyrophyllite most likely both crystallised under conditions of low-grade metamorphism in the central Nappamerri Trough. These authigenic clay minerals block pore throats and reduce effective permeability. Kaolin clays are present in virtually all sandstones in the study area but similar to the carbonates show no obvious tendency to increase in abundance with depth.

➢ *Mechanical compaction*. Although the effects of compaction are largely absent in clean, moderate to well sorted sandstones that were silicified early, there is abundant evidence for this type of diagenetic alteration in the more poorly sorted argillaceous sediments in the Cooper Basin. Mechanical compaction is evident from bent mica flakes, rearrangement of detrital grains and deformation of lithic fragments. This lead to denser grain packing and reduction of sediment porosities.

➢ *Chemical compaction*. During later diagenesis, chemical compaction resulted in sutured grain contacts and stylolites in some sandstones. Again, mostly the finer grained, poorly sorted clayey sediments were affected. Samples that experienced intense intergranular pressure solution are characterised by a distinct lack of authigenic quartz and have virtually no porosity.

➢ *Facies*. Core plug measurements derived from wells drilled in the depocentres of the basin are related to finer grained argillaceous sediments. This is because of the predominance of distal depositional regimes in this geologic setting, related to broad facies changes of strata from fluviatile to 'lake' environments (Stuart, 1976). The finer grained, more argillaceous nature of distal sediments is likely to be reflected in the porosity-permeability data.

➢ *Hydrodynamics and chemical ground water composition.* It is hypothesised that towards the interior of the basin, meteoric flushing was generally not as vigorous as near the basin margin, and that silica was gradually depleted from ground waters moving laterally due to precipitation along the margins. This resulted in a lesser overall extent of early reservoir silicification in basinal facies, leading to an increased porosity loss by compaction in many such sediments. The higher clay content of distal facies most likely isolated many detrital grains from water capable of precipitating quartz overgrowths.

The study highlights the need to know more regarding the interrelationship between sandstone silicification, depositional environment and differential subsidence. Meteoric fluid flux into the basin interior was probably facilitated by sand bodies with a high degree of interconnection. By implication, the degree of sand body interconnection, controlled by both rate of subsidence (Allen, 1978; Bridge & Leeder, 1979; Read & Dean, 1982; Stuart et al., 1988) and rate of avulsion (Leeder, 1978), may influence reservoir quality in fluvial sequences in the Cooper Basin. Texturally mature, moderately to well-sorted sandstones of medium to coarse grain size with low detrital clay contents and high initial porosities conducive to fluid flows are likely to have been the preferred migration conduits of the silica-enriched meteoric waters. This is considered the reason why the bulk of the commercial petroleum discoveries to date occur in channel and point bar sequences in the Cooper Basin. Early reservoir silicification lead to the suppression of compaction during later burial in many of these deposits; quartz cementation reduced but did not occlude original depositional porosity in marginal and midflank areas of the basin. Also, proximity to meteoric influences most likely promoted framework grain dissolution leading to the creation of secondary porosity in reservoir facies characterised by abundant primary porosity. Hence, point bar sequences provide excellent targets for petroleum exploration, including in marginal areas, along structural highs, and onlapping older strata near the depositional edge of the basin; such deposits may also occur as downflank exploration plays. However, towards the basin depocentres, sands of point bar origin grade laterally and intertongue with rocks more typical of deltaic and 'lake' deposition (Stuart, 1976). Excluding down-basin areas of increased sandstone percentage produced by structual growth, fluvial facies are more finer grained and argillaceous in these settings (Stuart, 1976), and hence likely to be characterised by lower overall reservoir quality. However, fine-grained, well-sorted facies of delta shoreline/distributary mouthbar origin locally have excellent reservoir character, departing from the broad rule of thumb that the best reservoir quality is generally associated with coarser sediments. In the present study, porosities in excess of 22 percent and permeabilities up to about 400

md have been recorded in such fine grained delta sediments. It is thought that detrital clays in these deposits were winnowed out by stream and wave action, enabling early reservoir silicification to take place before the delta front sediments were encased in shales in response to lake fluctuations controlled by differential subsidence and possible climatic fluctuations (cf. Stuart, 1976). The stratigraphic occurrence of the delta front sandstones is believed to have effectively isolated them from the cementing influence of later migrating fluids, resulting in the common preservation of abundant primary porosity in these deposits. Delta front sandstones are very common within the Permian sequence; they are found in the Patchawarra, Epsilon and Daralingie Formations, and are considered to offer excellent structural/stratigraphic potential for future petroleum exploration.

More knowledge is required regarding the influence of sedimentary facies and differential subsidence on quartz cementation. It is suggested that an oxygen isotope investigation of quartz overgrowths be carried out in order to study changes in groundwater composition during cementation, and delineate likely meteoric invasion pathways. Such work would provide important clues concerning the controls affecting silicification in the basin, in particular it would provide assessment of the relative importance of early silicification in relation to quartz cementation under conditions of deeper burial in sandstones of different origins (Schulz-Rojahn, 1990). For this, progressive gas extracts during isotopic analysis are required to estimate the isotope character of quartz overgrowth generations distinguished under CL. Temperature estimates of quartz overgrowth formation derived from isotope data could be integrated with fluid inclusion microthermometry and vitrinite reflectance data; such an approach would allow modelling of the timing of overgrowth formation in the Cooper Basin (Schulz-Rojahn, 1990). The work would enable a framework for quartz cement stratigraphy to be established relative to the basin's tectonic and sedimentational history. It is recommended oxygen isotope signatures of quartz cements be contrasted on the basis of (1) different overgrowth generations, (2) depositional regime, (3) structural elevation, (4) stratigraphic location, and (5) tectonic province. Average isotope values obtained for generic facies associations are to be projected onto basemaps and contoured; this may help identify source direction of migrating pore fluids, and delineation of high-quality reservoir facies in the subsurface (Schulz-Rojahn, 1990). Study results should be integrated with K-Ar, Rb-Sr and oxygen isotope studies of clay minerals, providing further constraints on the source and chemistry of migrating pore fluids in the Cooper Basin (Schulz-Rojahn, 1990).

Most hydrocarbon-producing intervals contain a complex mixture of porosity types. By comparing petrographic results with DST and production test data, a broad assessment was possible of the initial deliverability rates of the various porosity

groups. The reservoir sandstones characterised by the highest initial flow rates are those containing abundant primary porosity. Primary pores provide for a high degree of porosity interconnection, resulting in high effective rock permeabilities that contribute to numerous flow results of commercial significance. Sandstones dominated by primary porosity are capable of hydrocarbon flows in excess of 11 MMCFD (Daralingie) and of at least 1750 BOPD (Wancoocha). Such high-quality reservoir sandstones also tend to be those in which secondary porosity is most common. Secondary porosity contributes to permeability and enhances the storage capacity of many reservoir rocks for oil and gas.

The poorest reservoir potential is associated with rocks that are exclusively microporous. Microporous sandstones containing abundant kaolin are capable of low-order gas flows in the order of at least 20-500 MCFD prior to fracturing. However, where there are isolated remnants of primary pores in microporous sands, the efficiency of hydrocarbon recovery is much improved and flow rates several orders of magnitude higher are recorded, up to 2 MMCFD and more. Undoubtedly, micropores between individual kaolin booklets serve as storage space for gaseous hydrocarbons and contribute to long-term production in many petroleum fields. In the Moomba and Big Lake Fields, for example, microporosity accounts for much of the total porosity in reservoirs that have produced more than a trillion cubic feet of gas (Schulz-Rojahn et al., 1991); these fields contain nearly 40 percent of the proven and probable gas reserves in South Australia (Morton, 1989).

These findings offer encouragement to the petroleum industry for the drilling of deeper targets, despite the overall deterioration of reservoir quality with depth. Microporosity is abundant in the central Nappamerri Trough and other deep portions of the Cooper Basin where large hydrocarbon reserves may be located. By analogy with giant gas fields in North America, low-permeability clay-rich sequences may be commercially exploitable in the Cooper Basin. In North America, some of the largest gas fields with individual recoverable gas reserves of up to 9 TCF occur in downdip structural locations in sandstones with average reservoir permeabilities of less than 2 md (Table 5.12). These fields are characterised by an average well production of between 100 and 1000 MCFD, similar to many low-order DST flows recorded in the Cooper Basin. Importantly, such low volumes of hydrocarbon production can sometimes be maintained for decades (Laughrey & Harper, 1986) provided care is taken to ensure that a minimisation of formation damage occurs (section 5.4.2.3).

In the Cooper Basin, it is well-known that much of the central Nappamerri Trough is gas-saturated (Heath, 1989; Tupper & Burckhardt, 1990). Gaseous hydrocarbons (dominantly methane) are probably still being generated in this portion of the basin at the present time, as indicated by vitrinite reflectance data. Importantly,

the relatively closed nature of low-permeability microporous reservoirs in the Nappamerri Trough imposes likely constraints on the ability of natural gas to migrate appreciable distances from the interbedded source rocks over a short geologic time. This effectively removes temporal restrictions on hydrocarbon migration with respect to the development of trap structures in this part of the basin. Of significance in this context is that remnants of primary porosity have been recorded in core samples to depths up to 10,000 feet. Evidence from ditch cuttings suggests primary porosity may be present to even greater depths. It is interpreted that higher-quality reservoir facies are intercalated within sequences of low-permeability clastics of microporous nature in the basin depocentres. Such 'sweet spots' offer especially attractive targets for deep gas exploration, particularly in view of the fact that massive hydraulic fracture stimulation can increase flow results in 'tight' sandstone sequences by several orders of magnitude (cf. Stanley & Halliday, 1984).

The study results suggest that deep basin-centred gas resources in the central Nappamerri Trough and elsewhere are likely to play an important role in securing Australia's natural gas needs well into the 21st century. The Cooper Basin is particularly suited for the development of such resources since much of the required infra-structure is already in-place.

It is important that petrophysicists and explorationists investigating the petroleum potential of clay-rich sequences containing abundant microporosity be aware of potential problems encountered in well log interpretation. The clay minerals within the pore system of a reservoir affect the physical and electrochemical properties of the rock (eg. Wescott, 1983; Laughrey & Harper, 1986). The following potential key problems were identified:

➢ V_{clay} may be underestimated by the gamma ray log in kaolin-rich sandstones because of the low potassium content of these clays (Rider, 1986; Bowler, 1988).

➢ Log-derived porosities are likely to overestimate effective porosity in rocks with a high proportion of kaolin minerals (Schulz-Rojahn & Phillips, 1989; Schulz-Rojahn & Stuart, 1991).

➢ Productive zones may be by-passed because they appear water-wet. This is because clays are associated with bound water of irreducible nature which cannot presently be identified from resistivity logs, leading to pessimistic computation of S_w (Wescott, 1983; Ranganathan & Tye, 1986; Pittman, 1989).

➢ Misleading log calculations of S_w may lead to pessimistic assessment of hydrocarbons in-place, and influence perceptions of prospectivity in the Cooper Basin. The implication is that present-day hydrocarbon reserves in the central Nappamerri Trough and other deep portions of the Cooper Basin are probably considerably underestimated.

For these reasons, future research should be directed towards better understanding the influence of clay minerals on log response in the Cooper Basin and other petroleum provinces in Australia. In particular, research should be focused on methods of log identification of kaolin clay content in the Permian reservoir sandstones. Such work may best be accomplished using an array of wireline logs, including possibly the natural gamma ray spectrometry tool (NGT) that is not routinely run in the Cooper Basin. Log data should be integrated with diagenetic information, DST and production test results, and pressure build-up data from reservoir intervals. It is suggested initial research be focused on reservoir sandstones in the Moomba-Big Lake area, as here reservoir rocks have a generally high microporosity component; study results could be integrated with the existing NCPGG database and supplemented with diagenetic information derived from additional core material from other wells.

Evidence of liquid hydrocarbon migration is evident from core and ditch samples in several areas of the Cooper Basin. Oil migrated through, but was not trapped in the Permian sediments. Alternatively, liquid hydrocarbons were 'cracked' and converted to gas during metagenesis, leaving a bitumen residue.

Determination of the relative timing of hydrocarbon generation and migration in relation to mineral authigenesis was possible by detailed petrographic analysis. Although no differences in diagenetic history were detected between water-wet and hydrocarbon-bearing reservoir intervals, the possibility of diagenetic entrapment of hydrocarbons cannot be excluded in the Cooper Basin. Available evidence suggests the precipitation of several authigenic mineral phases occurred synchronous with, or postdated hydrocarbon generation and migration in some parts of the study area. Theoretically therefore, hydrocarbons that migrated into a structural or depositional trap could have been sealed by some of these diagenetic precipitates. Subsequent structural adjustments could leave the diagenetically sealed traps in seemingly unfavourable structural position (Schneeflock, 1978).

A hydrocarbon-derived origin for the carbonate cements in the Cooper/Eromanga Basins is unlikely. This is because there is a marked dissimilarity in the stable carbon isotope character of the carbonates and the hydrocarbons in these basins; hydrocarbon-derived carbonate cements should have an isotopically light

signature approaching the $\partial^{13}C$ of associated hydrocarbons because of the incorporation of carbon from that source into the carbonate lattice.

Cooper Basin siderites probably formed under a complex range of conditions involving a mixture of different carbon sources. Likely carbon sources include carbon derived from the atmosphere, thermal maturation reactions involving organic matter, and bacterial fermentation reactions and/or methanogenesis. Carbonate evolution progressed from low-Mg siderite → High-Mg siderite → Ankerite → Dolomite → Calcite. Calcite, and possibly ankerite and dolomite may have largely precipitated in response to post-Triassic influx of aquifer waters from the Eromanga Basin. Other carbonate minerals formed by precipitation and/or replacement. Micritic siderite precipitated near the sediment-surface interface at temperatures as low as about 15 °C. Later-formed siderites are associated with dead oil in some samples, suggesting precipitation at elevated temperatures; this is confirmed by isotope data, suggesting precipitation temperatures of up to about 70 °C or more. Siderite precipitation was continuous throughout the Permian and may have continued into the Late Cretaceous when burial depths of about 3000 to 6500 feet (1-2 km) were attained, as indicated by temperature data and burial subsidence plots. Ankerite, dolomite and calcite require more isotope work; for detailed temperature modelling, it is suggested the $\partial^{18}O$ character of modern formation waters in the Cooper Basin be investigated.

Importantly, massive carbonate-cemented zones in the Eromanga Basin may serve as a guide to commercial hydrocarbon accumulations. This is indicated from both isotopic evidence and theoretical considerations. Available data suggests the formation of intensely carbonate-cemented zones in the Eromanga Basin is controlled by the injection of Cooper Basin carbon dioxide into the Ca^{2+}-bearing Jurassic aquifers (J-aquifers). The carbon dioxide is considered to have provided a source of carbon required for carbonate precipitation. Hence, zones of intense carbonate cementation may reflect the preferred migration pathways of the carbon dioxide, and also the hydrocarbons since both are likely to have migrated updip along similar conduits. There is evidence in the available literature to suggest massive carbonate cements are prominent in main structure-flanking positions in at least several petroleum fields in the Eromanga Basin (cf. Anderson, 1985; Staughton, 1985; Wall, 1987).

It is strongly recommended that an attempt be made at mapping both the distribution and thickness of the carbonate-cemented zones in the Eromanga Basin. This could best be accomplished by integration of data from a variety of sources, such as log character, seismic amplitude anomalies, and lithological descriptions from core and ditch samples. Calcite-cemented zones are readily identifiable on wireline logs because of their high sonic velocities and high resistivities, as well as their

characteristic PEF response (Desbrandes, 1985; Rider, 1986). Carbonate isopach maps constructed for the Eromanga aquifers should be compared to geological maps produced from seismic and well log data showing the extent and thickness of the regional Triassic seal; they should further be compared to time structure maps showing the location of structural highs and major fault zones. This is to test the hypothesis that upward escape of carbon dioxide from the Cooper Basin into the Eromanga aquifers is facilitated in areas where there is no effective Triassic seal, along fault planes, and along structural highs where there is minimal separation between the Permian and Jurassic-Cretaceous sediments due to depositional thinning and/or erosion.

Evaluation of the concept that massive carbonate-cemented zones may serve as a guide to commercial hydrocarbon accumulations in the Eromanga Basin is probably best accomplished by noting differences in carbonate content between water-wet and hydrocarbon-bearing reservoir intervals. A further suggestion is that a statistical comparison be made between the presence and thickness of carbonate-cemented zones and the height of hydrocarbon column(s) in a number of selected petroleum fields.

If indeed there is a relationship between massive carbonate-cemented zones and commercial hydrocarbon accumulations, the direct detection of such zones on seismic sections through the study of amplitude anomalies may prove to be an invaluable new exploration tool. It is hoped that by delineating the extent of carbonate zones in the subsurface, explorationists may be able to better rank prospects and leads for drilling in the Eromanga Basin and elsewhere. The J-aquifer is present throughout the Great Artesian Basin area, occupying about one-fifth of the Australian landmass (Habermehl, 1980). Apart from the Eromanga Basin, the Great Artesian Basin also comprises the Surat and Carpentaria Basins as well as portions of the Bowen and Galilee Basins. These constituent basins are underlain by pre-Jurassic sediments of the Georgina, Amadeus, Pedirka, Drummond and other basins (Habermehl, 1980). An analoguous situation to the Cooper/Eromanga Basins may exist in these areas, and possibly elsewhere in the world.

Upward leakage of carbon dioxide from the Cooper Basin into the superjacent Eromanga sediments could also have potentially far-reaching implications for the mechanism of both primary and secondary hydrocarbon migration in the region. A CO_2 gas-drive mechanism may have controlled the mobilisation of hydrocarbons in the Permian sediments. Stripping of liquid hydrocarbons from coaly source beds was possibly facilitated by a CO_2-rich gas phase in the Patchawarra Trough (McKirdy, 1989). Hence, the possibility exists that both the hydrocarbon character and the present distribution of oil and gas pools in the Cooper/Eromanga Basins was to some extent influenced by the upward escape of carbon dioxide en route to the atmosphere.

To test these hypotheses, it is proposed that hydrocarbon composition and character be studied in relation to carbon dioxide abundances in the reservoirs of both the Cooper and Eromanga Basins. Further, an attempt should be made at identifying possible 'CO_2 chimneys' in the subsurface and comparing their distribution to that of known oil and gas pools in the two basins. The identification of such hypothesised 'CO_2 chimneys' could best be accomplished by delineating anomalous carbon dioxide levels in the subsurface that depart from regional CO_2 trends. For this, existing gas maps (eg. Hunt et al., 1986, 1989) showing the percentage molar volume of carbon dioxide within the main Permian reservoirs should be updated and revised. The work should then be extended to younger strata. In particular, detailed CO_2 contour maps for the hydrocarbon-bearing reservoir intervals of Jurassic age in the Eromanga Basin are required. It is hoped that areas of consistently high CO_2 levels at successive stratigraphic levels in the Eromanga Basin reflect sites of updip carbon dioxide migration; interpretation of CO_2 trends should occur in conjunction with all available geological and geophysical data relating to the areal extent of regional seals and the general reservoir quality of associated sediments. Especial attention should be devoted to fault zones since it is known that carbon dioxide concentrations in formation water locally are anomalously high in the vicinity of such structures in Eromanga reservoirs (eg. Habermehl, 1986b). It is possible that the delineation of 'CO_2 chimneys' in the subsurface may assist in establishing the preferred migration pathways of the hydrocarbons in this important petroleum province which in turn may help direct exploration activities to hitherto less well-explored regions.

It is evident that more research is required regarding the origin and evolution of the carbon dioxide in the Cooper/Eromanga Basins. The present study was able to highlight some of the complexities concerning this issue. Although isotopic data is ambiguous, such data in conjunction with geological considerations assisted in the re-evaluation of existing concepts. A dominant CO_2 origin involving the dissolution of carbonate cements in the Cooper Basin (Bodard et al., 1985; Wall, 1987; Hunt et al., 1989) is considered implausible. The present investigation was unable to ascertain the existence of zones of intense carbonate dissolution in the subsurface. Further, the highest carbon dioxide concentrations occur towards the basin depocentres where there is very little evidence of secondary porosity and reservoirs are generally 'tight'.

A dominant origin of the carbon dioxide in the Cooper Basin involving a granite source (Rigby & Smith, 1981) is also considered improbable. Granite basement in the Cooper Basin is invariably overlain by a thick weathering profile, suggesting the granites were exposed prior to the onset of Permo-Triassic sedimentation. Hence, even if the granite magmas were accompanied by a CO_2-rich phase during their ascent in the crust (Rigby & Smith, 1981), much if not all of the

carbon dioxide would have been lost to the atmosphere long before Cooper Basin sedimentation was initiated. Similarly, geological considerations downgrade the possibility that much of the carbon dioxide in the Cooper/Eromanga region was derived from the Warburton Basin limestones that underlie parts of the study area (Kantsler et al., 1983). There is no obvious relationship between carbon dioxide concentrations and the distribution of such rock types.

Instead, the possibility that much of the carbon dioxide in the study area was released from humic organic matter during organic maturation reactions (Schwebel et al., 1980) is upgraded. Arguments put forward by several workers (Rigby & Smith, 1981; Hunt et al., 1989) to argue against this possibility are considered invalid. The inferred mobility of the carbon dioxide gases is probably the key controlling factor in explaining present-day carbon dioxide concentrations in the Cooper/Eromanga Basins. This is contrary to the views of Schwebel et al. (1980) and Rigby & Smith (1981) who considered modern CO_2 levels to reflect solely the source of the carbon dioxide. The reservoir characteristics and the sealing capacity of associated sediments probably greatly influenced modern CO_2 concentrations. Carbon dioxide levels are high in the central Nappamerri Trough characterised by abundant microporosity but low towards the flankal areas and the structural highs of the southern Cooper Basin where abundant primary porosity is preserved. It follows that carbon dioxide concentrations may provide an indication of overall reservoir quality in the study area (cf. Figs. 2.7 a & b and Fig. 6.11).

The isotopic signature of the carbon dioxide gases is of limited use to infer their origin; there is considerable overlap in $\partial^{13}C$ values between various potential carbon sources (cf. Fig.6.8). Also, the isotopic signature of the carbon dioxide may have evolved over geologic time and with depth towards more heavier $\partial^{13}C$ values, a possibility that was not hitherto recognised in the published literature. Such an evolutionary trend could be due to a number of reasons, including temperature-related effects; the progressive removal of $^{12}C_{CO_2}$ from the reservoir system with time by carbonate precipitation; upward escape of $^{12}C_{CO_2}$ and/or addition of $^{13}C_{CO_2}$ with depth.

To understand the complexities of diagenesis in other Australian petroleum provinces, it is recommended that a combination of techniques be used, including optical petrography, cathodoluminescence, scanning electron microscopy, X-ray diffraction, electron microprobe work, and isotope geochemistry. The results should be integrated with sedimentological core descriptions and wireline log evaluation. Ditch cuttings are of limited use in the study of clay mineralogy and assessment of porosity types since there is evidence to suggest some clays (such as dickite) are

preferentially washed out in the stream of drilling mud that brings the cuttings to the surface.

Reference list *

Abdel-Wahab, A. & McBride, E.F., 1991 - Diagenetic controls of reservoir quality of Araba and Naqua diagenetic quartzarenites (Cambrian), Gebel Araba-Qabeliat, Southwest Sinai, Egypt. Am. Assoc. Petrol. Geol., Abstracts 75th Anniversay 1991 Annual Convention, Dallas, Texas, April 7-10, p. 68.

Airey, P.L., Calf, G.E., Campbell, B.L., Habermehl, M.A., Hartley, P.E. & Roman, D., 1979 - Aspects of the hydrology of the Great Artesian Basin, Australia. In: Isotope Hydrology, 1. Proc. Int. Symp. Isotope Hydrology, Neurenberg, Fed. Rep. Germany. International Atomic Energy Agency, Vienna, 205-219.

Ajdukiewicz, J.M., Paxton, S.T. & Szabo, J.O., 1991 - Deep porosity preservation in the Norphlet Formation, Mobile Bay, Alabama. Am. Assoc. Petrol. Geol., Abstracts 75th Anniversay 1991 Annual Convention, Dallas, Texas, April 7-10, p.69.

Aldahan, A.A. & Morad, S., 1986 - Mineralogy and chemistry of diagenetic clay minerals in Proterozoic sandstones from Sweden. Amer. J. Science, 286, 29-80.

Allard, P., Le Guern, F. & Sabroux, J.C., 1977 - Thermodynamic and isotopic studies in eruptive gases. Geotherm., 5, 37-40.

Allen, R.W.Jr., 1955 - Stratigraphic gas development in the Blanco Mesaverde pool of the San Juan Basin. In: Geology of parts of Paradox, Black Mesa and San Juan Basin. Four Corners Geol. Soc. Guidebook, 144-149.

Allen, J.R.L., 1965 - A review of the origin and characteristics of recent alluvial sediments. Sedimentol. Special Issue, 5, 89-191.

Allen, J.R.L., 1970 - Physical processes of sedimentation. Elsevier, New York. 248p.

Allen, J.R.L., 1978 - Studies in fluviatile sedimentation: an exploratory quantitative model for the architecture of avulsion-controlled alluvial suites. Sediment. Geol., 21, 129-147.

Almon, W.R., 1979 - A geologic appreciation of shaly sands. Soc. Prof. Well Log Analysts, 20th Annual Logging Symposium, WW 1-14.

Almon, W.R. & Schultz, A.L., 1979 - Electric log detection of diagenetically altered reservoirs and diagenetic traps. Trans. Gulf Coast Assoc. Geol. Soc., 29, 1-10.

Almon, W.R. & Davies, D.K., 1979 - Regional diagenetic trends in the Lower Cretaceous Muddy Sandstone, Powder River Basin. Soc. Econ. Palaeontologists and Mineralogists Spec. Publ., 26, 379-400.

Almon, W.R. & Davies, D.K., 1981 - Formation damage and the crystal chemistry of clays. In: F.J. Longstaffe (ed.), Short course in clays and the resource geologist, Mineral. Ass. Canada Short Course, Calgary, 1981, 81-103.

* All title abbreviations follow the guidelines outlined by Alkin, L.G., 1989 - Periodical title abbreviations, vols. I & II. Gale Research Inc., Detroit, 919p.

Al-Shaieb, Z. & Lilburn, R.A., 1982 - Geochemistry and isotopic composition of hydrocarbon-induced diagenetic aureole (HIDA), southwestern Oklahoma. Am. Assoc. Petrol. Geol. Bull., 66, 542-543.

Alsop, D.B., 1990 - The effect of diagenesis and facies distribution on reservoir quality in the Permian sandstones of the Toolachee Gas Field, southern Cooper Basin, South Australia. Unpublished Masters thesis, University of Adelaide, 74p.

Althaus, A., 1969 - Das System Al_2O_3-SiO_2-H_2O. Experimentelle Untersuchungen und Folgerungen für die Petrogenese der metamorphen Gesteine. Teil I: Apparative und experimentelle Grundlagen; die Stabilitätsbedingungen der hydroxylhaltigen Aluminium-Silikate. Neues Jahrbuch Mineralogie Abh., 111, 74-110.

Ambrose, G., Suttill, R. & Lavering, I., 1982 - A review of the Early Cretaceous Murta Member in the southern Eromanga Basin. In: P.S. Moore & T.J. Mount (eds.), Eromanga Basin Symposium Summary Papers. Eromanga Basin Symposium, Petrol. Expl. Soc. Aust. & Geol. Soc. Aust. Spec. Publ., Adelaide, 9-11th November 1982, 92-109.

Ambrose, G., Suttill, R. & Lavering, I., 1986 - The geology and hydrocarbon potential of the Murta Member (Mooga Formation) in the southern Eromanga Basin. Geol. Soc. Aust. Spec. Publ., 12, 71-84.

Anderson, A., 1985 - A geoseismic investigation of carbonate cementation of the Namur Sandstone of the Gidgelpa Field, Eromanga Basin. Unpubl. B.Sc.(Hons.) thesis, University of Adelaide, Australia, 47p.

Armstrong, J.D., 1983 - Cooper Basin petroleum - exploration and development. In: Permian geology of Queensland. Geol. Soc. Aust. & Geol. Surv. Qsld., Proc. Symp. Permian Geology of Queensland, Brisbane, 14-16th July 1982, p.1

Armstrong, J.D. & Barr, T.M., 1982 - The Eromanga Basin. In: P.S. Moore & T.J. Mount (eds.), Eromanga Basin Symposium Summary Papers. Eromanga Basin Symposium, Petrol. Expl. Soc. Aust. & Geol. Soc. Aust. Spec. Publ., Adelaide, 9-11th November 1982, 20-42.

Armstrong, J.D. & Barr, T.M., 1986 - The Eromanga Basin. An overview of exploration and potential. In: Contributions to the geology and hydrocarbon potential of the Eromanga Basin. Geol. Soc. Aust. Spec. Publ., 12, 25-38.

Atwater, G.I. & Miller, E.E., 1965 - The effect of decrease in porosity with depth on future development of oil and gas reserves in South Louisiana. Abstracts Am. Assoc. Petrol. Geol. Annual Meeting, New Orleans, 1965, p. 48.

Ayalon, A. & Longstaffe, F.J., 1988 - Oxygen isotope studies of diagenesis and pore-water evolution in the western Canada sedimentary basin: Evidence from the Upper Cretaceous Basal Belly River Sandstone, Alberta. J. Sediment. Petrol., 58, 489-505.

Baertschi, P., 1957 - Messung und Deutung relativer Häufigkeits-variationen von O^{18} und C^{13} in Karbonatgesteinen und Mineralen. Schweizer. Mineralog. Petrog. Mitt., 37 (1), 73-152.

Bahrig, B., 1989 - Stable isotope composition of siderites as an indicator of the palaeoenvironmental history of oil shale lakes. Palaeogeo. Palaeoclimatol. Palaeoecol., 70, 139-151.

Barker, C.E. & Dalziel, M.C., 1991 - Using cathodoluminescence to map regionally zoned carbonate cements occurring in diagenetic aureoles above oil reservoirs, Velma Oil Field, Oklahoma. Am. Assoc. Petrol. Geol., Abstracts 75th Anniversay 1991 Annual Convention, Dallas, Texas, April 7-10, p.73.

Bates, R.L. & Jackson, J.A., 1987 - Glossary of geology. 3rd edition. American Geological Institute, Alexandria, Virginia. 788p.

Bathurst, R.G.C., 1975 - Carbonate sediments and their diagenesis. Developments in Sedimentology, 12. Elsevier Scientific Publications, Amsterdam. 658p.

Battersby, D.G., 1976 - Cooper Basin oil and gas fields. In: R.B. Leslie, H.J. Evans & C.L. Knight (eds.), Economic Geology of Australia and New Guinea, 3. Petroleum. Australas. Inst. Min. Metall., Monogr. 7, 321-370.

Beddoes, L.R.Jr., 1973 - Oil and gas fields of Australia, Papua New Guinea and New Zealand. Tracer Petroleum and Mining Publications, Sydney, 391p.

Bentley, H.W., Phillips, F.M., Davis, S.N., Habermehl, M.A., Airey, P.L., Calf, G.E., Elmore, D., Gove, H.E. & Torgersen, T., 1986 - Chlorine-36 dating of very old groundwater, 1. The Great Artesian Basin, Australia. Water Resour. Res., 22 (13), 1991-2001.

Berman, R.G., Engi, M. & Brown, T.H., 1985 - Optimization of standard state properties and activity models for minerals: methodology and application to an 11 component system. Codata Symposium on Chemical Thermodynamics and Thermophysical Properties Databases, Paris 1985, 166-173.

Berner, R.A., 1964 - Stability fields of iron minerals in anaerobic sediments. J. Geol., 72, 826-834.

Berner, R.A., 1981 - Authigenic mineral formation resulting from organic matter decomposition in modern sediments. Fortschr. Mineral., 59, 117-135.

Bird, M.I. & Chivas, A.R., 1988a - Oxygen-isotope dating of the Australian regolith. Nature, 331, 513-516.

Bird, M.I. & Chivas, A.R., 1988b - Stable-isotope evidence for low-temperature kaolinitic weathering and post-formational hydrogen-isotope exchange in Permian kaolinites. Chem. Geology, 72, 249-265.

Bjørlykke, K., 1979 - Cementation of sandstones - a discussion. J. Sediment. Petrol., 49, 1358-1359.

Bjørlykke, K., 1983 - Diagenetic reactions in sandstones. In: A. Parker & B.W. Sellwood (eds.), Sediment diagenesis. Reidel, Dordrecht, 169-213.

Bjørlykke, K., 1984 - Formation of secondary porosity: How important is it? In: D.A. McDonald & R.C. Surdam (eds.), Clastic Diagenesis. Part 2. Aspects of Porosity Modification. Am. Assoc. Petrol. Geol. Mem., 37, 277-286.

Bjørlykke, K., 1988 - Sandstone diagenesis in relation to preservation, destruction and creation of porosity. In: G.V.Chilingarian & K.H.Wolf (eds.), Diagenesis, 2. Developments in Sedimentology, 41. Elsevier Scientific Publications, Amsterdam, 555-588.

Bjørlykke, K., 1991 - Prediction of diagenetic reactions and reservoir properties of North Sea reservoir sandstones. Am. Assoc. Petrol. Geol., Abstracts 75th Anniversay 1991 Annual Convention, Dallas, Texas, April 7-10, p. 79.

Bjørlykke, K., Elverhøi, A. & Malm, A.O., 1979 - Diagenesis in Mesozoic Sandstones from Spitzbergen and the North Sea - a comparison. Geol. Rundschau, 68, 1151-1171.

Bjørlykke, K., Mo, A. & Palm, E., 1988 - Modelling of thermal convection in sedimentary basins and its relevance to diagenetic reactions. Mar. Pet. Geol., 5, 338-351.

Bjørlykke, K., Ramm, M. & Saigal, G.C., 1989 - Sandstone diagenesis and porosity modification during basin evolution. Geol. Rundschau, 78 (1), 243-268.

Blatt, H., 1979 - Diagenetic processes in sandstones: In: P.A. Scholle & P.R. Schluger (eds.), Aspects of diagenesis, Soc. Econ. Palaeontologists and Mineralogists Spec. Publ., 26, 141-157.

Blatt, H., Middleton, G.V. & Murray, R.C., 1972 - Origin of sedimentary rocks. Prentice-Hall, New Jersey, 634p.

Bodard, J.M. & Wall, V.J., 1986 - Sandstone porosity patterns in the Latrobe Group, offshore Gippsland Basin. In: R.C. Glenie (ed.), Second South-Eastern Australia Oil Exploration Symposium, Melbourne, 14-15 November 1985, 137-154.

Boles, J.R., 1978 - Active ankerite cementation in the subsurface Eocene of southwest Texas. Contrib. Mineral. Petrol., 68, 13-22.

Boles, J.R. & Franks, S.G., 1979 - Clay diagenesis in Wilcox sandstones of southwest Texas: implications of smectite diagenesis on sandstone cementation. J. Sediment. Petrol., 49, 55-70.

Boles, J.R. & Ramseyer, K., 1987 - Diagenetic carbonate in Miocene sandstone reservoir, San Joaquin Basin, California. Am. Assoc. Petrol. Geol. Bull., 71 (12), 1475-1487.

Bone, Y. & Russell, N.J., 1988 - Correlation of vitrinite reflectivity with fluid inclusion microthermometry: Assessment of the technique in the Cooper/Eromanga Basins, South Australia. Aust. J. Earth Sci., 35, 567-570.

Botz, R.W., Hunt, J.W. & Smith, J.W., 1986 - Isotope geochemistry of minerals in Australian bituminous coal. J. Sediment. Petrol., 56 (1), 99-111.

Bowering, A.J.W. & Burnett, P.J., 1980 - Formation water salinities: Toolachee and Patchawarra-Tirrawarra Formations. Unpubl. report, Santos Ltd., 7p.

Bowering, A.J.W., 1982 - Hydrodynamics and hydrocarbon migration - a model for the Eromanga Basin. Aust. Pet. Explor. Assoc. J., 22 (1), 227-236.

Bowering, A.J.W. & Harrison, D.M., 1986 - The Merrimelia Oil and Gas Field - a case history. In: Contributions to the geology and hydrocarbon potential of the Eromanga Basin. Geol. Soc. Aust. Spec. Publ., 12, 183-194.

Bowler, J., 1988 - Wireline log evaluation for explorationists. Unpubl. course notes, Bowler Log Consulting Services Pty. Ltd., 73p.

Braithwaite, C.J.R., 1988 - Stylolites as open fluid conduits. Mar. Pet. Geol., 6 (1), 93-96.

Branson, R.W., 1989 - The development history and status of the Cooper and Eromanga Basins. In: B.J. O'Neil (ed.), q.v., 15-17.

Bridge, J.S. & Leeder, M.R., 1979 - A simulation model of alluvial stratigraphy. Sedimentol., 26, 617-644.

Brindley, G.W. & Porter, A.R.D., 1978 - Occurrence of dickite in Jamaica - ordered and disordered varieties. Amer. Mineral., 63, 554-562.

Broadhead, R.F., 1984 - Geology of gas production from 'tight' Abo red beds, east central New Mexico. Oil & Gas J., June 11, 147-158.

Broecker, W.S. & Olson, E.A., 1960 - Radiocarbon from nuclear tests, 2. Science, 132, 712-721.

Brooks, J.K., Hesp, W.R. & Rigby, D., 1971 - The natural conversion of oil to gas in sediments in the Cooper Basin. Aust. Pet. Explor. Assoc. J., 11 (1), 121-5.

Broussard, M.L. (ed.), 1975 - Deltas: models for exploration. Houston Geol. Soc., Houston, 555p.

Brown, C.A., Smagala, T.M. & Haefele, G.R., 1986 - Southern Piceance Basin model - Cozette, Corcoran and Rollins sandstones. In: C.W. Spencer & R.F. Mast (eds.), Geology of tight gas reservoirs. Am. Assoc. Petrol. Geol. Studies in Geology, 24, 207-219.

Bubenicek, L., 1983 - Diagenesis of iron-rich rocks. In: G. Larsen & G.V. Chilingar (eds.), q.v., 495-511.

Burley, S.D. & Kantorowicz, J.D., 1986 - Thin section and SEM textural criteria for the recognition of cement-dissolution porosity in sandstones. Sedimentol., 33, 587-604.

Cant, D.J., 1982 - Fluvial facies models and their application. In: P.A. Scholle & D. Spearing (eds.), Sandstone depositional environments. Amer. Assoc. Petrol. Geol. Mem., 31, 115-137.

Carothers, W.W. & Kharaka, Y.K., 1980 - Stable carbon isotopes of HCO_3 in oil-field waters - implications for the origin of CO_2. Geochim. Cosmochim. Acta, 44, 323-332.

Carothers, W.W., Adami, L.H. & Rosenbauer, R.J., 1988 - Experimental oxygen isotope fractionation between siderite-water and phosphoric acid liberated CO_2-siderite. Geochim. Cosmochim. Acta, 52, 2445-50.

Carroll, D., 1970 - Clay minerals: a guide to their X-ray identification. Geol. Soc. Amer. Special Publ., 126. 75p.

Chatterjee, N.D., Johannes, W. & Leistner, H., 1984 - The system CaO-Al_2O_3-SiO_2-H_2O: new phase equilibria data, some calculated phase relations, and their geological applications. J. Petrol., 27, 677-693.

Chivas, A.R., Barnes, I., Lupton, J. & Collerson, K., 1984 - Isotopic studies of south-east Australian CO_2-rich discharges: deep sources and shallow sources. Geol. Soc. Aust. Abstracts No. 12, 7th Aust. Geol. Convention, Sydney 1984, 2p.

Chopin, C. & Schreyer, W., 1983 - Magnesiocarpholite and magnesiochloritoid: two index minerals of pelitic blueschists and their preliminary phase relations in the modelsystem MgO-Al_2O_3-SiO_2-H_2O. Amer. J. Sci., 283-A, 72-96.

Clauer, N. & Lucas, J., 1970 - Mineralogie de la fraction fine des schistes de Steige-Vosges septentrionales. Bull. Groupe Fr. Argiles, 22, 223-235.

Claypool, G.E. & Kaplan, I.R., 1974 - The origin and distribution of methane in marine sediments. In: I.R. Kaplan (ed.), Natural gases in marine sediments. New York, Plenum Press, 99-140.

Clayton, R.N. & Degens, E.T., 1959 - Use of carbon isotope analyses of carbonates for differentiating fresh-water and marine sediments. Am. Assoc. Petrol. Geol. Bull., 43 (4), 890-897.

Coleman, M.L., 1976 - Deltas: processes of deposition and models for exploration. Continuing Education Publication Co.Ltd., Champaign, Illinois. 102p.

Coleman, J.M. & Gagliano, S.M., 1965 - Sedimentary structures: Mississippi River deltaic plain. In: G.V. Middleton (ed.), Primary sedimentary structures and their hydrodynamic interpretation. Soc. Econ. Palaeontologists and Mineralogists Spec. Publ. 12, 133-148.

Coleman, J.M. & Prior, D.B., 1980 - Deltaic sand bodies. Am. Assoc. Petrol. Geol. Continuing Education Course Notes Series, 15. 103p.

Coleman, J.M. & Prior, D.B., 1982 - Deltaic environments. In: P.A. Scholle & D. Spearing (eds.), Sandstone depositional environments. Am. Assoc. Petrol. Geol. Mem. 31. 206p.

Collerson, K.D., Ullman, W.J. & Torgersen, T., 1988 - Ground waters with unradiogenic $^{87}Sr/^{86}Sr$ ratios in the Great Artesian Basin, Australia. Geology, 16, 59-63.

Collinson, J.D., 1978 - Alluvial sediments. In: H.G. Reading (ed.), Sedimentary environments and facies. Blackwell Scientific Publications, Oxford, 15-60.

Connan, J. & Cassou, A.M., 1980 - Properties of gases and petroleum liquids derived from terrestrial kerogen at various maturation levels. Geochim. Cosmochim. Acta, 44, 1-23.

Cook, A.C., 1985 - Organic petrology of a suite of samples from McLeod-1. Keiraville Konsultants, unpubl. report for Delhi International Oil Corporation. 14p.

Cooper, B.J., 1981 - Carboniferous and Permian sediments in South Australia and their correlation. Quart. Geol. Notes No. 79, Geol. Survey of South Australia, 2-6.

Cosgrove, J.L., 1987 - South-west Queensland gas - a resource for the future. Aust. Pet. Explor. Assoc. J., 27 (1), 245-63.

Cox, R.E., 1984a - Stable carbon isotope composition of oils: Chookoo-2, Naccowlah South-1, Wilson-4, Wilson-5, Wilson-6. Unpublished AMDEL report F6357/4, Delhi Petroleum Pty. Ltd. 3p.

Cox, R.E., 1984b - Stable carbon isotope composition of oils: Tinpilla-1 and Gunna-1. Unpublished AMDEL report F6408/84 for Delhi Petroleum Pty. Ltd. 3p.

Craig, H., 1953 - The geochemistry of the stable carbon isotopes. Geochim. Cosmochim. Acta, 3, 53-92.

Craig, H., 1954 - Carbon 13 in plants and the relationships between carbon 13 and carbon 14 variations in nature. J. Geol., 62 (2), 115-149.

Craig, H., 1957 - Isotope standards for carbon and oxygen and correction factors for mass spectrometric analysis of carbon dioxide. Geochim. Cosmochim. Acta, 12, 133-149.

Craig, H., 1961a - Standards for reporting concentrations of deuterium and oxygen-18 in natural waters. Science, 133, 1833-1834.

Craig, H., 1961b - Isotopic variations in meteoric waters. Science, 133, 1702-1703.

Crowell, J.C., 1978 - Gondwana glaciation, cyclothems, continental positioning and climate change. Amer. J. Sci., 278, 1345-1372.

Crowell, J.C. & Frakes, L.A., 1971a - Late Palaeozoic glaciation. IV.Australia. Geol. Soc. Am. Bull., 82, 2515-40.

Crowell, J.C. & Frakes, L.A., 1971b - Late Palaeozoic glaciation of Australia. J. Geol. Soc. Aust., 17, 115-155.

Crowell, J.C. & Frakes, L.A., 1975 - The Late Palaeozoic glaciation. In: K.S.W. Campbell (ed.), Gondwana geology. Australian National University Press, Canberra, 313-31.

Curtis, C.D., 1967 - Diagenetic iron minerals in some British Carboniferous sediments. Geochim. Cosmochim. Acta, 31, 2109-2123.

Curtis, C.D. & Spears, D.A., 1968 - The formation of sedimentary iron minerals. Econ. Geol., 63, 257-270.

Curtis, C.D., Coleman, M.L. & Love, L.G., 1986 - Pore water evolution during sediment burial from isotopic and mineral chemistry of calcite, dolomite and siderite concretions. Geochim. Cosmochim. Acta, 50, 2321-2334.

Dansgaard, W., 1964 - Stable isotopes in precipitation. Tellus, 16 (4), 436-468.

Dapples, E.C., 1967a - Diagenesis of sandstone. In: G. Larsen & G.V. Chilingar (eds.), Diagenesis in sediments. Developments in Sedimentology, 8, Elsevier (Amsterdam), 91-126.

Dapples, E.C., 1967b - Silica as an agent in diagenesis. In: G. Larsen & G.V. Chilingar (eds.), Diagenesis in sediments. Developments in Sedimentology, 8, Elsevier (Amsterdam), 323-342.

Dapples, E.C., 1979a - Diagenesis of sandstones. In: G.Larsen & G.V. Chilingar (eds.), Diagenesis in sediments and sedimentary rocks, Developments in Sedimentology, 25A, 31-97.

Dapples, E.C., 1979b - Silica as an agent in diagenesis: In: G. Larsen & G.V. Chilingar (eds.), Diagenesis in sediments and sedimentary rocks, Developments in Sedimentology, 25A, 99-141.

Davies, D.K., 1980 - Sandstone reservoirs - their genesis, diagenesis and diagnosis for successful exploration and development. Petrol. Expl. Soc. Aust. Distinguished Lecturer Series. 93p.

Davis, S.W., 1964 - Silica in streams and ground water. Amer. J. Sci., 262, 870-890.

deBoer, R. & Collins, L.B., 1988 - Petrology and diagenesis of the Flag Sandstone, Harriet Field, Barrow Sub-basin. In: P.G. Purcell & R.R. Purcell (eds.), The North West Shelf, Australia. Proc. Petrol. Expl. Soc. Aust., Perth 1988, 225-235.

Deer, W.A., Howie, R.A. & Zussman, J., 1975 - An introduction to the rock-forming minerals (8th edition). Longman Group Limited, London, 528p.

Degens, E.T. & Epstein, S., 1964 - Oxygen and carbon isotope ratios in coexisting calcites and dolomites from recent and ancient sediments. Geochim. Cosmochim. Acta, 28, 23-44.

Deines, P., 1986 - The isotopic composition of reduced organic carbon. In: P. Fritz & J.Ch. Fontes (eds), Handbook of environmental isotope geochemistry, Elsevier Scientific Publishing Company, New York, 329-406.

Deischl, D.G., 1973 - The characteristics, history and development of the Basin Dakota gas field, San Juan Basin, New Mexico. In: Cretaceous and Tertiary rocks of the southern Colorado Plateau. Four Corners Geol. Soc. Guidebook, 168-173.

Denton, P.A., 1985 - Diagenetic history and reservoir evaluation of the Permian sandstones, Big Lake Field, southern Cooper Basin, South Australia. Unpubl. M.Sc. thesis, Department of Earth Sciences, Monash University, Australia. 123p.

Desborough, G.A., 1978 - A biogenic-chemical stratified lake model for the origin of oil shale of the Green River Formation: an alternative to the playa-lake model. Geol. Soc. Amer. Bull., 89, 961-971.

Desbrandes, R., 1985 - Encyclopedia of well logging. Institut Français du Pétrole Publications, Graham & Trotman Ltd., London. 584p.

Deuser, W.G. & Degens, E.T., 1967 - Carbon isotope fractionation in the system CO_2 (gas)-CO_2 (aqueous)-HCO_3^- (aqeous). Nature, 215, 1033-1035.

Devine, S.B. & Gatehouse, C.G., 1977 - Sandstone reservoir geometry of non-marine sediments in the Toolachee Gas Field. Aust. Pet. Explor. Assoc. J., 17 (1), 50-57.

Dickins, J.M., 1985 - Late Palaeozoic glaciation. BMR J. Aust. Geol. Geophys., 9, 163-169.

Dickinson, W.W., 1987 - An oxygen isotope model for interpreting carbonate diagenesis in nonmarine rocks (Green River Basin, Wyoming, U.S.A.). Chem. Geology, 65, 103-116.

Dickinson, W.W., 1988 - Isotopic and petrographic evidence for carbonate diagenesis in nonmarine sandstones, Green River Basin, Wyoming. J. Sediment. Petrol., 58 (2), 327-338.

Dimitrakopoulos, R. & Muehlenbachs, K., 1985 - ^{13}C-rich diagenetic carbonates associated with heavy-oil deposits. Am. Assoc. Pet. Geol. Bull., 69, p.847 [abstract].

Dimitrakopoulos, R. & Muehlenbachs, K., 1987 - Biodegradation of petroleum as a source of ^{13}C-enriched carbon dioxide in the formation of carbonate cement. Chem. Geology, 65, 283-291.

Dixon, S.A., Summers, D.M. & Surdam, R.C., 1989 - Diagenesis and preservation of porosity in Norphlet Formation (Upper Jurassic), southern Alabama. Am. Assoc. Pet. Geol. Bull., 73 (6), 707-728.

Donovan, T.J., 1974a - Petroleum microseepage at Cement, Oklahoma: Evidence and mechanism. Am. Assoc. Petrol. Geol. Bull., 58, 429-446.

Donovan, T.J., 1974b - Mineralogical evidence for buried hydrocarbons - a new exploration tool. Am. Assoc. Petrol. Geol. Bull., 58, p. 913 [abstract].

Donovan, T.J., Friedman, I. & Gleason, J.D., 1974 - Recognition of petroleum-bearing traps by unusual carbon isotopic compositions of carbonate-cemented surface rocks. Geology, 2, 351-354.

Doyle, H.A. & Howard, K.W., 1988 - History of seismic exploration in Australia. Petroleum in Australia: the first century. Aust. Petrol. Expl. Assoc. Spec. Publ. 286-291.

Draper, J.J., 1983 - Origin of pebbles in mudstones in the Denison Trough. In: Permian Geology of Queensland. Proc. Symp. on the Permian Geology of Queensland, Geol. Soc. Aust. & Geol. Surv. Qsld, Brisbane, 14-16th July 1982, 305-316.

Dresser Atlas, 1983 - Log interpretation charts. Dresser Atlas Publication. 237p.

Drong, H.J., 1979 - Diagenetische Veränderungen in den Rotliegend Sandsteinen im NW-Deutschen Becken. Geol. Rundschau, 68 (3), 1172-1183.

Duchscherer, W., 1982 - Geochemical exploration for hydrocarbons - no new tricks but an old dog. Oil & Gas J., July, 163-176.

Dulhunty, J.A., 1964 - Our Permian heritage in central eastern New South Wales. Jour. Proc. Royal Soc. New South Wales, 97 (5), 145-155.

Dutton, S.P. & Land, L.S., 1988a - Diagenetic history of a well-cemented quartzarenite, Lower Cretaceous Travis Peak Formation, East Texas. Geol. Soc. Amer. Bull., 100, 1271-1282.

Dutton, S.P. & Land, L.S., 1988b - Cementation and burial history of a low-permeability quartzarenite, Lower Cretaceous Travis Peak Formation, East Texas. Geol. Soc. Amer. Bull., 100, 1271-1282.

Eadington, P.J., Hamilton, P.J. & Green, P., 1989 - Hydrocarbon fluid history in relation to diagenesis in the Hutton Sandstone, south-west Queensland. In: B.J. O'Neil (ed.), q.v., 601-618.

Eberl, D. & Hower, J., 1976 - Kinetics of illite formation. Geol. Soc. Amer. Bull., 87, 1326-1330.

Edwards, N.M., 1985 - Hydrocarbon fields of the Naccowlah area, SW Queensland; diagenesis - its influence on reservoir quality. Unpubl. B.Sc. (Hons.) thesis, Department of Earth Sciences, Monash University, Australia. 95p.

Eglinton, G. & Murphy, M.T.J., 1969 - Organic geochemistry. Springer Verlag, Berlin-Heidelberg-New York, 828p.

Eleftheriou, J., 1990 - Reservoir quality of Permian sandstones in the Strzelecki-Kidman-Kerna area, Cooper Basin, South Australia. Unpubl. Masters thesis, University of Adelaide, Australia. 90p.

Elliot, T., 1978 - Deltas. In: H.G. Reading (ed.), Sedimentary environments and facies. Blackwell Scientific Publications, Oxford, 97-142.

Embleton, B.J.J., 1981 - A review of the palaeomagnetism of Australia and Antarctica. In: Palaeoreconstruction of the Continents. Am. Geophys. Union, Geodynamics Series 2, 77-92.

Embleton, B.J.J. & McElhinny, M.W., 1982 - Marine magnetic anomalies, palaeomagnetism and the drift history of Gondwanaland. Earth Planet. Sci. Letters, 58, 141-50.

Eslinger, E. & Pevear, D., 1988 - Clay minerals for petroleum geologists and engineers. Soc. Econ. Palaentologists and Mineralogists Short Course Notes No. 22. 83p.

Evans, P.R., 1966 - Palynological comparison of the Cooper and Galilee Basins. BMR Record 1966/222 (unpubl.). 23p.

Evans, P.R., 1988 - The formation of petroleum and geological history of Australia. Petroleum in Australia: the first century. Aust. Petrol. Expl. Assoc. Spec. Publ., 26-47.

Exon, N.F. & Senior, B.R., 1976 - The Cretaceous of the Eromanga and Surat Basins. BMR Jour. Aust. Geol.. Geophys., 1, 33-50.

Faehrmann, P., 1986 - 'Permian' and 'Jurassic' waters of the southern Cooper/Eromanga Basins: a discussion. Unpubl. report, Santos Ltd., 28p.

Fairburn, W.A., 1989 - The geometry of Toolachee unit 'C' fluvial sand trends, Moomba Field, Permian Cooper Basin, South Australia. In: B.J. O'Neil (ed.), q.v., 239-250.

Fanning, M., 1987 - Ella-1. K-Ar dating of drill core at 4190 feet 10 inches. Unpubl. Amdel report for Delhi Petroleum Pty. Ltd., 4p.

Faure, G., 1986 - Principles of isotope geology. 2nd edition, John Wiley & Sons, 589p.

Fisher, M.A., 1982 - Petroleum geology of the Norton Basin, Alaska. Am. Assoc. Petrol. Geol. Bull., 66 (3), 286-301.

Folk, R.L., 1965 - Some aspects of recrystallization in ancient limestones. In: L.C. Pray & R.C. Murray (eds.), Dolomitization and limestone diagenesis. Soc. Econ. Palaeontologists and Mineralogists Spec. Publ., 13, 14-48.

Fothergill, C.A., 1955 - The cementation of oil reservoir sands and its origin. Proc. 4th World Petroleum Conference, Rome, 1955, 301-314.

Frakes, L.A., 1979 - Climates throughout geologic time. Elsevier, Amsterdam, 301p.

Franks, S.G. & Forester, R.W., 1984 - Relationships among secondary porosity, pore-fluid chemistry and carbon dioxide, Texas Gulf Coast. Am. Assoc. Petrol. Geol. Mem. 32, 63-79.

Frey, M., 1978 - Progressive low-grade metamorphism of a black shale formation, central Swiss Alps, with special reference to pyrophyllite and margarite bearing assemblages. J. Petrol., 19, 93-135.

Frey, M., Saunders, J. & Schwander, H., 1988 - The mineralogy and metamorphic geology of low-grade metasediments, Northern Range, Trinidad. J. Geol. Soc. London, 145, 563-575.

Fritz, P., Binda, P.L., Folinsbee, F.E. & Krouse, H.R., 1971 - Isotopic composition of diagenetic siderites from Cretaceous sediments in western Canada. J. Sediment. Petrol., 41 (1), 282-288.

Fritz, P. & Fontes, J.C. (eds.), 1980 - Handbook of environmental isotope geochemistry, 1A. Elsevier, Amsterdam, 545p.

Fritz, P. & Fontes, J.C. (eds.), 1986 - Handbook of environmental isotope geochemistry, 1B. Elsevier, Amsterdam, 557p.

Fuex, A.N., 1977 - The use of stable isotopes in hydrocarbon exploration. J. Geochem. Explor., 7, 155-188.

Fullagar, P.K., 1989 - Petroleum exploration by geochemical and geophysical detection of vertical migration. Petrol. Expl. Soc. Aust., Special Lecture Series 1989, 118p.

Füchtbauer, H., 1967a - Der Einfluß des Ablagerungs-milieus auf die Sandstein-Diagenese im Mittleren Buntsandstein. Sediment. Geol., 1, 159-179.

Füchtbauer, H., 1967b - Influence of different types of diagenesis on sandstone porosity. Proc. 7th World Petroleum Congress, 2, 353-369.

Füchtbauer, H., 1974 - Zur Diagenese fluviatiler Sandsteine. Geol. Rundschau, 63, 904-925.

Füchtbauer, H., 1978 - Zur Herkunft des Quarzzementes. Abschätzung der Quarzauflösung in Silt- und Sandsteinen. Geol. Rundschau, 67, 991-1008.

Galimov, E.M., 1966 - Carbon isotopes in soil CO_2. Geochem. Int., 3, 889-897.

Gallagher, K., 1978 - Thermal conductivity and heat flow in the southern Cooper Basin. Exploration Geophysics, 5th Geophysical Conference and Exhibition, Perth, February 22-27, 18, 62-65.

Galloway, W.E., 1974 - Deposition and diagenetic alteration of sandstone in northeast Pacific arc-related basins: Implications for greywacke diagenesis. Geol. Soc. Amer. Bull., 85, 379-390.

Galloway, W.E. & Hobday, D.K., 1983 - Terrigeneous clastic depositional systems. Applications to petroleum, coal and uranium exploration. Springer Verlag, New York. 423p.

Garrels, R.M. & Christ, C.L., 1965 - Solutions, minerals and equilibria. Harper and Row, New York, 450p.

Gatehouse, C.G., 1972 - Formations of the Gidgealpa Group in the Cooper Basin. Aust. Oil & Gas J., 18 (12), 10-15.

Gatehouse, C.G., 1986 - The geology of the Warburton Basin in South Australia. Aust. J. Earth Sci., 33, 161-180.

Gilby, A.R. & Mortimore, I.R., 1989 - The prospects for Eromanga oil accumulations in the northern Cooper Basin region, Australia. In: B.J. O'Neil (ed.), q.v., 391-403.

Giles, M.R., 1987 - Mass transfer and problems of secondary porosity creation in deeply buried hydrocarbon reservoirs. Mar. Pet. Geol., 4, 188-204.

Glasmann, J.R., Clark, R.A., Larter, S., Briedis, N.A. & Lundegard, P., 1989 - Diagenesis and hydrocarbon accumulation, Brent Sandstone (Jurassic), Bergen High area, North Sea. Am. Assoc. Petrol. Geol. Bull., 73 (11), 1341-1360.

Gleadow, A., Duddy, I., Green, P. & Lovering, J., 1989 - Assessment of hydrocarbon resource potential by fission track techniques. Pet. Explor. Soc. Aust. J., 15, 38-40.

Goméz-Pugnaire, M., Sassi, F.P. & Visona, D., 1978 - Sobre la présencia de paragonite y pyrofilita en las filitas del complejo Nevado-Filabride en la Sierra de Baza (Cordilleras Beticas, España). Bol. Geol. Min., 89 (5), 468-474.

Gostin, V., 1973 - Lithological study of the Tirrawarra Sandstone. Unpubl. report for Delhi Int. Oil Corp. 21p.

Gould, K.W. & Smith, J.W., 1978 - Isotopic evidence for microbiologic role in genesis of crude oil from Barrow Island, Western Australia. Am. Assoc. Petrol. Geol. Bull., 62 (3), 455-462.

Gould, K.W. & Smith, J.W., 1979 - The genesis and isotopic composition of carbonates associated with some Permian Australian coals. Chem. Geology, 24, 137-150.

Gould, K.W. & Smith, J.W., 1980 - Isotopic studies of geochemical factors in outbursting. In: Symposium on the Occurrence, Prediction and Control of Outbursts in Coal Mines. Australas. Inst. Min. Metall., Melbourne, 85-98.

Gould, K.W. & Johnson, D.P., unpubl. - Isotopic evidence on the formation of carbonate concretions in Permian freshwater Coal Measures, Bowen Basin, Australia. CSIRO Division Mineral Physics & Mineralogy, 28p.

Gravestock, D.I. & Morton, J.G.G., 1984 - Geology of the Della Field, a perspective on the history of the Cooper Basin. Aust. Pet. Explor. Assoc. J., 24 (1), 266-277.

Gravestock, D.L. & Alexander, E.M., 1986 - Porosity and permeability of reservoirs and caprocks in the Eromanga Basin, South Australia. Aust. Pet. Explor. Assoc. J., 26 (1), 202-213.

Gravestock, D.I. & Alexander, E.M., 1988 - Eromanga Basin, South Australia core and well log study. NERDDC project 820, unpubl. report. 124p.

Gravestock, D.I. & Alexander, E.M., 1989 - Petrophysics of oil reservoirs in the Eromanga Basin, South Australia. In: B.J. O'Neil (ed.), q.v., 141-151.

Gravestock, D.I. & Morton, J.G.G., 1984 - Geology of the Della Field, a perspective on the history of the Cooper Basin. Aust. Pet. Explor. Assoc. J., 24 (1), 266-77.

Gravestock, D., Griffiths, M. & Hill, A., 1983 - The Hutton Sandstone - two separate reservoirs in the Eromanga Basin, South Australia. Aust. Pet. Explor. Assoc. J., 23, 109-119.

Gray, R.J. & Roberts, D.C., 1984 - A seismic model of faults in the Cooper Basin. Aust. Pet. Explor. Assoc. J., 24 (1), 421-428.

Green, P.M., Eadington, P.J., Hamilton, P.J. & Carmichael, D.C., 1989 - Regional diagenesis - an important influence in porosity development and hydrocarbon

accumulations within the Hutton Sandstone, Eromanga Basin. In: B.J. O'Neil (ed), q.v., 619-627.

Greer, W.J., 1965 - The Gidgealpa Gas Field. Aust. Pet. Explor. Assoc. J., 5, 65-68.

Gross, M.G., 1964 - Variations in the O^{18}/O^{16} and C^{13}/C^{12} ratios of diagenetically altered limestones in the Bermuda Islands. J. Geol., 72, 170-194.

Grund, R., 1966 - The glacigene sediments of the Coopers Creek Basin. Unpubl. B.Sc. (Hons.) thesis, University of Adelaide, Australia, 197p.

Guven, N., Hower, W.D. & Davies, D.K., 1980 - Nature of authigenic illite in sandstone reservoirs. J. Sediment. Petrol., 50, 761-766.

Haas, H. & Holdaway, M.J., 1973 - Equilibrium in the system Al_2O_3-SiO_2-H_2O involving the stability limits of pyrophyllite and thermodynamic data of pyrophyllite. Amer. J. Sci., 273, 449-464.

Habermehl, M.A., 1980 - The Great Artesian Basin, Australia. BMR Jour. Geol. Geophys., 5, 9-38.

Habermehl, M.A., 1983 - Hydrogeology and hydrochemistry of the Great Artesian Basin, Australia. In: Papers of the International Conference on Groundwater and Man, Australian Water Resources Council Conference Series, 8 (3), 83-98.

Habermehl, M.A., 1984 - Hydrogeology of the Great Artesian Basin. 1984 Yearbook of the Bureau of Mineral Resources, Canberra, 92-93.

Habermehl, M.A., 1986a - Mound spring deposits of the Great Artesian Basin, Australia. 12th International Sedimentological Congress, Abstracts, August 24-30th 1986, Canberra, 128-129.

Habermehl, M.A., 1986b - Regional groundwater movement, hydrochemistry and hydrocarbon migration in the Eromanga Basin. In: Gravestock, D.I., Moore, P.S. & Pitt, G.M. (eds.), Contributions to the geology and hydrocarbon potential of the Eromanga Basin. Geol. Soc. Aust. Spec. Publ. No.12, 353-76.

Habermehl, M.A., 1986c - Mound spring deposits of the Great Artesian Basin. Geol. Soc. Aust., Abstracts 8th Australian Geological Convention, Adelaide, 1986, p.90.

Habermehl, M.A., 1986d - The Great Artesian Basin - a groundwater resource. Geol. Soc. Aust., Abstracts 8th Australian Geological Convention, Adelaide, 1986, p. 91.

Hamilton, J.R. & Wilson, J.S., 1981 - Study of geopressured reservoir by drilling and producing a well in a limited geopressured water sand. Proc. 4th U.S. Gulf Coast Geopressured-Geothermal Energy Conference, Research and Development, 3: Centre for Energy Studies, University of Texas, Austin, 1137-1159.

Hamilton, N.J., 1989 - A review of the petrology and mineralogy of Permian sandstone, Cooper Basin, Australia. Unpubl. report, Santos Ltd. 23p.

Hancock, N. & Taylor, A.M., 1978 - Clay mineral genesis and oil migration in the Middle Jurassic Brent Formation. J. Geol. Soc. London, 135, 69-72.

Hankel, R.C., Davies, G.R. & Krouse, H.R., 1989 - Eastern Medicine Hat gas field: a shallow, Upper Cretaceous, bacteriogenic gas reservoir of southeastern Alberta. Canadian Petrol. Geol. Bull., 37 (1), 98-112.

Harder, H., 1974 - Illite mineral synthesis at surface temperatures. Chem. Geology, 14, 241-253.

Hawkins, P.J., 1978 - Relationship between diagenesis, porosity, reduction, and oil emplacement in late Carboniferous sandstone reservoirs, Bothamsall Oilfield, E. Midlands. J. Geol. Soc. London, 135, 7-24.

Hawlader, H.M., 1990a - Diagenesis and reservoir potential of volcanogenic sandstones - Cretaceous of the Surat Basin, Australia. Sediment. Geology, 66, 181-195.

Hawlader, H.M., 1990b - Reservoir properties of some Surat Basin sandstones as a function of diagenetic clay-mineral assemblage. Queensl. Govt. Min. J., April 1990, 180-189.

Hayes, J.B., 1970 - Polytypism of chlorite in sedimentary rocks. Clays & Clay Minerals, 18, 285-306.

Hayes, J.B., 1979 - Sandstone diagenesis - the hole truth: In: P. Scholle and P.R. Schluger, (eds.), Aspects of diagenesis, Soc. Econ. Palaeontologists and Mineralogists Spec. Publ., 26, 127-139.

Heald, M.T. & Larese, R.E., 1974 - Influence of coatings on quartz cementation. J. Sediment. Petrol., 44, 1269-1274.

Heath, R., 1989 - Exploration in the Cooper Basin. Aust. Pet. Explor. Assoc. J., 29, 366-378.

Heath, R., McIntyre, S. & Gibbins, N., 1989 - A Permian origin for Jurassic reservoired oil in the Eromanga Basin. In: B.J. O'Neil (ed.), q.v., 405-416.

Helgeson, H.C., Delany, J.M., Nesbitt, H.W. & Bird, D.K., 1978 - Summary and critique of the thermodynamic properties of rock-forming minerals. Amer. J. Sci., 278-A, 1-220.

Hemley, J.J. & Jones, W.R., 1964 - Chemical aspects of hydrothermal alteration with emphasis on hydrogen metasomatism. Econ. Geology, 59, 538-539.

Hendy, D.H., 1971 - The isotopic geochemistry of speleothems. I. The Calculation of the effects of different modes of formation on the isotopic composition of speleothems and their applicability as palaeoclimatic indicators. Geochim. Cosmochim. Acta, 35, 801-824.

Herczeg, A.L., Torgersen, T., Habermehl, M.A. & Chivas, A.R., 1988 - Geochemical evolution of groundwaters from the Great Artesian Basin, Australia. 9th Australian Geological Convention, Abstracts, University of Queensland, Brisbane, 186-187.

Ho, C. & Coleman, J.M., 1969 - Consolidation and cementation of Recent sediments in the Atchafalaya Basin. Geol. Soc. Amer. Bull., 80, 183-192.

Hoefs, J., 1973 - Stable isotope geochemistry. Springer Verlag, Berlin. 241p.

Holland, H.D. & Malinin, S.D., 1979 - The solubility and occurrence of nonore minerals. In: H.L. Barnes (ed.), Geochemistry of hydrothermal ore deposits (2nd ed.), New York, Wiley-Interscience Publishers, 461-508.

Hollingsworth, R.J.S., 1989 - The exploration history and status of the Cooper and Eromanga Basins. In: B.J. O'Neil (ed.), q.v., 3-13.

Hollingsworth, R.J.S., Barnes, R.G., Middleton, M.P. & Covil, M.W., 1976 - Tooroopie seismic survey by Seismograph Service Ltd. S. Aust. Dept. Mines and Energy Confidential Env. 2523 (unpubl.). 62p.

Holloway, J.R., 1976 - Fluids in the evolution of granitic magmas: consequences of finite CO_2 solubility. Geol. Soc. Amer. Bull., 87, 1513-1518.

Houseknecht, D.W., 1984 - Influence of grain size and temperature on intergranular pressure solution, quartz cementation, and porosity in a quartzose sandstone. J. Sediment. Petrol., 54, 348-361.

Houseknecht, D.W., 1987 - Assessing the relative importance of compaction processes and cementation to reduction of porosity in sandstones. Am. Assoc. Petrol. Geol. Bull., 71 (6), 633-642.

Houseknecht, D.W., 1988 - Intergranular pressure solution in four quartzose sandstones. J. Sediment. Petrol., 58, 228-246.

Hovland, M., Talbot, M.R., Qvale, H., Olaussen, S. & Aasberg, L., 1987 - Methane-related carbonate cements in pockmarks of the North Sea. J. Sediment. Petrol., 57 (5), 881-892.

Hower, J., Eslinger, E.V., Hower, M.E. & Perry, E.A., 1976 - Mechanism of burial metamorphism of argillaceous sediments. 1. Mineralogical and chemical evidence. Geol. Soc. Amer. Bull., 87, 725-737.

Huang, W.L., Bishop, A.M. & Brown, R.W., 1986 - The effect of fluid/rock ratio on feldspar dissolution and illite formation under reservoir conditions. Clay Minerals, 21, 585-601.

Hudson, J.D., 1977 - Stable isotopes and limestone lithification. Jour. Geol. Soc. London, 133, 637-660.

Huebner, M., 1981 - Carbon-13 isotope values for carbon dioxide gas and dissolved carbon species in springs and wells in the Geysers - Clear Lake region. In: R.J. McLaughlin & J.M. Donelly-Nolan (eds)., Research in the geysers - Clear Lake area, northern California. U.S. Geological Survey Prof. Pap. 1141, 211-213.

Hunt, J.W., Heath, R.S. & McKenzie, P.F., 1986 - Cooper Basin hydrocarbon characteristics and gas-liquids composition. Unpubl. report, Delhi Petroleum Pty. Ltd. 500p.

Hunt, J.W., Heath, R.S. & McKenzie, P.F., 1989 - Thermal maturity and other geological controls on the distribution and composition of Cooper Basin hydrocarbons. In: B.J. O'Neil (ed.), q.v, 509-523.

Hurst, A.R., 1980 - Occurrence of corroded authigenic kaolinite in a diagenetically modified sandstone. Clays & Clay Minerals, 28, 393-396.

Hurst, A.R., 1985 - Diagenetic chlorite formation in some Mesozoic shales from the Sleipner area of the North Sea. Clay Minerals, 20, 69-79.

Hurst, A. & Irwin, H., 1982 - Geological modelling of clay diagenesis in sandstones. Clays & Clay Minerals, 17, 5-22.

Hurst, V.J. & Kunkle, A.C., 1985 - Dehydroxylation, rehydroxylation, and stability of kaolinite. Clays & Clay Minerals, 33, 1-14.

Hutcheon, I., 1983 - Aspects of the diagenesis of coarse-grained siliciclastic rocks. Geosci. Canada, 10 (1), 4-14.

Ianovici, V., Neaçsu, G. & Neaçsu, V., 1981 - Pyrophyllite occurrences and their genetic relations with the kaolin minerals in Romania. Bull. Mineral., 104, 768-775.

Irwin, H., 1980 - Early diagenetic carbonate precipitation and pore fluid migration in the Kimmeridge Clay of Dorset, England. Sedimentol., 27, 577-591.

Irwin, H., Curtis, C.D. & Coleman, M., 1977 - Isotopic evidence for source of diagenetic carbonates formed during burial of organic-rich sediments. Nature, 269, 209-213.

Jakobsen, B.H., 1987 - Occurrence of pyrite and carbonate minerals in a lowland moor area. J. Sediment. Petrol., 57 (3), 530-536.

James, N.P. & Choquette, P.W., 1984 - Diagenesis 9. Limestones - the meteoric diagenetic environment. Geosci. Canada, 11, 161-194.

Jeffery, P.M., Compston, W., Greenhalgh, D. & De Laeter, J., 1955 - On the carbon-13 abundance of limestones and coals. Geochim. Cosmochim. Acta, 7, 255-286.

Jenkins, C.C., 1989 - Geochemical correlation of source rocks and crude oils from the Cooper and Eromanga Basins. In: O'Neil (ed.), q.v., 525-39.

Johnston, D.D. & Johnson, R.J., 1987 - Depositional and diagenetic controls on reservoir quality in First Wilcox Sandstone, Livingston Field, Louisiana. Am. Assoc. Petrol. Geol. Bull., 71 (10), 1152-1161.

Jonas, E.C. & McBride, E.F., 1977 - Diagenesis of sandstone and shale: application to exploration for hydrocarbons. University of Texas at Austin, Continuing Education Program, No.1, 120p.

Jones, F.O. & Owens, W.W., 1980 - A laboratory study of low-permeability gas sands. J. Petrol. Technology, September 1980, 1631-1640.

Kahle, C.F., 1965 - Possible role of clay minerals in the formation of dolomite. J. Sediment. Petrol., 35, 448-453.

Kantorowicz, J.D., Lievaart, L., Eylander, J.G.R. & Eigner, M.R.P., 1986 - The role of diagenetic studies in production operations. Clay Minerals, 21, 769-780.

Kantsler, A.J., Smith, G.C. & Cook, A.C., 1978 - Lateral and vertical rank variation: implications for hydrocarbon exploration. Aust. Pet. Explor. Assoc. J., 18 (1), 143-156.

Kantsler, A.J. & Cook, A.C., 1979 - Rank variation in the Cooper and Eromanga Basins, central Australia. Unpubl. report for Delhi Petroleum Pty Ltd. 43p.

Kantsler, A.J., Prudence, T.J.C., Cook, A.C. & Zwigulis, M., 1983 - Hydrocarbon habitat of the Cooper/Eromanga Basin, Australia. Aust. Pet. Explor. Assoc. J., 23 (1), 373-389.

Kantsler, A.J., Cook, A.C. & Zwigulis, M., 1986 - Organic maturation in the Eromanga Basin. Geol. Soc. Aust. Spec. Publ., 12, 305-322.

Kapel, A.J., 1966 - The Coopers Creek Basin. Aust. Pet. Explor. Assoc. J., 6 (1), 71-75.

Kapel, A.J., 1972 - The geology of the Patchawarra area, Cooper Basin. Aust. Pet. Explor. Assoc. J., 12 (1), 53-57.

Keeling, C.D., 1958 - The concentration and isotopic abundances of atmospheric carbon dioxide in rural areas. Geochim. Cosmochim. Acta, 13, 322-334.

Keighin, C.W., 1979 - Influence of diagenetic reactions on reservoir properties of the Neslen, Farrer, and Tuscher Formations, Uinta Basin, Utah. Soc. Petrol. Eng. Symp. Low-permeability gas reservoirs, Denver, May 20-22, 1979, paper SPE 7919, 77-84.

Keike, E.M. & Hartmann, D.J., 1973 - Scanning electron microscope application to formation evaluation. Transactions of the Gulf Coast Association of Geological Societies, 3, 60-67.

Kennicutt, M.C., Denoux, G.J., Brooks, J.M. & Sandberg,W.A., 1987 - Hydrocarbons in Mississippi fan and intraslope basin sediments. Geochim. Cosmochim. Acta, 51, 1457-1466.

Kharaka, Y.K., Carothers, W.W. & Rosenbauer, R.J., 1983 - Thermal decarboxylation of acetic acid: implications for origin of natural gas. Geochim. Cosmochim. Acta, 47, 397-402.

Kharaka, Y.F. & Carothers, W.W., 1986 - Oxygen and hydrogen isotope geochemistry of deep basin brines. In: P. Fritz & J. Ch. Fontes (eds.), Handbook of environmental isotope geochemistry, 2, 305-360.

Kingston, D.R., Dishroon, C.P. & Williams, P.A., 1983 - Global basin classification system. Am. Assoc. Petrol. Geol. Bull., 67, 2175-2193.

Kisch, H.J., 1983 - Mineralogy and petrology of burial diagenesis (Burial Metamorphism) and Incipient Metamorphism in Clastic Rocks. In: G.Larsen & G.V. Chilingar (eds.), q.v., 289-493.

Klemme, H.D., 1980 - Petroleum basins - classifications and characteristics. J. Petrol. Geol., 3, 187-207.

Knauss, K.G. & Wolery, T.J., 1988 - The dissolution kinetics of quartz as a function of pH and time at 70° C. Geochim. Cosmochim. Acta, 52, 4 3-53.

Koncz, I., 1983 - The stable carbon isotope composition of the hydrocarbon and carbon dioxide components of Hungarian natural gases. Acta Miner. Petrogr., 26 (1), 33-49.

Kossovskaya, A.G. & Shutov, V.D., 1970 - Main aspects of the epigenesis problem. Sedimentol., 15, 11-40.

Krauskopf, K.B., 1959 - The geochemistry of silica in sedimentary environments. In: Silica in sediments, Soc. Econ. Palaeontologists and Mineralogists Spec. Publ., 7, 4-20.

Kreulen, R., 1980 - CO_2-rich fluids during regional metamorphism on Naxos (Greece): carbon isotopes and fluid inclusions. Amer. J. Sci., 280, 745-771.

Kuang, K.S., 1985 - History and style of Cooper-Eromanga basin structures. Austr. Soc. Expl. Geophys. Bull., 16, 245-48.

Kunkler, J.L., 1969 - The sources of carbon dioxide in the zone of aeration of the Bandelier Tuff, near Los Alamos, New Mexico. U.S. Geol. Surv., Prof. Paper, 650-B, 185-188.

Kvenvolden, K.A. & Claypool, G.E., 1980 - Origin of gasoline range hydrocarbons and their migration by solution in carbon dioxide in Norton Basin, Alaska. Am. Assoc. Petrol. Geol. Bull., 64, 1078-1086.

Kvenvolden, K.A. & Pettinga, J.R., 1989 - Hydrocarbon gas seeps of the convergent Hikurangi margin, North Island, New Zealand. Mar. Pet. Geol., 6, 2-8.

Kvenvolden, K.A. & Squires, R.M., 1967 - Carbon isotopic composition of crude oils from Ellenburger Group (Lower Ordovician), Permian Basin, west Texas and eastern New Mexico. Am. Assoc. Petrol. Geol. Bull., 5 (7), 1293-1303.

Laier, T., 1988 - Hydrocarbon gases in the crystalline rocks of the Gravberg-1 well, Swedish deep gas project. Mar. Pet. Geol., 5, 370-377.

Lambeck, K. & Stephenson, R., 1986 - The post-Palaeozoic uplift history of southeastern Australia. Aust. J. Earth Sci., 33, 253-270.

Lambert-Aikhionbare, D.O., 1982 - Relationship between diagenesis and pore fluid chemistry in Niger Delta oil-bearing sands. J. Pet. Geol., 4, 287-298.

Land, L.S., 1983 - The application of stable isotopes to studies of the origin of dolomite and to problems of diagenesis of clastic sediments. In: M.A. Arthur, T.F. Anderson, I.R. Kaplan, J.Veizer & L.S. Land (eds.), Stable isotopes in sedimentary geology. Soc. Econ. Palaeontologists and Mineralogists Short Course Series, 10, p. 4-1 to 4-22.

Land, L.S., 1984 - Frio Sandstone diagenesis, Texas Gulf Coast: a regional isotopic study. In: Clastic Diagenesis, Part 2, Aspects of Porosity Modification, Am. Assoc. Petrol. Geol. Mem., 37, 47-62.

Land, L.S. & Dutton, S.P., 1978 - Cementation of a Pennsylvanian deltaic sandstone: isotopic data. J. Sediment. Petrol., 48, 1167-1176.

Land, L.S. & Dutton, S.P., 1979 - Cementation of sandstone - reply. J. Sediment. Petrol., 49, 1359-1361.

Larsen, G. & Chilingar, G.V., 1983 - Diagenesis in sediments and sedimentary rocks, 2. Developments in Sedimentology 25B, Elsevier Scientific Publishing Company, Amsterdam. 572p.

Laughrey, C.D. & Harper, J.A., 1986 - Comparisons of Upper Devonian and Lower Silurian tight formations in Pennsylvania - geological and engineering characteristics. In: C.W. Spencer & R.F. Mast (eds.), Geology of tight gas reservoirs. Am. Assoc. Petrol. Geol. Studies in Geology, 24, 9-43.

Law, B.E., Pollastro, R.M. & Keighin, C.W., 1986 - Geologic characterization of low-permeability gas reservoirs in selected wells, Greater Green River Basin, Wyoming, Colorado and Utah. In: C.W. Spencer & R.F. Mast (eds.), Geology of tight gas reservoirs. Am. Assoc. Petrol. Geol. Studies in Geology, 24, 253-269.

Laws, R.A., 1989 - Preface. In: B.J. O'Neil (ed.), The Cooper and Eromanga Basins, Australia. Proceedings of the Cooper and Eromanga Basins Conference, Adelaide, 26-27 June 1989, v-vi.

Lebedew, W.C., Owsjannikov, W.M., Mogilewskij, G.A. & Bogdanow, W.M., 1969 - Fraktionierung der Kohlenstoffisotope durch mikrobiologische Prozesse in der biochemischen Zone. Z. Angew. Geol., 15, 621-624.

Lécolle, M. & Roger, G., 1976 - Métamorphisme regional hercynien de 'faible degrèe' dans la province pyrito-cuprifère de Huelva (Espagne). Consequences petrologiques. Soc. Geol. France Bull., Ser.7, 18 (6), 1687-1698.

Leeder, M.R., 1973 - Sedimentology and palaeogeography of the Upper Old Red Sandstone in the Scottish Border Basin. Scott. J. Geol., 9, 117-144.

Leeder, M.R., 1978 - A quantitative stratigraphic model for alluvium, with special reference to channel deposit density and interconnectedness. In: A.D. Miall (ed.), Fluvial sedimentology: Canadian Soc. Pet. Geol. Memoir 5, 587-596.

Lerman, A., 1979 - Geochemical processes, water and sediment environments. J. Wiley and Sons, Toronto. 220p.

Lindner, A.W., 1986 - Oil and gas developments in Australia in 1985. Am. Assoc. Petrol. Geol. Bull., 70 (10), 1611-1624.

Livingstone, D.A., 1963 - Data on geochemistry: chemical composition of rivers and lakes. U.S. Geol.. Surv. Prof. Paper, 440-G, 64p.

Lombardi, G. & Sheppard, S.M.F., 1977 - Petrographic and isotope studies of the altered acid volcanics of the Tolfa-Cerite area, Italy: The genesis of the clays. Clay Minerals, 12, 147-161.

Long, M., 1977 - Infill drilling expands in New Mexico. Oil & Gas J., March 21, 62-63.

Loucks, R.G., Dodge, M.M. & Galloway, W.E., 1984 - Regional controls on diagenesis and reservoir quality in Lower Tertiary sandstones along the Texas Gulf Coast. In: D.A. McDonald & R.C. Surdam (eds.), Clastic Diagenesis. Part 2. Aspects of Porosity Modification. Am. Assoc. Petrol. Geol. Mem., 37, 15-45.

Loughnan, P.F. & Roberts, F.I., 1986 - Dickite- and kaolinite-bearing sandstones and conglomerates in Illawarra Coal Measures of the Sydney Basin, New South Wales. Aust. J. Earth Sci., 33, 325-332.

Lowenstam, H.A., 1964 - Palaeotemperatures of the Permian and Cretaceous Periods. In: A.E.M. Nairn (ed.), Problems in palaeoclimatology. Interscience, London, 227-248.

Lundegard, P.D. & Land, L.T., 1986 - Carbon dioxide and organic acids: their role in porosity enhancement and cementation, Palaeogene of the Texas Gulf Coast. In: D.L. Gautier (ed.), Roles of organic matter in sediment diagenesis. Soc. Econ. Palaeontologists and Mineralogists Spec. Publ., 38, 129-146.

Lyon, G.L. & Hulston, J.R., 1984 - Carbon and hydrogen isotopic compositions of New Zealand geothermal gases. Geochim. Cosmochim. Acta, 48, 1161-1171.

Magara, K., 1976 - Water expulsion from clastic sediments during compaction, direction and volumes. Am. Assoc. Petrol. Geol. Bull., 60, 543-553.

Magara, K., 1981 - Fluid dynamics for cap-rock formation in the Gulf Coast. Am. Assoc. Petrol. Geol. Bull., 65, 1334-1343.

Magus, D.J., Bratrud, T.F., Molnar, E.L. & Wiltshire, M.J., 1983 - Low permeability sandstones in Australia can be fracture stimulated. Aust. Pet. Explor. Assoc. J., 16 (2), 176-190.

Marshall, D.J., 1988 - Cathodoluminescence of geological materials. Unwin Hyman Boston, 146p.

Martin, C.A., 1967a - The Gidgealpa and Merrimelia Formations in the Cooper's Creek Basin. Aust. Oil & Gas J., 14 (2), 29-35.

Martin, C.A., 1967b - Moomba - a South Australian gas field. Aust. Pet. Explor. Assoc. J., 7 (2), 124-129.

Martin, K.R., 1980 - A preliminary account of diagenesis and reservoir quality in the Toolachee Formation, Cooper Basin. Unpubl. report, Santos Ltd. 22p.

Martin, K.R. & Hamilton, N.J., 1981 - Diagenesis and reservoi quality, Toolachee Formation, Cooper Basin. Aust. Pet. Explor. Assoc. J., 21, 143-154.

Masters, J.A., 1979 - Deep basin gas trap, western Canada. Am. Assoc. Petrol. Geol. Bull., 63 (2), 152 - 181.

Matsumoto, R. & Iijima, A., 1981 - Origin and diagenetic evolution of Ca-Mg-Fe carbonates in some coalfields of Japan. Sedimentol., 28, 239-259.

Matuszçzak, R.A., 1973a - Wattenberg Field, Denver Basin, Colorado. Mountain Geologist, 10 (3), 99-105.

Matuszçzak, R.A., 1973b - Wattenberg Field, Denver Basin, Colorado. Am. Assoc. Petrol. Geol. Mem. 24, 136-144.

Maxwell, J.C., 1964 - Influence of depth, temperature, and geologic age on porosity of quartzose sandstones. Am. Assoc. Petrol. Geol. Bull., 48 (5), 697.

May, H.M., Helmke, P.A. & Jackson, M.L., 1979 - Gibbsite solubility and thermodynamic properties of hydroxy-aluminium ions in aqeous solution at 25°C. Geochim. Cosmochim. Acta, 43, 861-868.

McBride, E.F., 1987 - Diagenesis of the Maxon Sandstone (Early Cretaceous), Marathon region, Texas: a diagenetic quartzarenite. J. Sediment. Petrol., 57, 98-107.

McBride, E.F., 1989 - Quartz cement in sandstones: a review. Earth Sci. Reviews, 26, 69-112.

McCrea, J.M., 1950 - On the isotopic chemistry of carbonates and a palaeotemperature scale. J. Chem. Phys., 18, 849-857.

McElhinny, M.W., 1969 - The palaeomagnetism of the Permian of southeast Australia and its significance regarding the problem of intercontinental correlation. Geol. Soc. Aust. Spec. Publ., 2, 61-67.

McKenzie, D., 1978 - Some remarks on the development of sedimentary basins. Earth Planet. Sci. Letters, 40, 25-32.

McKirdy, D.M., 1982a - Geochemical and isotopic correlation of six Mesozoic oils from the Eromanga/Cooper Basin. Unpubl. Amdel report F2187/83, Delhi Petroleum Pty. Ltd. 30p.

McKirdy, D.M., 1982b - Petroleum geochemistry and source-rock potential of the Cooper Basin and superjacent Eromanga Basin. Unpubl. report, Delhi Petroleum Pty. Ltd. 61p.

McKirdy, D.M., 1982c - Petroleum geochemistry and source-rock potential of the Arrowie, Pedirka, Cooper and Eromanga Basins, Central Australia. Unpubl. report, Delhi Petroleum Pty. Ltd. 61p.

McKirdy, D.M., 1982d - Aspects of the source rock and petroleum geochemistry of the Eromanga Basin. In: P.J. Moore & T.J. Mount (eds.), Eromanga Basin Symposium, Adelaide, 9th-11th November 1982, Geol. Soc. Aust. & Petrol. Expl. Soc. Aust. Spec. Publ., 258-259.

McKirdy, D.M., 1984 - Notes on the source affinity and thermal maturity of Eromanga Basin crude oils. Unpubl. report, Delhi Petroleum Pty. Ltd. 4p.

McKirdy, D.M., 1985 - Rapid evaluation of non-marine petroleum source rocks. National Energy Research Development and Demonstration Program, Project 261. End grant technical report. 36p.

McKirdy, D.M., 1987 - Oil correlation study, ATP 267P, Eromanga Basin, Queensland. Unpubl. Amdel report F6473/87 for Pancontinental Petroleum Ltd. 45p.

McKirdy, D.M., 1989 - Geochemistry of oils and condensates associated with CO_2-rich natural gas in the Otway and Cooper Basins. CSIRO Marine Laboratories, 1989 Australian Organic Geochemistry Conference, April 13-14, Hobart, Tasmania [abstract].

Menhennitt, C.E., 1985 - Diagenesis and its influence on the reservoir sandstones of the Jackson Oilfield. Unpubl. B.Sc. (Hons.) thesis, Department of Earth Sciences, Monash University, Australia. 112p.

Meszoly, G.F.J., Bodard, J.M. & Wall, V.J., 1986 - Diagenesis and porosity in the Eastern View Group, Bass Basin. In: R.C. Glenie (ed.), Second south-eastern Australia oil exploration symposium. Petrol. Expl. Soc. Austr. Spec. Publ., 303-313.

Miall, A.D., 1977 - A review of the braided river depositional environment. Earth Sci. Review, 13 (1), 1-62.

Miall, A.D. (ed.), 1978 - Fluvial sedimentology. Canadian Soc. Pet. Geologists, Calgary, Alberta. 859p.

Miall, A.D., 1984 - Deltas. In: R.G. Walker (ed.), Facies models, Geosci. Canada, Reprint Series 1, 105-118.

Michaels, A.S. & Lin, C.S., 1954 - Permeability of kaolinite. Ind. Eng. Chemistry, 46 (6), 1239-1246.

Michaelsen, B.H. & McKirdy, D.M., 1989 - Organic facies and petroleum geochemistry of the lacustrine Murta Member (Mooga Formation) in the Eromanga Basin, Australia. In: B.J. O'Neil (ed.), q.v., 541-558.

Middleton, M.F., 1979 - Heat flow in the Moomba, Big Lake and Toolachee Gas Fields of the Cooper Basin and implications for hydrocarbon maturation. Aust. Soc. Explor. Geophys. Bull., 10 (2), 149-155.

Middleton, M.F., 1980 - A model of intracratonic basin formation, entailing deep crustal metamorphism. Geophys. J. Royal Astr. Soc., 62, 1-14.

Middleton, M.F. & Boardman, M.H., 1983 - Tartulla - case history of a Permian discovery. Geol. Soc. Aust. & Geol. Sur. Queensl., Proc. Symp. on the Permian Geology of Queensland, Brisbane 14-16th July, 1982, 335-342.

Middleton, M.F. & Hunt, J.W., 1988 - Influence of tectonics on Permian coal rank patterns in Australia. Unpubl. report for Cooper Basin Consortium Group of Companies, 14p.

Milliken, K.L., Land, L.S. & Loucks, R.G., 1981 - History and burial diagenesis determined from isotope geochemistry, Frio Formation, Brazoria County, Texas. Am. Assoc. Petrol. Geol. Bull. , 65 (8), 1397-1413.

Moore, P.S. & Castro, C., 1984 - Petroleum exploration in fluvio-lacustrine sequences, with examples from the Cooper and Eromanga Basins. Unpubl. report, Delhi Petroleum Pty. Ltd., 19p.

Moore, P.S. & Pitt, G.M., 1984 - Cretaceous of the Eromanga Basin - implications for hydrocarbon exploration. Aust. Pet. Explor. Assoc. J., 358-376.

Morad, S. & Aldahan, A.A., 1987a - Diagenetic replacement of feldspars by quartz in sandstones. J. Sediment. Petrol., 57, 488-493.

Morad, S. & Aldahan, A.A., 1987b - A SEM study of diagenetic kaolinitization and illitization of detrital feldspars in sandstones. Clay Minerals, 22, 237-243.

Morton, J.G.G., 1989 - Petrophysics of Cooper Basin reservoirs in South Australia. In: B.J. O'Neil (ed.), q.v., 153-163.

Morton, J., 1990 - A reply to Porter's review. Petr. Expl. Soc. Aust. Jour., 16, 39-41.

Mount, T.J., 1982 - Geology of the Dullingari Murta Oilfield. In: P.S. Moore & T.J. Mount (eds.), Eromanga Basin Symposium Summary Papers. Eromanga Basin Symposium, Petrol. Expl. Soc. Austr. & Geol. Soc. Aust., Adelaide 9-11th November, 1982, 356-375.

Mozely, P.S., 1989 - Complex compositional zonation in concretionary siderite: implications for geochemical studies. J. Sediment. Petrol., 59, 815-818.

Münnich, K.O. & Vogel, J.C., 1959 - C^{14}-Altersbestimmung von Süsswasser-Kalkablagerungen. Naturw., 46 (5), 168-169.

Nelson, R.A., 1981 - Significance of fracture sets associated with stylolite zones. Am. Assoc. Petrol. Geol. Bull. , 65, 2417-2425.

Nickel, E., 1978 - The present status of cathode luminescence as a tool in sedimentology. Minerals Sci. Eng., 10, 73-100.

Norton, C., 1985 - The comparison of gas compositions throughout the South Australian portion of the Cooper Basin and the relationship to thermal regimes. Unpubl. report, Santos Ltd., 58p.

Nugent, O.W., 1969 - Sedimentation and petroleum potential of the Jurassic sequence in the southwestern Great Artesian Basin. Aust. Pet. Explor. Assoc. J., 9 (2), 97-107.

Oana, S. & Deevey, E.S., 1960 - Carbon-13 in lake waters and its possible bearing on palaeolimnology. Am. J. Sci., 235A, 253-272.

O'Driscoll, E.S.T., 1983 - Deep tectonic foundations of the Eromanga Basin. Aust. Pet. Explor. Assoc. J., 23 (1), 5-17.

Oehler, D.Z. & Sternberg, B.K., 1984 - Seepage-induced anomalies, "false" anomalies, and implications for electrical prospecting. Am. Assoc. Petrol. Geol. Bull., 68, 1121-1145.

O'Neil, B.J. (ed.), 1989 - The Cooper and Eromanga Basins, Australia. Proceedings of the Cooper and Eromanga Basins Conference, Adelaide, 26-27 June 1989: Petroleum Exploration Society of Australia, Society of Petroleum Engineers, Australian Society of Exploration Geophysicists (S.A. branches), 664p.

O'Shea, K.J. & Frape, S.K., 1988 - Authigenic illite in the Lower Silurian Cataract Group sandstones of Southern Ontario. Bull. Canadian Pet. Geol., 36, 153-167.

Papalia, N., 1969 - The Nappamerri Formation. Aust. Pet. Explor. Assoc. J., 9 (2), 108-110.

Passmore, V.L., 1989 - Petroleum accumulations of the Eromanga Basin: a comparison with other Australian Mesozoic accumululations. In: B.J. O'Neil (ed.), q.v., 371-389.

Paten, R.J., 1969 - Palynologic contributions to petroleum exploration in Permian formations of the Cooper Basin. Aust. Pet. Explor. Assoc. J., 9 (1), 79-87.

Paton, I.M. & Zwigulis, M., 1988 - The Merrimelia Field - a Cooper Basin case history. Petroleum in Australia: the first century. Aust. Petrol. Expl. Assoc. Spec. Publ., 139-151.

Payne, J.N., 1968 - Hydrological significance of the lithofacies of the Sparta sand in Arkansas, Louisiana, Mississippi and Texas. Geol. Surv., Prof. Pap. 569, C1-C17.

Pearson, F.J. & Hanshaw, B.B., 1970 - Sources of dissolved carbonate in ground water and their effects on carbon-14 dating. In: Isotope Hydrology, International Atomic Energy Agency, Vienna, 271-286.

Pearson, M.J. & Small, J.S., 1988 - Illite-smectite diagenesis and palaeotemperatures in northern North Sea Quarternary to Mesozoic shale sequences. Clay Minerals, 23, 109-132.

Pecanek, H.T. & Paton, I.M., 1984 - The Development of the Tirrawarra Oil and Gas Field. Aust. Pet. Explor. Assoc. J., 24 (1), 278-88.

Perry, E.A., 1974 - Diagenesis and the K/Ar dating of shales and clay minerals. Geol. Soc. Amer. Bull., 85, 827-830.

Perry, E.A. & Hower, J., 1970 - Burial diagenesis in Gulf Coast pelitic sediments. Clays & Clay Minerals, 18, 165-177.

Pettijohn, F.J., Potter, P.E. & Siever, R., 1972 - Sand and sandstone. Springer-Verlag, Berlin, 617p.

Philp, R.P., Gilbert, T.D. & Friedrich, J., 1981 - Bicyclic sequiterpenoids and diterpenoids in Australian crude oils. Geochim. Cosmochim. Acta, 45, 1173-80.

Pianalto, E.I., 1985 - The Tirrawarra oil and gas field, Cooper Basin, South Australia. Postdepositional evolution and reservoir quality. Unpubl. B.Sc. (Hons.) thesis, Department of Earth Sciences, Monash University, Australia. 93p.

Pinchin, J. & Bayly, M., 1989 - Lateral changes in seismic velocities and their effect on depth prediction. In: O'Neil, B.J. (ed.), q.v., 197-203.

Pitman, J.K., Fouch, T.D. & Goldhaber, M.B., 1982 - Depositional setting and diagenetic evolution of some Tertiary unconventional reservoir rocks, Uinta Basin, Utah. Am. Assoc. Petrol. Geol. Bull., 66, 1581-1596.

Pitt, G.M., 1986 - Geothermal gradients, geothermal histories and the timing of thermal maturation in the Eromanga-Cooper Basins. In: Gravestock, D.I., Moore, P.S. & Pitt, G.M. (eds.), Contributions to the geology and hydrocarbon potential of the Eromanga Basin. Geol. Soc. Aust. Spec. Publ., 12, 323-351.

Pittman, E.D., 1979 - Porosity, diagenesis and productive capability of sandstone reservoirs. In: P.A. Scholle & P.R. Schluger (eds.), Aspects of diagenesis. Soc. Econ. Palaeontologists and Mineralogists Spec. Publ. 26, 159-173.

Pittman, E.D., 1989 - Problems related to clay minerals in reservoir sandstones. In: J.F. Mason & P.A. Dickey (eds.), Oil field development techniques. Proceedings of the Daqing International Meeting, 1982. Am. Assoc. Petrol. Geol. Studies in Geology, 28, 237-244.

Pittman, E.D. & King, G.E., 1986 - Petrology and formation damage control, Upper Cretaceous sandstone, offshore Gabon. Clay Minerals, 21, 781-790.

Pollard, J.E., 1988 - Trace fossils in coal-bearing sequences. J. Geol. Soc. London, 145, 339-350.

Porter, C.R., 1973 - Comments - isosalinity maps, Cooper Basin, South Australia. Unpublished report for Delhi International Oil Corp., 4p.

Porter, C.R., 1974 - Permian waters of the Cooper Basin: their salinity, composition, genetic characteristics. Unpubl. report, Santos Ltd., 37p.

Porter, C.R., 1976 - An empirical approach to the determination of porosity, shale percentage, and permeability of Permian sandstones in the Cooper Basin, South Australia. Aust. Pet. Explor. Assoc. J., 16 (1), 111-115.

Porter, C.R., 1990 - A review of 'Petrophysics of Cooper Basin Reservoirs in South Australia'. Pet. Explor. Soc. Aust. J., 16, 37-38.

Porter, C.R. & Crocker, H., 1972 - Petrophysics of the Cooper Basin, South Australia. Aust. Pet. Explor. Assoc. J., 12 (1), 23-27.

Postma, D., 1977 - The occurrence and chemical composition of recent Fe-rich mixed carbonates in a river bog. J. Sediment. Petrol., 47 (3), 1089-1098.

Postma, D., 1981 - Formation of siderite and vivianite and the pore-water composition of a recent bog sediment in Denmark. Chem.Geology, 31, 225-244.

Postma, D., 1982 - Pyrite and siderite formation in brackish and freshwater swamp sediments. Amer. J. Sci., 282, 1151-1183.

Powell, C.McA. & Veevers, J.J., 1987 - Namurian uplift in Australia and South America triggered the main Gondwana glaciation. Nature, 326, 177-179.

Powell, T.G. & McKirdy, D.M., 1972 - The geochemical characterisation of Australian crude oils. Aust. Pet. Explor. Assoc. J., 12 (1), 125-31.

Powell, T.G. & McKirdy, D.M., 1973 - Relationship between ratio of pristane to phytane, crude oil composition and geological environment in Australia. Nature Phys. Sci., 243, 37-39.

Powell, T.G. & McKirdy, D.M., 1975 - Geologic factors controlling crude oil composition in Australia and Papua New Guinea. Am. Assoc. Petrol. Geol. Bull., 59, 1176-97.

Powell, T.G. & McKirdy, D.M., 1976 - Geochemical character of crude oils from Australia and Papua New Guinea. In: R.B. Leslie, H.J. Evans & C.L. Knight (eds.), Economic geology of Australia and Papua New Guinea - 3. Petroleum. Aust. Inst. Min. Metall., Monograph 7, 18-29.

Powis, G.D., 1989 - Revision of Triassic stratigraphy at the Cooper Basin to Eromanga Basin transition. In: B.J. O'Neil (ed.), q.v., 265-277.

Price, P.L., 1973 - Cooper Basin palynology. Mines Administration Pty. Ltd., palynological report No. 13-95 (unpubl.). 23p.

Prikryl, J.D., Posey, H.H. & Kyle, J.R., 1988 - A petrographic and geochemical model for origin of calcite cap rock at Damon Mound Salt Dome, Texas, U.S.A. Chem. Geology, 74, 67-97.

Pritchard, R.L.A., 1973 - History of Mesaverde development in the San Juan Basin. In: Cretaceous and Tertiary rocks of the southern Colorado Plateau. Four Corners Geol. Soc. Guidebook, 174-177.

Pye, K., 1984 - SEM analysis of siderite cements in intertidal marsh sediments, Norfolk, England. Marine Geology, 56, 1-12.

Pyecroft, M., 1973 - The Della Field, Cooper Basin, South Australia. Aust. Pet. Explor. Assoc. J., 13 (1), 58-67.

Ramseyer, K., Baumann, J., Matter, A. & Mullis, J., 1988 - Cathodoluminescence colours of alpha-quartz. Mineral. Mag., 52, 669-677.

Randal, M.A., 1978 - Hydrogeology of the southeastern Georgina Basin and environs, Queensland and Northern Territory. Geol. Surv. Qsld Publ. 366, 116p.

Randel, M.A., 1983 - Petroleum exploration in Permian Basins - history and future trends. In: Permian Geology of Queensland, Proceedings, Geol. Soc. Aust., Queensland Division, Australia, 33-42.

Ranganathan, V. & Tye, R.S., 1986 - Petreography, diagenesis, and facies controls on porosity in Shannon Sandstone, Hartzog Draw Field, Wyoming. Am. Assoc. Petrol. Geol. Bull., 70 (1), 56-69.

Rao, C.P., 1981 - Cold-water carbonates: Recent, last glacial and Permian Tasmanian examples. In: Sediments through the ages. 5th Australian Geological Convention, Perth 1981, Geol. Soc. Aust., p.56 [abstract].

Read, W.A. & Dean, J.M., 1982 - Quantitative relationships between numbers of fluvial cycles, bulk lithological composition and net subsidence in a Scottish Namurian basin. Sedimentol., 29, 181-200.

Reading, H.G., 1978 - Sedimentary environments and facies. Blackwell Scientific Publications, Oxford. 557p.

Reed, B.L. & Hemley, J.J., 1966 - Occurrences of pyrophyllite in the Kekiktuk conglomerate, Brooks Range, Northeast Alaska. U. S. Geol. Surv. Prof. Paper 550-C, p. 162-166.

Rider, M.H., 1986 - The geological interpretation of well logs. John Wiley & Sons, New York, 175p.

Rigby, D. & Smith, J.W., 1981 - An isotopic study of gases and hydrocarbons in the Cooper Basin. Aust. Pet. Explor. Assoc. J., 21 (1), 222-229.

Rightmire, C.T. & Hanshaw, B.B., 1973 - Relation between the carbon isotope composition of soil-CO_2 and dissolved carbonate species in groundwater. Water Resour. Res., 9, 958-967.

Ritger, S., Carson, B. & Suess, E., 1987 - Methane-derived authigenic carbonates formed by subduction-induced pore-water expulsion along the Oregon/Washington margin. Geol. Soc. Amer. Bull., 98, 147-156.

Roberts, D.C., Carroll, P.G. & Sayers, J., 1990 - The Kalladeina Formation - a Warburton Basin Cambrian carbonate play. Aust. Pet. Explor. Assoc. J., 30 (1), 166-183.

Rosenbaum, J. & Sheppard, S.M.F., 1986 - An isotopic study of siderites, dolomites and ankerites at high temperatures. Geochim. Cosmochim. Acta, 50, 1147-1150.

Russell, N.J. & Bone, Y., 1989 - Palaeogeothermometry of the Cooper and Eromanga Basins, South Australia. In: O'Neil, B.J. (ed.), q.v., 559-581.

Sackett, W.M., 1964 - The depositional history and isotopic carbon composition of marine sediments. Marine Geology, 2, 173-185.

Salter, G.B., 1989 - The role of fracture stimulation in the development of the Tirrawarra Field. In: B.J. O'Neil (ed.), q.v., 131-137.

Sansome, A., 1988 - A review of the reservoir sands, Patchawarra Formation in the Daralingie Field area, southern Cooper Basin, South Australia. Unpubl. B.Sc. (Hons.) thesis, National Centre for Petroleum Geology & Geophysics, University of Adelaide, Australia. 43p.

Sarkisyan, S.G., 1972 - Origin of authigenic clay minerals and their significance in petroleum geology. Sediment. Geol., 7, 1-22.

Sass, J.H. & Lachenbruch, A.H., 1979 - Thermal regime of the Australian continental crust. In: M.W. McElhinny (ed.), The earth - its origin, structure and evolution. London, Academic Press, 301-351.

Schmidt, V., McDonald, D.A. & Platt, R.L., 1977 - Pore geometry and reservoir aspects of secondary porosity in sandstones. Canadian Pet. Geol. Bull., 25, 271-290.

Schmidt, V. & McDonald, D.A., 1979a - The role of secondary porosity in the course of sandstone diagenesis. Soc. Econ. Palaeontologists and Mineralogists Spec. Pub. 26, 175-208.

Schmidt, V. & McDonald, D.A., 1979b - Texture and recognition of secondary porosity in sandstones. Soc. Econ. Palaeontologists and Mineralogists Spec. Publ., 26, 209-225.

Schneeflock, R., 1978 - Permeability traps in Gatchell (Eocene) Sand of California. Am. Assoc. Petrol. Geol. Bull., 62 (5), 848-853.

Scholefield, T., 1983 - Carbonate investigation of the Mooga Formation (Namur Sandstone Member) in the Merrimelia Field, Eromanga Basin. Unpubl. report, S. Aust. Dept. Mines and Energy. 45p.

Scholefield, T., 1989 - The stratigraphy and hydrocarbon potential of the northern Eromanga Basin. In: B.J. O'Neil (ed.), q.v., 417-427.

Schulz-Rojahn, J.P. & Phillips, S.E., 1989 - Diagenetic alteration of Permian reservoir sandstones in the Nappamerri Trough and adjacent areas, southern Cooper Basin. In: B.J. O'Neil (ed.), q.v., 629-645.

Schulz-Rojahn, J.P., 1990 - Oxygen isotopic investigation of quartz cement in Permian sandstones of the Cooper Basin in relation to tectonic activity and sedimentation. Unpubl. ARC Research Proposal, Department of Geology & Geophysics, University of Adelaide, Australia. 8p.

Schulz-Rojahn, J.P., Alsop, D., Eleftheriou, J., Thomas, A., Farrow, B., Lemon, N., Phillips, S.E. & Stuart, W.J., 1991 - Diagenetic reservoir evaluation, southern Cooper Basin. In: Exploration in a Changing Environment. Austr. Soc. Expl. Geophys. 8th Conference & Geol. Soc. Aust. Expl. Symp., Sydney 1991, No. 30, p. 180 [abstract].

Schulz-Rojahn, J.P. & Stuart, W.J., 1991 - Controls on porosity and permeability distribution in the southern Cooper Basin, Australia: Implications for petroleum exploration. Am. Assoc. Petrol. Geol., Abstracts 75th Anniversay 1991 Annual Convention, Dallas, Texas, April 7-10, p.204 [abstract].

Schwebel, D.A., Devine, S.B. & Riley, M., 1980 - Source maturity and gas composition relationships in the southern Cooper Basin. Aust. Pet. Explor. Assoc. J., 20 (1), 191-200.

Schwertmann, U., Carlson, L. & Murad, E., 1987 - Properties of iron oxides in two finnish lakes in relation to the environment of their formation. Clays & Clay Minerals, 35, 297-304.

Scott, G.L., Brannigan, J.P. & Mitchell, S.T., 1983 - Pecos Slope Abo Field of Chaves County, New Mexico. Roswell Geological Society and New Mexico Bureau of Mines and Mineral Resources. Guidebook for field trip to the Abo red beds (Permian), central and south-central New Mexico, p.73.

Selley, R.C., 1978 - Porosity gradients in North Sea oil-bearing sandstones. J. Geol. Soc. London, 135, 119-132.

Senior, B.R. & Habermehl, M.A., 1980 - Structure, hydrodynamics and hydrocarbon potential, central Eromanga Basin, Queensland, Australia. BMR J. Aust. Geol. Geophys., 5, 47-55.

Senior, B.R., Mond, A. & Harrison, P.L., 1978 - Geology of the Eromanga Basin. BMR Bull. 167. 102p.

Serra, O., 1979 - Diagraphies différées. Bases de l'interprétation. Tome 1: Acquisition des données diagraphiques. Bull. Centre Rech. Expl.-Prod. Elf Aquitaine, Mem.1, Technip, Paris, 328p.

Serra, O., 1985 - Sedimentary environments from wireline logs. Schlumberger, 211p.

Shibaoka, M., Bennett, A.J.R. & Gould, K.W., 1973 - Diagenesis of organic matter and occurrence of hydrocarbons in some Australian sedimentary basins. Aust. Pet. Explor. Assoc. J., 13, 73-80.

Shibaoka, M., Saxby, J.D. & Taylor, G.H., 1978 - Hydrocarbon generation in Gippsland Basin, Australia - comparison with Cooper Basin, Australia. Am. Assoc. Petrol. Geol. Bull. , 62 (7), 1151-58.

Sibley, D.F. & Blatt, H., 1976 - Intergranular pressure solution and cementation of the Tuscarora orthoquartzite. J. Sediment. Petrol., 46, 881-896.

Sibson, R.H., Moore, J.McM. & Rankin, A.H., 1975 - Seismic pumping - a hydrothermal fluid transport mechanism. J. Geol. Soc. London,131, 653-659.

Siegel, D.I., Chamberlain, S.C. & Dossert, W.P., 1987 - The isotopic and chemical evolution of mineralization in septarian concretions: Evidence for episodic palaeohydrogeologic methanogenesis. Geol. Soc. Amer. Bull., 99, 385-394.

Siever, R., 1959 - Petrology and geochemistry od silica cementation in some Pennsylvanian sandstones. In: H.A. Ireland (Ed.), Silica in sediments. Soc. Econ. Palaeontologists and Mineralogists Spec. Publ., 7, 55-79.

Siever, R., 1962 - Silica solubility, 0-200 °C, and the diagenesis of siliceous sediments. J. Geology, 70, 127-150.

Siever, R., 1979 - Plate tectonics and sandstone diagenesis. J. Geology, 87, 127-155.

Silverman, S.R., 1964 - Investigations of petroleum origin and evolution mechanisms by carbon isotope studies. In: Isotopic and cosmic chemistry: Amsterdam, North-Holland Publishing Co., 92-102.

Silverman, S.R. & Epstein, S., 1958 - Carbon-isotopic compositions of petroleums and other sedimentary organic materials. Am. Assoc. Petrol. Geol. Bull., 42 (5), 998-1012.

Smale, D. & Trueman, N.A., 1965 - The mineralogy and petrology of the Permian sandstones at Gidgealpa, South Australia. Aust. Pet. Explor. Assoc. J., 5, 152-158.

Smith, J.T. & Ehrenberg, S.N., 1989 - Correlation of carbon dioxide abundance with temperature in clastic hydrocarbon reservoirs: relationship to inorganic chemical equilibrium. Mar. Pet. Geol., 6 (2), 129-136.

Smith, J.W., 1978 - Carbonates: a guide to hydrocarbons. J. Geochem. Explor., 10, 103-107.

Smith, J.W. & Gould, K.W., 1980 - An isotopic study of the role of carbon dioxide in outbursts in coal mines. J. Geochemistry, 14, 27-32.

Smith, J.W., Rigby, D., Schmidt, P.W. & Clark, D.A., 1983 - D/H ratios of coals and the palaeolatitude of their deposition. Nature, 302, 322-323.

Smyth, M., 1979 - Hydrocarbon generation in the Fly Lake-Brolga area of the Cooper Basin. Aust. Pet. Explor. Assoc. J., 19 (1), 108-114.

Smyth, M., 1983 - Nature of source material for hydrocarbons in Cooper Basin, Australia. Am. Assoc. Petrol. Geol. Bull., 67 (9), 1422-1428.

Sommer, F., 1978 - Diagenesis of Jurassic sandstones in the Viking Graben. J. Geol. Soc. London, 135, 63-67.

Spencer, C.W., 1985 - Geologic aspects of tight gas reservoirs in the Rocky Mountain Region. J. Petrol. Technology, July 1985, 1308-1314.

Spencer, C.W., 1989 - Review of characteristics of low-permeability gas reservoirs in Western United States. Am. Assoc. Petrol. Geol. Bull., 73 (5), 613-629.

Sprigg, R.C., 1958 - Petroleum prospects of western parts of Great Australian Artesian Basin. Bull. Am. Assoc. Petrol. Geol. Bull., 42, 2465-2491.

Sprigg, R.C., 1961 - On the structural evolution of the Great Artesian Basin. Aust. Pet. Explor. Assoc. J., 1, 37-56.

Sprigg, R.C., 1966 - Palaeogeography of the Australian Permian in relation to oil search. Aust. Pet. Explor. Assoc. J., 6, 17-29.

Sprunt, E.S., 1981 - Causes of quartz luminescence colors. Scanning Electron Microscopy, 1, 525-535.

Srodon, J. & Eberl, D.D., 1984 - Illite. In: S.W. Bailey (ed.), Micas. Reviews in Mineralogy, 13, 495-544.

Stahl, W.J., 1977 - Carbon and nitrogen isotopes in hydrocarbon research and exploration. Chem. Geology, 20, 121-149.

Stahl, W.J. & Carey, B.D., 1975 - Source-rock identification by isotope analyses of natural gases from fields in the Val Verde and Delaware Basins, West Texas. Chem. Geology, 16, 257-267.

Stanley, D.J. & Halliday, G., 1984 - Massive hydraulic fracture stimulation of Early Permian gas reservoirs, Big Lake Field, Cooper Basin. Aust. Pet. Explor. Assoc. J., 24 (1), 180-195.

Stanmore, P.J., 1989 - Case studies of stratigraphic and fault traps in the Cooper Basin, Australia. In: B.J. O'Neil (ed.), q.v., 361-369.

Stanmore, P.J. & Johnstone, E.M., 1988 - The search for stratigraphic traps in the Southern Patchawarra Trough, South Australia. Aust. Pet. Explor. Assoc. J., 28 (1), 156-66.

Staughton, D.B., 1985 - The diagenetic history and reservoir quality evaluation of the Strzelecki hydrocarbon field, Cooper/Eromanga Basins, South Australia. Unpubl. B.Sc. (Hons.) thesis, Department of Earth Sciences, Monash University, Australia. 180p.

Stern, P.A., 1984 - The Merrimelia hydrocarbon field, Cooper-Eromanga Basins: diagenesis and reservoir evolution. Unpubl. B.Sc. (Hons.) thesis, Department of Earth Sciences, Monash University, Australia. 159p.

Stevens, G.R. & Clayton, R.N., 1971 - Oxygen isotope studies on Jurassic and Cretaceous belemnites from New Zealand and their biogeographic significance. New Zealand J. Geol. Geophys., 14, 829-897.

Steveson, B.G. & Spry, A.H., 1973 - Nature of porosity in some indurated Permian sandstones from the Cooper Basin. Aust. Pet. Explor. Assoc. J., 13 (1), 86-90.

Stuart, W.J., 1976 - The genesis of Permian and Lower Triassic reservoir sandstones during phases of southern Cooper Basin development. Aust. Pet. Explor. Assoc. J., 16 (1), 37-47.

Stuart, W.J., Kennedy, S. & Thomas, A.D., 1988 - Influence of structural growth and other factors on the configuration of fluviatile sandstones, Permian Cooper Basin. Aust. Pet. Explor. Assoc. J., 28 (1), 255-265.

Stuart, W.J., Farrow, B.B., Lemon, N.L. & Phillips, S.E., 1990 - Porosity and permeability in Permian sandstones: southern Cooper Basin. Final report, NERDDC Project No. 1175, National Centre for Petroleum Geology & Geophysics, University of Adelaide, Australia. 104p.

Sun, S.S. & Eadington, P.J., 1987 - Oxygen-isotope evidence for the mixing of magmatic and meteoric waters during tin mineralisation in the Mole Granite, New South Wales, Australia. Econ. Geology, 82, 43-52.

Taylor, G.H., Liu, S.Y. & Smyth, M., 1988 - New light on the origin of Cooper Basin oil. Aust. Pet. Explor. Assoc. J., 28 (1), 303-9.

Taylor, G.H., Liu, S.Y. & Diessel, C.F.K., 1989 - The cold-climate origin of inertinite-rich Gondwana coals. Int. J. Coal Geology, 11, 1-22.

Taylor, S., Solomon, G., Tupper, N., Evanochko, J., Horton, G., Waldeck, R. & Phillips, S., 1991 - Flank plays and faulted basement: new directions for the Cooper Basin. Aust. Pet. Explor. Assoc. J., 31 (1), 56-73.

Thomas, A., 1990 - The diagenesis of Permian arenaceous and argillaceous units in the Moomba Gas Field, southern Cooper Basin, South Australia. Unpubl. Masters thesis, University of Adelaide, Australia. 161p.

Thomas, B.M., 1982 - Land plant source rocks for oil and their significance in Australian basins. Aust. Pet. Explor. Assoc. J., 22 (1), 164-178.

Thomas, J.B., 1981 - Classification and diagenesis of clay minerals in tight gas sandstones: case studies in which clay mineral properties are crucial to drilling fluid selection, formation evaluation and completion techniques. In: F.J. Longstaffe (ed.), Short course in clays and the resource geologist. Mineral. Ass. Canada Short Course, Calgary 1981, 104-118.

Thomas, R.D. & Ward, D.C., 1972 - Effect of overburden pressure and water saturation on gas permeability of tight sandstone cores. J. Petrol. Technology, February 1972, 120-124.

Thompson, A.B., 1970 - A note on the kaolinite-pyrophyllite equilibrium. Amer. J. Sci., 268, 454-458.

Thornton, R.C.N., 1973 - Lithofacies study on the Toolachee Formation. Gidgealpa-Moomba-Big Lake area, Cooper Basin, South Australia. Aust. Pet. Explor. Assoc. J., 13 (1), 41-48.

Thornton, R.C.N., 1978 - Regional lithofacies and palaeogeography of the Gidgealpa Group. Aust. Pet. Explor. Assoc. J., 18, 52-63.

Thornton, R.C.N., 1979 - Regional stratigraphic analysis of the Gidgealpa Group, Southern Cooper Basin, Australia. Geol. Surv. S. Aust. Bull. 49, 140p.

Tieh, T.T., Berg, R.R., Popp, R.K., Brasher, J.E. & Pike, J.D., 1986 - Deposition and diagenesis of Upper Miocene arkoses, Yowlumne and Rio Viejo Fields, Kern County, California. Am. Assoc. Petrol. Geol. Bull., 70 (8), 953-969.

Tissot, B.P. & Welte, D.H., 1978 - Petroleum formation and occurrence - a new approach to oil and gas exploration. Springer Verlag, Berlin, 538p.

Towe, K.M., 1962 - Clay mineral diagenesis as a possible source of silica cement in sedimentary rocks. J. Sediment. Petrol., 32, 26-28.

Trevena, A.S. & Clark, R.A., 1986 - Diagenesis of sandstone reservoirs of Pattani Basin, Gulf of Thailand. Am. Assoc. Petrol. Geol. Bull., 70 (3), 299-308.

Trigueiro, D., 1990 - Canadian find praised: basin theory works again. Am. Assoc. Petrol. Geol. Bull. Explorer, May 1990, p.40.

Tucker, M.E., 1981 - Sedimentary petrology: an introduction. Blackwell Scientific Publications, London, 252p.

Tupper, N.P. & Burckhardt, D.M., 1990 - Use of the methylphenanthrene index to characterise expulsion of Cooper and Eromanga Basin oils. Aust. Pet. Explor. Assoc. J., 30 (1), 373-385.

Usdowski, E., 1982 - Reactions and equilibria in the systems CO_2-H_2O and $CaCO_3$-CO_2-H_2O (O°-50°C) - a review. N. Jb. Miner. Abh. 144 (2), 148-171.

Van Krevelen, D.W. & Schuyer, J., 1957 - Coal science. Aspects of coal constitution. Elsevier, Amsterdam. 212p.

Veevers, J.J., 1984 - Phanerozoic earth history of Australia. Oxford Geological Science Series, Oxford University Press, New York, 418p.

Vegh, E., 1975 - Comparison between core and log (determined by C.R. Porter's method 1973) porosity and permeability in the Cooper Basin. Unpubl. report, Santos Ltd. 13p.

Velde, B. & Kornprobst, J., 1969 - Stabilité des silicates d'alumine hydrates. Contrib. Mineral. Petrol., 21, 63-74.

Velde, B. & Medhioub, M., 1988 - Approach to chemical equilibrium in diagenetic chlorites. Contrib. Mineral. Petrol., 98, 122-127.

Vincent, P.W., Mortimore, I.R. & McKirdy, D.M., 1985 - Hydrocarbon generation, migration and entrapment in the Jackson-Naccowlah area, ATP 259P, southwestern Queensland. Aust. Pet. Explor. Assoc. J., 25 (1), 62-84.

Von Engelhardt, W., 1967 - Interstitial solution and diagenesis in sediments. In: G. Larsen & G.V. Chilingar (Eds.), Diagenesis in sediments. Developments in Sedimentology, 8, Elsevier, Amsterdam, 503-522.

Walker, R.G. & Cant, D.J., 1984 - Sandy fluvial systems. In: R.G. Walker (ed.), Facies models. Geosci. Canada, Reprint Series 1, 71-89.

Walker, T.R., 1960 - Carbonate replacement of detrital crystalline silicate minerals as a source of authigenic silica in sedimentary rocks. Geol. Soc. Amer. Bull., 71, 145-152.

Wall, V.J., 1987 - Hydrocarbon reservoir quality in the Cooper/Eromanga Basins. Final report, NERDDC Project No. 808 (ref.84/4067). Department of Earth Sciences, Monash University, Australia. 129p.

Walls, J.D., Nur, A.M. & Bourbie, T., 1982 - Effects of pressure and partial water saturation on gas permeability in tight sands: experimental results. J. Petrol. Technology, April 1982, 930-936.

Walsh, R.N.E., 1985 - Depositional and diagenetic controls on porosity distribution in the Gidgealpa Group: Gidgealpa Field, Cooper Basin, South Australia. Unpubl. B.Sc. (Hons.) thesis, Department of Earth Sciences, Monash University, Australia. 119p.

Watts, A.B., Karner, G.D. & Steckler, M.S., 1982 - Lithospheric flexure and the evolution of sedimentary basins. Phil. Trans. Royal Soc. London, A305, 249-281.

Weaver, C.E. & Pollard, L.D., 1973 - The chemistry of clay minerals. Developments in Sedimentology, 15. Elsevier Sci. Publ. Company, Amsterdam. 213p.

Webb, A.W., 1974 - Geochronology of stratigraphically significant rocks from South Australia. Unpubl. progress report 7. S. Aust. Dept. Mines and Energy Open File Env. 1689, 5p.

Wescott, W.A., 1983 - Diagenesis of Cotton Valley Sandstone (Upper Jurassic), East Texas: Implications for tight gas formation pay recognition. Am. Assoc. Petrol. Geol. Bull., 67 (6), 1002-1013.

Wieland, B., 1979 - Zur Diagenese und schwachen Metamorphose eozäner siderolithischer Gesteine des Helvetikums. Schweiz. Mineral. Petrogr. Mitt., 59, 41-66.

Wild, E.K., 1987 - The sedimentology and reservoir quality of the Kinnerton Sandstone Formation, U.K. and the Tirrawarra Sandstone, S.Australia. Unpubl. Ph.D. thesis, Department of Geology, University of Bristol, England (2 volumes).

Willey, J.D., 1974 - The effect of pressure on the solubility of amorphous silica in seawater at 0 °C: Marine Chemistry, 2, 239-250.

Williams, B.P.J. & Wild, E.K., 1984a - The Tirrawarra Sandstone and Merrimelia Formation of the southern Cooper Basin, South Australia - the sedimentation and evolution of a glaciofluvial system. Aust. Pet. Explor. Assoc. J., 24 (1), 377-392.

Williams, B.P.J. & Wild, E.K., 1984b - Late Carboniferous-Early Permian sandstone reservoir facies analysis in hydrocarbon exploration of the Gidgealpa Group, southern Cooper Basin. Geol. Soc. Aust. Abstracts, 7th Australian Geological Convention, Sydney, 12, 553.

Williams, B.P.J., Wild, E.K. & Suttill, R.J., 1985 - Paraglacial aeolianites: potential new hydrocarbon reservoirs, Gidegalpa Group, southern Cooper Basin. Aust. Pet. Explor. Assoc. J., 25 (1), 291-310.

Wiltshire, M.J., 1989 - Mesozoic stratigraphy and palaeogeography, eastern Australia. In: B.J. O'Neil (ed.), q.v., 279-291.

Winkler, H.G.F., 1964 - Das P-T Feld der Diagenese und niedrigtemperierten Metamorphose aufgrund von Mineralreaktionen. Beitr. Mineral. Petrol., 10, 70-93.

Winkler, H.G.F., 1965 - Die Genese der metamorphen Gesteine. Springer Verlag, Berlin, 218p.

Winkler, H.G.F., 1970 - Abolition of metamorphic facies, introduction of the four divisions of metamorphic stage, and of a classification based on isograds in common rocks. Neues Jahrbuch Mineralogie Monatsh., 5, 189-248.

Winkler, H.G.F., 1979 - Petrogenesis of metamorphic rocks. Springer, New York. 348p.

Wood, J.R. & Hewlett, T.A., 1982 - Fluid convection and mass transfer in porous sandstones - a theoretical model. Geochim. Cosmochim. Acta, 46, 1707-1713.

Wopfner, H., 1960 - On some structural development in the central part of the Great Australian Artesian Basin. Trans. Roy. Soc. S. Aust., 83, 179-193.

Wopfner, H., 1966 - A case history of the Gidgealpa Gas Field, South Australia. Aust. Oil & Gas J., 12 (11), 29-53.

Woronick, R.E & Land, L.S., 1985 - Late burial diagenesis, Lower Cretaceous Pearsall and Lower Glen Rose Formations, south Texas. In: N. Schneidermann & P.M. Harris (eds.), Carbonate cements. Soc. Econ. Palaeontologists and Mineralogists Spec. Pub., 37, 265-275.

Yew, C.C. & Mills, A.A., 1989 - The occurrence and search for Permian oil in the Cooper Basin, Australia. In: B.J. O'Neil (ed.), q.v., 339-359.

Youngs, B.C., 1975 - The hydrology of the Gidgealpa Formation of the western and central Cooper Basin. Geol. Surv. S. Aust. Report of Investigations 43, 35p.

Yurtsever, Y. & Gat, J.R., 1981 - Atmospheric waters. In: J.R. Gat & Gonfiantini, R. (eds.), Stable isotope hydrology: Deuterium and Oxygen-18 in the water cycle. International Atomic Energy Agency, Vienna, 103-42.

Zaykov, V.V., Udachin, V.N. & Sinyakovskaya, I.V., 1988 - Pyrophyllite deposits. Intern. Geology Rev., 30, 90-103.

Zieglar, D.L. & Spotts, J.H., 1978 - Reservoir and source-bed history of Great Valley, California. Am. Assoc. Petrol. Geol. Bull., 62 (5), 813-826.

Hutcheon, I.E., 1989 - Application of chemical and isotopic analyses of fluid to problems in sandstone diagenesis. In: I.E. Hutcheon (ed.), Short course in burial diagenesis. Mineral Association of Canada, Montreal, 279-310.

Surdam, R.C., Crossey, L.J., Hagen, E.S. & Heasler, H.P., 1989 - Organic-inorganic interactions and sandstone diagenesis. Bull. Am. Assoc. Petrol. Geol., 73 (1), 1-23.

Acknowledgements

Many people assisted in all phases of this study. I wish to express my heartfelt appreciation to the numerous individuals whose assistance, technical expertise and support made this work possible. I warmly thank the Cooper Basin Consortium Group of Companies for giving me access to technical reports and databases. In particular, I am indebted to the management of Santos Ltd. for its generous logistical support throughout the course of this project. I also wish to thank the following individuals and organisations for their assistance:

- the Cooper Basin development and exploration teams, the library staff, the staff in the drafting department, and the members of the Exploratory Studies Group at Santos Ltd., especially Mr. S. Aufderheide, Ms. D.M. Burckhardt, Mr. H. Griffiths, Mr. N. Hamilton, Mr. G. Hanisch, Dr. R.S. Heath, Mr. M. Henderson, Mr. S. Maguire, Ms. R. McLean, Mr. E. Montague, Mr. S. Taylor, Mr. N.P. Tupper, and Mr. R. Young;

- Dr. S.E. Phillips (Amdel Core Services Ltd.);

- The SADME Core Library, in particular Mr. B. Logan and his staff;

- the Electron Optical Centre of the University of Adelaide;

- the Department of Geology and Geophysics, University of Adelaide, for preparing some of the thin sections, running the XRD traces, printing some of the photomicrographs, and for assistance with CL work and coal microscopy, namely Mr. R. Barrett, Mr. E. Bleys, Dr. Y. Bone, Mr. B. Michaelsen, Mr. W. Mussared, Ms. D. Padley, Mr. G. Trevallyan, and Dr. K. Turnbull;

Major funding was generously provided by NERDDC (project no. 1175) and SENRAC, and a Geology and Geophysics Research Scholarship made available by the NCPGG. I warmly thank Drs. M. Brennan (Santos Ltd.), D. McKirdy, P. Tindale and M. Wallace (University of Adelaide) for a critical review of the study results. Last but not least, I also wish to express my sincere appreciation to my supervisors Dr. W.J. Stuart (Director, NCPGG) and Prof. L.A. Frakes (Douglas Mawson Professor, University of Adelaide) for their constructive criticism of this thesis, as well as their encouragement and full-hearted support thoughout the years.